EVALUATING THE BEHAVIOR OF LATERALLY LOADED PILES UNDER A SCOURED CONDITION BY MODEL TESTS

By

Omar K. Ismael

Submitted to the Department of Civil, Environmental, and Architectural Engineering and Graduate Faculty of the University of Kansas in partial fulfillment of the requirements for the degree of Master's in Science

Dr. Jie Han, Chairperson

Committee Members:

Dr. Anil Misra

Dr. Robert L. Parsons

Date Defended: May 14, 2014

The Thesis Committee for Omar K. Ismael certifies that this is the approved version of the following thesis:

EVALUALTING THE BEHAVIOR OF LATERALLY LOADED PILES UNDER A SCOURED CONDITION BY MODEL TESTS

Committee:

Dr. Jie Han, Chairperson

Dr. Anil Misra

Dr. Robert L. Parsons

Date Approved: May 19, 2014

Acknowledgment

First of all, I would like to express my appreciation to the Higher Committee for Education Development in Iraq (HCED Iraq) for sponsoring me and giving me this great opportunity to study for my Master's degree at such a well-known university - the University of Kansas.

Second of all, I would like to express my sincerely appreciation to my advisor Dr. Jie Han for giving me this wonderful opportunity to work with him in the field of soil-structure interaction in which I am interested. Without his guidance, support, and encouragement, this project would not have been possible to complete and performed as it looks now. Also, I would like to thank Dr. Anil Misra and Dr. Robert L. Parsons for their advices and support.

Furthermore, I would like to thank everyone who supported and helped me by their advice and time along the process of this research. Also, I would like to thank the technicians of the University of Kansas for helping me in doing the modifications for the test box and building the timber slope blocks.

Finally, I would like to express my appreciation for my wonderful family for their support, understanding, and encouragements from my first day in the United State until this moment.

Table of Contents

Abstract

Scour removes soil around piles supporting waterfront structures and changes the behavior of laterally loaded piles from flow wave, earthquake, and wind. Limited experimental studies have been conducted so far on the behavior of laterally loaded piles under a scoured condition. To evaluate their behavior under a scoured condition, model tests of laterally loaded piles were conducted in this study to investigate the effects of the scour depth, scour slope, and scour width under both static and repeated loading. Total of 41 tests were conducted in this study.

For the static loading phase, the scour depth ranged from 0 to 500 mm with a 100-mm increment and a test was conducted for each scour depth. The scour slope ranged from 0 to 30 degrees with a 15-degree slope increment and for each slope increment four tests were conducted with scour depths ranged from 200 to 500 mm. The scour widths were 0, 240, 400, and 667 mm and for each scour width four tests were conducted with scour depths ranged from 200 to 500 mm. On the other hand, only three tests were conducted to investigate the effect of the scour depth, scour slope, and scour width under repeated loading. The scour depths were 200 and 400 mm, the scour slopes were 0 and 30 degrees, and the scour widths were 0 and 667 mm. Two-way loading was the method of applying repeated loads and a safety factor of 2.0 was applied for the ultimate lateral load capacities of the piles calculated using Broms' method. Pile failure was defined when the lateral displacement at the point where the lateral load was applied reached 20% the diameter of the pile.

The static loading test results showed that the ultimate lateral load capacities from the experimental work were close to those obtained from Broms' method. The ultimate lateral load

capacities decreased significantly as the scour depth increased. At the same scour depth, the increased scour slope increased the ultimate lateral load capacities for the pile. Furthermore, at a constant scour depth, the increased scour width decreased the ultimate lateral load capacities for the pile. On the other hand, the repeated loading test results showed that the lateral displacement at the point where the lateral load acted was decreased as the scour depth and the scour width increased. Furthermore, the results also showed that the lateral displacement at the point where the lateral load acted increased as the scour slope increased.

List of Figures

List of Tables

Chapter One

Introduction

1.1. Background

Scour of soils around piles and piers that support waterfront structures and bridges may cause failure of these structures and result in costly losses. Such failure may pose a danger to public safety. According to Lagasse *et al.* (2007), scour caused 60% of the bridge failures in the United States. In 1993, the flood in the upper Mississippi basin caused 23 bridges to fail with an estimated loss of $15 million. In 1994, the flooding induced by the Alberto storm in Georgia caused damage to over 500 bridges (Richardson & Davis, 2001). The Georgia Department of Transportation (GADOT) reported a total loss of $130 million **(**Richardson & Davis, 2001). Figure 1.1 shows how deep the scour depth can be in real life. Thus, clearly scour is a serious problem for waterfront structures.

Figure 1.1 Bridge Scour in Iran (Institute for Hydromechanics (IfH), 1994)

Studies (Lin *et al.*, 2010; Ni *et al.*, 2011; Mostafa, 2012) have investigated numerically the effect of the scour on the behavior of the laterally loaded piles. So far, only limited experimental studies evaluate the behavior of laterally loaded piles in sand under scoured conditions. To answer why the scour may cause the failure to the structural elements, one should investigate the effect of the scour from geotechnical and structural perspectives. From a geotechnical point of view, when the scour removes soil around the piles, the stress history of the soil changes (Daniels *et al.*, 2007; Hughes *et al.*, 2007a; Hughes *et al.*, 2007b). As the scour depth increases, the stresses decrease because of the removal of the overburden soils during the scour process. This in turn leads the soil to an over-consolidated condition from a normally consolidated soil. These new conditions make the soil unable to provide the required support for the structural elements which lead to the failure of these elements. On the other hand and from a structural perspective, when the scour removes the soil around the pile, the unsupported length for the pile will increase. This increases the slenderness of the pile if it is considered as a column and decreases the capacity of the pile to support the loads from the superstructure. Furthermore, the increment in the unsupported length of the pile increases the chance of buckling due to the removal of the lateral loads acting on the pile. As a result, failure may happen to these structural elements.

1.2. Research Objectives

This study was to evaluate the behavior of laterally loaded piles under a scoured condition, to determine the load capacities of the scoured piles, and to examine the effects of key influence factors. The effects of scour on the piles were investigated in this study by conducting reduced-scale model experiments inside a 1400 × 400 × 830 mm test box in laboratory under the following scoured conditions:

1. Scour depth: Scour depth ranged from 0 to 500 mm in 100-mm increment and a test was conducted for each scour depth.
2. Scour slope: For each scour depth, the scour slope ranged from 0 to 30 degrees with 15-degree increment and a test was conducted for each scour slope. The investigated scour depths were 200, 300, 400, and 500 mm.
3. Scour width: For each scour depth, the scour width was 0, 240, 400, and 667 mm. The investigated scour depths were 200, 300, 400, and 500 mm.

Furthermore, the effect of loading type was investigated: static and cyclic or repeated loading.

In this study, the following effects were specifically investigated:

1. Effect of scour depth on the behavior of the laterally loaded piles.
2. Effect of scour slope on the behavior of the laterally loaded piles with a constant scour depth.
3. Effect of scour depth on the behavior of the laterally loaded piles with a constant scour slope.
4. Effect of scour width on the behavior of the laterally loaded piles with a constant scour depth.
5. Effect of scour depth on the behavior of the laterally loaded piles with a constant scour width.
6. Effect of loading type on the behavior of the laterally loaded piles by comparing experiments having the same scour depth, the same scour slope, or the same scour width.

7. Effect of scour slope on the behavior of the laterally loaded piles with a constant scour depth under cyclic loading.
8. Effect of scour width on the behavior of laterally loaded piles with a constant scour depth under cyclic loading.

1.3. Organization

Chapter 1 presents a brief introduction for this study. Chapter 2 presents a literature review of scour concepts, basic sand properties, past studies on the behavior of laterally loaded piles without scour, and past studies on the effects of scour on the behavior of the laterally loaded piles. Chapter 3 discusses the materials used in the experiments, the preparations for the experiments, and the setup for each group of the experiments. Chapter 4 provides the data from the experimental work. Chapter 5 presents the analysis and comparison of the test results from the experimental work. Chapter 6 provides the conclusions of this study and recommendations for future studies.

Chapter 2

Literature Review

2.1. Introduction

In this chapter, the literature review summarizes the research on the behavior of laterally loaded piles under scoured conditions. The literature review consists of three sections: (1) Section 2.2 introduces scour in sand in terms of origin, types, and geometry, (2) Section 2.3 discusses research on laterally loaded piles without scour, and (3) Section 2.4 discusses research on laterally loaded piles under scoured conditions.

2.2. Scour in sand

The discussion of scour in sand includes the following three aspects: scour definition, scour types, and geometry of scour holes.

2.2.1. Scour definition

Scour is described as the removal of soils by flowing water from the stream bed and banks and around bridge piers and abutments. The scour rate depends on the type of the bed soil. Rapid scour rates exist in loose granular soils, while low rates exist in cohesive or cemented soils. So scour in sandy soils is a major issue. However, ultimate scour depth in cohesive or cemented soils can be as great as the ultimate scour depth in loose granular soils (Richardson & Davis, 2001). Thus, scour in cohesive soils can be a long-term problem.

2.2.2. Scour Types

Scour can be divided into three major types: long-term aggradation or degradation of the river bed, general scour, and local scour. These three types are also known as: general scour, contraction scour, and local scour respectively by Melville and Coleman (2000) as shown in

Figure 2.1. Channel migration is also considered as a scour type by Richardson and Davis (2001).

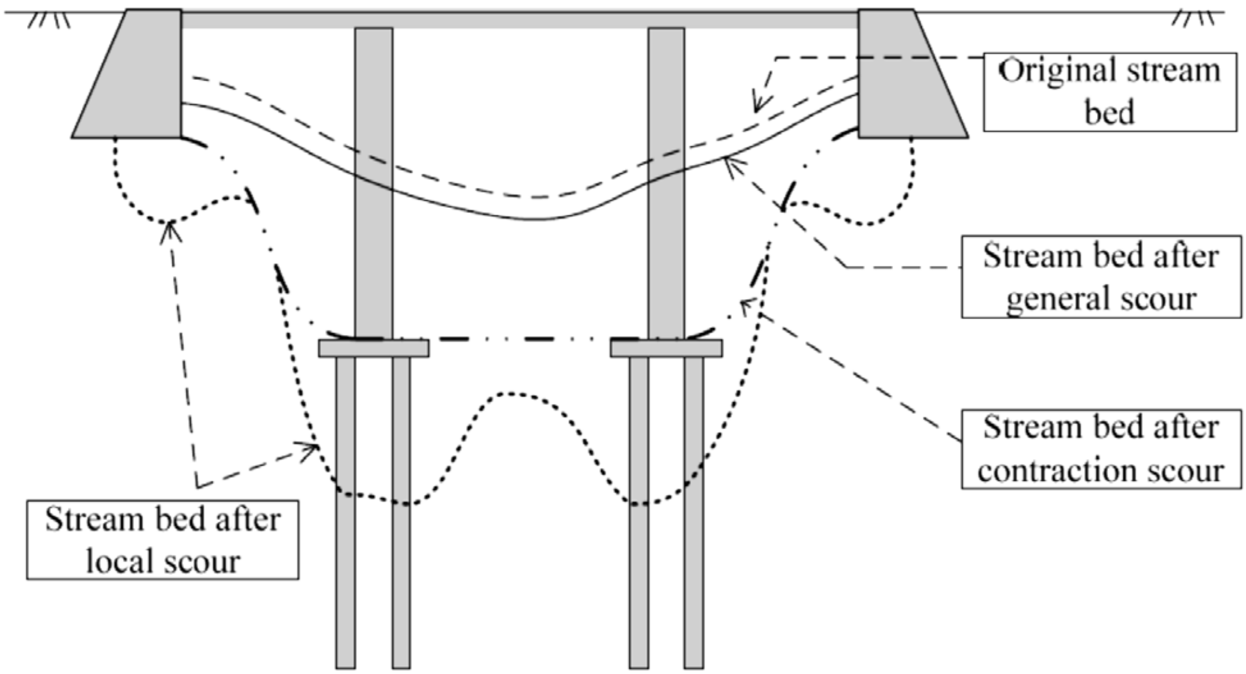

Figure 2.1 Scour types that might occur at a bridge (Lin, 2012)

Long-term aggradation or degradation of the river bed: Naturally or human-induced causes affect current characteristics of the river on which the bridge is located, change the long-term stream elevation. These changes are known as aggradation and degradation. Aggradation is the deposition of materials upstream of a bridge from channels or watersheds, while degradation is the process of lowering the streambed and happens because of a shortage in the supply of upstream sediment (Richardson & Davis, 2001).

General scour: General scour on the other hand refers to uniform or non-uniform dropping across the bed of a stream at the bridge. A contraction in the flow or other conditions such as flow around a bend may cause general scour. This contraction scour occurs when a reduction in the flow area happens either because of a bridge or by a natural constriction in the stream. When the flow area decreases, the average flow velocity and bed shear stress increase because of continuity which leads to a removal of materials from the stream bed. In riverine areas, when the flow area increases by scour and the velocity decreases and the sediment rate equals the transport rate, contraction scour can reach equilibrium so that it becomes a short-term scour. In coastal areas on the other hand, equilibrium cannot be reached due to tidal effects so that contraction scour can be considered a long-term scour (Richardson & Davis, 2001).

Local scour at the piers or abutments: Piers and abutments increase flow velocity around them, which in turn removes materials around these submerged structural elements and develops a scour hole. This mechanism is known as vertices, which include a horseshoe vortex and a wake vortex as shown in Figure 2.2. The pileup of the flow on the upstream surface of pier or abutment causes a horseshoe vertex, which leads to a stream acceleration removing materials around the submerged structural element. A wake vortex refers to the vertical removal of materials which occurs downstream of the obstruction. Its intensity diminishes as the downstream distance increases. Once an equilibrium is reached between erosion forces from vertices and resistance forces from bed materials, local scour ceases (Richardson & Davis, 2001).

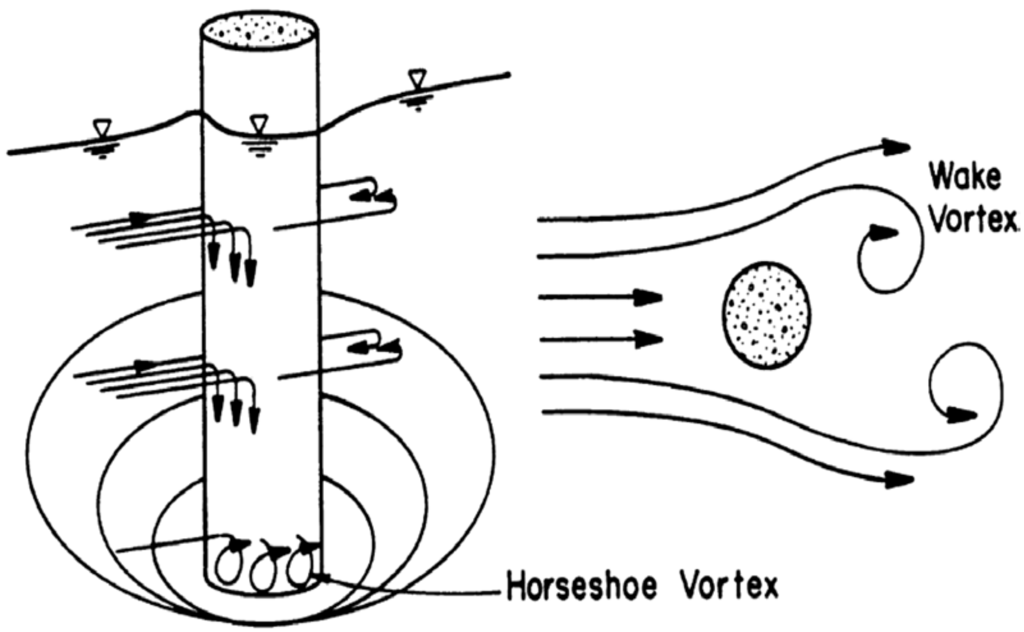

Figure 2.2 Schematic representation of local scour at cylindrical pier (Richardson & Davis, 2001)

2.2.3. Geometry of Scour Holes

Scour depth

Total scour depth results from the contributions of different scour types at the bridge pier or abutment. Many studies (Laursen, 1963; Raudkivi, 1986; Richardson & Davis, 2001; Shen *et al.*, 1969) have proposed a number of equations for calculating the scour depth. Most of the studies focused on the calculation of local scour depth because it significantly affects the total scour depth. Melville and Coleman (2000) presented a detailed method for calculating the total scour depth. A comparison of 22 scour equations was made by Mueller (1996). He found that the HEC-18 equation (Richardson & Davis, 2001) gave a conservative prediction for scour depth. The HEC-18 equation is widely used in design and it considers the characteristics of riverbed materials, bed configuration, fluid properties, characteristics of flow, and the geometry of the pier and footing as components to calculate the local scour, as shown in the equation below:

$$\frac{y_s}{y_1} = 2.0K_1K_2K_3K_4\left(\frac{a}{y_1}\right)^{0.65} Fr_1^{0.43} \qquad 2.1$$

where, y_s = scour depth (m); y_1 = flow depth directly upstream of the pier (m); K_1 = correction factor for pier nose shape; K_2 = correction factor for angle of attack of flow; K_3 = correction factor for bed condition; K_4 = correction factor for armoring by bed material size; a = pier width (m); L = pier length (m); Fr_1 = Froude number directly upstream of the pier = $\frac{V_1}{(gy_1)^{1/2}}$; V_1 = mean velocity of flow directly upstream of the pier (m/s); g = acceleration of gravity (i.e., 9.81 m/s^2).

Scour width

According to Richardson & Davis (2001), the following equation can be used to estimate the top width of a scour hole in cohesionless soils:

$$W = y_s \times \left(K + Cot(\theta)\right) \qquad 2.2$$

where, W = top width of the scour hole form each side of the footing (m); y_s = scour depth (m); K = bottom width of the scour hole related to the scour depth (m); θ = angle of repose of the bed material ranging from about 30° to 44°.

2.3. Laterally loaded piles in sand without a scour hole

Many methods have been proposed to calculate the ultimate lateral load capacity for a pile without scour and they differ in their methodology of the analysis. The complexity of these methods also varies from equations that are ready to be used, like Broms' method to complex analytical and numerical solutions such as 3D continuum modeling.

In this study, Broms' method was adopted in the calculation of the ultimate lateral load capacity of the pile because this method is simple and includes the distance between the soil surface and the point where the lateral loads act in the proposed equations, This distance represents the total scour depth in this study. Brom's method can be used for both short and long piles. Furthermore, this method gives an equation for the two boundary conditions of pile head (free head and fixed head pile). According to this method, the pile failure takes place when a pile displaces at the point where the lateral loads act a distance equal to 20% times the diameter of the pile and the load required to reach this displacement is defined as the ultimate lateral load capacity of that pile (Broms, 1964).

In addition to the previous methods, Lee et al. (2011) proposed a method for analyzing the laterally loaded rigid piles in cohesionless soil nonlinearly. Their method assumes that a linear increment in the ultimate soil resistance and the modulus of horizontal subgrade reaction with depth. They validated their method by comparing the results obtained from the solution with laboratory model and field tests. They also compared their results with those gotten form 3D finite element analysis, which gave confidence in applying this method in actual problems.

The effects of influence factors, such as the geometry of the pile, the characteristics of the materials of the pile, and the properties of the soil around the pile, on the behavior of the laterally loaded pile were investigated numerically and experimentally by many researchers (Phanikanth *et al.*, 2010; Salini and Girish, 2009; Lee *et al.*, 2011). Phanikanth *et al.* (2010) evaluated the response of a single pile under lateral loads in cohesionless soils considering the factors such as pile length, pile radius, soil density, and soil type. Using finite difference techniques coded into MATLAB, they calculated the ultimate loads and pile deflections to ensure that these values remained within the serviceability requirements accounted for in the design. They observed that when loose sand changed from a dry state to a submerged state, the deflection of a short rigid pile increased about 58%. The increase in the deflection for medium and dense sands was 30% and 27% respectively when these soils changed from a dry to a submerged condition. They also found that the deflection of a short rigid pile in loose sand under a dry condition was increased by 2.69 times the deflection in dense sand under a dry condition. Under a submerged condition, the same pile in loose sand deflected about 3.57 times its deflection in dense sand.

The lateral load capacity of the pile was studied by Salini and Girish (2009) using laboratory experiments on model piles made from mild steel and aluminum pipes installed in dry river sand. Factors such as pile length, pile diameter, and soil density were considered in this study and the load-displacement curves were obtained. When pile diameter, pile roughness, pile length, pile weight, and soil density increased, the lateral load capacity of the pile increased. Furthermore, the lateral load capacity of a group pile was more than that of a single pile and the mild steel pile had a higher lateral load capacity than the aluminum pile.

In addition to the previous studies, the effect of the multilayered sand conditions on the behavior of the laterally loaded pile was investigated experimentally by Lee *et al.* (2011). The lateral load capacities for the laterally loaded pile under this condition were also investigated and then the results were compared to those form laterally loaded pile with uniform sand conditions. Series of model tests were conducted in a calibration chamber using two model piles with different lengths. Relying on the analysis of the results, they found that the lateral behavior of the pile was affected by the conditions of the soil at the top and the bottom of the pile, while in the middle part the effect was smaller.

A good design for the piles supporting waterfront structures includes the effect of the lateral loads on the behavior of the pile, while a better design takes in consideration the effect of the cyclic lateral loads on the behavior of the pile to simulate the effect of the current waves, earthquakes, and winds. As a result, the lateral behavior of group pile and isolated single pile subjected to two-way cyclic loading in sand were investigated by Brown et al. (1988). A submerged firm to dense sand was compacted around the piles and the piles were equipped extensively with strain gages to record any variation in the soil resistance within the group. The results indicated that the deflection for the group was larger than the deflection for the single isolated pile for the same lateral load. Furthermore, they found that the method of applying the load (two-way cyclic) had a densification effect on the soil around the pile. Due to this effect, the loss in the soil resistance was small.

Long and Vanneste (1994) proposed two methods for predicting the effect of the repeated lateral load on the behavior of a pile based on 34 full-scale cyclic loading experiments on two drilled piles in Tampa. They found that the effect of the repeated loads on the behavior of the pile in sand was greater than what was predicted by the *p-y* method. The first method was based on a closed-form solution for a beam on an elastic foundation with a linearly increasing soil reaction modulus (LISM) while the second method considered the degradation of static *p-y* (DSPY). The DSPY method can be applied for the nonlinear static *p-y* or for predicting the effect of the repeated lateral load on the behavior of the pile.

2.4. Laterally loaded piles in sand with a scour hole

Limited studies investigated the effect of the scour on the behavior of the laterally loaded pile. Most of the past studies investigated the effect of the scour numerically and only a few investigated the effect of the scour on the behavior of the pile experimentally. Ni *et al.* (2011) investigated numerically the effect of scour on the lateral response of piles in sand. The effects of influence factors such as soil stiffness, pile head fixity, and the pile slenderness ratio on the lateral load capacity of an isolated pile subjected to scour were also investigated. The results showed that when the scour depth reached 1.3 to 2.4 times the pile diameter, the lateral load capacity of the pile reached almost 50% of the lateral load capacity of a pile that is not subjected to scour. Piles with a fixed head can resist more lateral loads; in other words, reduction in lateral load capacity of a fixed-headed pile is smaller than that of a free-headed pile. Ni *et al.* (2011) also found that the effect of the pile slenderness ratio decreased when the slenderness ratio was greater than 10. Thus, the effect of scour is more serious for the short piles because they have a slenderness ratio less than 10.

Furthermore, Mostafa (2012) studied the effects of local and global scour on lateral response of single piles in soils. Numerical analyses using the finite element model in the software program PLAXIS and the Winkler model in the software program LPILE were performed. Parameters such as soil type, scour depth, pile dimension, pile material, magnitude of lateral load, and load eccentricity were investigated. The results showed that scour effects for piles installed in sand were significantly larger than those for the piles installed in clay. He also found that global scour had an impact on pile bending moment and lateral displacement. Furthermore, the results indicated that when the scour depth ranged from 1 to 3 times the pile diameter, the lateral displacement at the pile head and the bending moment increased significantly when compared to those for the same pile without scour.

The effect of the scour on the behavior of laterally loaded piles in sand was studied by Lin *et al.* (2010) considering the stress history under of the sand. They found that the reduction in the lateral load capacity of the pile was due to the change in the stress history of the soil. As the scour removes the soil around the pile, the soil stress history changes from a normally consolidated to an over-consolidated state and this change causes the reduction in the lateral capacity of the pile. On the other hand, they found the stiffness of the remaining soil increased because of the change of the stress history of the soil. This means that when considering the stress history of the soil, the required depth of the embedment around the pile can be reduced.

Kishore *et al.* (2008) investigated the effect of the scour on the behavior of laterally loaded piles experimentally. They simulated the piles by using PVC and aluminum pipe piles. The tests were conducted in clay bed and a scour hole was established around the pile and some of them were in a submerged condition. The results from the experimental work were compared to those from the finite element model. They found that the lateral load capacity was reduced by 15 to 23 % and the bending moment was increased 18 to 22 % when compared to those without scour. Also, when the soil was submerged, the lateral load capacity of the pile was not affected significantly.

In a summary of this chapter, one can see that the scour is a serious problem that can cause costly losses and even pose risks on the public safety. A few studies investigated this engineering problem; however, most of them were numerical investigations. Because of the limitation of studies on this type of problem, a study was conducted in this research to investigate the effect of the scour on the behavior of the laterally loaded piles experimentally.

Chapter 3

Laboratory Model Tests

3.1. Introduction

In this chapter, the materials, the preparation of the test box and the pile, and the setup of the experiments are outlined. Section 3.1 provides a blueprint for this chapter. Section 3.2 presents the materials and their properties. Section 3.3 discusses the test box and the modification of the test box. Section 3.4 describes the instrumentation. Section 3.5 describes the scheme for the experiment.

3.2. Materials

Kansas River sand was used in this research. The gradation of the Kansas River sand is shown in Figure 3.1. Based on the ASTM standards D4254-00 and D4253-00, this sand had the minimum and maximum density values of 16.02 kN/m^3 and 18.85 kN/m^3 respectively. A manual steel compacter with a 200-mm drop distance was used in this study to compact each sand layer up to the required density as shown in Figure 3.2.

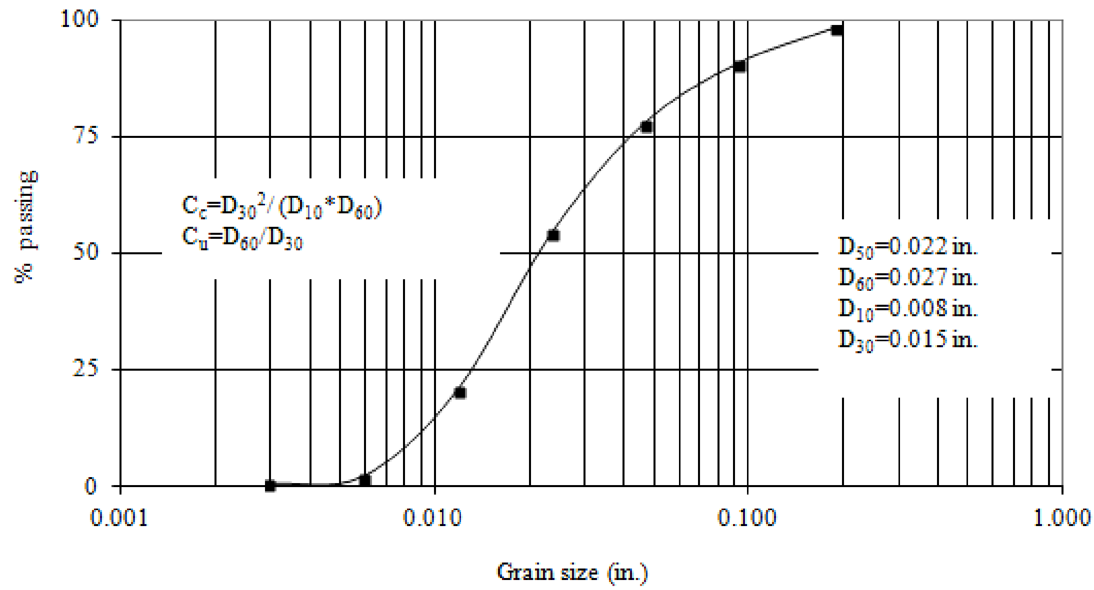

Figure 3.1 Grain Size Distribution of Kansas River Sand (Khatri, 2012)

Figure 3.2 Manual Steel Compacter

An aluminum pipe with an outer diameter of 63.5 mm and a length of 915 mm length was used as a test pile. The wall thickness of the pipe was 2 mm. The pile length to diameter ratio was 14.41. The bending stiffness of the model pile (EI) was 12.929 kN×m^2.

3.3 Test box

The test box had interior dimensions of 1400 × 400 × 830 mm and was made of three sides of wood and one side of plexiglass as shown in Figure 3.3. This box can be divided into two parts, the base part with interior dimensions of 1400 × 400 × 400 mm and the upper part with interior dimensions of 1400 × 400 × 430 mm. The thickness of the plexiglass was 25 mm.

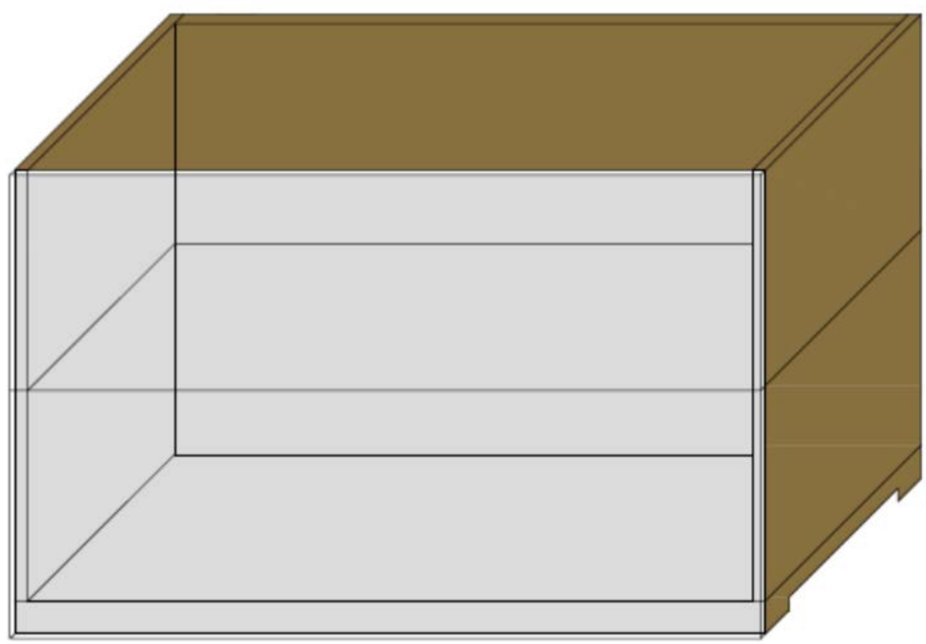

Figure 3.3 Illustration of the Test Box

Two scissor manual jacks were used to support the long sides of the box laterally to prevent any lateral deformation especially for the plexiglass side as shown in Figure 3.4.

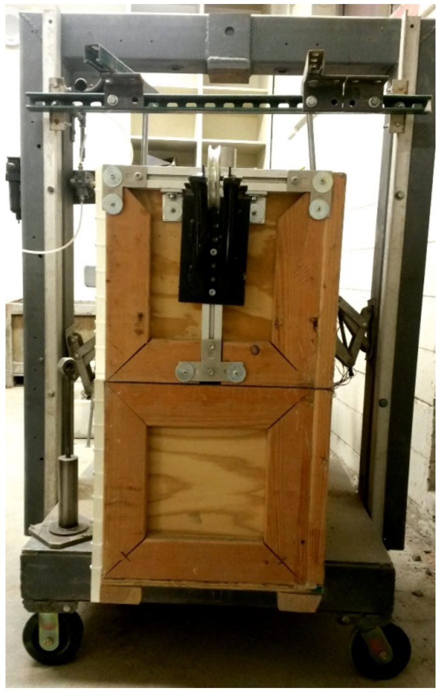

Figure 3.4 Lateral Support of the Box

In order to apply lateral loads to the pile, the upper part of the box was modified as shown In Figure 3.5. In this modified system, weights were used to apply lateral loads to the pile through a pulley system. A pulley with bearing balls was used to reduce the friction generated in the pulley itself from the pressure of the cable when the loads were applied. Two triangular steel frames carried the pulley in a stable position during the experiment. These two frames were welded to a steel plate containing holes in order to fasten the entire steel frame to the short side of the upper part of the box.

On the short side of the upper part of the box, an 80/20 extruded aluminum section was fixed to make the entire steel frame movable so it could be fastened at any required elevation. This elevation was the position of the pulley required to make the cable perfectly horizontal to prevent the generation of any vertical components on the pile that might cause a change in the behavior of the pile as shown in Figure 3.5. The weight used was 10 kg (98.1 N) or 5 kg (49 N).

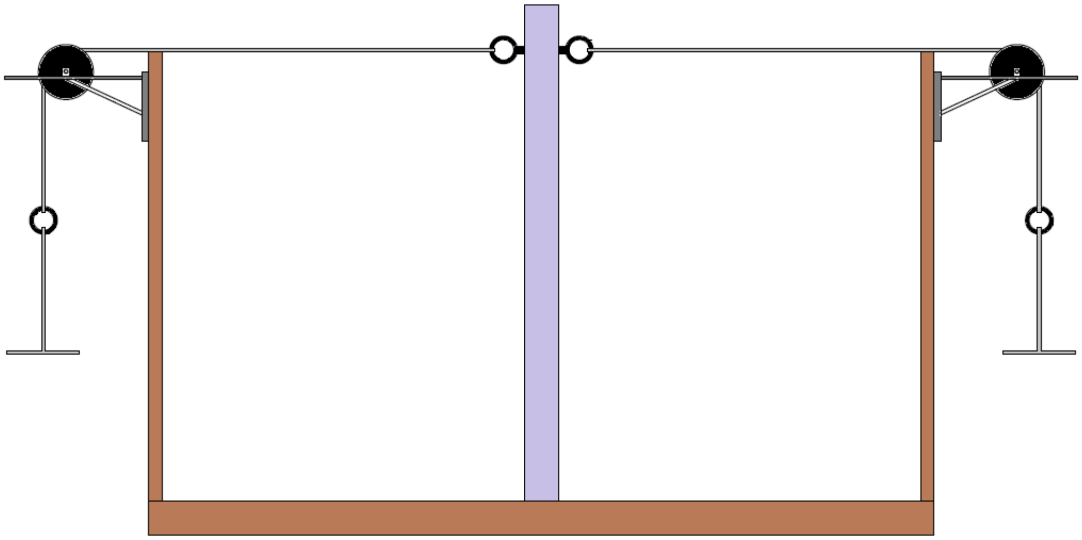

Figure 3.5 Modified Test Box with A Loading Mechanism

This system was modified on both short sides of the upper part of the box to use the same box for both static and cyclic loading experiments, which will be discussed later.

3.4 Instrumentation

Two displacement transducers (type CDP-100), one with a measuring capacity of 100-mm displacement and the other with a measuring capacity of 25-mm displacement, were used to measure pile deflections. An aluminum frame was used to fasten the transducers at the required location as shown in Figure 3.6.

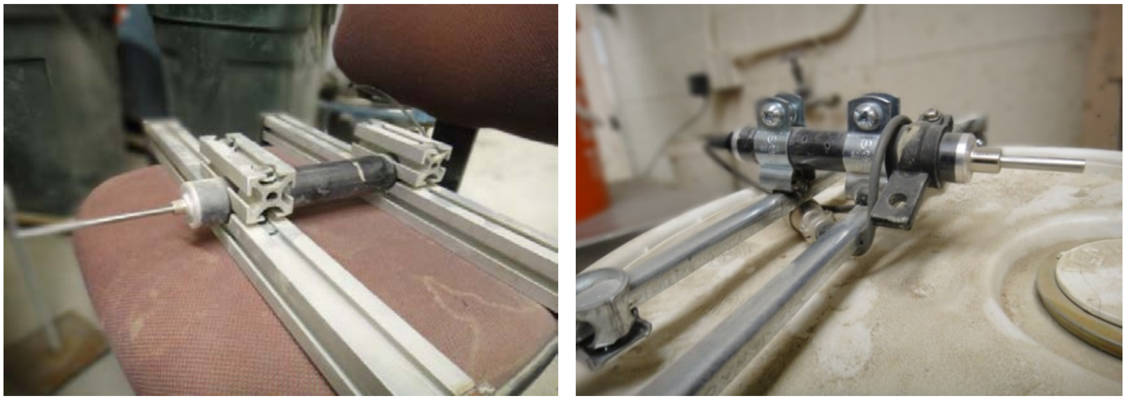

(a) **(b)**

Figure 3.6 Displacement Transducers: (a) Transducer with 100-mm Capacity and (b) Transducer with 25-mm Capacity

Three type DC-204R dynamic strain recorders as shown in Figure 3.7, each with four channels for a total of twelve channels, were used to measure the two displacement transducers and 10 strain gages on the pile.

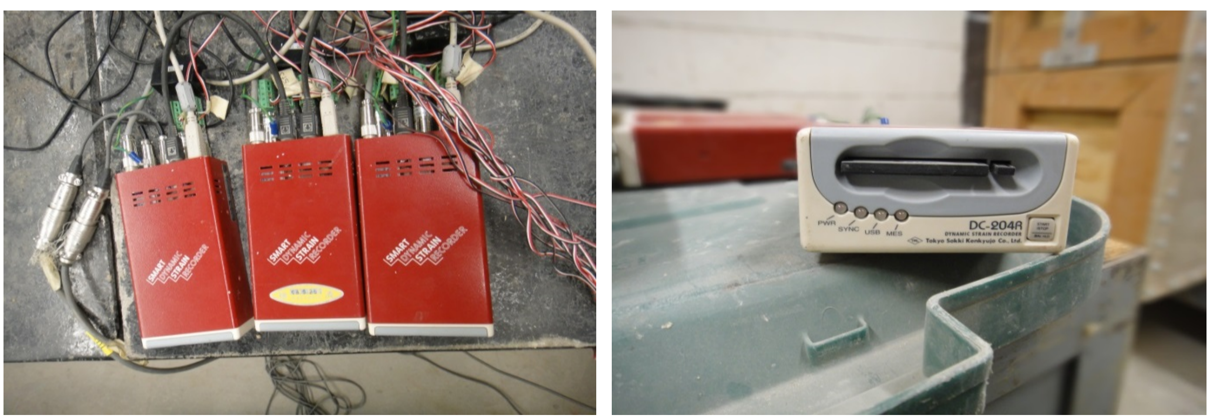

(a) **(b)**

Figure 3.7 Strain Recorders: (a) Recorders Used in Experiments and (b) Recorder Name

Ten strain gages (type of C2A-13-250LW-120) with grid resistance 120±0.6% ohms were attached on the pile to measure the strains during tests. The following procedures were adopted to prepare the pile and install strain gauges.

The pile preparation includes installation of strain gages and the distribution of the stain gages in the pile.

Surface preparation of the pile included the following steps:

- Use the acid and sand paper grade 320 to smoothen the pile surface where the strain gages would be placed. Move the sand paper in one direction to get uniform smooth surface.
- Use the neutralizer with the gauze pads to clean the surface from the residuals of the sand paper and the aluminum.
- Use the acid and sand paper grade 400 to get the smoothened surface. Also, move the sand paper in one direction to get uniform smooth surface.
- Use the neutralizer with gauze pads to clean the surface. Move the gauze from the center of the cleaned area to the outside to get a clean surface and prevent any contamination.

Installation of the strain gages included the following steps:

- Put a strain gage on a clean surface of a glass plate.
- Place a tape over the strain gage and then remove the tape with a shallow angle to ensure that the strain gage stays by the tape.
- Place the strain gage on the cleaned smooth surface of the pile.
- Add Cyanoacrylate Glue (type CN Adhesive as shown in Figure 3.8) to the surface beneath the strain gage.
- Press and hold a gauze pad on the strain gage to ensure that the strain gage is in contact with the surface and that any excessive glue has squeezed out under the strain gage.

- Remove the tape the next day to make sure that this type of glue has cured enough to fix the strain gage on the pile surface.
- Use an ohmmeter to check if the strain gage works.
- Use the coating paste (type N-1 (YH07L)) over the strain gage and the surrounding area to prevent any contact between the strain gage and the sand that may cause damage for the strain gage.
- Put a gauze pad over the coating paste as an additional protection for the strain gage and use electric tape to fix it over the pile surface.
- Repeat all the above steps for each one of the ten strain gages used on the pile as shown in Figure 3.9.

Figure 3.8 CN Adhesive Glue

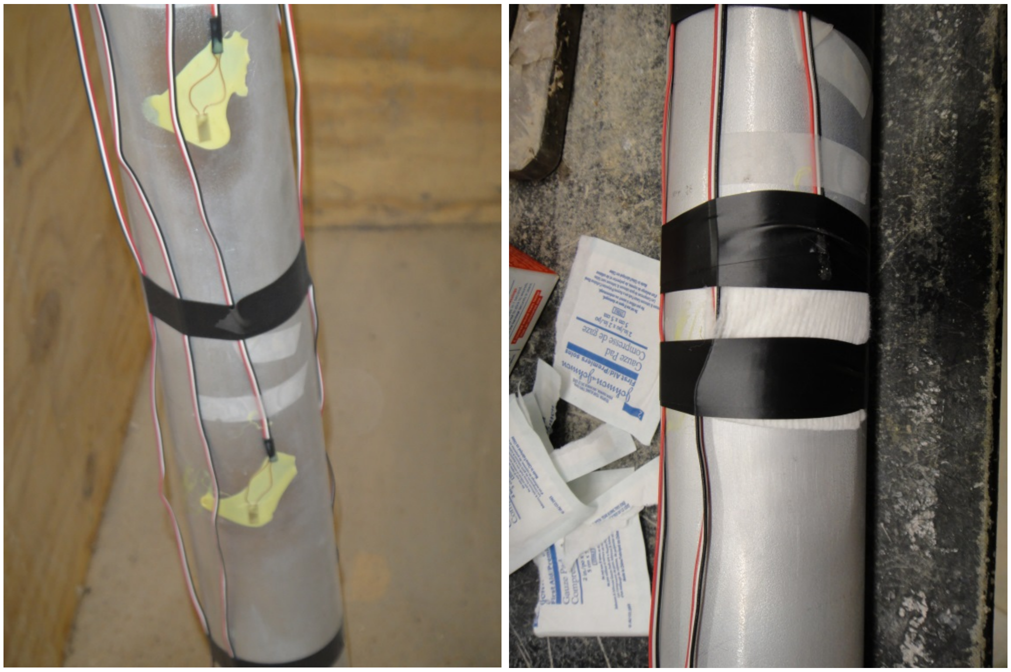

Figure 3.9 Installations and Protection of the Strain Gages

Ten strain gages were sufficient for the experiments. Five of them were placed along the pile surface that faced the cable where the loads were applied, while the rest of them were spread along the pile surface away from the loading surface on the opposite side of the pile.

For each surface, the strain gages were distributed starting from the base of the pile to the top where the loads would be applied. The first strain gage was placed at a distance of 19 mm from the base of the pile. The second strain gage was at a distance of 191-mm from the center of the first strain gage. The rest of the strain gages were distributed at space of 191-mm from each other as shown in Figure 3.10.

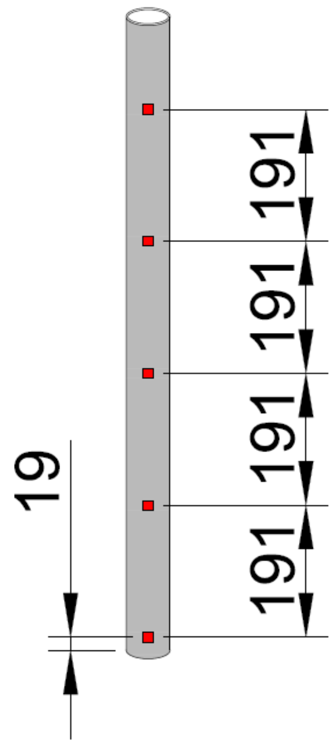

Figure 3.10 Strain Gages Distribution on the Pile (All Dimensions are in mm)

3.5. Scheme for experimental tests

The schedme for experimental tests consists of three parts: (1) pile base effect, (2) static loading tests, and (3) repeated loading tests.

3.5.1. Pile base effect

Four experiments were conducted to evaluate the effect of the base of the box on the behavior of the pile by changing the distance between the base of the box and the toe of the pile. By using a scour depth of 400 mm, all the experiments were completed in the same test box. The selected scour slope was zero to ensure that the test results could be compared with Broms' method. The distance between the box base and the toe of the pile ranged from 0 to 150 mm with a 50-mm increment for each experiment as shown in Figure 3.11. The loads were applied statically and the loads were increased whenever one of the following criteria was reached: the displacement was stable or 5-minute time period passed.

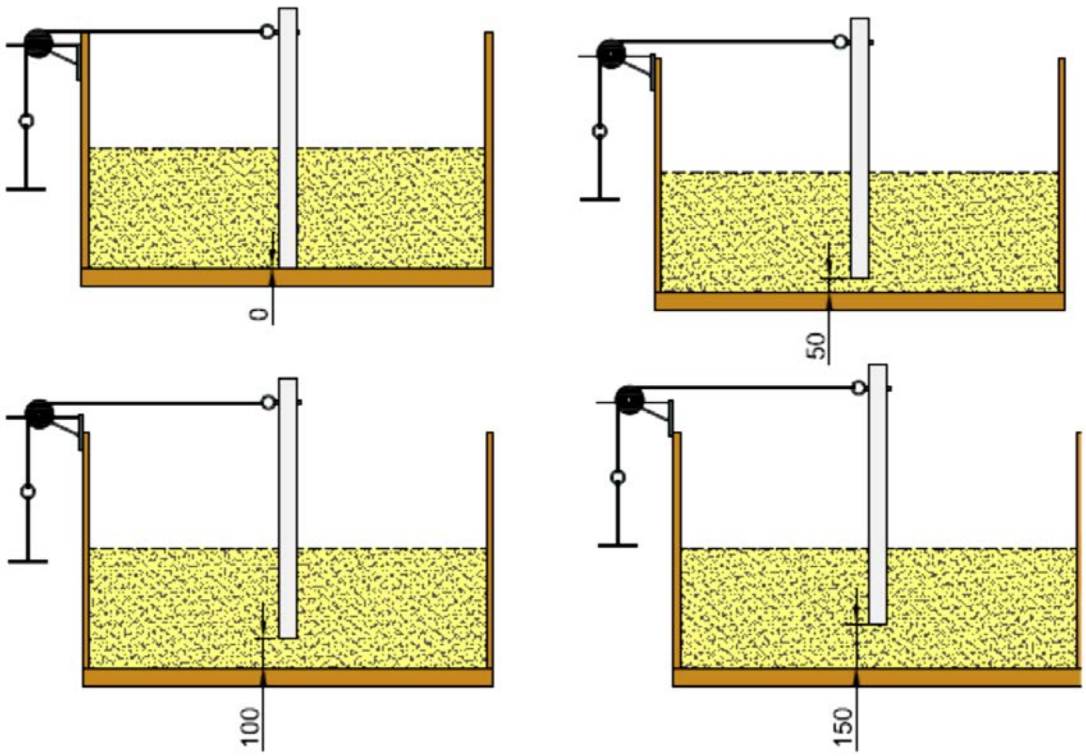

Figure 3.11 Experiments for the Base Pile Effect (All Dimensions are in mm)

The general setup for this type of experiments can be summarized in the following steps:

- Place the pile in the middle point of the box using a measuring tape.
- Use a steel cable to hold the pile in its location by tightening the cable around the pile and the steel rods in the sides of the box to prevent any pile movment.
- Divide total height of the sand to be used in the experiment into equal lift thickness (100 mm each).
- Weight the sand needed for each lift by knowing the required relative density of the sand (Dr = 70%) and the volume of that lift. Place the sand inside the box .

- Use a piece of timber to spread the sand in the box and around the pile to get a uniform level of sand. Then use the manual steel compactor to compact the sand in the box until the sand occupied the 100-mm layer.
- Repeat the two previous steps until the required height of sand for that experiment was reached.
- Connect the cable to the pile using a bolt through the hole in the pile. Then place the two displacment trasducers in the required positions. Make sure that the tip of the displacment transducers touched the pile and there was no gap in between.
- Connect the displacment transducers and the strain gages to the dynamic data recorders. Then connect these recorders to a laptop that has a program to operate and collect the required data from the recorders.
- Apply the loads according to the crateria of loading that is defined previously.

3.5.2. Static Loading Tests

In these tests, loads were applied statically and increased whenever one of the following criteria was reached: the displacement was stable or 5-minute time period passed.

The general setup for this type of test can be summarized in the following steps:

- Place the pile in the middle point of the box using a measuring tape.
- Use a steel cable to hold the pile in its location by tightening the cable around the pile and the steel rods in the sides of the box to prevent any pile movment.
- Divide total height of the sand to be used in the experiment into equal lifts (100 mm each).

- Weight the sand needed for each lift by knowing the required relative density for the sand (Dr = 70%) and the volume of that layer. Place the sand inside the box
- Use a piece of timber to spread the sand in the box and around the pile to get a uniform level of sand. Then use the manual steel compactor to compact the sand in the box until the sand occupied the 100-mm layer.
- Repeat the two previous steps until the required height of sand for that experiment was reached.
- Connect the cable to the pile using a bolt through the hole in the pile. Then place the two displacment trasducers in the required positions. Make sure that the tip of the displacment transducers touched the pile and there was no gap in between.
- Connect the displacment transducers and the strain gages to the dynamic data recorders. Then connect these recorders to a laptop that has a program to operate and collect the required data from the recorders.
- Apply the loads according to the crateria of loading that is defined previously.

Key influence factors, such as scour depth, scour slope, and scour width, were investigated in the static loading tests. An experiment was conducted for each changed factor. Static loading tests can be divided into three major groups, each investigating one key factor. These groups of tests are: scour depth experiments, scour slope experiments, and scour width experiments.

Scour Depth Experiments

In this group of experiments, the scour slope was set to zero and the scour width was set to 667 mm. This group focused on the effect of the scour depth on the behavior of the pile. Scour depth can be defined as the vertical distance from the point where the load was applied to the sand surface. Scour depth ranged from 0 to 500 mm as shown in Figure 3.12.

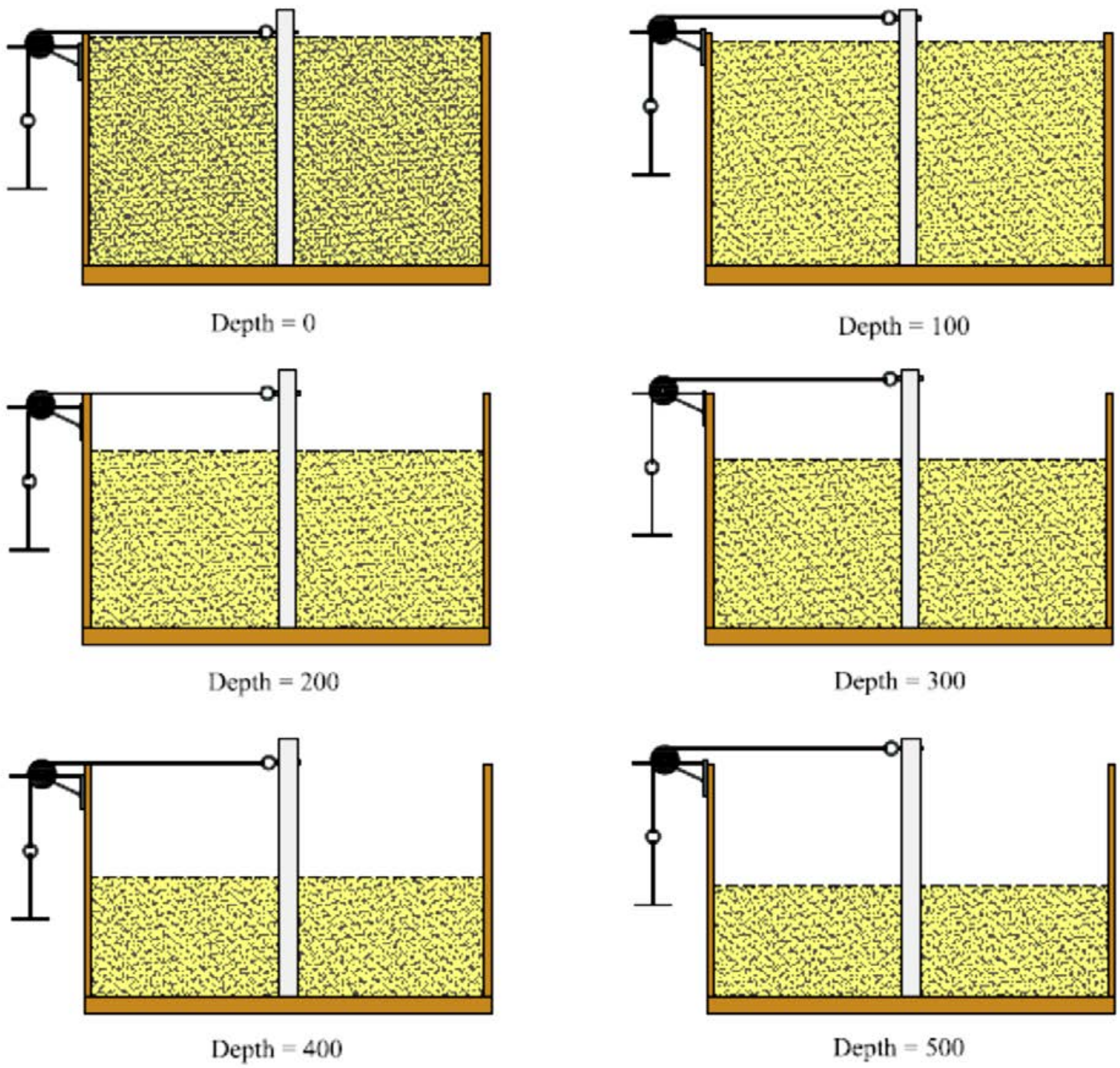

Figure 3.12 Scour Depth Experiments (All Dimensions are in mm)

Scour Slope Experiments

In these experiments, the effects of the scour slope on the behavior of the laterally loaded piles were investigated. Scour slope can be defined as the angle from the horizon to the sand surface. The scour slope was maintained using wood frames built according to the required dimensions. Relying on this definition, this group of experiments was divided into three parts where the first part consisted of experiments with the following scour depths: 200, 300, 400, and 500 mm and a scour slope equaling to 0 degree as shown in Figure 3.13. The second part consisted of experiments with the same scour depths as the first part but with a scour slope equaling to 15 degrees as shown in Figure 3.14 and the third part consisted of expirements with the same scour depth as the first part but with a scour slope of 30 degrees instead of 0 degree as shown in Figure 3.15. These three parts were to study the effect of the scour slope on the behavior of the pile with a constant scour depth. Also, the effect of the scour depth on the behavior of the pile with a constant scour slope was studied.

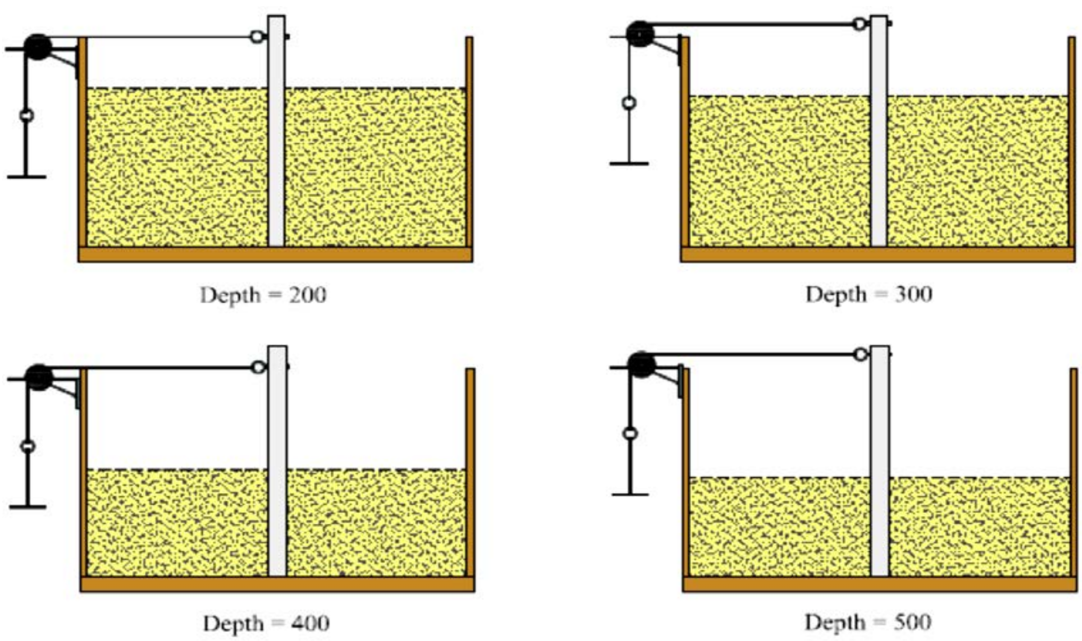

Figure 3.13 Experiments with 0-Degree Scour Slope (All Dimensions are in mm)

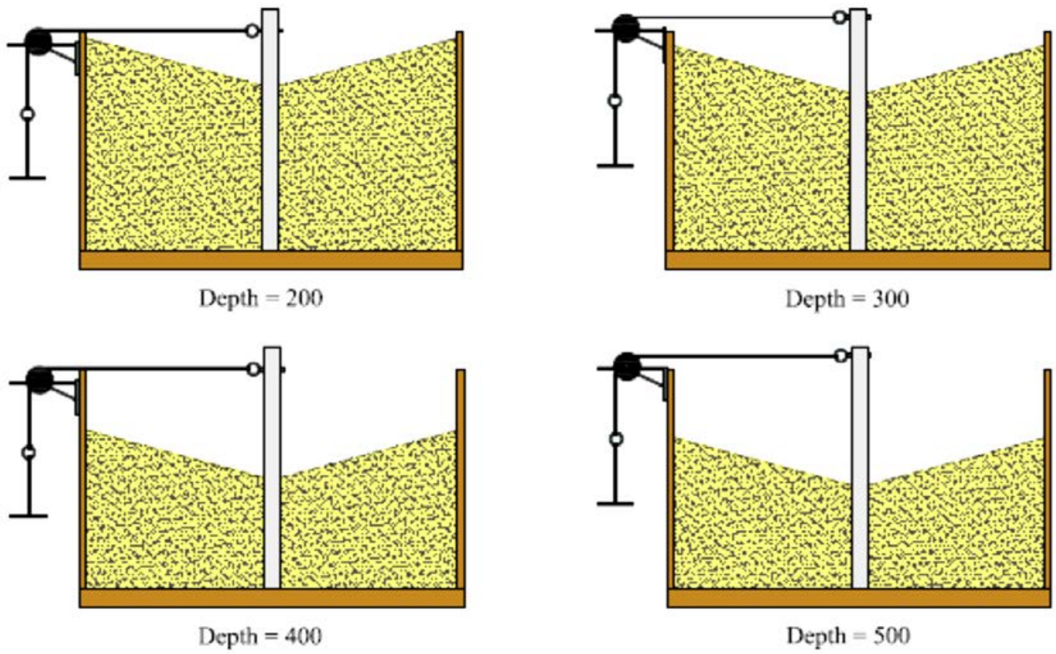

Figure 3.14 Experiments with 15-Degree Scour Slope (All Dimensions are in mm)

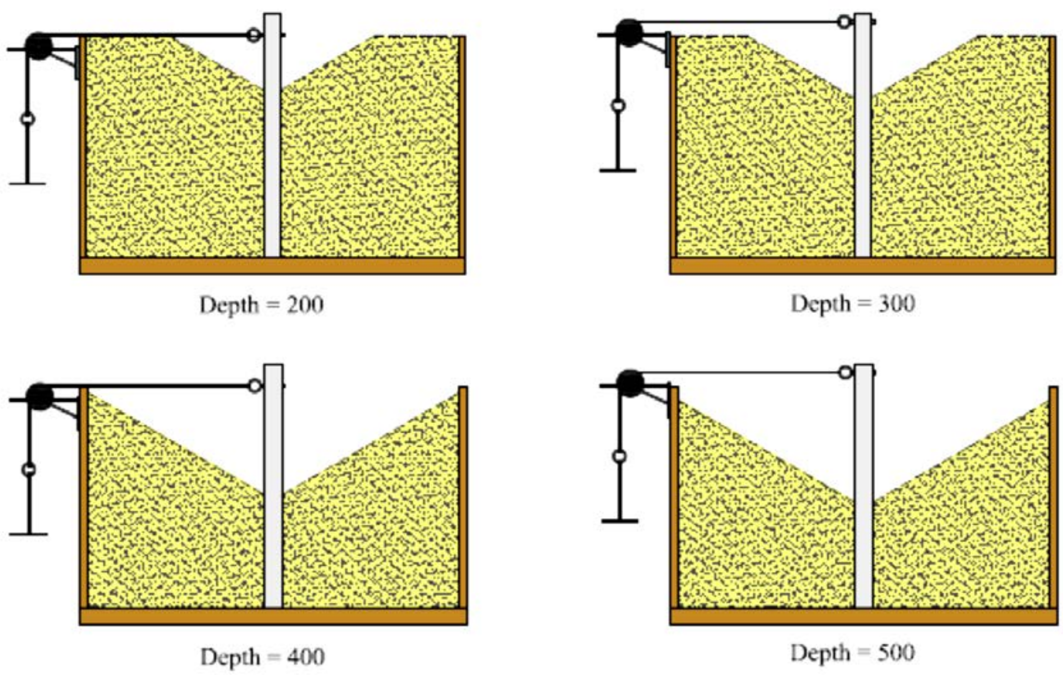

Figure 3.15 Experiments with 30-Degree Scour Slope (All Dimensions are in mm)

Scour Width Experiments

In these experiments, the effects of the scour width on the behavior of the laterally loaded piles were investigated. Scour width can be defined as the horizontal distance from the pile to the piont at which the slope in the sand starts. Using this definition, these experiments can be divided into four groups, each of which had four experiments with scour depths ranging from 200 to 500 mm. The first group had a scour width of 0 mm as shown in Figure 3.16, the second group had a scour width of 240 mm as shown in Figure 3.17, the third group had a scour depth of 400 mm as shown in Figure 3.18, and the last group had a scour depth of 667 mm as shown in Figure 3.19. These experiments were to evaluate the effects of the scour width on the behavior of the pile with a constant scour depth. Furthermore, the effect of the scour depth on the behavior of the pile with a constant scour width was invistegated.

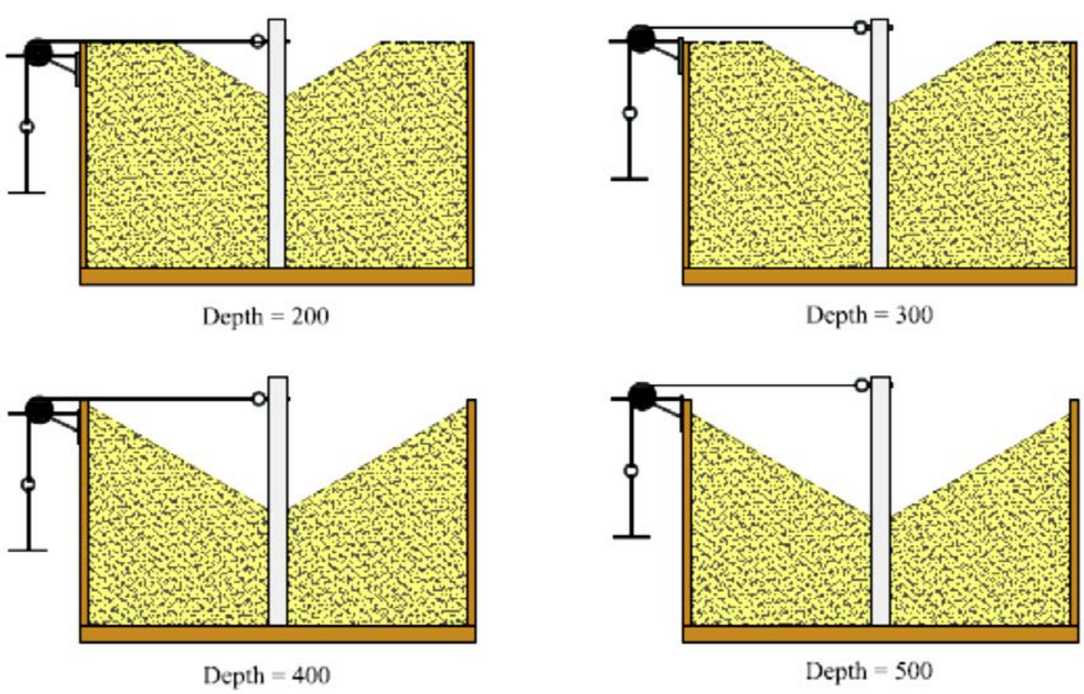

Figure 3.16 Experiments with 0-mm Scour Width (All Dimensions are in mm)

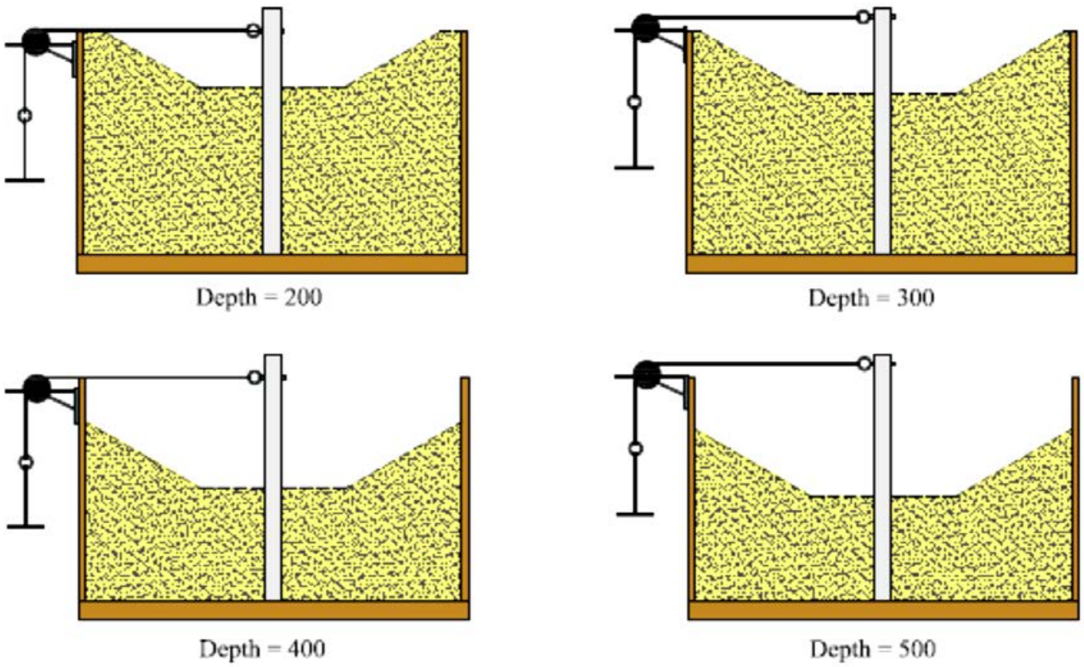

Figure 3.17 Experiments with 240-mm Scour Width (All Dimensions are in mm)

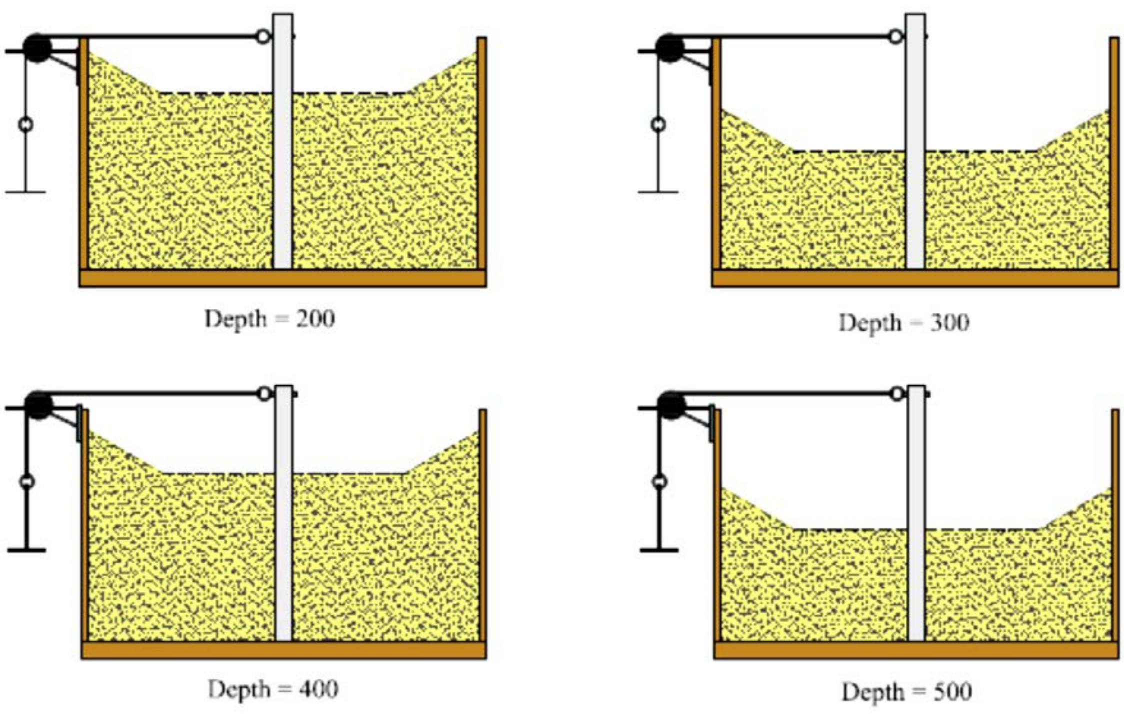

Figure 3.18 Experiments with 400-mm Scour Width (All Dimensions are in mm)

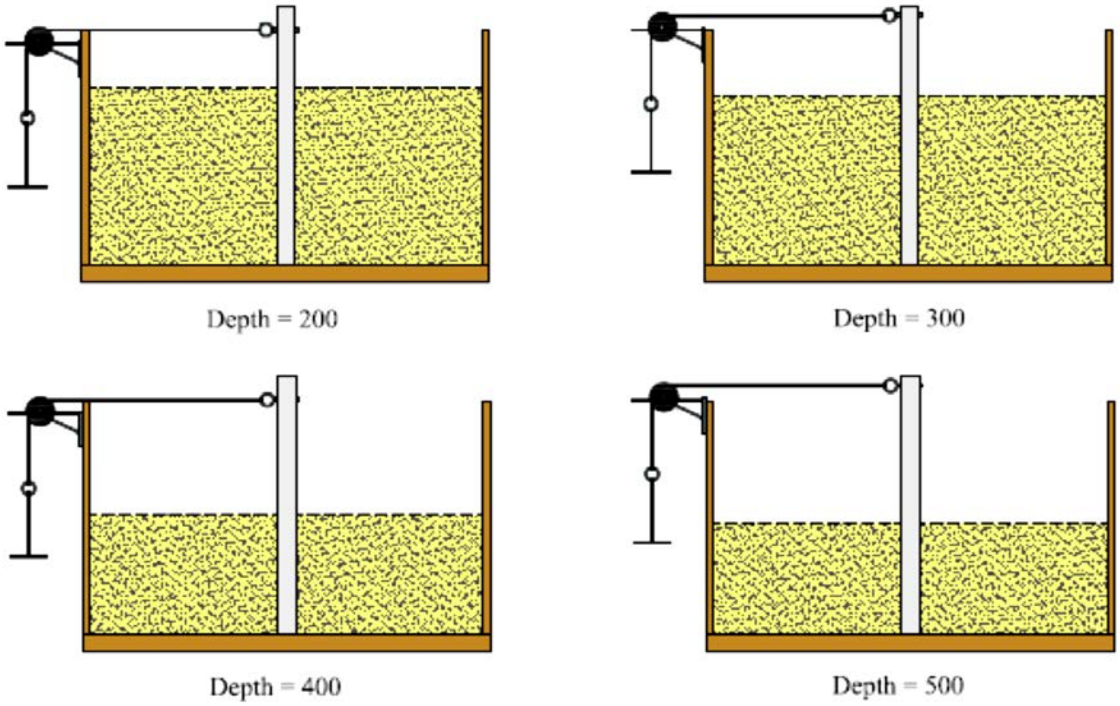

Figure 3.19 Experiments with 667-mm Scour Width (All Dimensions are in mm)

3.5.3. Repeated Loading Experiments

These experiments were to study the effect of the repeated loading on the behavior of the laterally loaded pile under scour conditions. The loading was applied repeatedly on each side of the test box. A safety factor of 2 was applied to the ultimate load capacity estimated using Brom's method to determine the repeated load. Three experiments were conducted to invistegate the effect of the scour depth, scour slope, and scour width on the repeated behavior of the laterally loaded pile under scour conditions as shown in Figure 3.20. The loading phase in these experiments was as follows:

- Apply the loads on one side of the box, then wait for one minute.
- Use a time interval of 5-15 seconds between unloading one side and loading the other side. Then repeat the previous step.

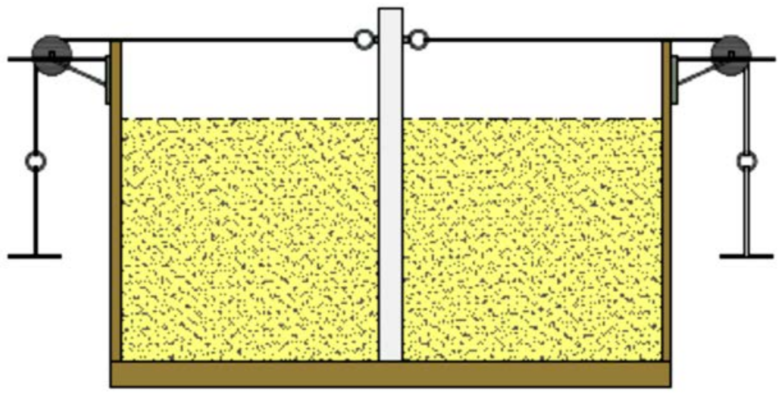

Depth = 200 mm, Slope = 0 degree, Width = 667 mm

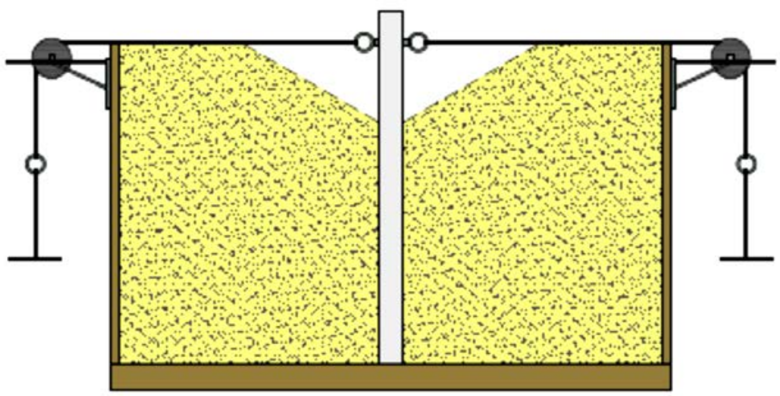

Depth = 200 mm, Slope = 30 degrees, Width = 0 mm

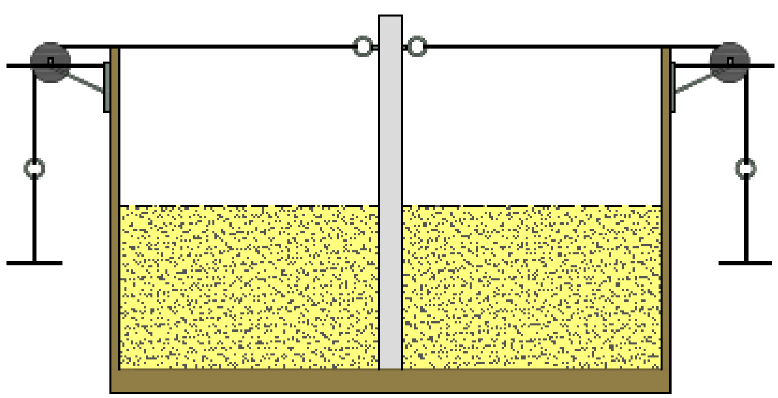

Depth = 400 mm, Slope = 0 degree, Width = 667 mm

Figure 3.20 Repeated Loading Experiments

The general setup for this type of experiments can be summarized in the following steps:

- Place the pile in the middle of the box using a measuring tape.
- Use a steel cable to hold the pile in its location by tightening the cable around the pile and the steel rods in the sides of the box to prevent any pile movment.
- Divide total height of the sand to be used in the experiment into equal lift thickness (100 mm each).
- Weight the sand needed for each lift by knowing the required relative density of the sand (Dr = 70%) and the volume of that lift. Place the sand inside the box.
- Use a piece of timber to spread the sand in the box and around the pile to get a uniform level of sand. Then using the manual steel compactor to compact the sand in the box until the sand occupied the 100-mm layer.
- Repeat the two previous steps until the required height of sand for that experiment was reached.
- Connect the cables to the pile using a bolt through the hole in the pile. Then place the two displacment trasducers in the required positions. Make sure that the tip of the displacment transducers touched the pile and there was no gap in between.
- Connect the displacment transducers and the strain gages to the dynamic data recorders. Then connect these recorders to a laptop that has a program to operate and collect the required data from the recorders.
- Apply the loads according to the crateria of loading that is defined previously.

Chapter Four

Experimental Data

4.1. Introduction

This chapter presents the data collected from the experiments. Based on the groups of experiments that were defined in the previous chapter, this chapter is divided into three sections: Section 4.2 presents the data from the experiments investigating the effect of pile base. Section 4.3 presents the data from the static loading experiments, and Section 4.4 presents the data from the repeated loading experiments.

4.2. Data for pile toe effect

Four experiments were conducted for the investigation of pile toe effect. The data for each experiment is presented in each sub-section. The data were collected from the dynamic strain recorders and then averaged for each load.

4.2.1. 0-mm base distance

Figure 4.1 presents the measured compressive strains from the strain gauges on the pile under the lateral load when the pile had 0-mm base distance. In this figure, the letter “C” represents the compression side and Numbers 1 to 5 represent the locations of the strain gages (i.e., C1 means the strain gage on the compression side of the pile and was close to the point where the lateral load was applied).

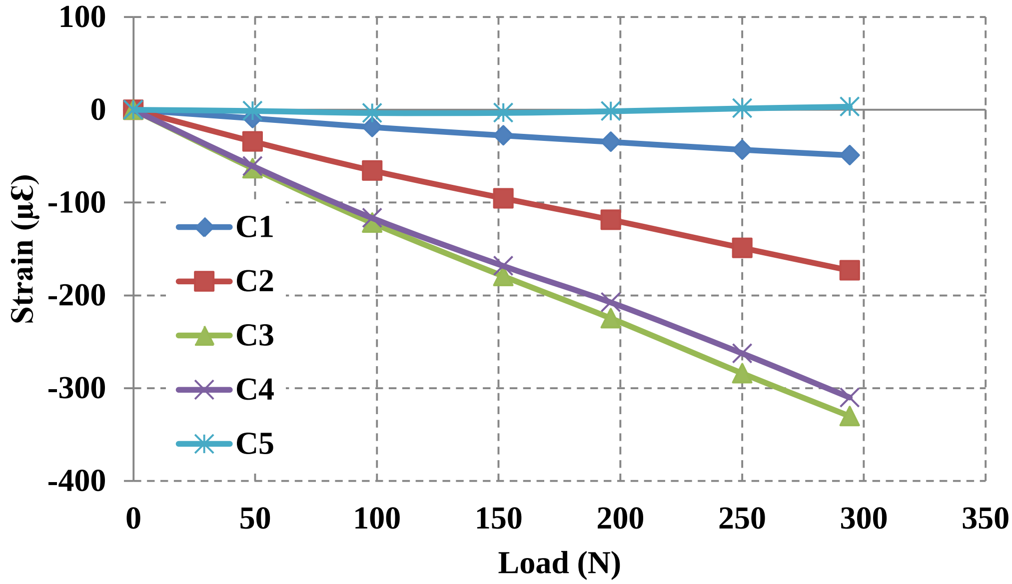

Figure 4.1 Compression Strain vs. Load for the Pile with 0-mm Base Distance

Figure 4.2 shows the measured strains from the strain gages on the tension side of the pile. The letter "T" represents the tension side of the pile and Numbers 1 to 5 represent the locations of the strain gages.

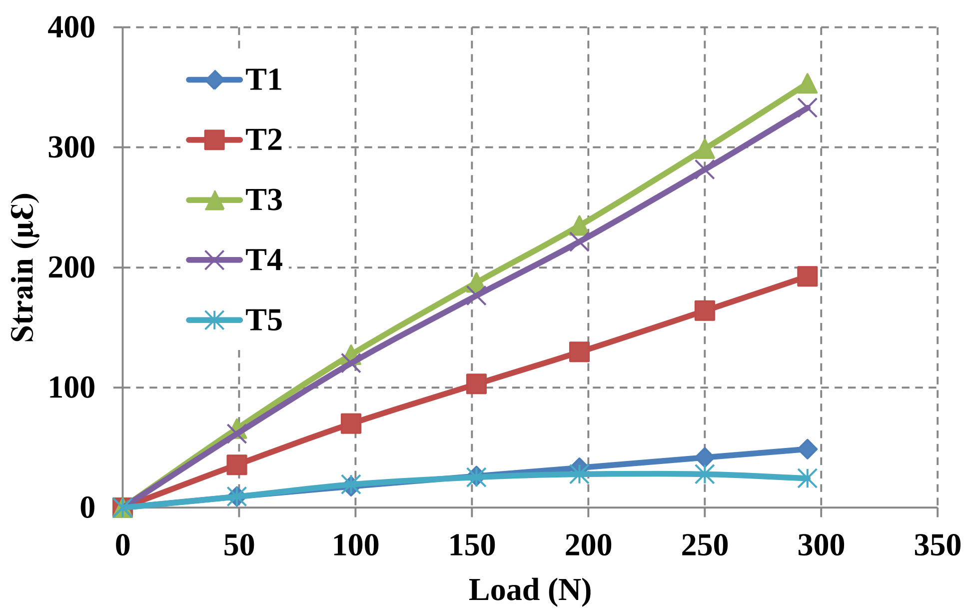

Figure 4.2 Tension Strain vs. Load for the Pile with 0-mm Base Distance

Figure 4.3 shows the measured displacements from the transducers with the load. DT1 was located at the upper level while DT2 was located at the lower level.

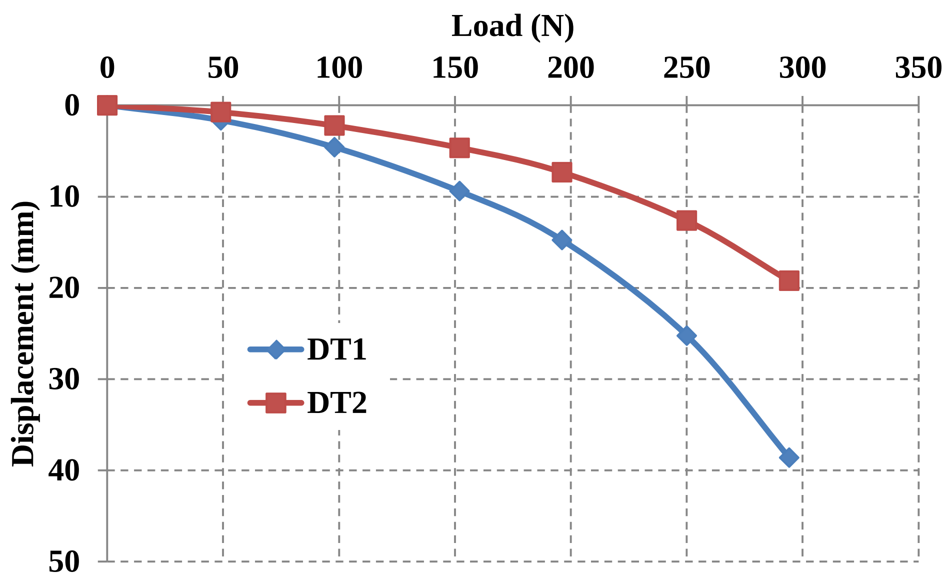

Figure 4.3 Lateral Displacements vs. Load for the Pile with 0-mm Base Distance

4.2.2. 50-mm base distance

Figure 4.4 presents the measured compressive strains from the strain gauges on the pile under the lateral load when the pile had 0-mm base distance.

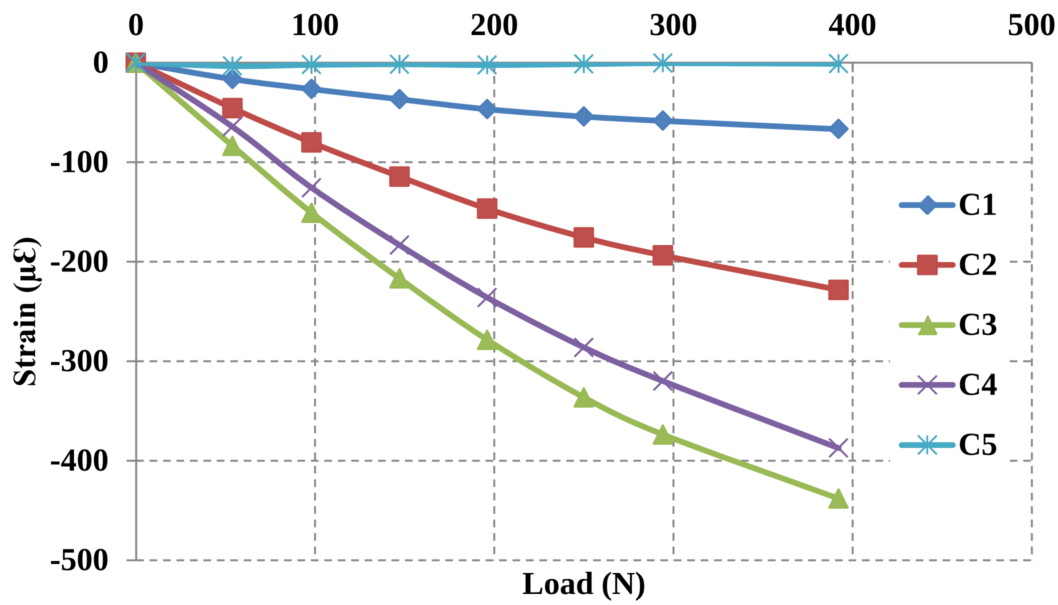

Figure 4.4 Compression Strain vs. Load for the Pile with 50-mm Base Distance

Figure 4.5 shows the measured strains from the strain gages on the tension side of the pile.

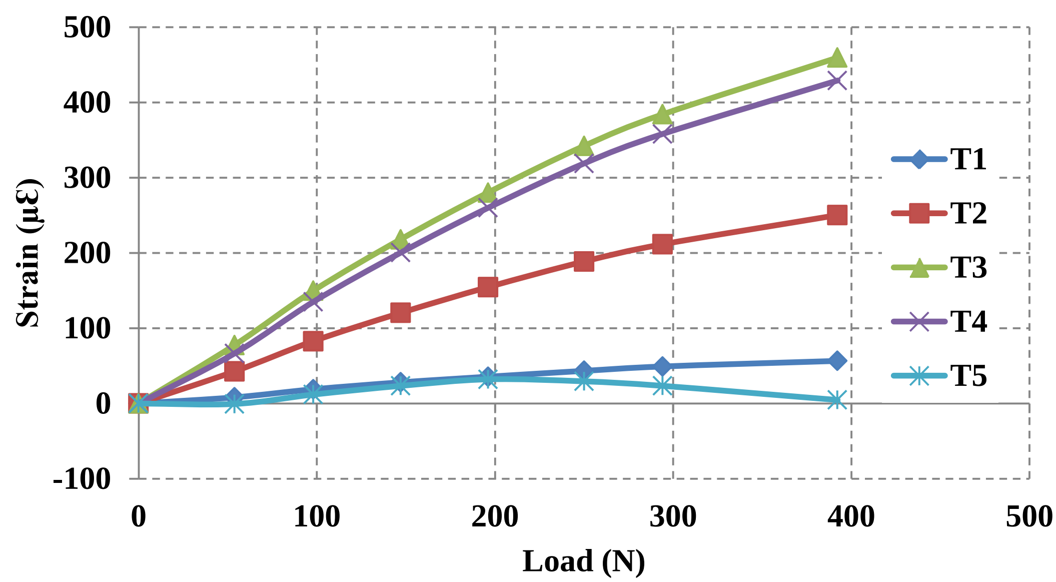

Figure 4.5 Tension Strain vs. Load for the Pile with 50-mm Base Distance

Figure 4.6 shows the measured displacements from the transducers with the load. DT1 was located at the upper level while DT2 was located at the lower level.

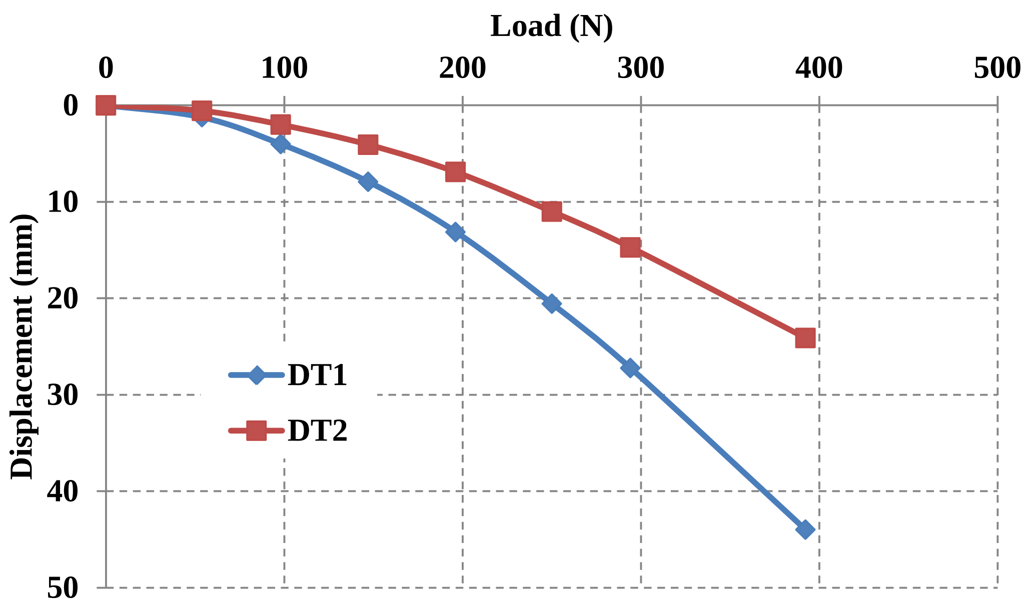

Figure 4.6 Lateral Displacements vs. Load for the Pile with 50-mm Base Distance

4.2.3. 100-mm base distance

Figure 4.7 presents the measured compressive strains from the strain gauges on the pile under the lateral load when the pile had 0-mm base distance.

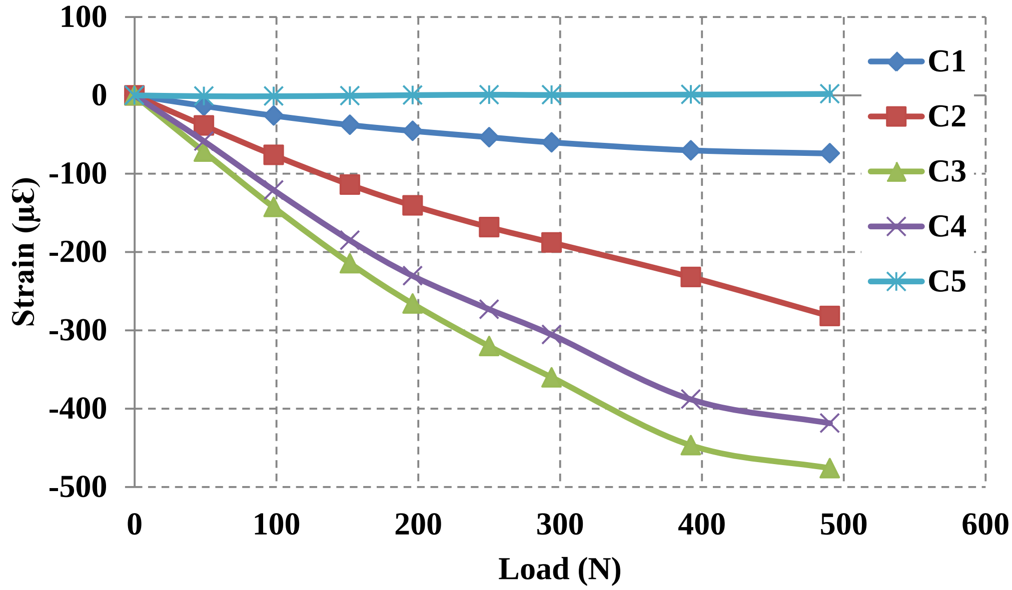

Figure 4.7 Compression Strain vs. Load for the Pile with 100-mm Base Distance

Figure 4.8 shows the measured strains from the strain gages on the tension side of the pile.

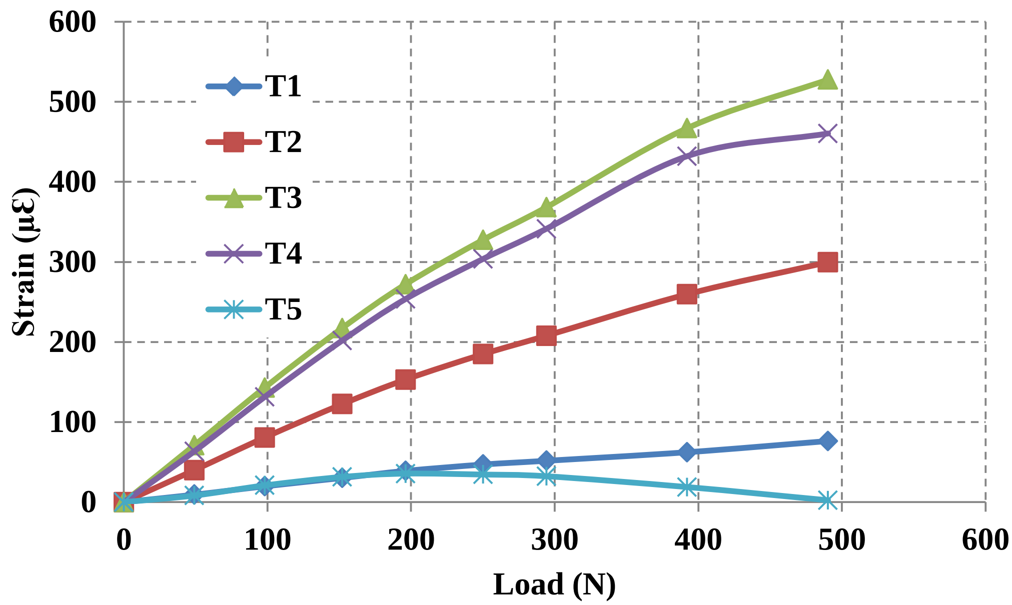

Figure 4.8 Tension Strain vs. Load for the Pile with 100-mm Base Distance

Figure 4.9 shows the measured displacements from the transducers with the load. DT1 was located at the upper level while DT2 was located at the lower level.

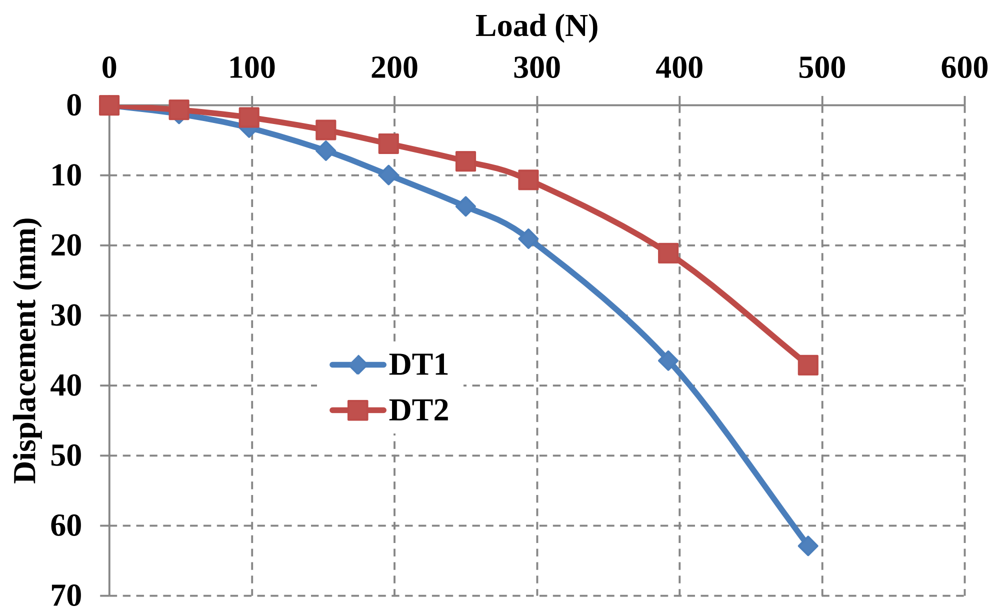

Figure 4.9 Lateral Displacements vs. Load for the Pile with 100-mm Base Distance

4.2.4. 150-mm base distance

Figure 4.10 presents the measured compressive strains from the strain gauges on the pile under the lateral load when the pile had 0-mm base distance.

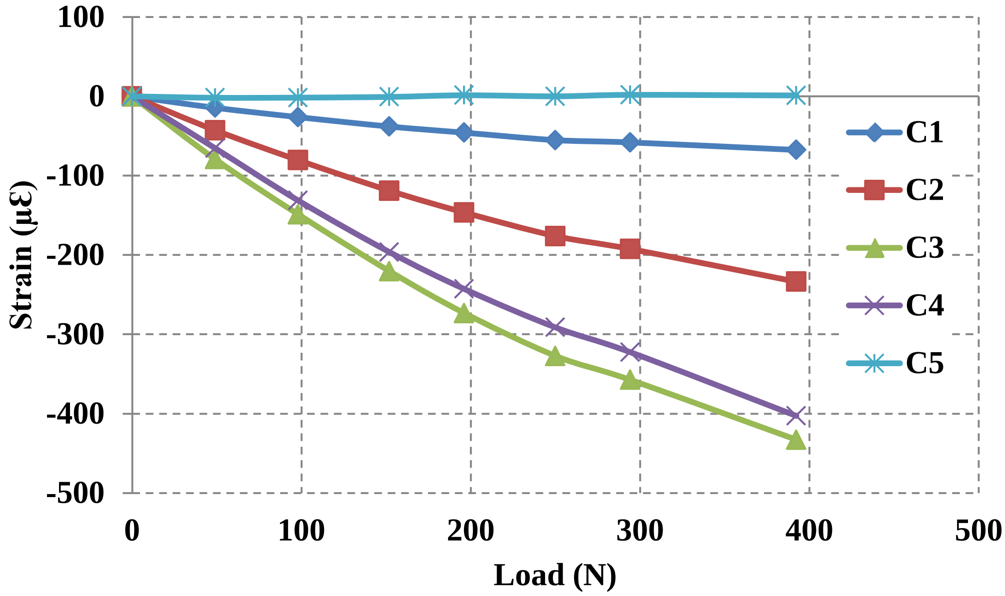

Figure 4.10 Compression Strain vs. Load for the Pile with 150-mm Base Distance

Figure 4.11 shows the measured strains from the strain gages on the tension side of the pile.

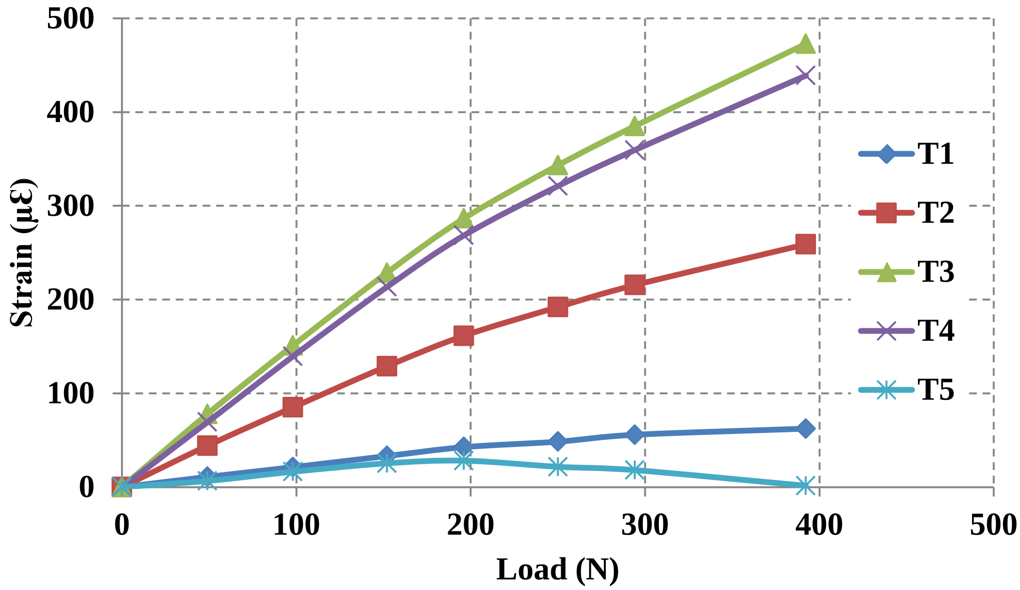

Figure 4.11 Tension Strain vs. Load for the Pile with 150-mm Base Distance

Figure 4.12 shows the measured displacements from the transducers with the load. DT1 was located at the upper level while DT2 was located at the lower level.

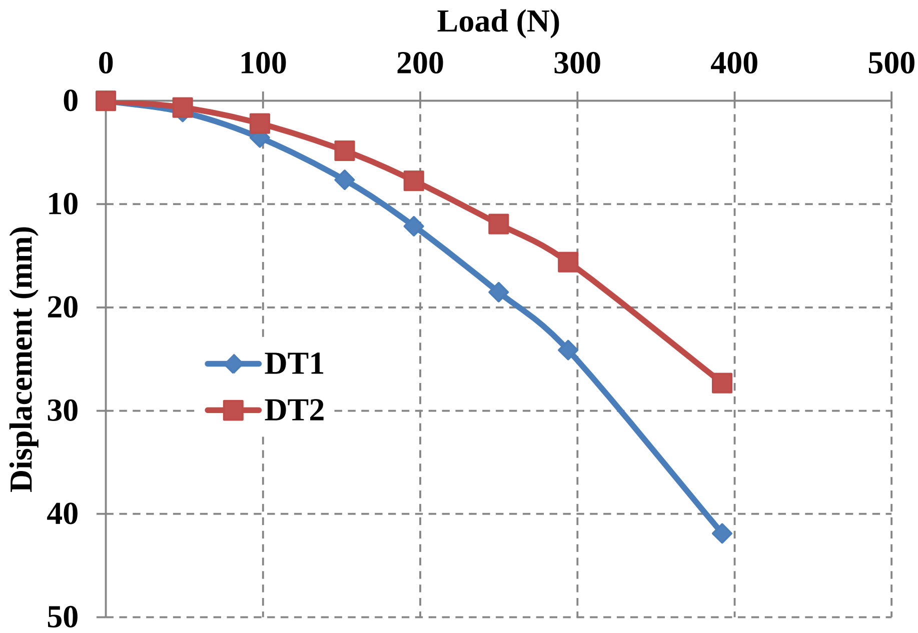

Figure 4.12 Lateral Displacements vs. Load for the Pile with 150-mm Base Distance

4.3. Static loading experiments

This section includes the data of the tests to investigate the effects of scour depth, scour slope, and scour width on the behavior of laterally loaded piles.

4.3.1. Scour depth

Six tests were conducted to evaluate the scour depth effect.

0-mm scour depth

Figures 4.13, 4.14, and 4.15 show the measured strains from the strain gages on the compression side, the strains on the tension side, and the displacements from the transducers with the load respectively.

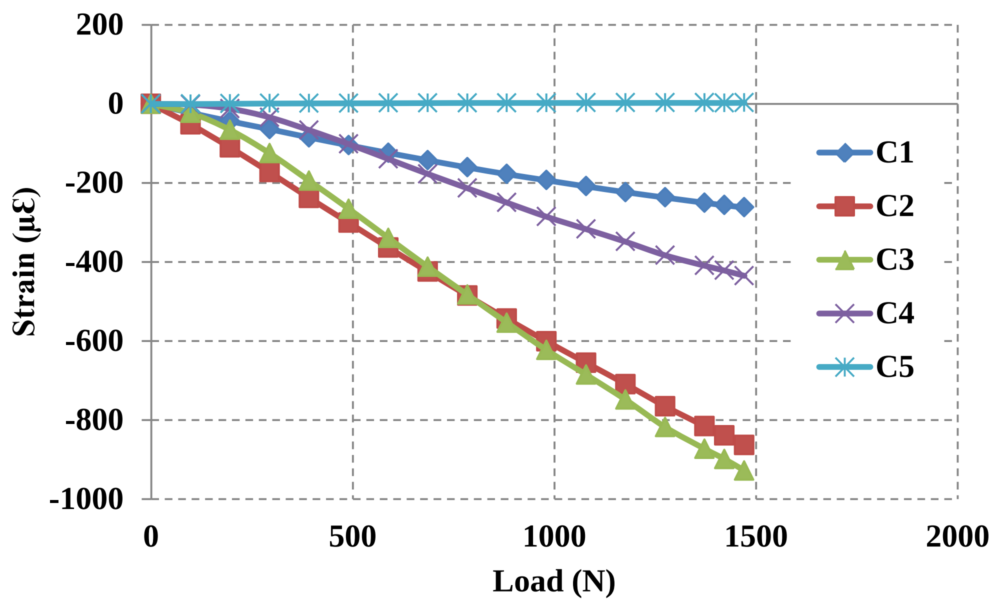

Figure 4.13 Compression Strain vs. Load for the Pile with 0-mm Scour Depth

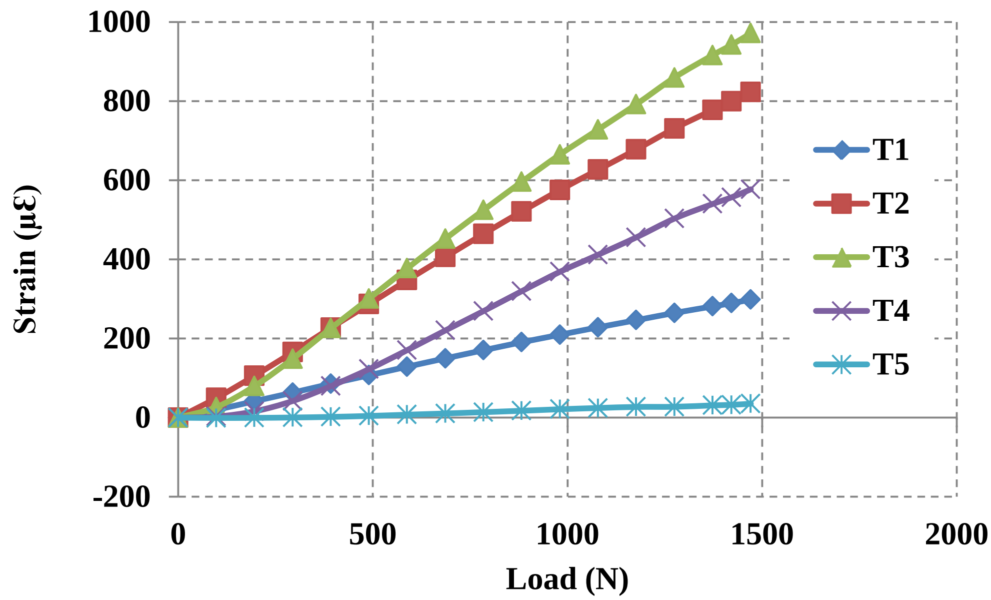

Figure 4.14 Tension Strain vs. Load for the Pile with 0-mm Scour Depth

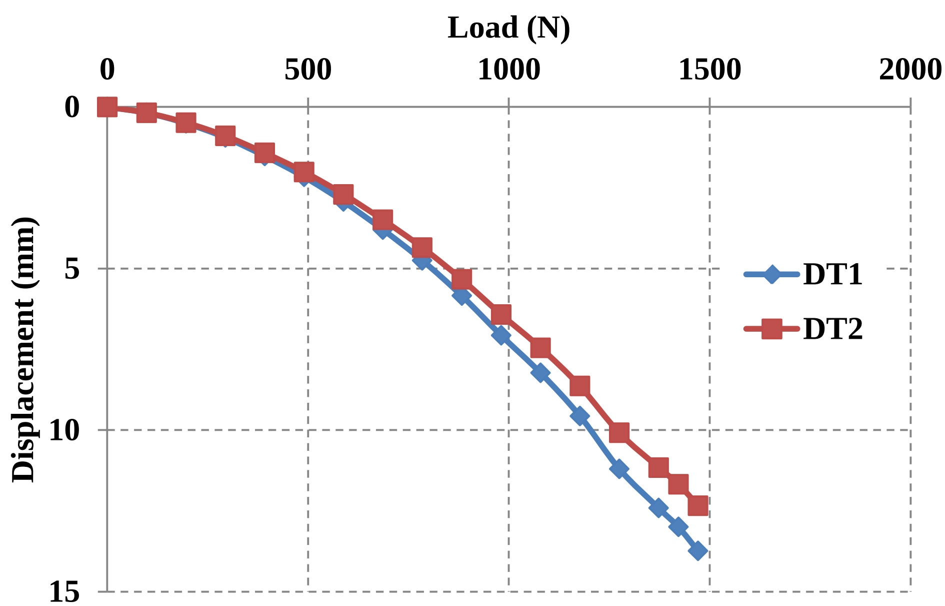

Figure 4.15 Lateral Displacements vs. Load for the Pile with 0-mm Scour Depth

100-mm scour depth

Figures 4.16, 4.17, and 4.18 show the measured strains from the strain gages on the compression side, the strains on the tension side, and the displacements from the transducers with the load respectively.

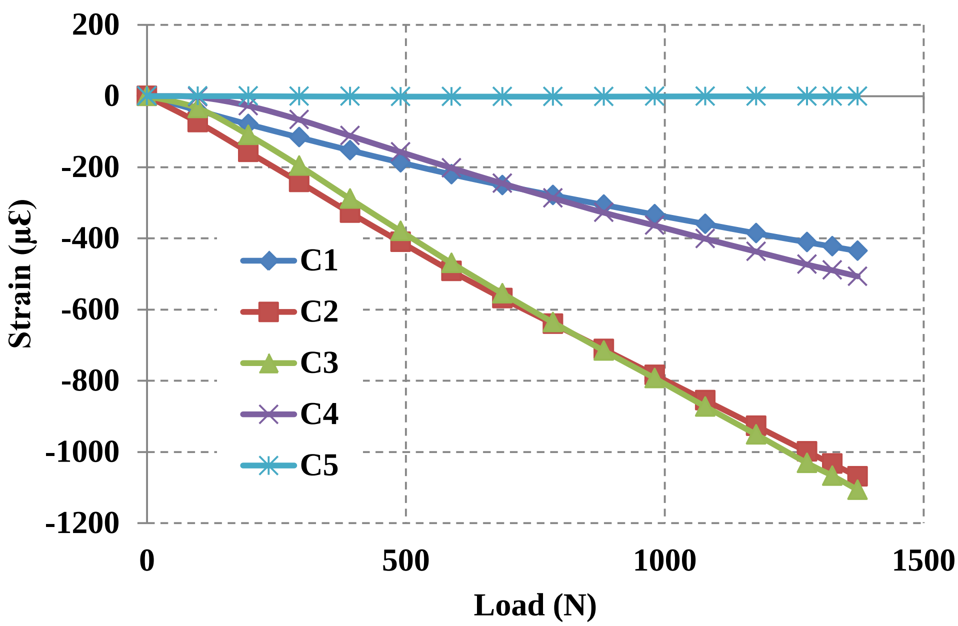

Figure 4.16 Compression Strain vs. Load for the Pile with 100-mm Scour Depth

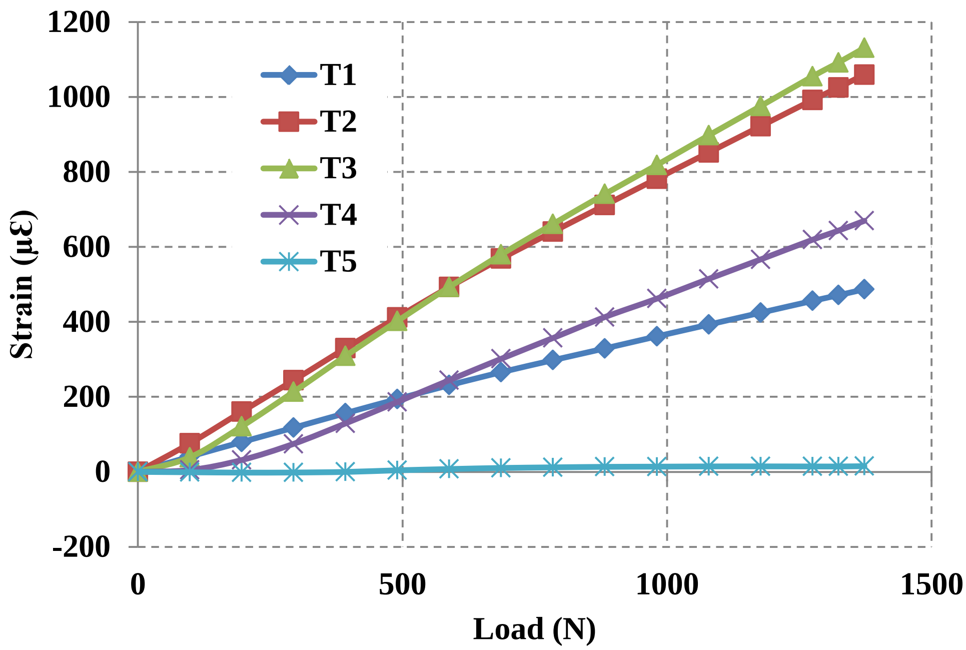

Figure 4.17 Tension Strain vs. Load for the Pile with 100-mm Scour Depth

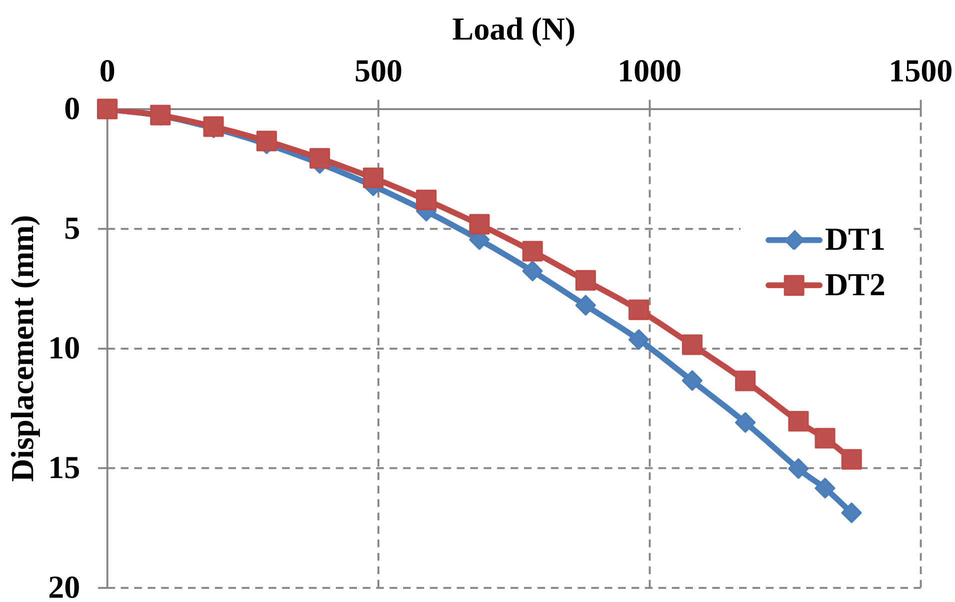

Figure 4.18 Lateral Displacements vs. Load for the Pile with 100-mm Scour Depth

200-mm scour depth

Figures 4.19, 4.20, and 4.21 show the measured strains from the strain gages on the compression side, the strains on the tension side, and the displacements from the transducers with the load respectively.

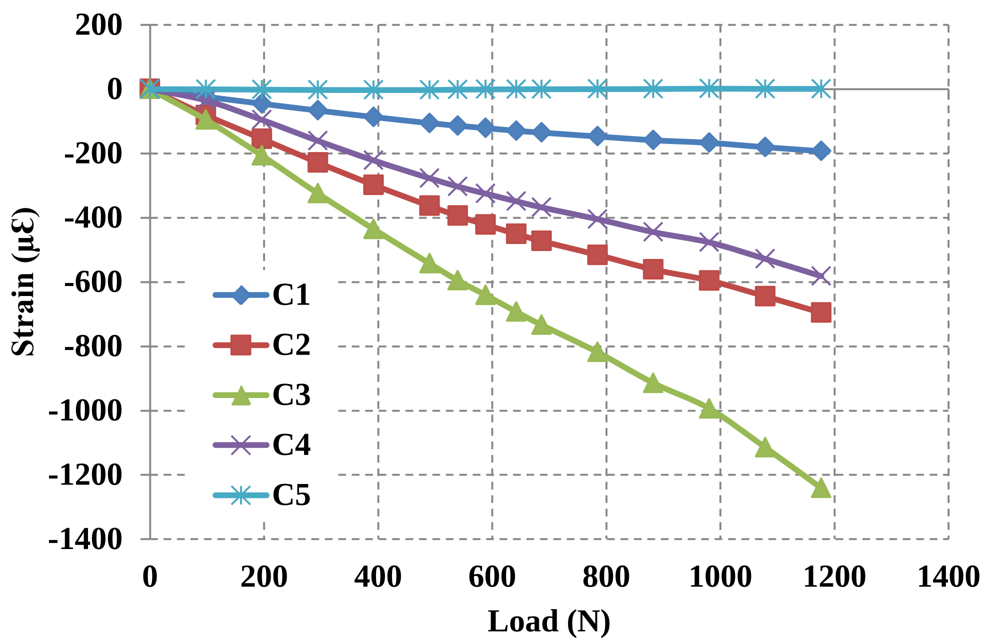

Figure 4.19 Compression Strain vs. Load for the Pile with 200-mm Scour Depth

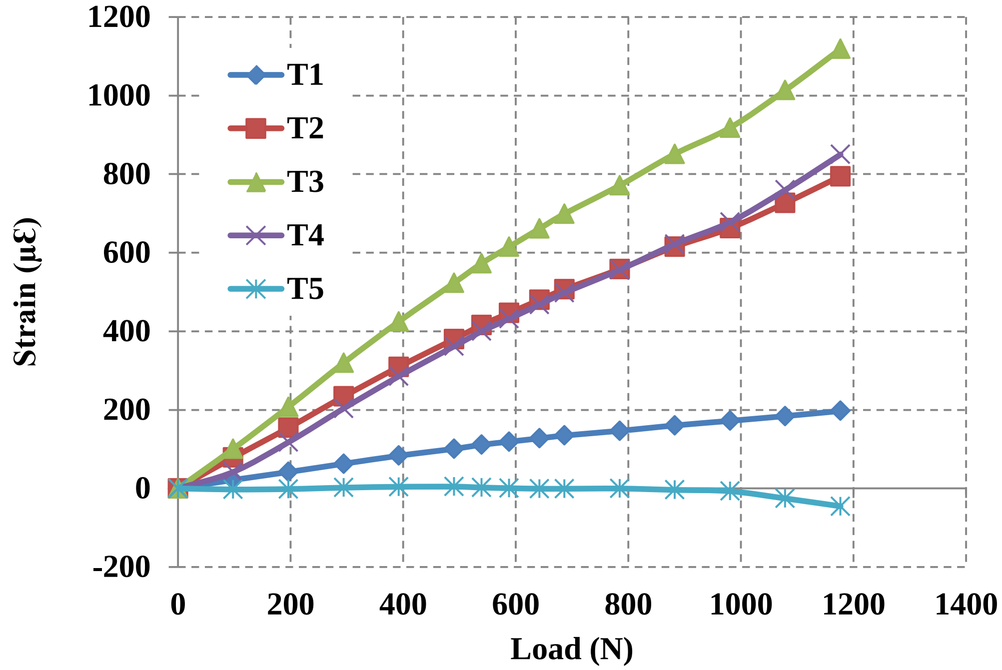

Figure 4.20 Tension Strain vs. Load for the Pile with 200-mm Scour Depth

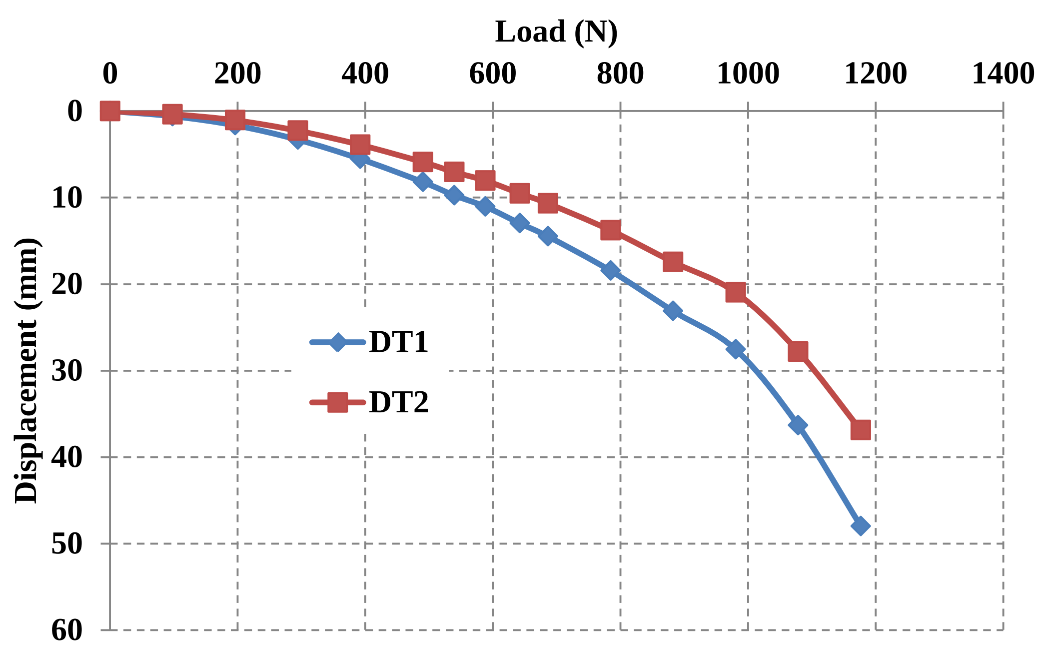

Figure 4.21 Lateral Displacements vs. Load for the Pile with 200-mm Scour Depth

300-mm scour depth

Figures 4.22, 4.23, and 4.24 show the measured strains from the strain gages on the compression side, the strains on the tension side, and the displacements from the transducers with the load respectively.

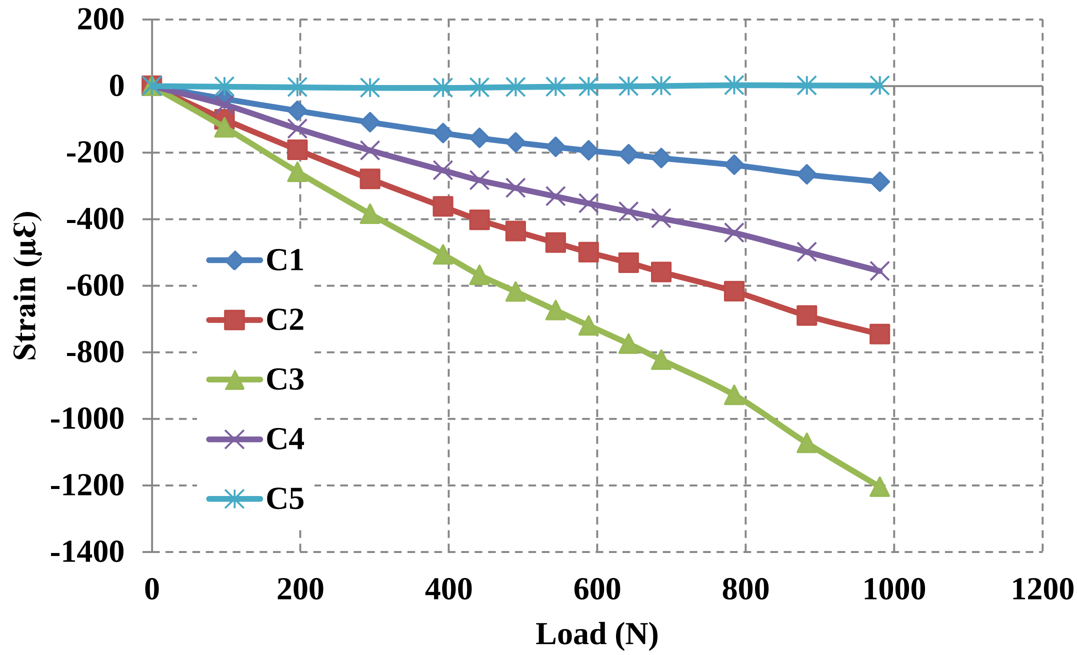

Figure 4.22 Compression Strain vs. Load for the Pile with 300-mm Scour Depth

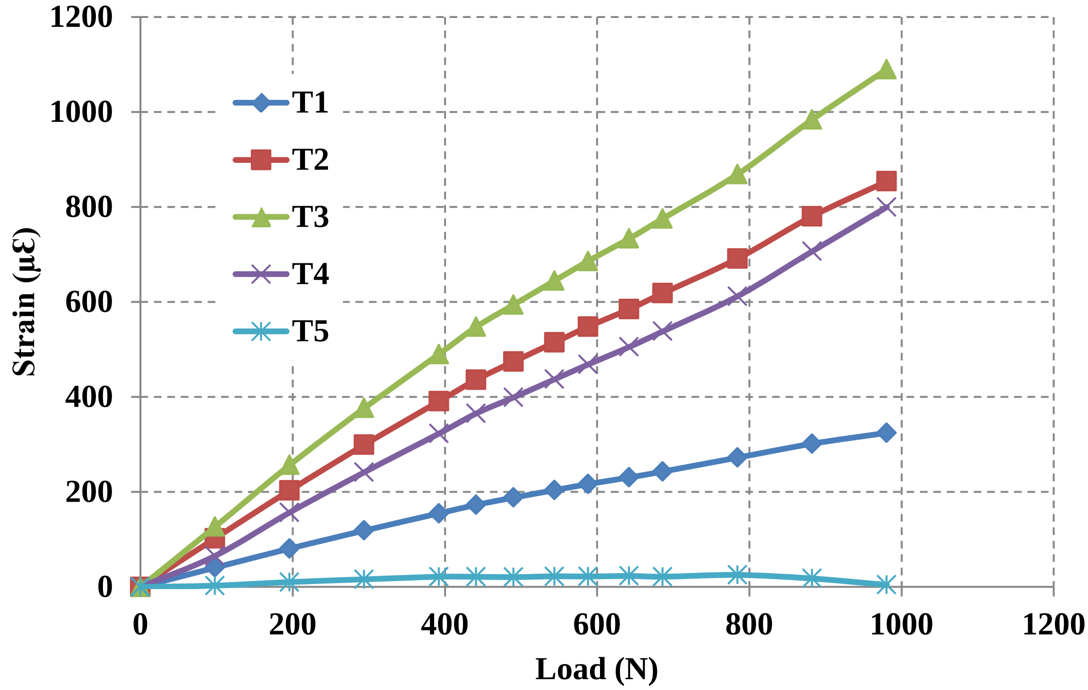

Figure 4.23 Tension Strain vs. Load for the Pile with 300-mm Scour Depth

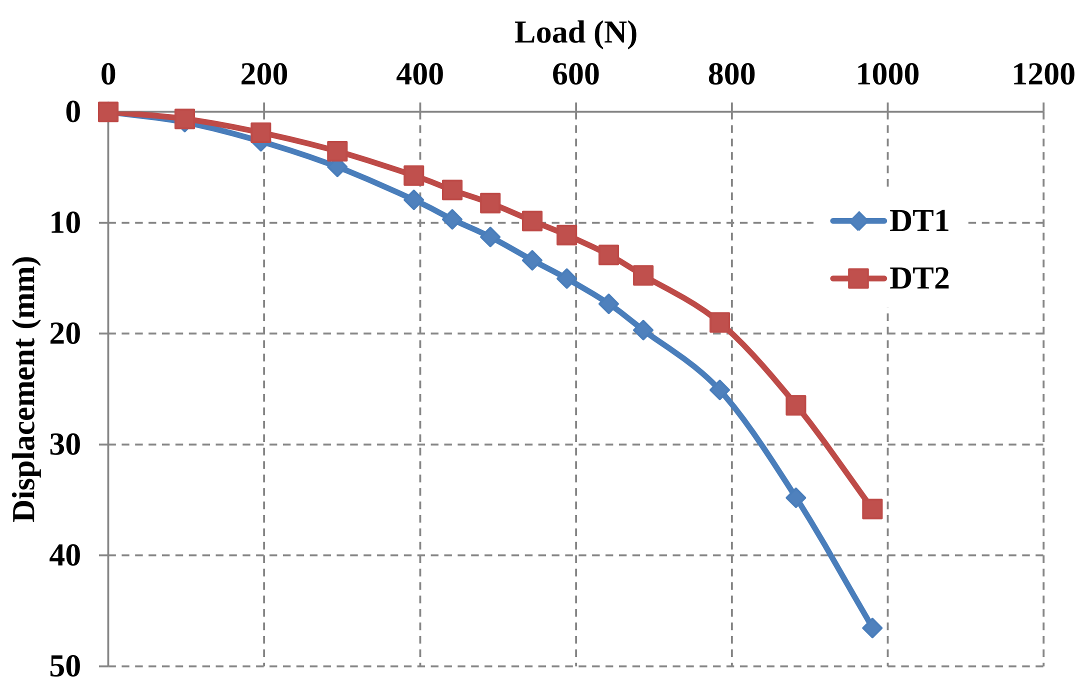

Figure 4.24 Lateral Displacements vs. Load for the Pile with 300-mm Scour Depth

400-mm scour depth

Figures 4.25, 4.26, and 4.27 show the measured strains from the strain gages on the compression side, the strains on the tension side, and the displacements from the transducers with the load respectively.

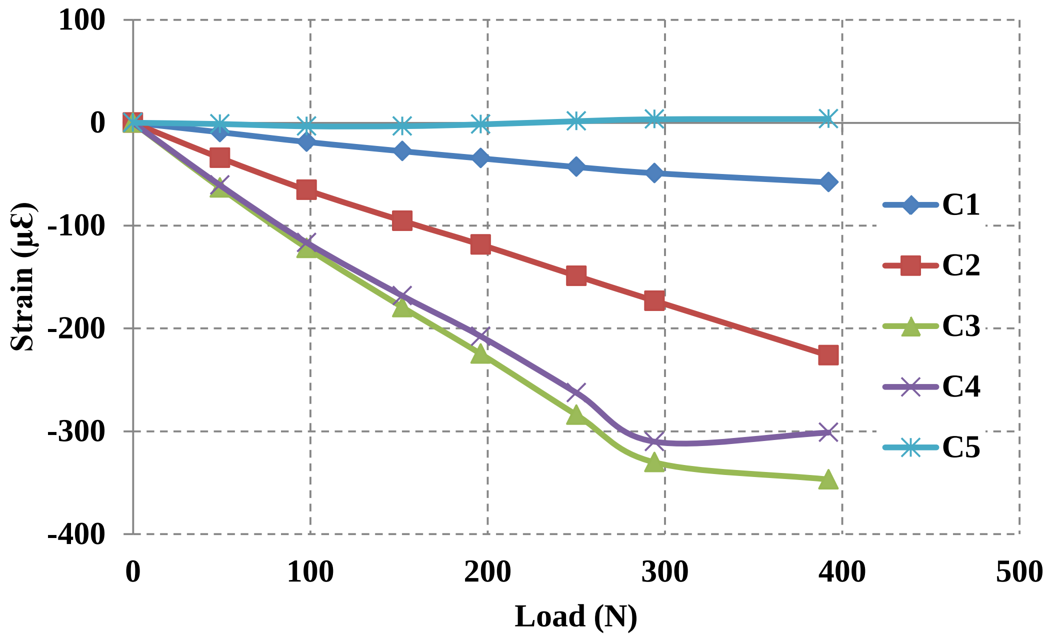

Figure 4.25 Compression Strain vs. Load for the Pile with 400-mm Scour Depth

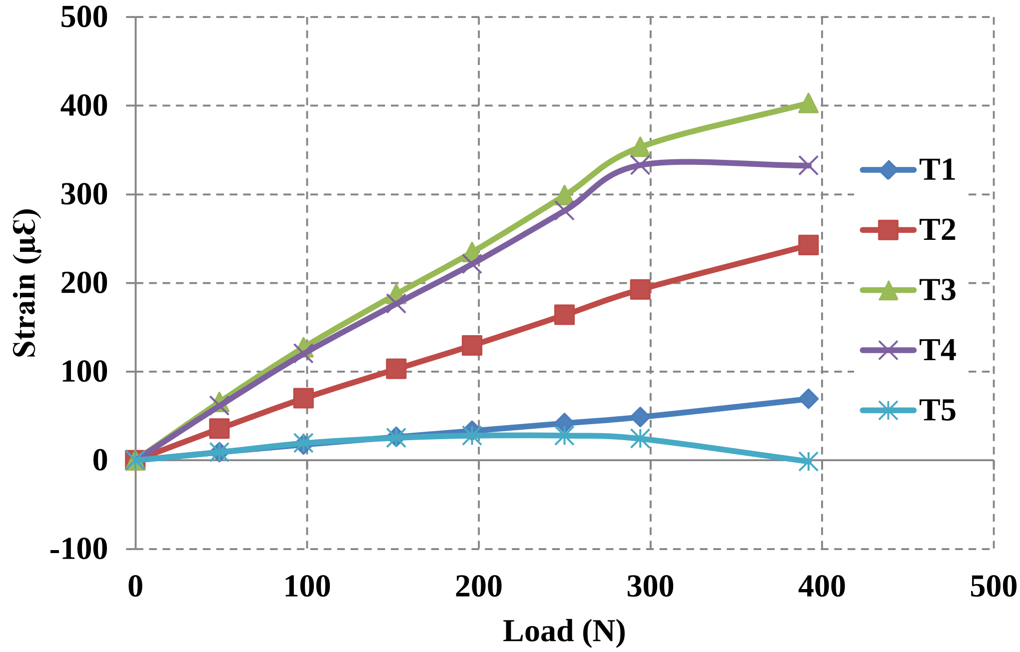

Figure 4.26 Tension Strain vs. Load for the Pile with 400-mm Scour Depth

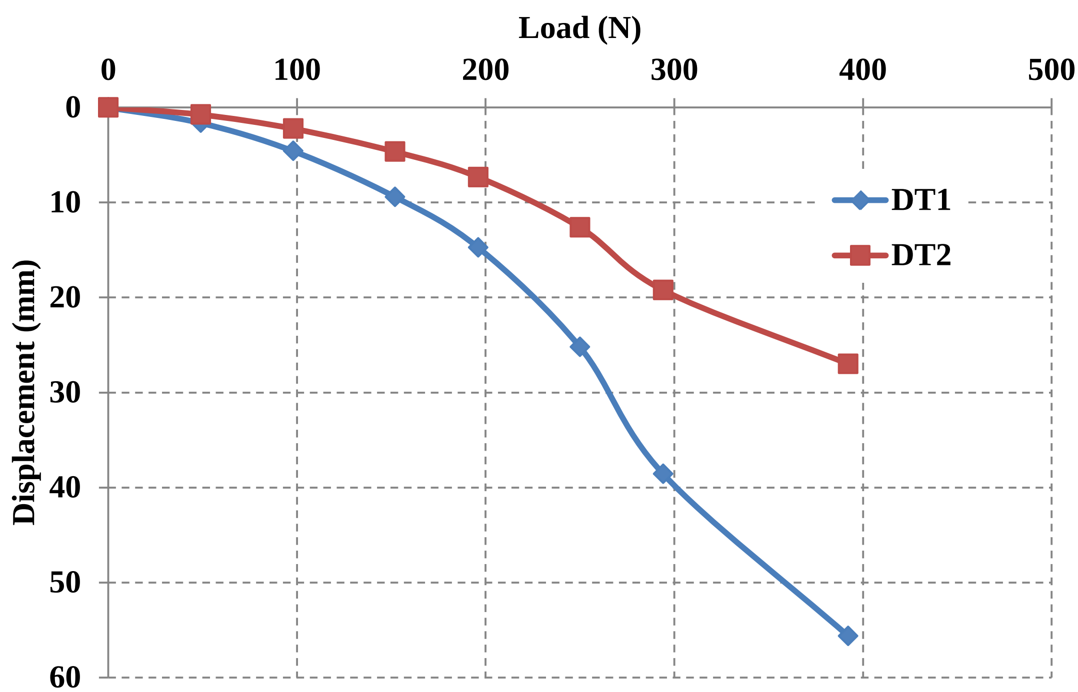

Figure 4.27 Lateral Displacements vs. Load for the Pile with 400-mm Scour Depth

500-mm scour depth

Figures 4.28, 4.29, and 4.30 show the measured strains from the strain gages on the compression side, the strains on the tension side, and the displacements from the transducers with the load respectively.

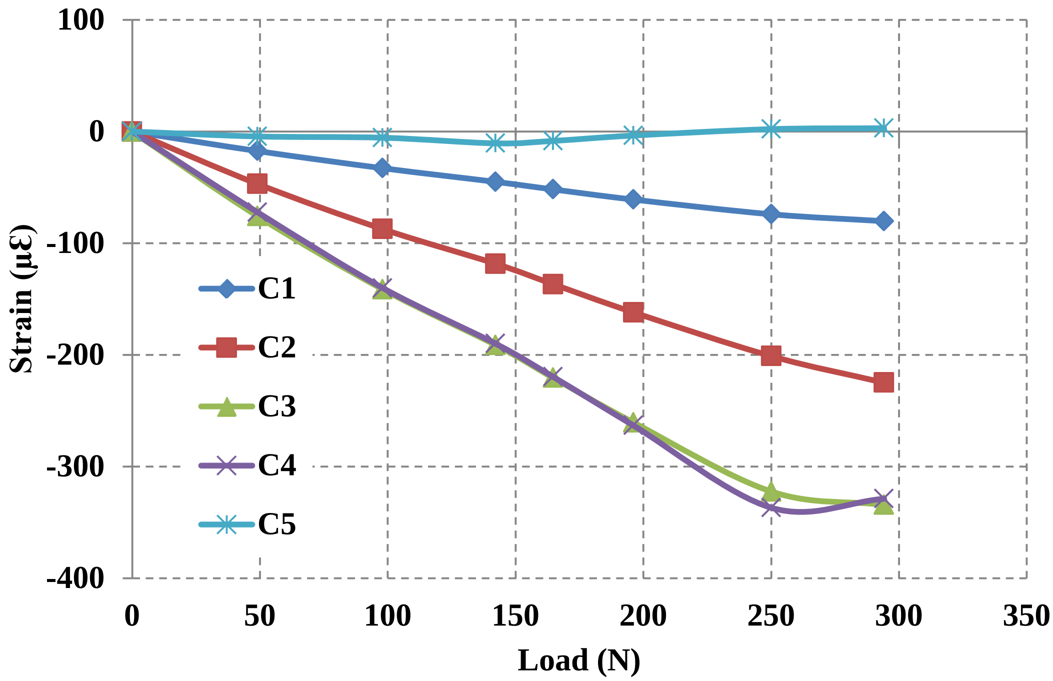

Figure 4.28 Compression Strain vs. Load for the Pile with 500-mm Scour Depth

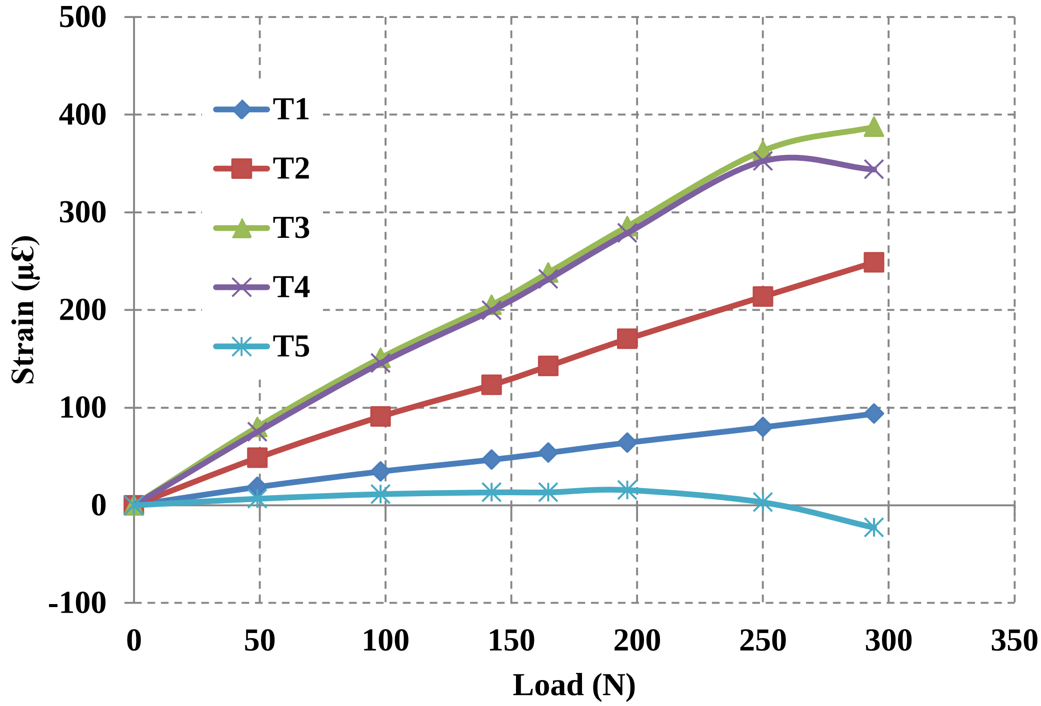

Figure 4.29 Tension Strain vs. Load for the Pile with 500-mm Scour Depth

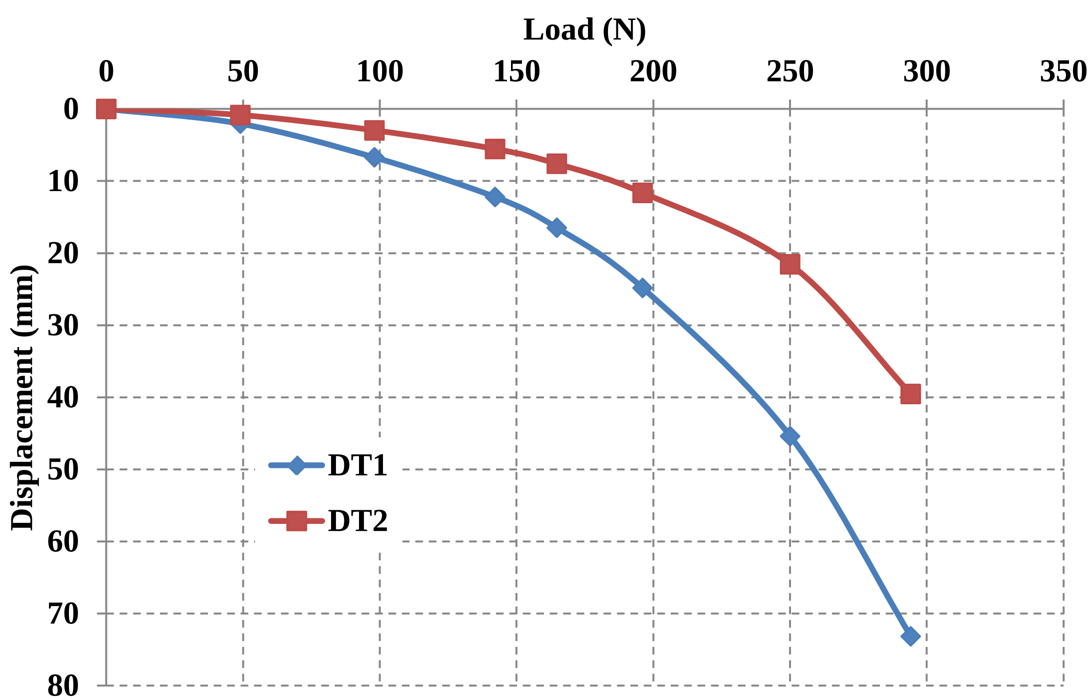

Figure 4.30 Lateral Displacements vs. Load for the Pile with 500-mm Scour Depth

4.3.2. Scour slope

Experimental tests were conducted for scour holes at three different scour slope angles: 0, 15, and 30 degrees.

0-degree scour slope

At 0-degree scour slope angle, four tests were conducted at different scour depths ranging from 200 to 500 mm.

200-mm scour depth. Figures 4.31, 4.32, and 4.33 show the measured strains from the strain gages on the compression side, the strains on the tension side, and the displacements from the transducers with the load respectively.

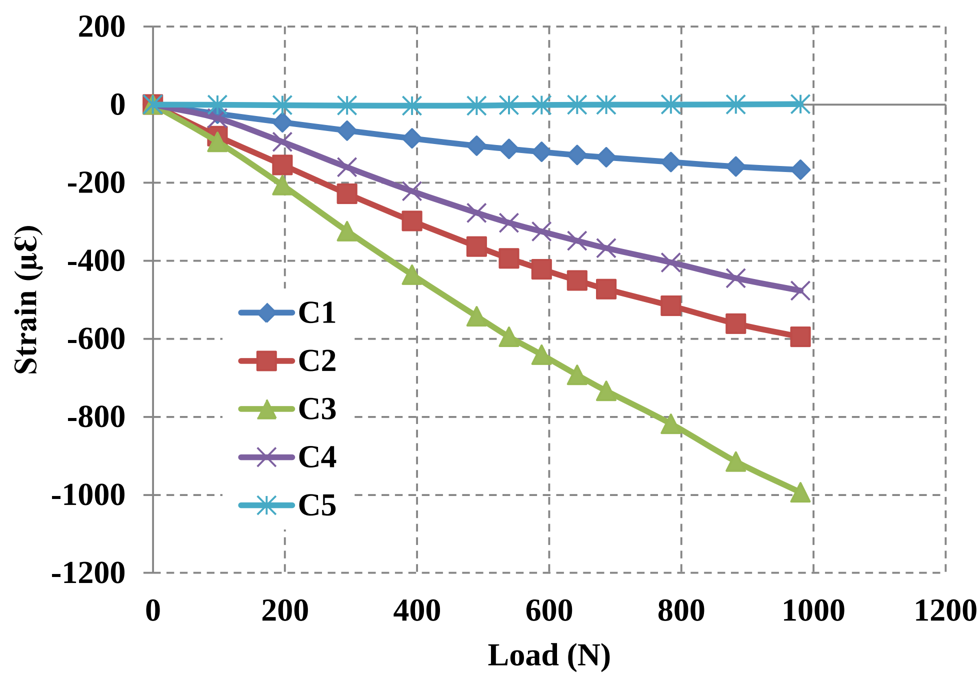

Figure 4.31 Compression Strain vs. Load for the Pile with 0-degree Scour Slope and 200-mm Scour Depth

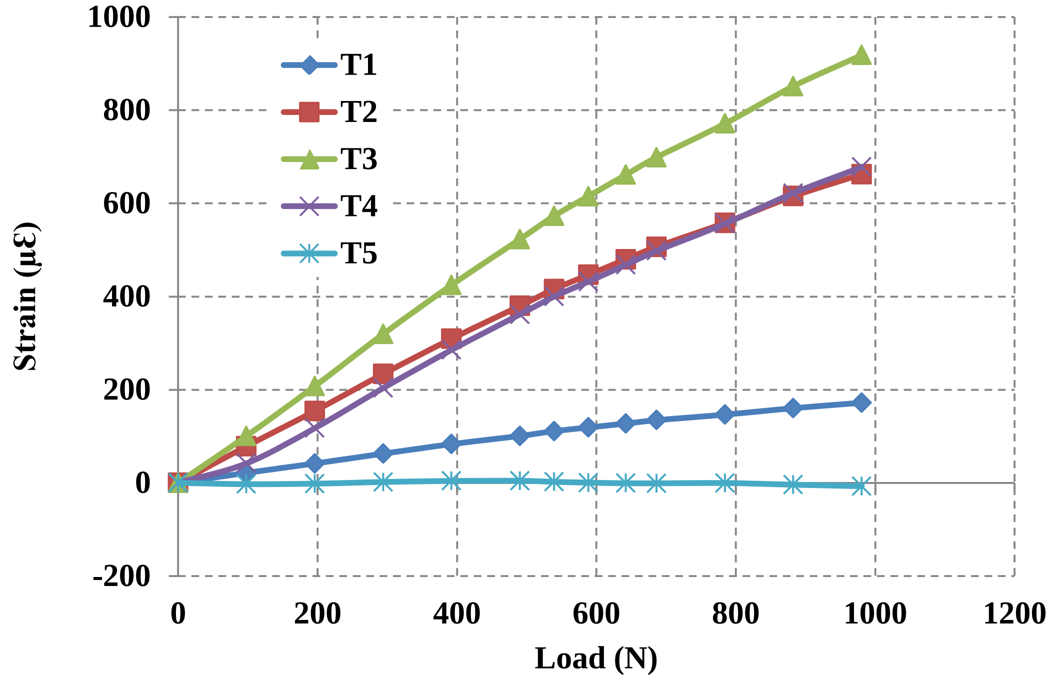

Figure 4.32 Tension Strain vs. Load for the Pile with 0-degree Scour Slope and 200-mm Scour Depth

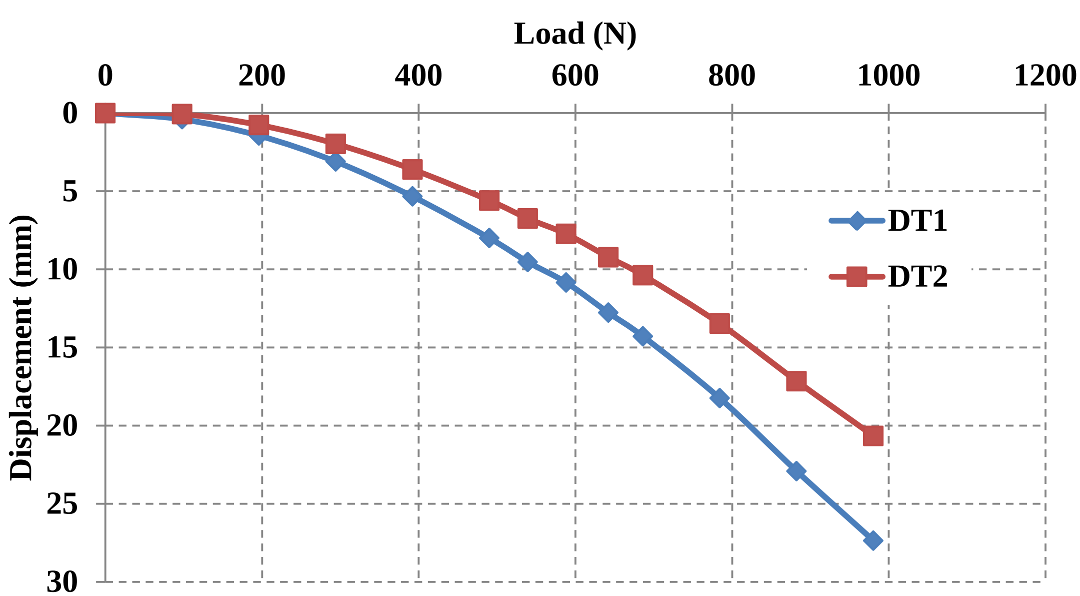

Figure 4.33 Lateral Displacements vs. Load for the Pile with 0-degree Scour Slope and 200-mm Scour Depth

300-mm scour depth. Figures 4.34, 4.35, and 4.36 show the measured strains from the strain gages on the compression side, the strains on the tension side, and the displacements from the transducers with the load respectively.

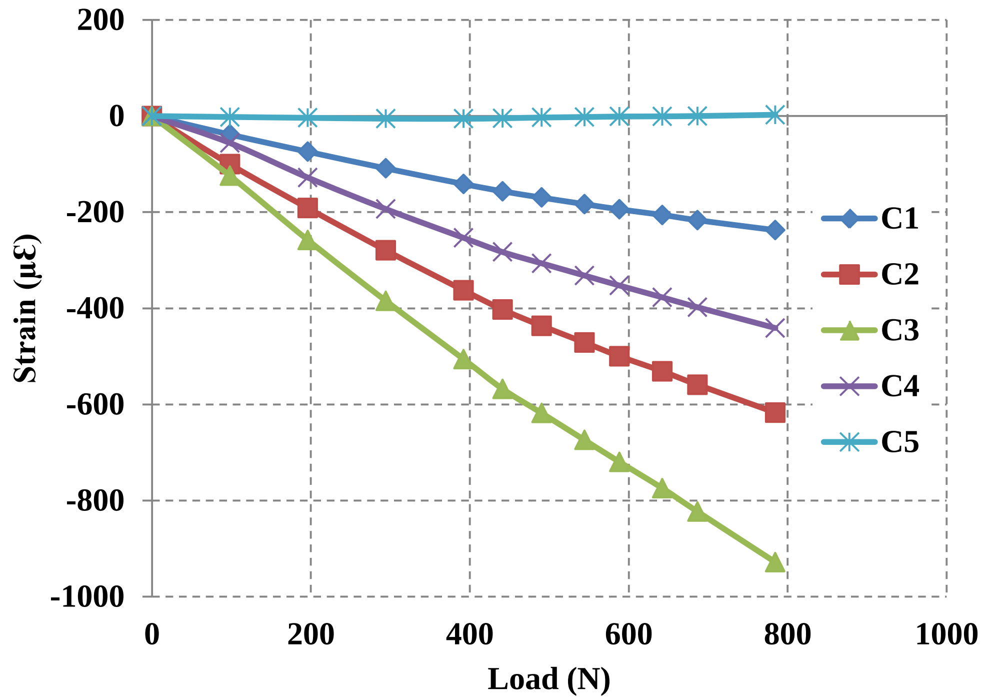

Figure 4.34 Compression Strain vs. Load for the Pile with 0-degree Scour Slope and 300-mm Scour Depth

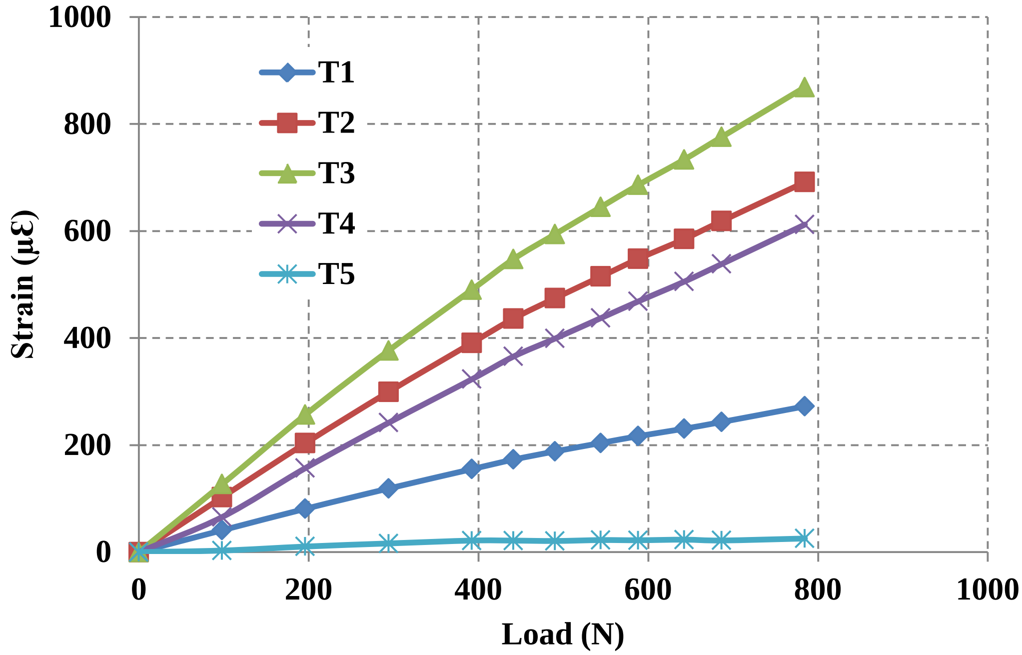

Figure 4.35 Tension Strain vs. Load for the Pile with 0-degree Scour Slope and 300-mm Scour Depth

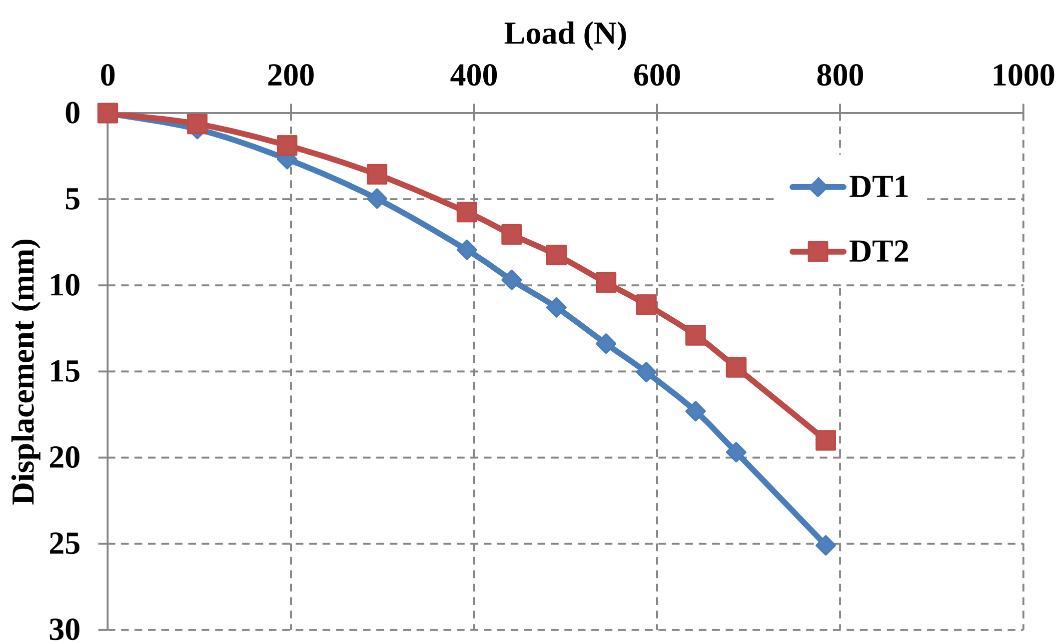

Figure 4.36 Lateral Displacements vs. Load for the Pile with 0-degree Scour Slope and 300-mm Scour Depth

400-mm scour depth. Figures 4.37, 4.38, and 4.39 show the measured strains from the strain gages on the compression side, the strains on the tension side, and the displacements from the transducers with the load respectively.

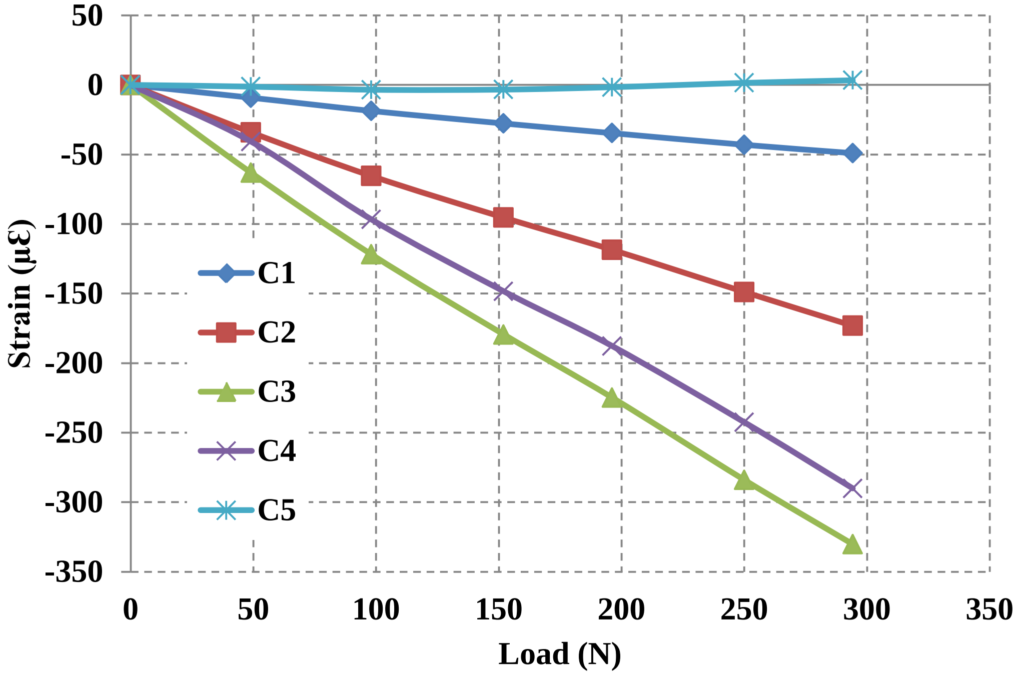

Figure 4.37 Compression Strain vs. Load for the Pile with 0-degree Scour Slope and 400-mm Scour Depth

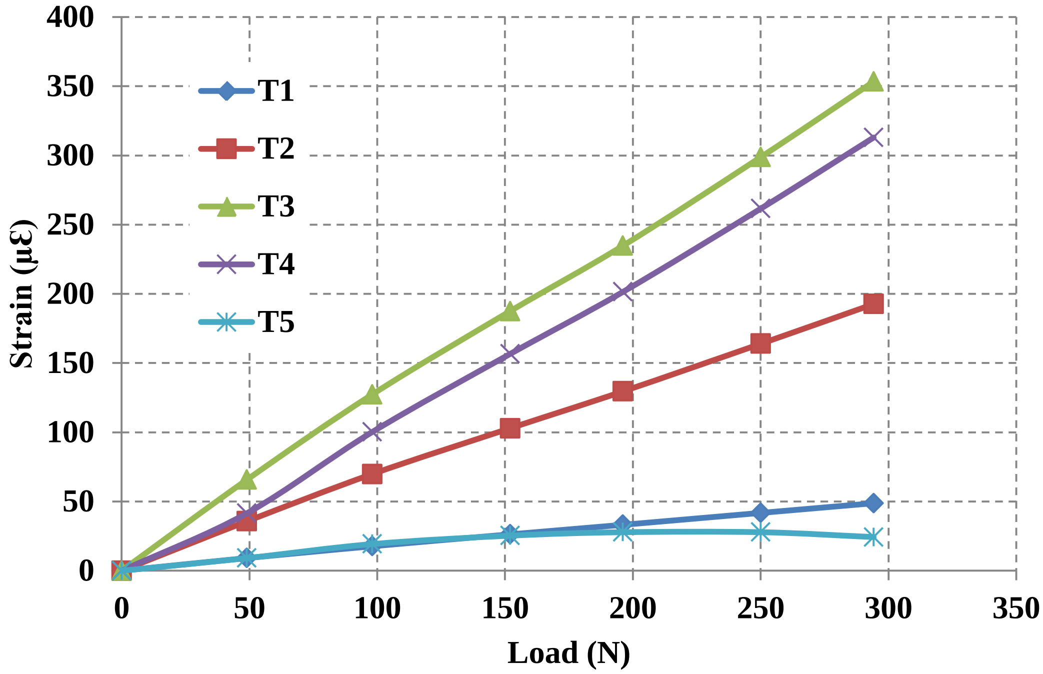

Figure 4.38 Tension Strain vs. Load for the Pile with 0-degree Scour Slope and 400-mm Scour Depth

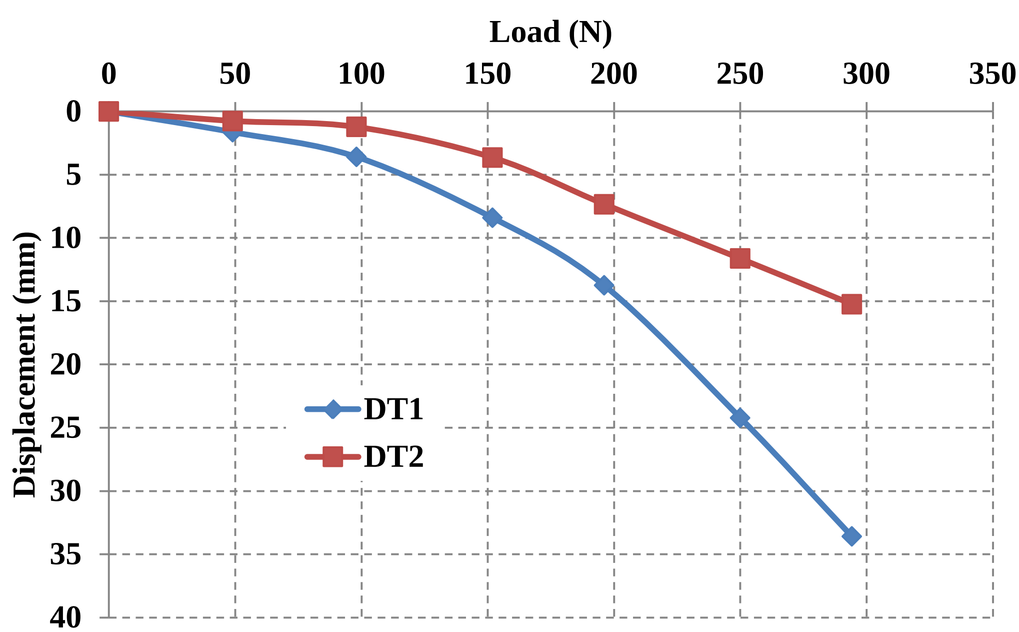

Figure 4.39 Lateral Displacements vs. Load for the Pile with 0-degree Scour Slope and 400-mm Scour Depth

500-mm scour depth. Figures 4.40, 4.41, and 4.42 show the measured strains from the strain gages on the compression side, the strains on the tension side, and the displacements from the transducers with the load respectively.

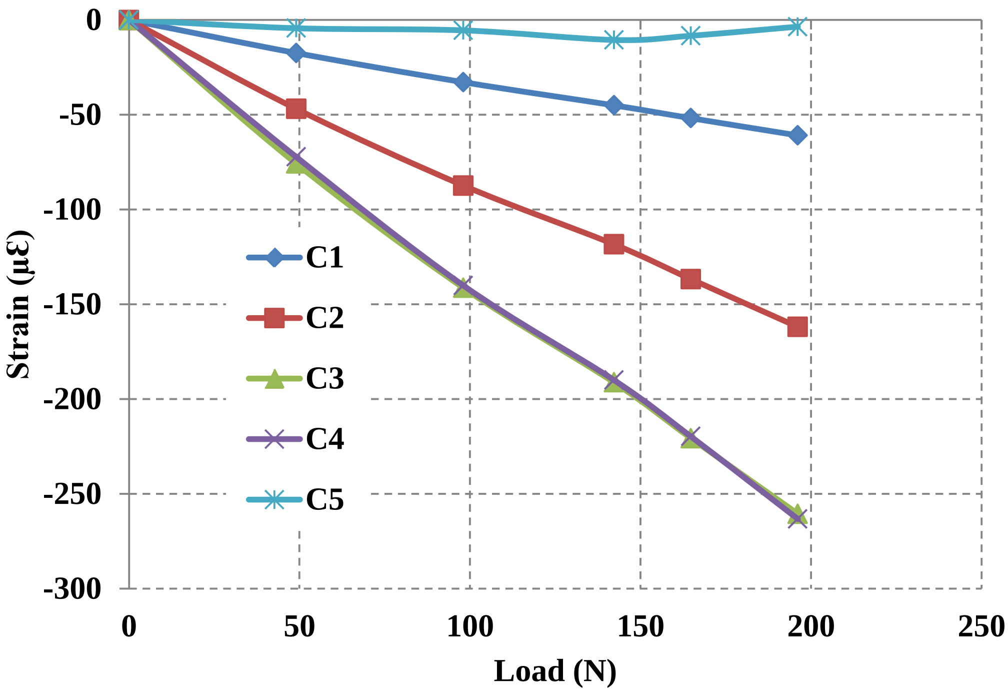

Figure 4.40 Compression Strain vs. Load for the Pile with 0-degree Scour Slope and 500-mm Scour Depth

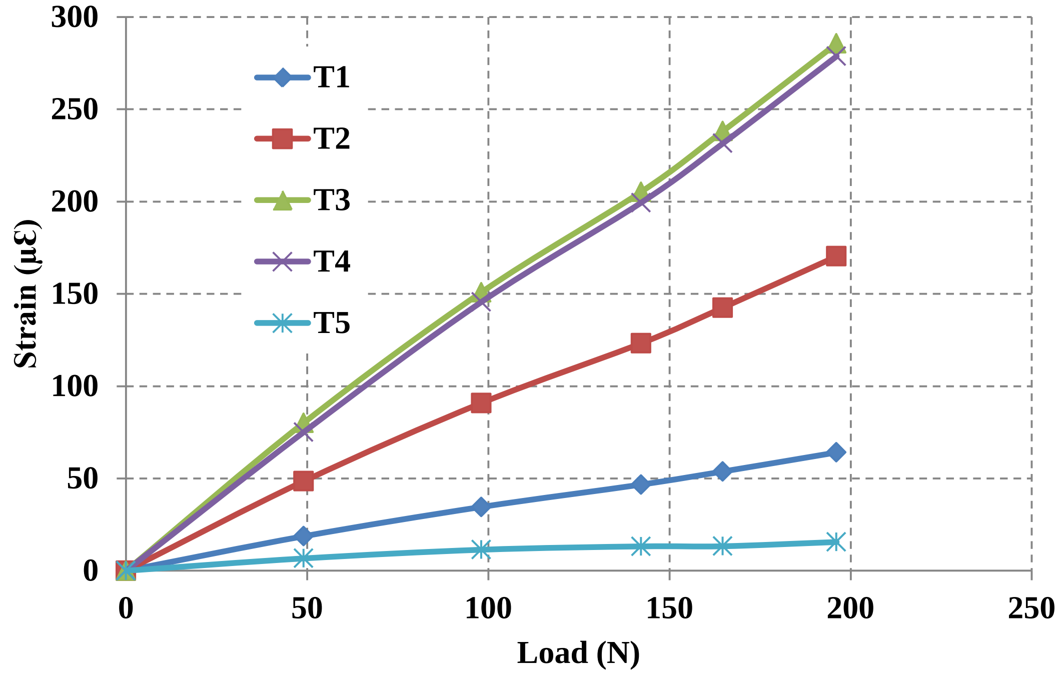

Figure 4.41 Tension Strain vs. Load for the Pile with 0-degree Scour Slope and 500-mm Scour Depth

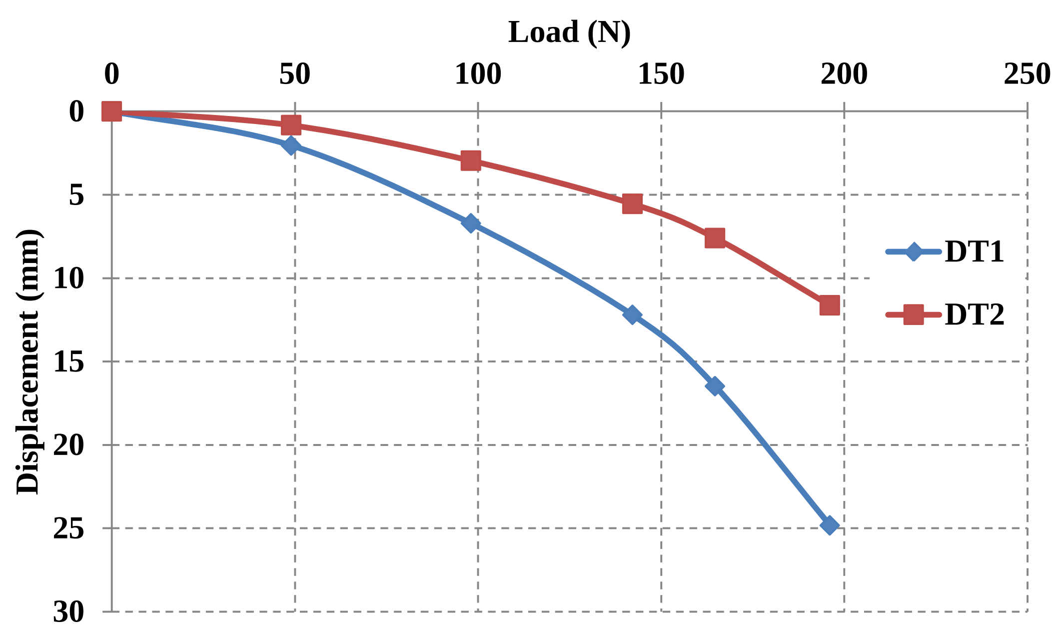

Figure 4.42 Lateral Displacements vs. Load for the Pile with 0-degree Scour Slope and 500-mm Scour Depth

15-degree scour slope

At 15-degree scour slope angle, four tests were conducted at different scour depths ranging from 200 to 500 mm.

200-mm scour depth. Figures 4.43, 4.44, and 4.45 show the measured strains from the strain gages on the compression side, the strains on the tension side, and the displacements from the transducers with the load respectively.

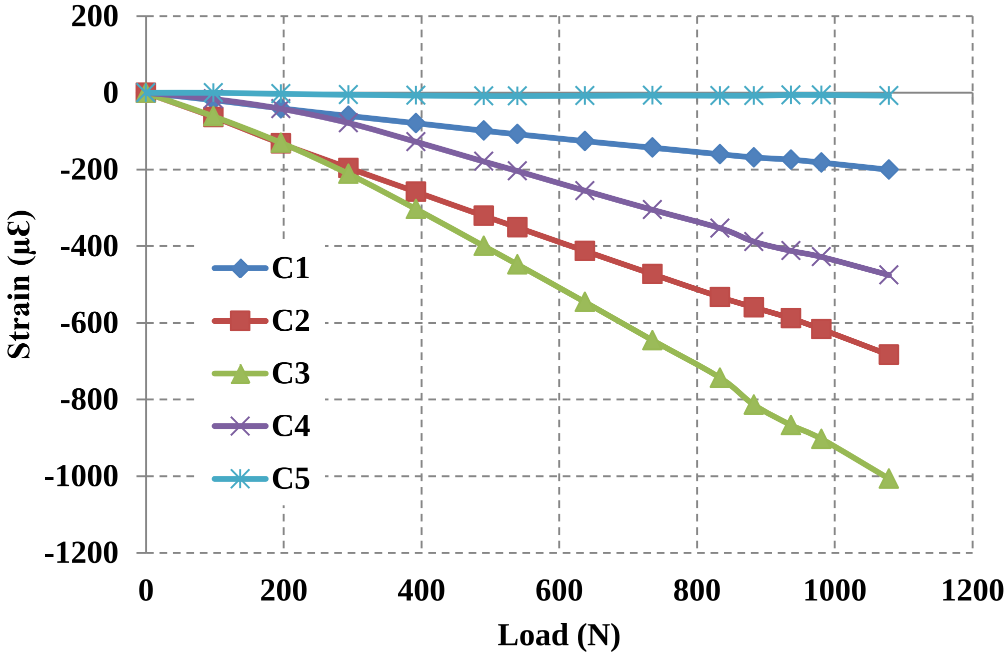

Figure 4.43 Compression Strain vs. Load for the Pile with 15-degree Scour Slope and 200-mm Scour Depth

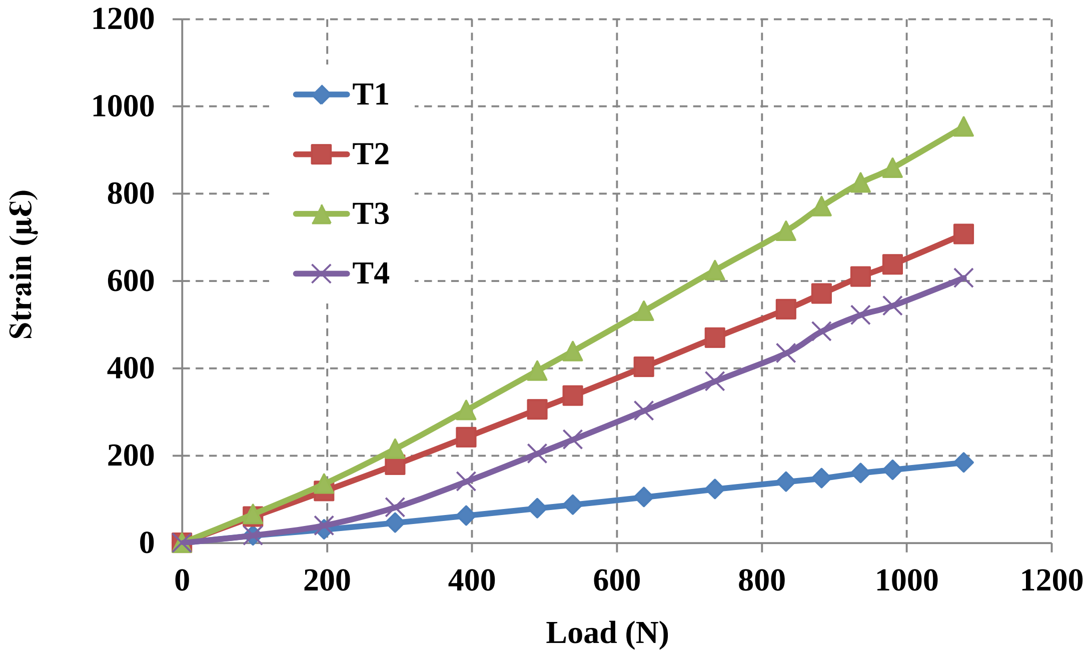

Figure 4.44 Tension Strain vs. Load for the Pile with 15-degree Scour Slope and 200-mm Scour Depth

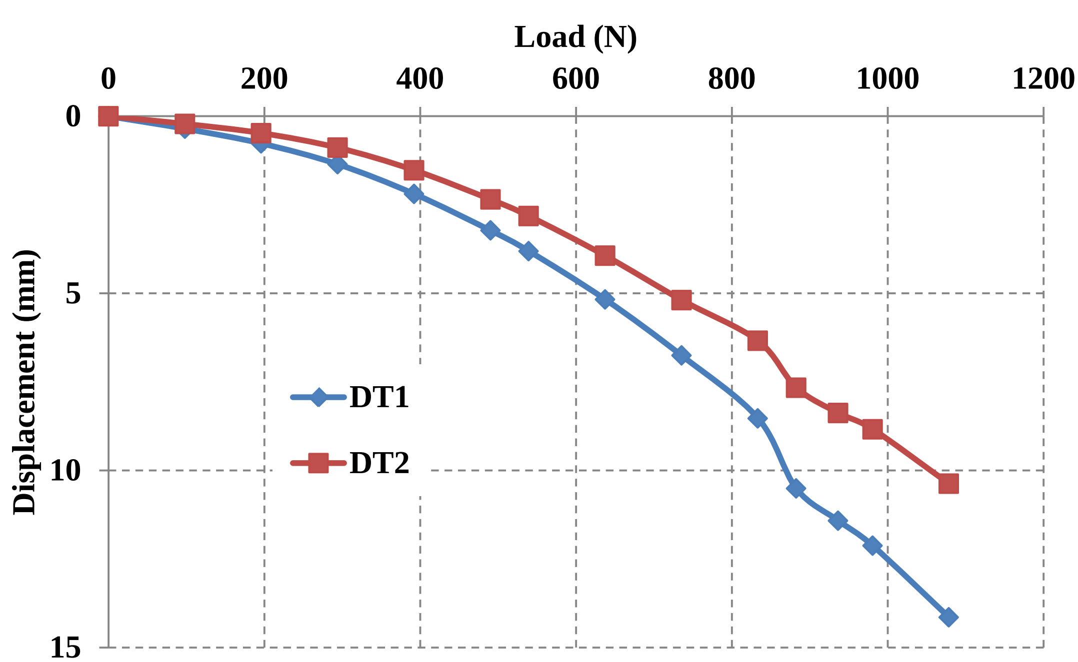

Figure 4.45 Lateral Displacements vs. Load for the Pile with 15-degree Scour Slope and 200-mm Scour Depth

300-mm scour depth. Figures 4.46, 4.47, and 4.48 show the measured strains from the strain gages on the compression side, the strains on the tension side, and the displacements from the transducers with the load respectively.

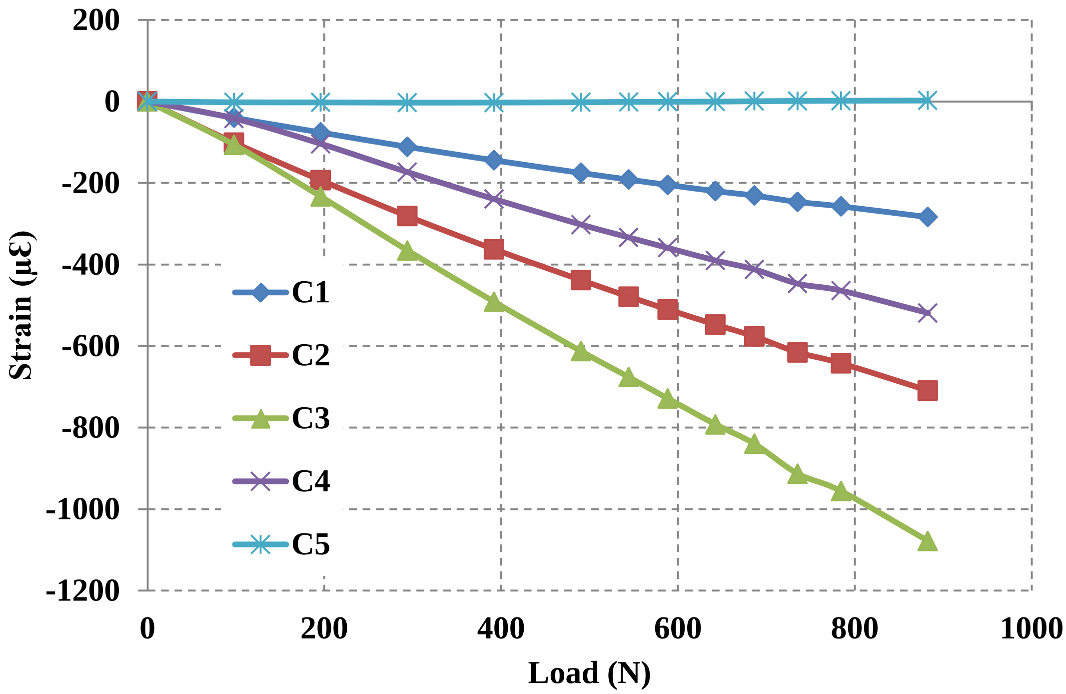

Figure 4.46 Compression Strain vs. Load for the Pile with 15-degree Scour Slope and 300-mm Scour Depth

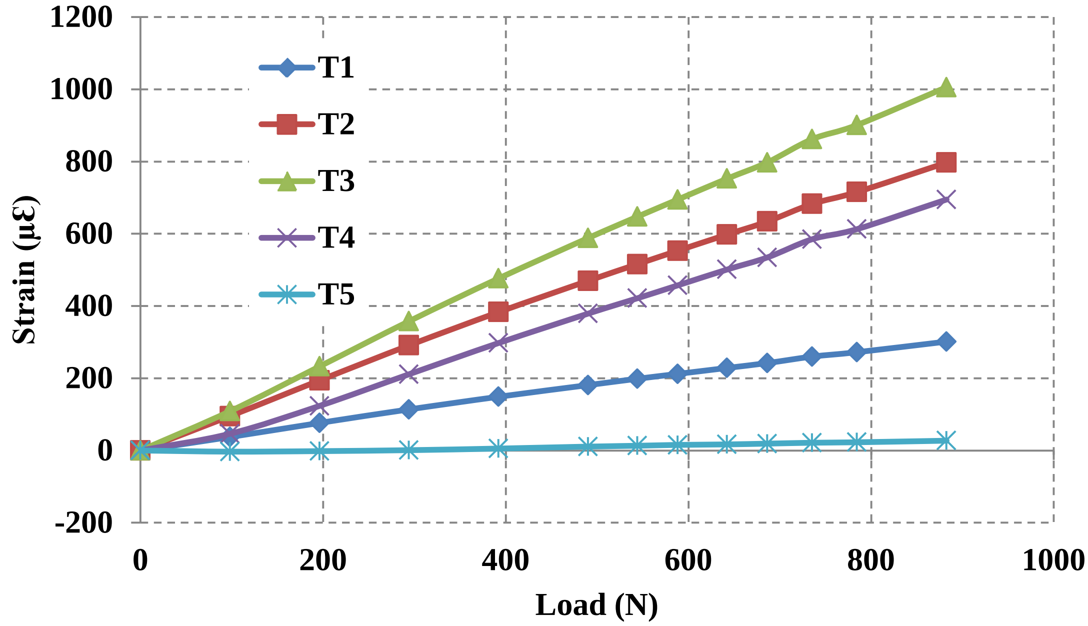

Figure 4.47 Tension Strain vs. Load for the Pile with 15-degree Scour Slope and 300-mm Scour Depth

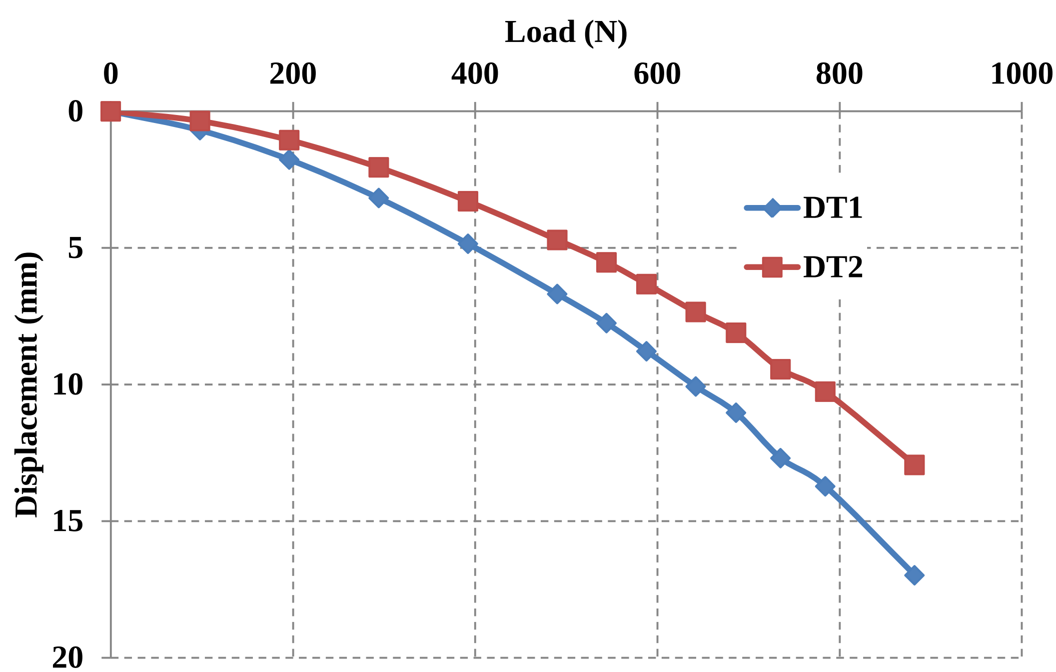

Figure 4.48 Lateral Displacements vs. Load for the Pile with 15-degree Scour Slope and 300-mm Scour Depth

400-mm scour depth. Figures 4.49, 4.50, and 4.51 show the measured strains from the strain gages on the compression side, the strains on the tension side, and the displacements from the transducers with the load respectively.

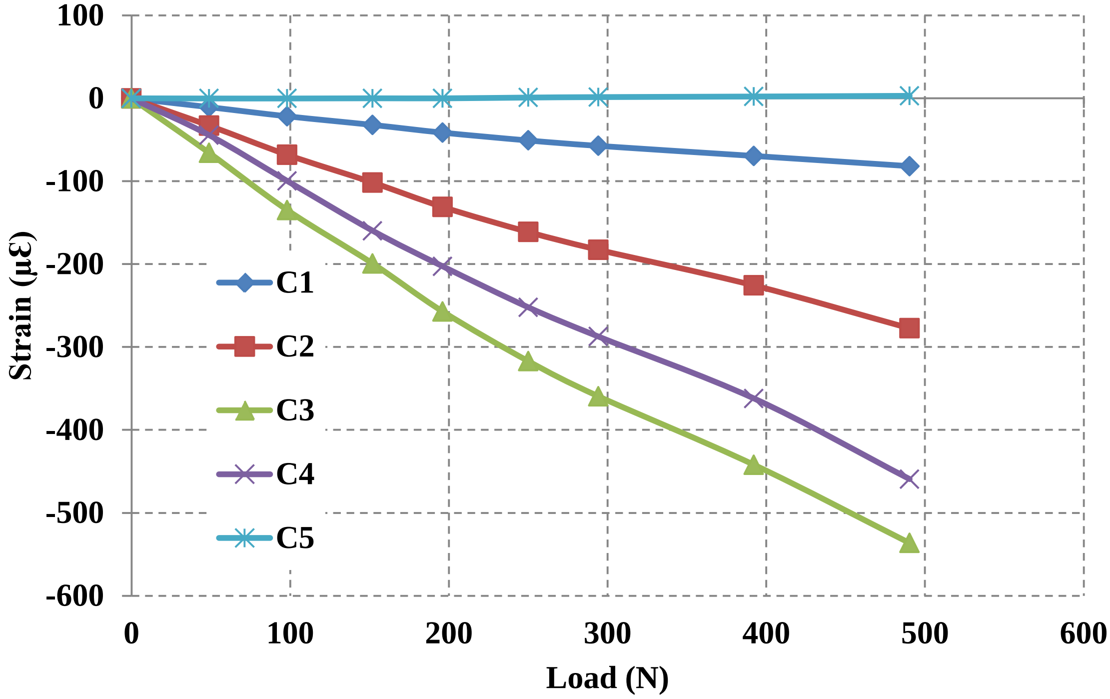

Figure 4.49 Compression Strain vs. Load for the Pile with 15-degree Scour Slope and 400-mm Scour Depth

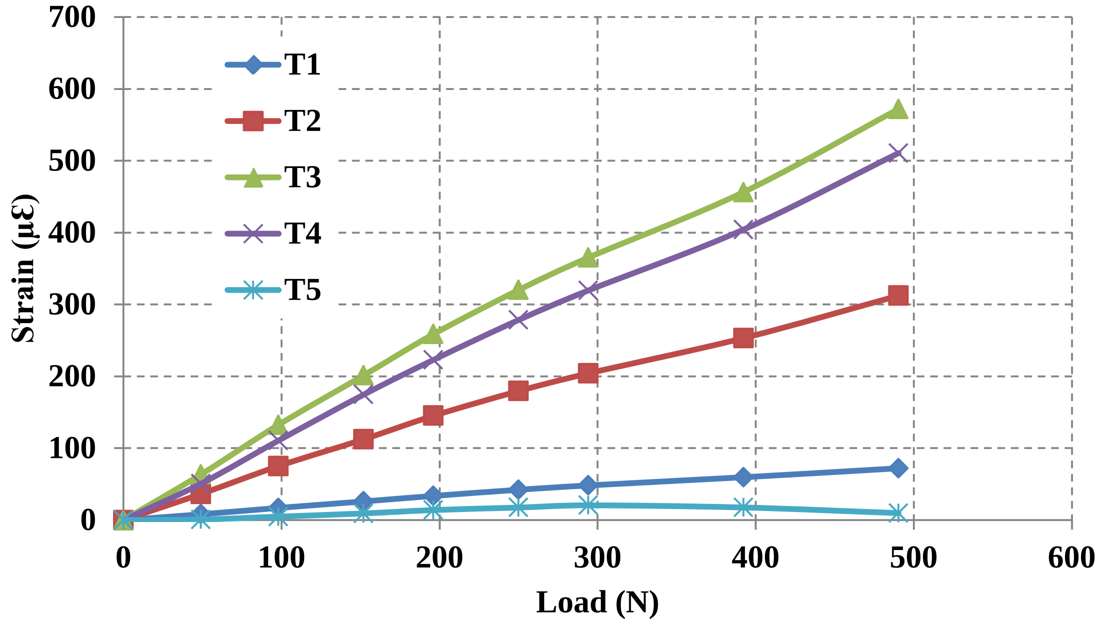

Figure 4.50 Tension Strain vs. Load for the Pile with 15-degree Scour Slope and 400-mm Scour Depth

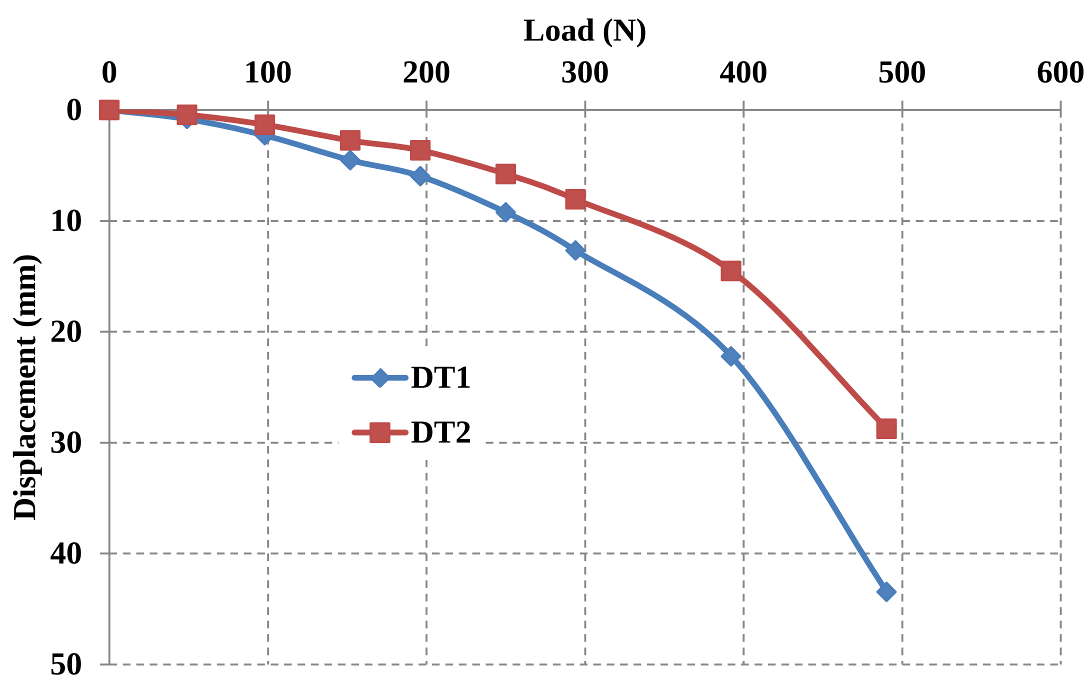

Figure 4.51 Lateral Displacements vs. Load for the Pile with 15-degree Scour Slope and 400-mm Scour Depth

500-mm scour depth. Figures 4.52, 4.53, and 4.54 show the measured strains from the strain gages on the compression side, the strains on the tension side, and the displacements from the transducers with the load respectively..

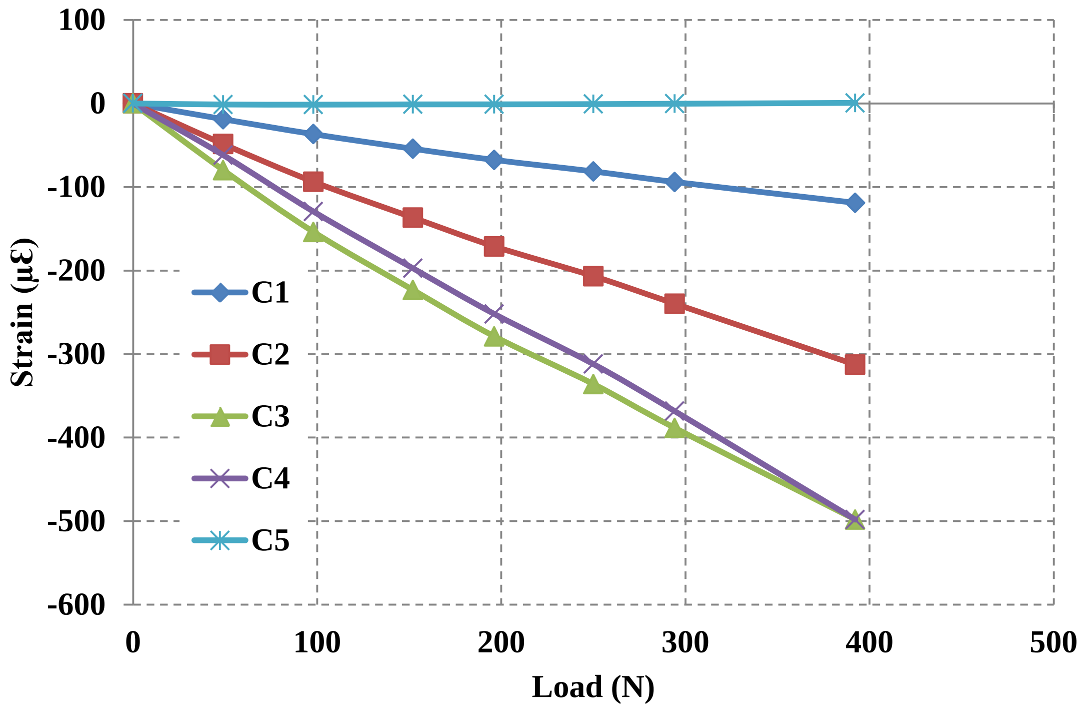

Figure 4.52 Compression Strain vs. Load for the Pile with 15-degree Scour Slope and 500-mm Scour Depth

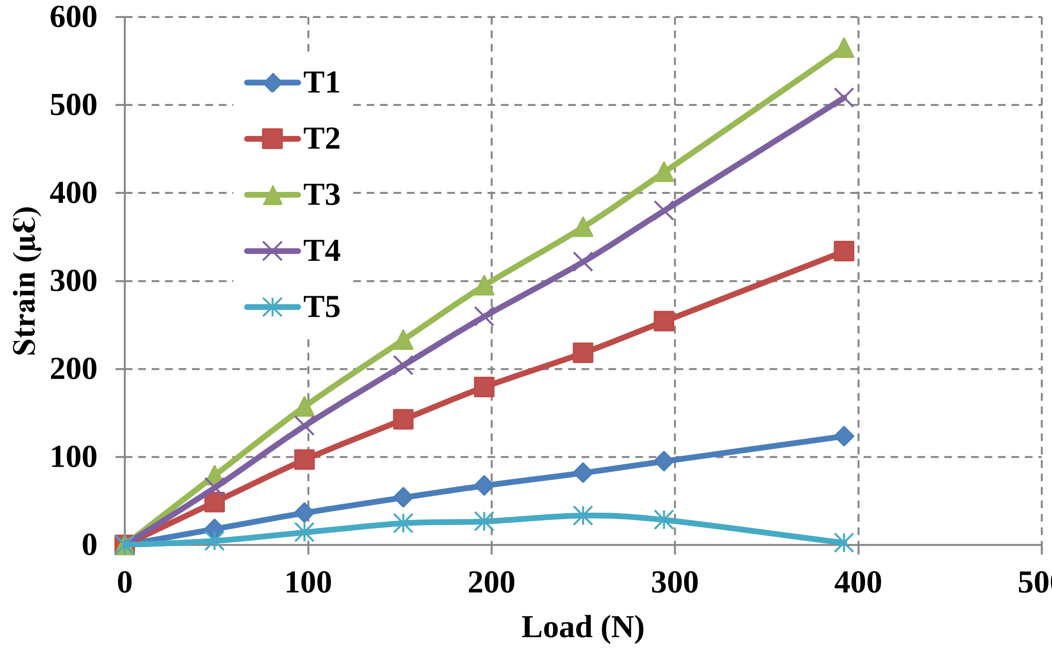

Figure 4.53 Tension Strain vs. Load for the Pile with 15-degree Scour Slope and 500-mm Scour Depth

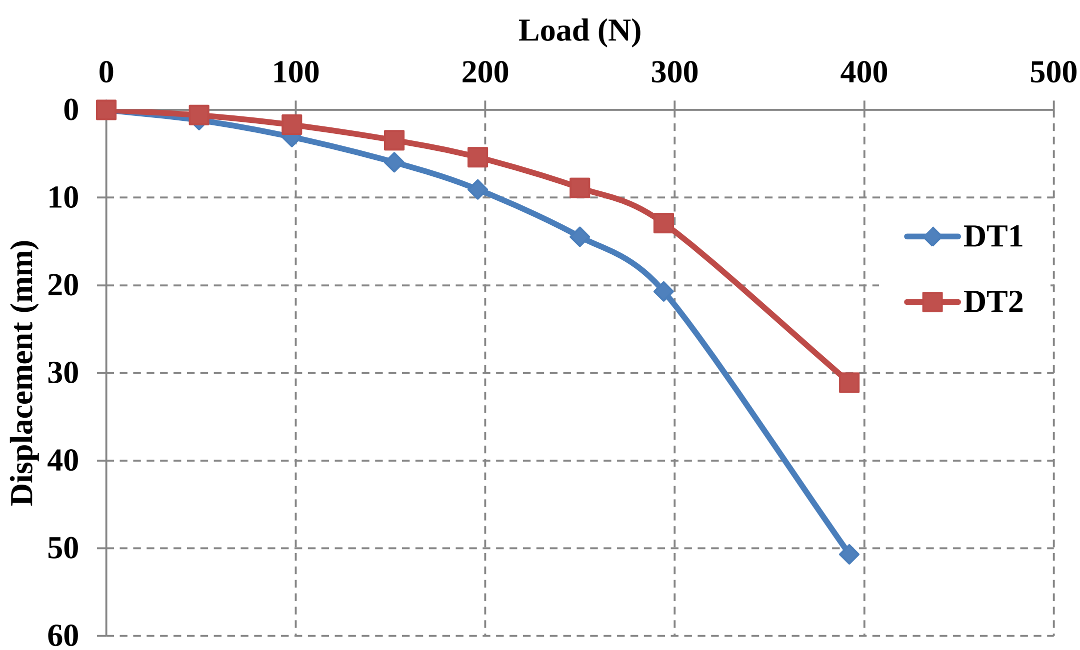

Figure 4.54 Lateral Displacements vs. Load for the Pile with 15-degree Scour Slope and 500-mm Scour Depth

30-degree scour slope

At 30-degree scour slope angle, four tests were conducted at different scour depths ranging from 200 to 500 mm.

200-mm scour depth. Figures 4.55, 4.56, and 4.57 show the measured strains from the strain gages on the compression side, the strains on the tension side, and the displacements from the transducers with the load respectively.

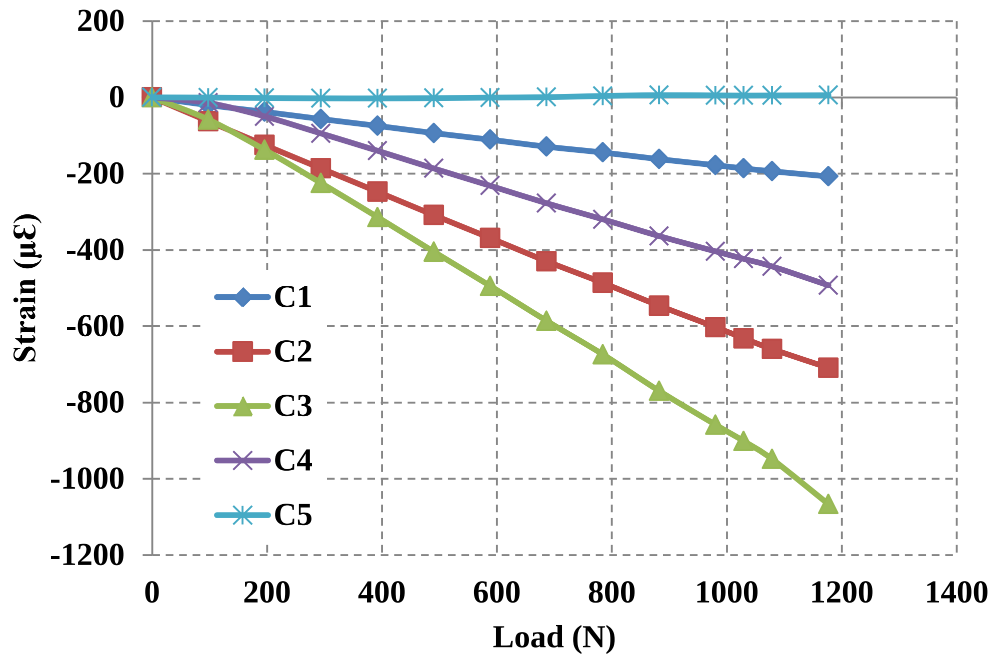

Figure 4.55 Compression Strain vs. Load for the Pile with 30-degree Scour Slope and 200-mm Scour Depth

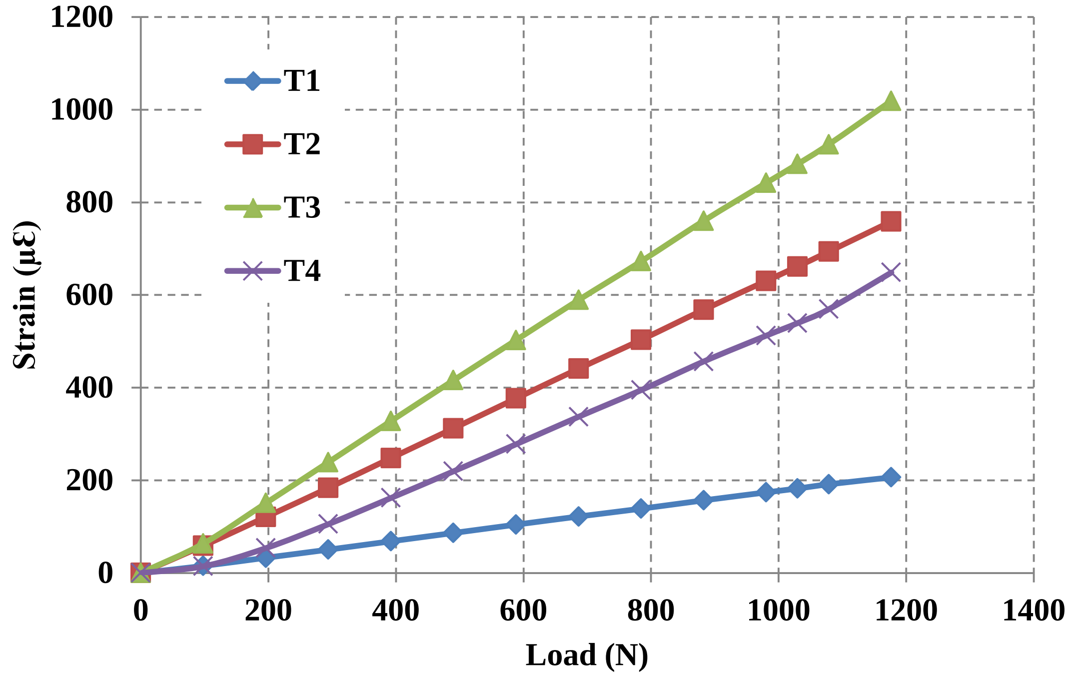

Figure 4.56 Tension Strain vs. Load for the Pile with 30-degree Scour Slope and 200-mm Scour Depth

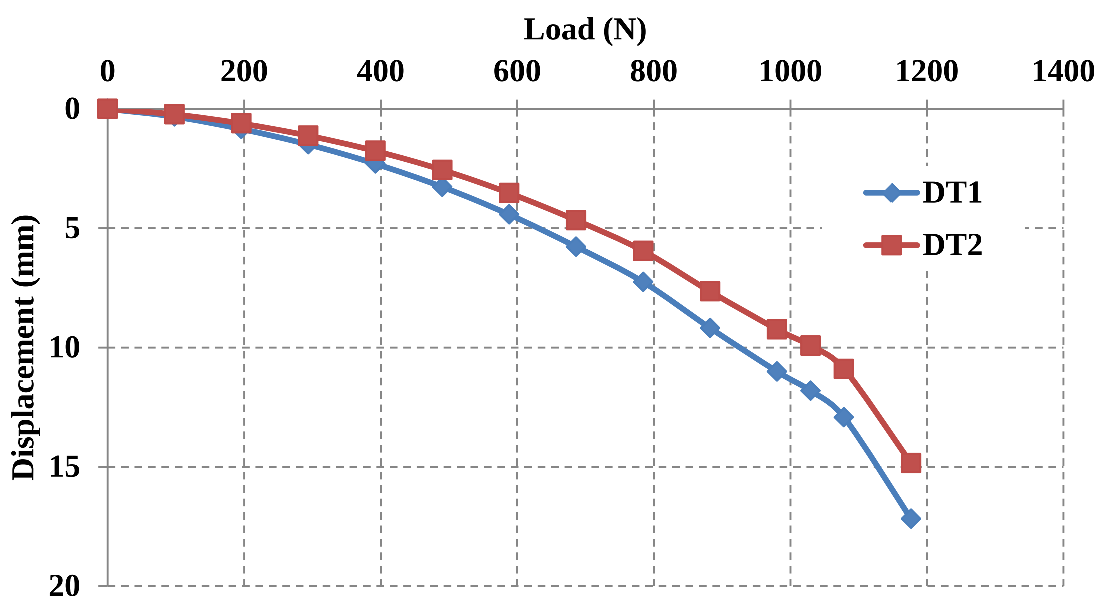

Figure 4.57 Lateral Displacements vs. Load for the Pile with 30-degree Scour Slope and 200-mm Scour Depth

300-mm scour depth. Figures 4.58, 4.59, and 4.60 show the measured strains from the strain gages on the compression side, the strains on the tension side, and the displacements from the transducers with the load respectively.

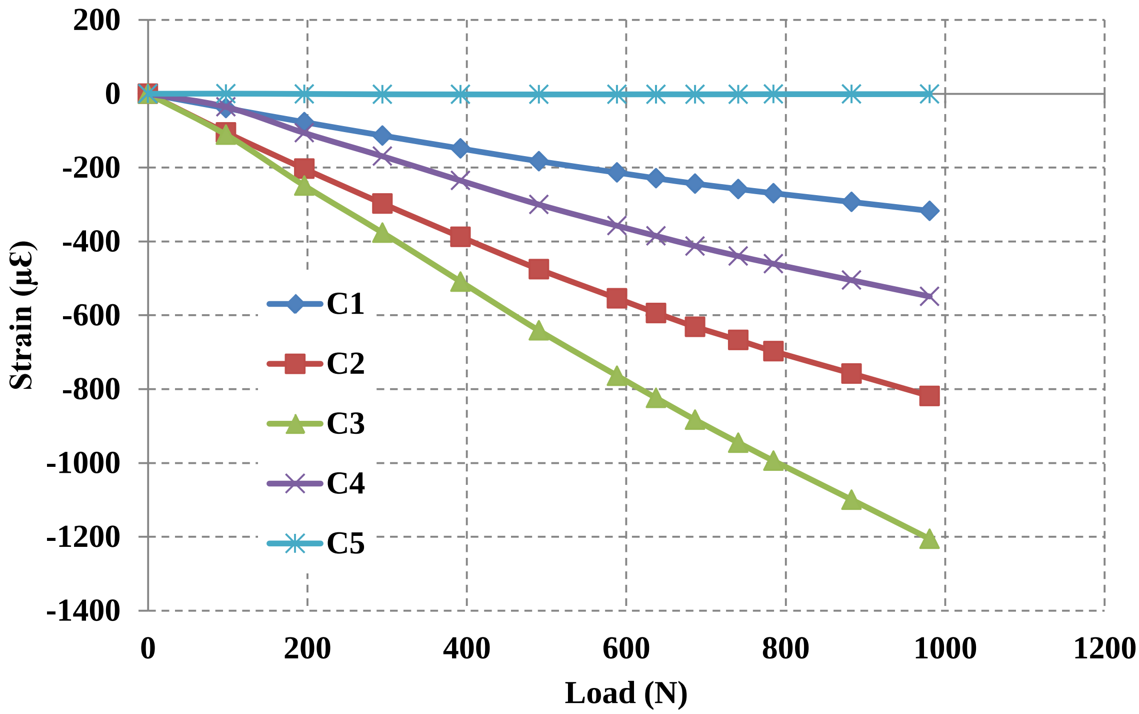

Figure 4.58 Compression Strain vs. Load for the Pile with 30-degree Scour Slope and 300-mm Scour Depth

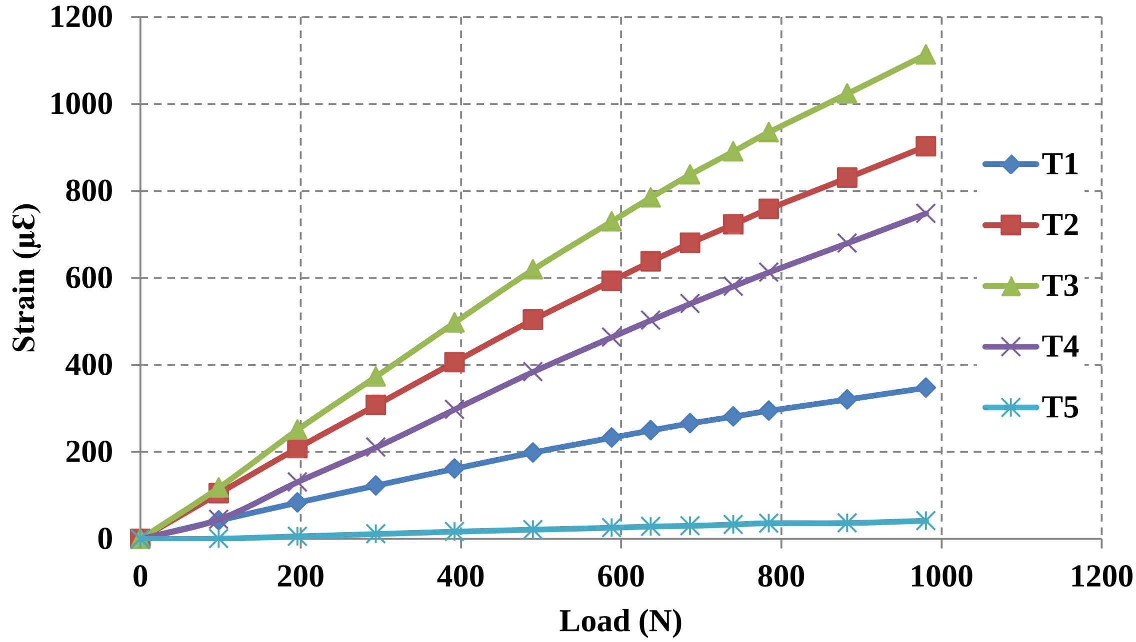

Figure 4.59 Tension Strain vs. Load for the Pile with 30-degree Scour Slope and 300-mm Scour Depth

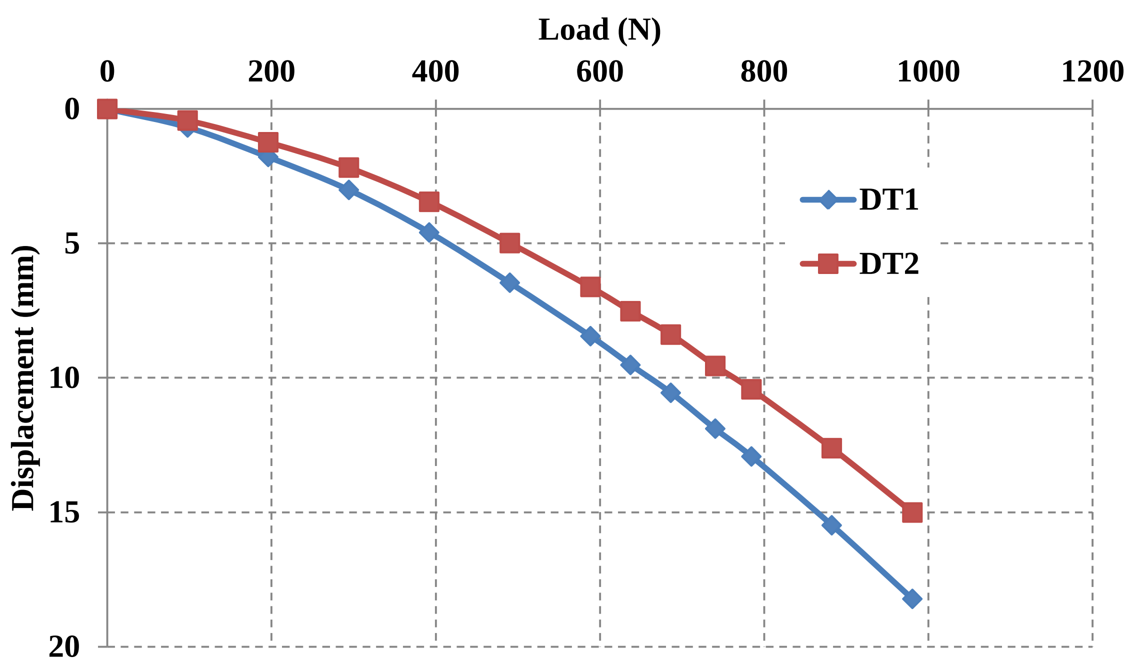

Figure 4.60 Lateral Displacements vs. Load for the Pile with 30-degree Scour Slope and 300-mm Scour Depth

400-mm scour depth. Figures 4.61, 4.62, and 4.63 show the measured strains from the strain gages on the compression side, the strains on the tension side, and the displacements from the transducers with the load respectively.

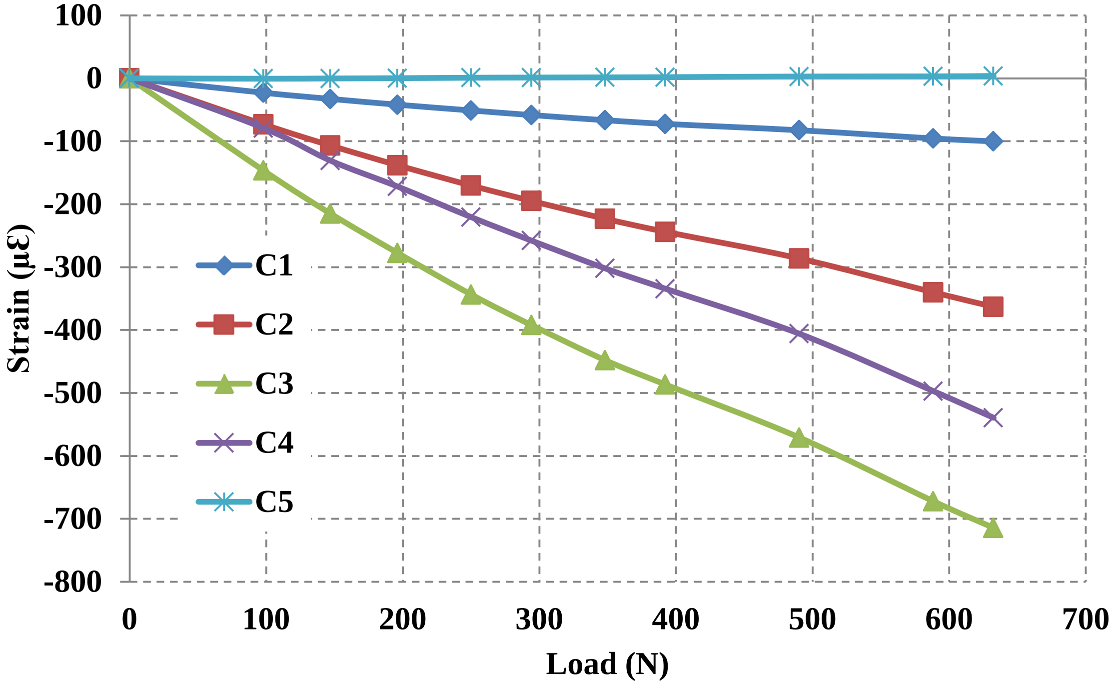

Figure 4.61 Compression Strain vs. Load for the Pile with 30-degree Scour Slope and 400-mm Scour Depth

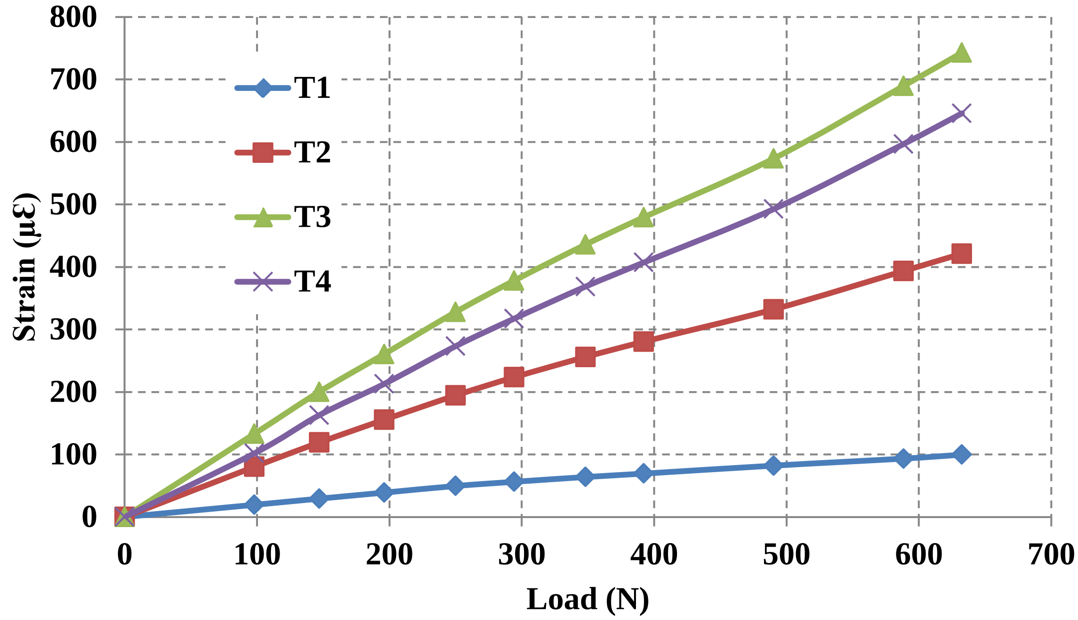

Figure 4.62 Tension Strain vs. Load for the Pile with 30-degree Scour Slope and 400-mm Scour Depth

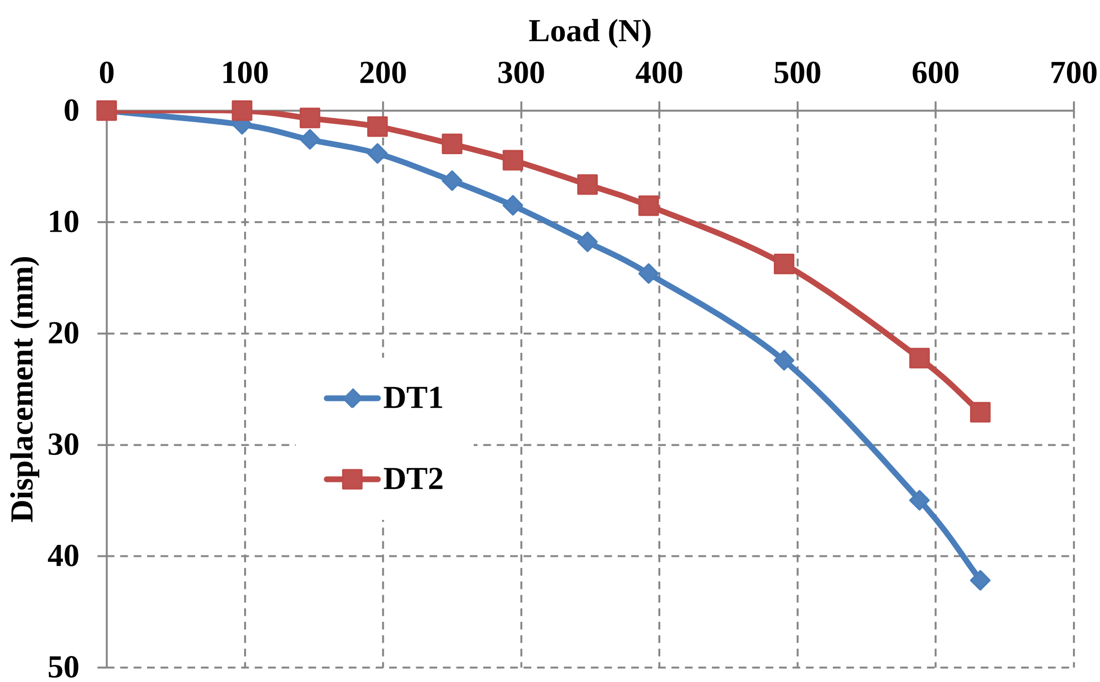

Figure 4.63 Lateral Displacements vs. Load for the Pile with 30-degree Scour Slope and 400-mm Scour Depth

500-mm scour depth. Figures 4.64, 4.65, and 4.66 show the measured strains from the strain gages on the compression side, the strains on the tension side, and the displacements from the transducers with the load respectively.

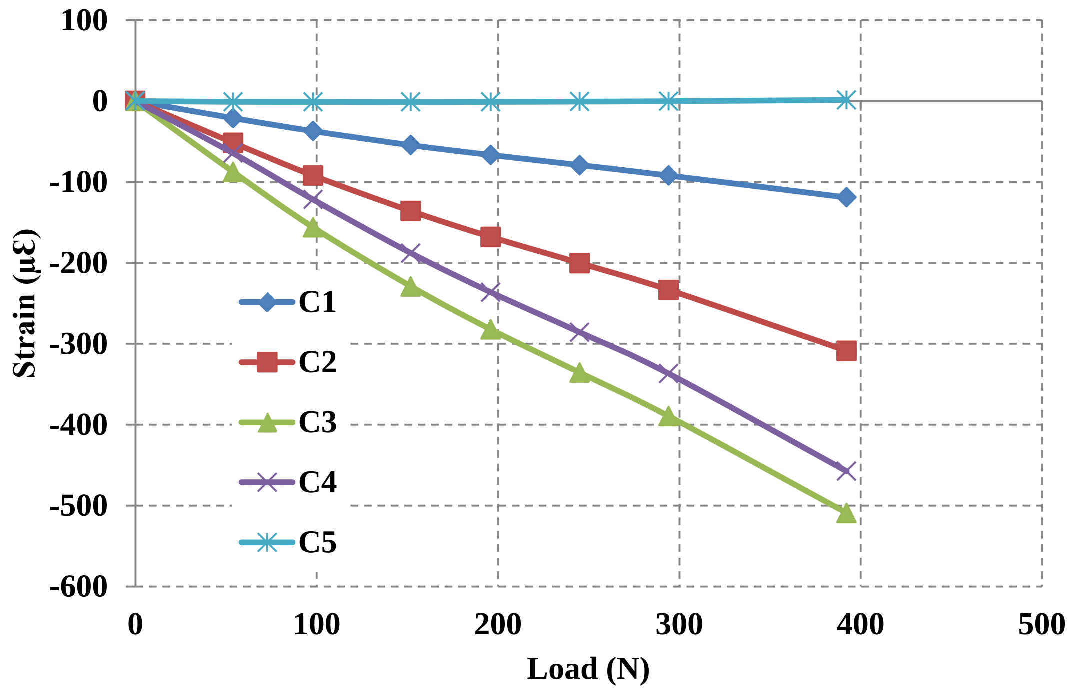

Figure 4.64 Compression Strain vs. Load for the Pile with 30-degree Scour Slope and 500-mm Scour Depth

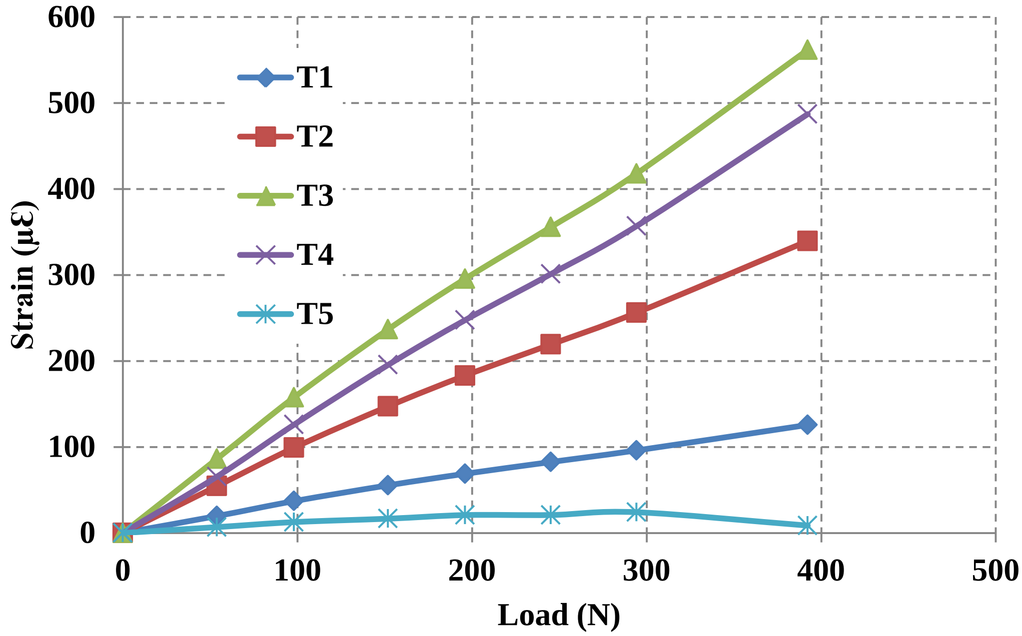

Figure 4.65 Tension Strain vs. Load for the Pile with 30-degree Scour Slope and 500-mm Scour Depth

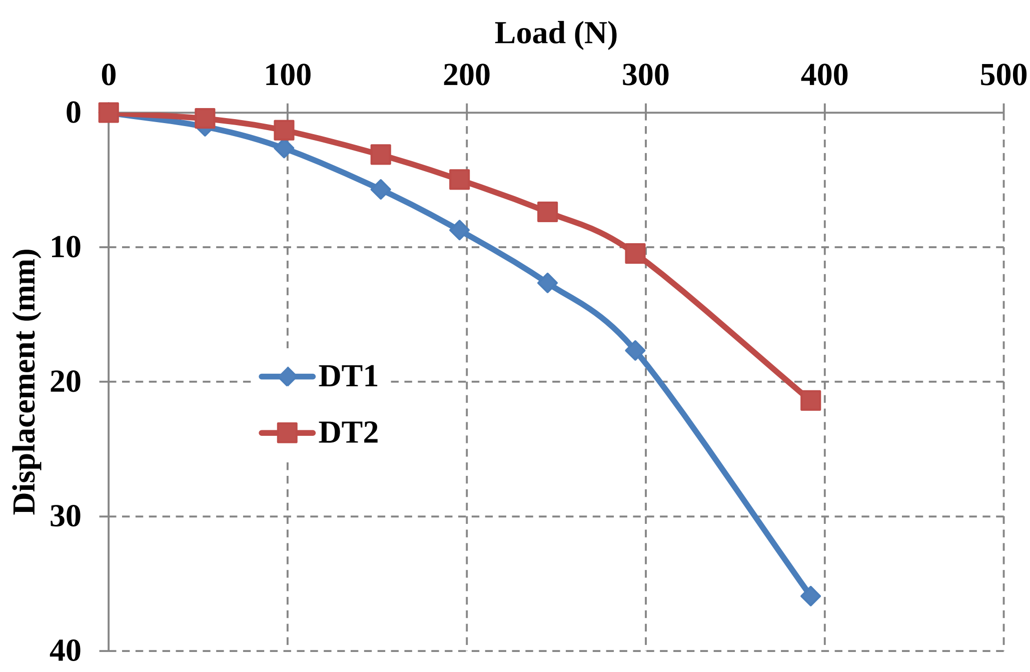

Figure 4.66 Lateral Displacements vs. Load for the Pile with 30-degree Scour Slope and 500-mm Scour Depth

4.3.3. Scour width

Experimental tests were conducted with laterally loaded piles at four different scour widths: 0, 240, 400, and 667 mm.

0-mm scour width

At 0-mm scour width, four tests were conducted at different scour depths ranging from 200 to 500 mm.

200-mm scour depth. Figures 4.67, 4.68, and 4.69 show the measured strains from the strain gages on the compression side, the strains on the tension side, and the displacements from the transducers with the load respectively.

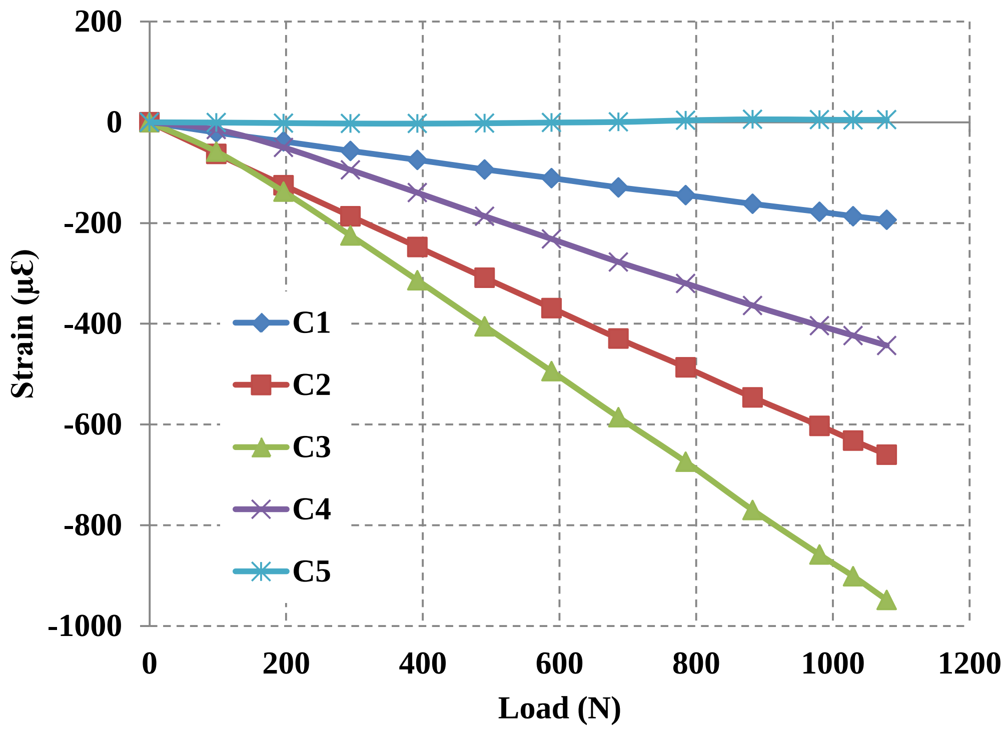

Figure 4.67 Compression Strain vs. Load for the Pile with 0-mm Scour Width and 200-mm Scour Depth

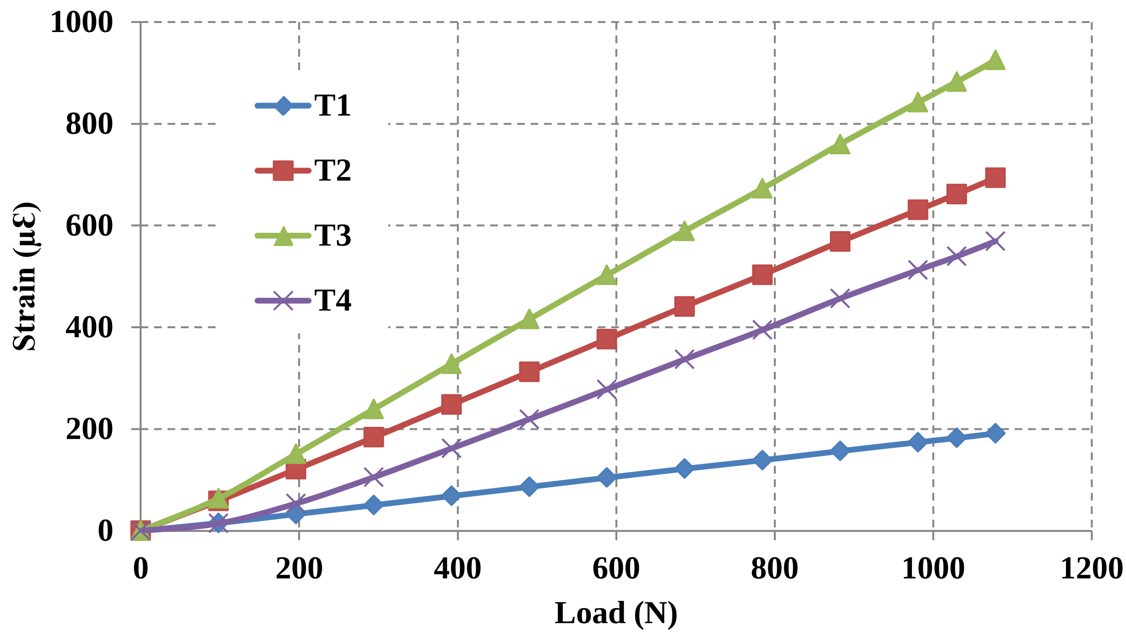

Figure 4.68 Tension Strain vs. Load for the Pile with 0-mm Scour Width and 200-mm Scour Depth

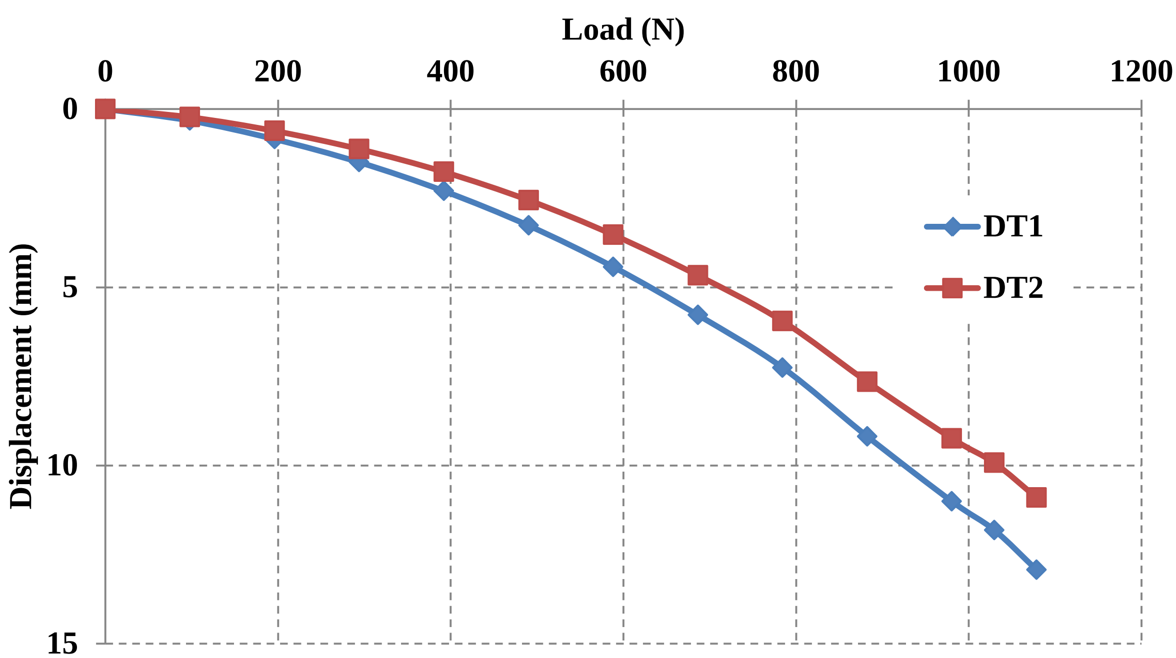

Figure 4.69 Lateral Displacements vs. Load for the Pile with 0-mm Scour Width and 200-mm Scour Depth

300-mm scour depth. Figures 4.70, 4.71, and 4.72 show the measured strains from the strain gages on the compression side, the strains on the tension side, and the displacements from the transducers with the load respectively.

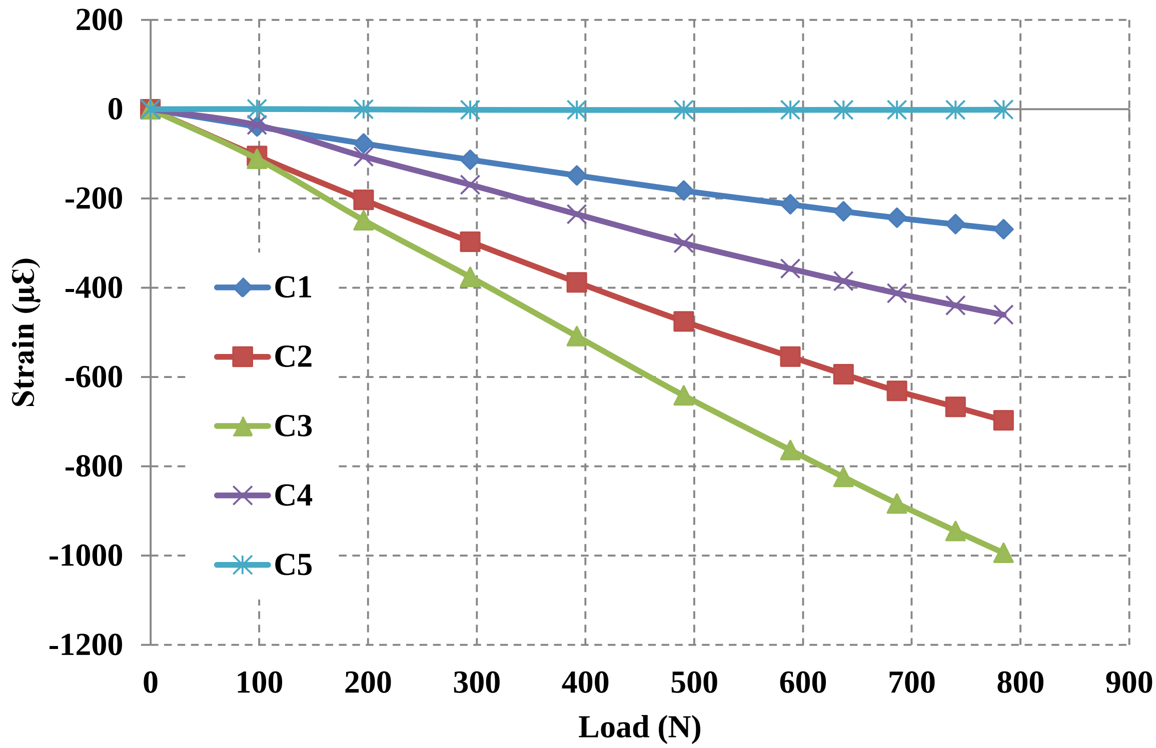

Figure 4.70 Compression Strain vs. Load for the Pile with 0-mm Scour Width and 300-mm Scour Depth

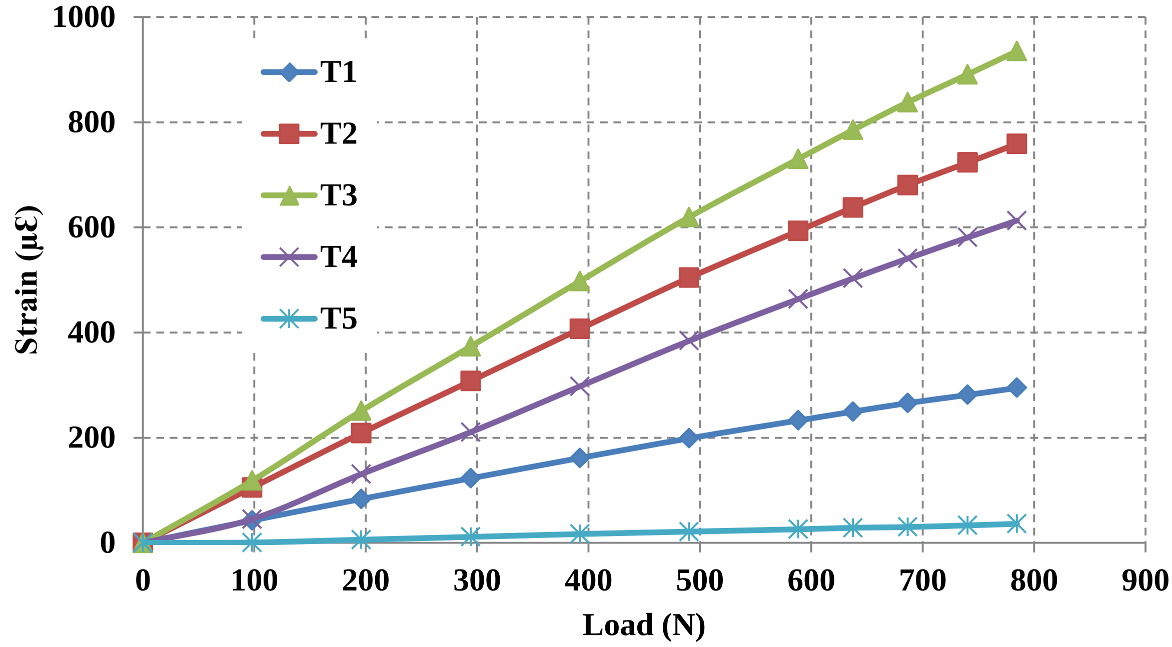

Figure 4.71 Tension Strain vs. Load for the Pile with 0-mm Scour Width and 300-mm Scour Depth

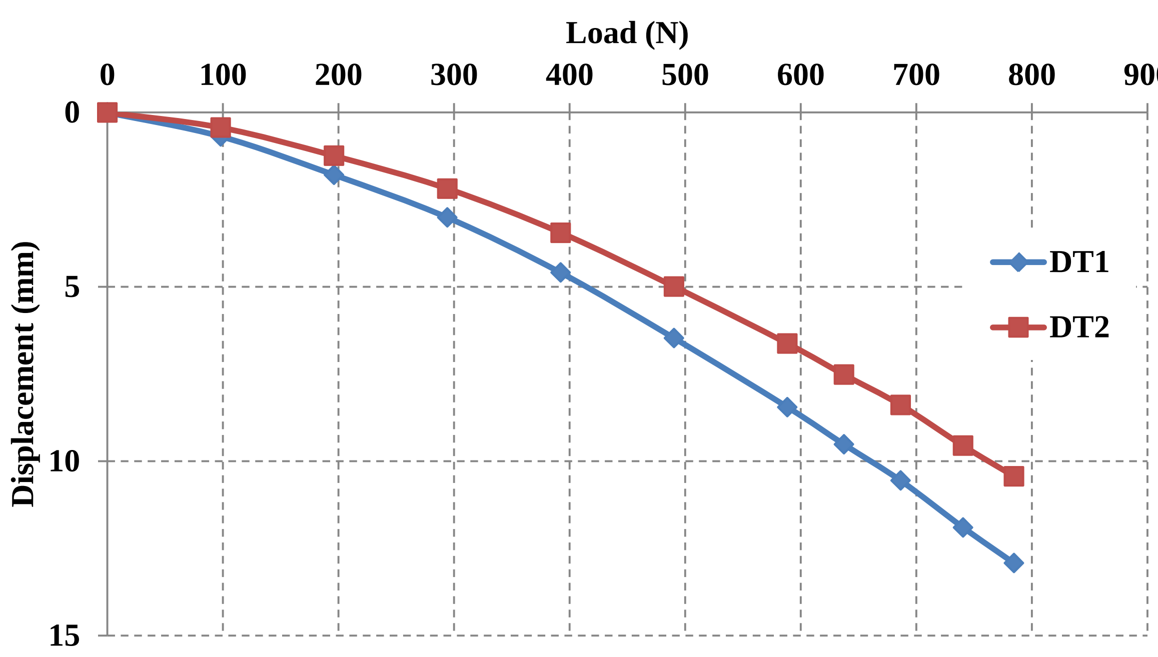

Figure 4.72 Lateral Displacements vs. Load for the Pile with 0-mm Scour Width and 300-mm Scour Depth

400-mm scour depth. Figures 4.73, 4.74, and 4.75 show the measured strains from the strain gages on the compression side, the strains on the tension side, and the displacements from the transducers with the load respectively.

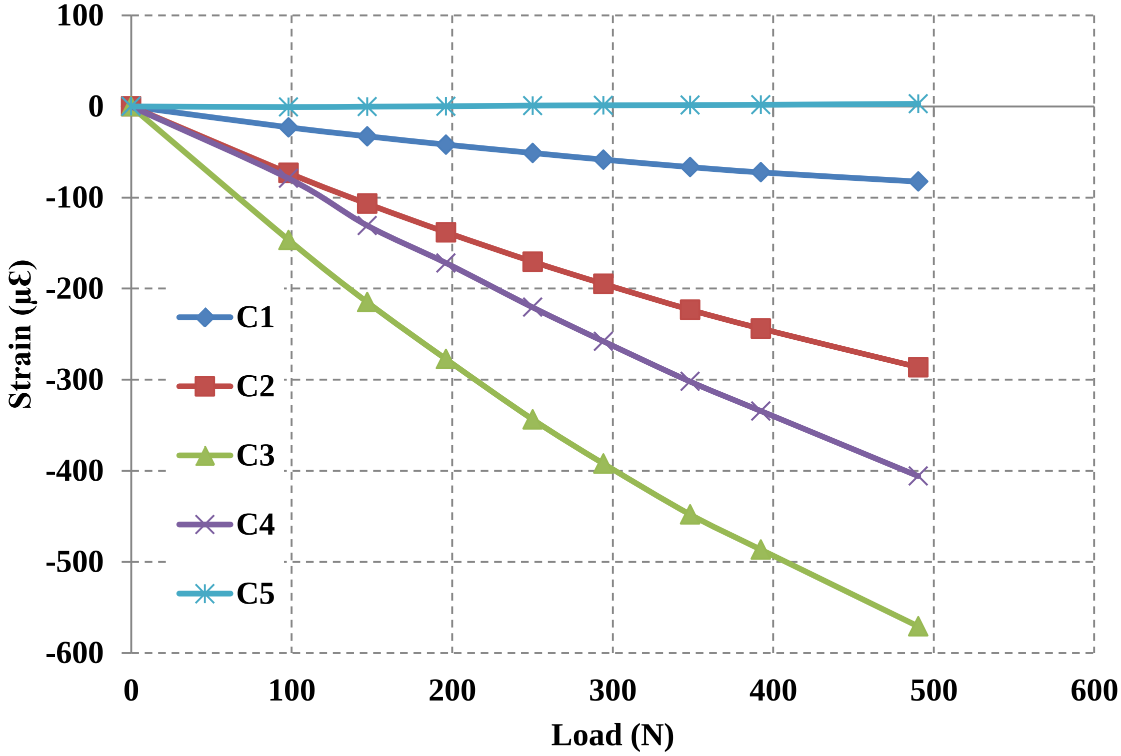

Figure 4.73 Compression Strain vs. Load for the Pile with 0-mm Scour Width and 400-mm Scour Depth

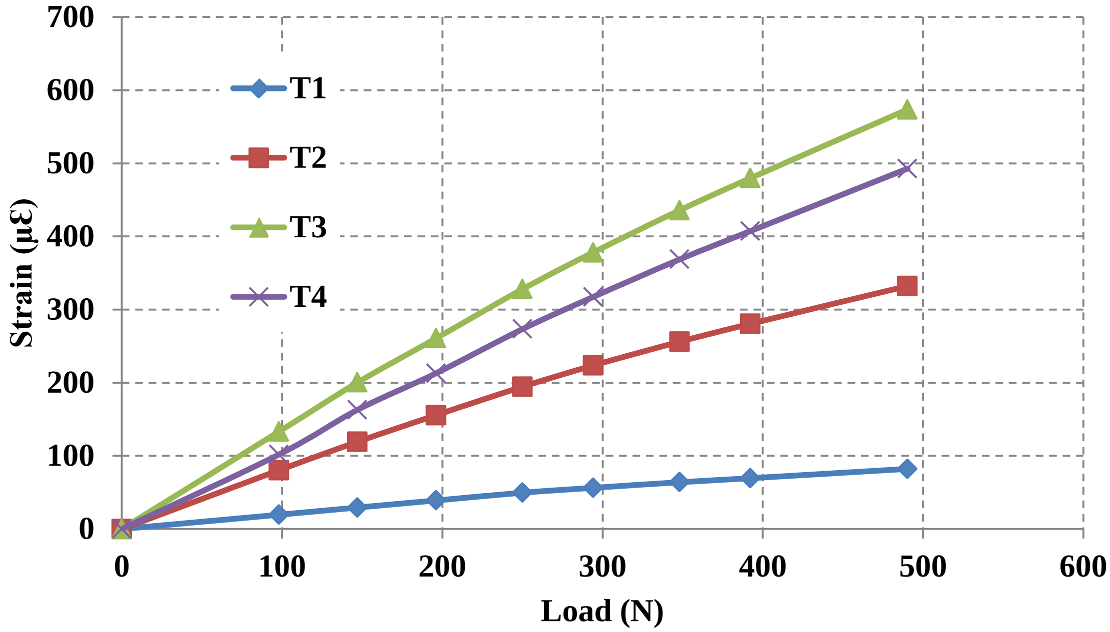

Figure 4.74 Tension Strain vs. Load for the Pile with 0-mm Scour Width and 400-mm Scour Depth

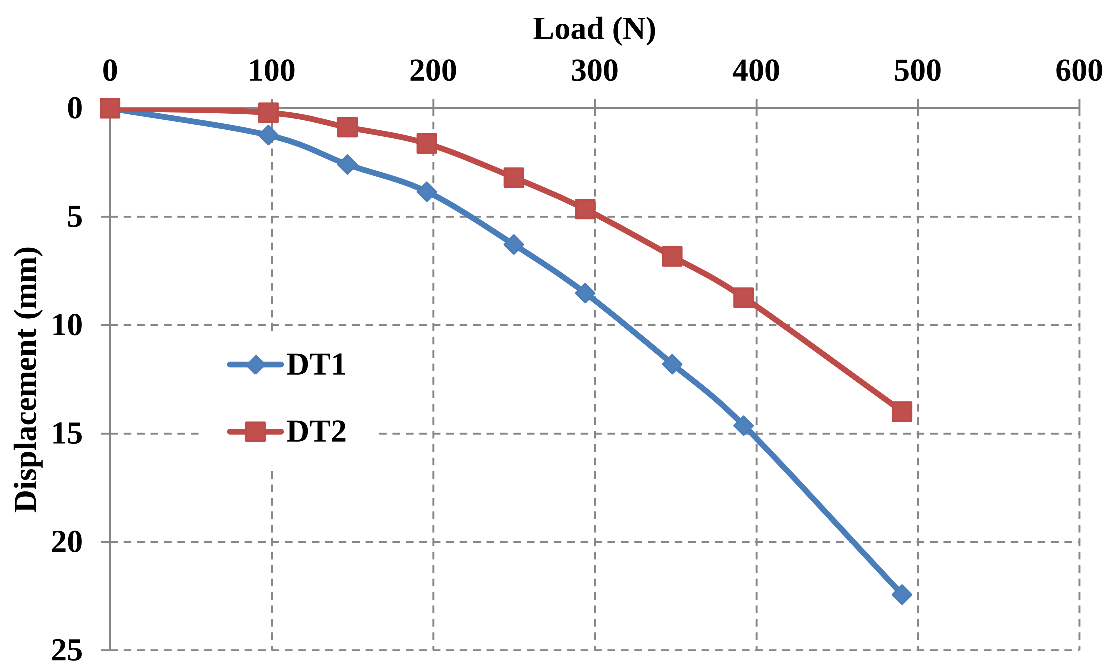

Figure 4.75 Lateral Displacements vs. Load for the Pile with 0-mm Scour Width and 400-mm Scour Depth

500-mm scour depth. Figures 4.76, 4.77, and 4.78 show the measured strains from the strain gages on the compression side, the strains on the tension side, and the displacements from the transducers with the load respectively.

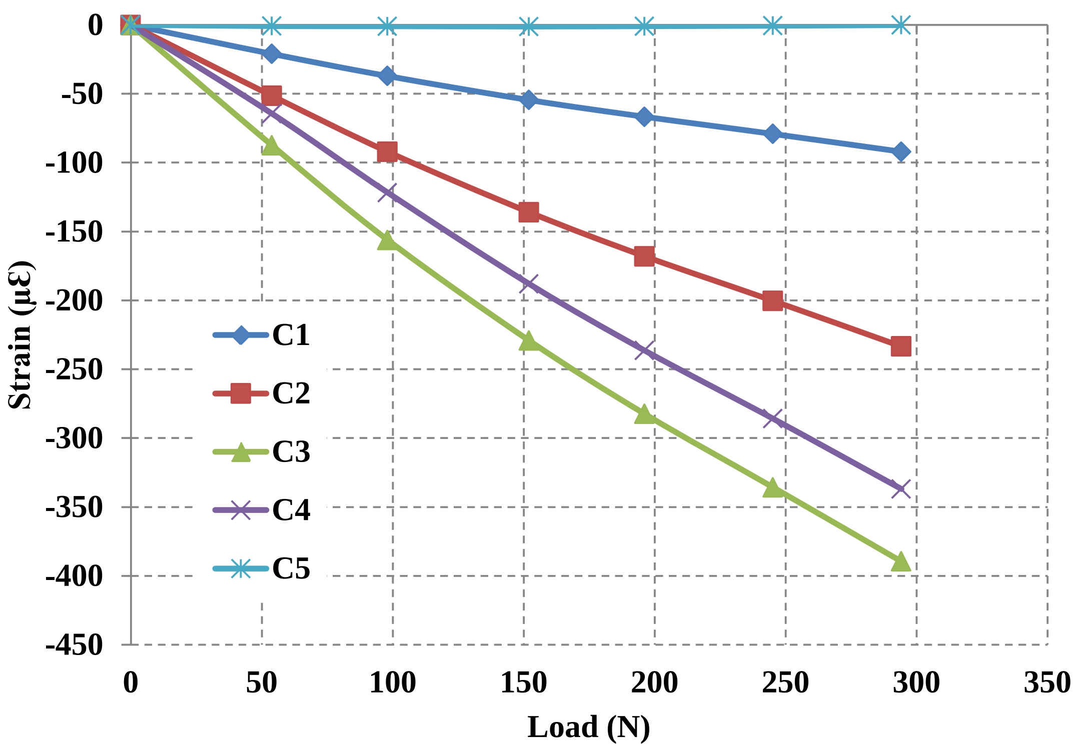

Figure 4.76 Compression Strain vs. Load for the Pile with 0-mm Scour Width and 500-mm Scour Depth

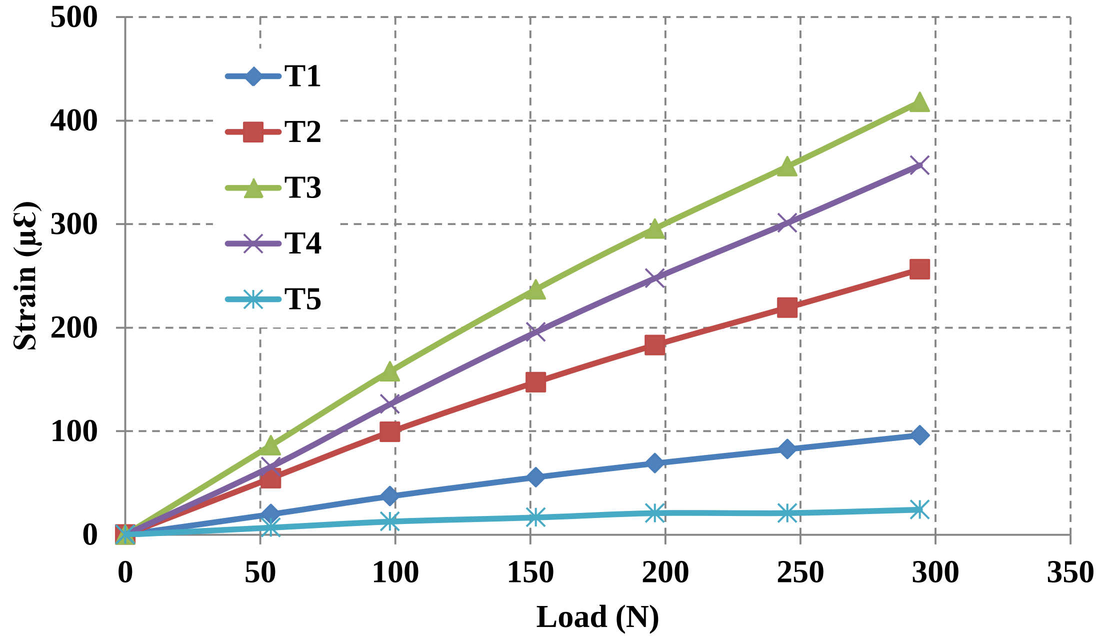

Figure 4.77 Tension Strain vs. Load for the Pile with 0-mm Scour Width and 500-mm Scour Depth

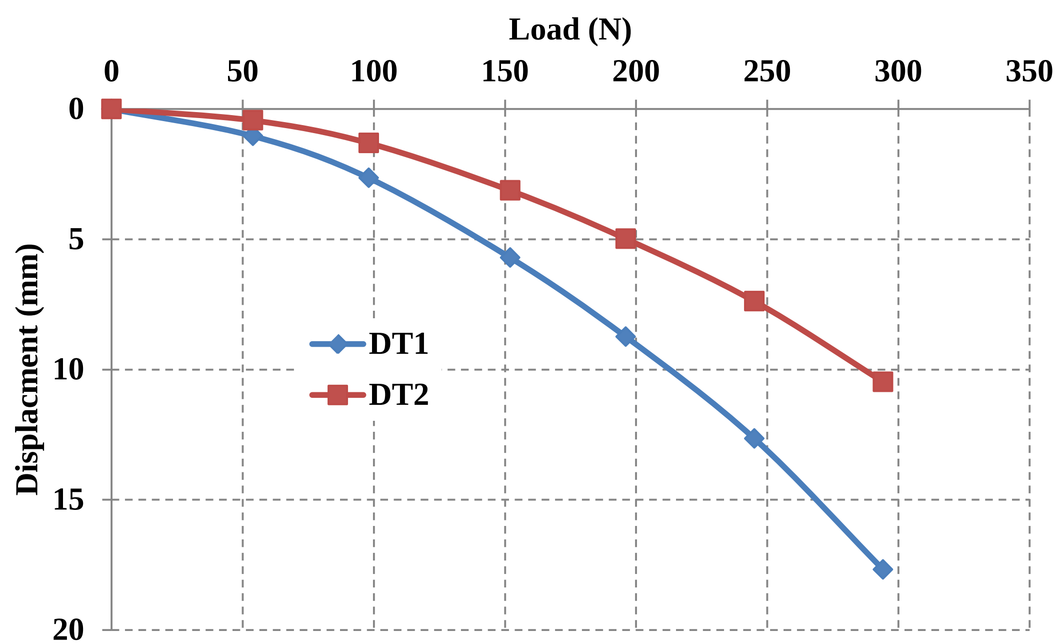

Figure 4.78 Lateral Displacements vs. Load for the Pile with 0-mm Scour Width and 500-mm Scour Depth

240-mm scour width

At 240-mm scour width, four tests were conducted at different scour depths ranging from 200 to 500 mm.

200-mm scour depth. Figures 4.79, 4.80, and 4.81 show the measured strains from the strain gages on the compression side, the strains on the tension side, and the displacements from the transducers with the load respectively.

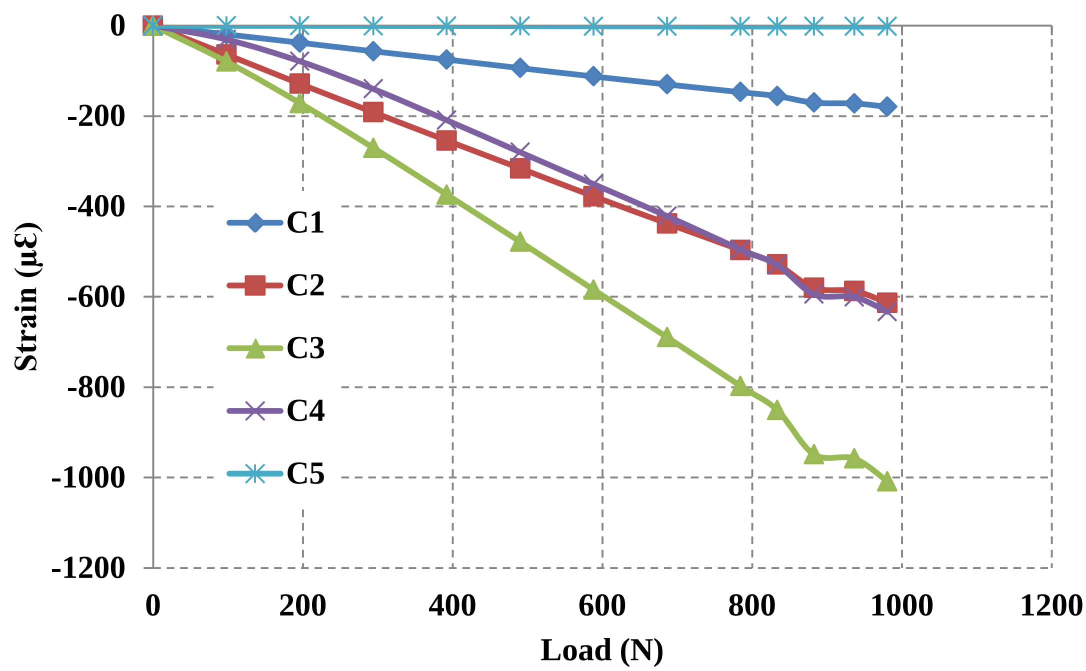

Figure 4.79 Compression Strain vs. Load for the Pile with 240-mm Scour Width and 200-mm Scour Depth

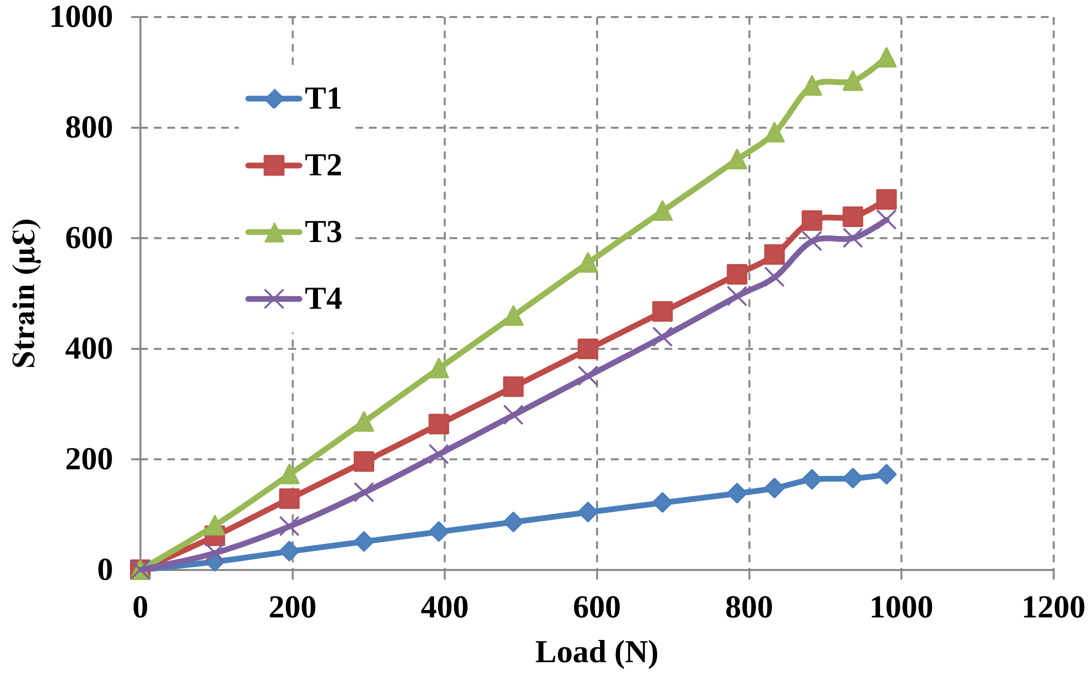

Figure 4.80 Tension Strain vs. Load for the Pile with 240-mm Scour Width and 200-mm Scour Depth

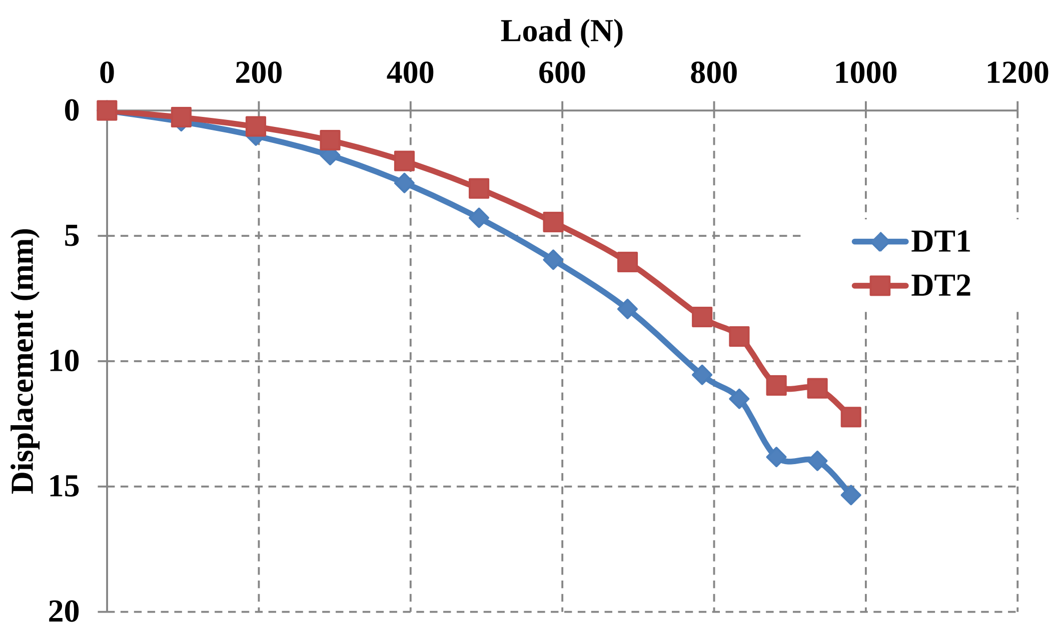

Figure 4.81 Lateral Displacements vs. Load for the Pile with 240-mm Scour Width and 200-mm Scour Depth

300-mm scour depth. Figures 4.82, 4.83, and 4.84 show the measured strains from the strain gages on the compression side, the strains on the tension side, and the displacements from the transducers with the load respectively.

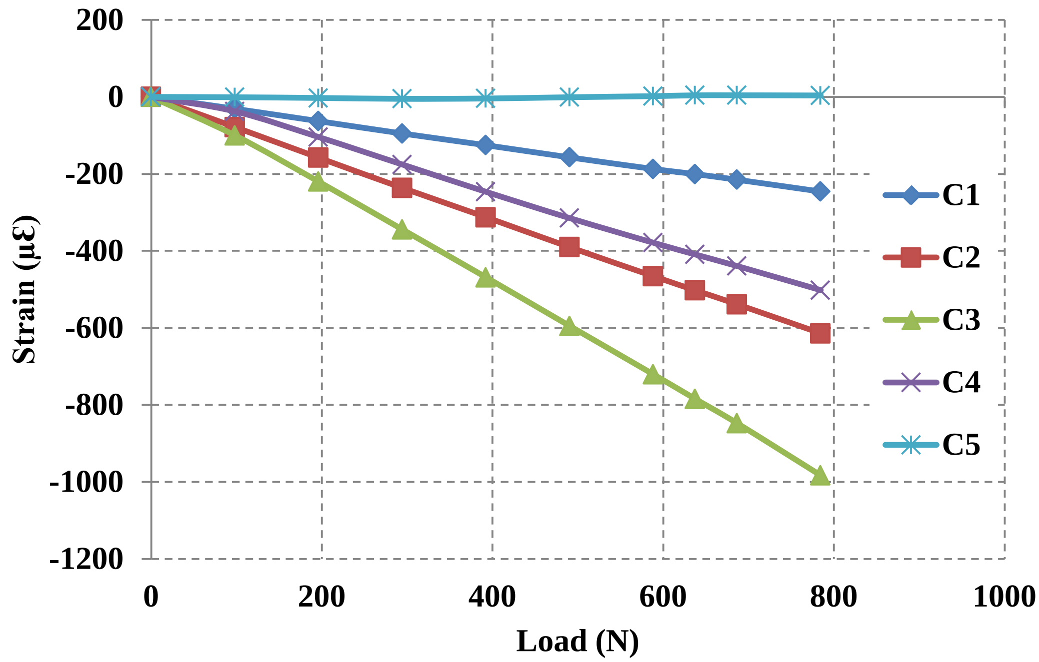

Figure 4.82 Compression Strain vs. Load for the Pile with 240-mm Scour Width and 300-mm Scour Depth

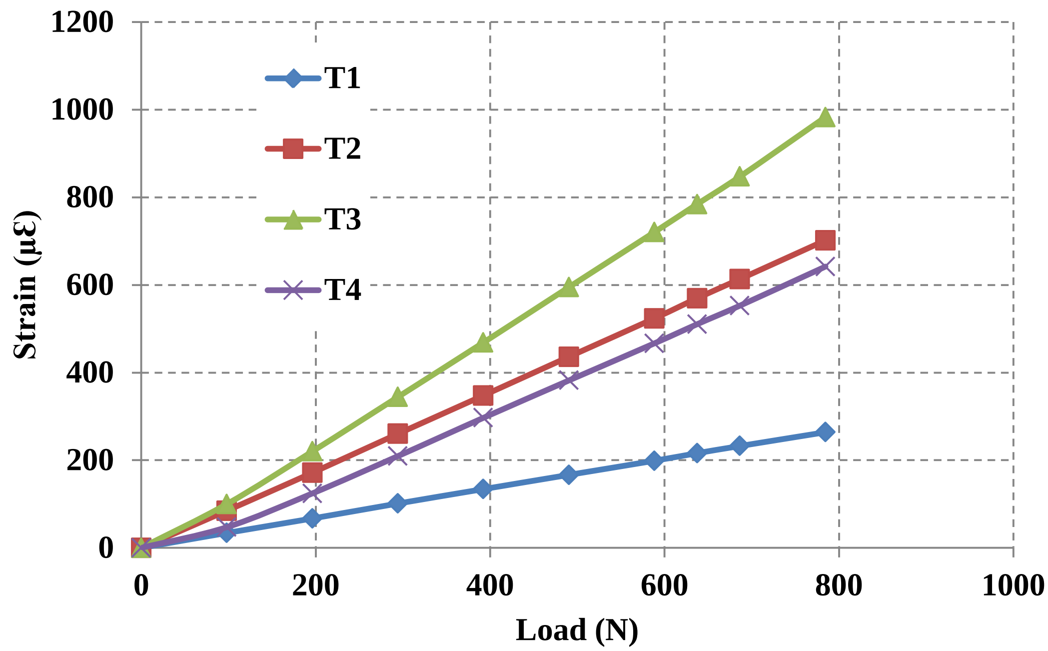

Figure 4.83 Tension Strain vs. Load for the Pile with 240-mm Scour Width and 300-mm Scour Depth

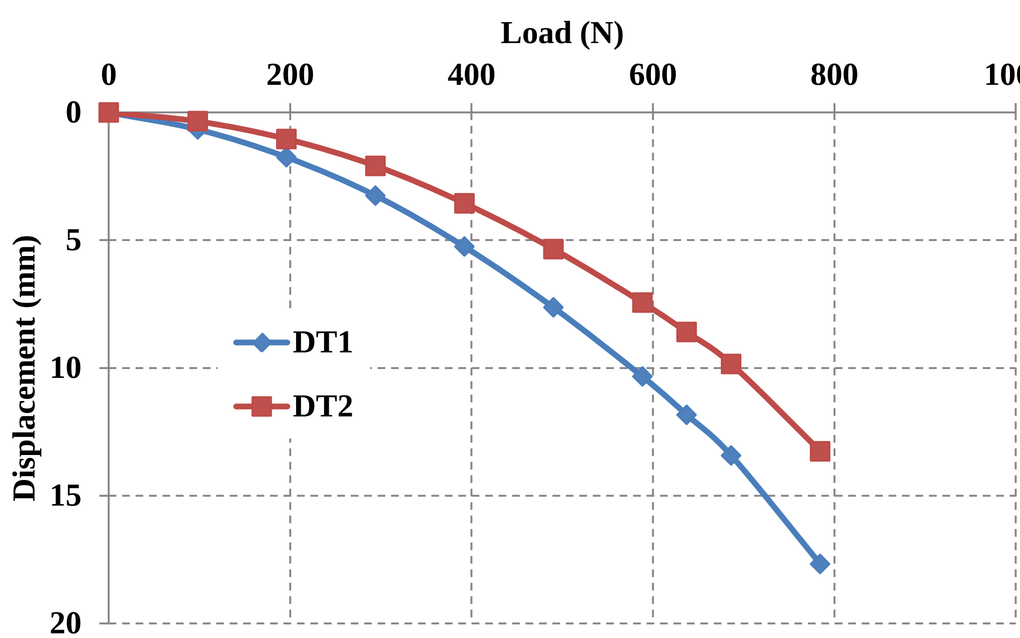

Figure 4.84 Lateral Displacements vs. Load for the Pile with 240-mm Scour Width and 300-mm Scour Depth

400-mm scour depth. Figures 4.85, 4.86, and 4.87 show the measured strains from the strain gages on the compression side, the strains on the tension side, and the displacements from the transducers with the load respectively.

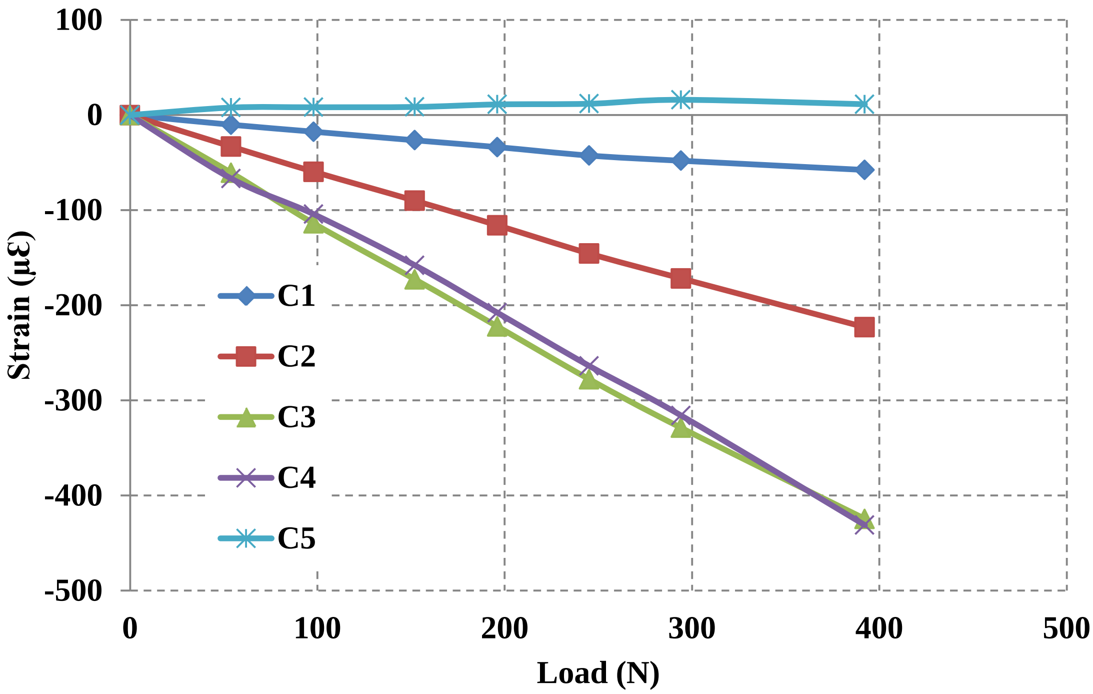

Figure 4.85 Compression Strain vs. Load for the Pile with 240-mm Scour Width and 400-mm Scour Depth

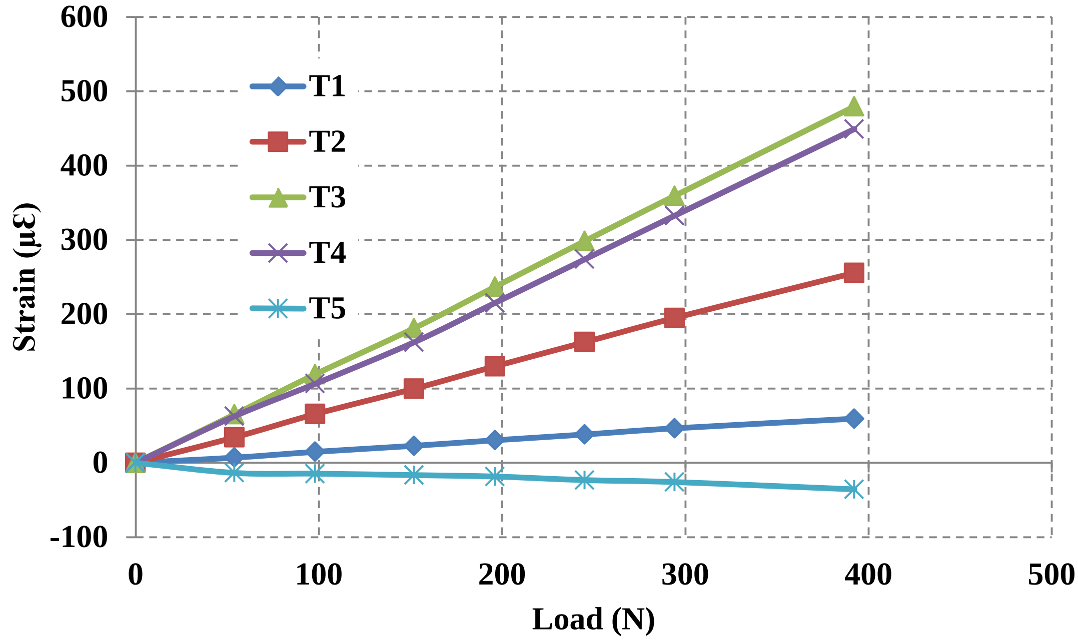

Figure 4.86 Tension Strain vs. Load for the Pile with 240-mm Scour Width and 400-mm Scour Depth

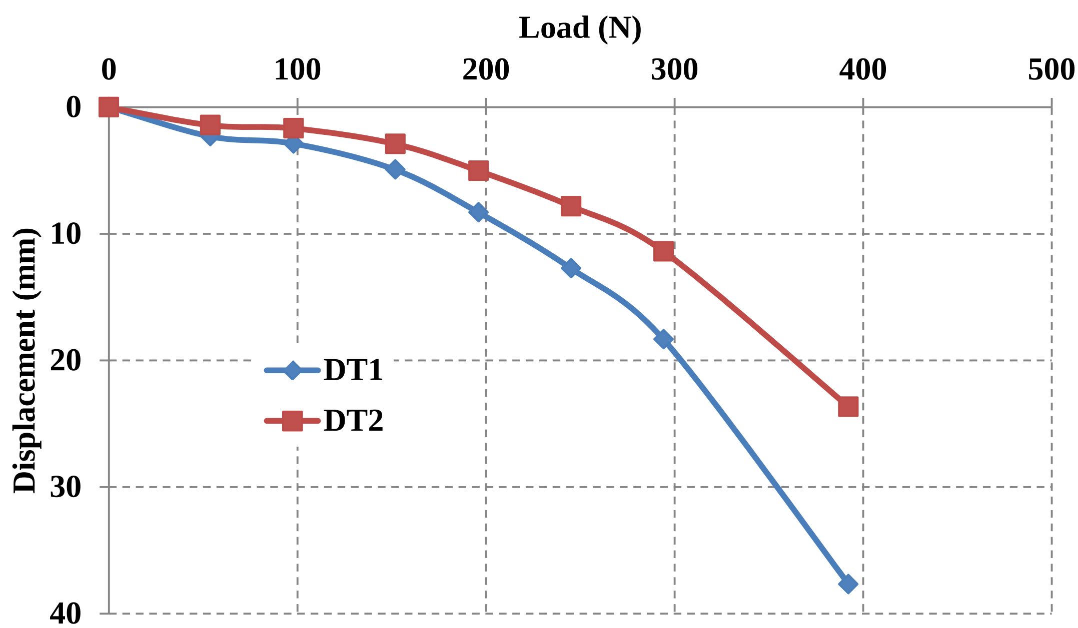

Figure 4.87 Lateral Displacements vs. Load for the Pile with 240-mm Scour Width and 400-mm Scour Depth

500-mm scour depth. Figures 4.88, 4.89, and 4.90 show the measured strains from the strain gages on the compression side, the strains on the tension side, and the displacements from the transducers with the load respectively.

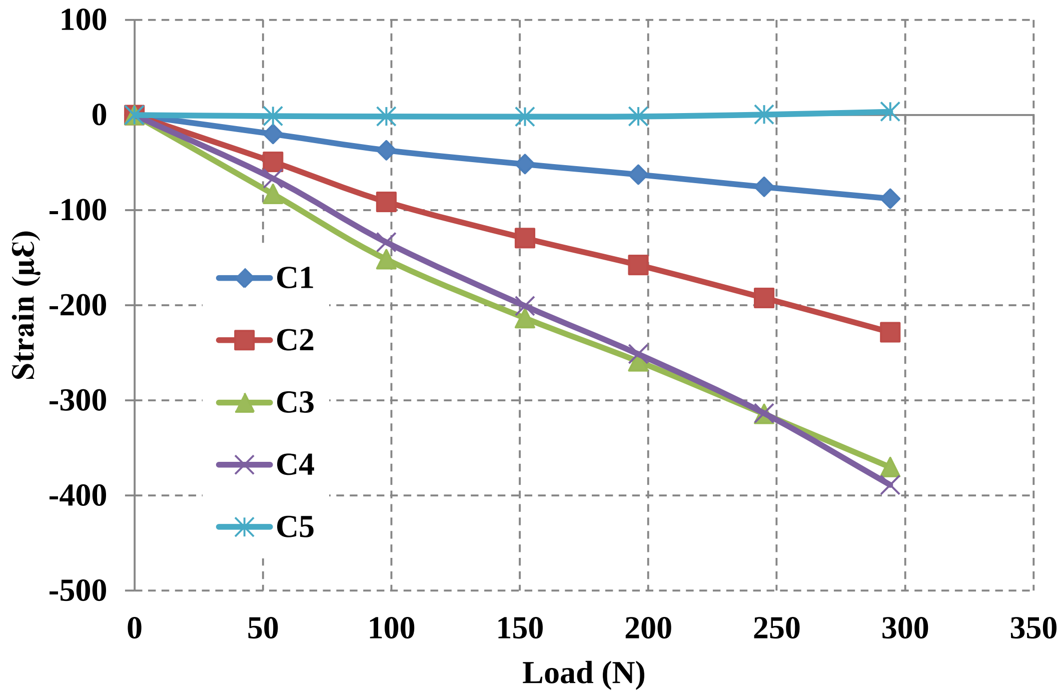

Figure 4.88 Compression Strain vs. Load for the Pile with 240-mm Scour Width and 500-mm Scour Depth

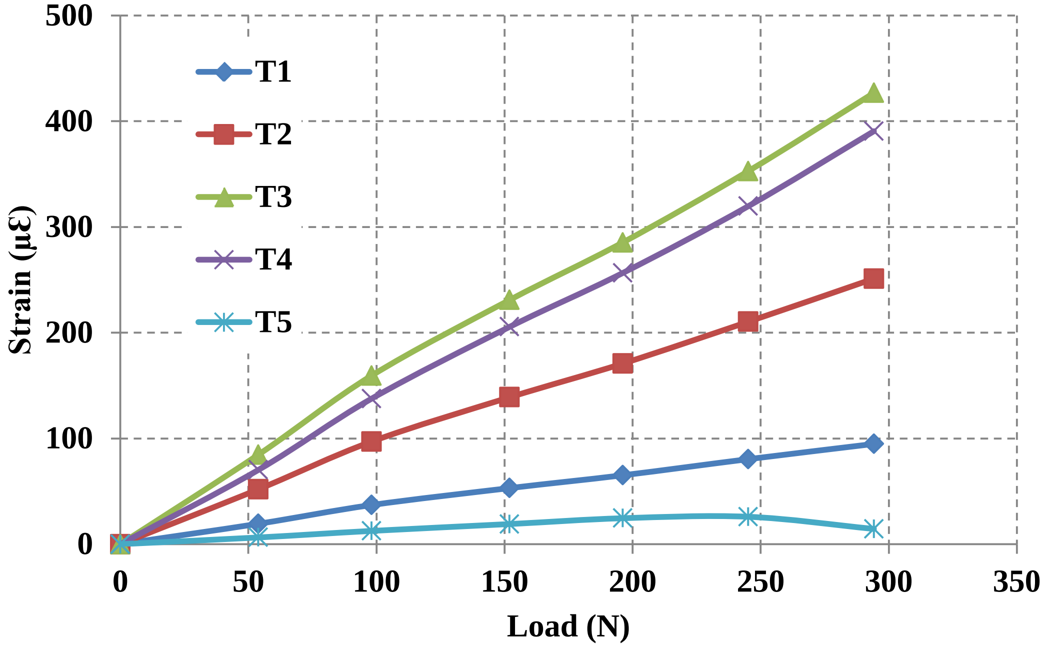

Figure 4.89 Tension Strain vs. Load for the Pile with 240-mm Scour Width and 500-mm Scour Depth

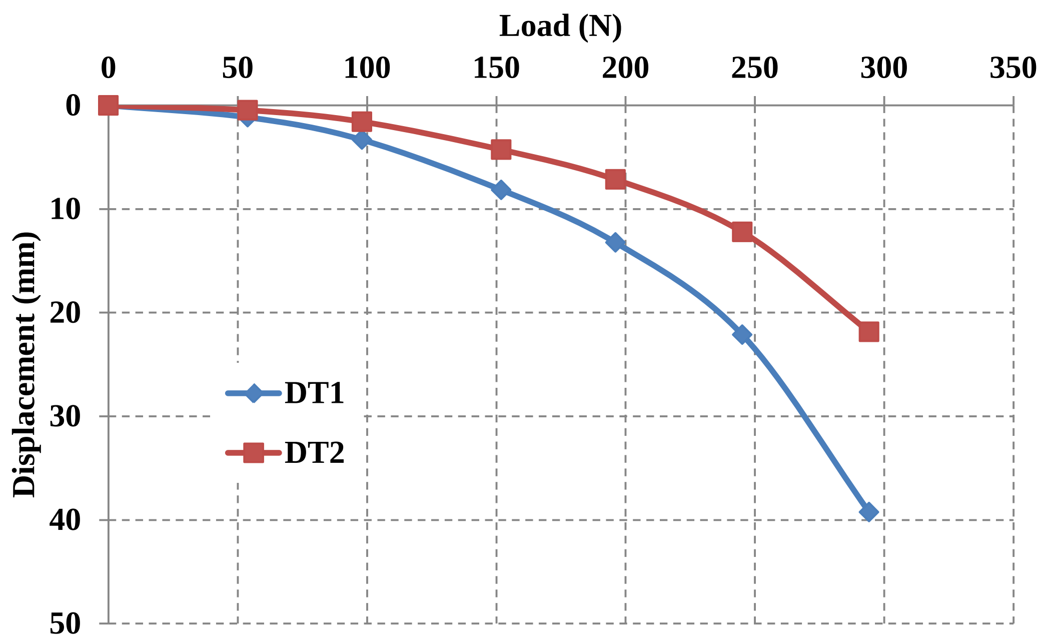

Figure 4.90 Lateral Displacements vs. Load for the Pile with 240-mm Scour Width and 500-mm Scour Depth

400-mm scour width

At 400-mm scour width, four tests were conducted at different scour depths ranging from 200 to 500 mm.

200-mm scour depth. Figures 4.91, 4.92, and 4.93 show the measured strains from the strain gages on the compression side, the strains on the tension side, and the displacements from the transducers with the load respectively.

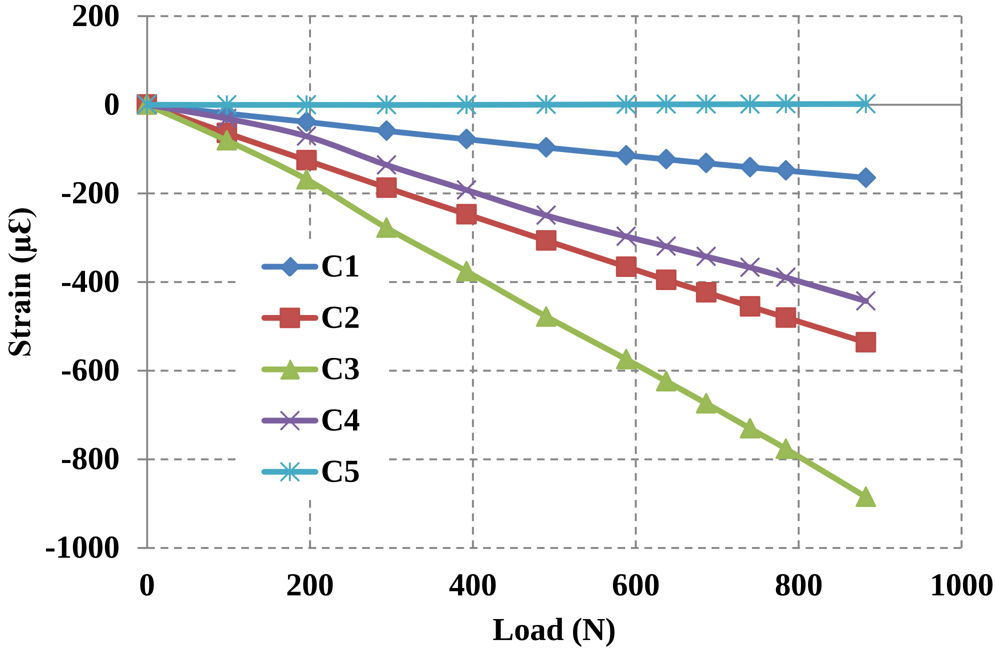

Figure 4.91 Compression Strain vs. Load for the Pile with 400-mm Scour Width and 200-mm Scour Depth

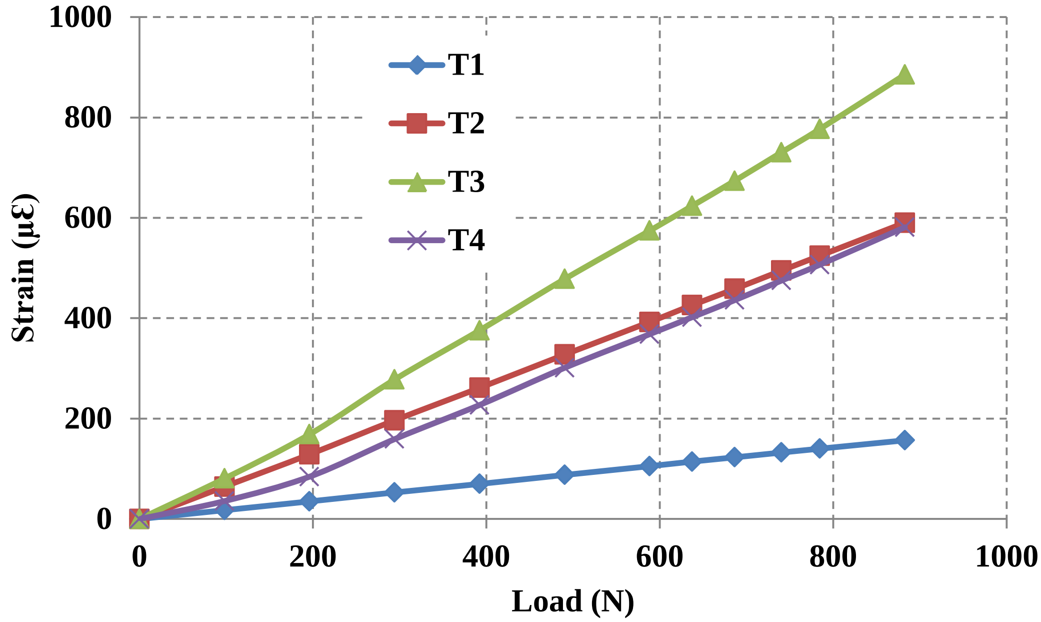

Figure 4.92 Tension Strain vs. Load for the Pile with 400-mm Scour Width and 200-mm Scour Depth

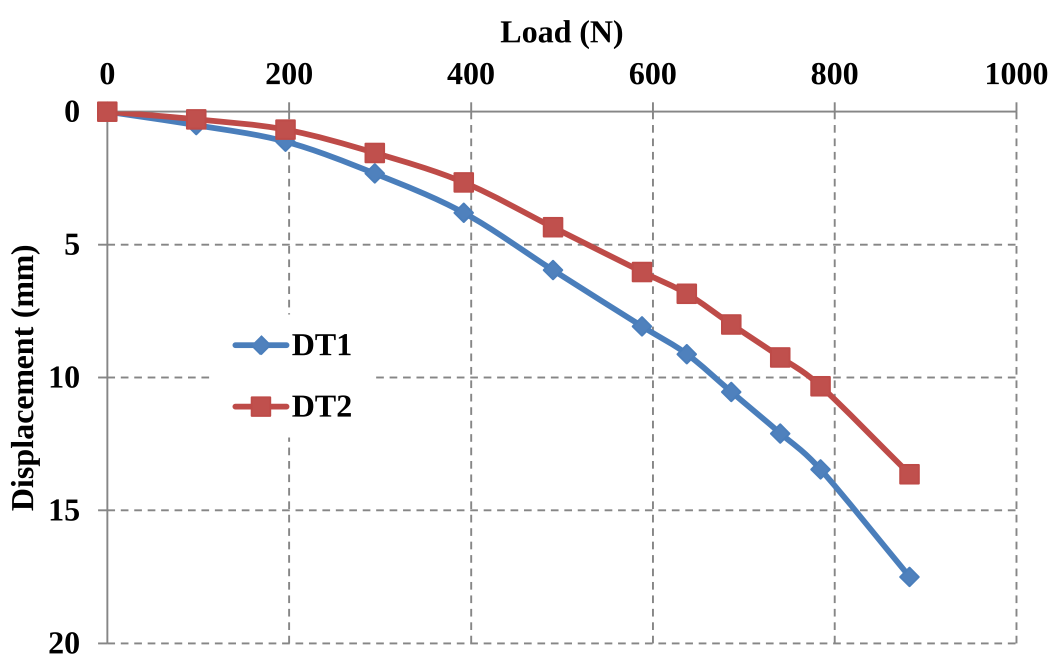

Figure 4.93 Lateral Displacements vs. Load for the Pile with 400-mm Scour Width and 200-mm Scour Depth

300-mm scour depth. Figures 4.94, 4.95, and 4.96 show the measured strains from the strain gages on the compression side, the strains on the tension side, and the displacements from the transducers with the load respectively.

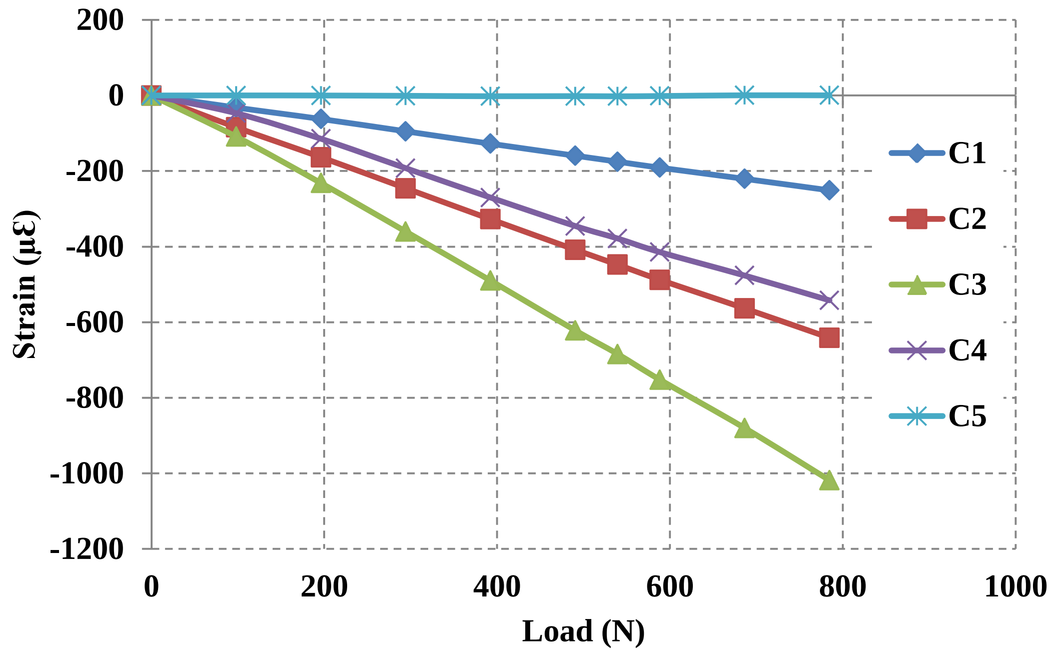

Figure 4.94 Compression Strain vs. Load for the Pile with 400-mm Scour Width and 300-mm Scour Depth

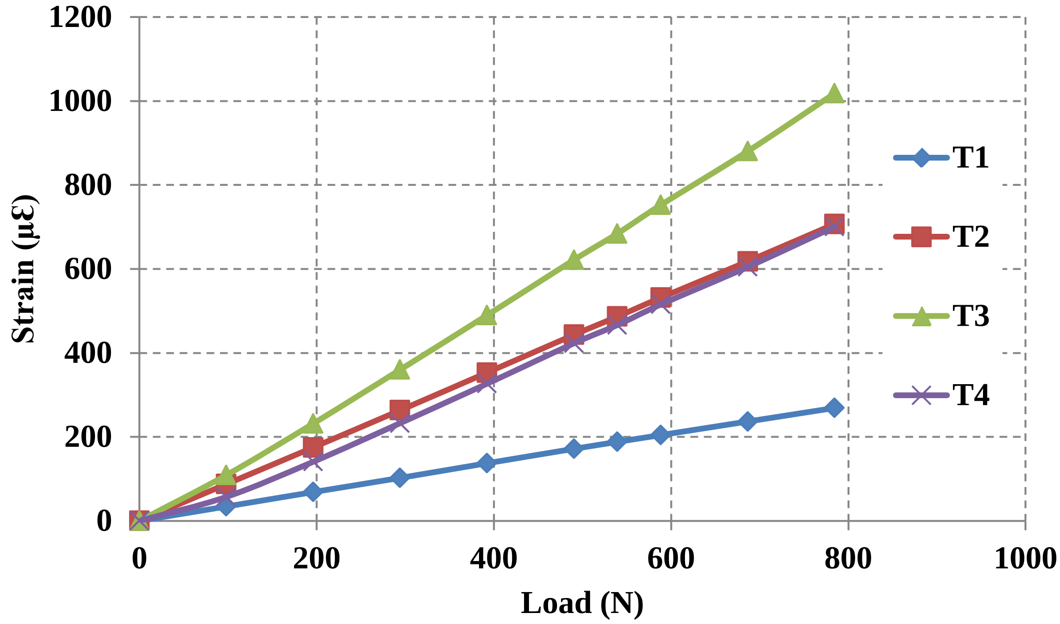

Figure 4.95 Tension Strain vs. Load for the Pile with 400-mm Scour Width and 300-mm Scour Depth

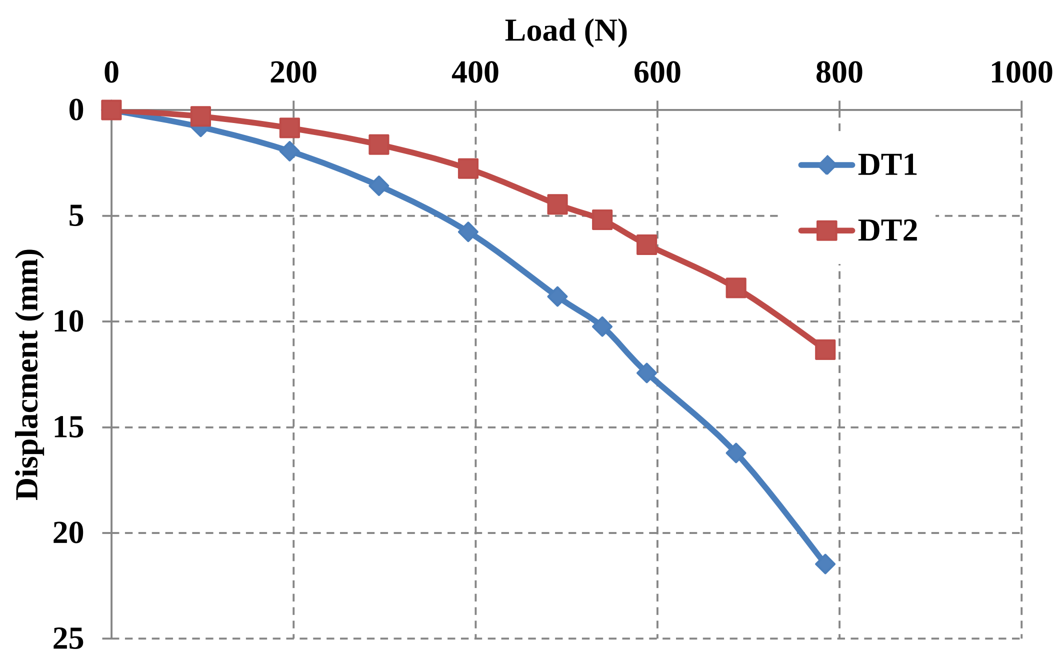

Figure 4.96 Lateral Displacements vs. Load for the Pile with 400-mm Scour Width and 300-mm Scour Depth

400-mm scour depth. Figures 4.97, 4.98, and 4.99 show the measured strains from the strain gages on the compression side, the strains on the tension side, and the displacements from the transducers with the load respectively.

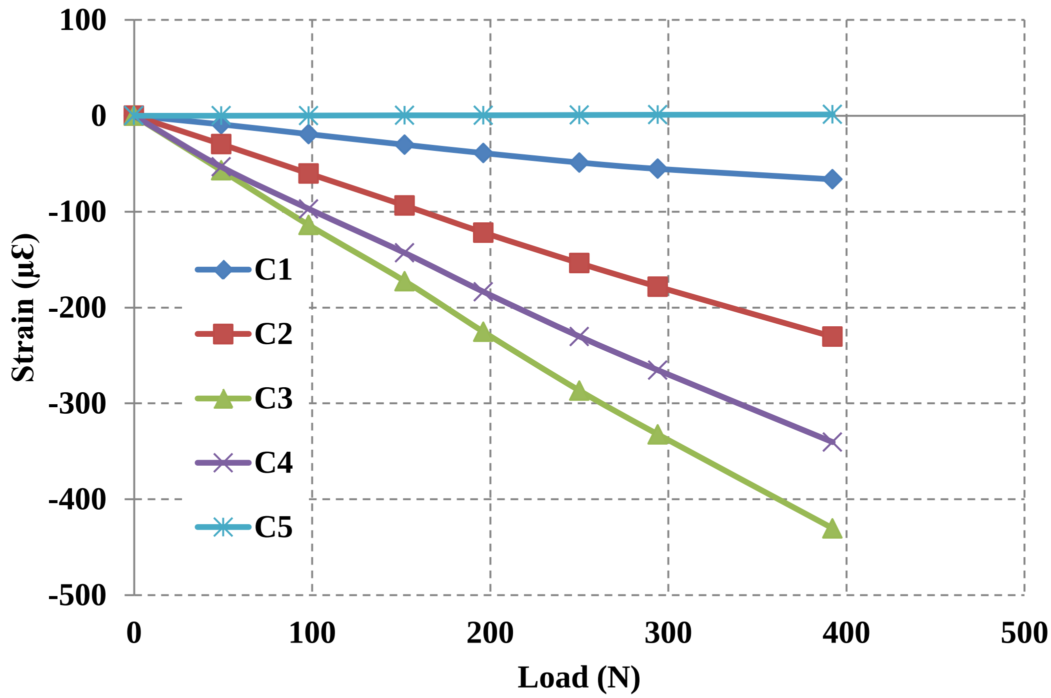

Figure 4.97 Compression Strain vs. Load for the Pile with 400-mm Scour Width and 400-mm Scour Depth

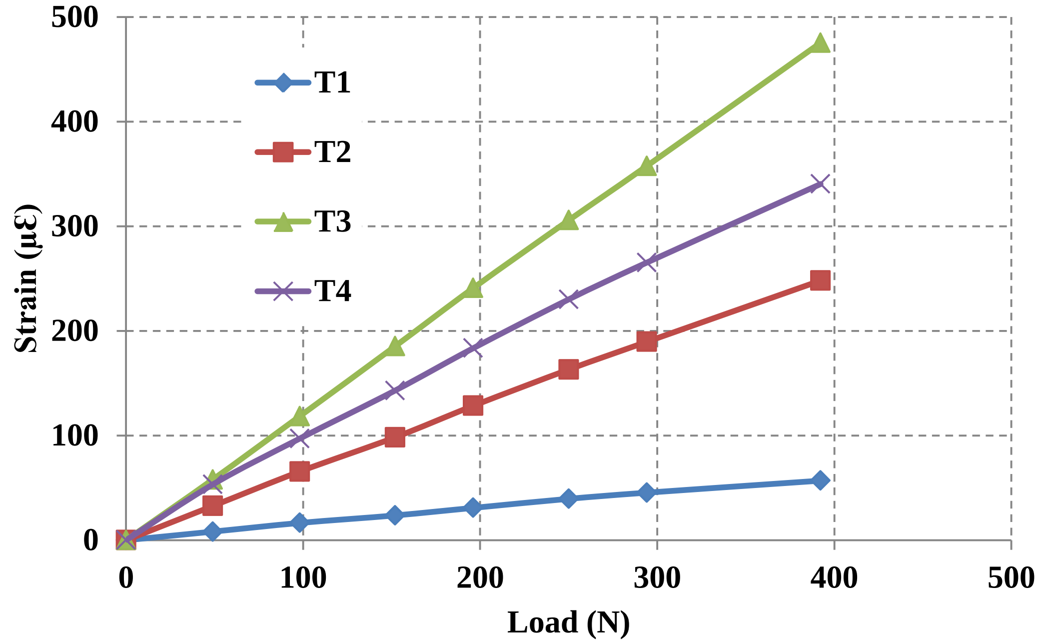

Figure 4.98 Tension Strain vs. Load for the Pile with 400-mm Scour Width and 400-mm Scour Depth

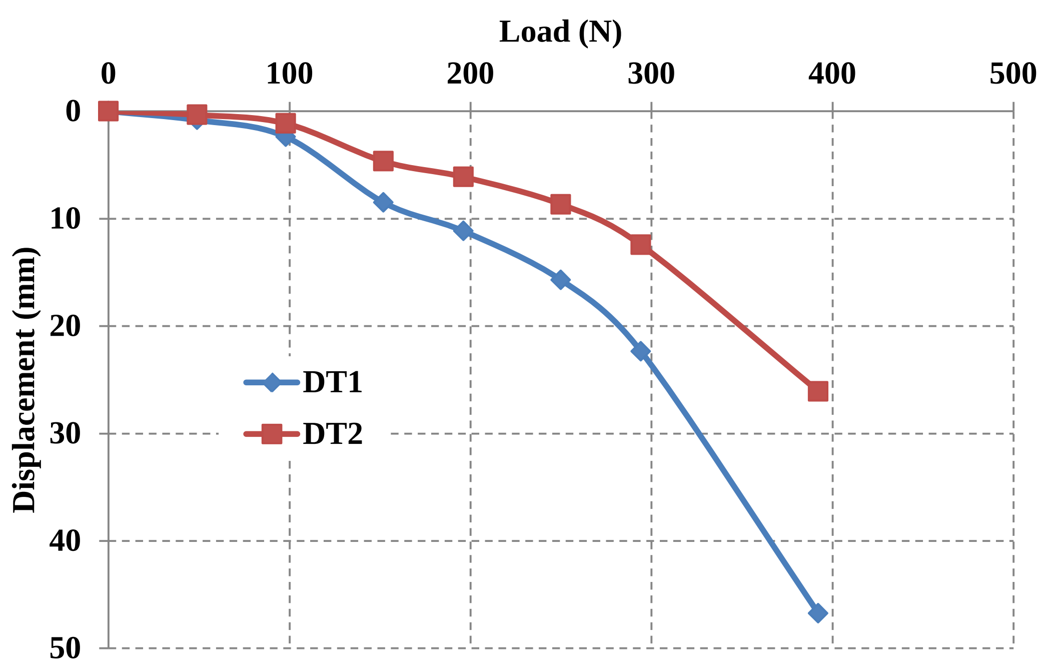

Figure 4.99 Lateral Displacements vs. Load for the Pile with 400-mm Scour Width and 400-mm Scour Depth

500-mm scour depth. Figures 4.100, 4.101, and 4.102 show the measured strains from the strain gages on the compression side, the strains on the tension side, and the displacements from the transducers with the load respectively.

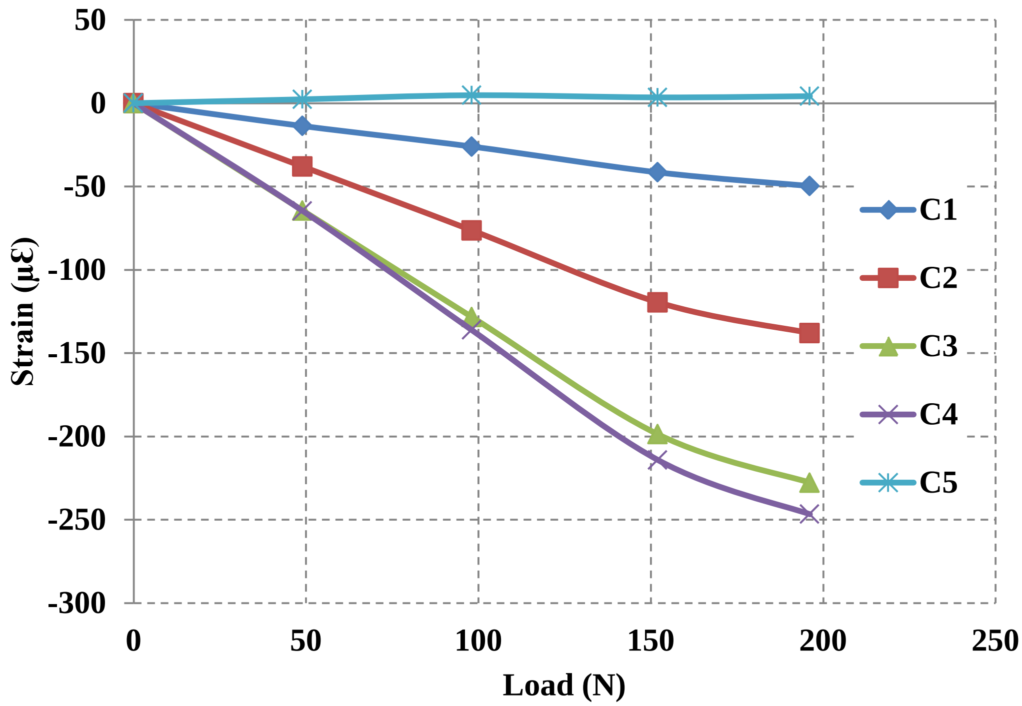

Figure 4.100 Compression Strain vs. Load for the Pile with 400-mm Scour Width and 500-mm Scour Depth

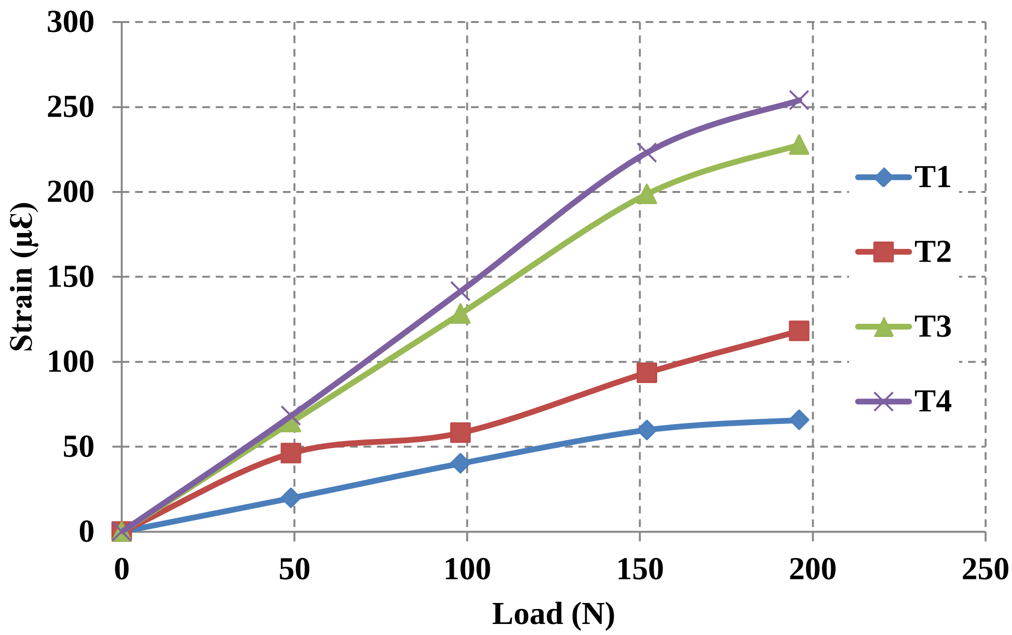

Figure 4.101 Tension Strain vs. Load for the Pile with 400-mm Scour Width and 500-mm Scour Depth

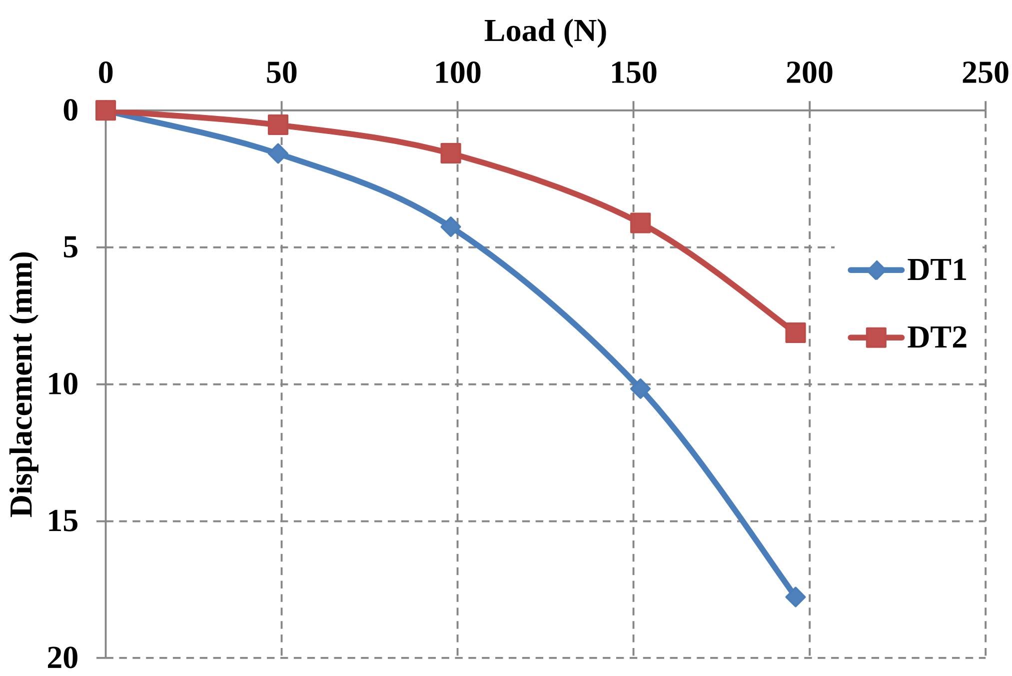

Figure 4.102 Lateral Displacements vs. Load for the Pile with 400-mm Scour Width and 500-mm Scour Depth

667-mm scour width

At 677-mm scour width, four tests were conducted at different scour depths ranging from 200 to 500 mm.

200-mm scour depth. Figures 4.103, 4.104, and 4.105 show the measured strains from the strain gages on the compression side, the strains on the tension side, and the displacements from the transducers with the load respectively.

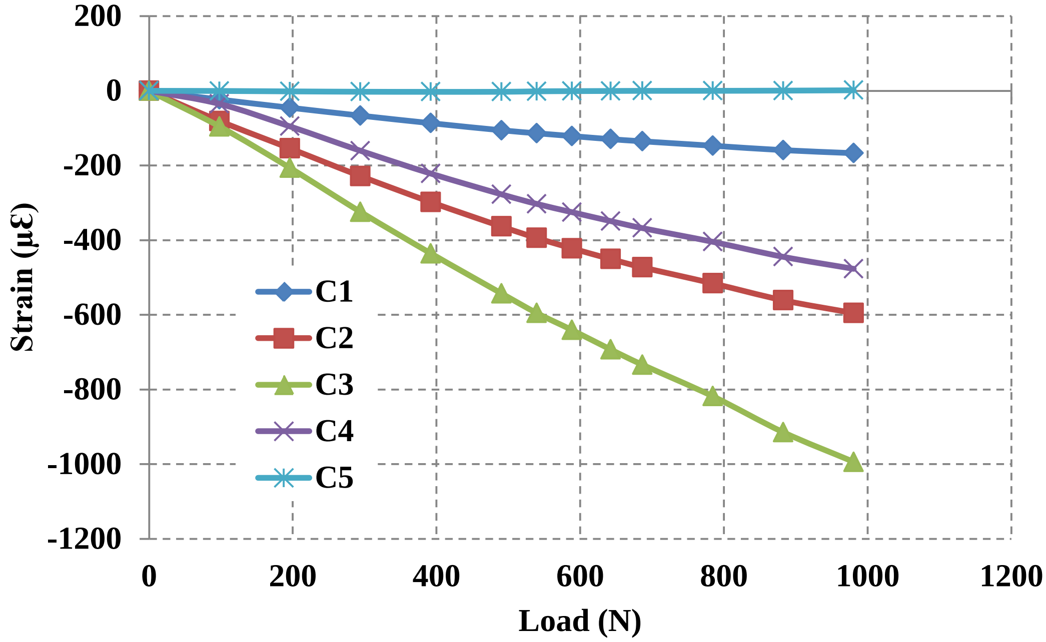

Figure 4.103 Compression Strain vs. Load for the Pile with 667-mm Scour Width and 200-mm Scour Depth

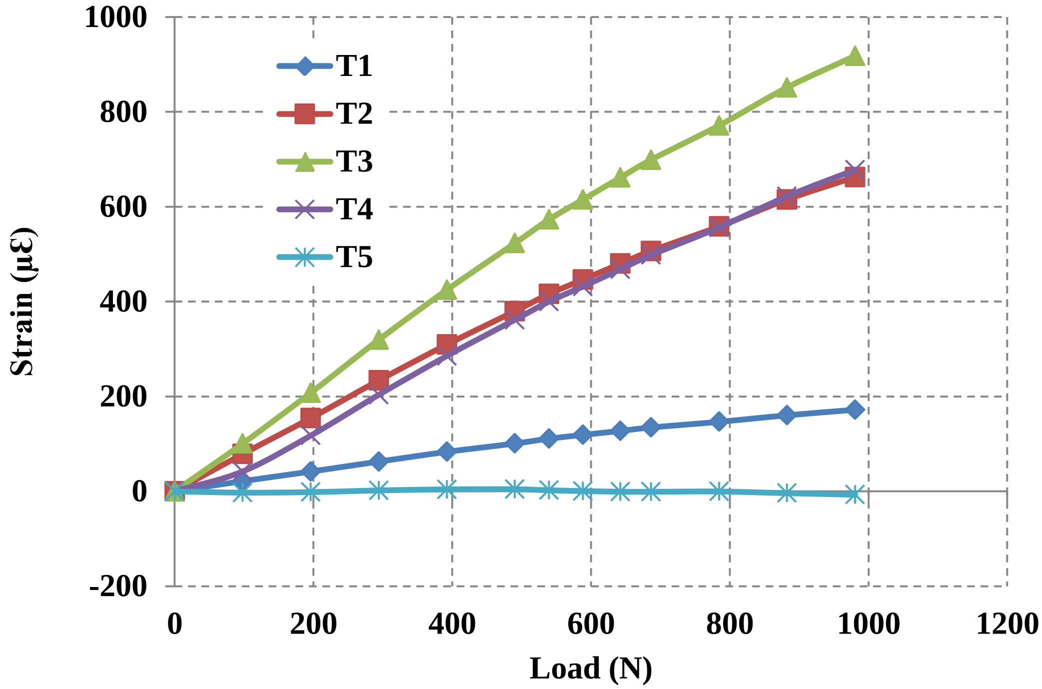

Figure 4.104 Tension Strain vs. Load for the Pile with 667-mm Scour Width and 200-mm Scour Depth

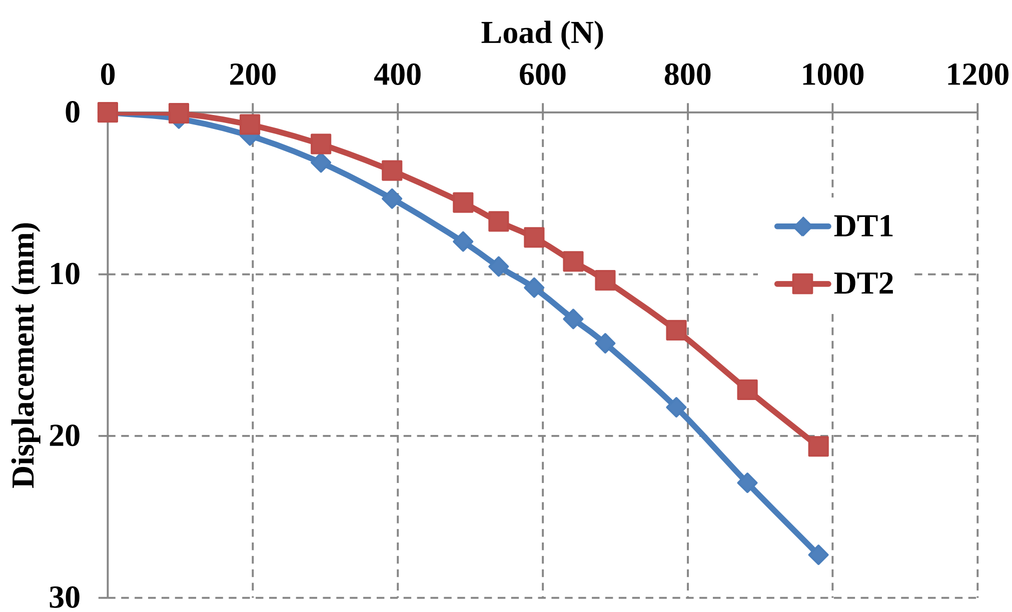

Figure 4.105 Lateral Displacements vs. Load for the Pile with 667-mm Scour Width and 200-mm Scour Depth

300-mm scour depth. Figures 4.106, 4.107, and 4.108 show the measured strains from the strain gages on the compression side, the strains on the tension side, and the displacements from the transducers with the load respectively.

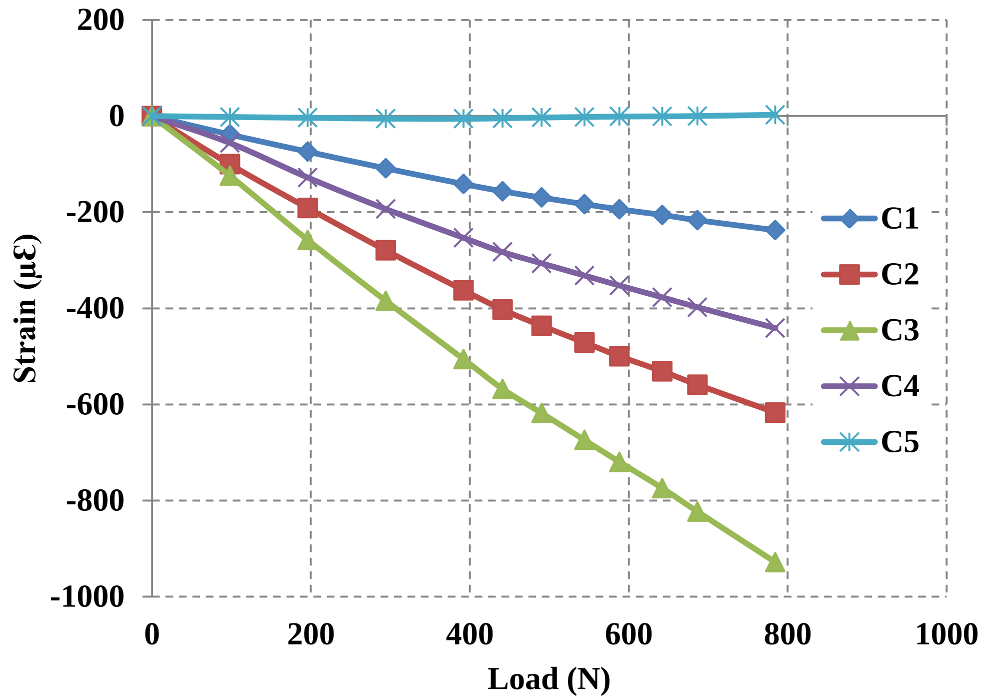

Figure 4.106 Compression Strain vs. Load for the Pile with 667-mm Scour Width and 300-mm Scour Depth

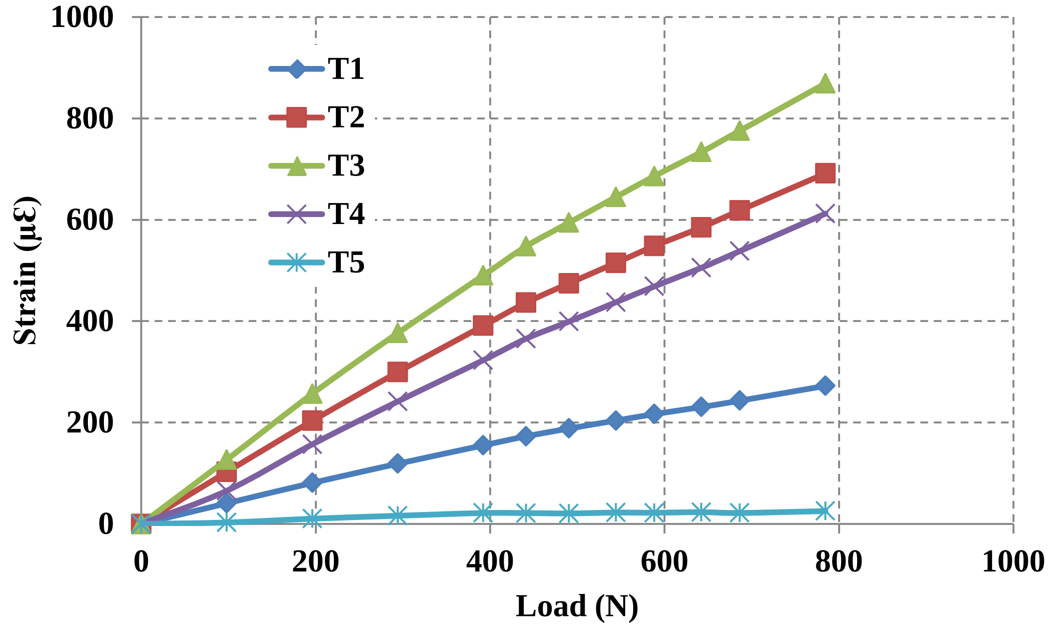

Figure 4.107 Tension Strain vs. Load for the Pile with 667-mm Scour Width and 300-mm Scour Depth

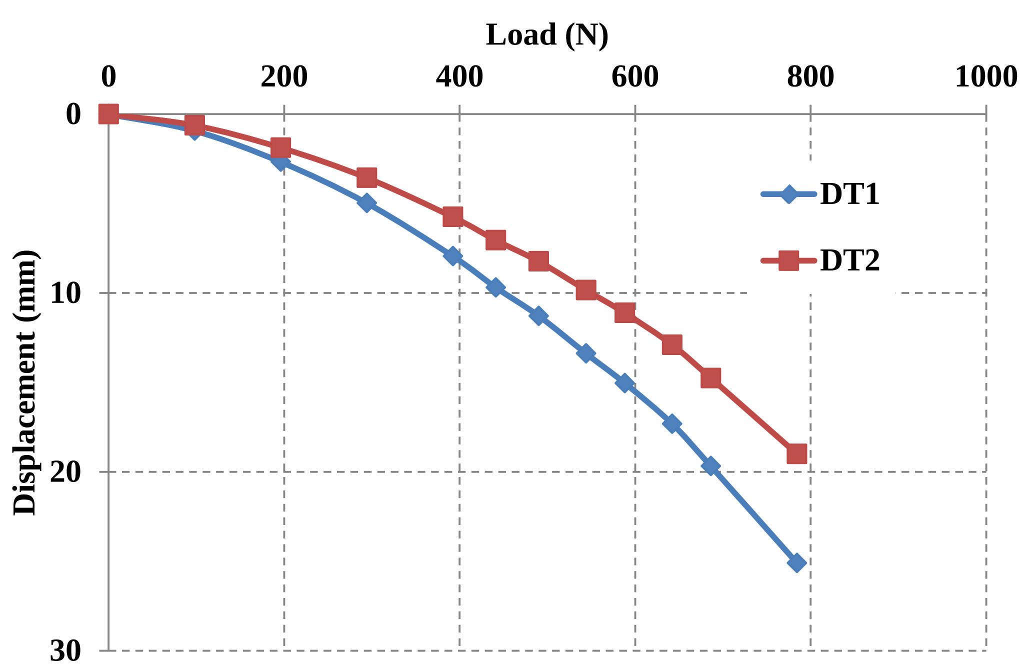

Figure 4.108 Lateral Displacements vs. Load the Pile with 667-mm Scour Width and 300-mm Scour Depth

400-mm scour depth. Figures 4.109, 4.110, and 4.111 show the measured strains from the strain gages on the compression side, the strains on the tension side, and the displacements from the transducers with the load respectively.

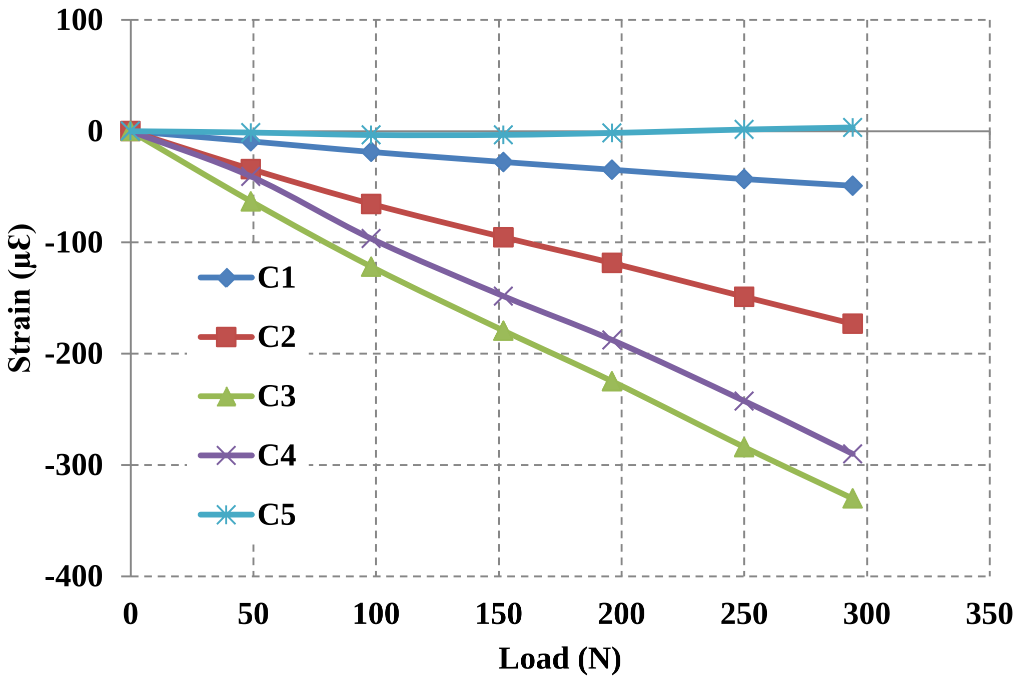

Figure 4.109 Compression Strain vs. Load for the Pile with 667-mm Scour Width and 400-mm Scour Depth

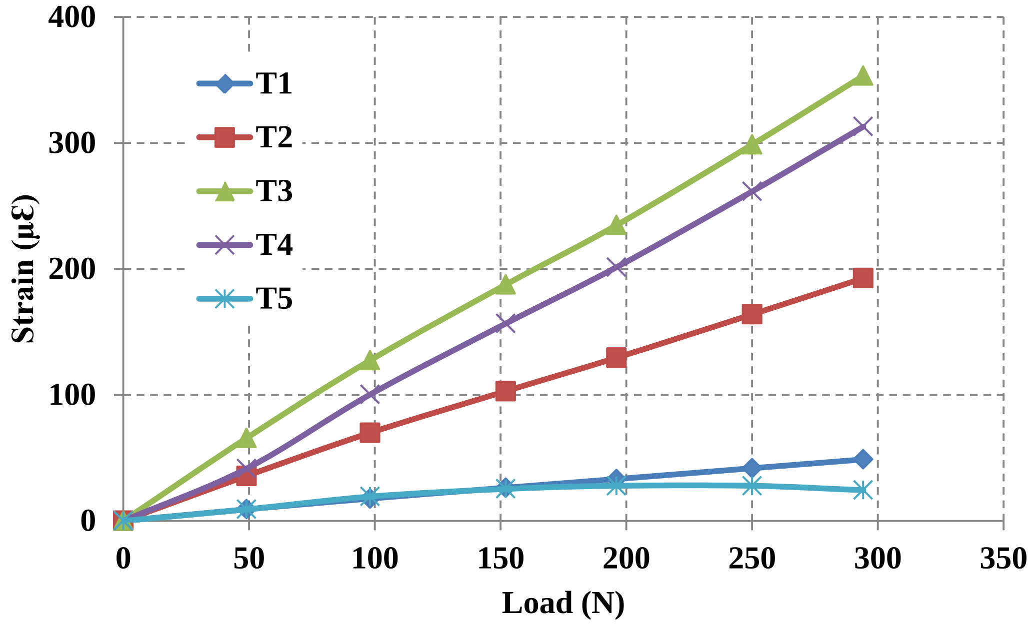

Figure 4.110 Tension Strain vs. Load for the Pile with 667-mm Scour Width and 400-mm Scour Depth

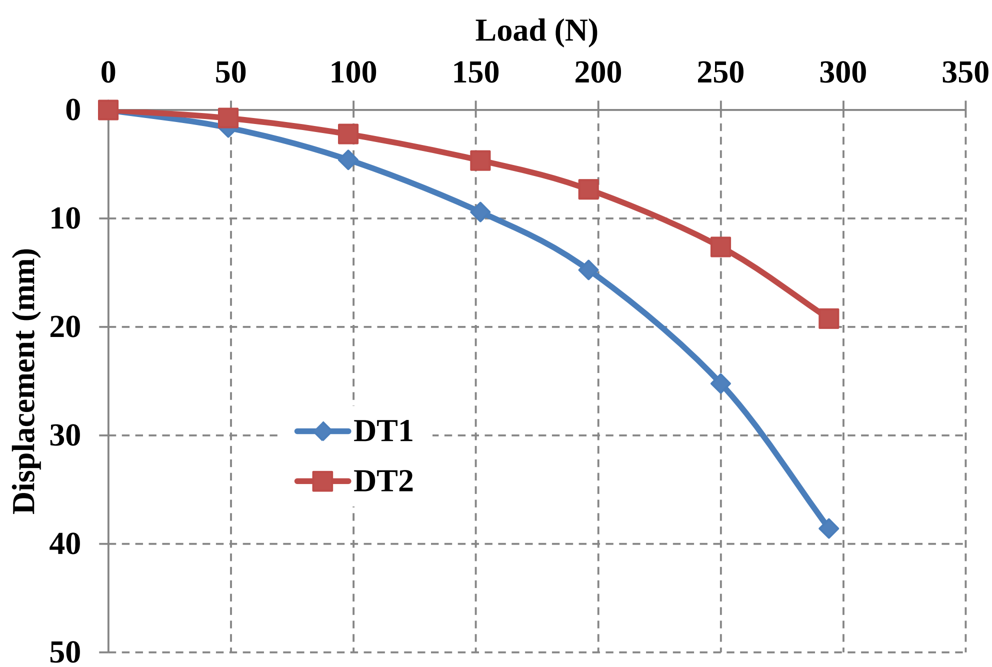

Figure 4.111 Lateral Displacements vs. Load for the Pile with 667-mm Scour Width and 400-mm Scour Depth

500-mm scour depth. Figures 4.112, 4.113, and 4.114 show the measured strains from the strain gages on the compression side, the strains on the tension side, and the displacements from the transducers with the load respectively.

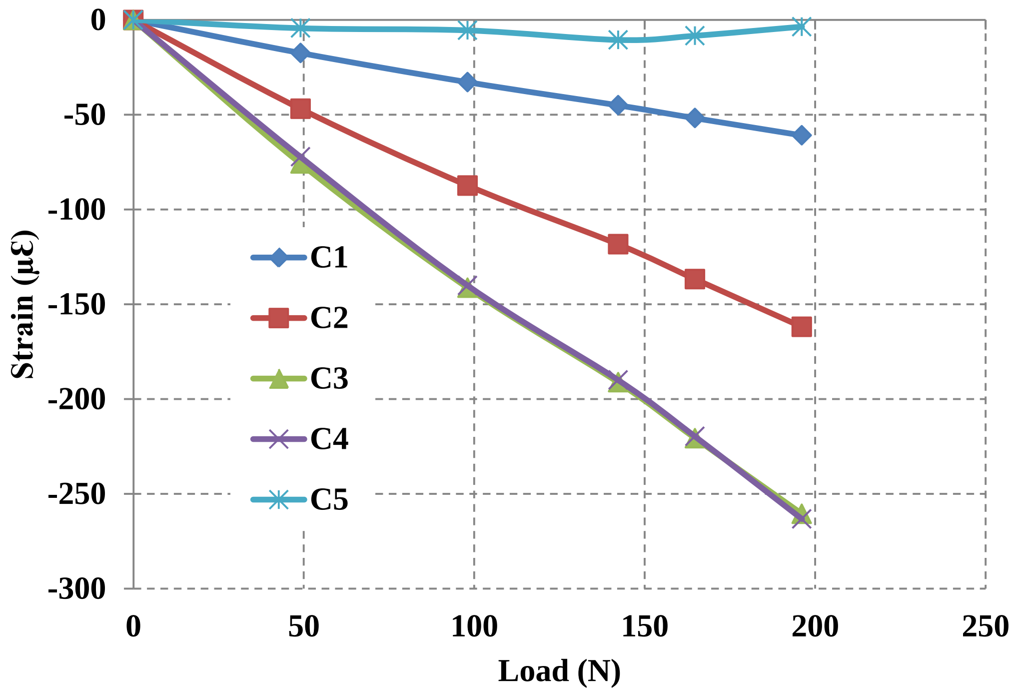

Figure 4.112 Compression Strain vs. Load for the Pile with 667-mm Scour Width and 500-mm Scour Depth

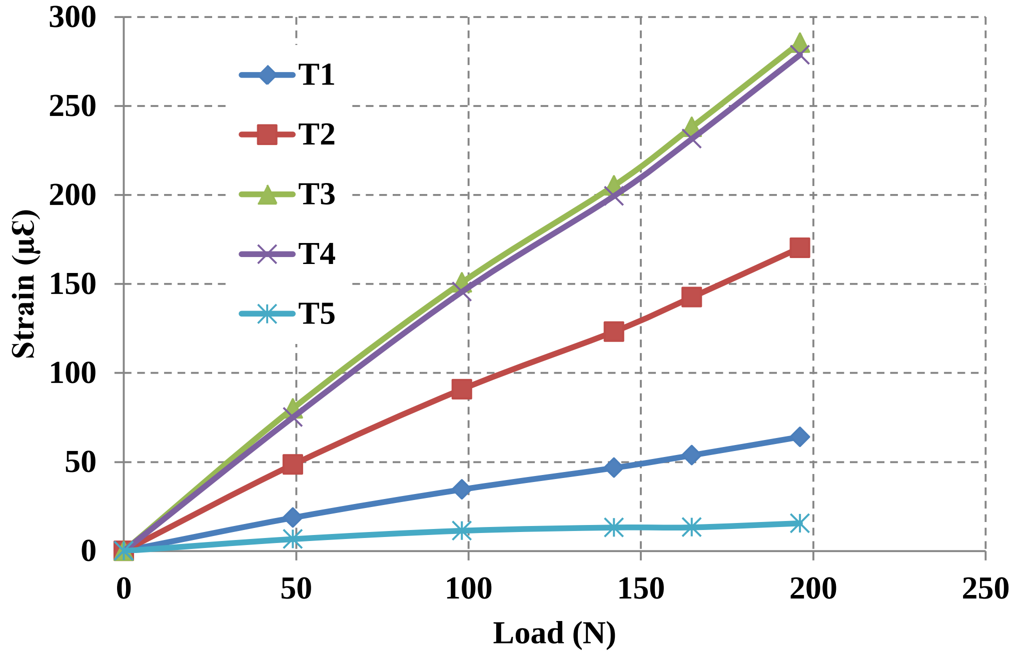

Figure 4.113 Tension Strain vs. Load for the Pile with 667-mm Scour Width and 500-mm Scour Depth

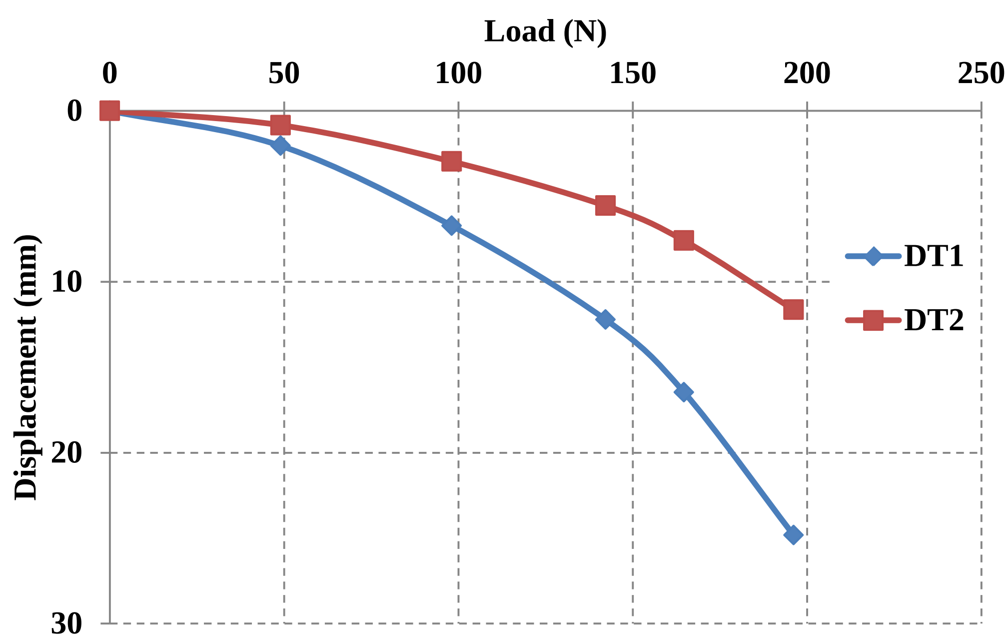

Figure 4.114 Lateral Displacements vs. Load for the Pile with 667-mm Scour Width and 500-mm Scour Depth

4.4. Repeated loading experiments

The following three repeated loading tests were conducted: (1) Repeated test 1, scour depth = 200 mm, scour slope = 0 degree, and scour width = 667 mm; (2) Repeated test 2, scour depth = 200 mm, scour slope = 30 degrees, and scour width = 0 mm; (3) Repeated test 3, scour depth = 400 mm, scour slope = 0 degree, and scour width = 667 mm.

4.4.1. Repeated test 1

Figure 4.115 presents the measured strains from the strain gages on the front side (i.e., the first loading side) of the pile with the number of load cycles. In this figure, the letter “F” represents the front side (the first loading side) and Numbers 1 to 5 represent the locations of the strain gages starting from the top of the pile to its toe. Figure 4.116 presents the measured strains from the strain gages form the back side (i.e., the second loading side) of the pile with the number of load cycles (i.e., 180 degrees between these two sides). In this figure, the letter “B” represents the back side (the second loading side). Figure 4.117 presents the measured lateral displacement of the pile with the number of load cycles from the two transducers.

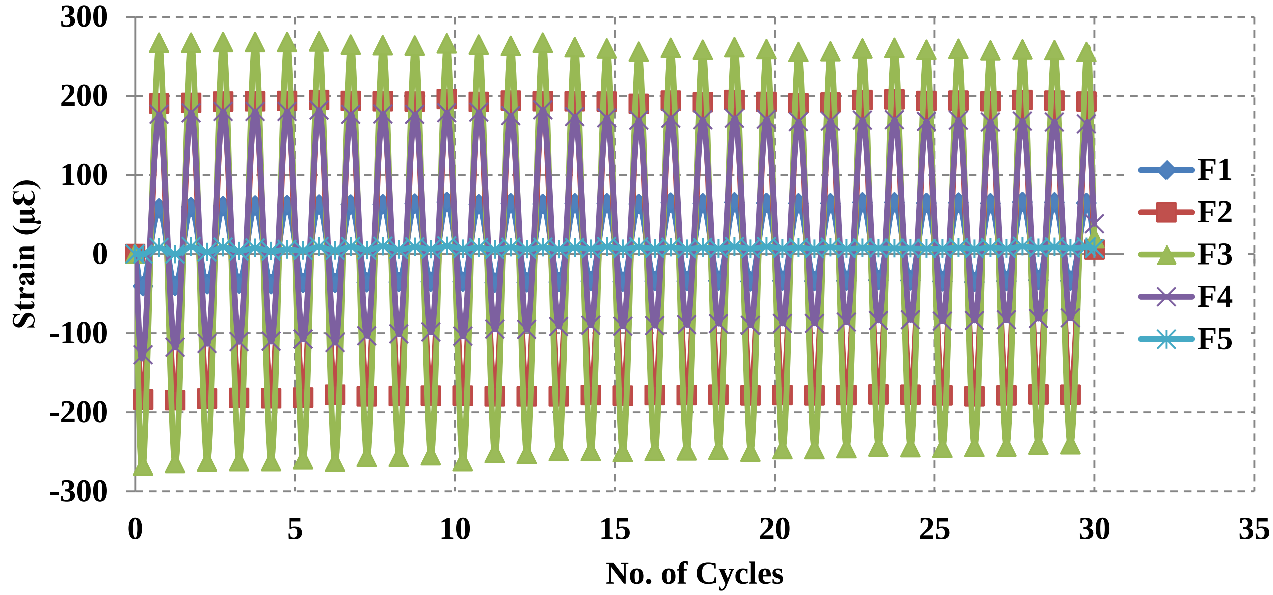

Figure 4.115 Front Side Strain with Number of Load Cycles for Repeated Test 1

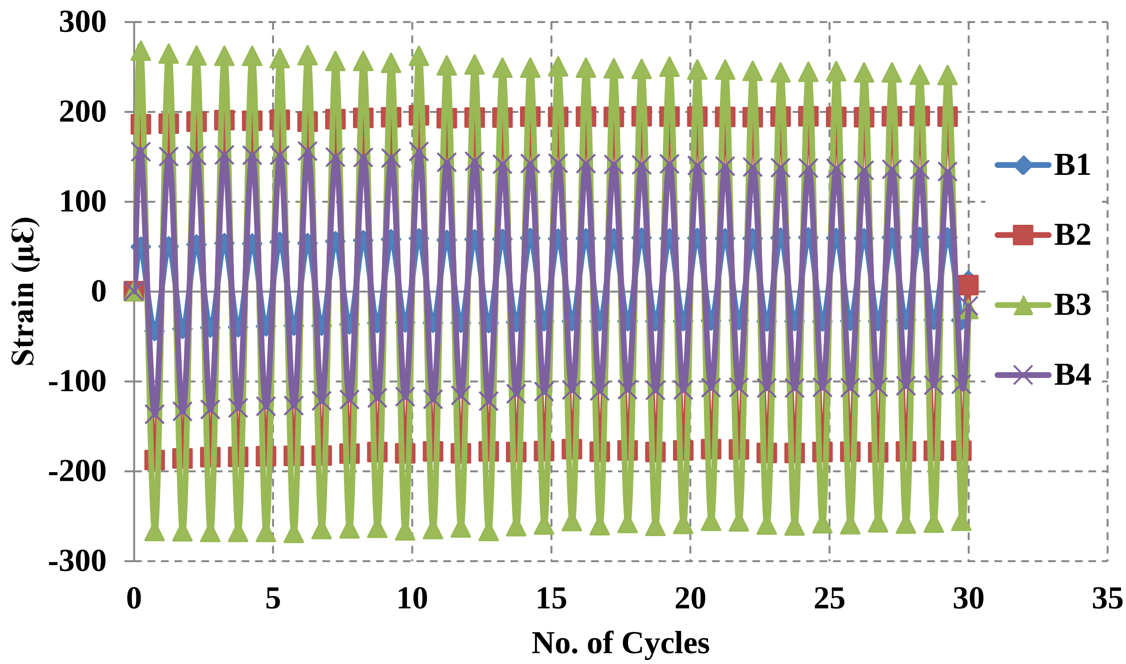

Figure 4.116 Back Side Strain with Number of Load Cycles for Repeated Test 1

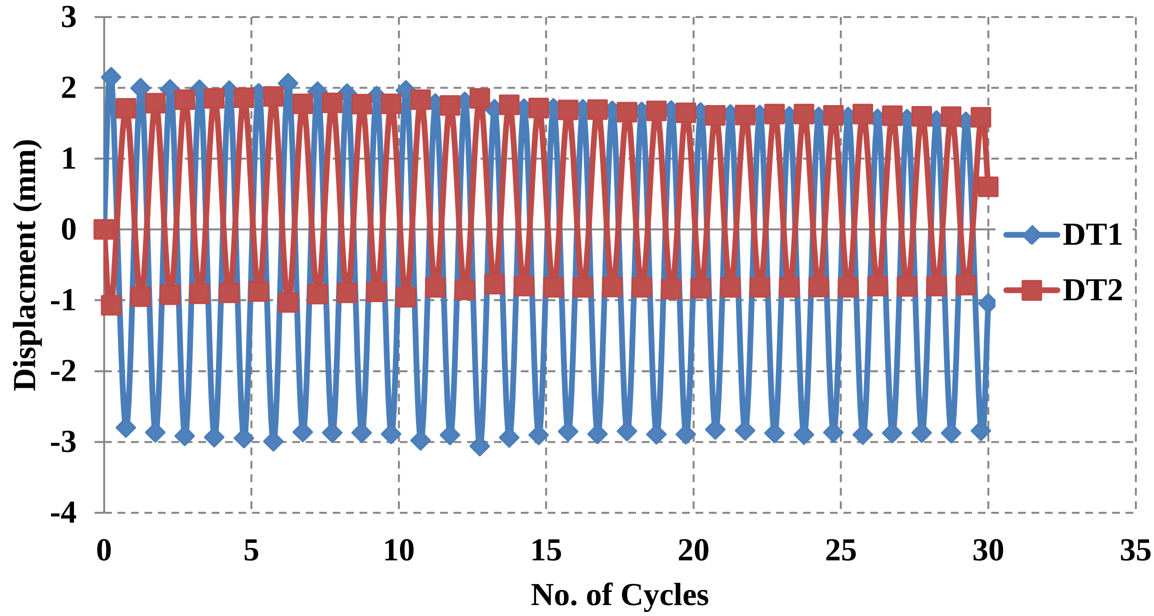

Figure 4.117 Lateral Displacements with Number of Load Cycles for Repeated Test 1

4.4.2. Repeated test 2

Figure 4.118 presents the measured strains from the strain gages on the front side (i.e., the first loading side) of the pile with the number of load cycles. Figure 4.119 presents the measured strains from the strain gages form the back side (i.e., the second loading side) of the pile with the number of load cycles (i.e., 180 degrees between these two sides). Figure 4.120 presents the measured lateral displacement of the pile with the number of load cycles from the two transducers.

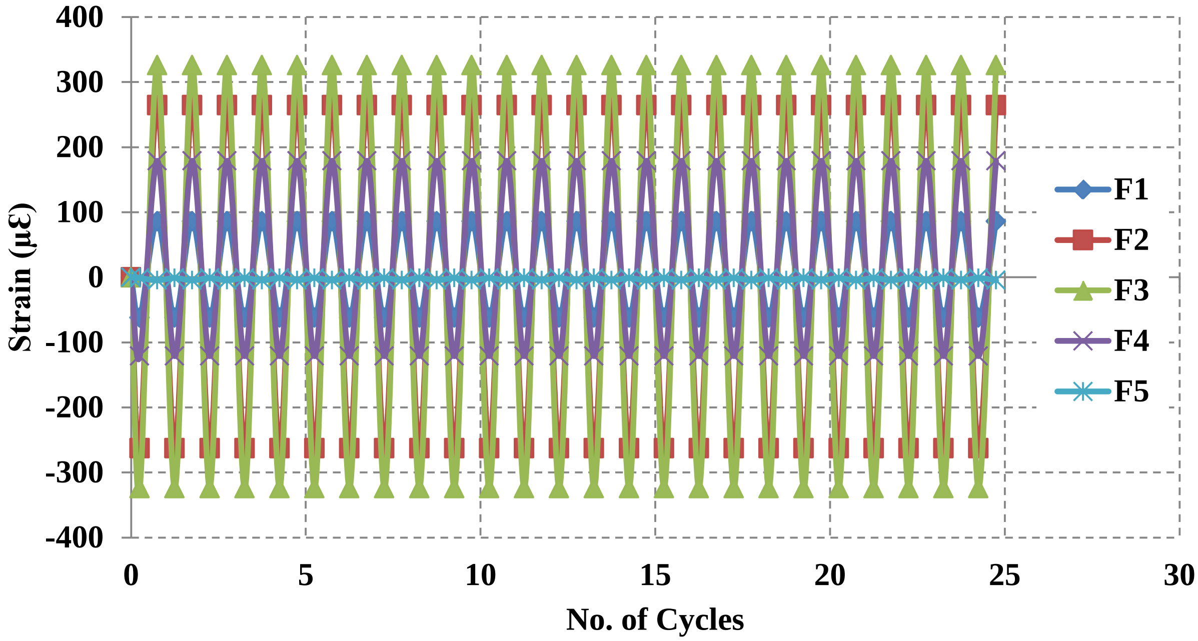

Figure 4.118 Front Side Strain with Number of Load Cycles for Repeated Test 2

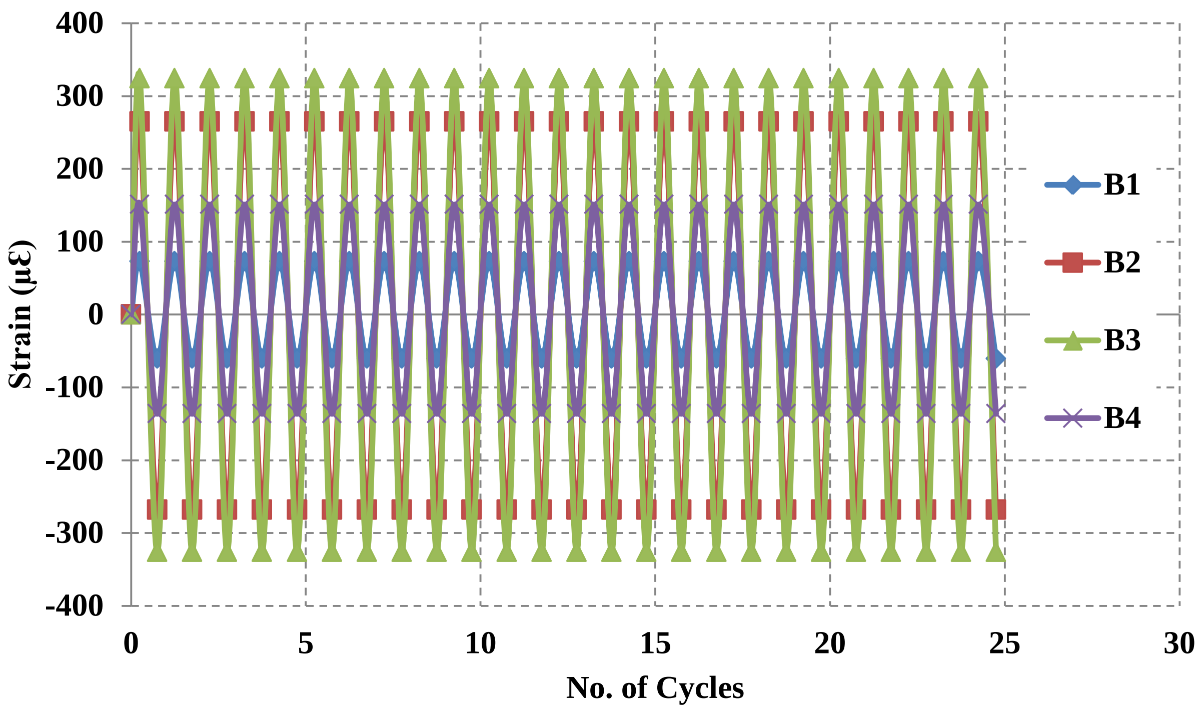

Figure 4.119 Back Side Strain with Number of Load Cycles for Repeated Test 2

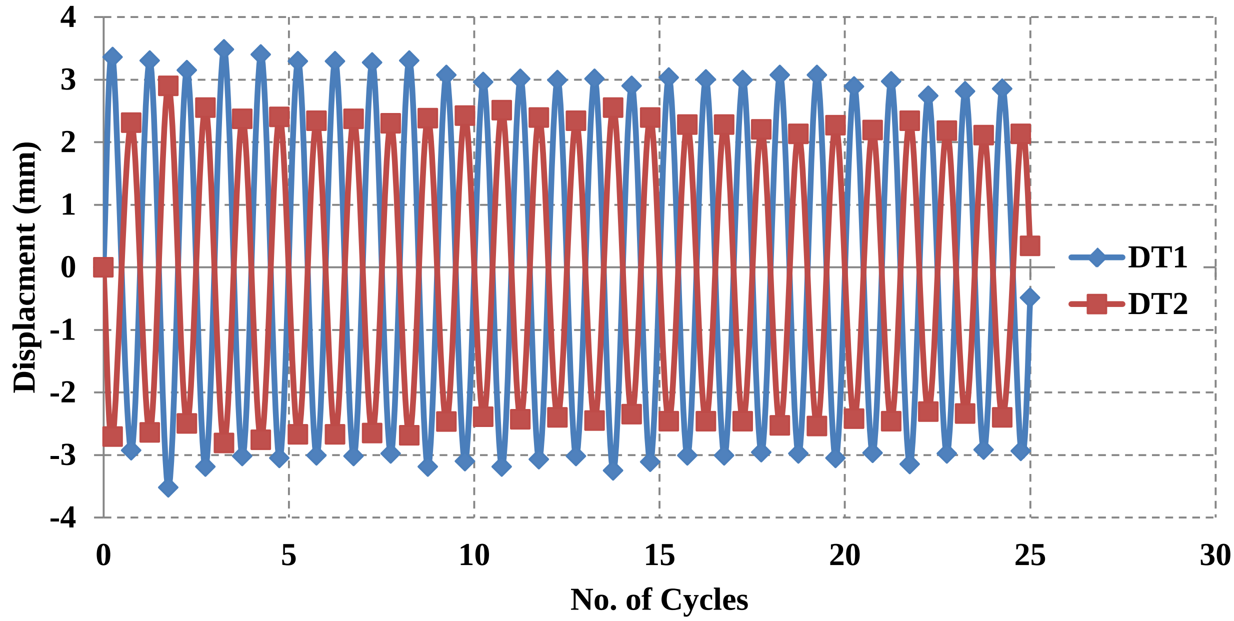

Figure 4.120 Lateral Displacements with Number of Load Cycles for Repeated Test 2

4.4.3. Repeated test 3

Figure 4.121 presents the measured strains from the strain gages on the front side (i.e., the first loading side) of the pile with the number of load cycles. Figure 4.122 presents the measured strains from the strain gages form the back side (i.e., the second loading side) of the pile with the number of load cycles (i.e., 180 degrees between these two sides). Figure 4.123 presents the measured lateral displacement of the pile with the number of load cycles from the two transducers.

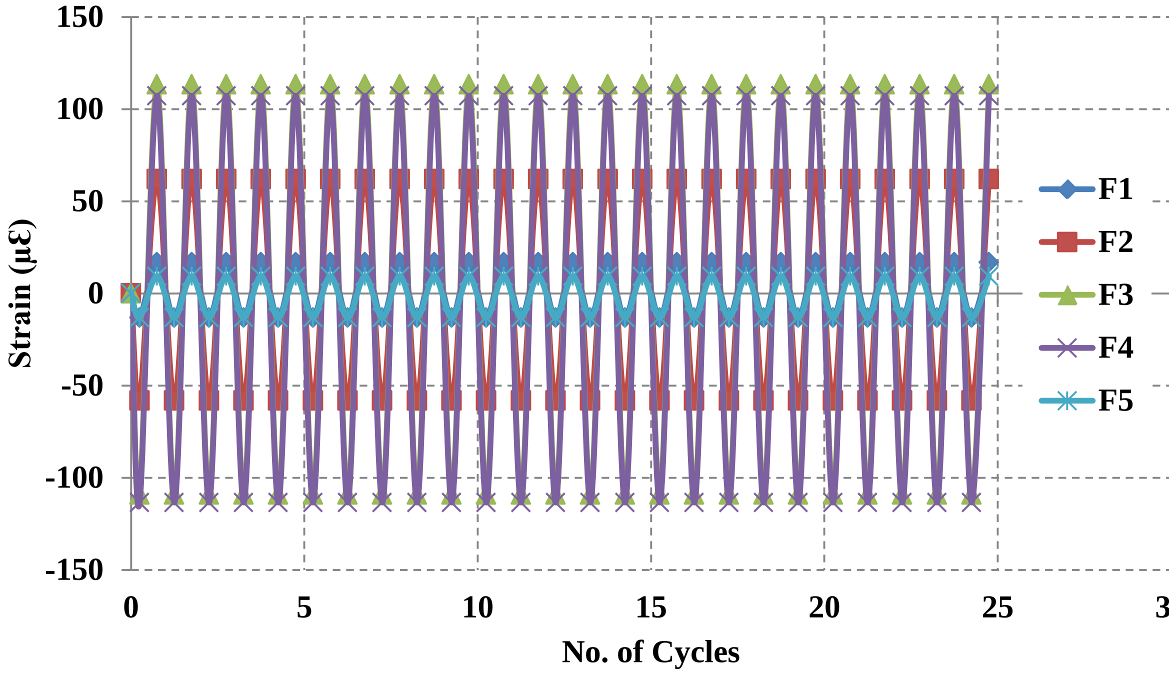

Figure 4.121 Front Side Strain with Number of Load Cycles for Repeated Test 3

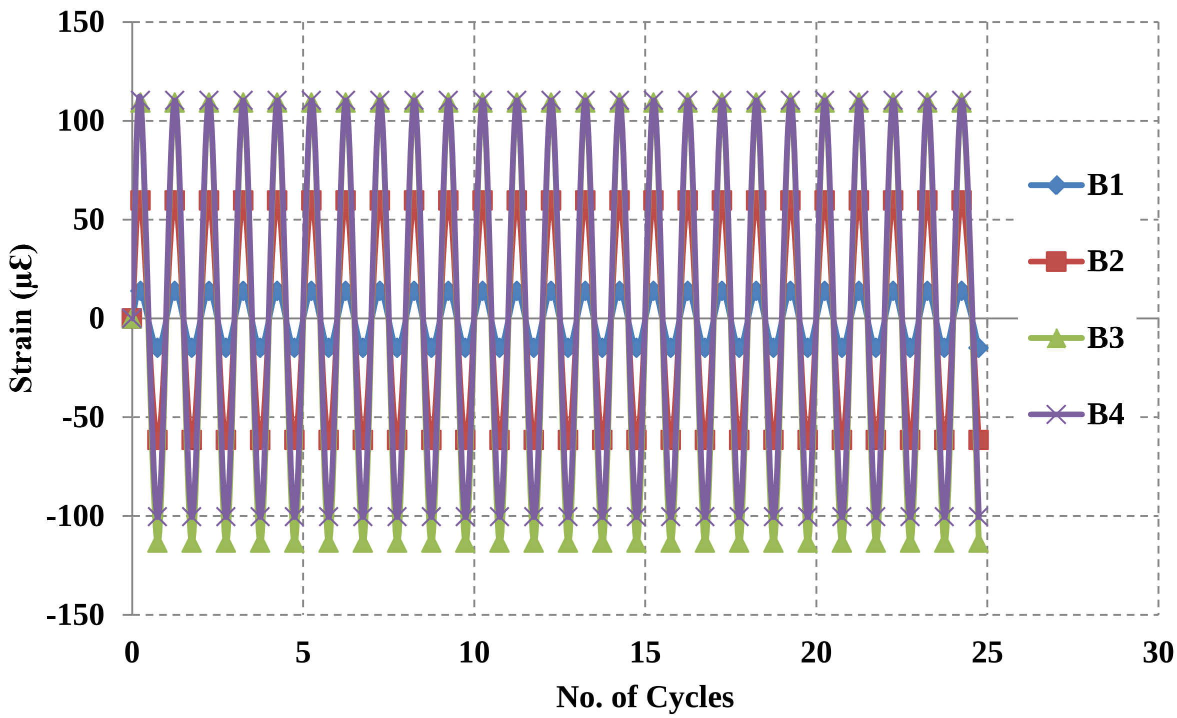

Figure 4.122 Back Side Strain with Number of Load Cycles for Repeated Test 3

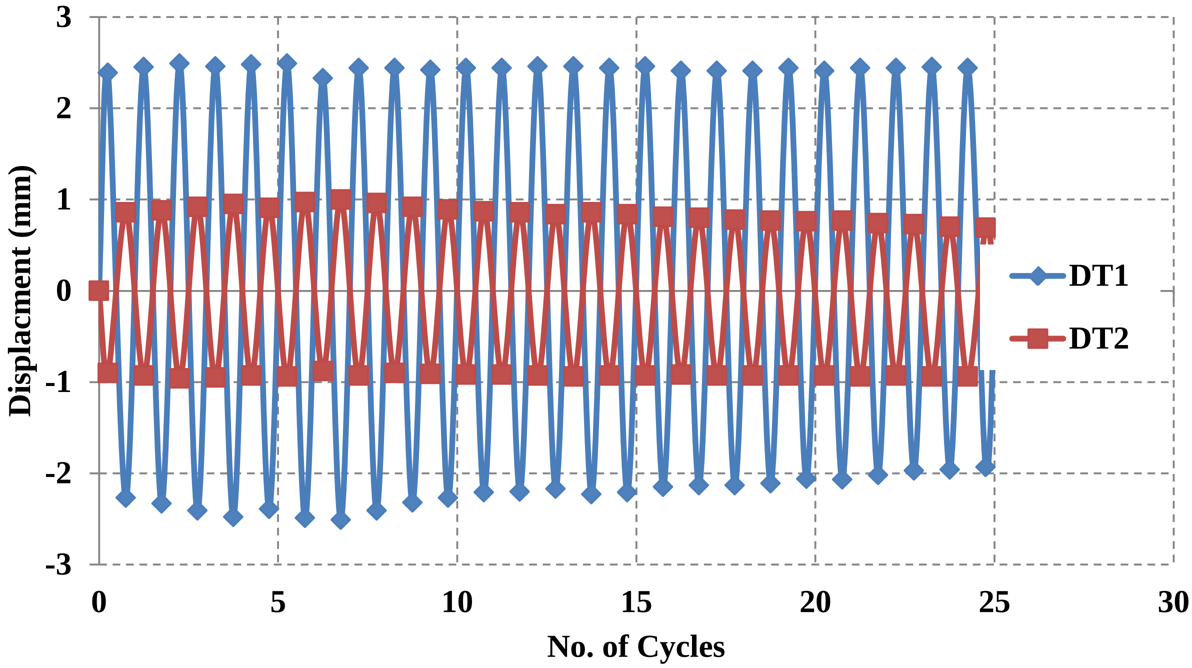

Figure 4.123 Lateral Displacements with Number of Load Cycles for Repeated Test 3

Chapter Five

Data Analysis

5.1. Introduction

This chapter presents the analysis of the data from the experimental work and discusses the comparisons among test results. Section 5.2 presents the calculations for the lateral load capacity of the pile using Broms' method. Section 5.3 discusses the methods adopted for analyzing the data of the experiments. Section 5.4 presents the analysis of the pile toe effect. Section 5.5 provides the analysis of the static loading test results. Section 5.6 presents the analysis of the repeated loading test results.

5.2. Broms' Method Calculations

Broms' method is considered one of the important and commonly used methods to calculate the ultimate lateral load capacity of a pile because it is theoretically derived and sound, simple for calculations, and generally accurate as compared with experimental data. This method includes the distance between the ground surface and the point of loading, which was considered as the scour depth in this study. The ultimate lateral load capacity of a pile is considered as the load required for failure of the pile. Broms (1964) defined the load required to displace the pile laterally to 20% times the pile diameter as the ultimate load.

In this method, a pile is treated as a short (rigid) or long (flexible) pile using the following criterion and the corresponding equations should be used to estimate the lateral load capacity for the pile:

$$D/d \lesseqgtr 20 \tag{5.1}$$

where $D =$ the length of the pile (m); $d =$ the diameter of the pile (m). If the ratio of the length to the diameter of the pile is less than 20, the pile is considered as a short pile. Otherwise, the pile is treated as a long pile. In this study, the length of the aluminum pile $(D) = 0.9$ m and the outer-diameter of the pile $(d) = 0.064$ m. According to the length to diameter ratio of the pile, $L/d = 14.1 < 20$, the test pile is considered as a short (rigid) pile. Therefore, the following equation proposed by Broms (1964) can be used to calculate the lateral load capacity for the test pile:

$$P_u = \frac{\gamma_s \times L^3 \times d \times K_p}{2(e + L)} \tag{5.2}$$

where $P_u =$ the ultimate lateral load capacity for the short pile (N); $\gamma_s =$ the unit weight of the sand (kN/m^3); $L =$ the embedment length of the pile (m); $k_p =$ the coefficient of passive earth pressure calculated using the Rankine earth pressure theory; $e =$ eccentricity of the lateral load measured from the surface of the sand to the point where the lateral load acts on the pile (m),.

In this study, the eccentricity represents the scour depth, $\gamma_s = 17.91$ kN/m^3, $d = 0.063$ m, the angle of internal friction $(\emptyset) = 37$ degree for the Kansas River sand (Khatri, 2012), and $K_p = \frac{1+\sin(\emptyset)}{1-\sin(\emptyset)} = 4.02$. The eccentricity and the embedment length vary according to the scour depth.

5.3. Methods for Experimental Data Analysis

The methods for analyzing experimental data depend on type of measurement. From the displacement transducers, the lateral displacements of the pile under a load were recorded using the dynamic strain recorders for every 0.1 sec during the test. The readings were averaged to get one average displacement for each load. The lateral displacement at the point of loading was estimated by interpolating the displacements from the two transducers based on the rotation of a rigid pile.

From the strain gages distributed along the pile, the strains along the pile were recorded using the dynamic strain recorders for every 0.1 sec during the experiment. For each load, the strain data was averaged to get one strain at one location under that load. Based on Hooke's Law, Eq. (5.3) converts a strain to a stress:

$$\sigma = \varepsilon \times E_p \qquad 5.3$$

in which $\sigma =$ the stress in the pile due to the application of the lateral load (kN/m^2); $\varepsilon =$ the measured average strain on the pile from the strain gages; and $E_p =$ the modulus of elasticity of the pile (kN/m^2). In this study, the modulus of elasticity for the aluminum pile $(E_p) = 69 \times 10^6$ kN/m^2.

Using the relationship between the stress and the moment presented in Eq. (5.4), the moment on a pile section under each load can be calculated.

$$M = \frac{\sigma \times I_p}{C_p} \qquad 5.4$$

in which $M =$ the bending moment on a pile section due to the application of the lateral load (kN×m); $I_p =$ the moment of inertia of the pile (m^4); $C_p =$ the distance from the extreme fiber to the neutral axis of the pile (m). In this study, the moment of inertia of the pile with an outer-diameter of 0.064 m and an inner diameter of 0.060 mm is $(I_p) = \frac{\pi \times ((outer\ diameter)^4 - (inner\ diameter)^4)}{64} = 1.874 \times 10^{-7}$ m^4 and $C_p = 0.032$ m due to the symmetry of the pile.

In the analysis, for the ultimate load capacity, the moment profile from the strain gages along the pile was drawn and the trend line equation for the profile was found. To obtain the deflection profile of the pile, the equation for the moment profile was integrated twice. The displacement readings from the displacement transducers were used as the boundary conditions to find the unknown terms in the deflection equation. Then the deflection profile of the pile was drawn. To obtain the shear stress profile of the pile, the equation for the moment curve was derived once. Based on the analysis, the data for each experiment resulted in four figures: the lateral load-displacement curve, the moment profile, the deflection profile, and the shear stress profile along the pile. The figures for totally 41 experiments are provided in Appendix A.

5.4. Analysis of Pile Toe Effect

The effect of pile toe on the lateral behavior of the pile was investigated by changing the distance between the pile toe and the bottom of the test box in the model pile tests. Figure 5.1 shows the lateral load-displacement curves of these tests. The ultimate lateral load capacity for each test at pile failure was found from Figure 5.1 and is shown in Table 5.1.

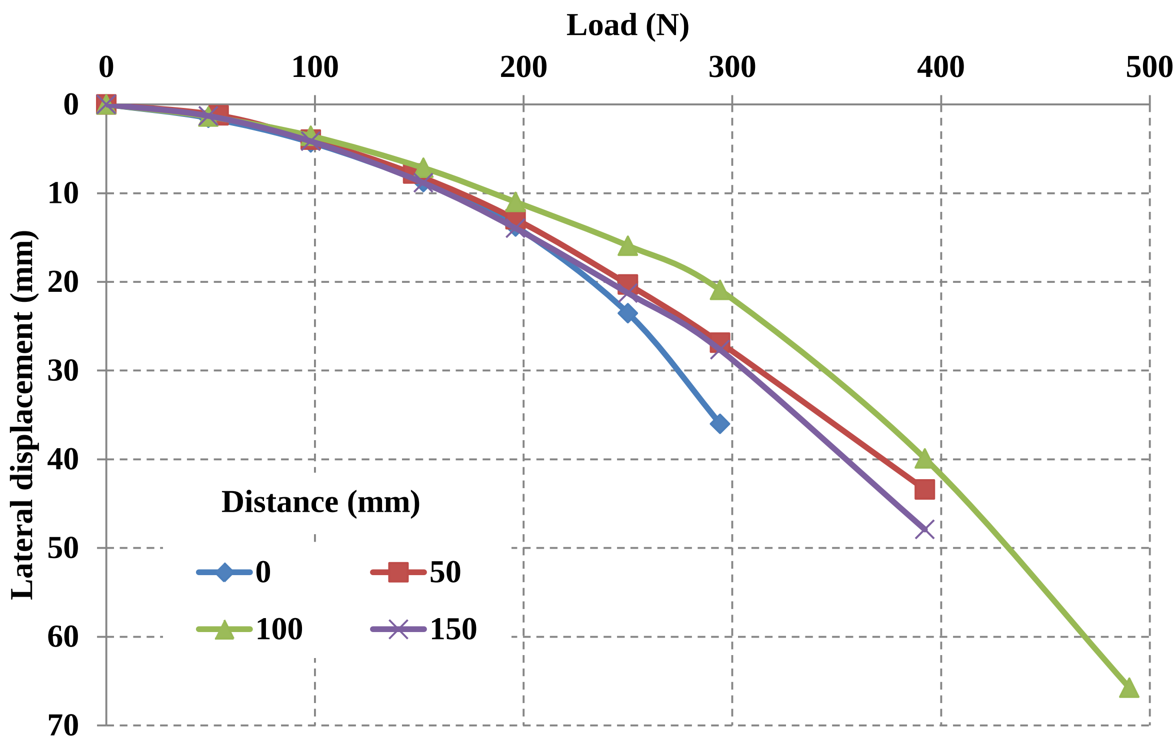

Figure 5.1 Effect of the Pile Toe Distance on the Lateral Load-Displacement Curves

Table 5.1 Effect of the Distance between the Pile Toe and the Box Base

Distance between the pile toe and the box base (mm)	Ultimate lateral load at failure (N)
0	181
50	186
100	206
150	181

Figures 5.2, 5.3, and 5.4 present the moment, lateral displacement, and shear force profiles along the pile at different pile toe distances, respectively. Figure 5.2 shows that the maximum moments happened at approximately 0.4 m above the toe. Figure 5.3 shows that the lateral displacements of the pile were nearly linearly. This result implies that the pile behaved as

rigid and rotated under lateral loading. Figure 5.4 shows that the maximum shear force occurred at the toe.

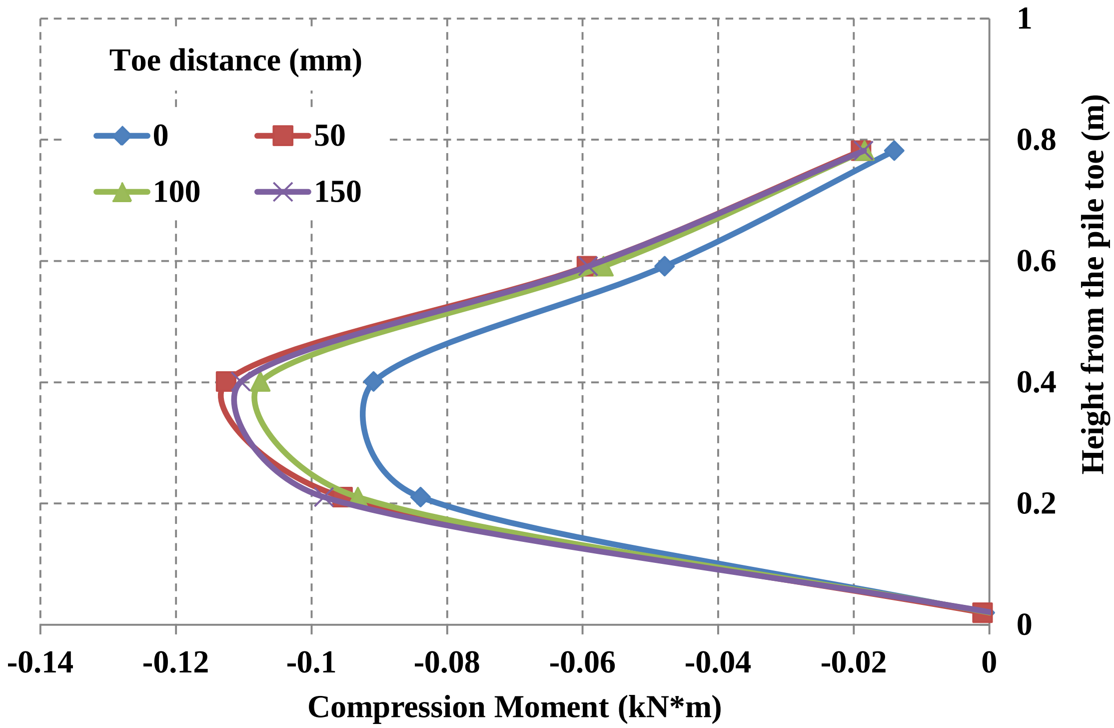

Figure 5.2 Effect of the Pile Toe Distance on Moment Profiles along the Pile

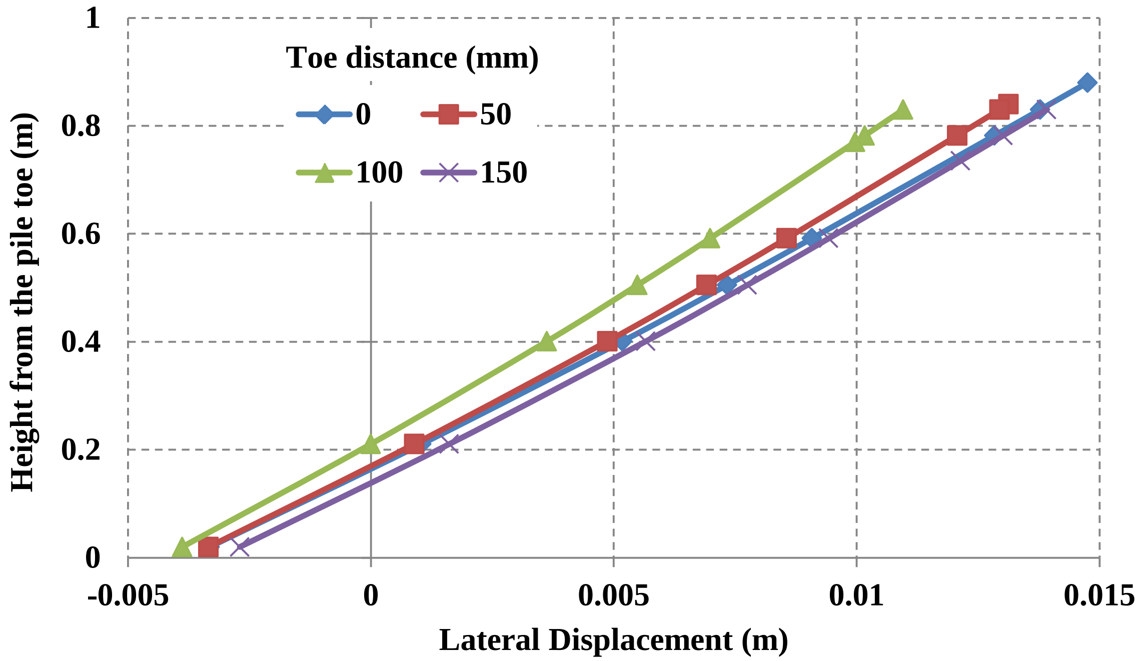

Figure 5.3 Effect of the Pile Toe Distance on Lateral Displacement Profiles along the Pile

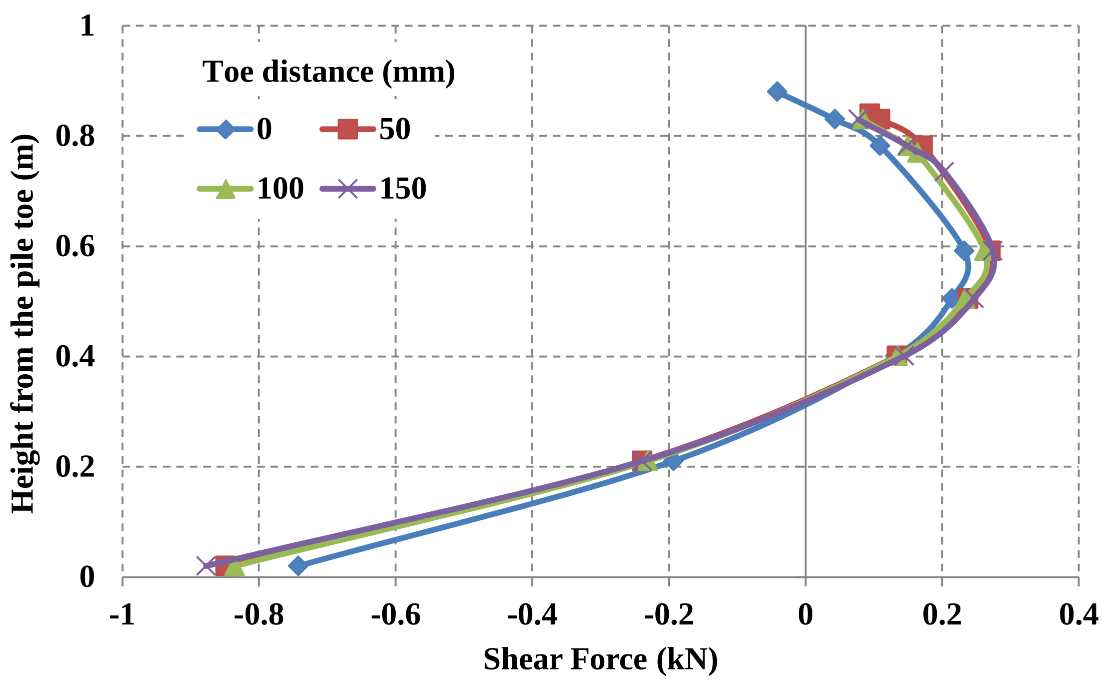

Figure 5.4 Effect of the Pile Toe Distance on Shear Force Profiles along the Pile

The results in Figures 5.1 to 5.4 show that the distance between the pile toe and the box base had a minor effect on the behavior of the pile. Therefore, the pile with a 0-mm toe distance to the box base was used for the rest of the tests.

5.5. Analysis of Static Loading Test Results

This section discusses and compares the results from the static loading tests under different scour conditions. Section 5.5.1 presents the effect of the scour depth on the behavior of the laterally loaded pile under a horizontally scoured condition. Section 5.5.2 shows the effect of the scour slope on the behavior of the laterally loaded pile. Section 5.5.3 presents the effect of the scour width on the behavior of the laterally loaded pile. Since scour depth, scour slope, and scour width are related, one factor is varied for analysis while other factors are fixed.

5.5.1. Horizontal scour

Figure 5.5 presents the effect of scour depth on the lateral load-displacement curves of the laterally loaded piles in sand under a horizontally scoured condition. It is shown that the displacement increased with an increase of the lateral load and the rate of displacement increase accelerated at the higher load. At the same lateral load, the displacement increased with an increase of the scour depth. The increased pile displacement resulted from the reduced soil resistance due to the increased scour depth. The curves have clear yielding points for the piles when the scour depths were equal or larger than 200 mm. The load capacity decreased significantly when the scour depth increased from 100 mm to 200 mm or larger.

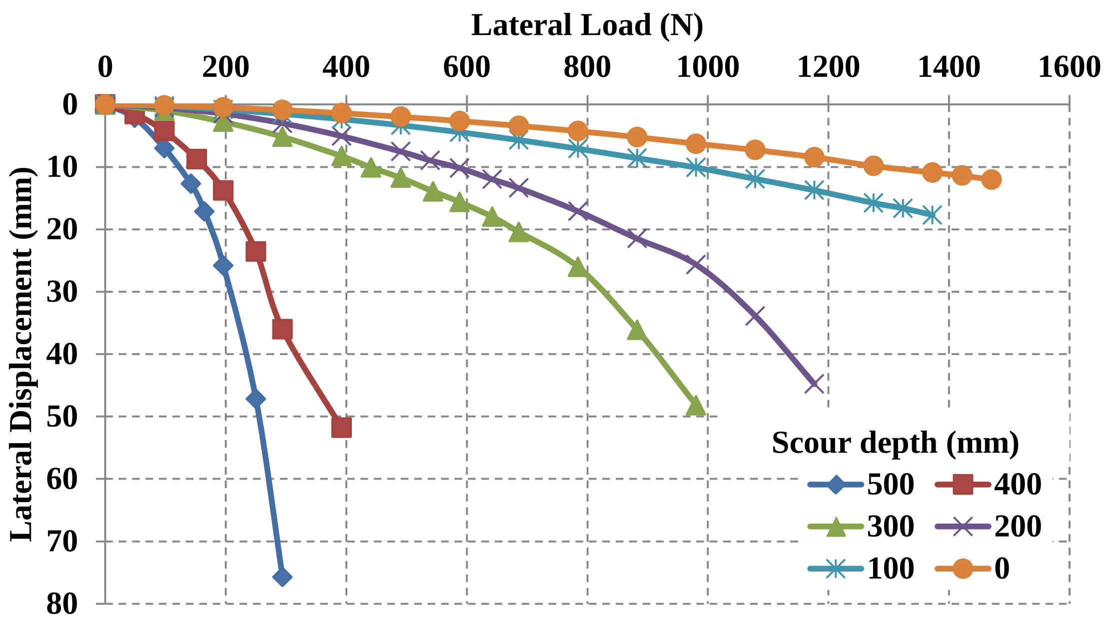

Figure 5.5 Effect of Scour Depth on the Lateral Load- Displacement Curves

From Figure 5.5, the ultimate load capacities of the pile were determined at the lateral displacement equal to 20% pile diameter. A comparison between the measured and calculated ultimate load capacities for the piles is shown in Table 5.2, which shows Broms' method reasonably predicted the ultimate load capacities of the laterally loaded piles in sand under a horizontally scoured condition.

Table 5.2 Measured and Calculated Ultimate Lateral Load Capacities for Piles

Scour depth (mm)	Embedment Length (m)	Broms' ultimate lateral load (N)	Experimental ultimate lateral load (N)
0	0.83	1452	1466
100	0.80	1291	1084
200	0.63	613	642
300	0.60	544	495
400	0.43	181	181
500	0.40	162	137

Based on the measured ultimate lateral load capacities of the model piles at different scour depths as presented in Table 5.1, the relationship between the ultimate lateral load capacity ratio and the scour depth to pile diameter ratio was established as shown in Figure 5.6 and is presented in the following equation:

$$\frac{P_{us}}{P_u} = 4 \times 10^{-3} \times \left(\frac{d_s}{D}\right)^3 + 5.8 \times 10^{-3} \times \left(\frac{d_s}{D}\right)^2 + 0.1884 \times \left(\frac{d_s}{D}\right) + 1.0026 \qquad 5.5$$

where $P_{us} =$ ultimate lateral load capacity for the pile under a horizontal scour condition; $P_u =$ ultimate lateral load capacity for the pile without scour; $d_s =$ scour depth (i.e., the distance between the top surface of the soil to the point where the lateral load acts on the pile); and $D =$ pile diameter.

This relationship indicates that the ultimate lateral load capacity ratio with and without scour decreased with the scour depth to pile diameter ratio. Figure 5.6 shows that when the scour depth was three times the pile diameter, the ultimate lateral load capacity was reduced by 50% from the pile capacity without scour.

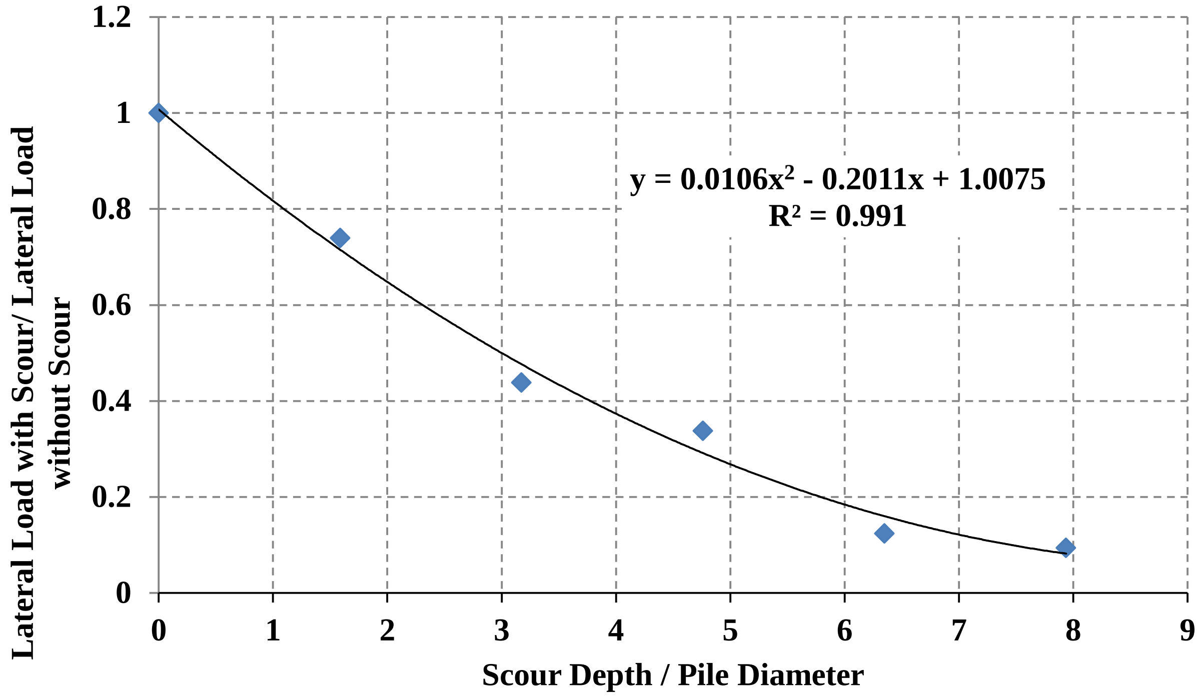

Figure 5.6 Ultimate Lateral Load Capacity Ratio to the Scour Depth to Pile Diameter Ratio

Figures 5.7, 5.8, and 5.9 present the effect of the scour depth on the moment, lateral displacement, and shear force profiles along the pile respectively at the pile failure. Figure 5.7 shows that the maximum moment decreased and happened at a lower depth with an increase of the scour depth. Figure 5.8 shows that the lateral displacements along the pile were nearly linear. Figure 5.9 shows that the maximum shear force transferred from a positive value at the point where the lateral load acted to the negative value at the pile toe with an increase of the scour depth because of the loss of the soil resistance due to the increase of the scour depth. Furthermore, the shear force decreased due to the reduction of the lateral load capacity with an increase of the sour depth.

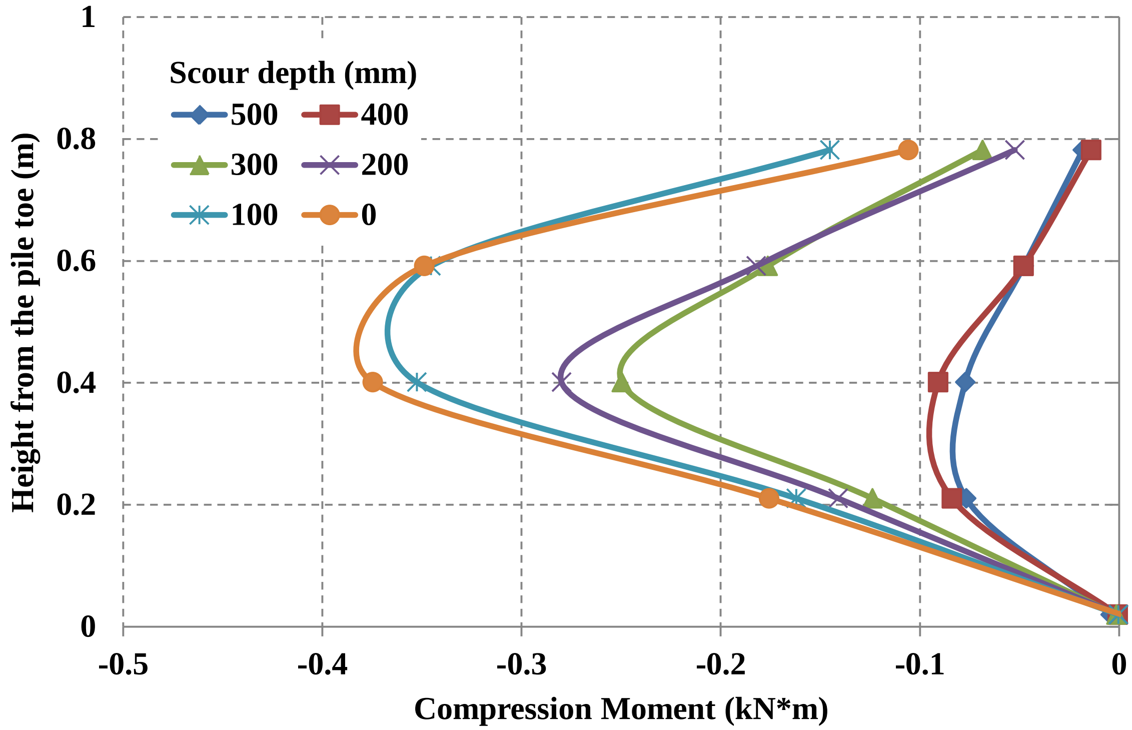

Figure 5.7 Effect of Scour Depth on the Moment Profiles along the Pile

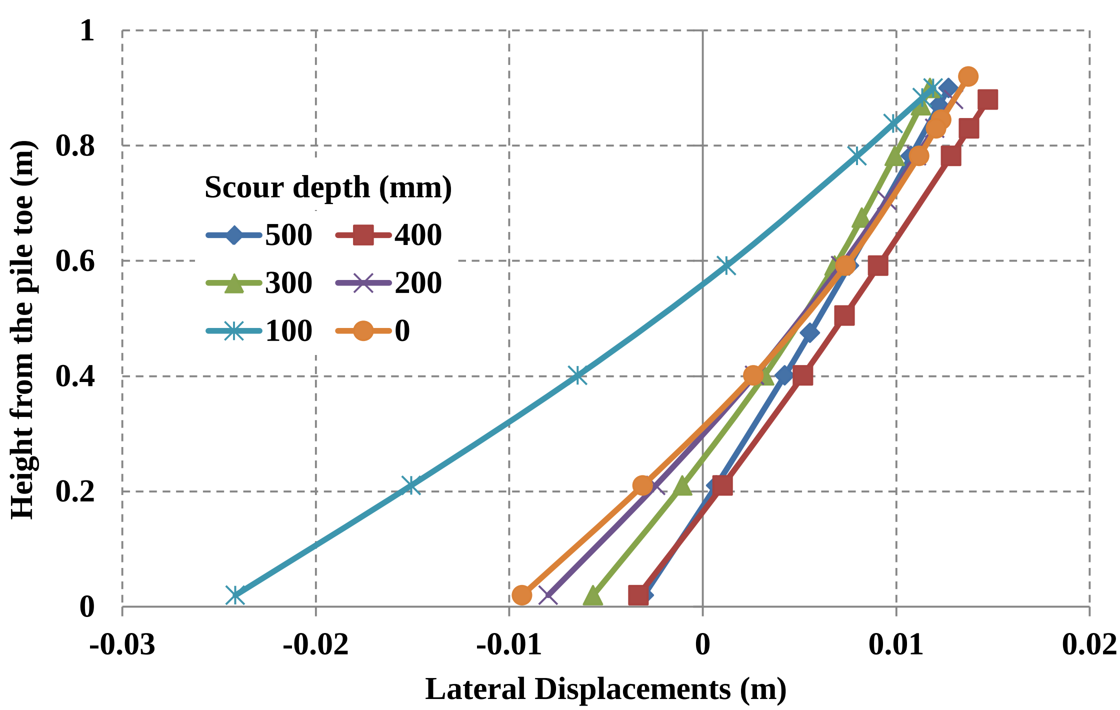

Figure 5.8 Effect of Scour Depth on the Lateral Displacement Profiles along the Pile

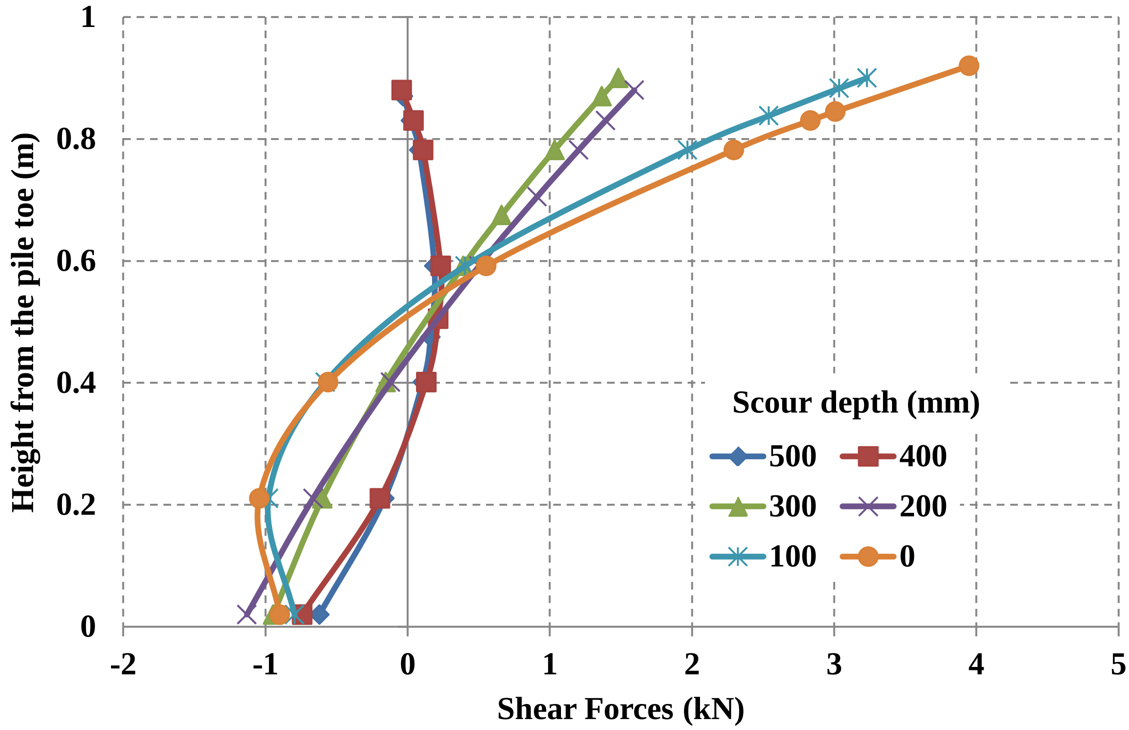

Figure 5.9 Effect of Scour Depth on the Shear Force Profiles along the Pile

5.5.2. Combined scour depth and scour slope effects

This section presents the effect of the scour slope on the behavior of the laterally loaded pile in sand under a sloped, scoured condition. The effect of the scour depth on the behavior of the laterally loaded pile at a constant scour slope is presented first. The scour slope effect on the behavior of the laterally loaded pile at a constant scour depth is presented afterwards.

Scour depth

The effects of scour depth on the behavior of laterally loaded piles at the scour slopes ranging from 0 to 30 degrees are presented below.

0-degree scour slope. Figure 5.10 presents the effect of the scour depth on the lateral load-displacement curves. Figure 5.10 shows that the increased scour depth increased the lateral displacement. Also it shows that at a constant lateral load, the increase of the scour depth increased the lateral displacement.

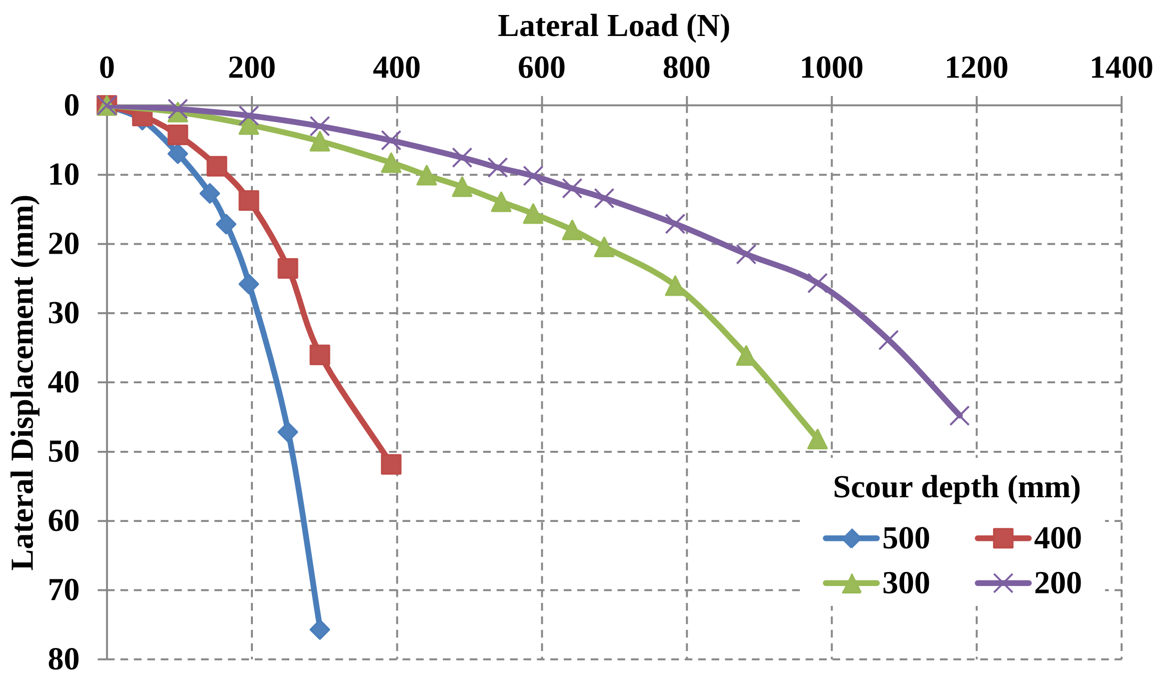

Figure 5.10 Effect of Scour Depth on the Lateral Load-Displacement Curves for the Pile with 0-degree Scour Slope

Figures 5.11, 5.12, and 5.13 present the effect of the scour depth on the moment, lateral displacement, and shear force profiles along the pile respectively at 0-degree scour slope. Figure 5.11 shows that the maximum moment decreased and went towards the pile toe with the increase of the sour depth. Figure 5.12 shows that the lateral displacements were nearly linear. Figure 5.13 shows that the maximum shear force transferred from a positive value at the point where the lateral load acted to the negative value at the pile toe with an increase of the scour depth because of the loss of the soil resistance due to the increase of the scour depth.

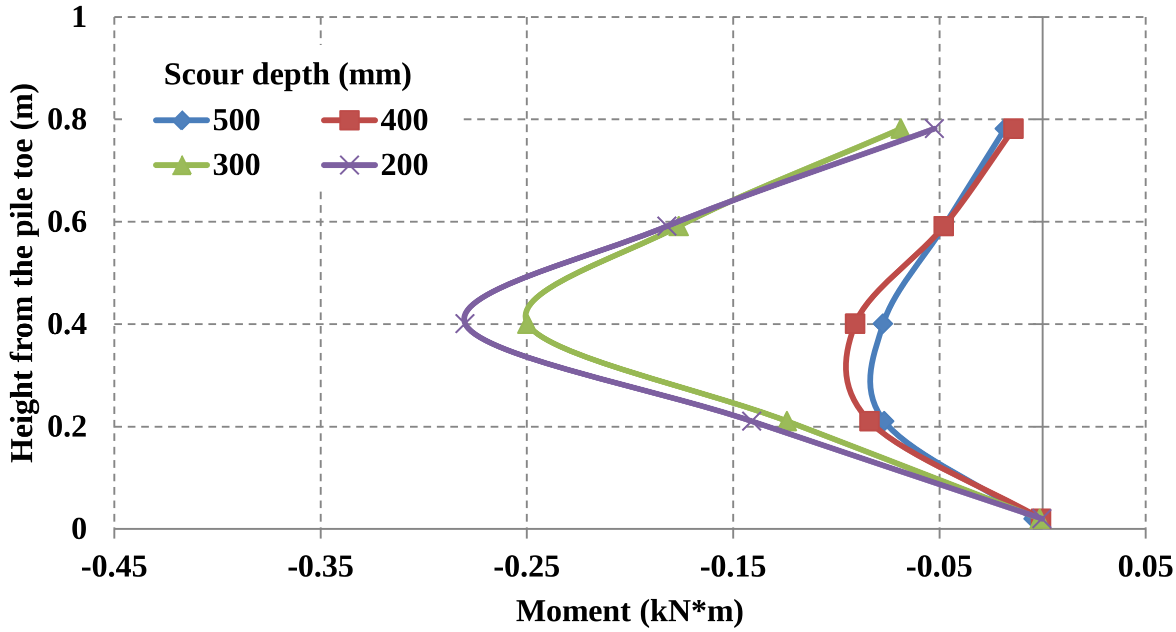

Figure 5.11 Effect of Scour Depth on the Moment Profiles along the Pile with 0-degree Scour Slope

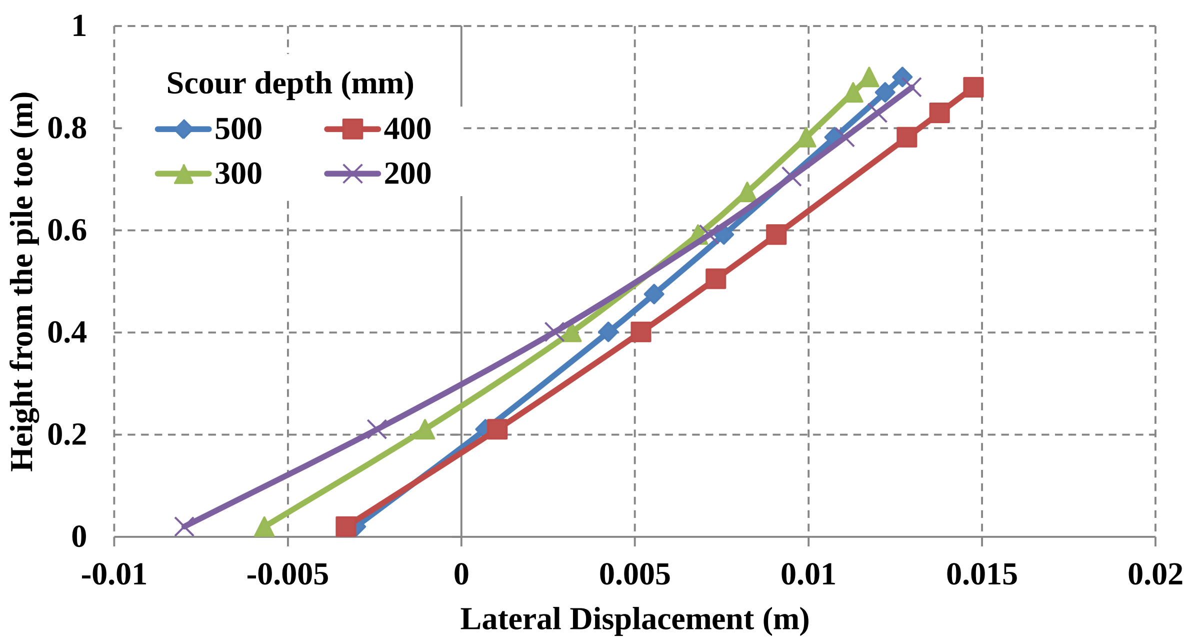

Figure 5.12 Effect of Scour Depth on the Lateral Displacement Profiles along the Pile with 0-degree Scour Slope

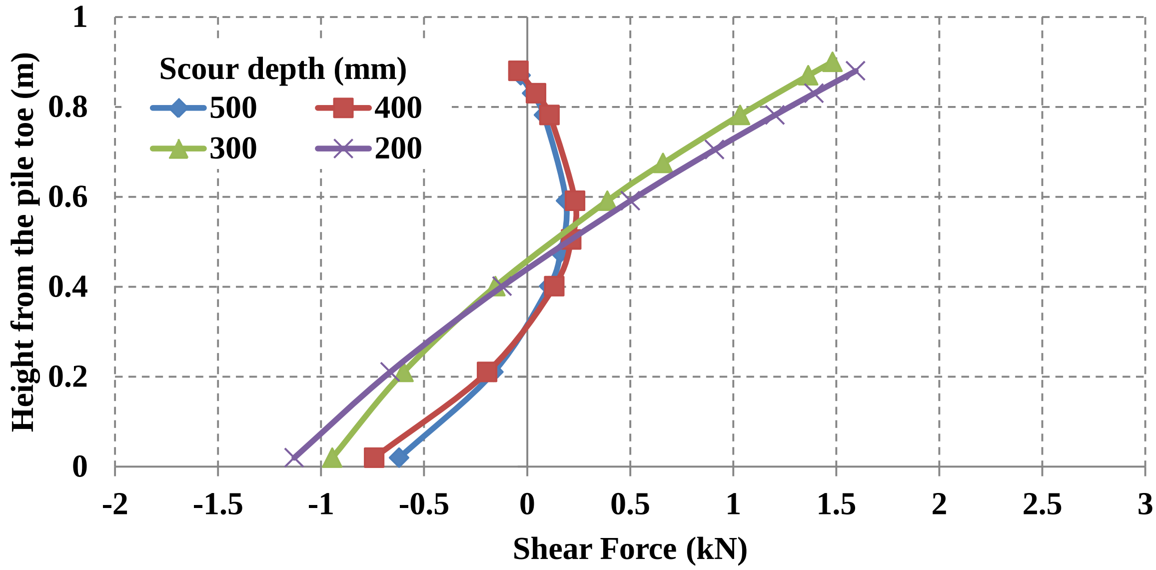

Figure 5.13 Effect of Scour Depth on the Shear Force Profiles along the Pile with 0-degree Scour Slope

15-degree scour slope. Figure 5.14 presents the effect of the scour depth on the lateral load-displacement curves. It shows that the increased sour depth increased the lateral displacement.

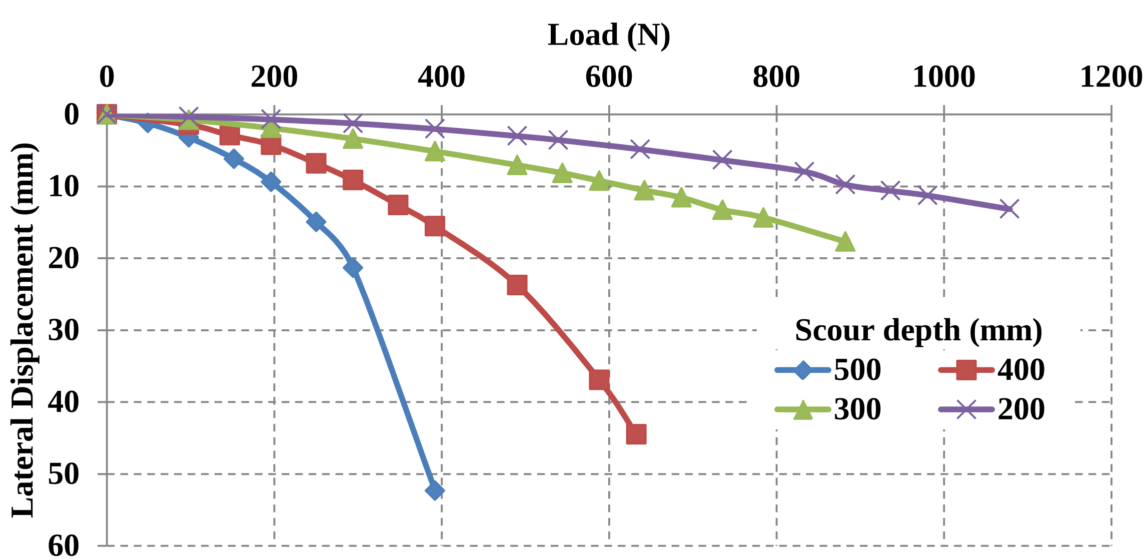

Figure 5.14 Effect of Scour Depth on the Load-Lateral Displacement Curves for the Pile with 15-degree Scour Slope

Figures 5.15, 5.16, and 5.17 present the effect of the scour depth on the moment, lateral displacement, and shear force profiles along the pile respectively at 15-degree scour slope. Figure 5.15 shows that the maximum moment decreased and went towards the pile toe with the increase of the sour depth. Figure 5.16 shows that the lateral displacements were nearly linear. Also, it shows that the increased scour depth increased the lateral movement of the pile because of the loss of the soil resistance around the pile due to the increase of the scour depth. Figure 5.17 shows that the maximum shear force transferred from a positive value at the point where the lateral load acted to the negative value at the pile toe with an increase of the scour depth because of the loss of the soil resistance due to the increase of the scour depth.

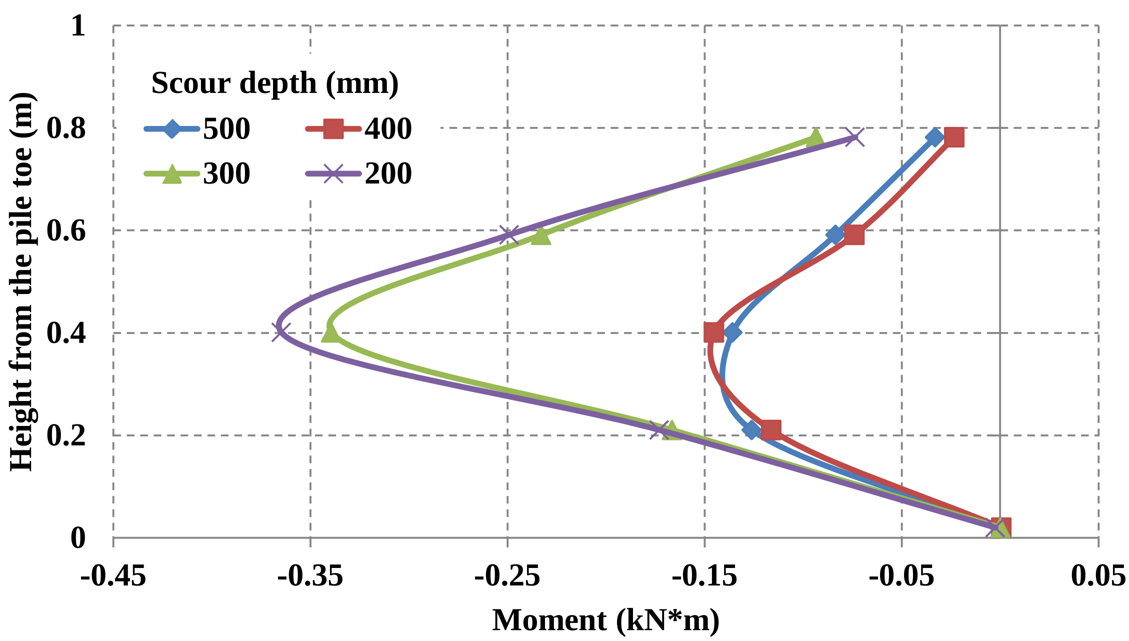

Figure 5.15 Effect of Scour Depth on the Moment Profiles along the Pile with 15-degree Scour Slope

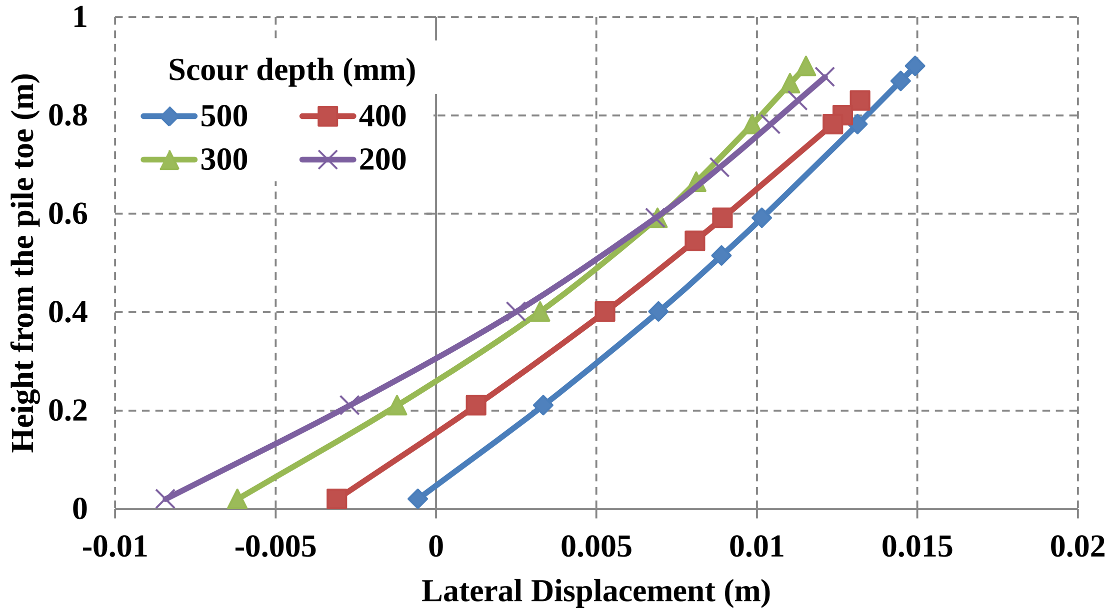

Figure 5.16 Effect of Scour Depth on the Lateral Displacement Profiles along the Pile with 15-degree Scour Slope

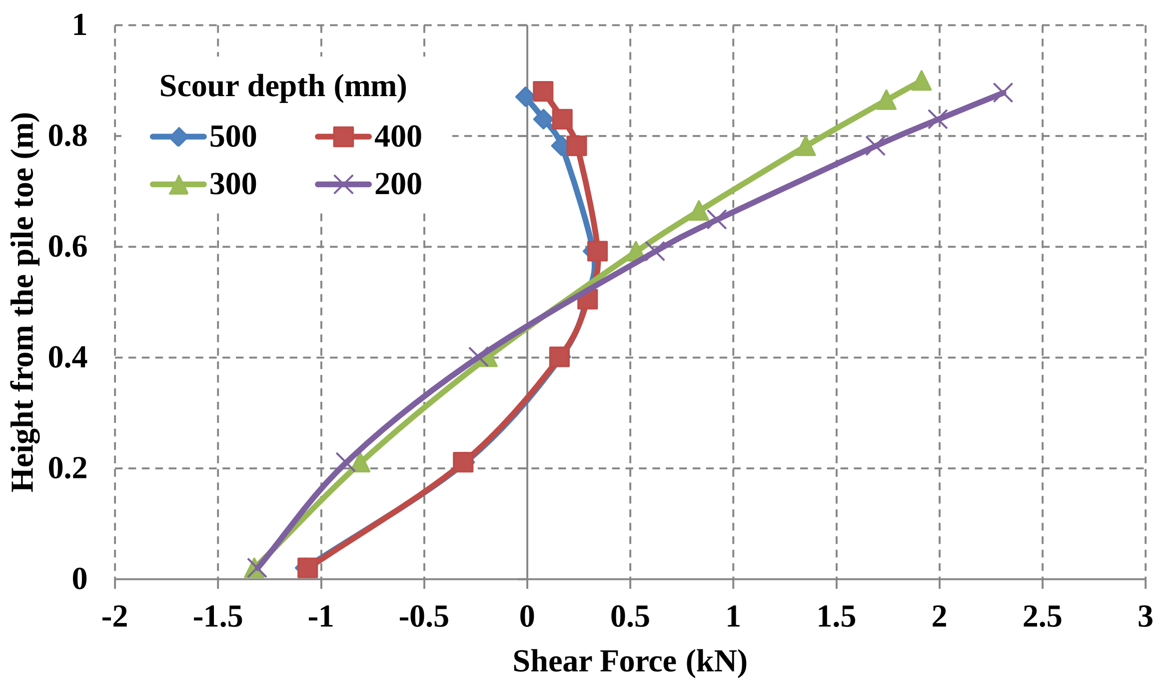

Figure 5.17 Effect of Scour Depth on the Shear Force Profiles along the Pile with 15-degree Scour Slope

30-degree scour slope. Figure 5.18 presents the effect of the scour depth on the lateral load-displacement curves. Also, it shows that the increased scour depth increased the lateral displacement.

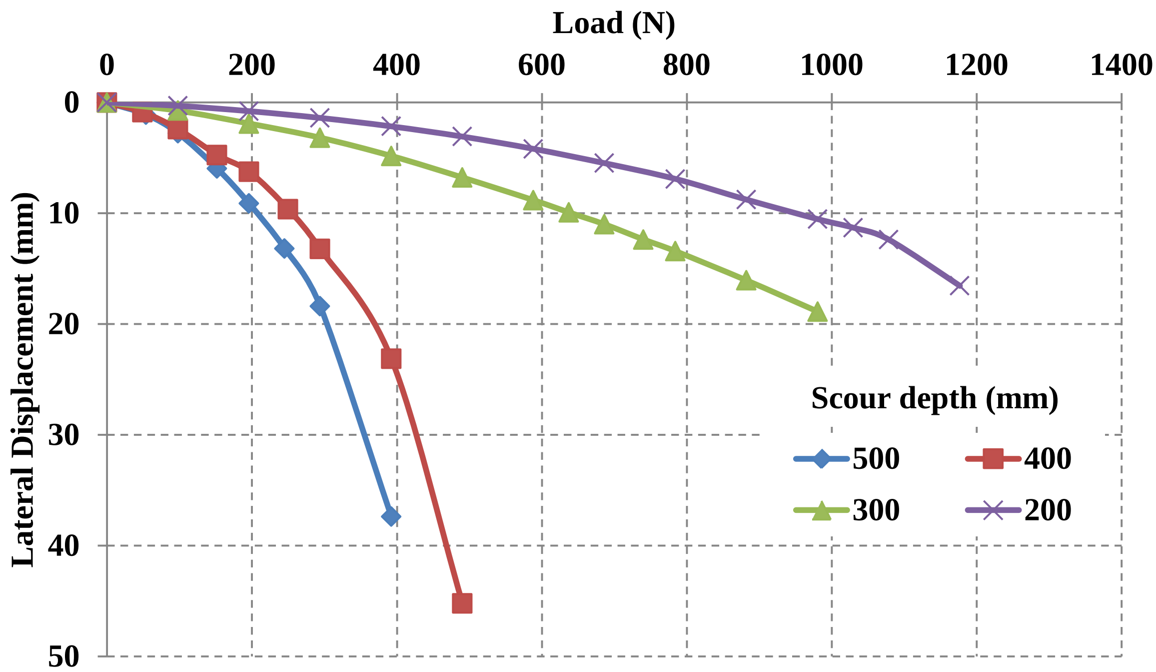

Figure 5.18 Effect of Scour Depth on the Load-Lateral Displacement Curves for the Pile with 30-degree Scour Slope

Figures 5.19, 5.20, and 5.21 present the effect of the scour depth on the moment, lateral displacement, and shear force profiles along the pile respectively at 30-degree scour slope. These figures showed similar behavior as in Figures 5.15, 5.16, and 5.17. Figure 5.22 shows the relation between the lateral load capacities ratio with and without scour and the ratio of the scour depth to pile diameter at each scour slope. Figure 5.22 also shows that at the same ratio of scour depth to pile diameter, the increased scour slope increased the ratio of the lateral load capacities with and without scour.

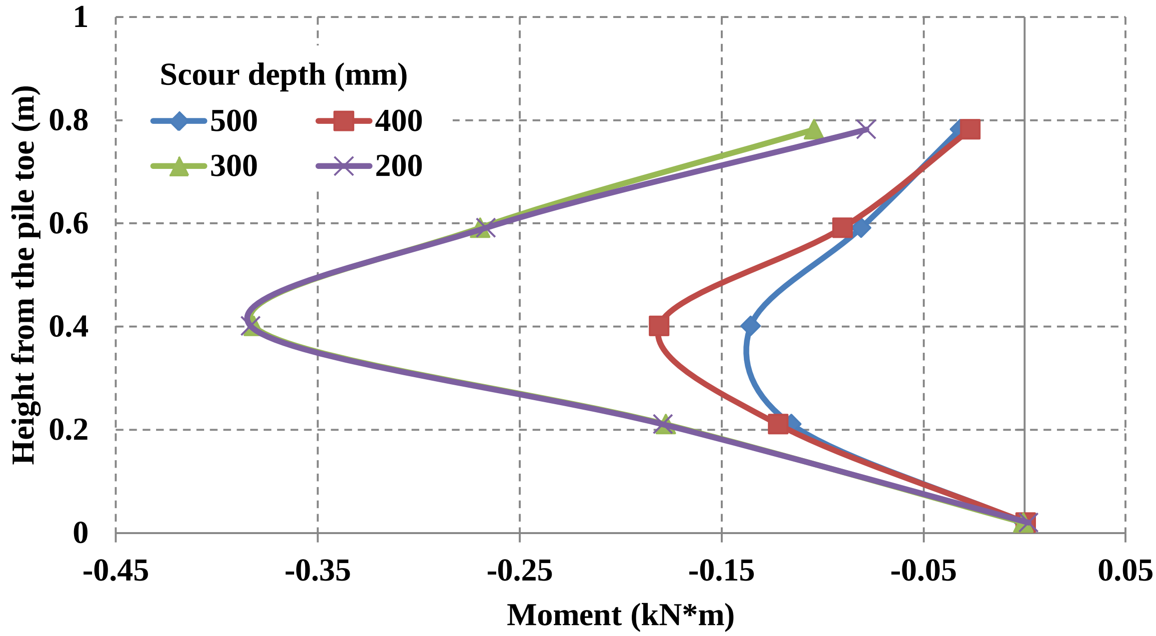

Figure 5.19 Effect of Scour Depth on the Moment Profiles along the Pile with 30-degree Scour Slope

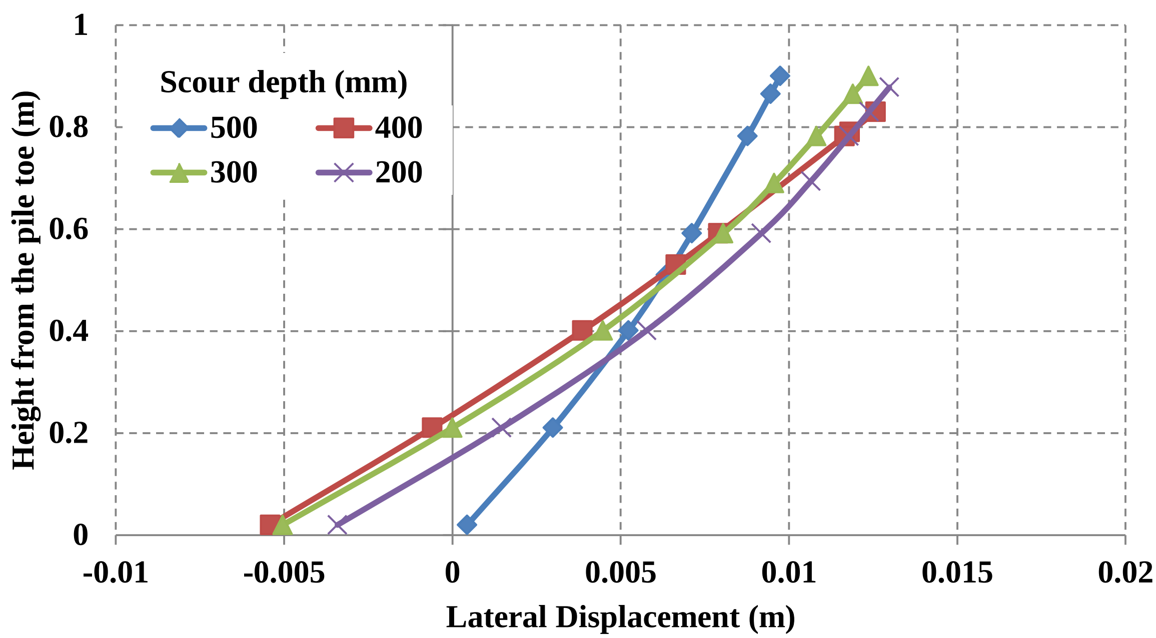

Figure 5.20 Effect of Scour Depth on the Lateral Displacement Profiles along the Pile with 30-degree Scour Slope

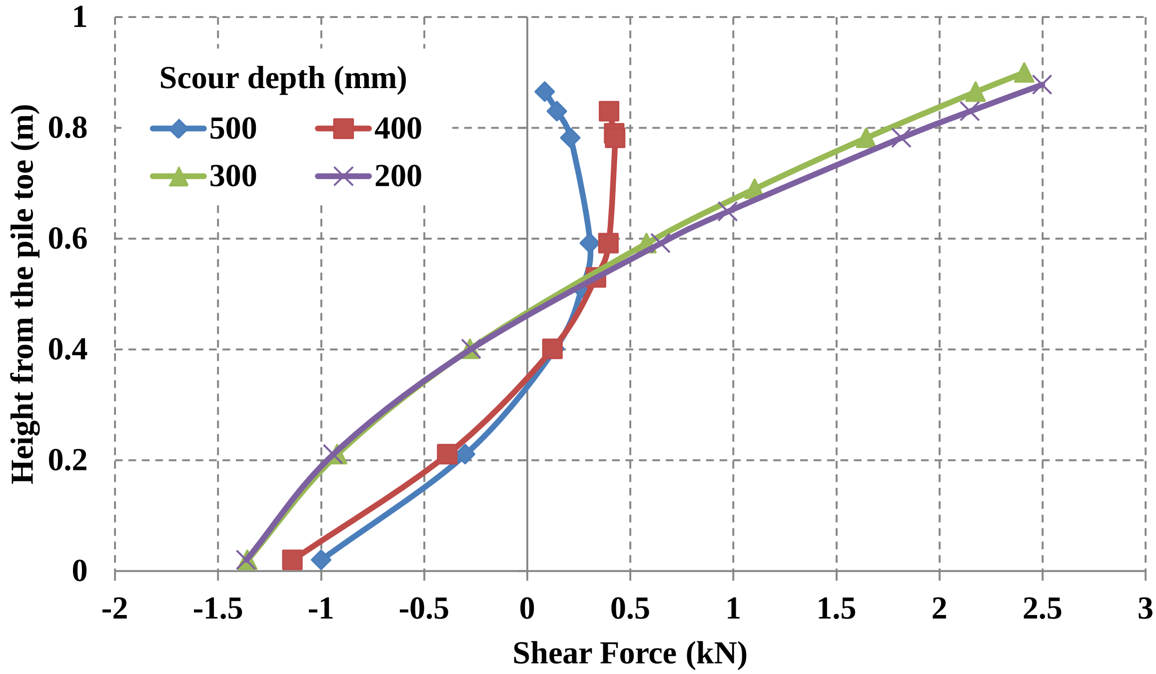

Figure 5.21 Effect of Scour Depth on the Shear Force Profiles along the Pile with 30-degree Scour Slope

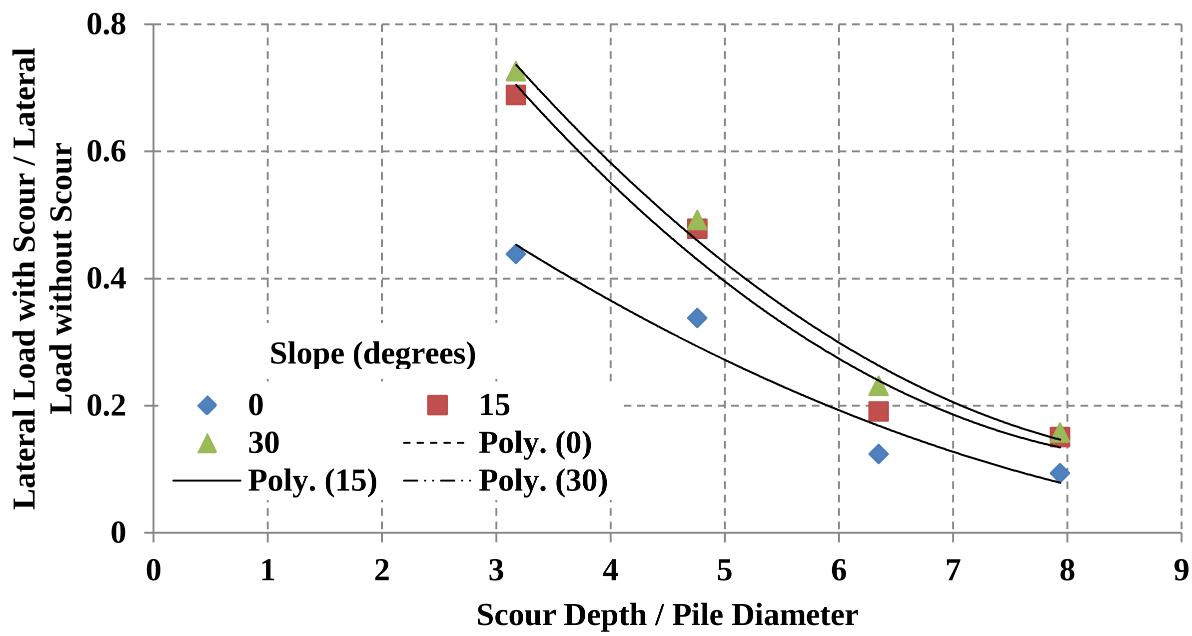

Figure 5.22 Ultimate Lateral Load Capacity Ratio versus the Scour Depth to Pile Diameter Ratio for Each Scour Slope

Scour slope

The scour slope effect was investigated at the following scour depths: 200, 300, 400, and 500 mm.

200-mm scour depth. Figures 5.23, 5.24, 5.25, and 5.26 present the effect of the scour slope on the lateral load-displacement curves, the moment profiles, the lateral displacement profiles, and the shear force profiles along the pile respectively. These figures show that the scour slopes of 15 and 30^o resulted in the similar behavior of the laterally loaded pile. At the same lateral load, the pile with a scour slope of 0^o had much larger lateral displacement due to less confinement. The increase of the slope angle provided more confinement to the pile thus increased the load capacity, the bending moment, and shear force at the higher load and the same lateral displacement. Figure 5.25 shows that the pile was more confined as the scour slope increased which led to various lateral displacements at the pile toe.

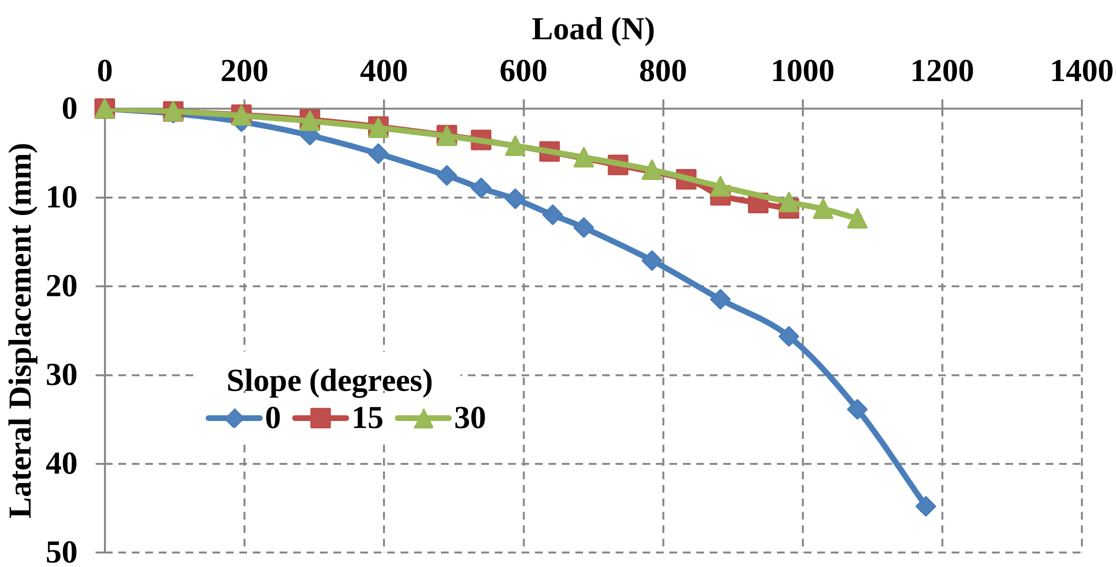

Figure 5.23 Effect of Scour Slope on the Load-Lateral Displacement Curves for the Pile with 200-mm Scour Depth

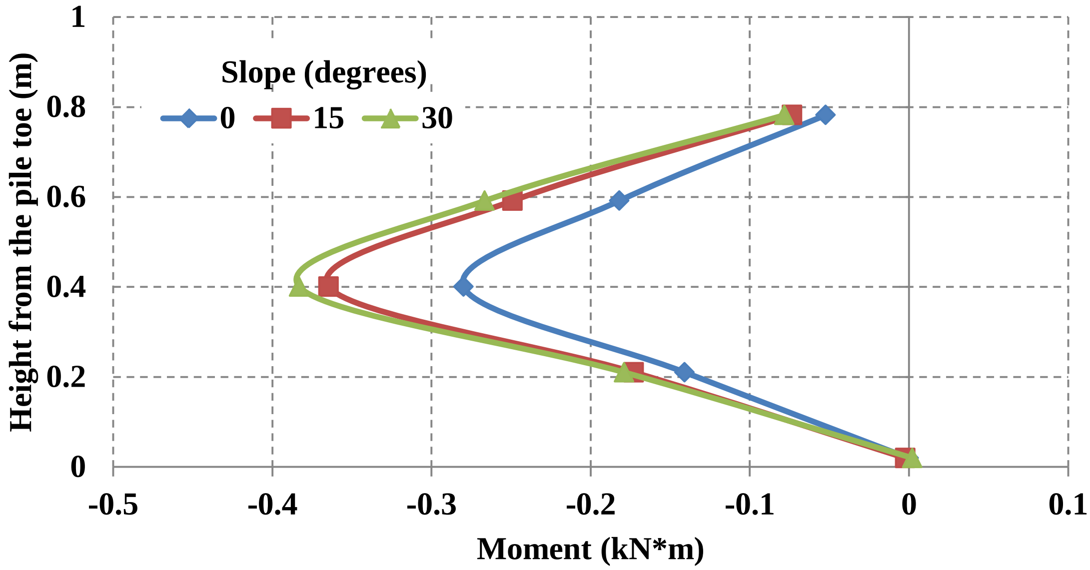

Figure 5.24 Effect of Scour Slope on the Moment Profiles along the Pile with 200-mm Scour Depth

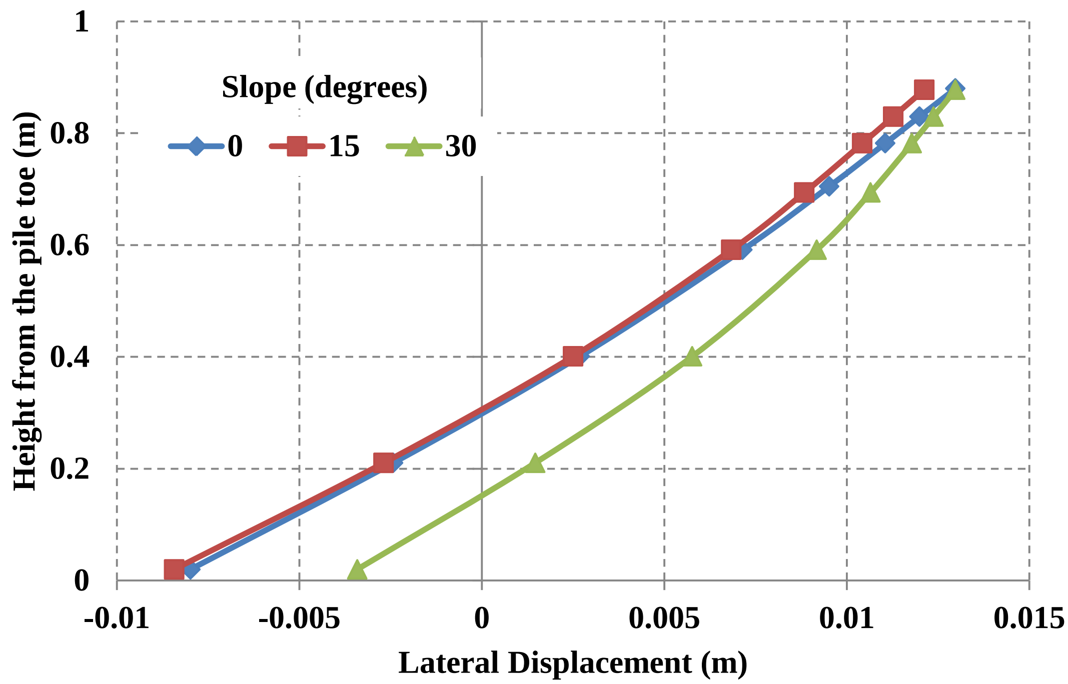

Figure 5.25 Effect of Scour Slope on the Lateral Displacement Profiles along the Pile with 200-mm Scour Depth

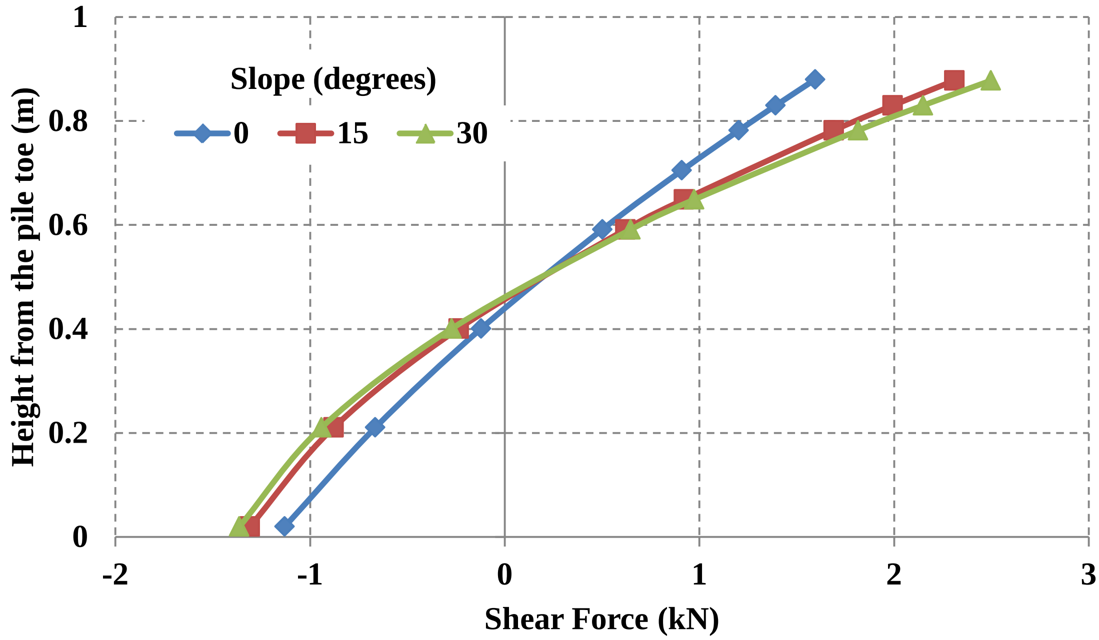

Figure 5.26 Effect of Scour Slope on the Shear Forces along the Pile with Scour Depth of 200 mm

300-mm scour depth. Figures 5.27, 5.28, 5.29, and 5.30 present the effect of the scour slope on the lateral load-displacement curves, the moment profiles, the lateral displacement profiles, and the shear force profiles along the pile respectively. These figures show the similar behavior of the laterally loaded piles as those in Figures 5.23, 5.24, 5.25, and 5.26.

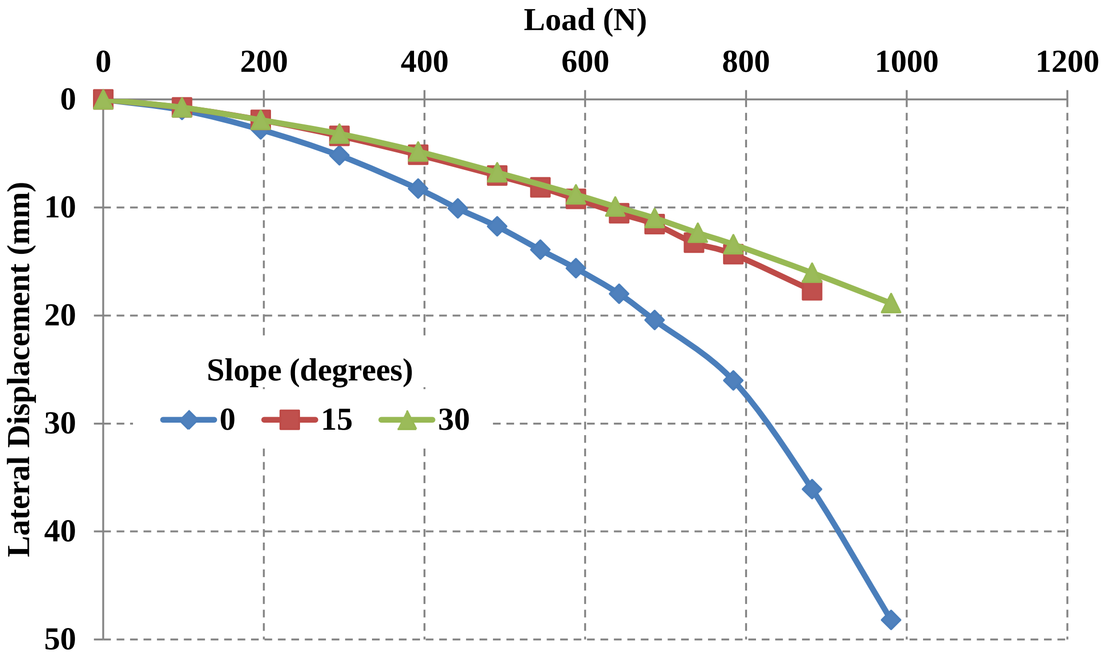

Figure 5.27 Effect of Scour Slope on the Load-Lateral Displacement Curves for the Pile with 300-mm Scour Depth

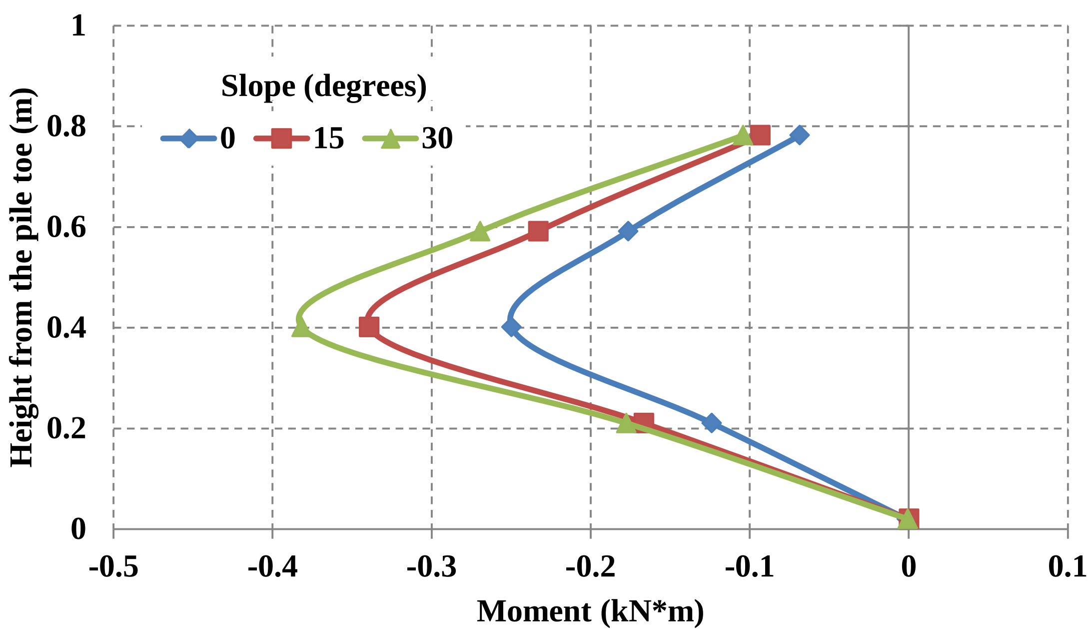

Figure 5.28 Effect of Scour Slope on the Moment Profiles along the Pile with 300-mm Scour Depth

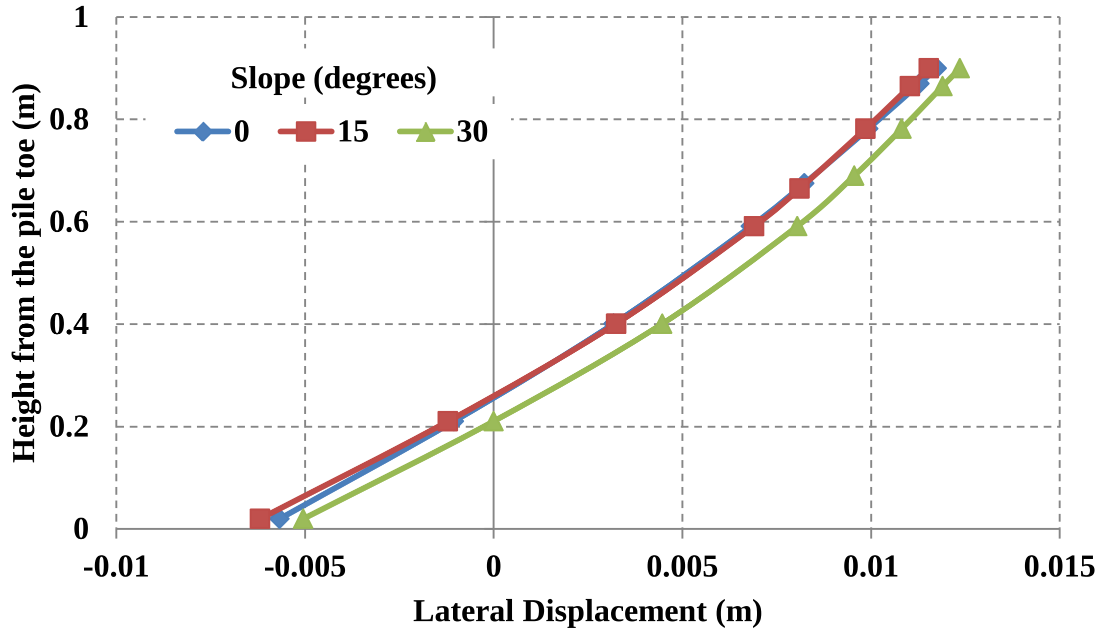

Figure 5.29 Effect of Scour Slope on the Lateral Displacement Profiles along the Pile with 300-mm Scour Depth

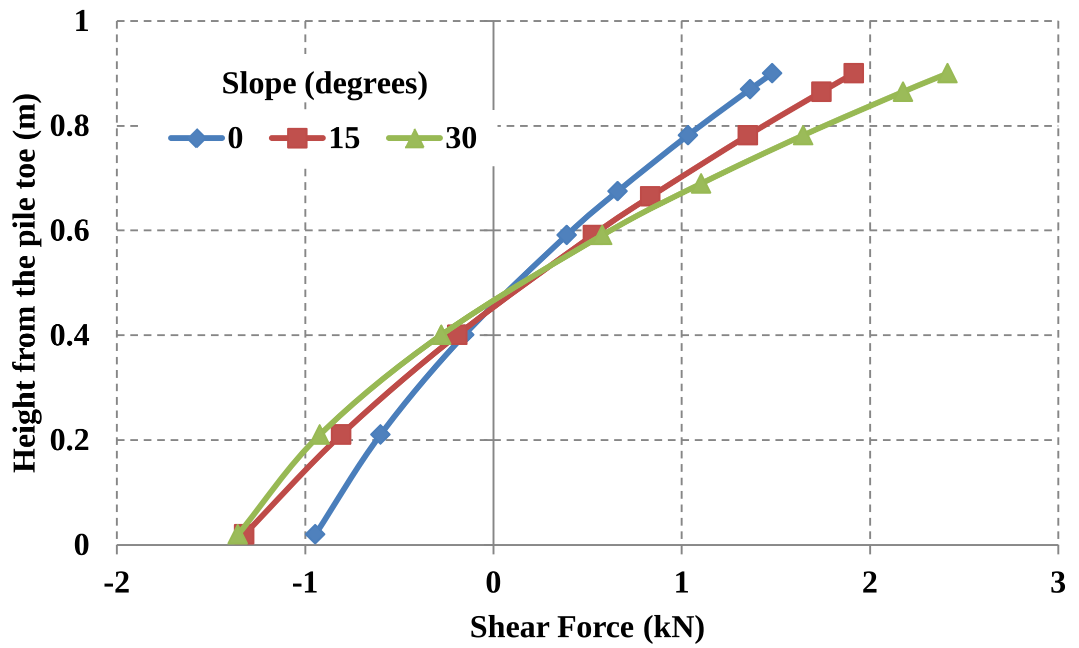

Figure 5.30 Effect of Scour Slope on the Shear Force Profiles along the Pile with 300-mm Scour Depth

400-mm scour depth. Figures 5.31, 5.32, 5.33, and 5.34 present the effect of the scour slope on the lateral load-displacement curves, the moment profiles, the lateral displacement profiles, and the shear force profiles along the pile respectively. These figures show that the increased scour slope decreased the lateral displacement because of the increase in the soil resistance due to the increase of the scour slope. The rate of the lateral displacement increased at the higher lateral loads. The maximum moment and the maximum shear force increased with the increase of the scour slope because of the increase of the soil resistance around the pile. The lateral displacements along the pile were nearly linear.

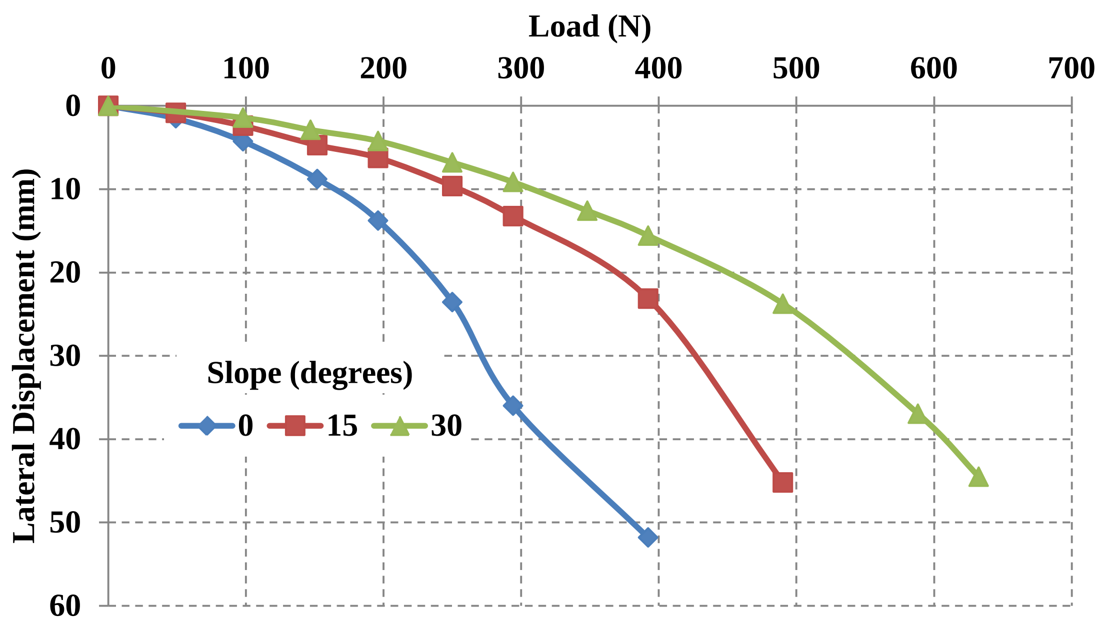

Figure 5.31 Effect of Scour Slope on the Load-Lateral Displacement Curves the Pile with 400-mm Scour Depth

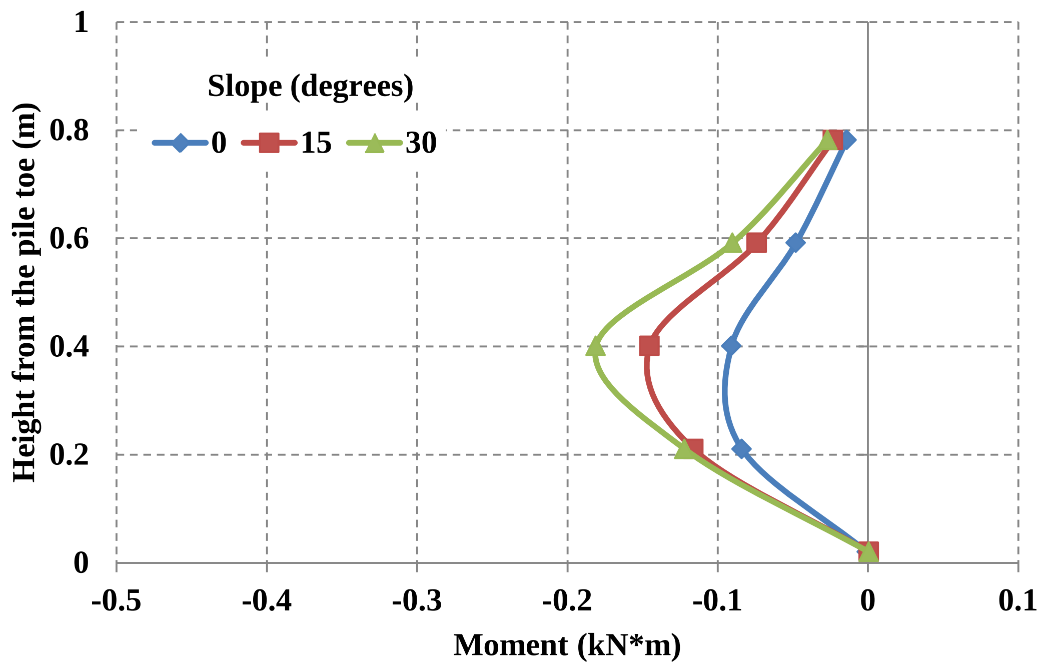

Figure 5.32 Effect of Scour Slope on the Moment Profiles along the Pile with 400-mm Scour Depth

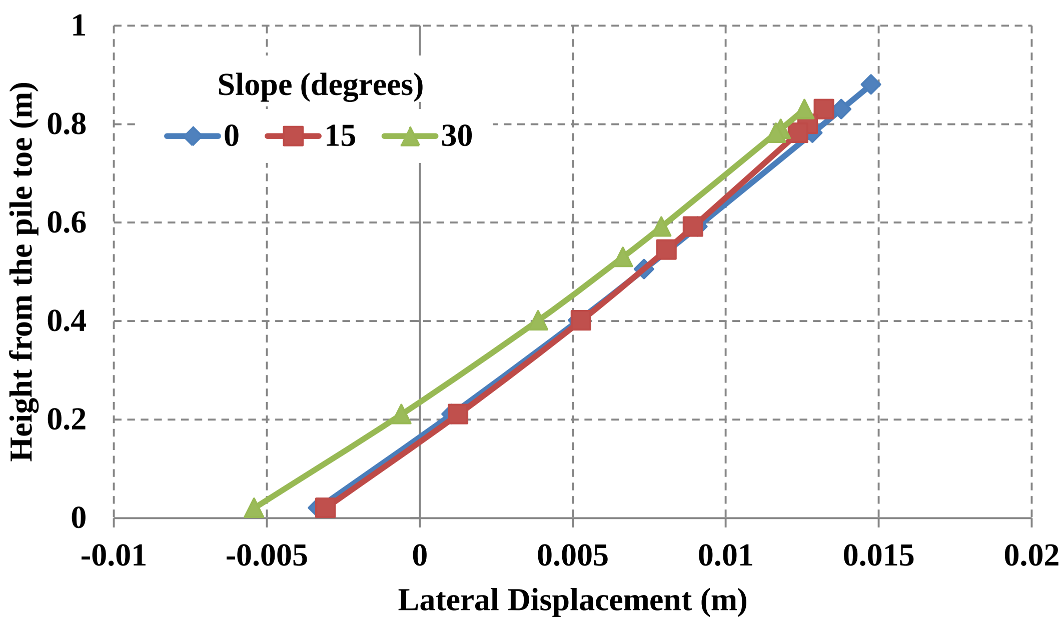

Figure 5.33 Effect of Scour Slope on the Lateral Displacement Profiles along the Pile with 400-mm Scour Depth

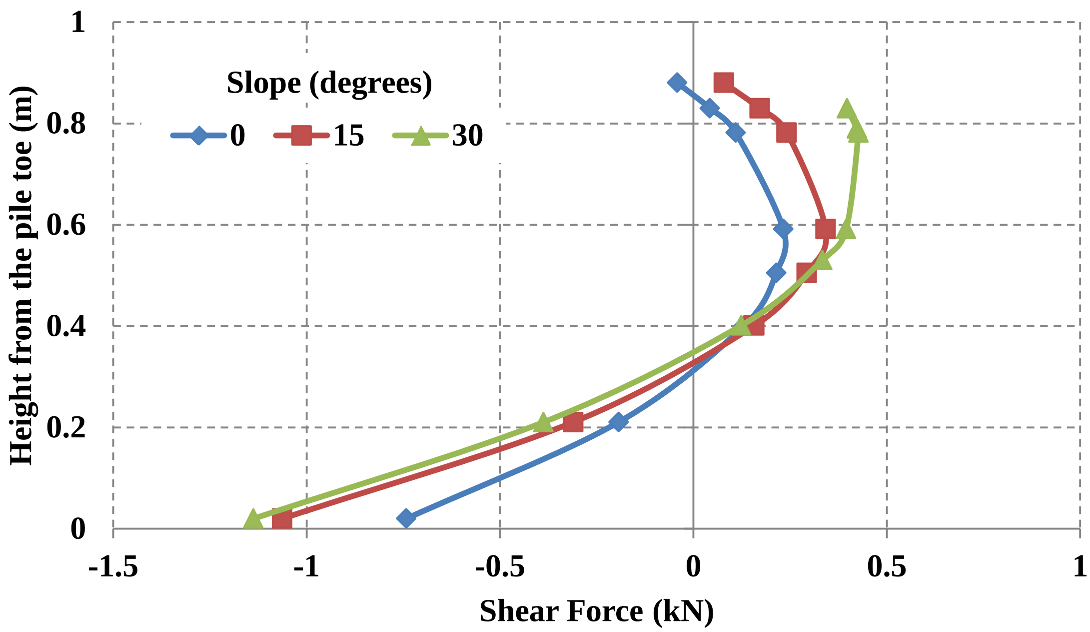

Figure 5.34 Effect of Scour Slope on the Shear Force Profiles along the Pile with 400-mm Scour Depth

500-mm scour depth. Figures 5.35, 5.36, 5.37, and 5.38 present the effect of the scour slope on the lateral load-displacement curves, the moment profiles, the lateral displacement profiles, and the shear force profiles along the pile respectively. These figures show similar behavior as shown in Figure 5.31, 5.32, 5.33, and 5.34.

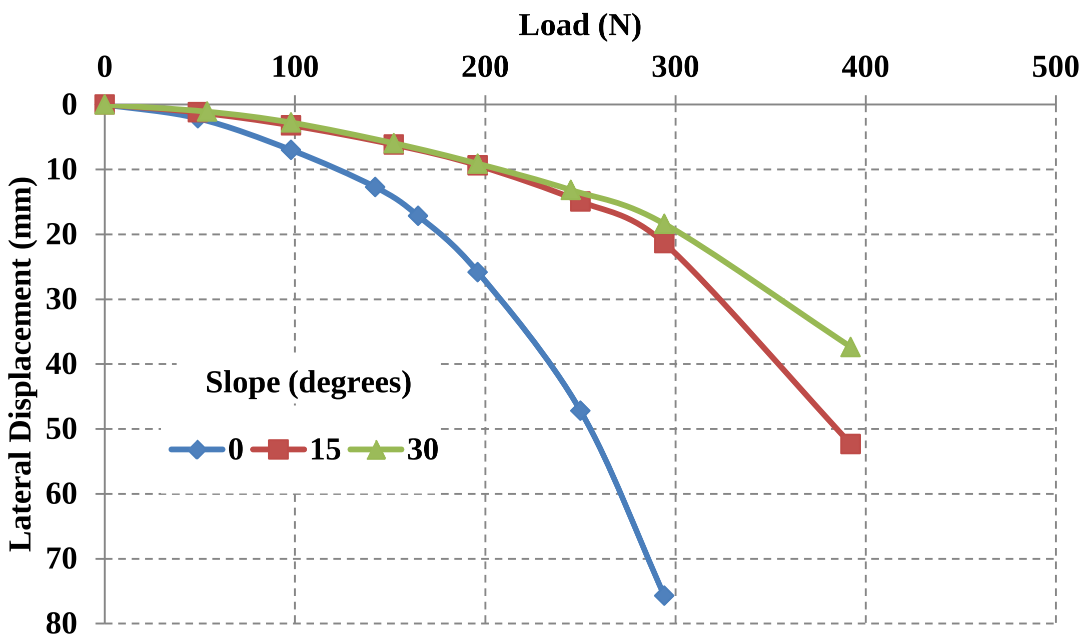

Figure 5.35 Effect of Scour Slope on the Load-Lateral Displacement Curves the Pile with 500-mm Scour Depth

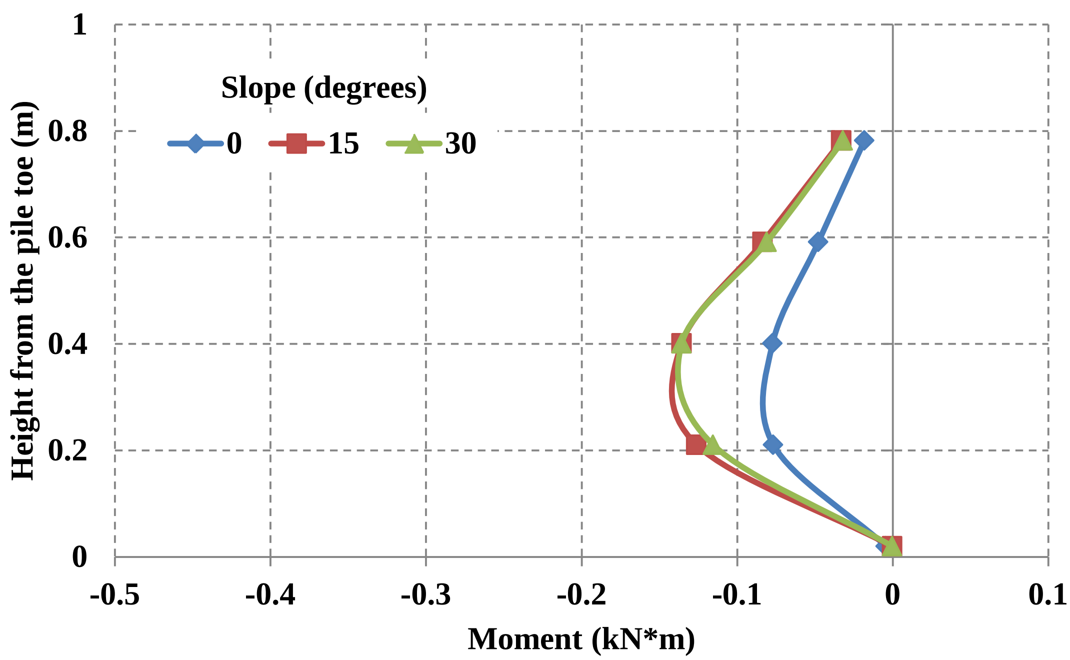

Figure 5.36 Effect of Scour Slope on the Moment Profiles along the Pile with 500-mm Scour Depth

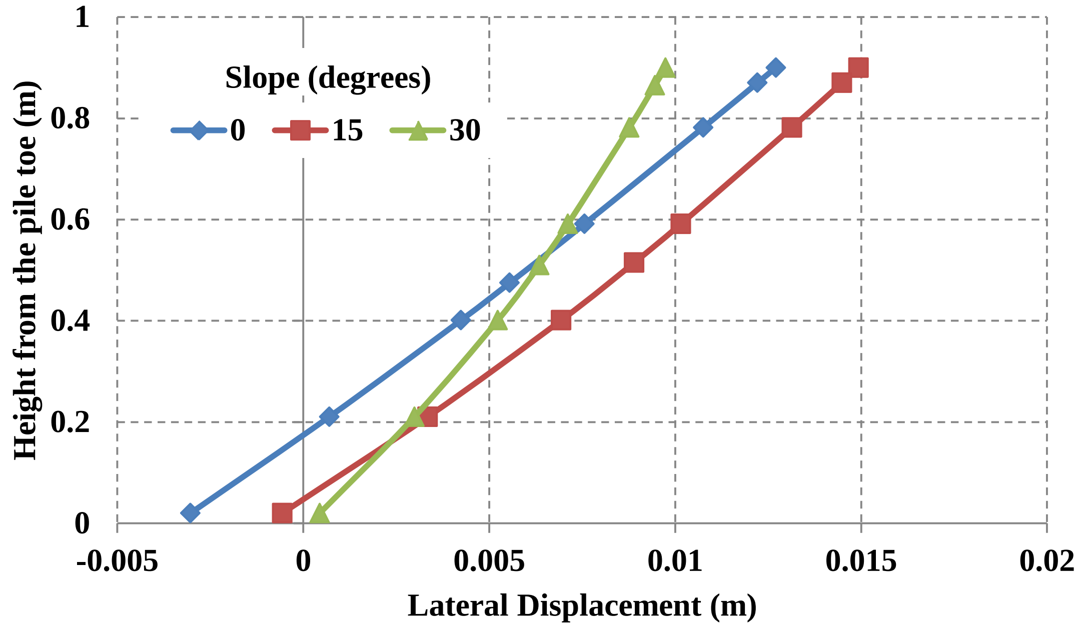

Figure 5.37 Effect of Scour Slope on the Lateral Displacement Profiles along the Pile with 500-mm Scour Depth

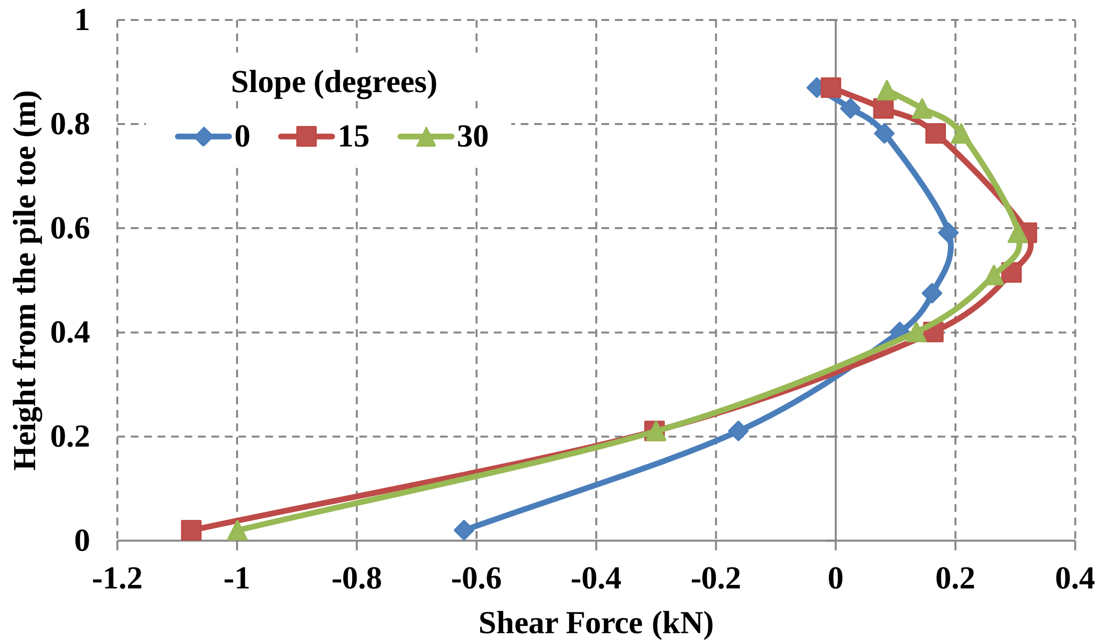

Figure 5.38 Effect of Scour Slope on the Shear Force Profiles along the Pile with 500-mm Scour Depth

Figure 5.39 shows the relation between the lateral load capacity ratio with and without scour and the scour slope for each ratio of the scour depth to the pile diameter. It is shown that the increase of the scour slope increased the ratio of lateral load capacity with scour to that without scour; however, the increase was small after the scour slope angle was greater than 15^o. Figure 5.39 also shows that the lateral load capacity ratio increased with the decrease of the scour depth to pile diameter ratio.

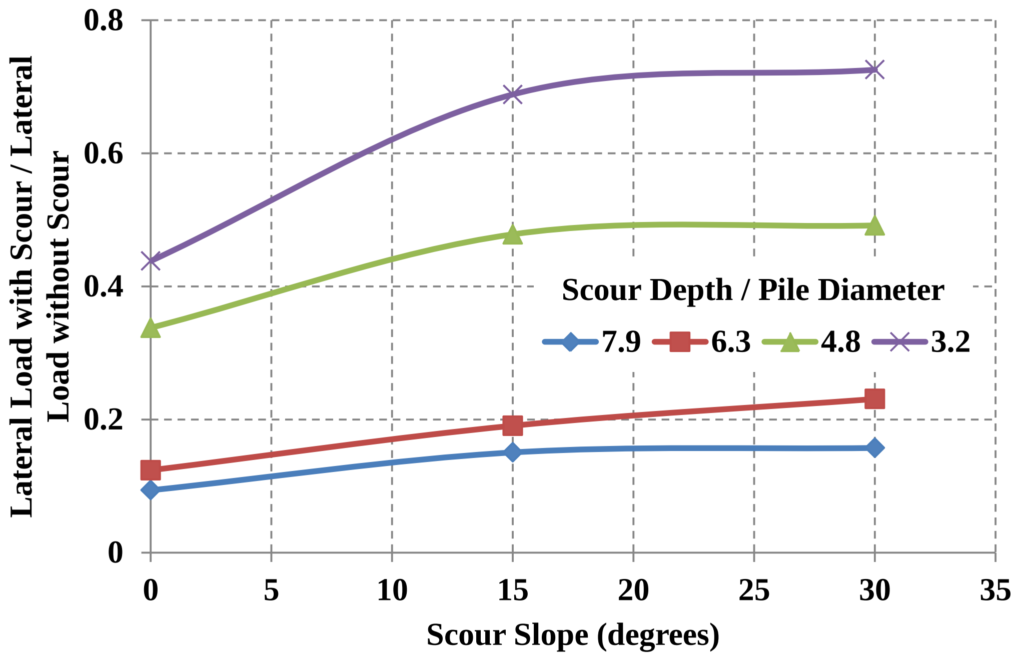

Figure 5.39 Ultimate Lateral Load Capacity Ratio to the Scour slope for Each Ratio of The Scour Depth to the Pile Diameter

5.5.3. Combined scour width and scour depth effects

Both scour width and scour depth affect the behavior of laterally loaded piles. In the following section, the effect of the scour depth on the behavior of the laterally loaded pile with a constant scour width is presented first. The scour width effect on the behavior of the laterally loaded pile with a constant scour depth is presented afterwards.

Scour depth

The effect of scour depth is presented below at four scour widths: 0, 240, 400, and 667 mm.

0-mm scour width. Figure 5.40 presents the effect of the scour depth on the lateral load-displacement curves. Also, it shows that the increased scour depth increased the lateral displacement. At the same lateral load, the lateral displacements increased with an increase of the scour depth because of the reduction in the confinement around the pile.

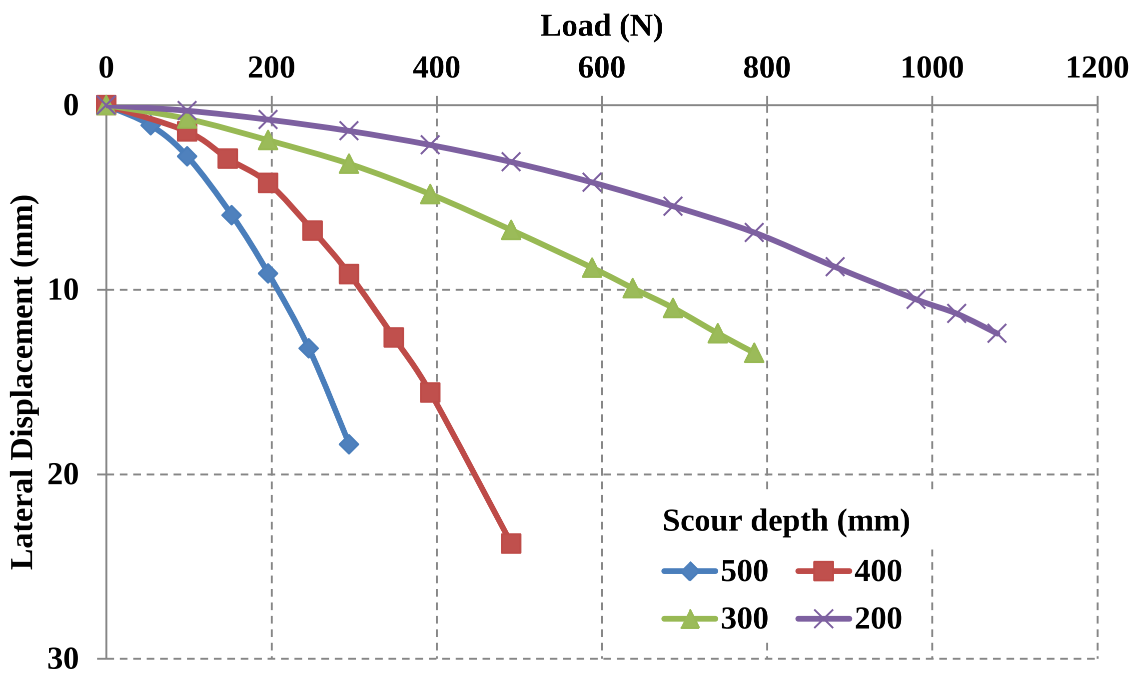

Figure 5.40 Effect of Scour Depth on the Lateral Load-Displacement Curves for the Pile with 0-mm Scour Width

Figures 5.41, 5.42, and 5.43 present the effect of the scour depth on the moment, lateral displacement, and shear force profiles along the pile with 0-mm scour width respectively. These figures show that the maximum moment decreased and went towards the pile toe with the increase of the scour depth. It is also shown that the scour depth of 200 mm and 300 mm resulted in a similar behavior of the laterally loaded pile. The maximum shear force transferred from a positive value at the point where the lateral load acted to the negative value at the pile toe.

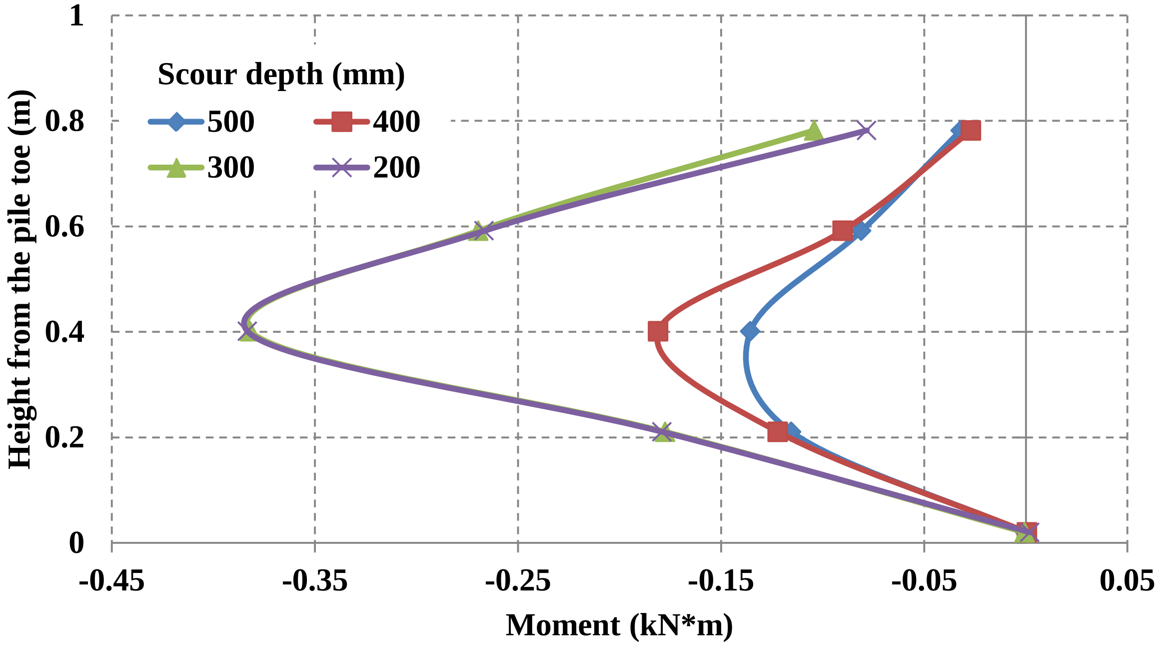

Figure 5.41 Effect of Scour Depth on the Moment Profiles along for the Pile with 0-mm Scour Width

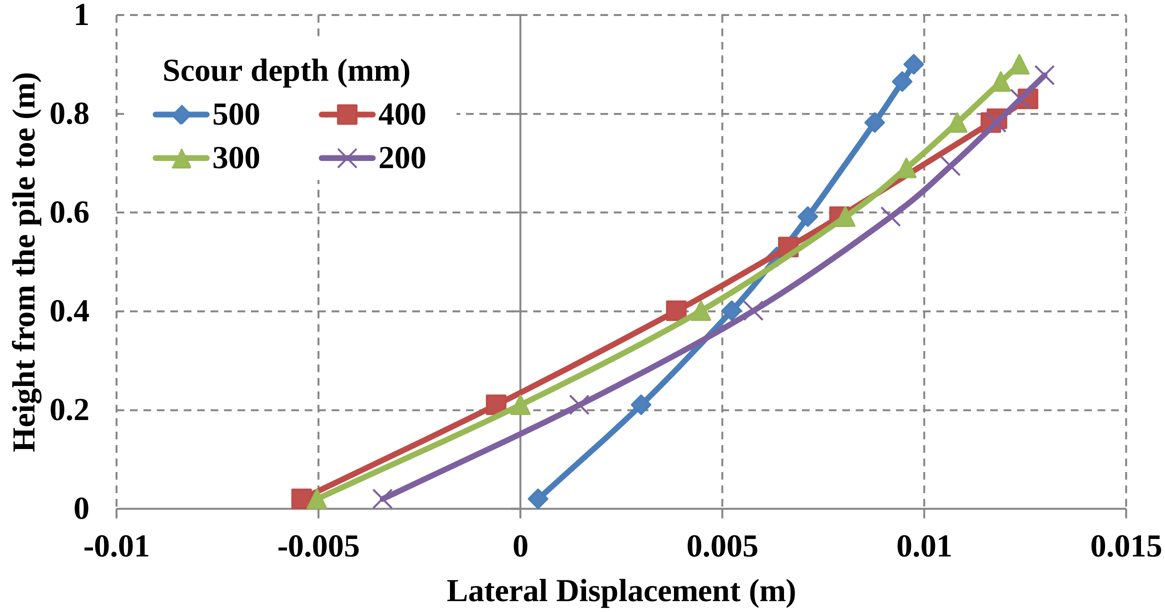

Figure 5.42 Effect of Scour Depth on the Lateral Displacement Profiles along for the Pile with 0-mm Scour Width

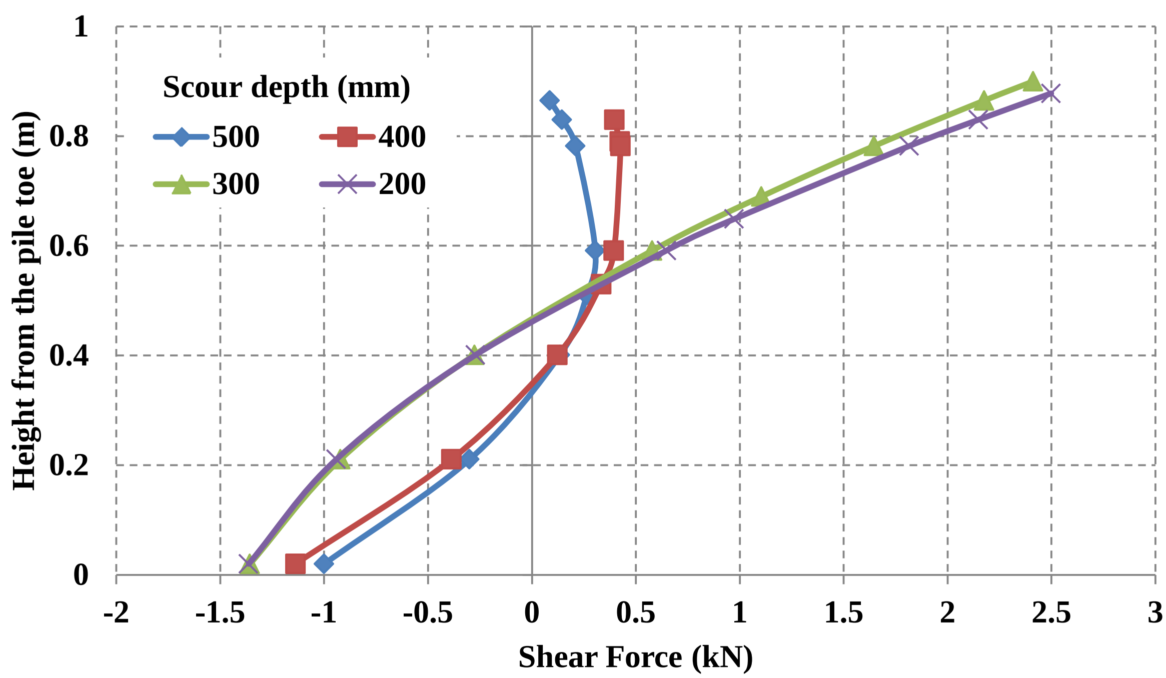

Figure 5.43 Effect of Scour Depth on the Shear Force Profiles along for the Pile with 0-mm Scour Width

240-mm scour width. Figure 5.44 presents the effect of the scour depth on the lateral load-displacement curves. Also, it shows that the increased scour depth increased the lateral displacement. At the same lateral load, the lateral displacements increased with an increase of the scour depth because of the reduction in the confinement around the pile. Figures 5.45, 5.46, and 5.47 present the effect of the scour depth on the moment, lateral displacement, and shear force profiles along the pile with 240-mm scour width respectively. These figures show that the maximum moment decreased and went towards the pile toe with the increase of the scour depth. It is also shown that the lateral displacement profiles along the pile were nearly linear. The maximum shear force transferred from a positive value at the point where the lateral load acted to the negative value at the pile toe.

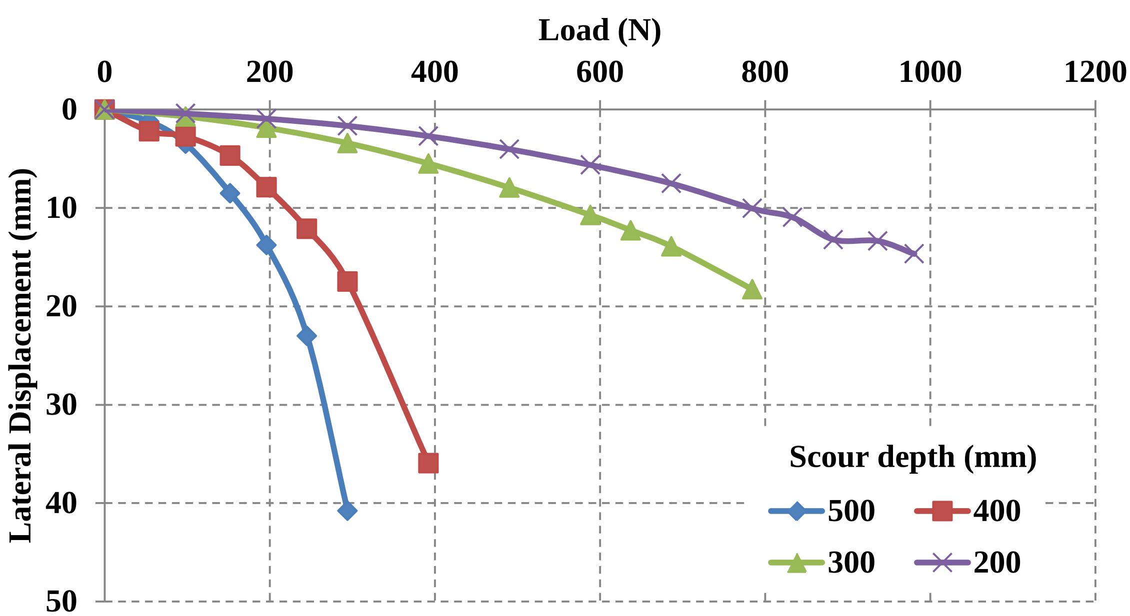

Figure 5.44 Effect of Scour Depth on the Load-Lateral Displacement Curves for the Pile with 240-mm Scour Width

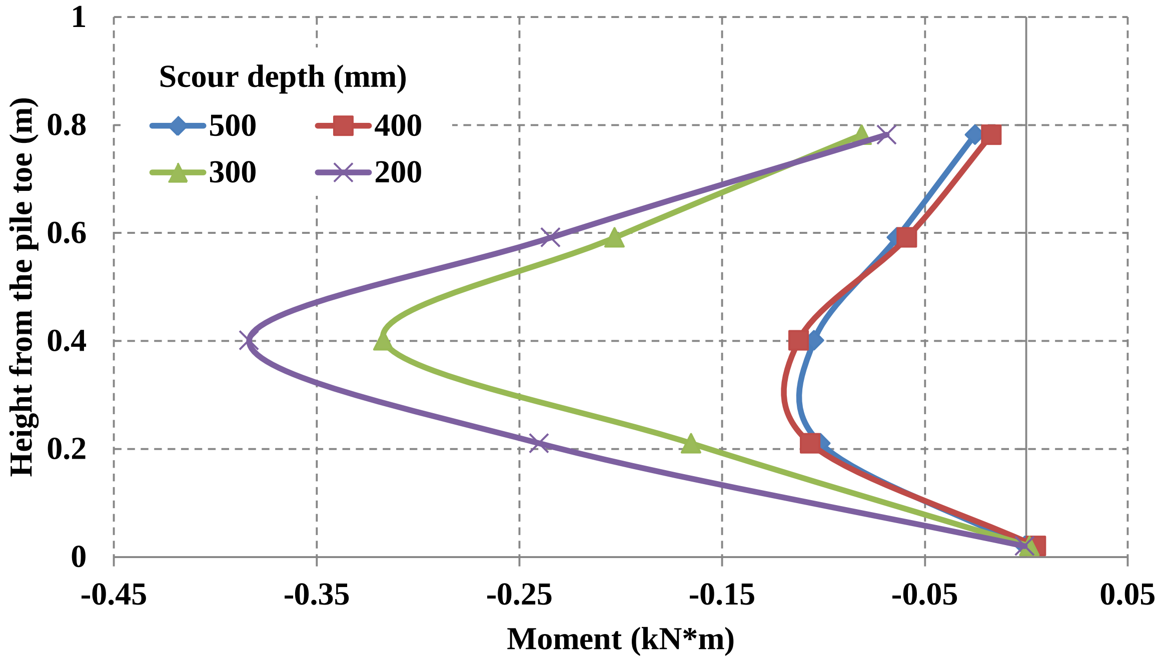

Figure 5.45 Effect of Scour Depth on the Moment Profiles along for the Pile with 240-mm Scour Width

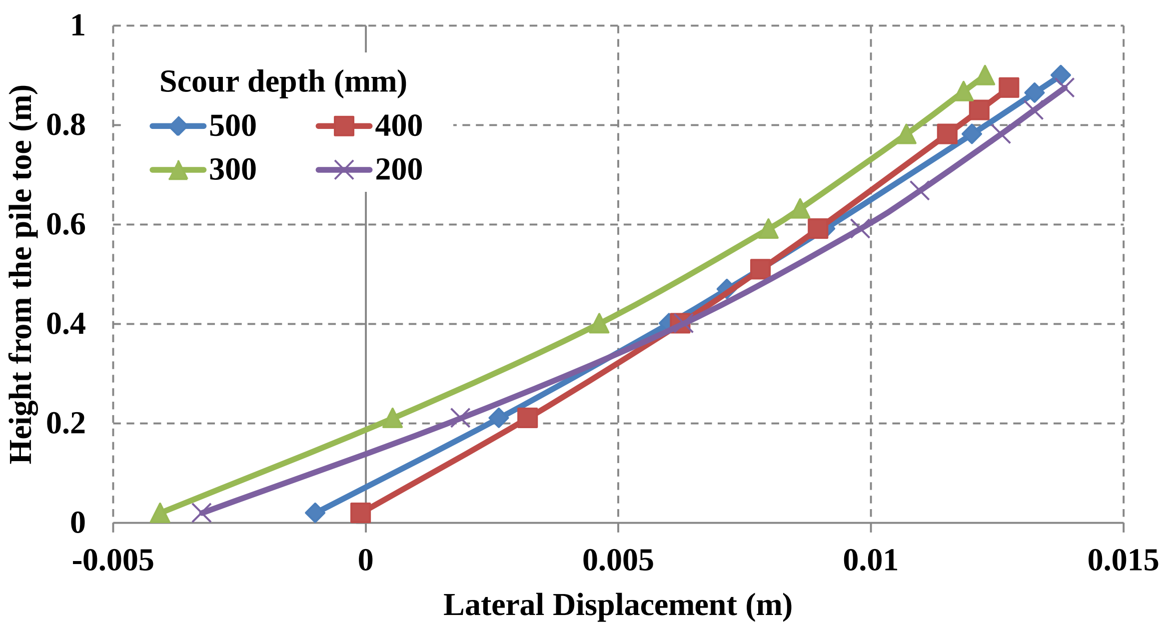

Figure 5.46 Effect of Scour Depth on the Lateral Displacement Profiles along for the Pile with 240-mm Scour Width

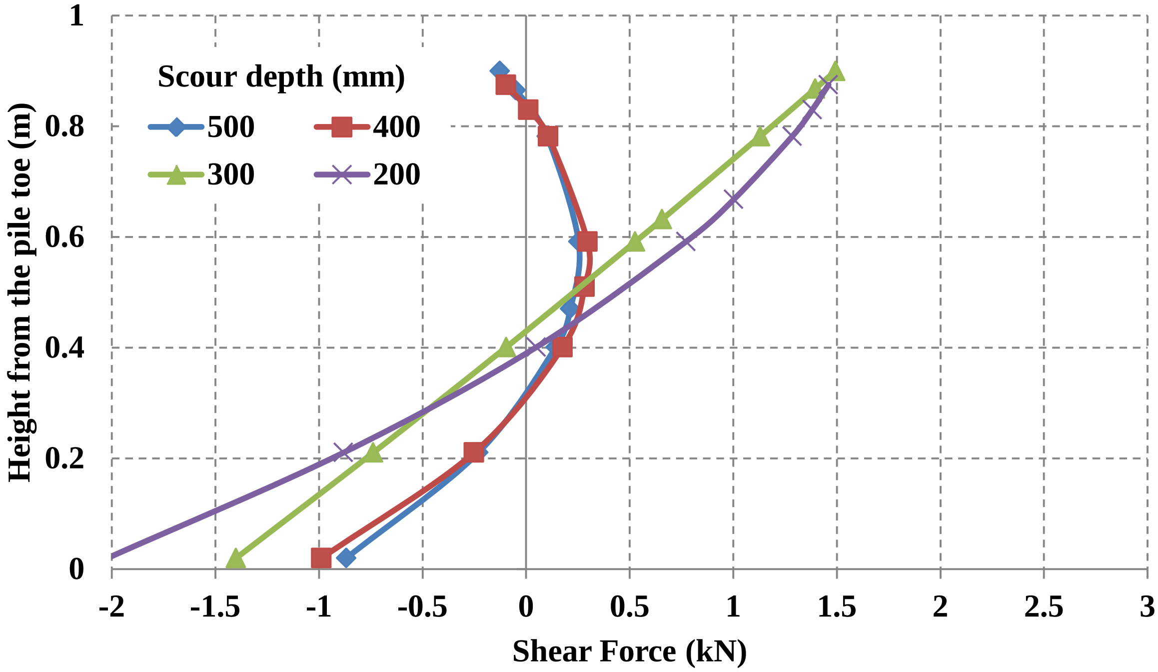

Figure 5.47 Effect of Scour Depth on the Shear Force Profiles along for the Pile with 240-mm Scour Width

400-mm scour width. Figures 5.48, 5.49, 5.50, and 5.51 present the effect of the scour depth on the lateral load-displacement curves and the moment, lateral displacement, and shear force profiles along the pile with 400-mm scour width respectively. These figures show similar behavior as shown in Figures 5.44, 5.45, 5.46, and 5.47.

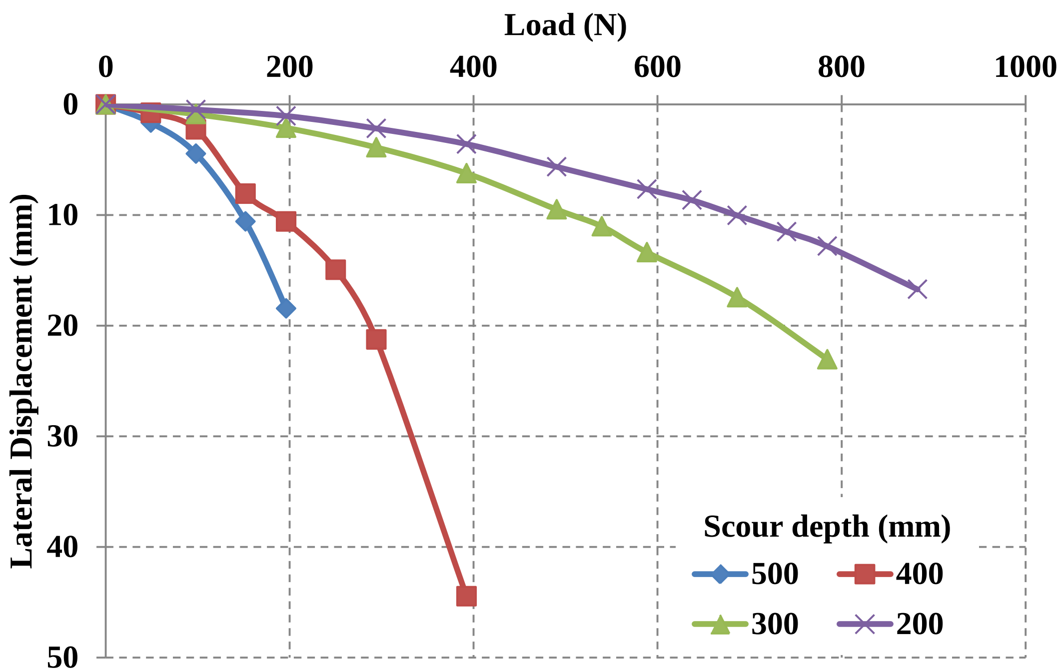

Figure 5.48 Effect of Scour Depth on the Load-Lateral Displacement Curves for the Pile with 400-mm Scour Width

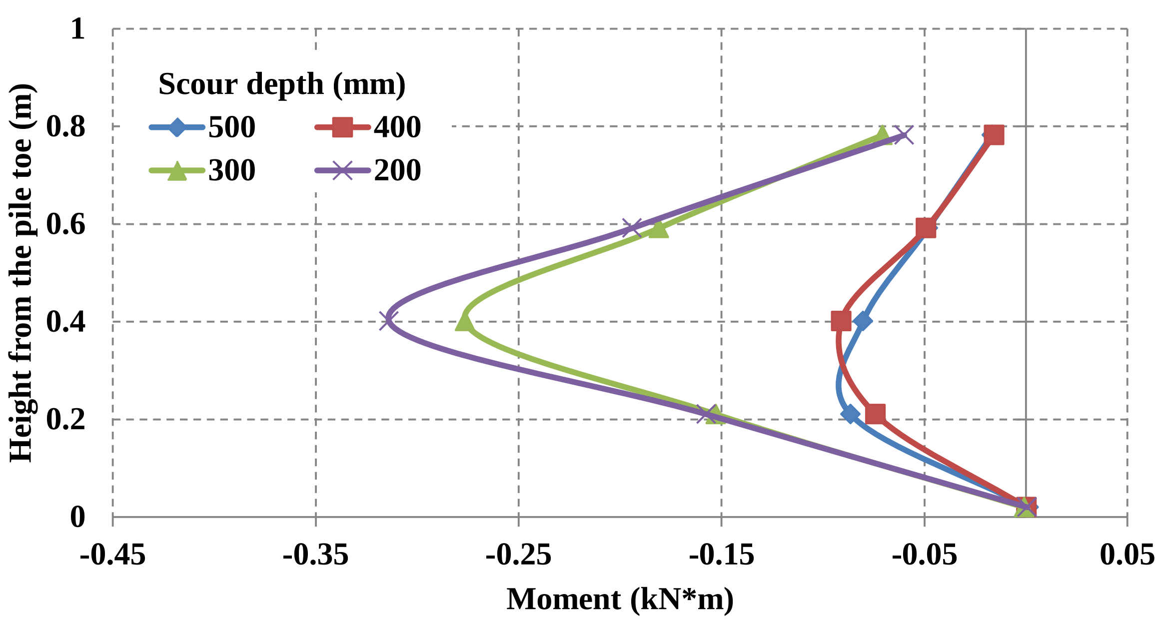

Figure 5.49 Effect of Scour Depth on the Moment Profiles along for the Pile with 400-mm Scour Width

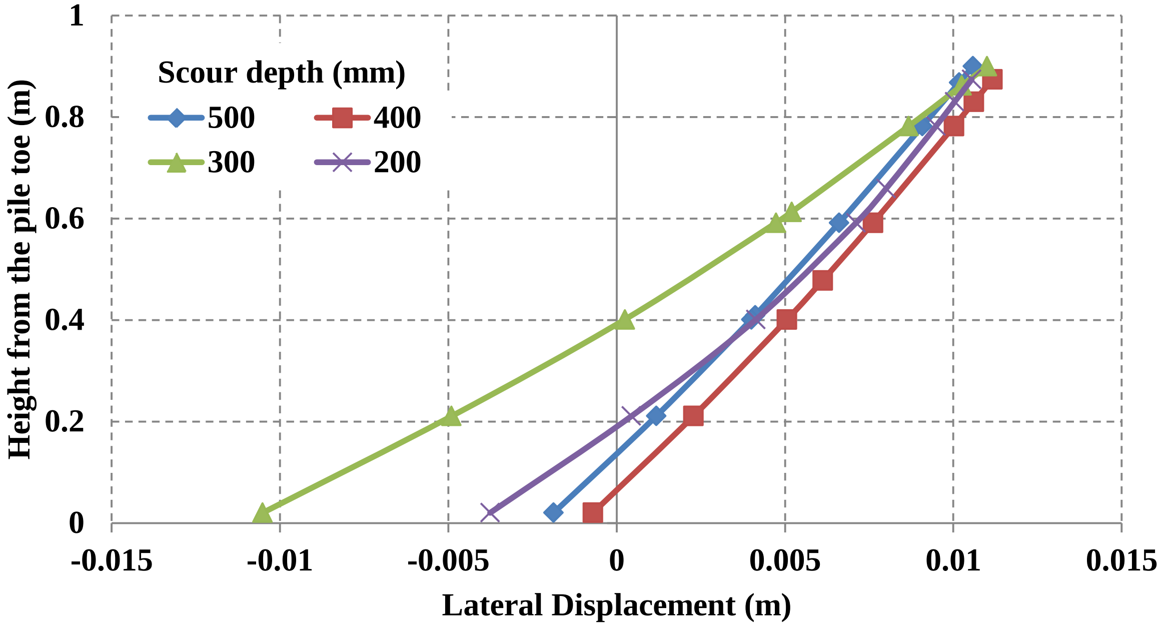

Figure 5.50 Effect of Scour Depth on the Lateral Displacement Profiles along for the Pile with 400-mm Scour Width

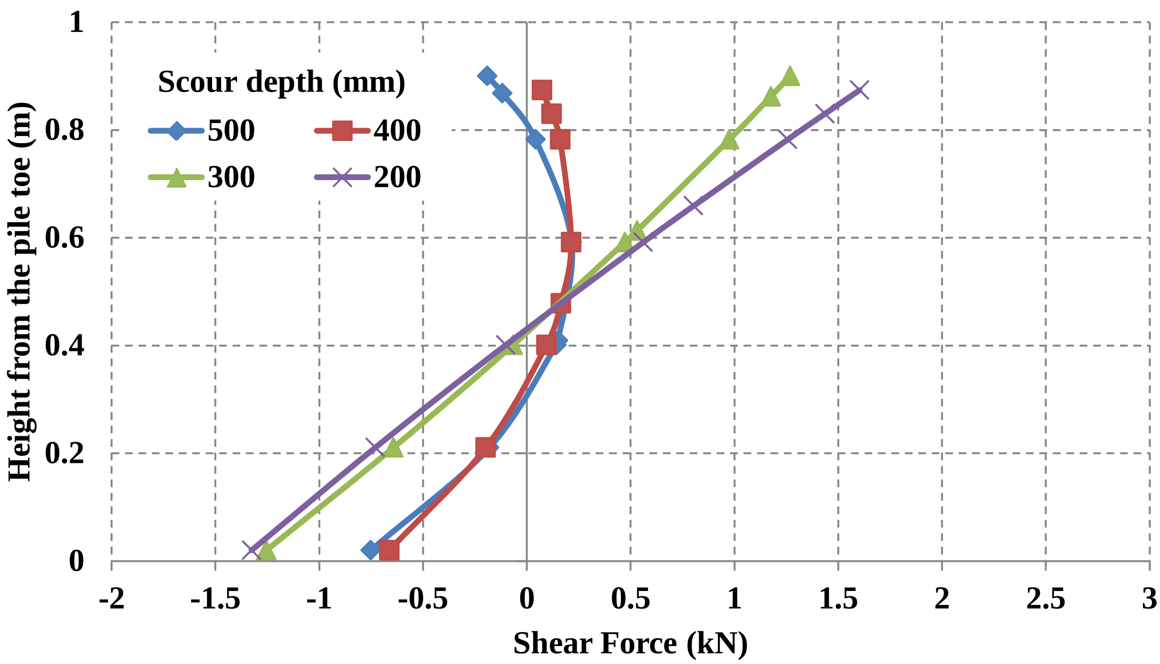

Figure 5.51 Effect of Scour Depth on the Shear Force Profiles along for the Pile with 400-mm Scour Width

667-mm scour width. Figures 5.52, 5.53, 5.54, and 5.55 present the effect of the scour depth on the lateral load-displacement curves and the moment, lateral displacement, and shear force profiles along the pile with 667-mm scour width respectively. These figures show similar behavior as shown in Figures 5.44, 5.45, 5.46, and 5.47.

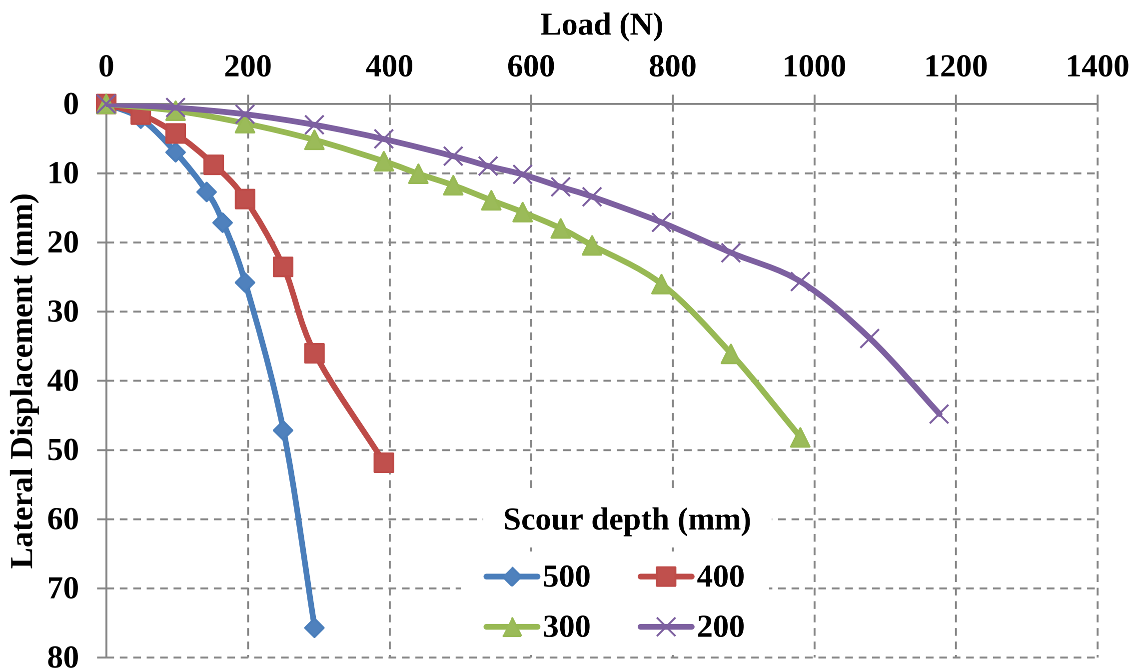

Figure 5.52 Effect of Scour Depth on the Load-Lateral Displacement Curves for the Pile with 667-mm Scour Width

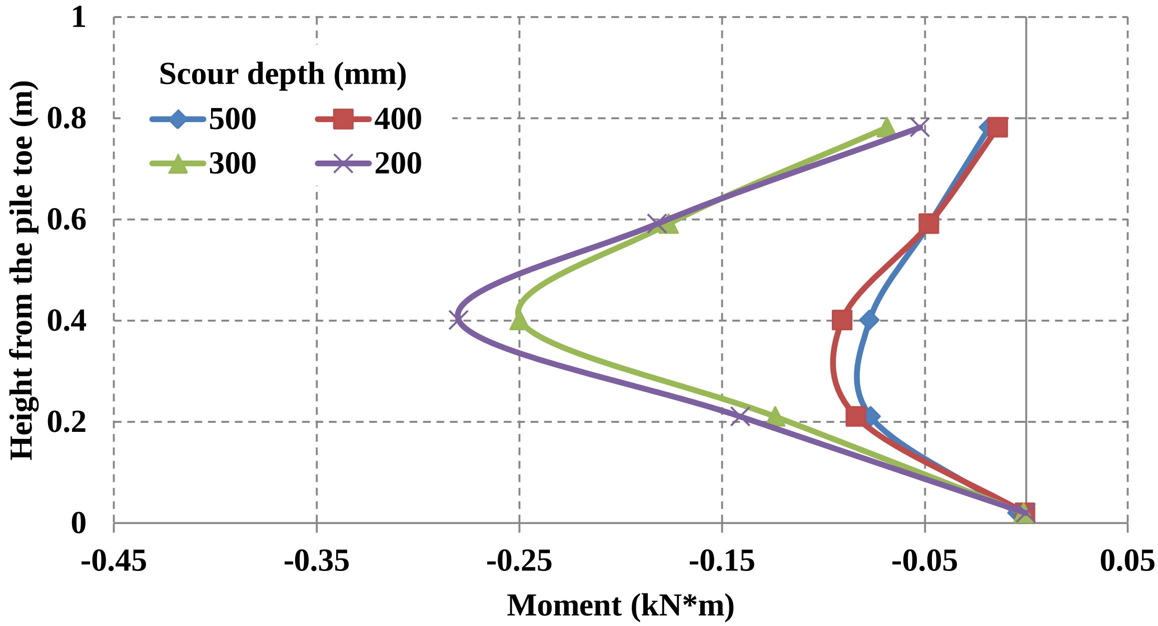

Figure 5.53 Effect of Scour Depth on the Moment Profiles along for the Pile with 667-mm Scour Width

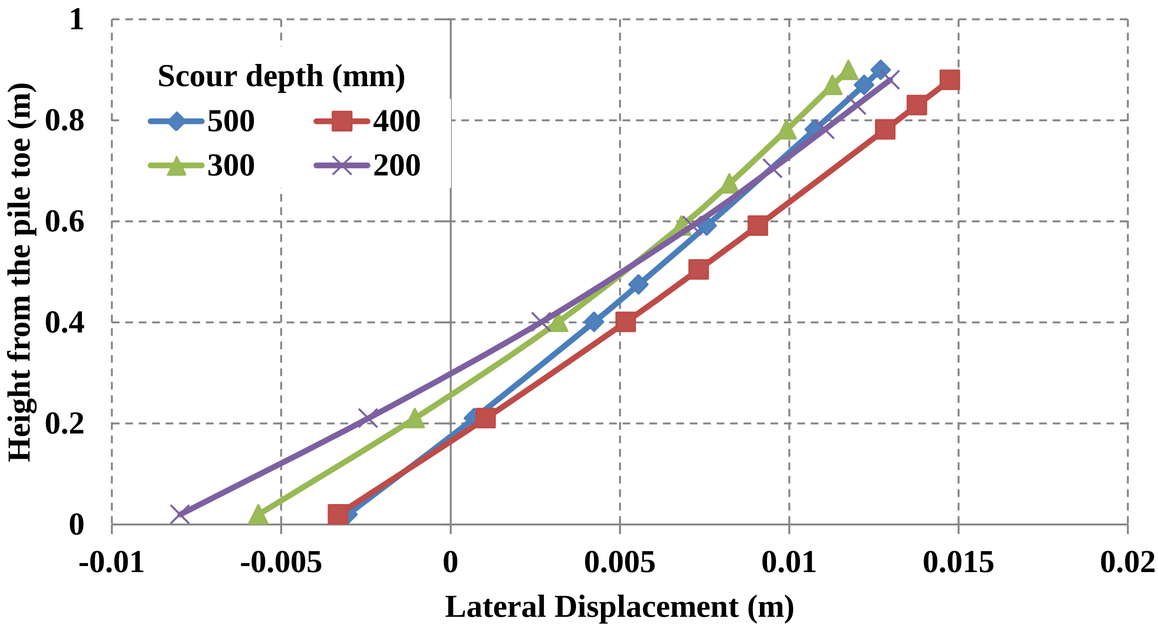

Figure 5.54 Effect of Scour Depth on the Lateral Displacement Profiles along for the Pile with 667-mm Scour Width

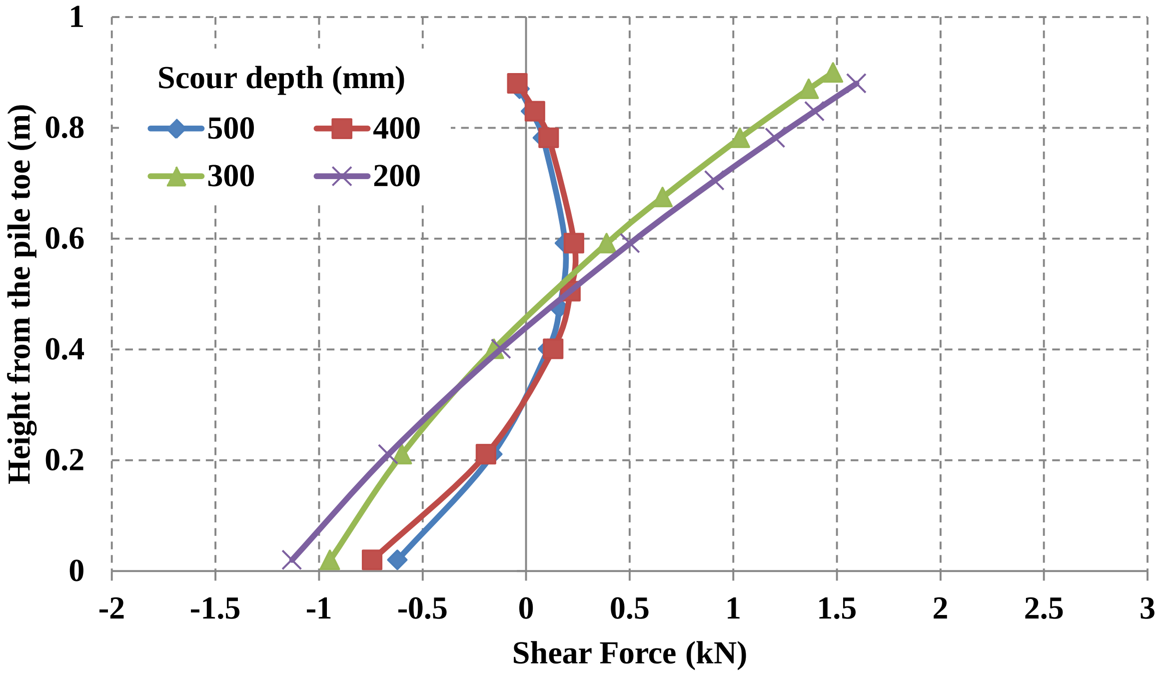

Figure 5.55 Effect of Scour Depth on the Shear Force Profiles along for the Pile with 667-mm Scour Width

Figure 5.56 shows the relation between the ultimate lateral load capacity ratio with and without scour and the ratio of the scour depth to the pile diameter for each ratio of the scour width to the pile diameter. It is shown that the lateral capacity ratio decreased with an increase of the scour depth to pile diameter ratio and the scour width to pile diameter ratio.

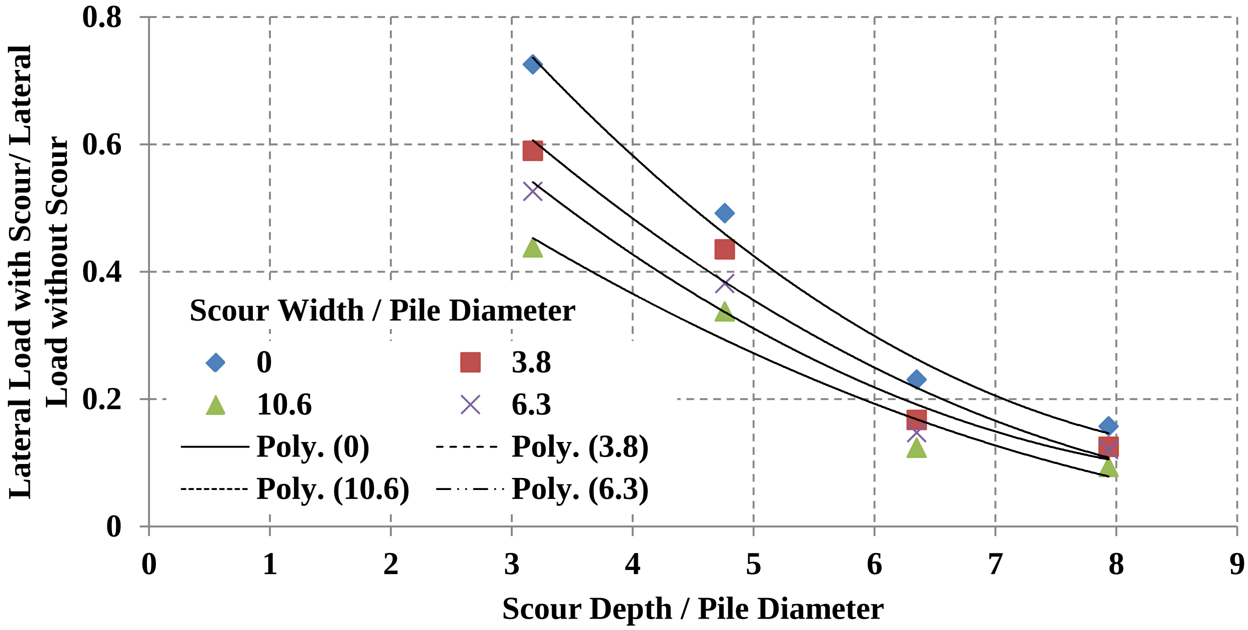

Figure 5.56 Ultimate Lateral Load Capacity Ratio verses the Ratio of the Scour Depth to the Pile Diameter for Each Ratio of the Scour Width to the Pile Diameter

Scour width

The effect of scour width is presented below at four different scour depths: 200, 300, 400, and 500 mm.

200-mm scour depth. Figures 5.57, 5.58, 5.59, and 5.60 present the effect of the scour width on the lateral load-displacement curves and the moment, lateral displacement, and shear force profiles along the pile with 200-mm scour depth respectively. These figures show the increased scour width decreased the lateral displacement because of the reduction in the soil resistance around the pile due to the decreased soil confinement. The maximum moment decreased with an increase of the scour width. The lateral displacement profiles along the pile were nearly linear. It is also shown that changing the scour width resulted in a similar behavior of the shear force profiles.

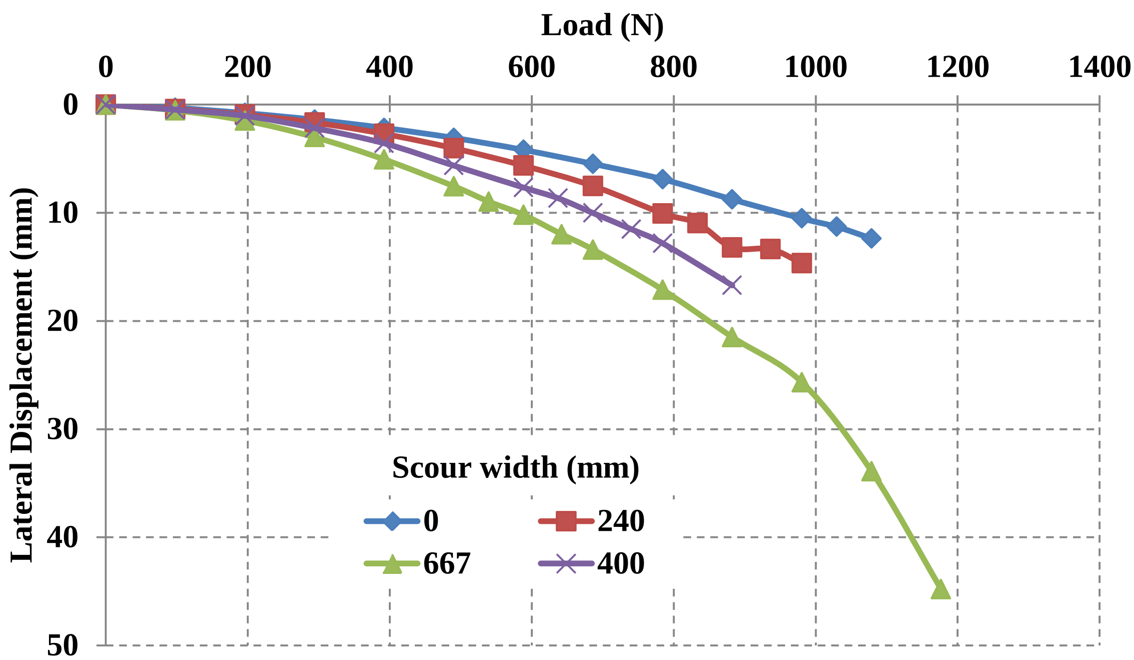

Figure 5.57 Effect of Scour Width on the Load-Lateral Displacement Curves for the Pile with 200-mm Scour Depth

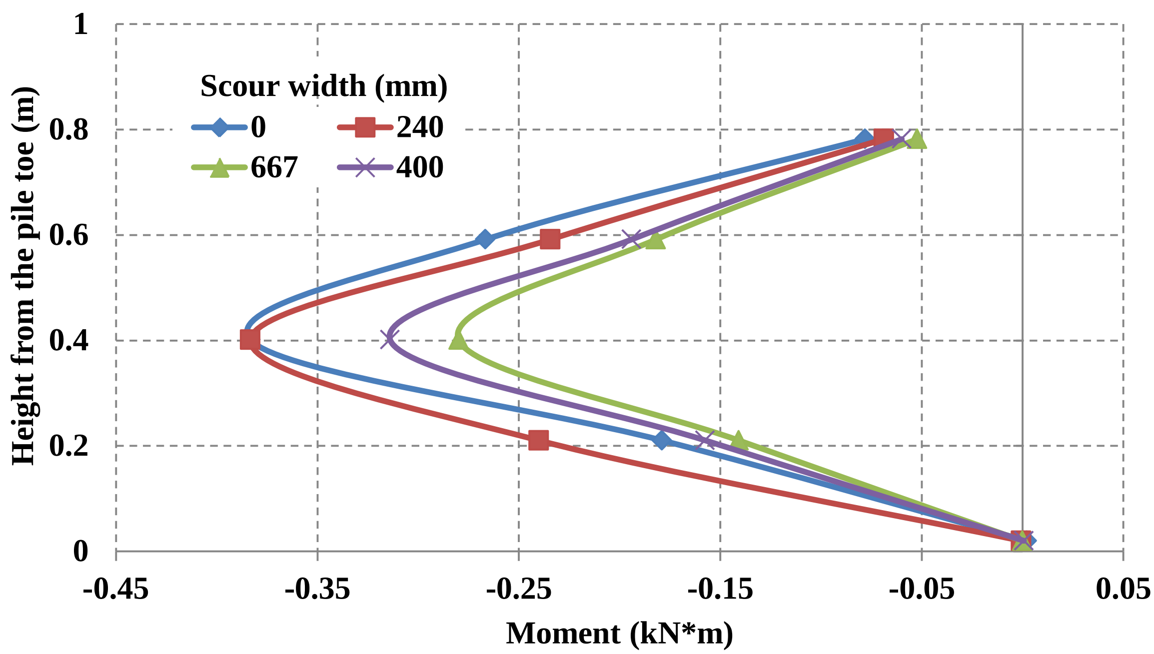

Figure 5.58 Effect of Scour Width on the Moment Profiles along for the Pile with 200-mm Scour Depth

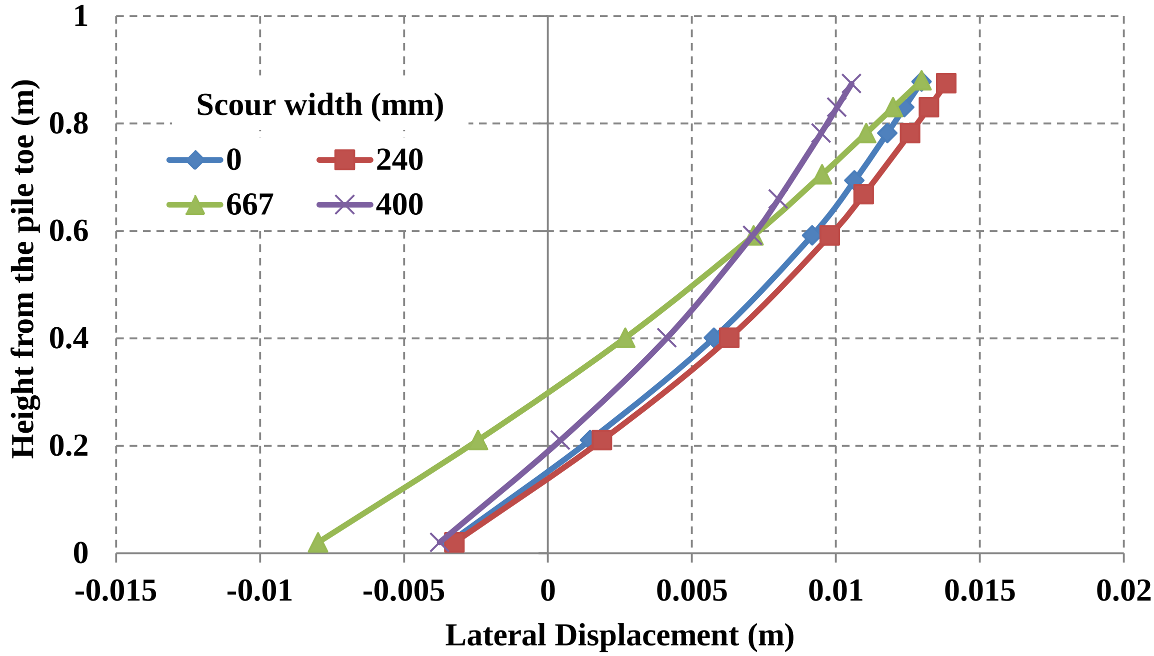

Figure 5.59 Effect of Scour Width on the Lateral Displacement Profiles along for the Pile with 200-mm Scour Depth

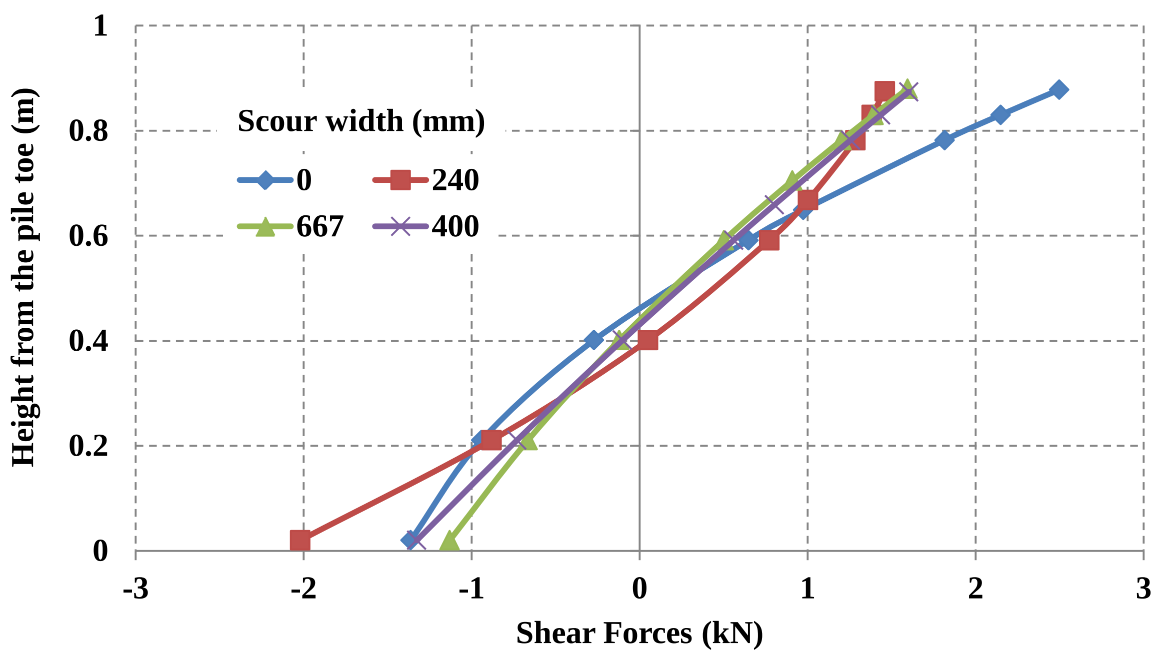

Figure 5.60 Effect of Scour Width on the Shear Force Profiles along for the Pile with 200-mm Scour Depth

300-mm scour depth. Figures 5.61, 5.62, 5.63, and 5.64 present the effect of the scour width on the lateral load-displacement curves and the moment, lateral displacement, and shear force profiles along the pile with 300-mm scour depth respectively. These figures show similar behavior as shown in Figures 5.57, 5.58, 5.59, and 5.60.

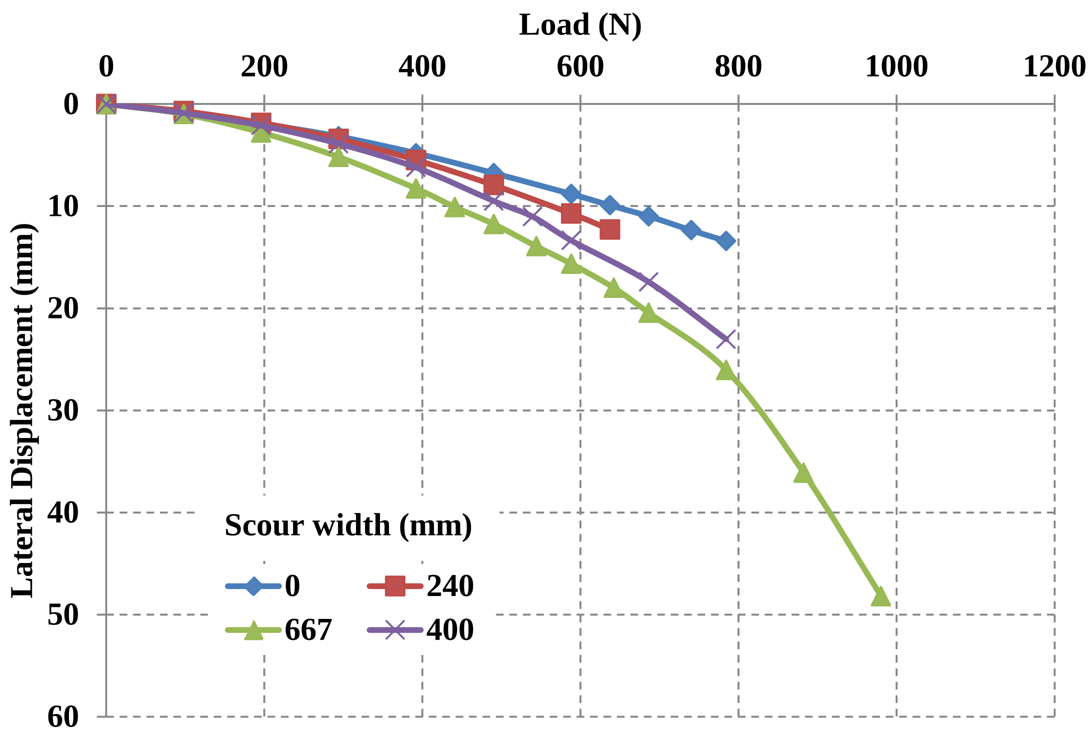

Figure 5.61 Effect of Scour Slope on the Load-Lateral Displacement Curves for the Pile with 300-mm Scour Depth

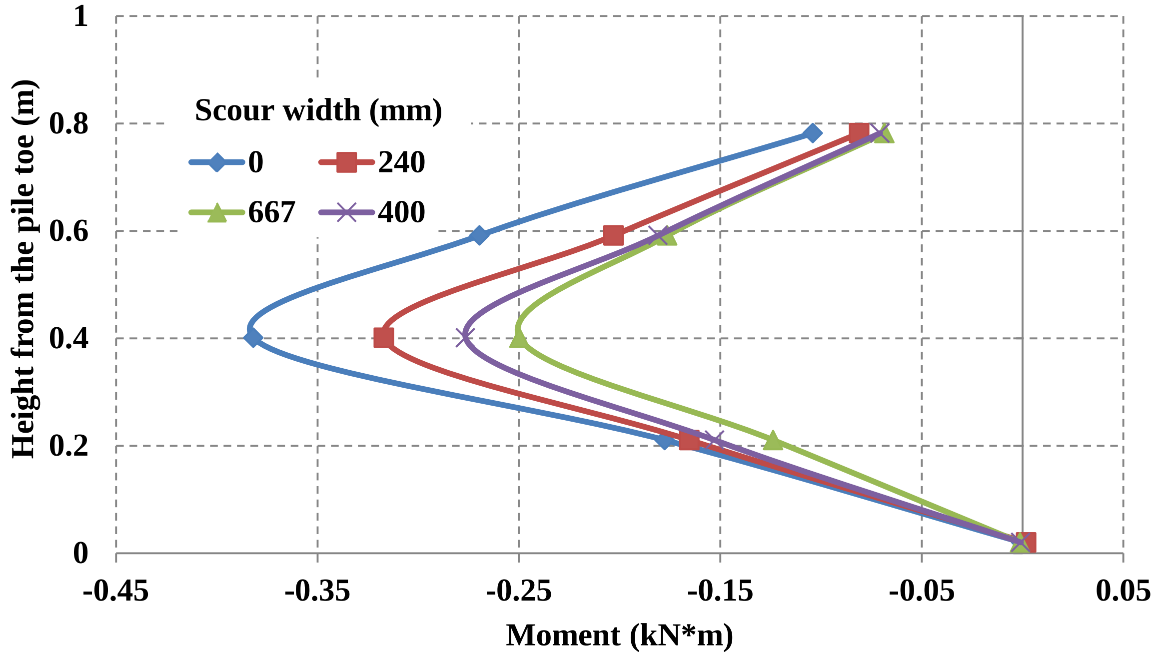

Figure 5.62 Effect of Scour Slope on the Moment Profiles along for the Pile with 300-mm Scour Depth

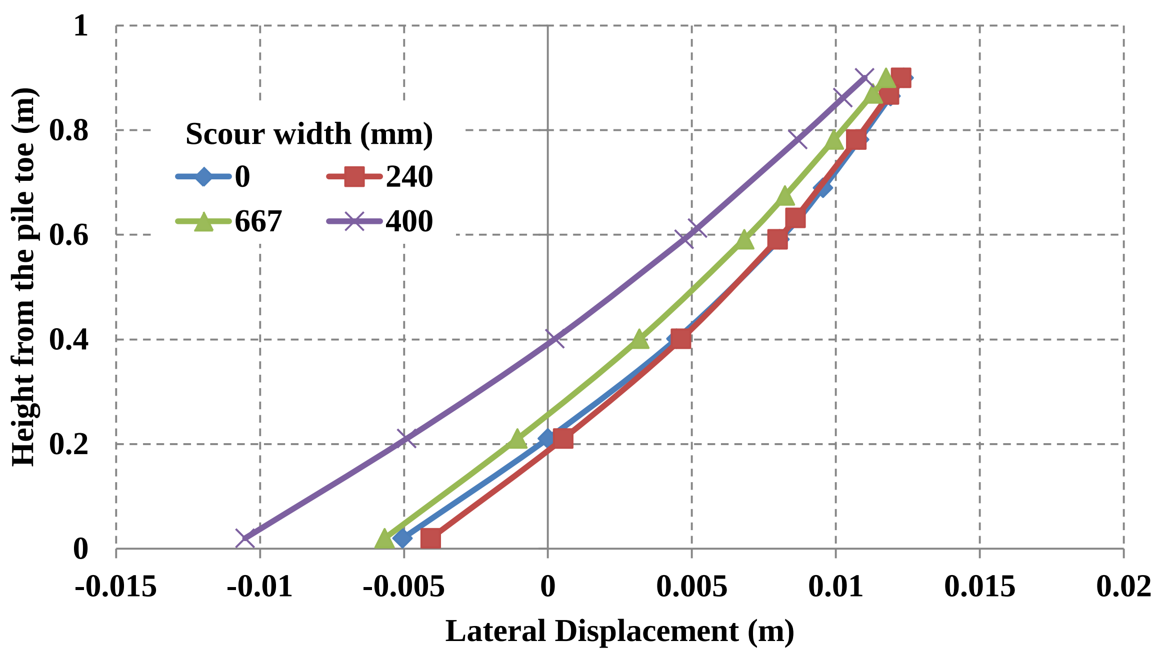

Figure 5.63 Effect of Scour Slope on the Lateral Displacement Profiles along for the Pile with 300-mm Scour Depth

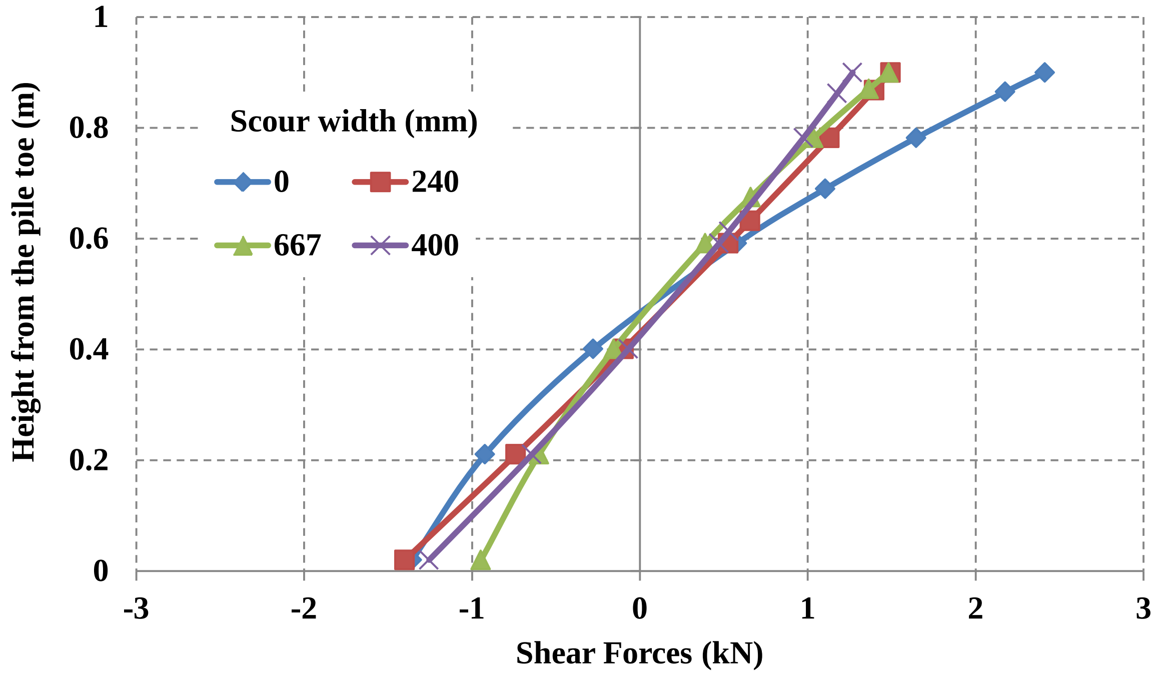

Figure 5.64 Effect of Scour Slope on the Shear Force Profiles along for the Pile with 300-mm Scour Depth

400-mm scour depth. Figures 5.65, 5.66, 5.67, and 5.68 present the effect of the scour width on the lateral load-displacement curves and the moment, lateral displacement, and shear force profiles along the pile with 400-mm scour depth respectively. These figures show the increased scour width decreased the lateral displacement because of the reduction in the soil resistance around the pile due to the decreased soil confinement. The maximum moment decreased and went towards the pile toe with an increase of the scour width. The lateral displacement profiles along the pile were nearly linear. It is also shown that changing the scour width resulted in a similar behavior of the shear force profiles.

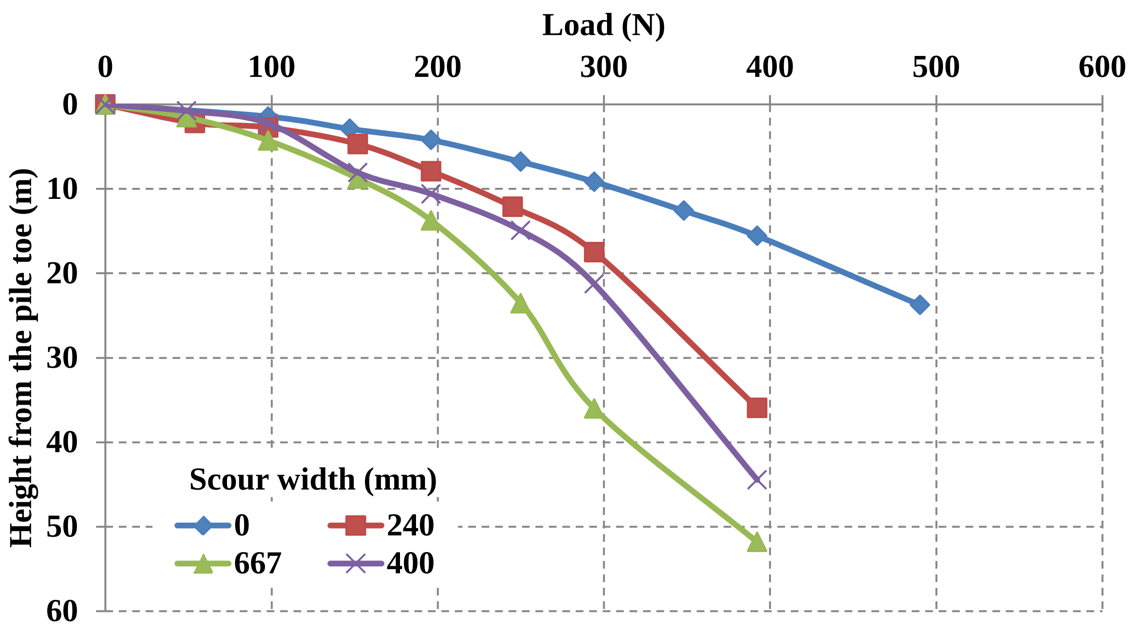

Figure 5.65 Effect of Scour Slope on the Load-Lateral Displacement Curves for the Pile with 400-mm Scour Depth

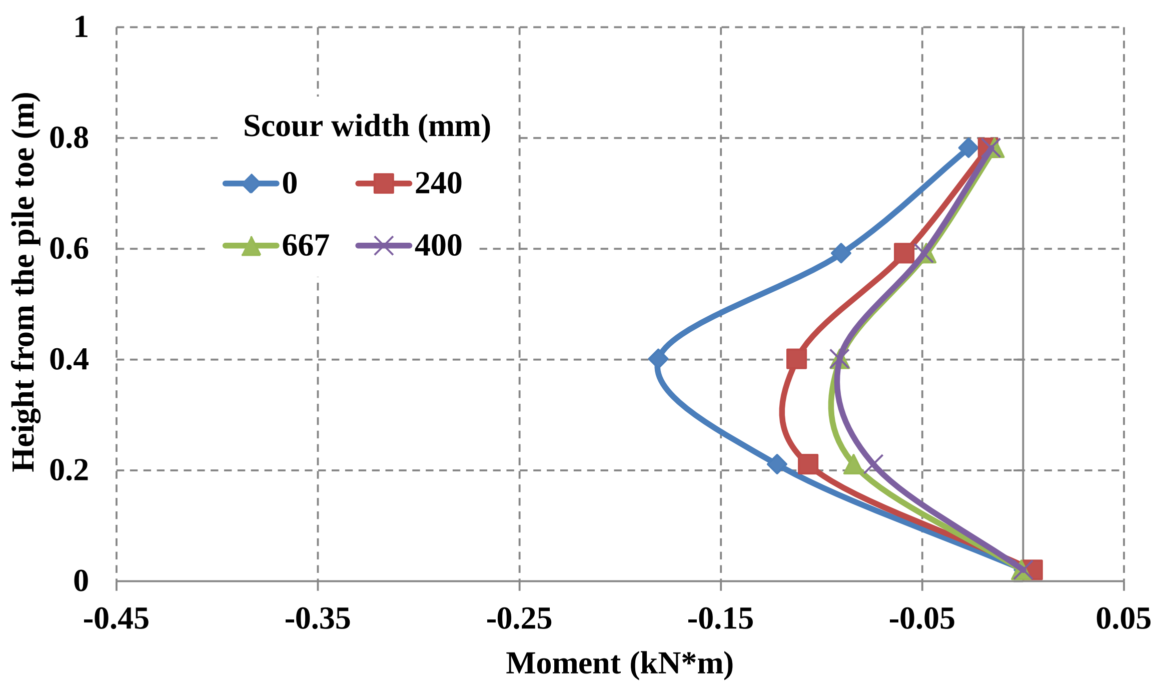

Figure 5.66 Effect of Scour Slope on the Moment Profiles along for the Pile with 400-mm Scour Depth

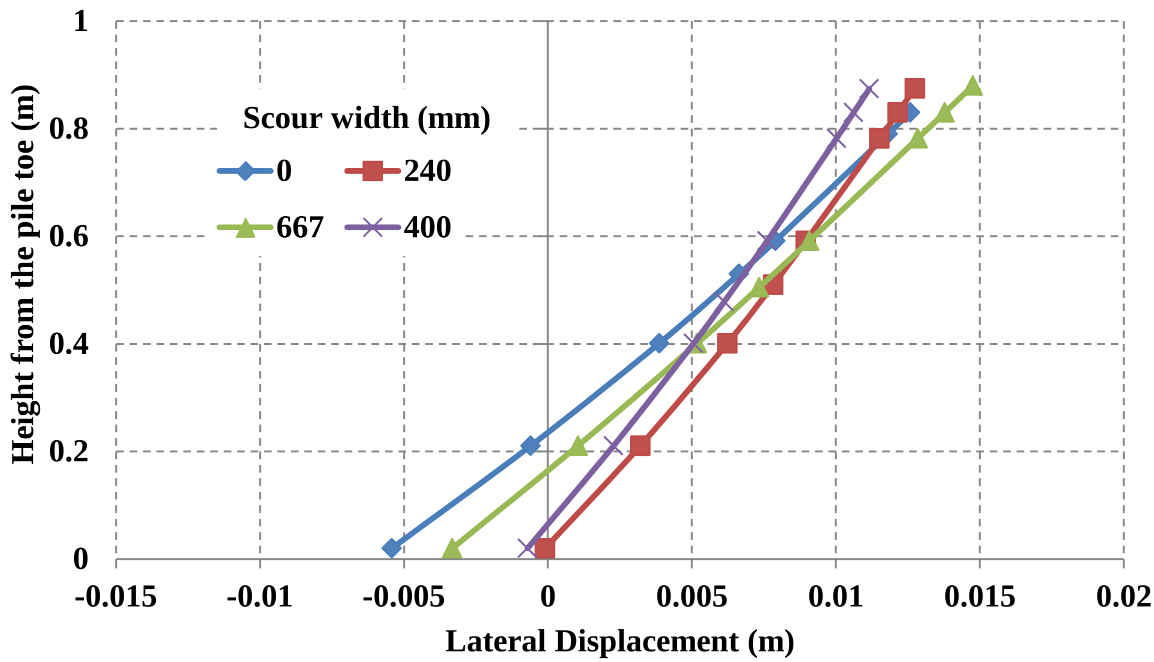

Figure 5.67 Effect of Scour Slope on the Lateral Displacement Profiles along for the Pile with 400-mm Scour Depth

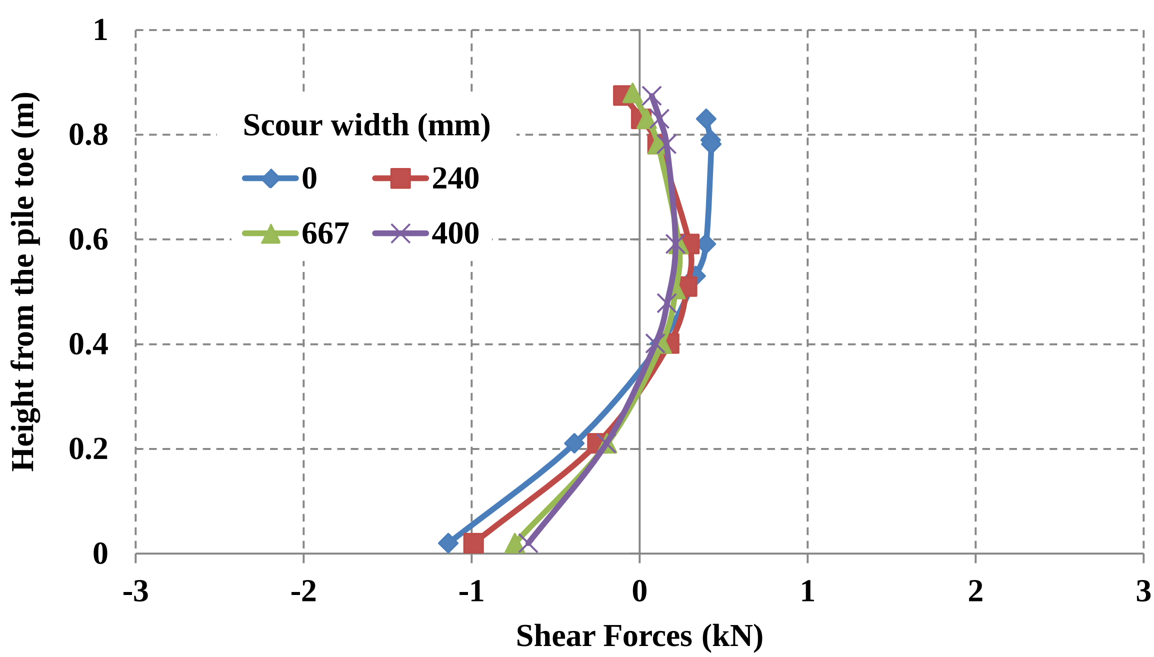

Figure 5.68 Effect of Scour Slope on the Shear Force Profiles along for the Pile with 400-mm Scour Depth

500-mm scour depth. Figures 5.69, 5.70, 5.71, and 5.72 present the effect of the scour width on the lateral load-displacement curves and the moment, lateral displacement, and shear force profiles along the pile with 500-mm scour depth respectively. These figures show similar behavior as shown in Figures 5.65, 5.66, 5.67, and 5.68.

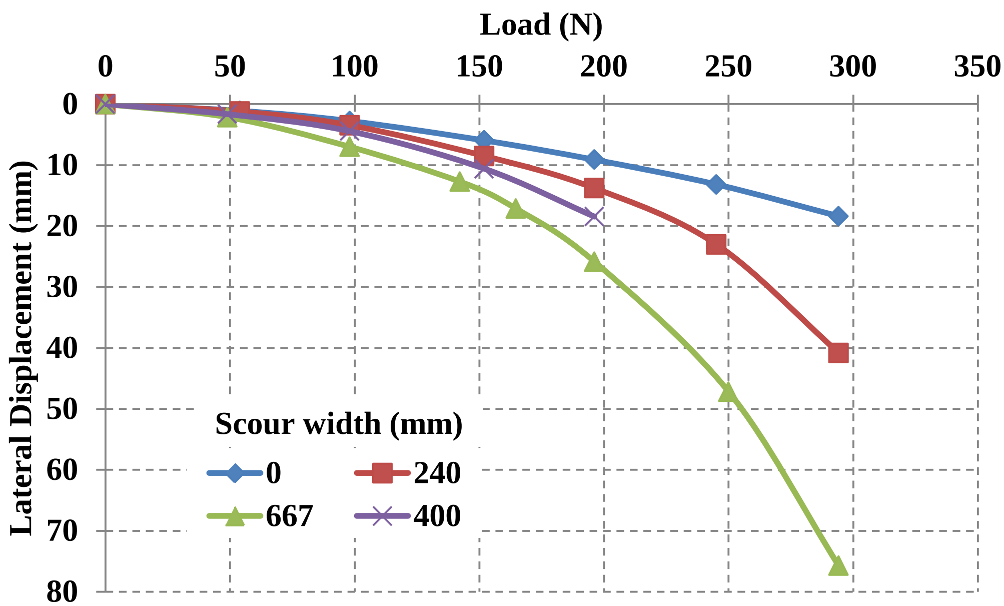

Figure 5.69 Effect of Scour Slope on the Load-Lateral Displacement Curves for the Pile with 500-mm Scour Depth

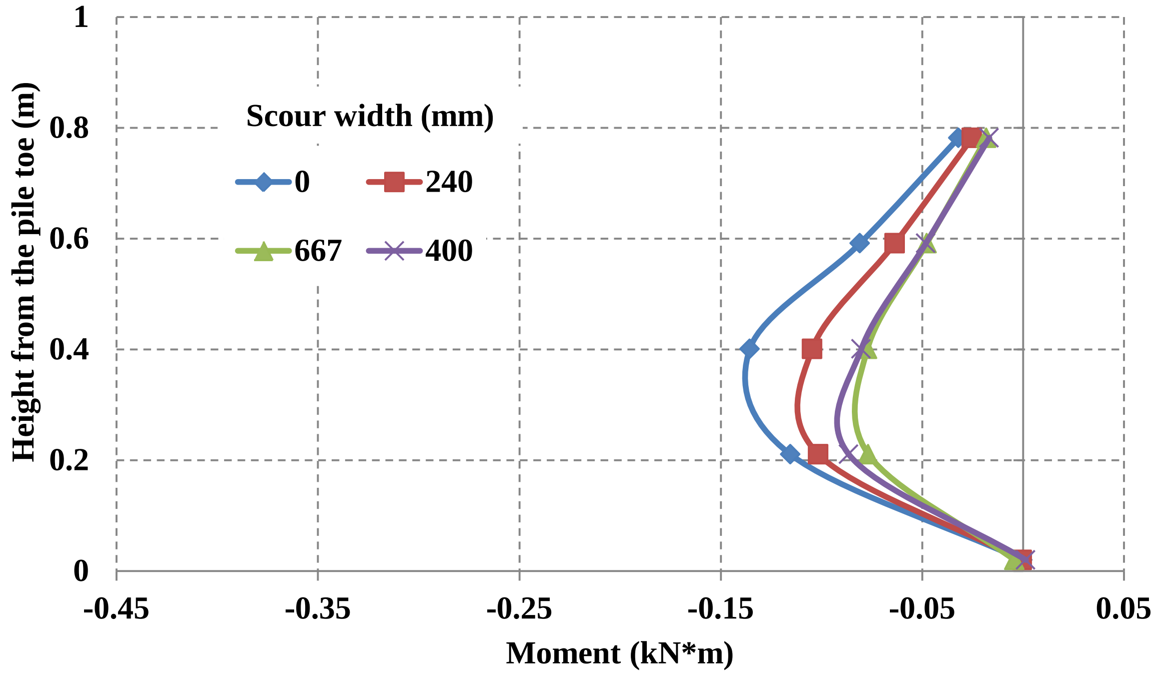

Figure 5.70 Effect of Scour Slope on the Moment Profiles along for the Pile with 500-mm Scour Depth

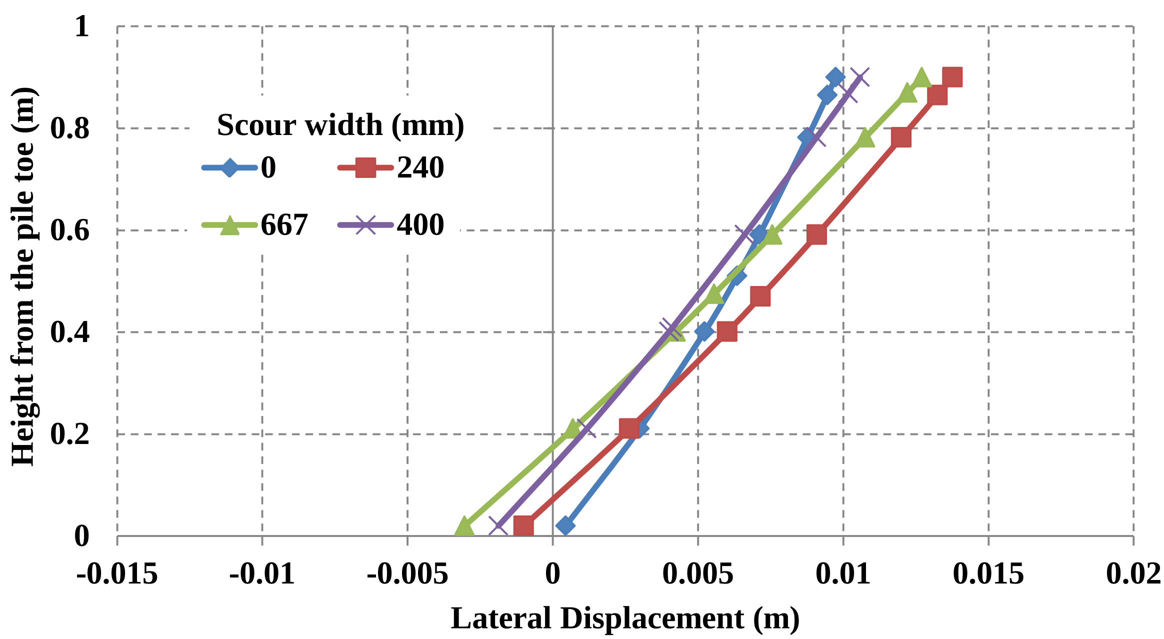

Figure 5.71 Effect of Scour Slope on the Lateral Displacement Profiles along for the Pile with 500-mm Scour Depth

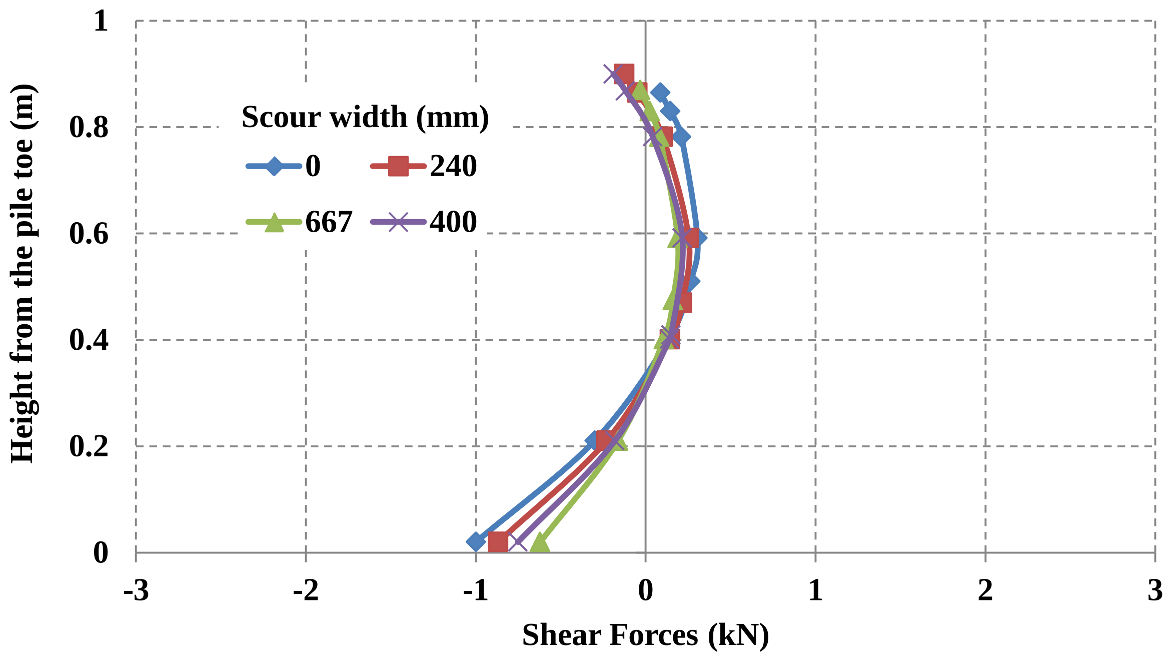

Figure 5.72 Effect of Scour Slope on the Shear Force Profiles along for the Pile with 500-mm Scour Depth

Figure 5.73 compares the effect of the scour width on the ultimate lateral load capacity of the pile for each scour depth. It is shown that the ratio of lateral load capacity without scour to that with scour decreased with an increase of the scour width to pile diameter ratio and the scour depth to pile diameter ratio.

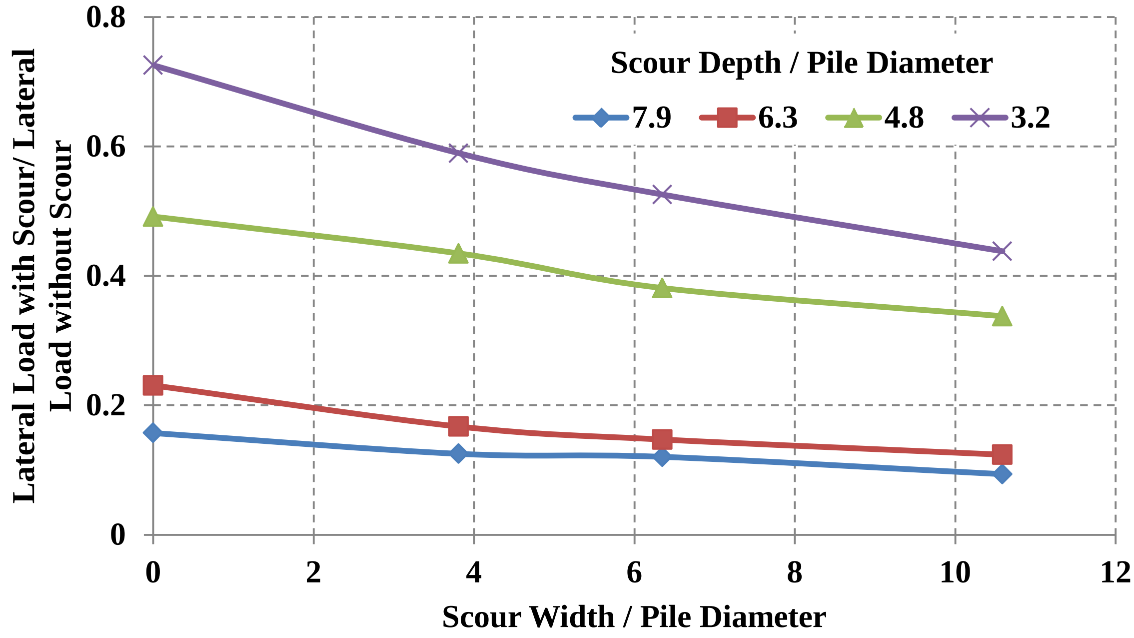

Figure 5.73 Ultimate Lateral Load Capacity Ratio verses the Ratio of Scour Width to the Pile Diameter for Each Ratio of the Scour Depth to the Pile Diameter

5.6. Analysis of Repeated Loading Test Results

This section evaluates the effect of scour depth, scour slope, and scour width on the behavior of the laterally loaded pile under repeated loading.

5.6.1. Scour depth effect

Two model pile tests were conducted with scour depths of 200 mm and 400 mm. In these tests, the scour width was 667 mm and the scour slope was 0 degree. The magnitude of load applied on the pile with the scour depth of 200 mm was 294 N while that with the scour depth of 400 mm was 98 N. Figure 5.74 presents the effect of the scour depth on the lateral displacement with the number of repeated load. It is also shown that the lateral displacement decreased with an increase of the scour depth because the lateral load capacity decreased due to the increase of the scour depth. Furthermore, it is shown that the lateral displacements deceased with the number of repeated load because of the soil densification after the load application (two-way repeated loading).

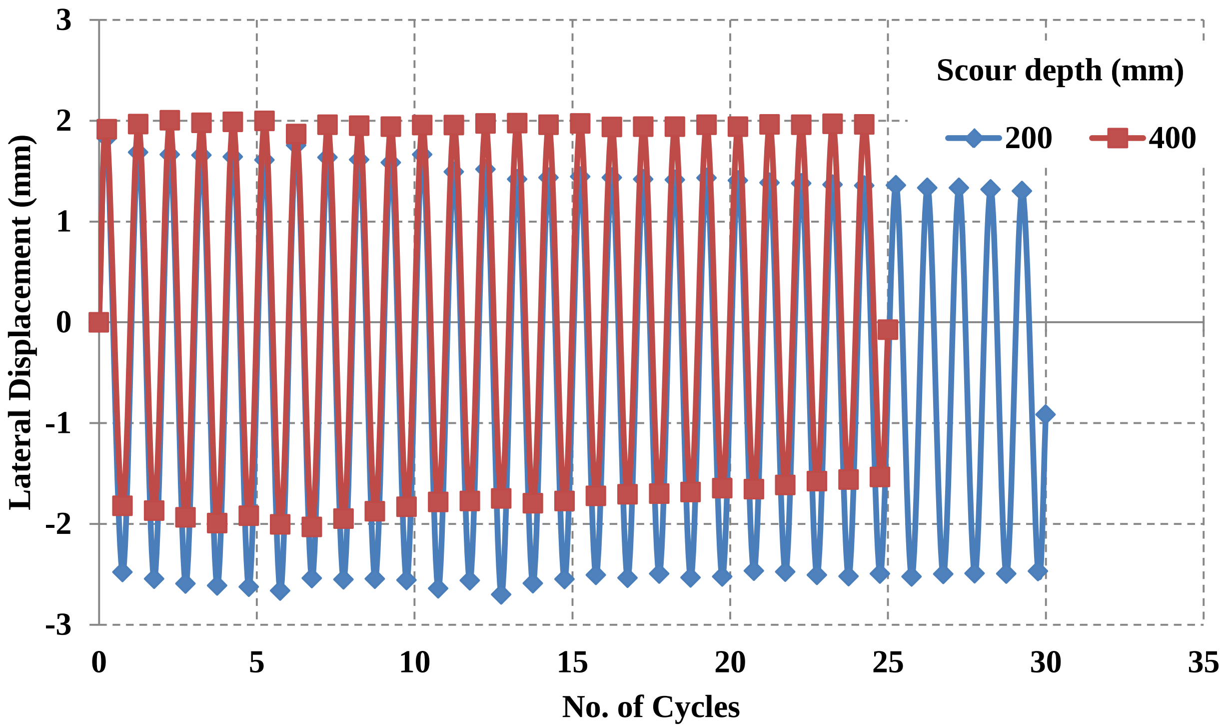

Figure 5.74 Scour Depth Effect on the Cyclic Behavior of the Laterally Loaded Pile

5.6.2. Scour slope effect

Two model pile tests were conducted with scour slopes of 0 and 30 degrees. In these tests, the scour depth was 200 mm and the scour widths were 667 and 0 mm respectively. The magnitude of load applied on the pile with the scour slope of 0^{o} was 294 N while that with the scour slope of 30^{o} was 441 N. Figure 5.75 presents the effect of the scour slope on the lateral displacement with the number of repeated load. It is also shown that the lateral displacement increased with an increase of the scour depth because of the increase in the soil confinement as the scour slope increased. Furthermore, it is shown that the lateral displacements deceased with the number of repeated load because of the soil densification after the load application (two-way repeated loading).

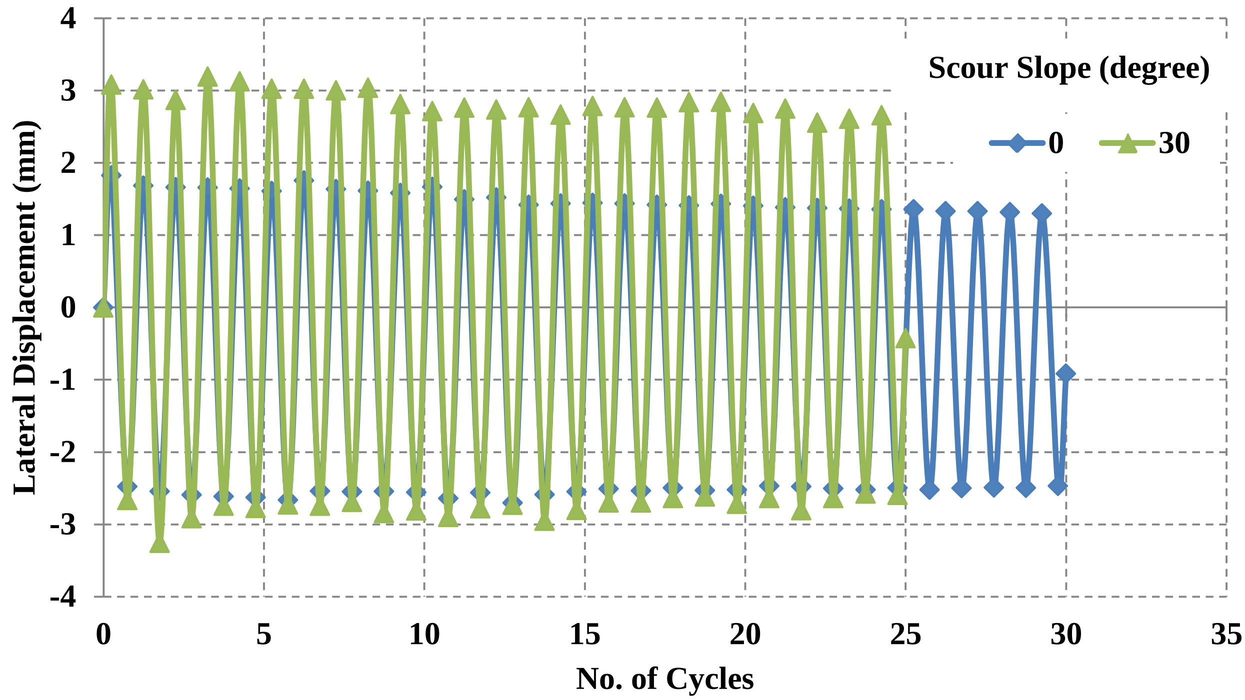

Figure 5.75 Scour Slope Effect on the Cyclic Behavior of the Laterally Loaded Pile

5.6.3. Scour width effect

Two model pile tests were conducted with scour widths of 0 and 667 mm. In these tests, the scour depth was 200 and the scour slope was 30 degrees. The magnitude of load applied on the pile with the scour width of 0 was 441 N while that with the scour width of 667 mm was 294 N. Figure 5.76 presents the effect of the scour width on the lateral displacement with the number of repeated load. It is also shown that the lateral displacement decreased with an increase of the scour width because the lateral load capacity decreased due to the increase of the scour width. Furthermore, it is shown that the lateral displacements deceased with the number of repeated load because of the soil densification after load application (two-way repeated loading).

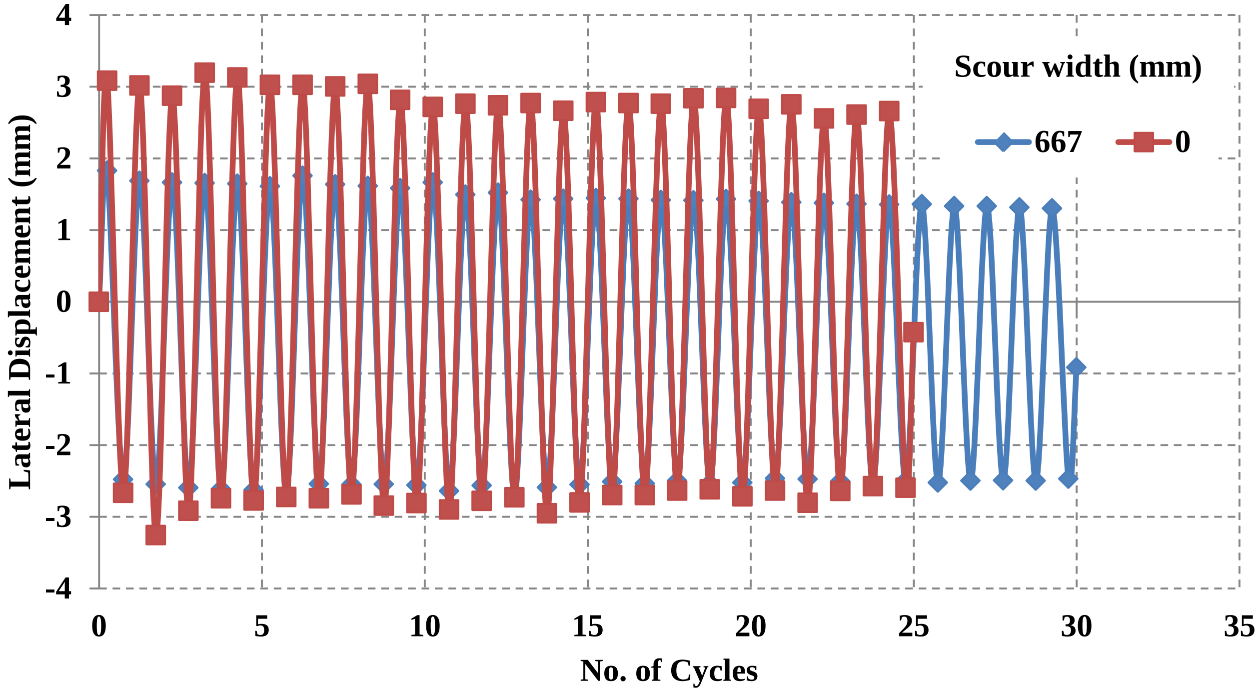

Figure 5.76 Scour Width Effect on the Cyclic Behavior of the Laterally Loaded Pile

Chapter Six

Conclusions and Recommendations

6.1. Introduction

Totally 41 model pile tests were conducted in this study to investigate the behavior of laterally loaded piles in dry sand under scoured conditions. Section 6.2 summarizes the test results with conclusions on the effect of the pile toe distance on the behavior of the laterally loaded pile. Section 6.3 summarizes the test results from the static loading tests with conclusions on the effects of scour depth, scour width, and scour slope on the behavior of laterally loaded piles. Section 6.4 summarizes the test results from the repeated loading tests with conclusions on the effects of scour depth, scour width, and scour slope on the behavior of laterally loaded piles. Section 6.5 presents the recommendations for future work on this research topic.

6.2. Effect of Pile Toe Distance

- Test results show that the distance between the pile toe and the box base had a minor effect on the behavior of the laterally-loaded pile, including the lateral displacement, the moment, and the shear force along the pile.

6.3. Static Loading Tests

6.3.1 Horizontal scour

- Test results show that the increase of scour depth significantly reduced the ultimate load capacity of a laterally loaded pile. The reduction of the ultimate load capacity of the pile resulted from the loss in the confinement around the pile as the scour depth increased.

- A relationship developed in this study indicates that the ultimate lateral load capacity ratio with scour decreased with the scour depth to pile diameter ratio
- Broms' method for a short (rigid) pile in sand well predicted the ultimate lateral load capacity of a pile as compared with the experimental data obtained from the model pile tests in this study.
- As the scour depth reached ½ the thickness of the soil layer, the ultimate lateral load capacity decreased to about 90% the ultimate lateral load capacity of the pile without scour.
- As the scour depth increased, the maximum moment and shear force at pile failure decreased because the ultimate load capacity decreased.
- As the scour depth increased, the maximum moment went towards the pile toe and the maximum shear force transferred from a positive value at the point where the load acted to the negative value at the toe of the pile.

6.3.2. Sloped scour

- At the same scour depth, as the scour slope increased, the ultimate lateral load capacity of the pile increased because the soil confinement around the pile increased as the scour slope increased.
- At the same scour depth, as the scour slope increased, the maximum moment and the shear force at the pile failure increased.
- At the same scour slope, as the scour depth increased, the ultimate lateral load capacity of the pile decreased due to the loss of the confinement around the pile.

- At the same scour slope, as the scour depth increased, the maximum moment and shear force at the pile failure decreased.
- A relationship between the ultimate lateral load capacity ratio with and without scour and the scour depth to pile diameter ratio at different scour slopes was established based on the model test results.

6.3.3. Scour Width

- At the same scour depth, as the scour width increased, the ultimate lateral load capacity of the pile decreased due to the loss of the soil confinement around the pile.
- At the same scour depth, as the scour width increased, the maximum moment and shear force at the pile failure decreased.
- At the same scour width, as the scour depth increased, the ultimate lateral load capacity of the pile decreased due to the loss of the soil confinement around the pile.
- At the same scour width, as the scour depth increased, the maximum moment and shear force at pile failure decreased.
- A relationship between the ultimate lateral load capacity ratio with and without scour and the scour width to pile diameter ratio at different scour depths was established based on the model test results.
- A relationship between the ultimate lateral load capacity ratio with and without scour and the scour depth to pile diameter ratio at different scour widths was established based on the model test results.
- The results show that changing the scour width had a minor effect on the shear force profiles along the pile with a constant scour depth.

6.4. Repeated Loading Tests

- As the scour depth increased, the lateral displacement at the point where the load acted decreased because of the soil densification around the pile by applying the repeated loads (two-way repeated loading).
- As the scour slope decreased, the lateral displacement at the point where the load acted decreased because of the soil densification around the pile by applying the repeated loads (two-way repeated loading).
- As the scour width decreased, the lateral displacement at the point where the load acted decreased because of the soil densification around the pile by applying the repeated loads (two-way repeated loading).
- As the number of the repeated loading increased, the lateral displacement decreased slightly for each cycle. This reduction in the lateral displacement resulted from the soil densification by applying the repeated loading (two-way repeated loading).

6.5. Future Work

This research was focused on static loading tests. More pile model tests need to be done on repeated loading tests to understand the behavior of the laterally loaded piles under repeated loading to account for the effects of scour depth, scour slope, and scour width. The test results obtained in this research should be verified by large-scale or field tests and numerical analyses.

Referances

Broms, B. B. (1964). Lateral Resistance of Piles in Cohesionless Soils. *ASCE Journal of the Soil Mechanics and Foundation Division*, *90*(SM3, Part 1), 123-156.

Brown, D. A., Morrison, C., & Reese, L. C. (1988). Lateral load behavior of pile group in sand. *Journal of Geotechnical Engineering*, *114*(11), 1261-1276.

Institute for Hydromechanics (IfH). Hydrulic Channel, Bridge Piers, Iran. *http://www.ifh.uni-karlsruhe.de/lehre/gerinnehydraulik/Diashow/dia_C1.htm*.

Khatri, D. K. (2012), *Laboratory Evaluation of the Behavior of Steel-Reinforced High Density Polyethylene (SRHDPE) Pipes*. Master's Thesis, the University of Kansas.

Kishore, Y. N., Rao, S. N., & Mani, J. (2008). *Influence of the Scour on Laterally Loaded Piles.* Paper presented at the The 12th International Conference of International Association for Computer Methods and Advances in Geomechanics.

Lagasse, P. F., Clopper, P. E., Zevenbergen, L. W., & Girard, L. G. (2007). Countermeasures to protect bridge piers from scour *NCHRP Report 593*. ,National cooperative highway research program: Transportation Research Board of The National Academies, Washington, D.C.

Laursen, E. M. (1963). Analysis of Relief Bridge Scour. *Journal of Hydraulic Divison, ASCE, 89*(3), 93-118.

Lee, J., Kyung, D., Hong, J., & Kim, D. (2011). Experimental investigation of laterally loaded piles in sand under multilayered conditions. *Soils & Foundations, 51*(5), 915-927.

Lin, C. (2012). *Evaluation of Lateral Behavior of Pile-Supported Bridges under Scour Conditions.* Ph.D. Dissertation, the University of Kansas.

Lin, C., Bennett, C., Han, J., & Parsons, R. L. (2010). Scour effects on the response of laterally loaded piles considering stress history of sand. *Computers and Geotechnics*, *37*(7), 1008-1014.

Long, J., & Vanneste, G. (1994). Effects of cyclic lateral loads on piles in sand. *Journal of Geotechnical Engineering, 120*(1), 225-244.

Melville, B. W., & Coleman, S. E. (2000). *Bridge scour*. Highlands Ranch (Colorado): Water Resources Publications, LCC.

Mostafa, Y. E. (2012). Effect of Local and Global Scour on Lateral Response of Single Piles in Different Soil Conditions. *Engineering*, *4*(6), 297-306.

Mueller, D. S. (1996). *Local Scour at Bridge Piers in Nonuniform Sediment Under Dynamic Conditions.* (Dissertation in partial fulfillment of the requirements for the Degree of Doctor of Philosophy), Colorado State University, Fort Collins, CO.

Ni, S.-H., Huang, Y.-H., & Lo, K.-F. (2011). Numerical Investigation of the Scouring Effect on the Lateral Response of Piles in Sand. *Journal of Performance of Constructed Facilities, 26*(3), 320-325.

Phanikanth, V., Choudhury, D., & Reddy, G. R. (2010). Response of single pile under lateral loads in cohesionless soils. *Electron. J. Geotech. Eng., USA, 15(H),* 813-830.

Raudkivi, A. (1986). Functional Trends of Scour at Bridge Piers. *Journal of Hydraulic Engineering, 112*(1), 1-13. doi: doi:10.1061/(ASCE)0733-9429(1986)112:1(1)

Richardson, E., & Davis, S. (2001). Evaluating Scour at Bridges . Federal Highway Administration, Hydraulic Engineering Circular No. 18. *Publication FHWA NHI*, 01-001.

Salini, U., & Girish, M. (2009). Lateral Load Capacity of Model Piles on Cohesionless Soil. *14 , Bund. P*.

Shen, H., Schneider, V., & Karaki, S. (1969). Local scour around bridge piers. *Journal of the Hydraulics Division, ASCE, 95*(HY6), 1919-1940.

Appendix A

Experimental Results

A.1. Introduction

This appendix includes the results from the analysis of the data of the experiments. Section A.2 presents the results for the experiments investigate the effect of pile toe distance. Section A.3 presents the results for the static loading experiments. Section A.4 presents the results for the repeated loading experiments.

A.2. Test data for pile toe distance effect

A.2.1. 0-mm pile toe distance

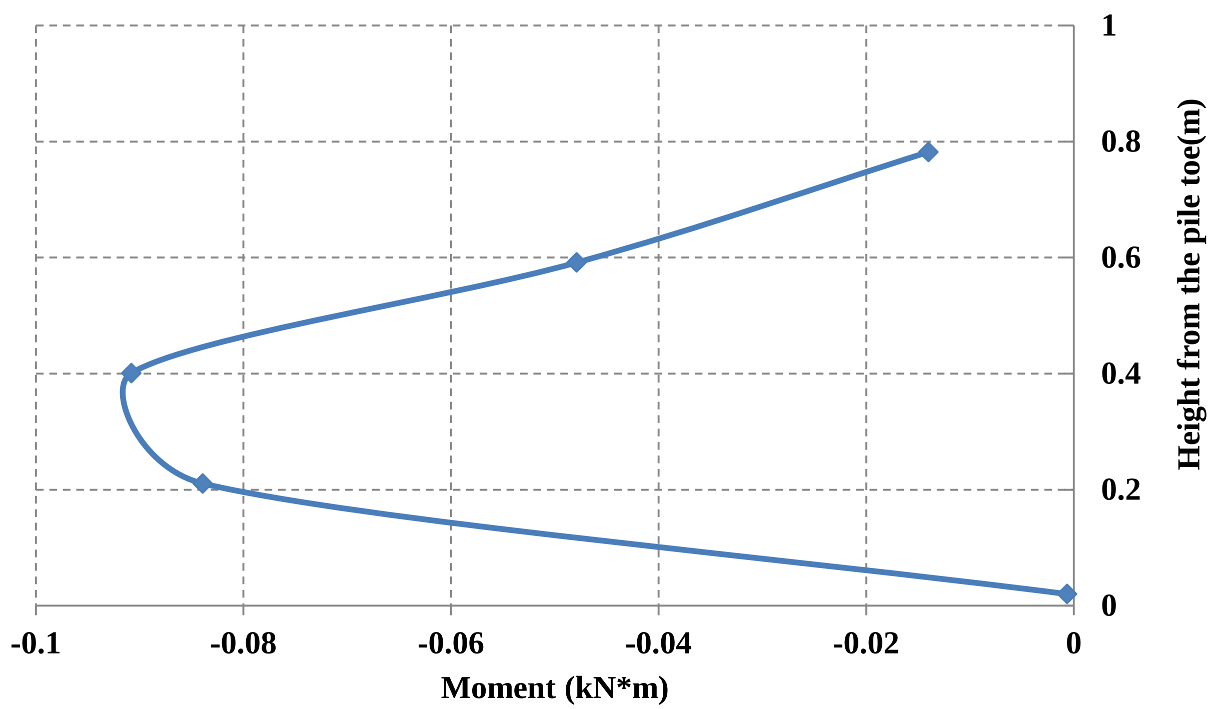

Figure A.1 Moment along the Pile for Toe Distance = 0 mm

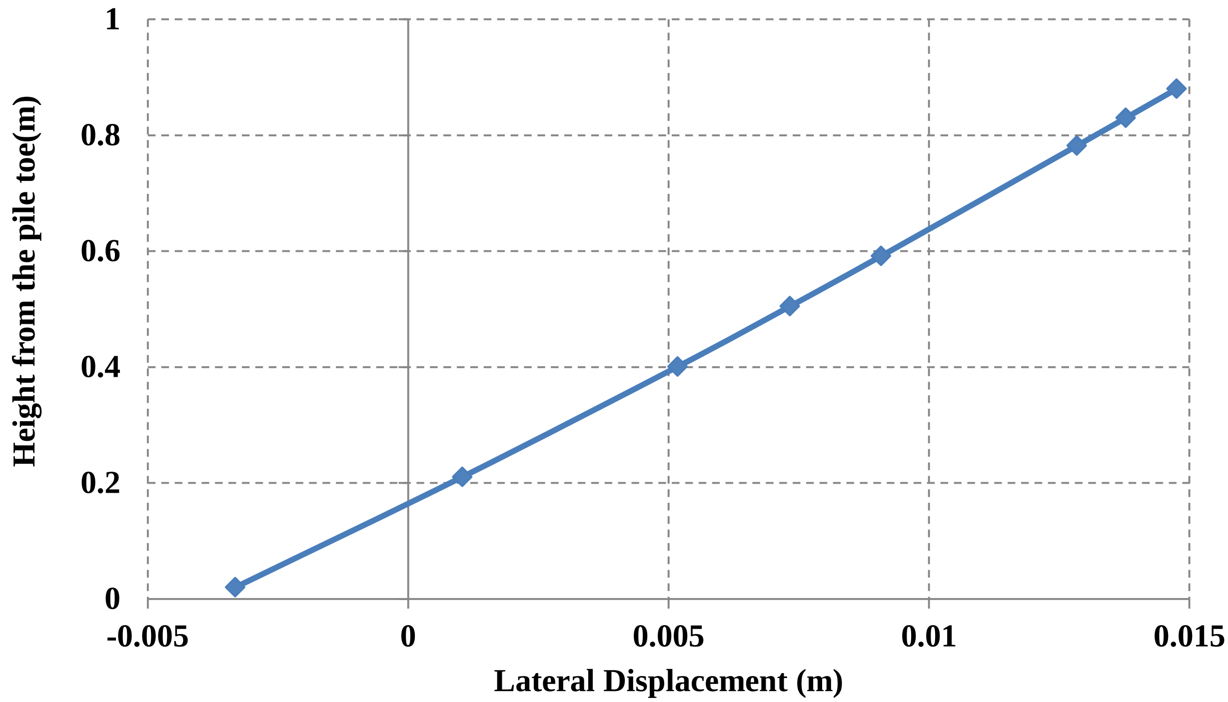

Figure A.2 Lateral Displacement along the Pile for Toe Distance = 0 mm

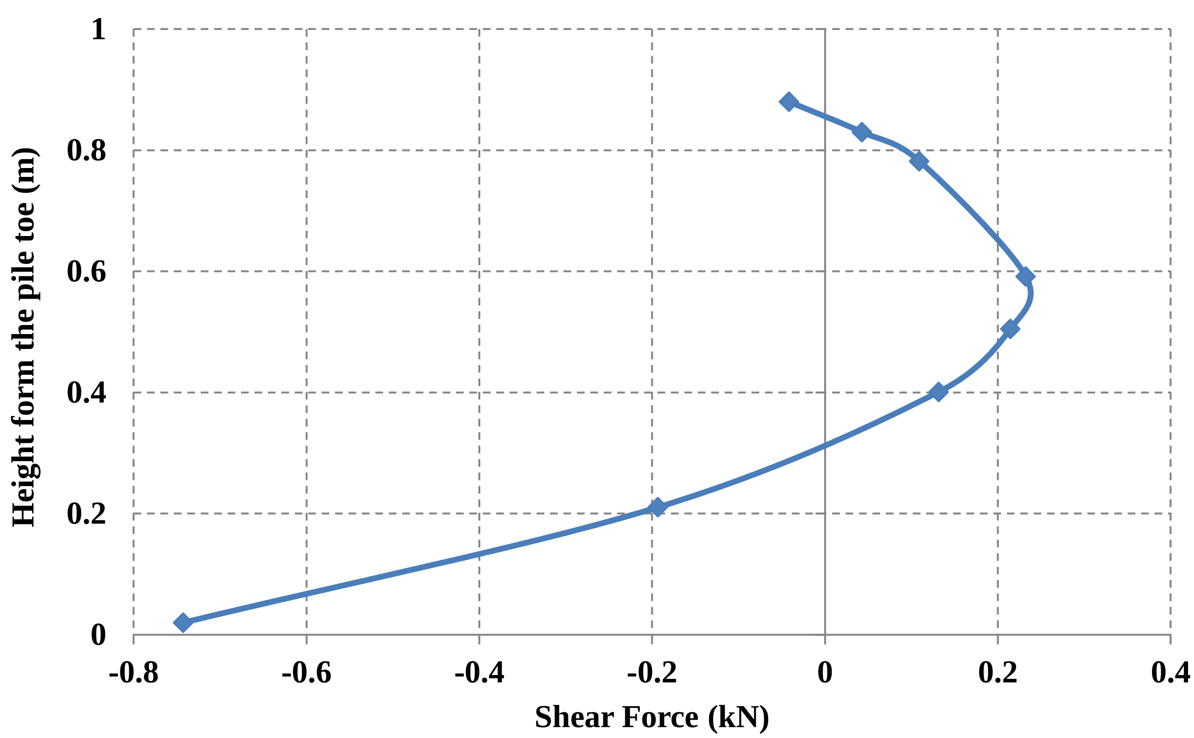

Figure A.3 Shear Force along the Pile for Toe Distance = 0 mm

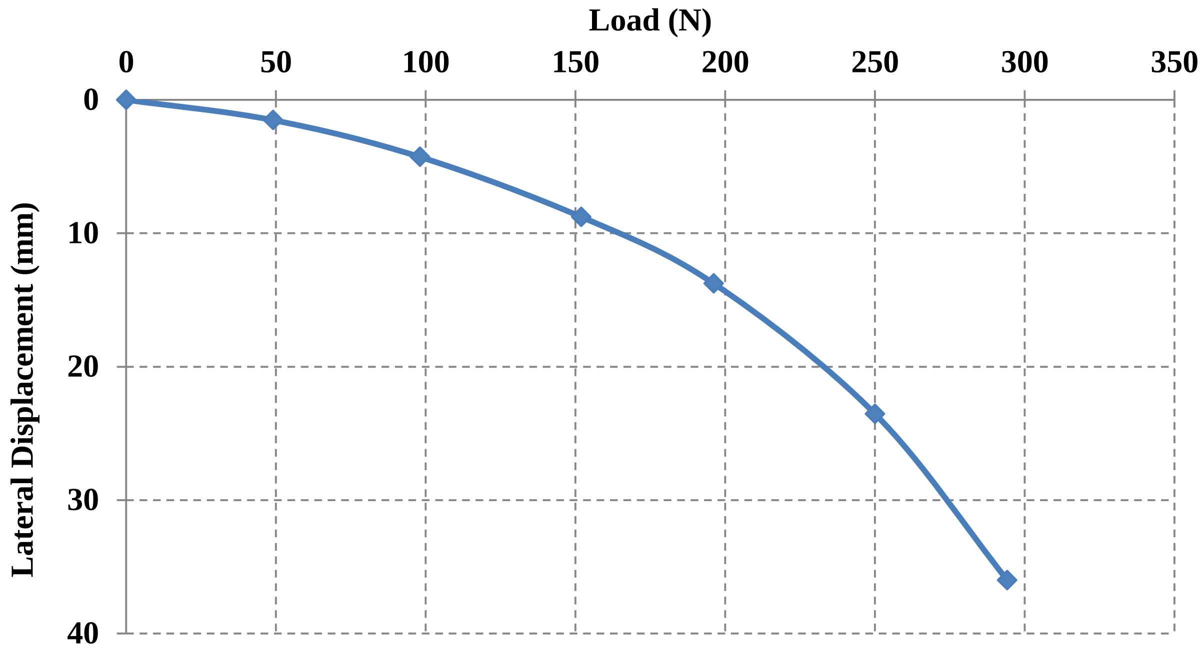

Figure A.4 Lateral Displacements vs. Load for Toe Distance = 0 mm

A.2.2. 50-mm pile toe distance

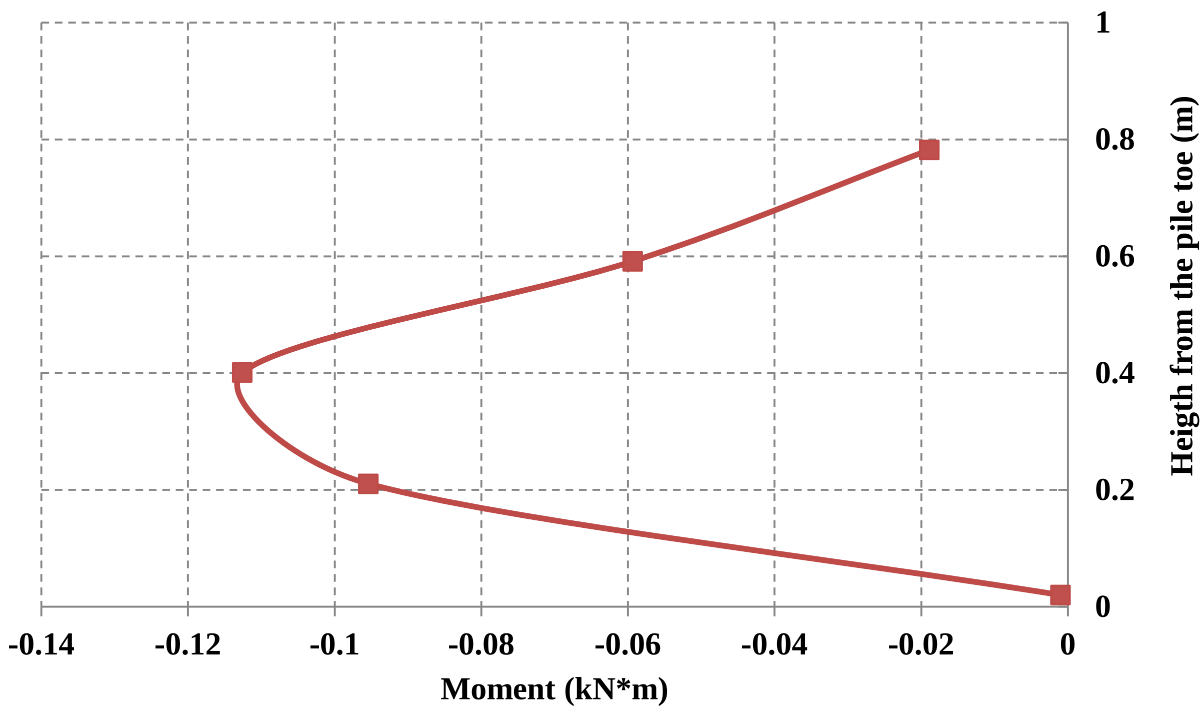

Figure A.5 Moment along the Pile for Toe Distance = 50 mm

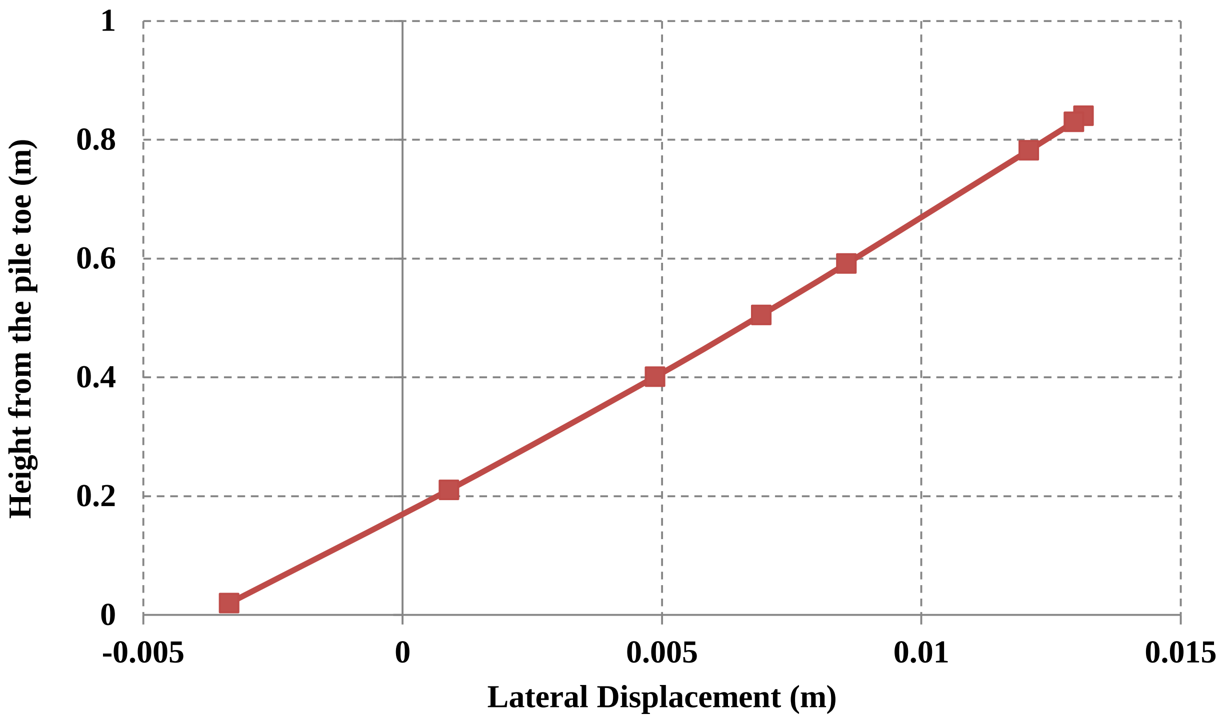

Figure A.6 Lateral Displacement along the Pile for Toe Distance = 50 mm

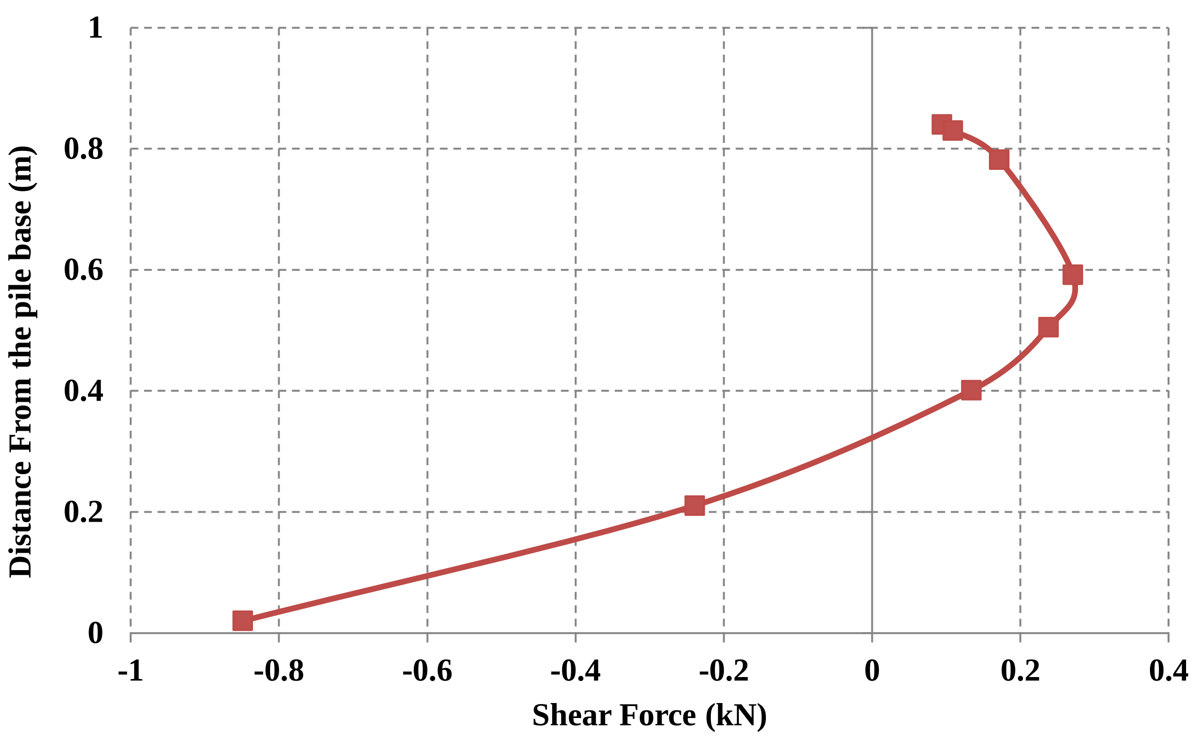

Figure A.7 Shear Force along the Pile for Toe Distance = 50 mm

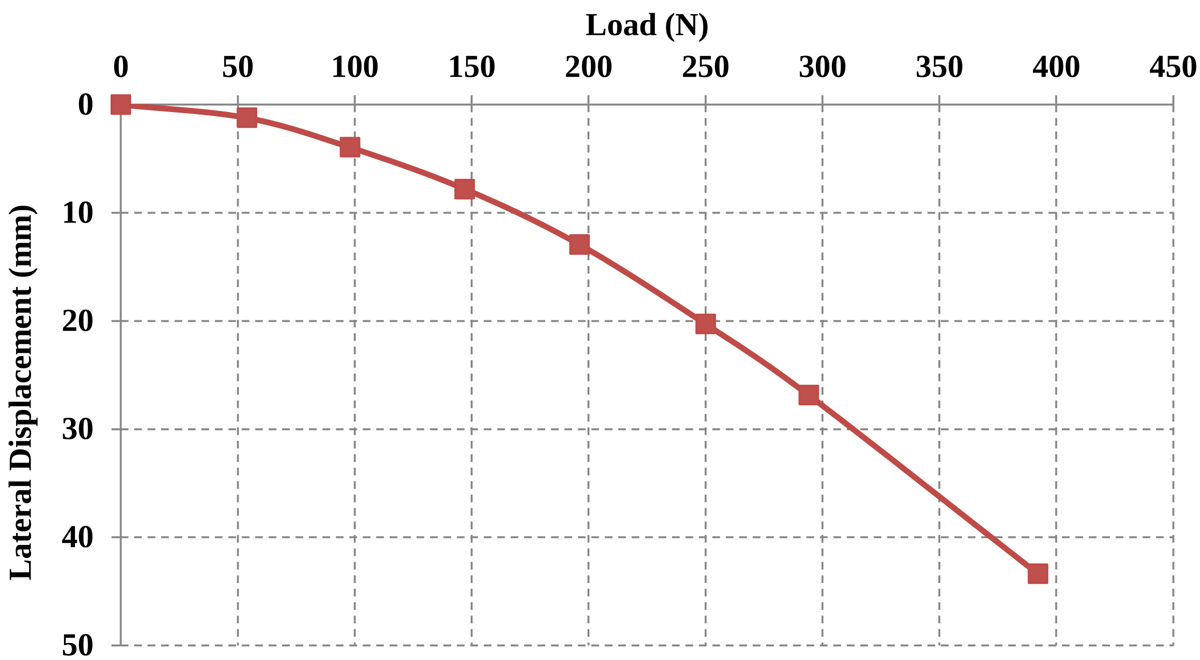

Figure A.8 Lateral Displacements vs. Load for Toe Distance = 50 mm

A.2.3. 100-mm pile toe distance

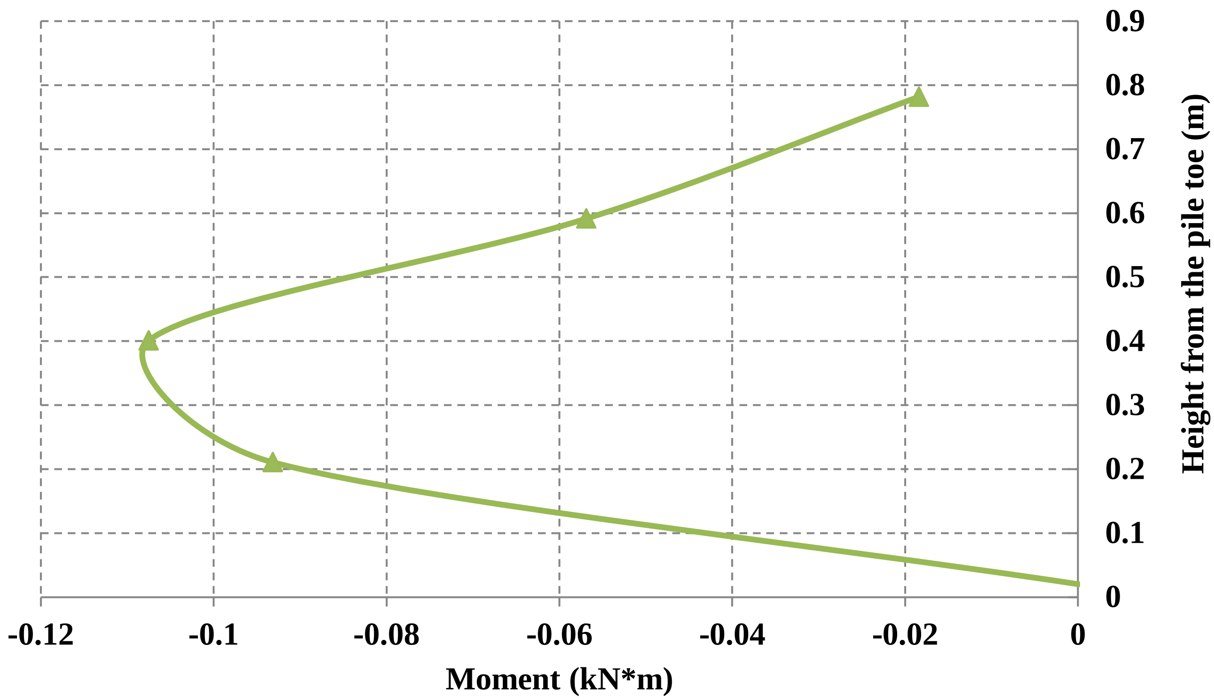

Figure A.9 Moment along the Pile for Toe Distance = 100 mm

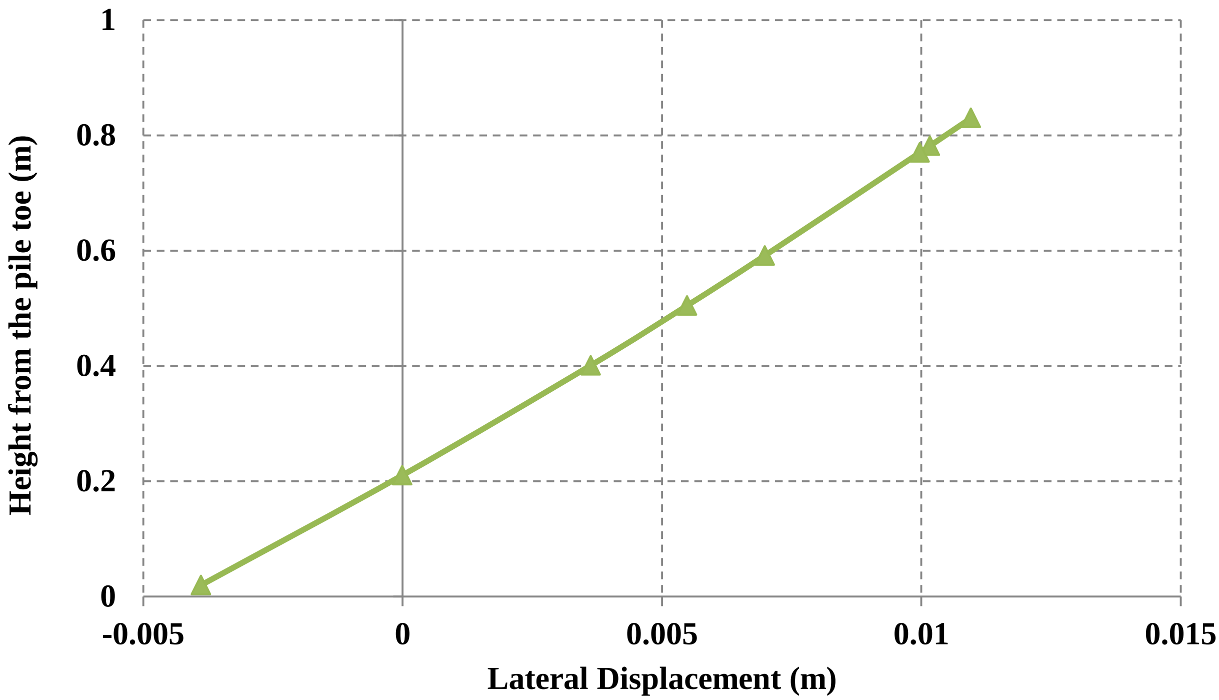

Figure A.10 Lateral Displacement along the Pile for Toe Distance = 100 mm

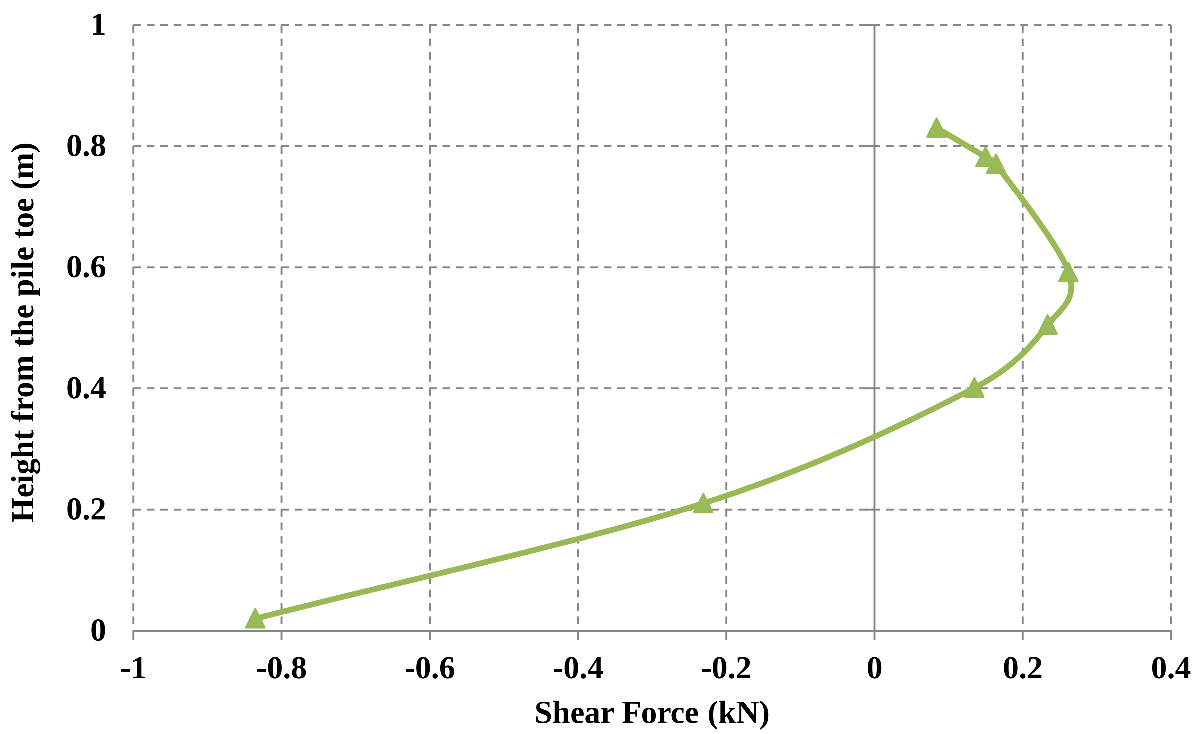

Figure A.11 Shear Force along the Pile for Toe Distance = 100 mm

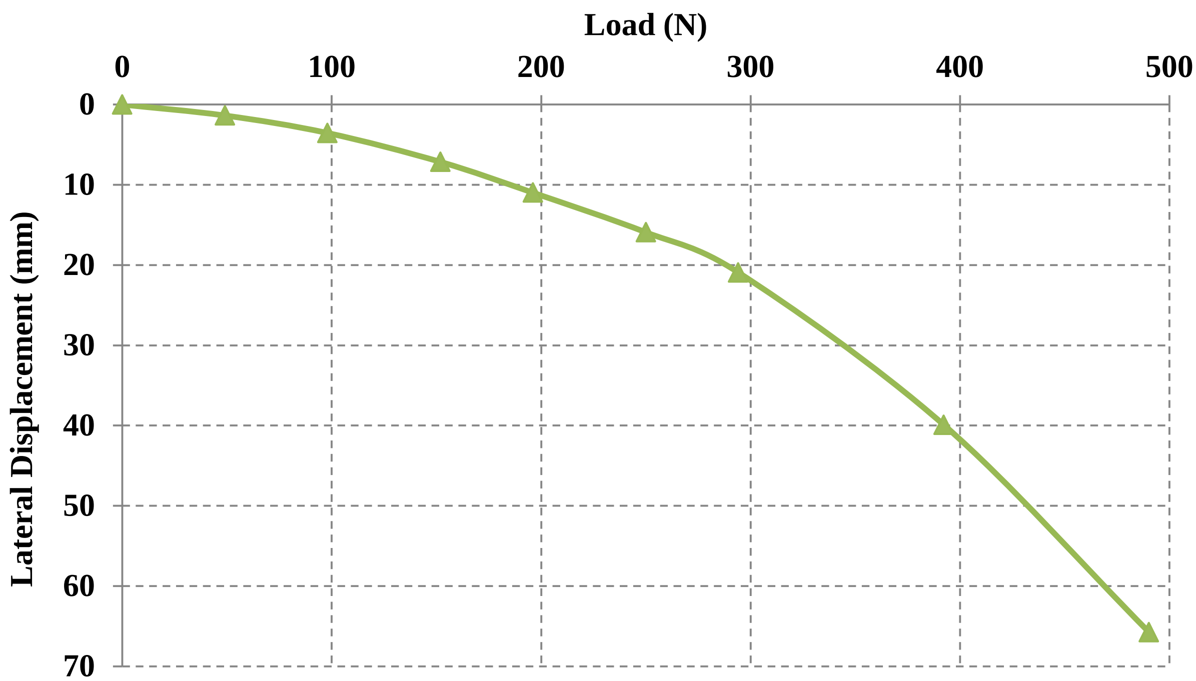

Figure A.12 Lateral Displacements vs. Load for Toe Distance = 100 mm

A.2.4. 150-mm pile toe distance

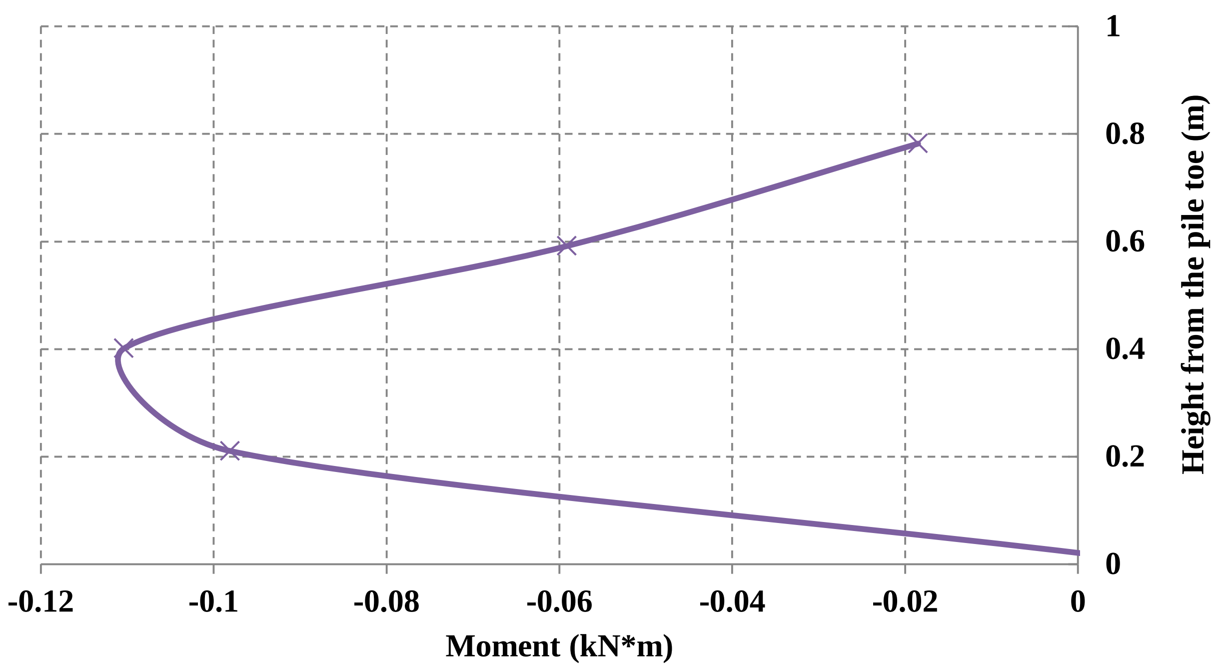

Figure A.13 Moment along the Pile for Toe Distance = 150 mm

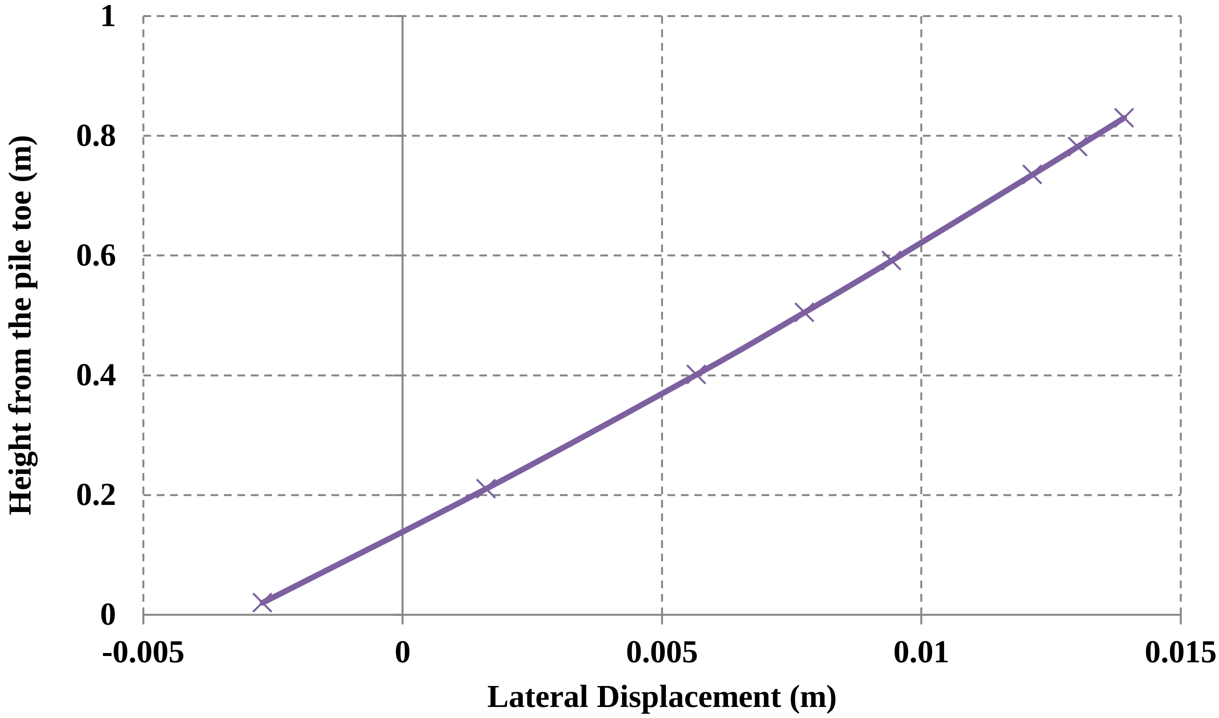

Figure A.14 Lateral Displacement along the Pile for Toe Distance = 150 mm

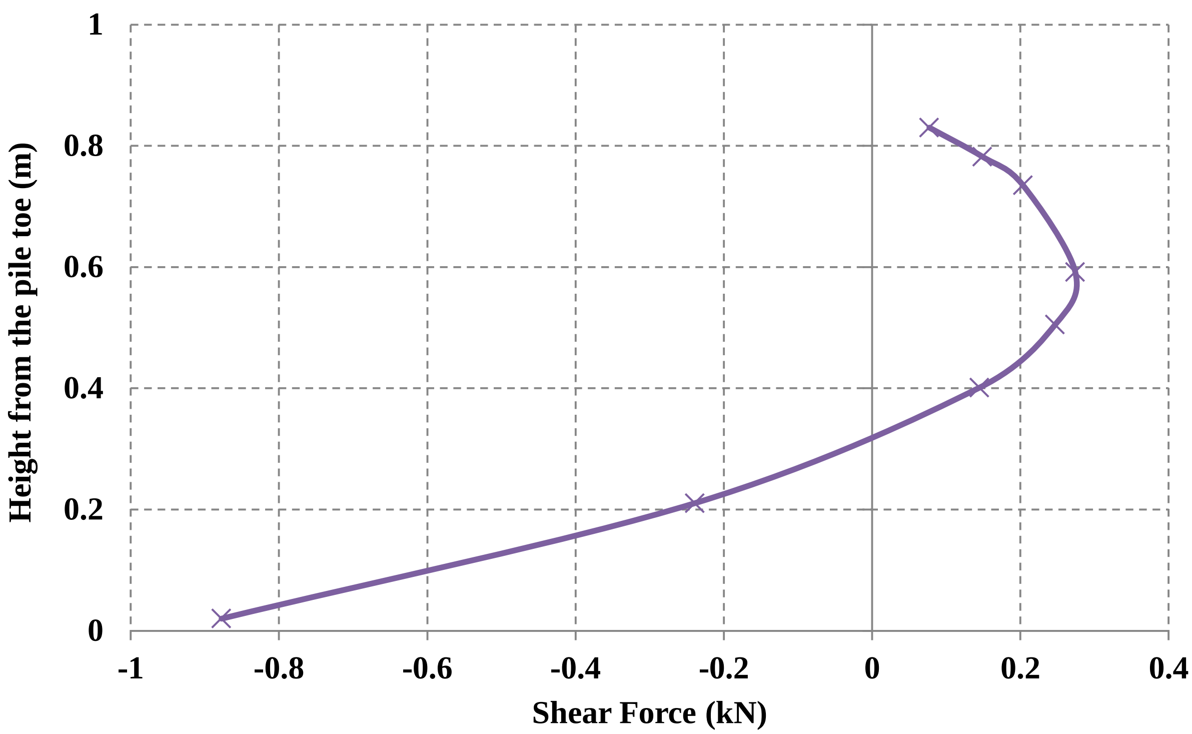

Figure A.15 Shear Force along the Pile for Toe Distance = 150 mm

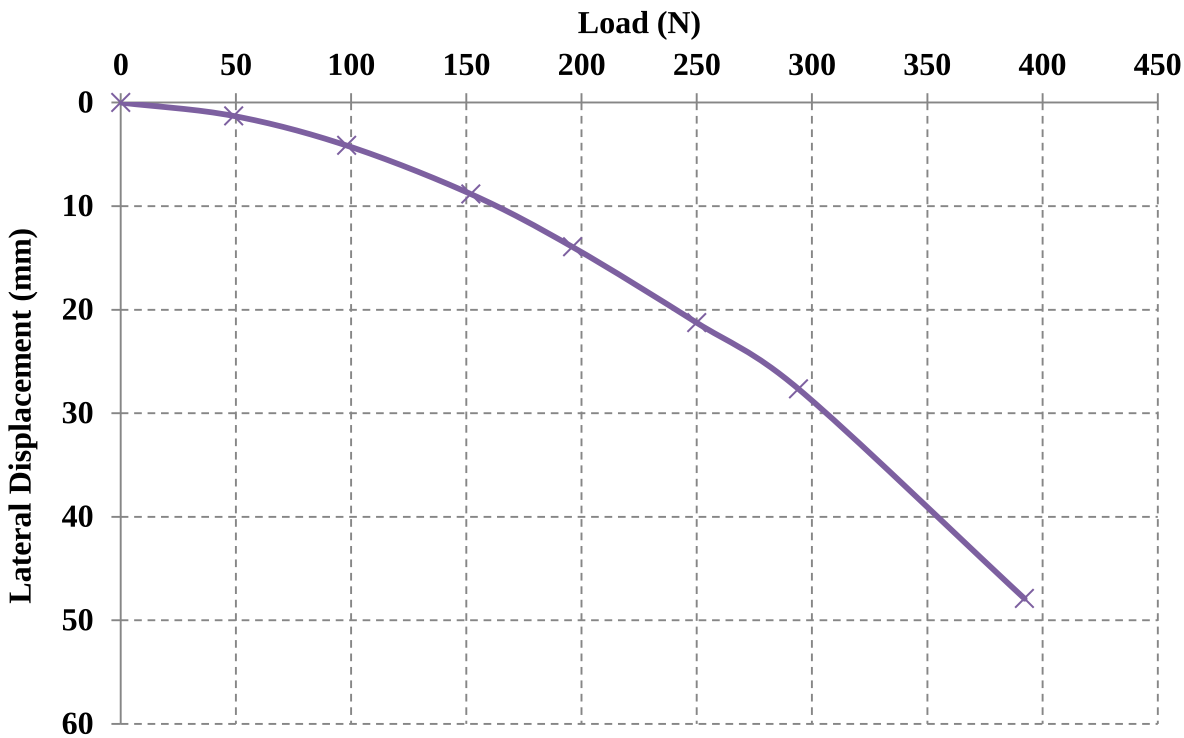

Figure A.16 Lateral Displacements vs. Load for Toe Distance = 150 mm

A.3. Static loading experiments

A.3.1. Horizontal scour

0-mm scour depth

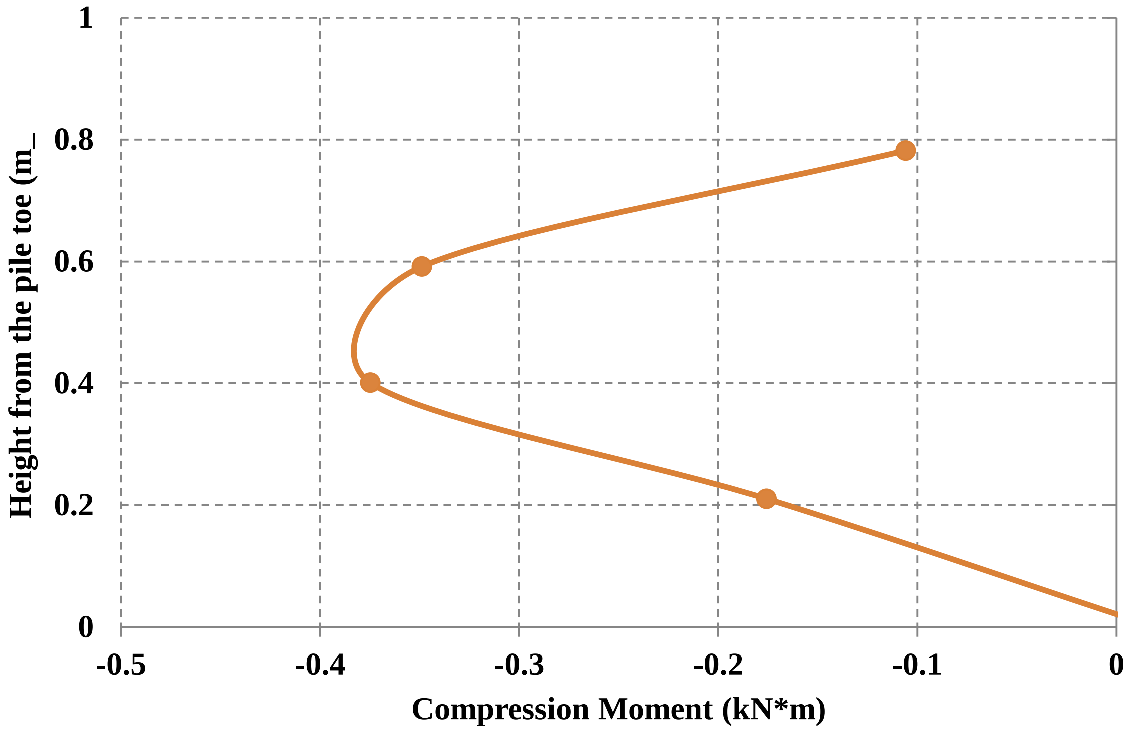

Figure A.17 Moment along the Pile for Scour Depth = 0 mm

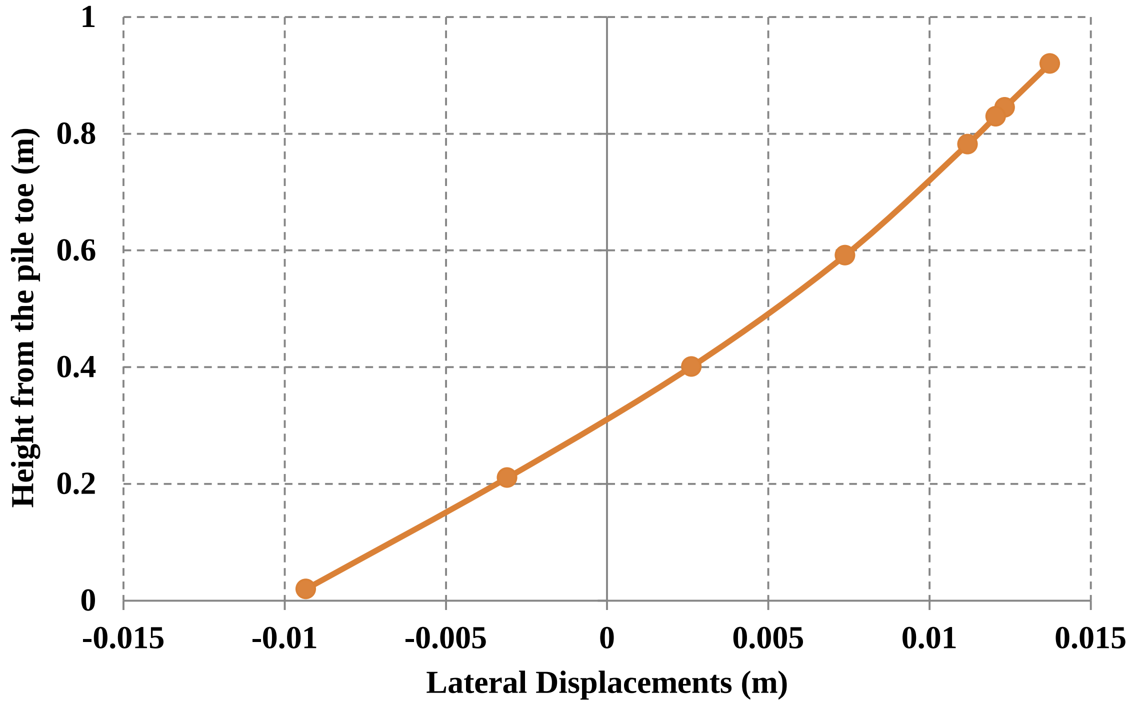

Figure A.18 Lateral Displacement along the Pile for Scour Depth = 0 mm

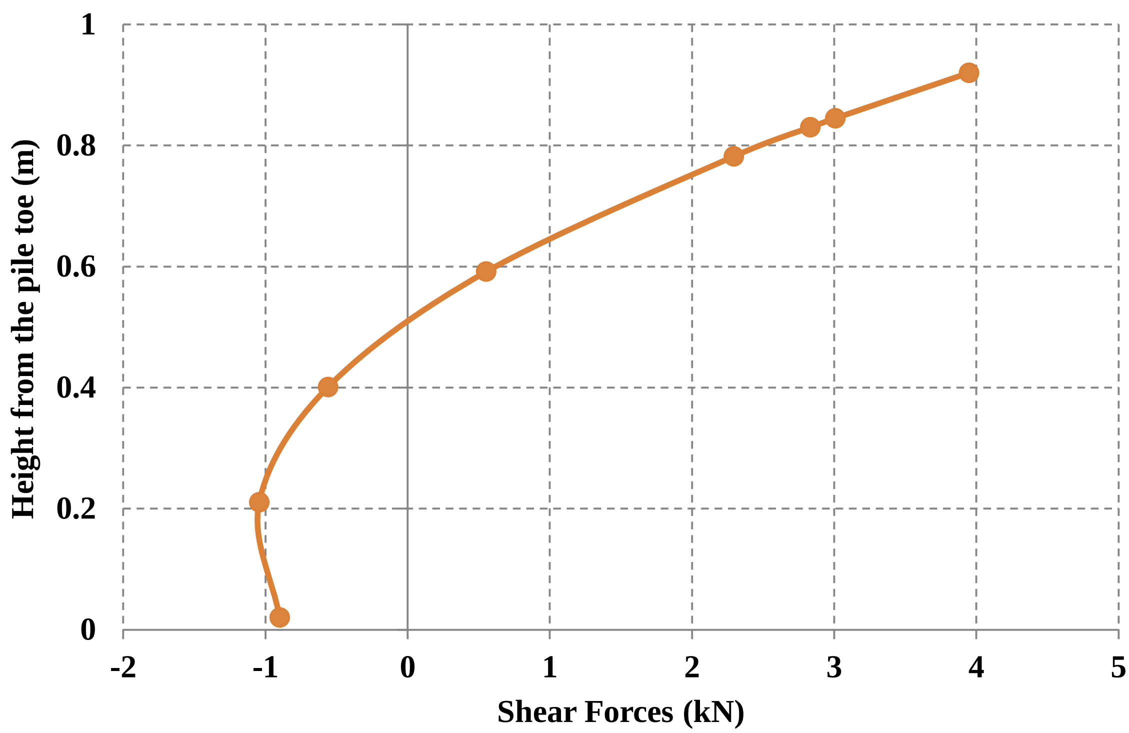

Figure A.19 Shear Force along the Pile for Scour Depth = 0 mm

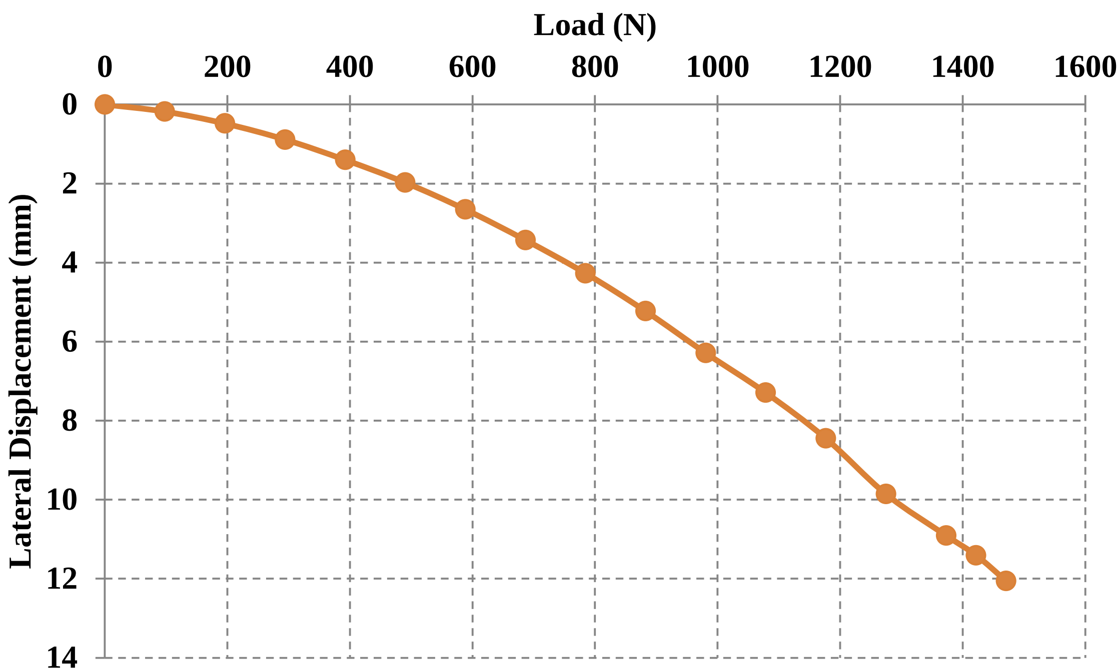

Figure A.20 Lateral Displacements vs. Load for Scour Depth = 0 mm

100-mm scour depth

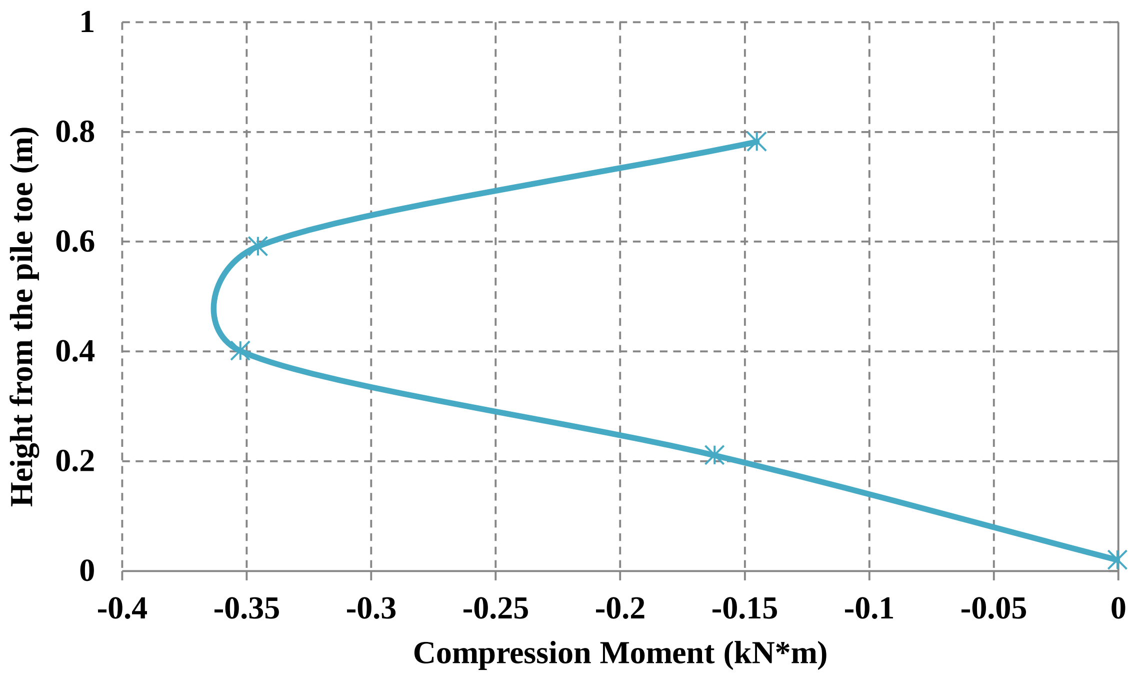

Figure A.21 Moment along the Pile for Scour Depth = 100 mm

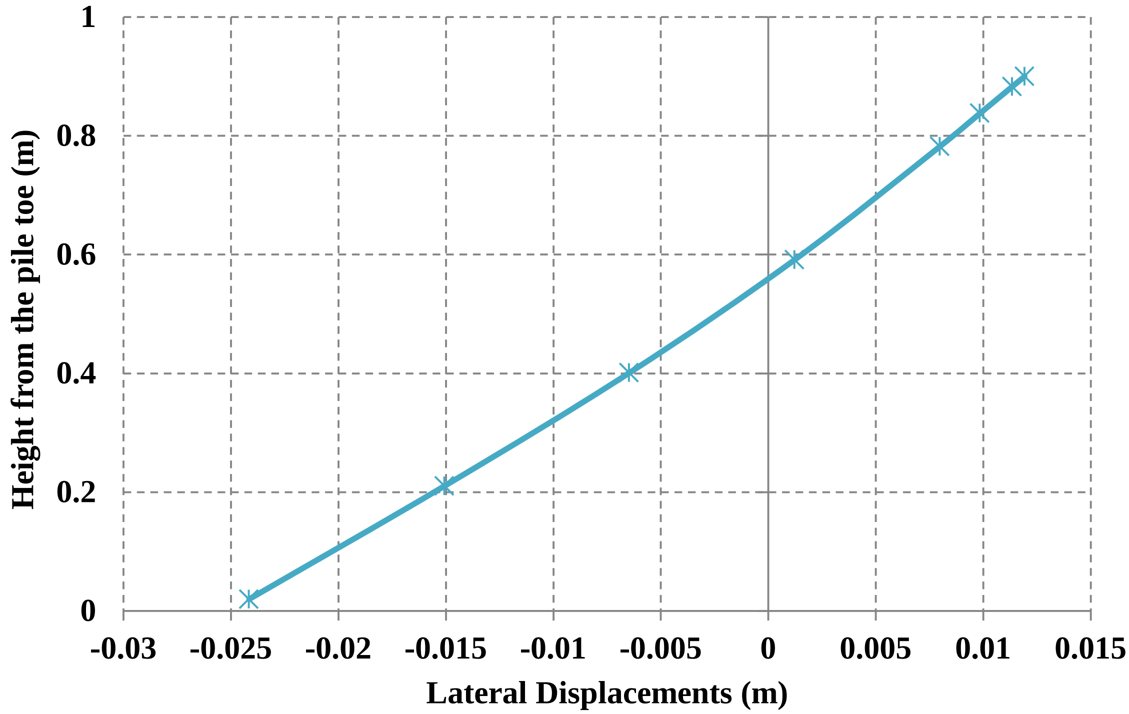

Figure A.22 Lateral Displacement along the Pile for Scour Depth = 100 mm

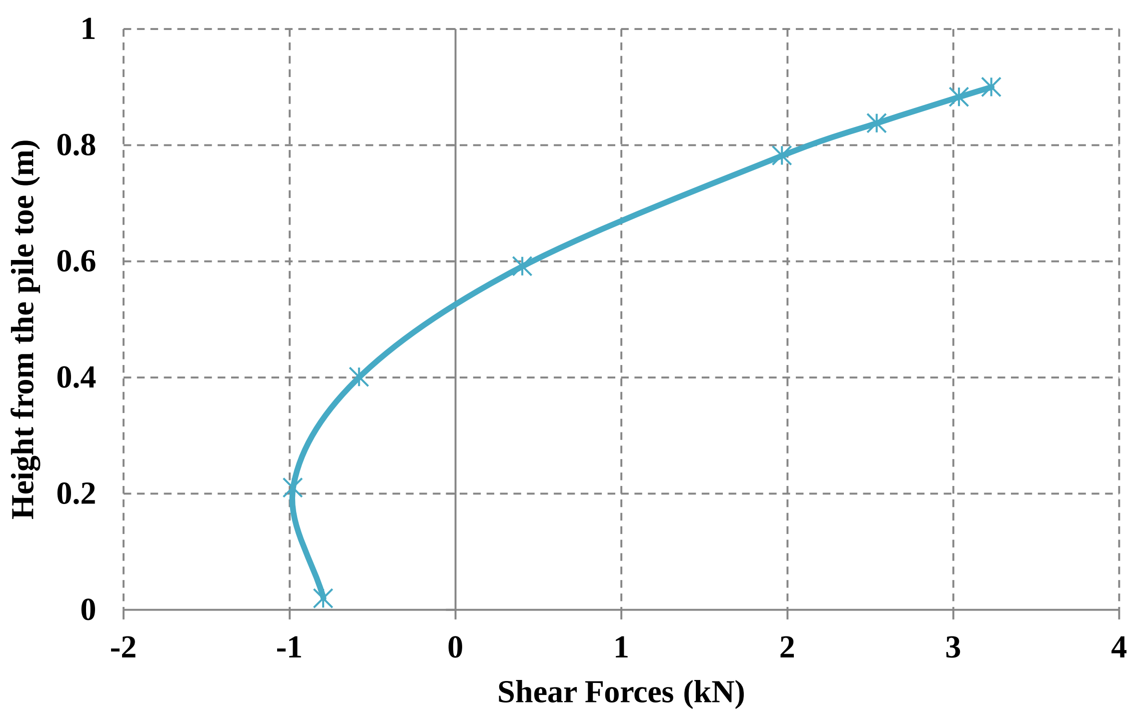

Figure A.23 Shear Force along the Pile for Scour Depth = 100 mm

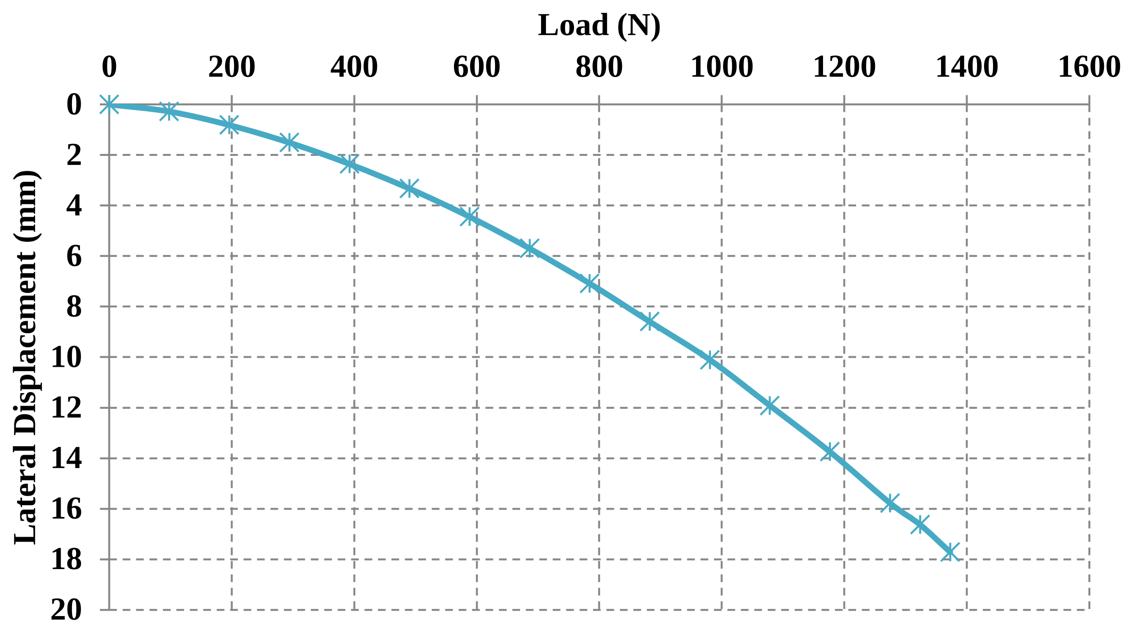

Figure A.24 Lateral Displacements vs. Load for Scour Depth = 100 mm

200-mm scour depth

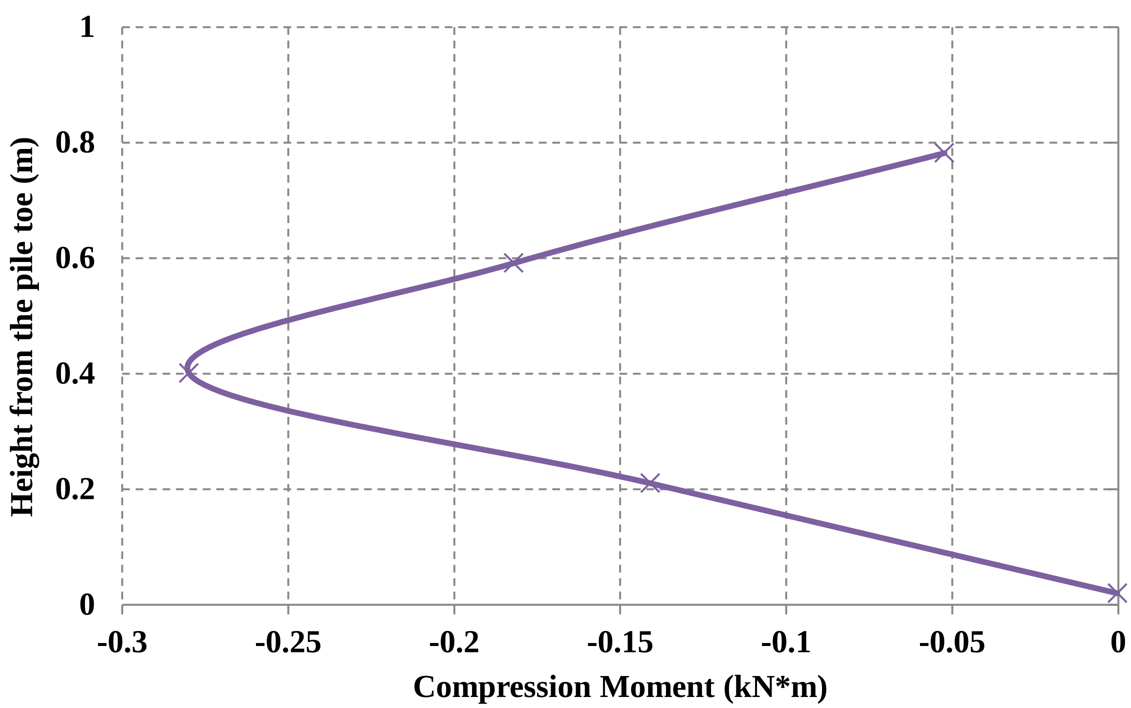

Figure A.25 Moment along the Pile for Scour Depth = 200 mm

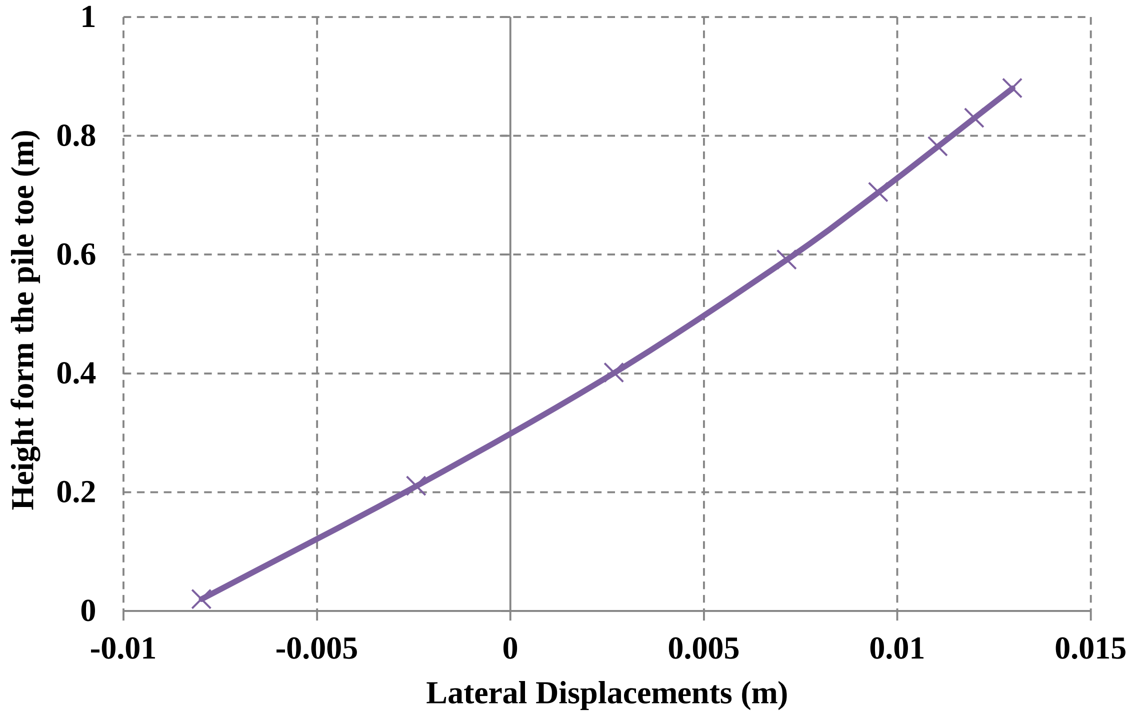

Figure A.26 Lateral Displacement along the Pile for Scour Depth = 200 mm

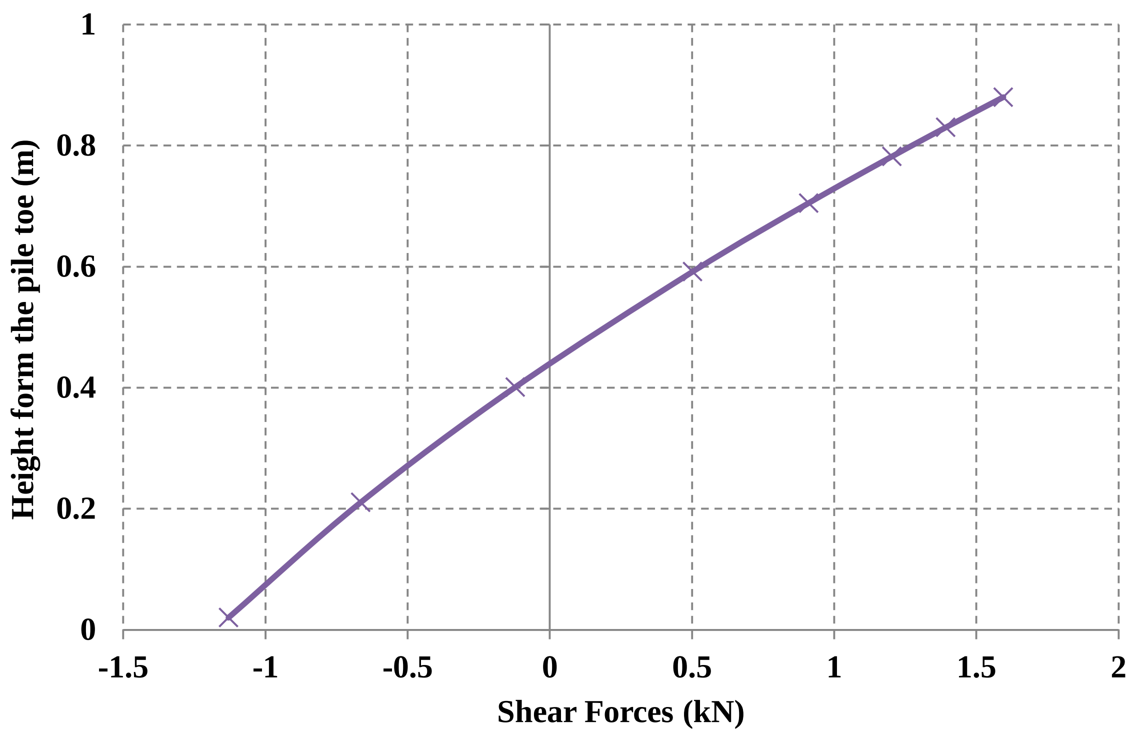

Figure A.27 Shear Force along the Pile for Scour Depth = 200 mm

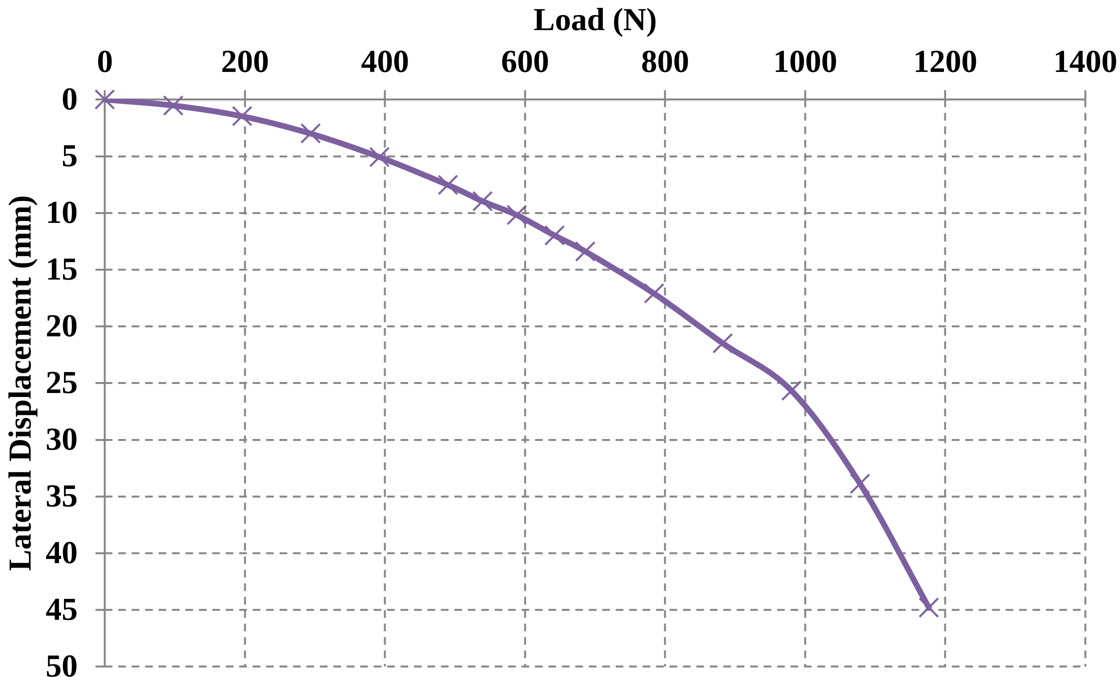

Figure A.28 Lateral Displacements vs. Load for Scour Depth = 200 mm

300-mm scour depth

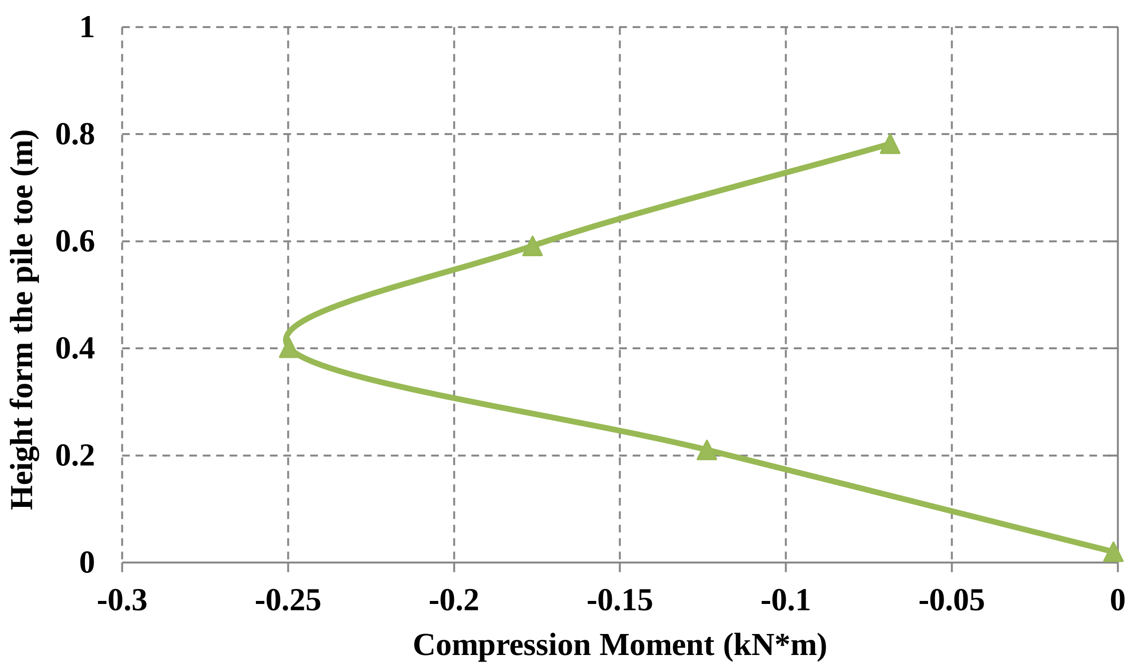

Figure A.29 Moment along the Pile for Scour Depth = 300 mm

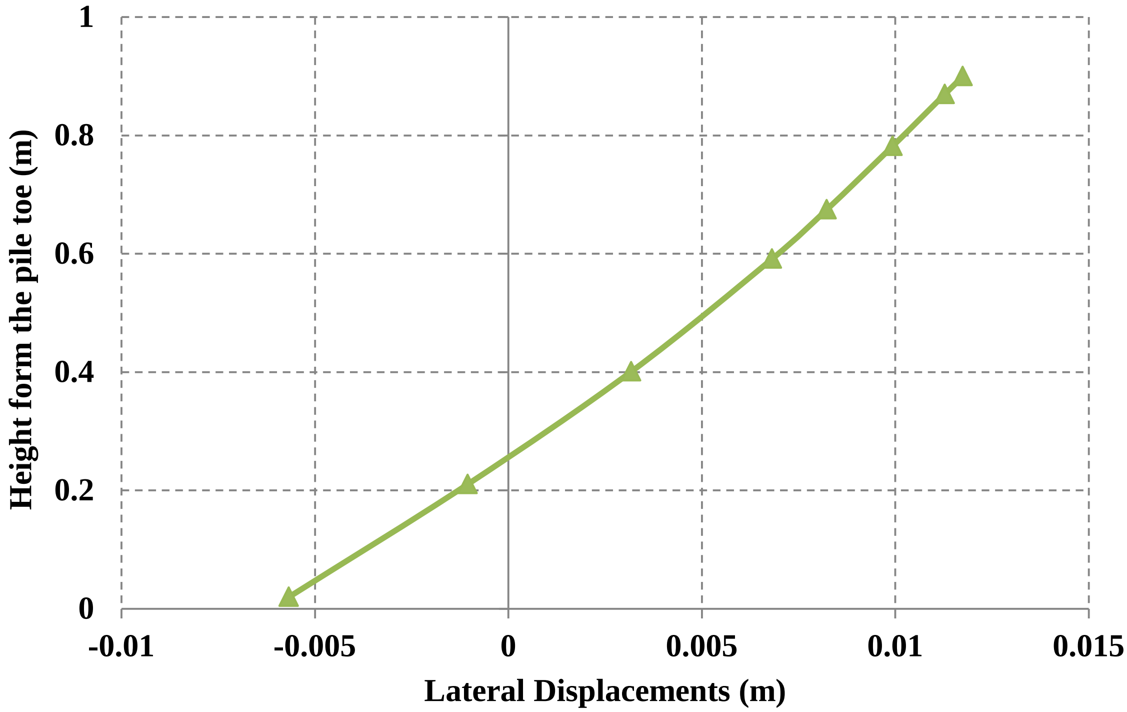

Figure A.30 Lateral Displacement along the Pile for Scour Depth = 300 mm

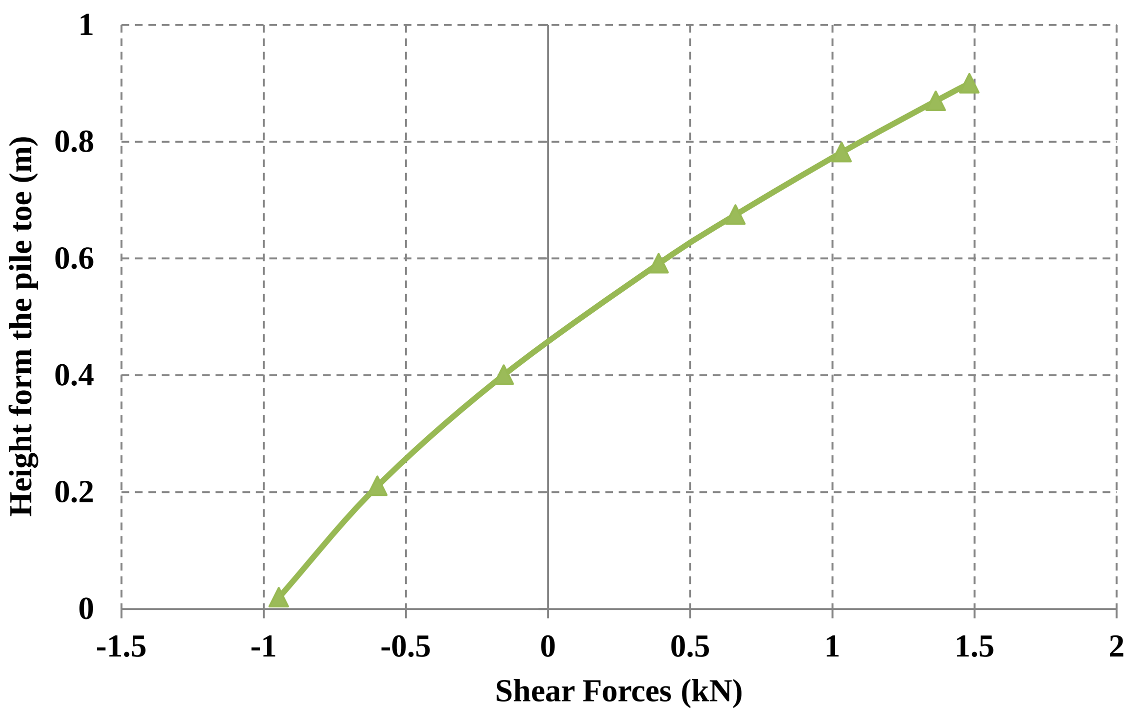

Figure A.31 Shear Force along the Pile for Scour Depth = 300 mm

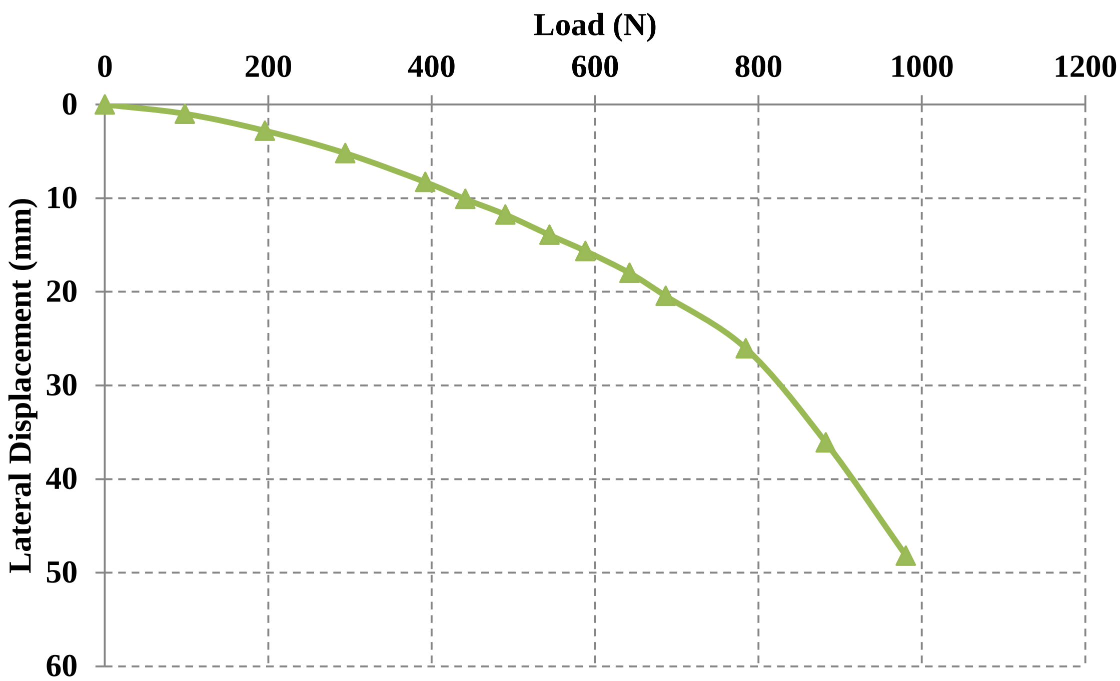

Figure A.32 Lateral Displacements vs. Load for Scour Depth = 300 mm

400-mm scour depth

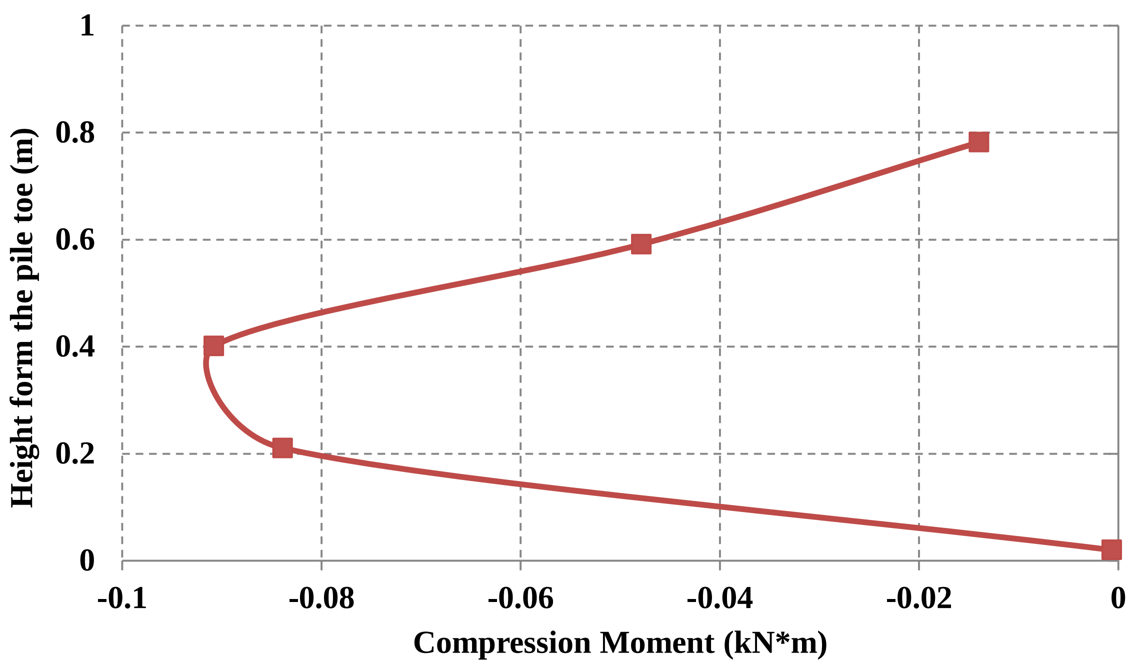

Figure A.33 Moment along the Pile for Scour Depth = 400 mm

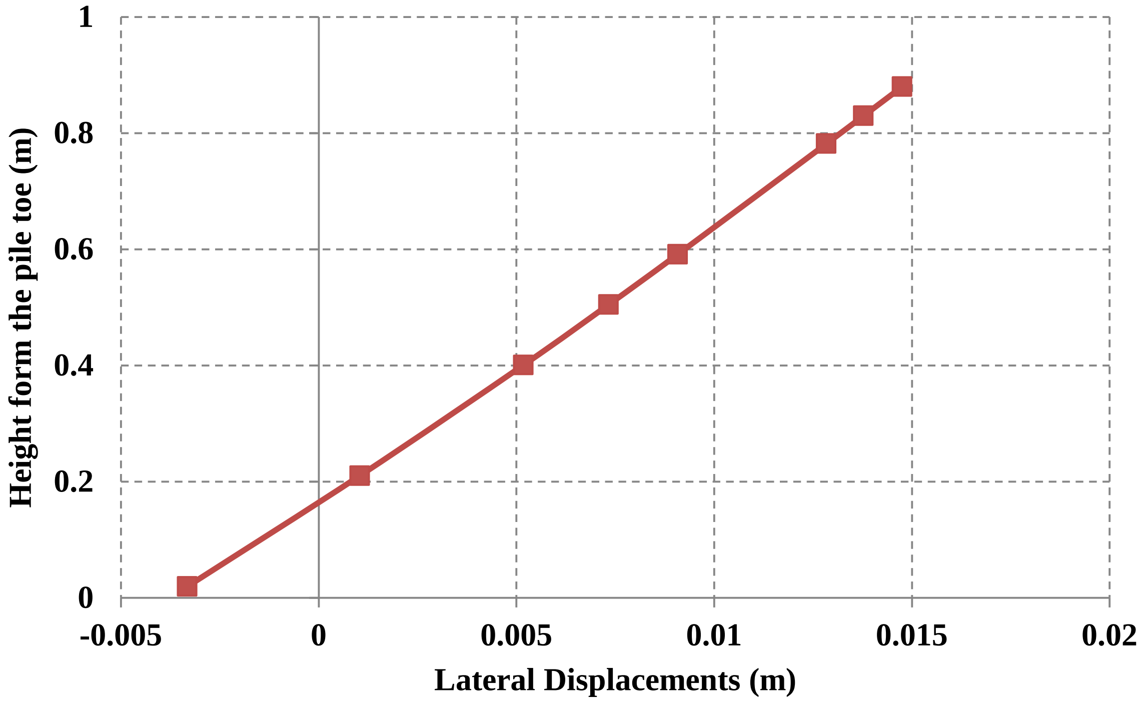

Figure A.34 Lateral Displacement along the Pile for Scour Depth = 400 mm

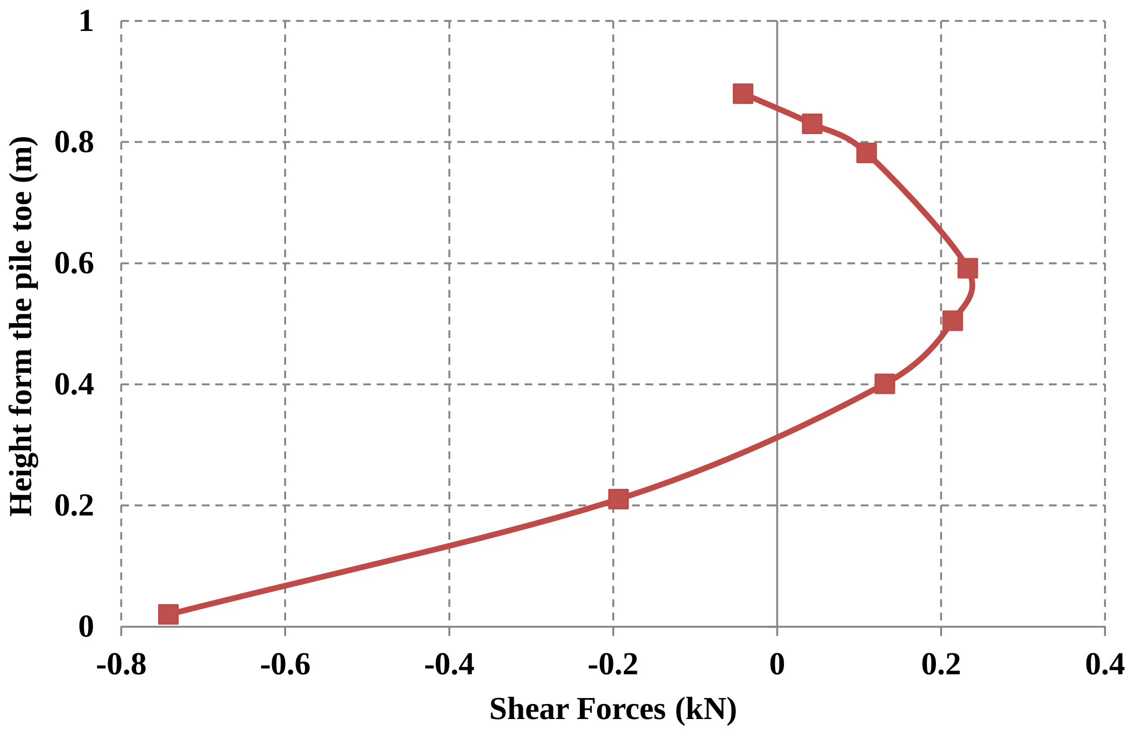

Figure A.35 Shear Force along the Pile for Scour Depth = 400 mm

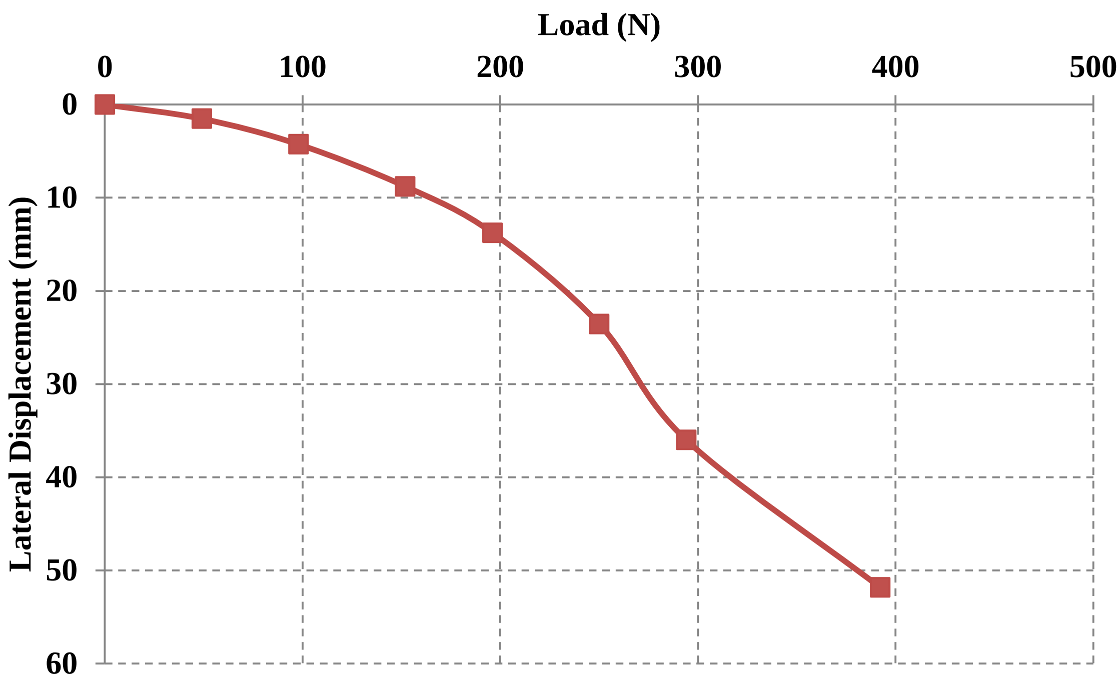

Figure A.36 Lateral Displacements vs. Load for Scour Depth = 400 mm

500-mm scour depth

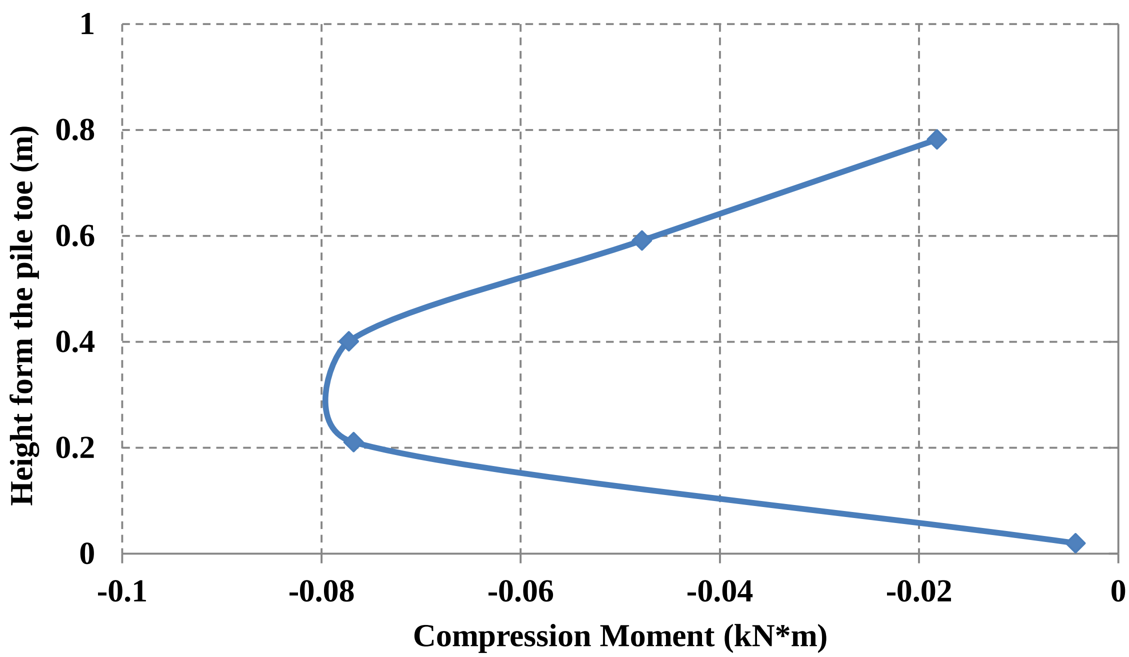

Figure A.37 Moment along the Pile for Scour Depth = 500 mm

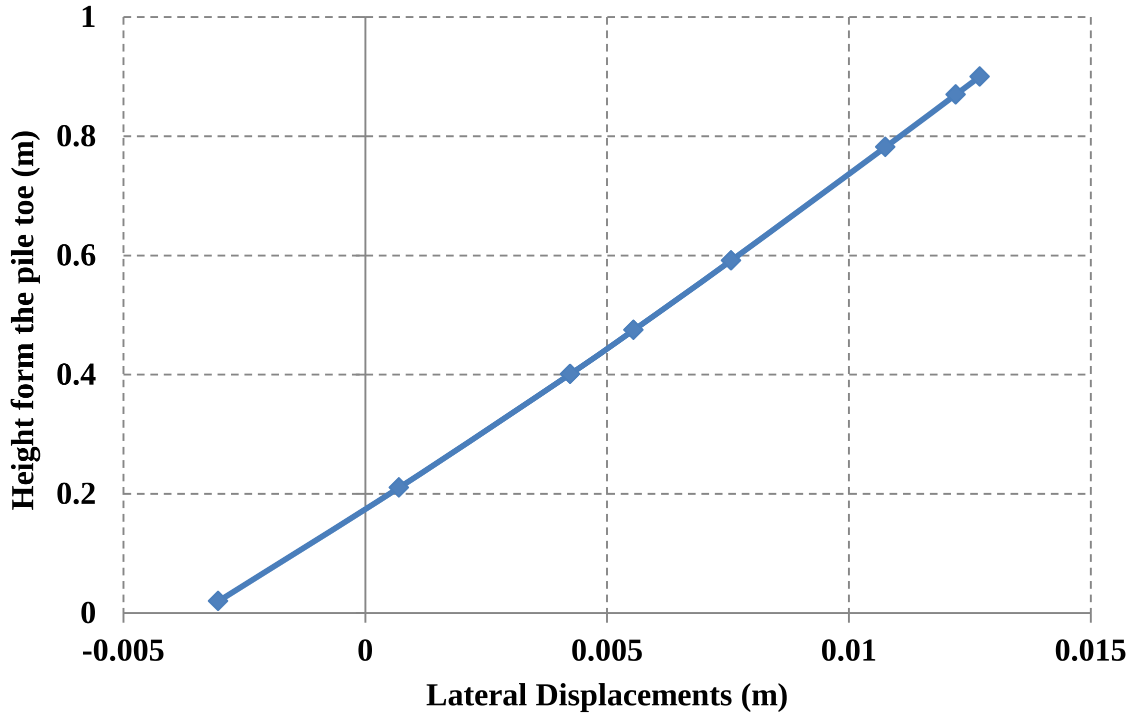

Figure A.38 Lateral Displacement along the Pile for Scour Depth = 500 mm

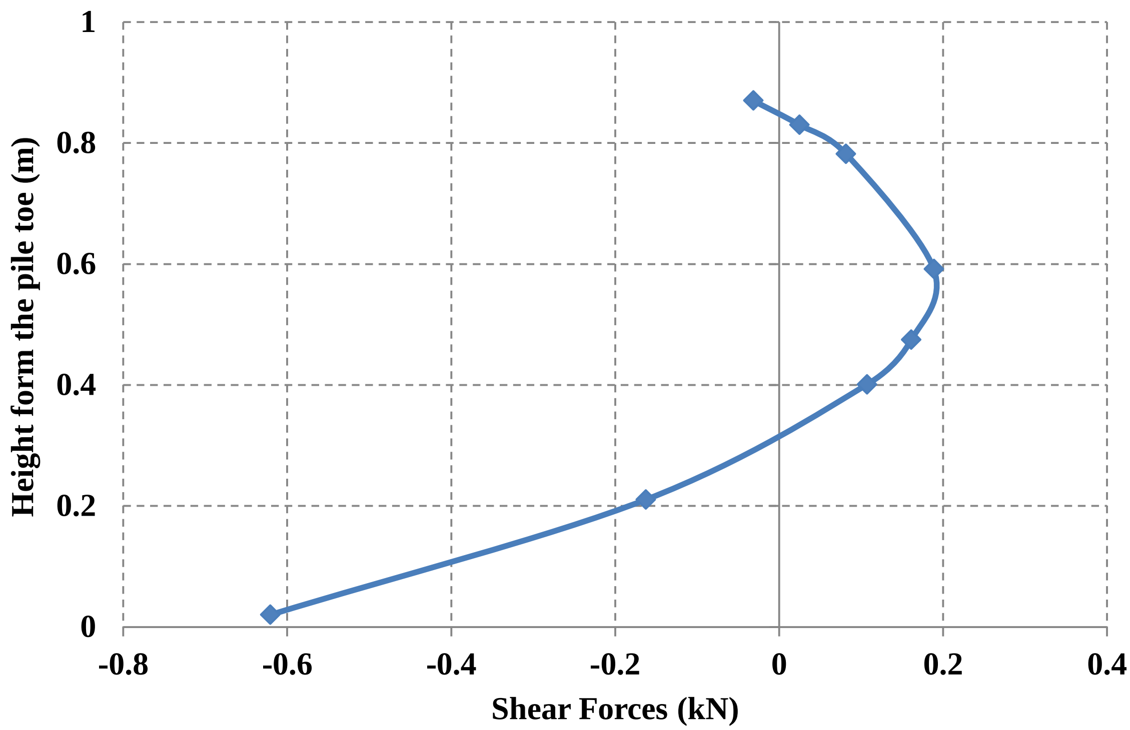

Figure A.39 Shear Force along the Pile for Scour Depth = 500 mm

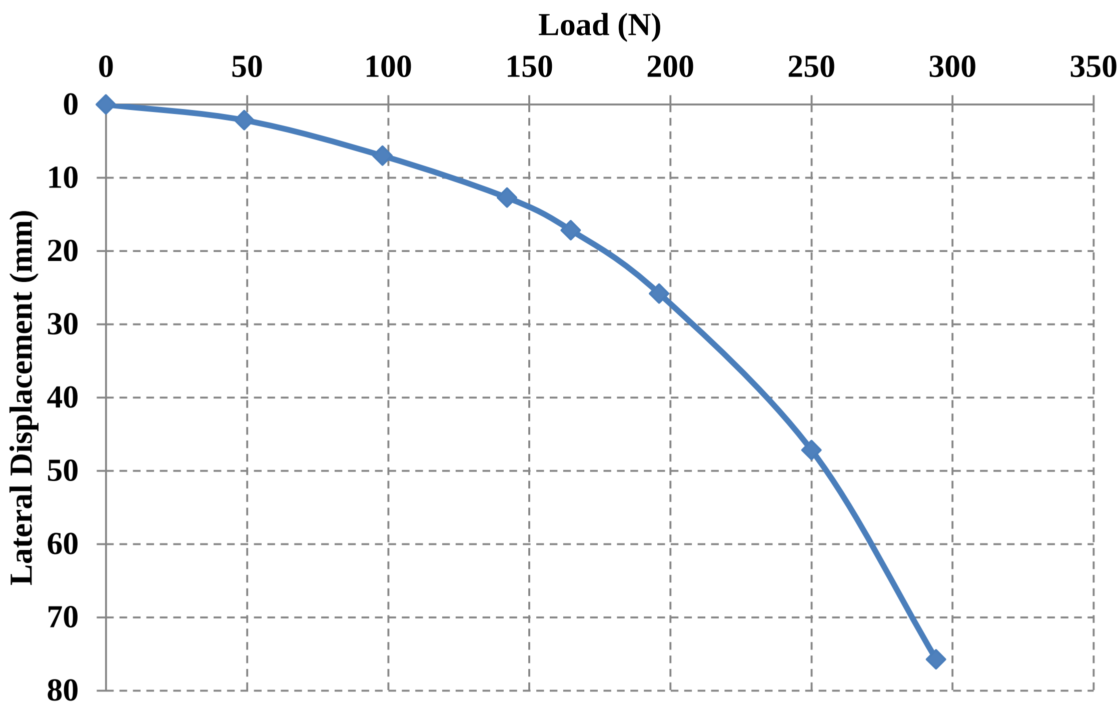

Figure A.40 Lateral Displacements vs. Load for Scour Depth = 500 mm

A.3.2. Combined scour slope and scour depth effect

A.3.2.1. 0-degree scour slope

200-mm scour depth

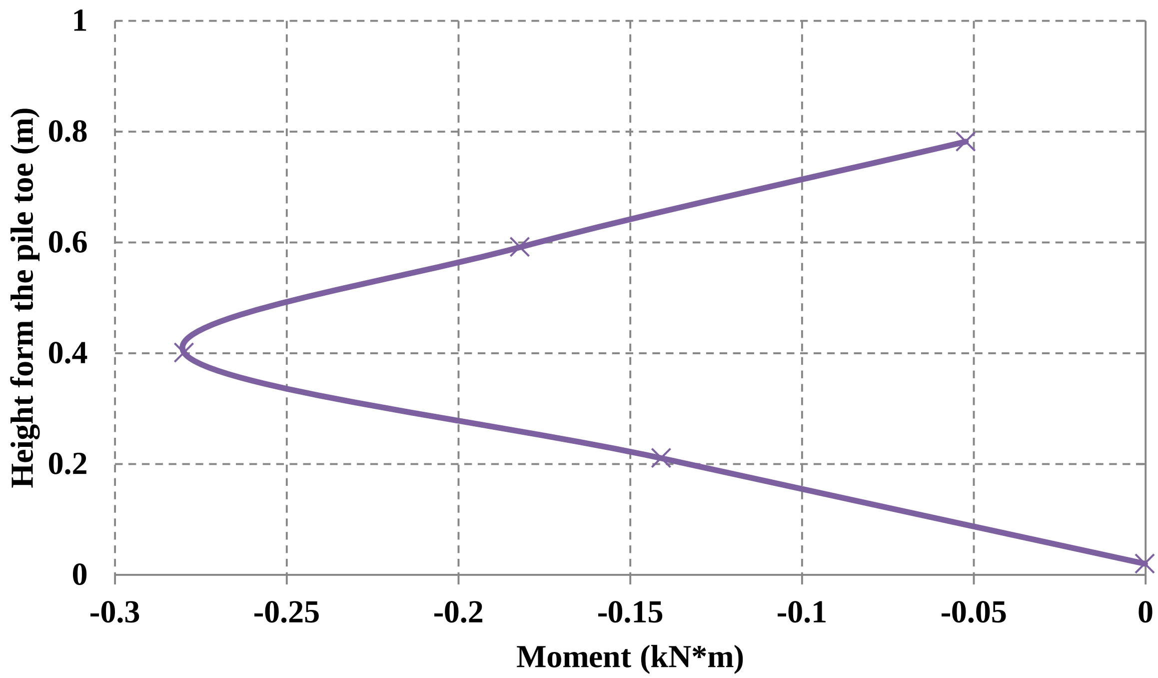

Figure A.41 Moment along the Pile for Scour Depth = 200 mm and Slope = 0 Degree

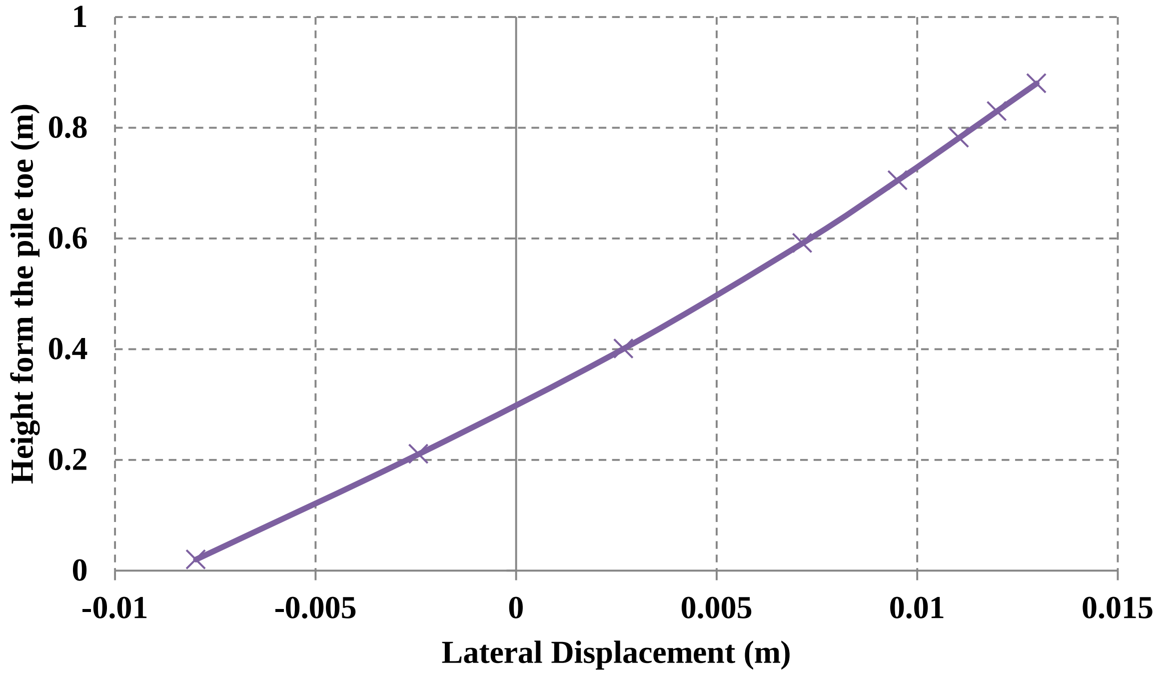

Figure A.42 Lateral Displacement along the Pile for Scour Depth = 200 mm and Slope = 0 Degree

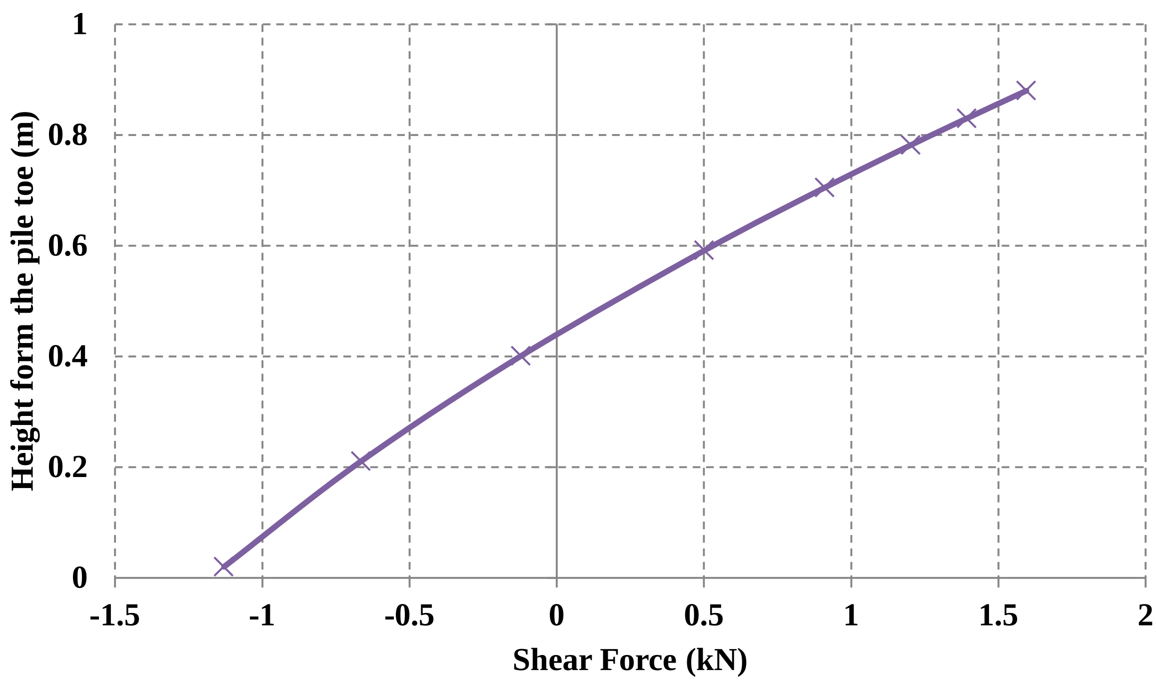

Figure A.43 Shear Force along the Pile for Scour Depth = 200 mm and Slope = 0 Degree

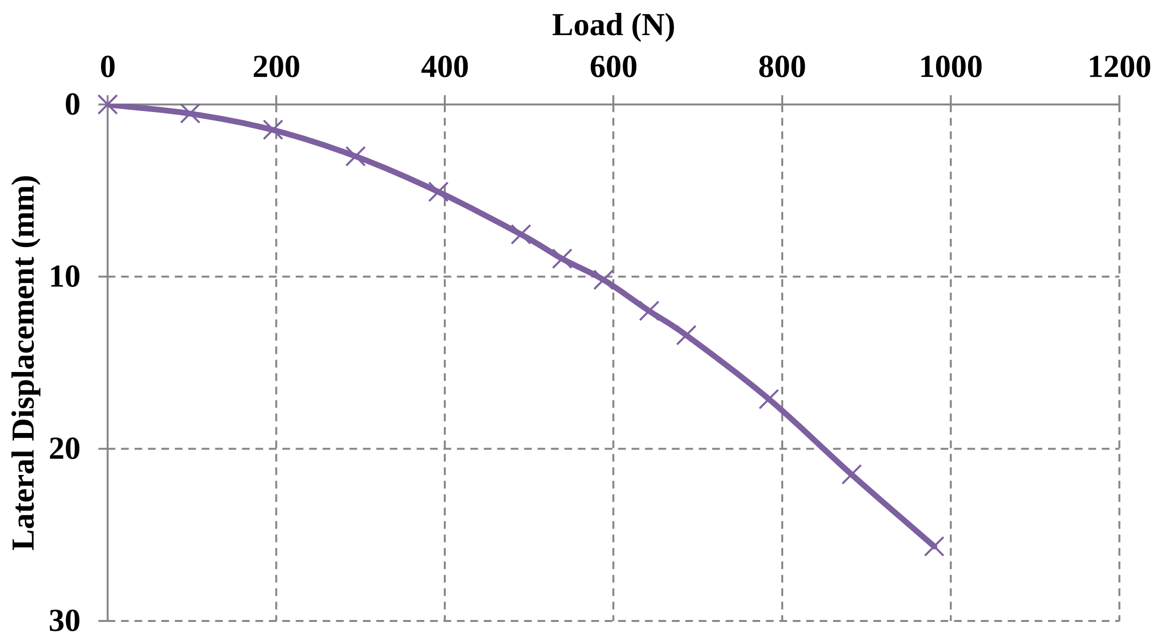

Figure A.44 Lateral Displacements vs. Load for Scour Depth = 200 mm and Slope = 0 Degree

300-mm scour depth

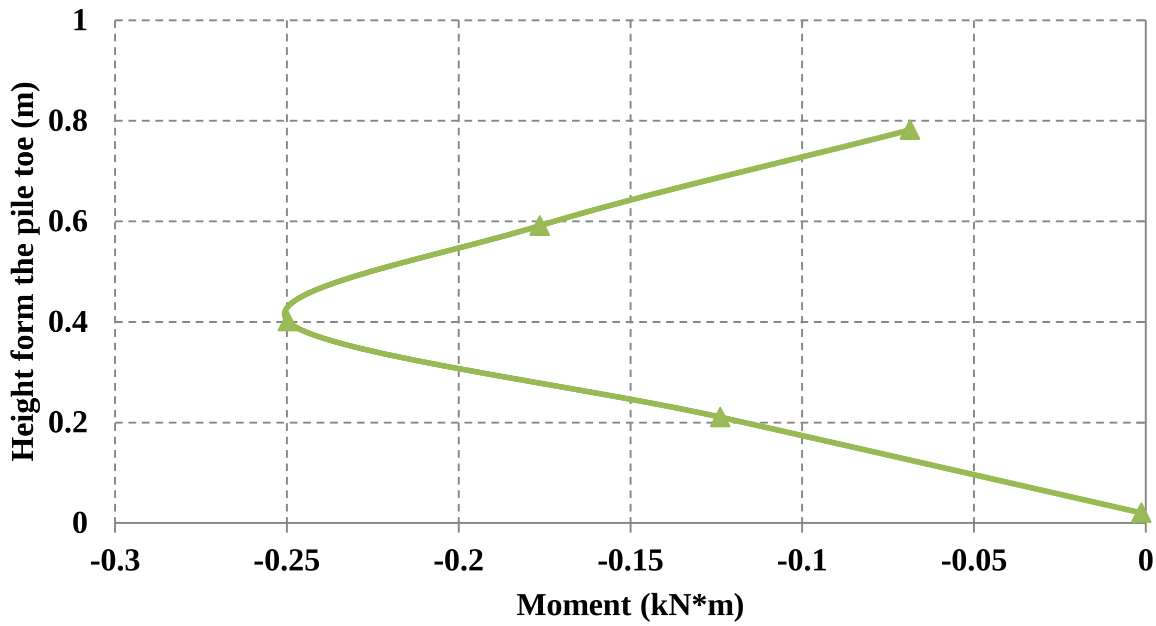

Figure A.45 Moment along the Pile for Scour Depth = 300 mm and Slope = 0 Degree

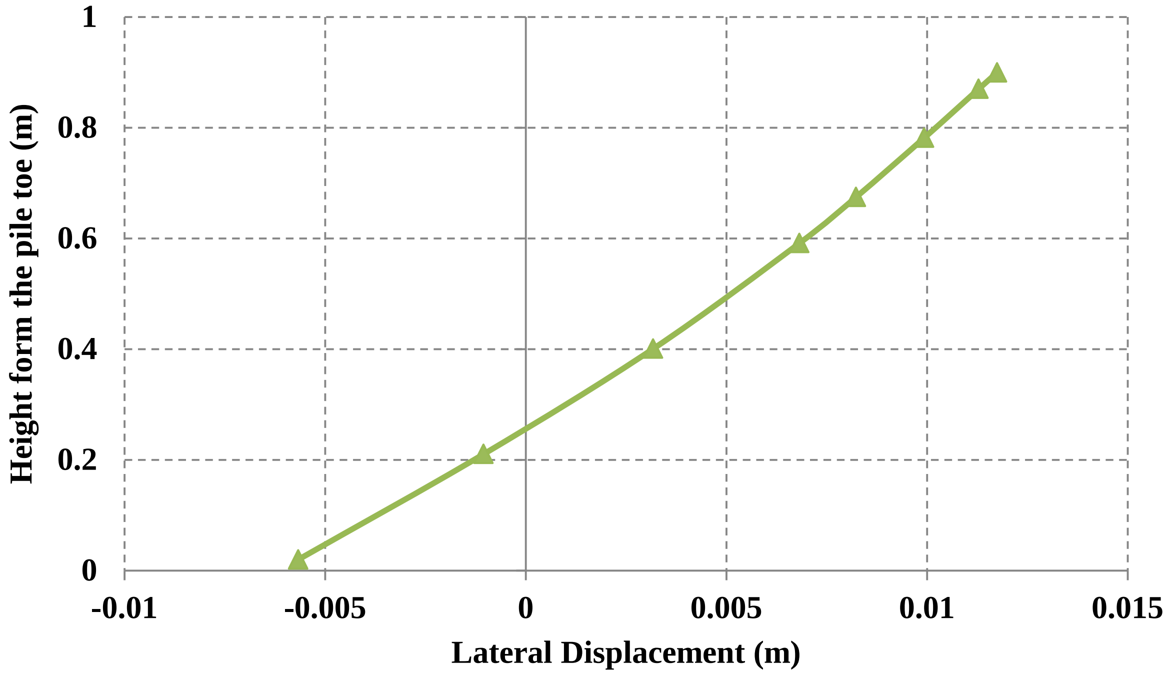

Figure A.46 Lateral Displacement along the Pile for Scour Depth = 300 mm and Slope = 0 Degree

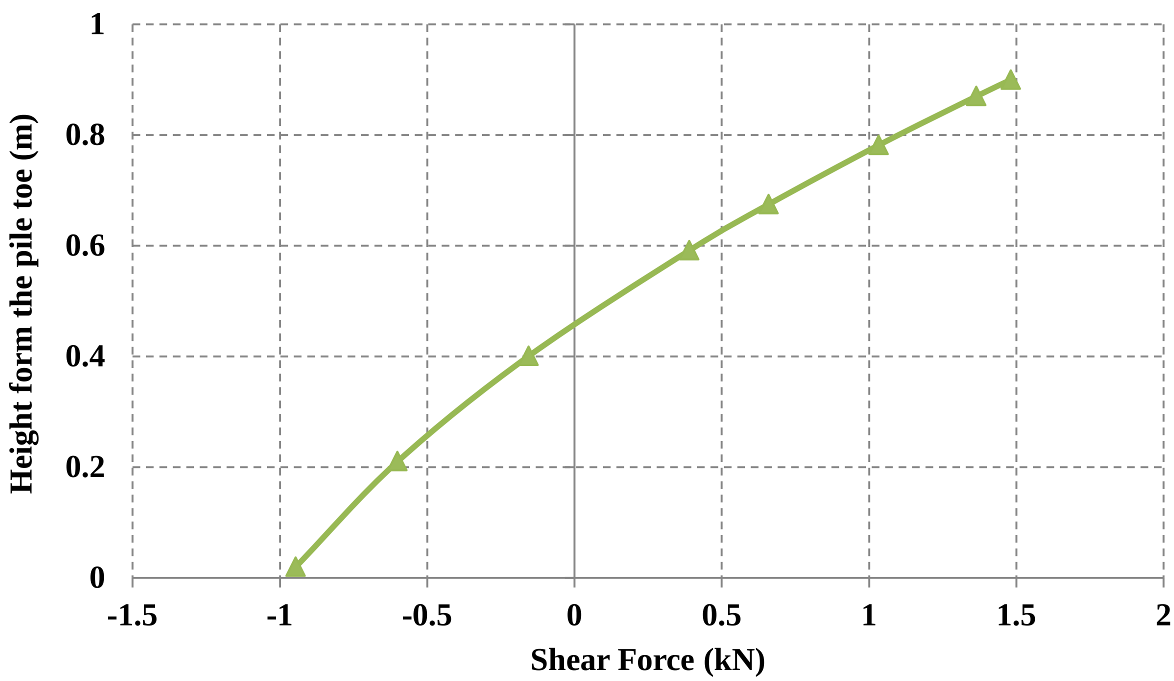

Figure A.47 Shear Force along the Pile for Scour Depth = 300 mm and Slope = 0 Degree

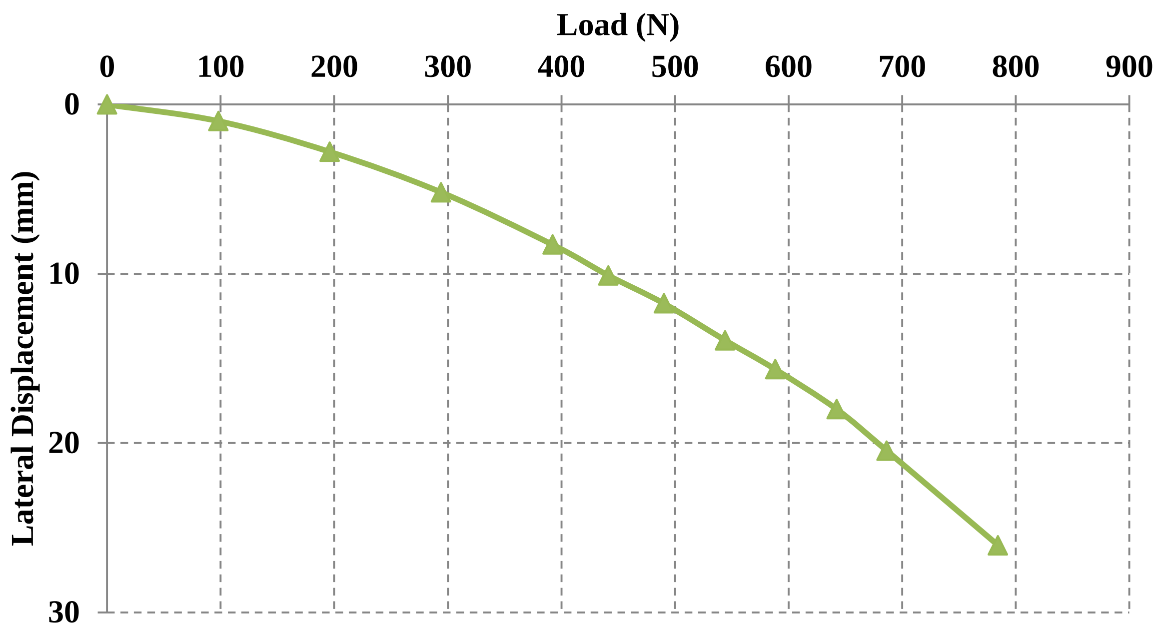

Figure A. 48 Lateral Displacements vs. Load for Scour Depth = 300 mm and Slope = 0 Degree

400-mm scour depth

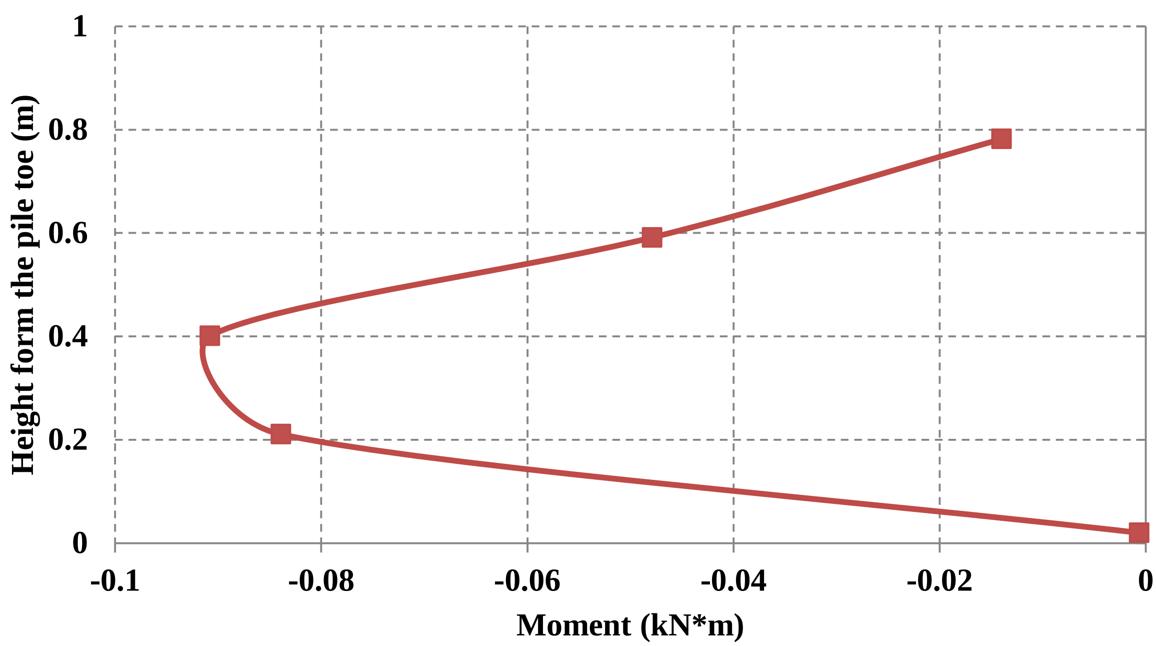

Figure A.49 Moment along the Pile for Scour Depth = 400 mm and Slope = 0 Degree

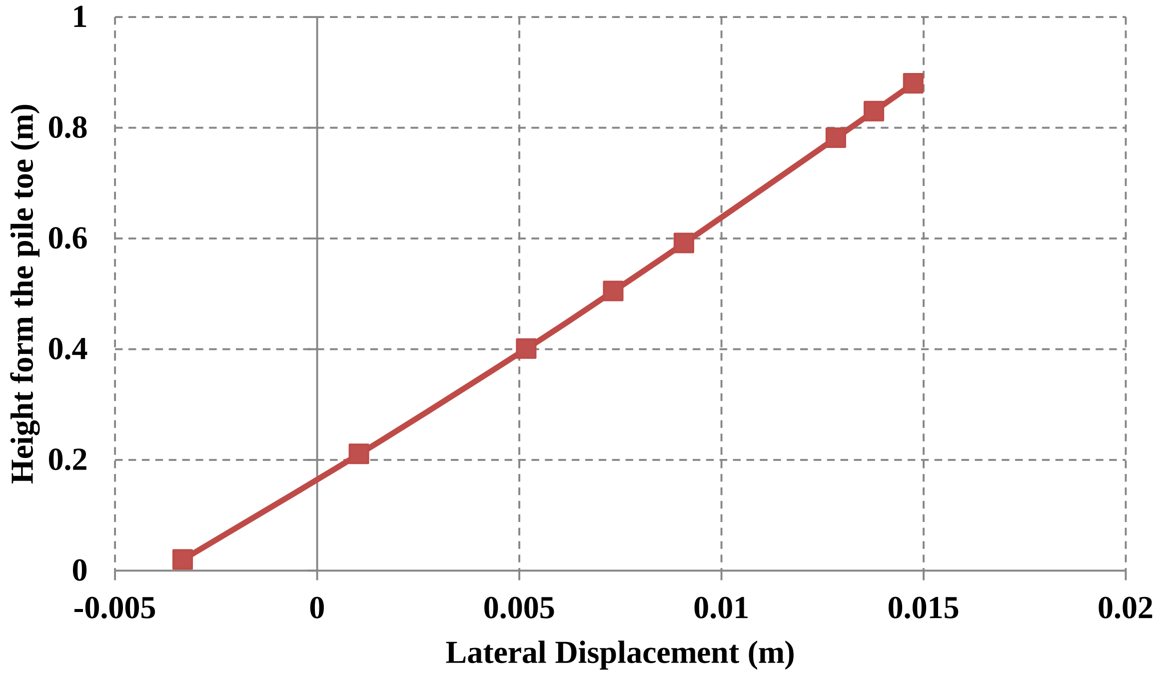

Figure A.50 Lateral Displacement along the Pile for Scour Depth = 400 mm and Slope = 0 Degree

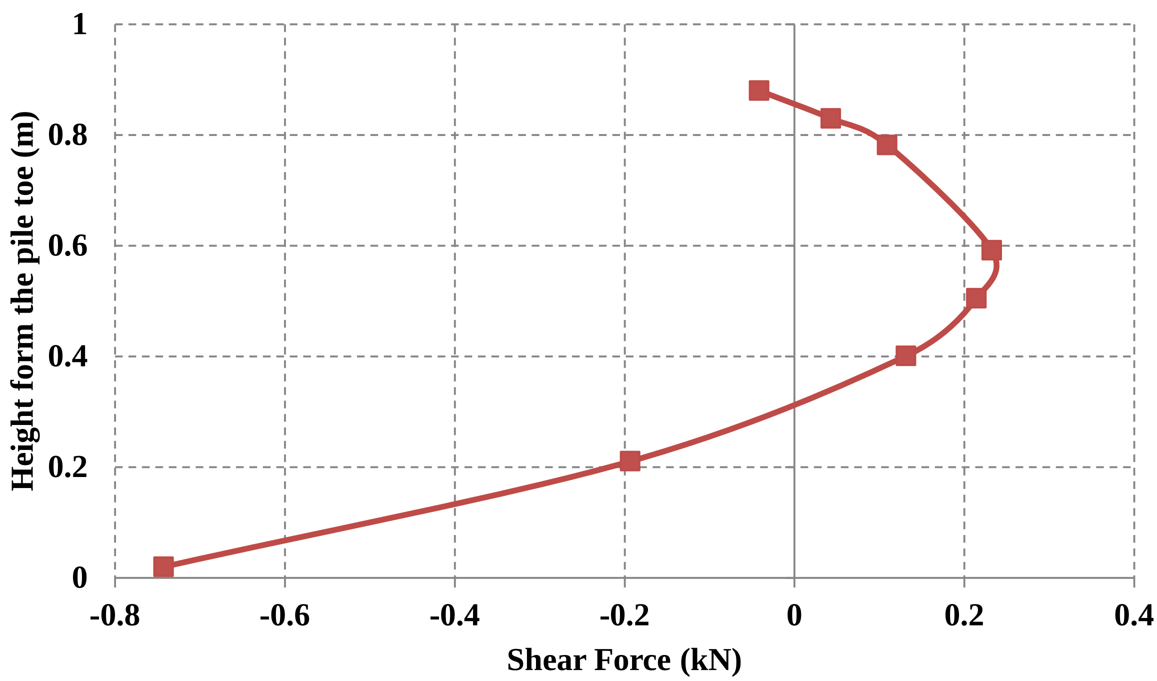

Figure A.51 Shear Force along the Pile for Scour Depth = 400 mm and Slope = 0 Degree

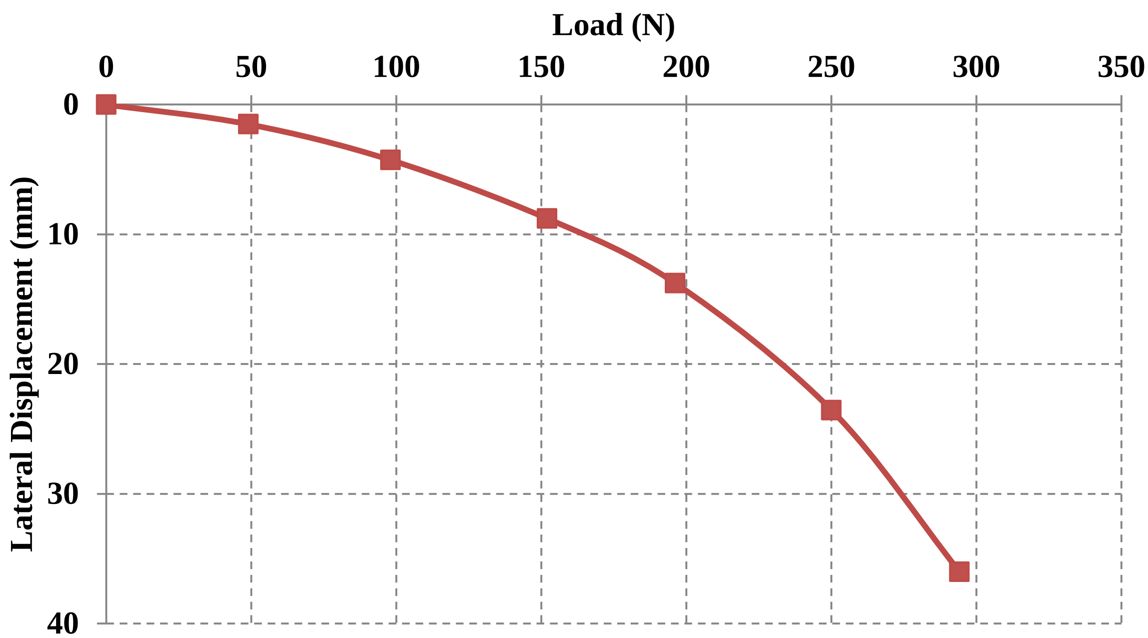

Figure A.52 Lateral Displacements vs. Load for Scour Depth = 400 mm and Slope = 0 Degree

500-mm scour depth

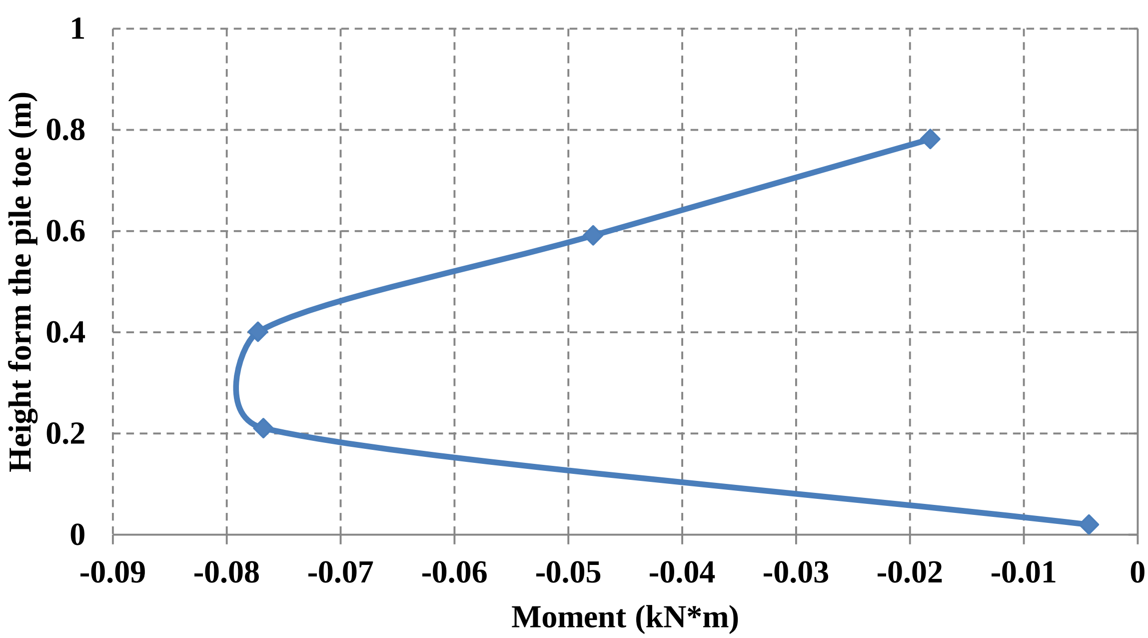

Figure A.53 Moment along the Pile for Scour Depth = 500 mm and Slope = 0 Degree

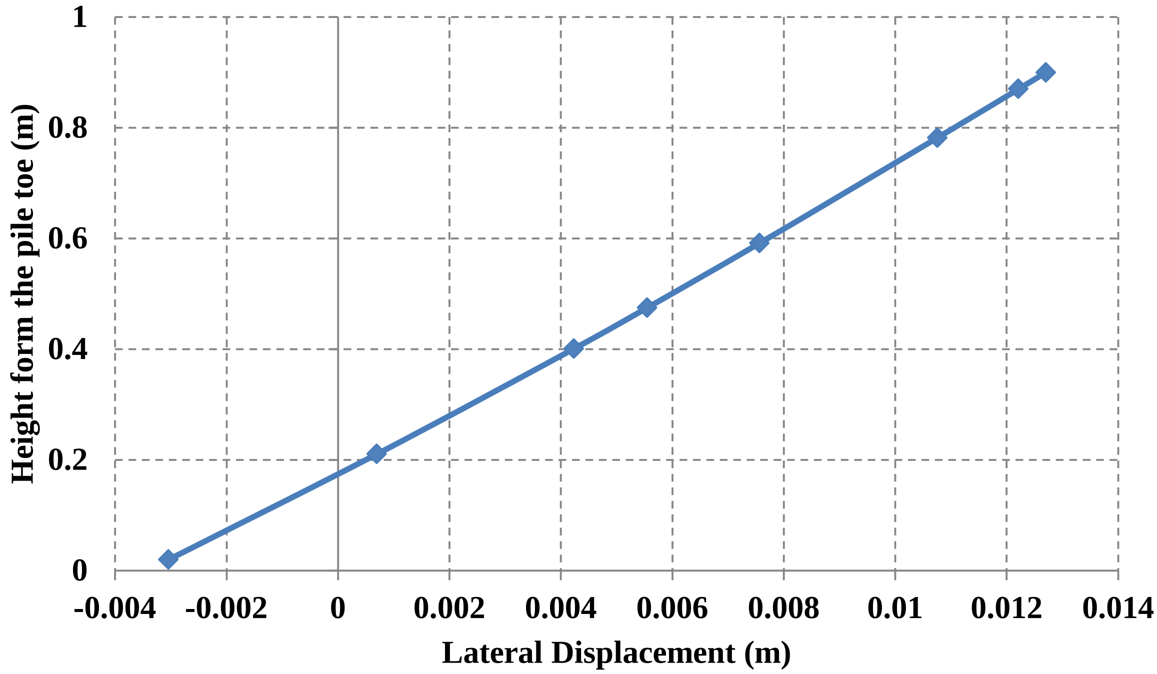

Figure A.54 Lateral Displacement along the Pile for Scour Depth = 500 mm and Slope = 0 Degree

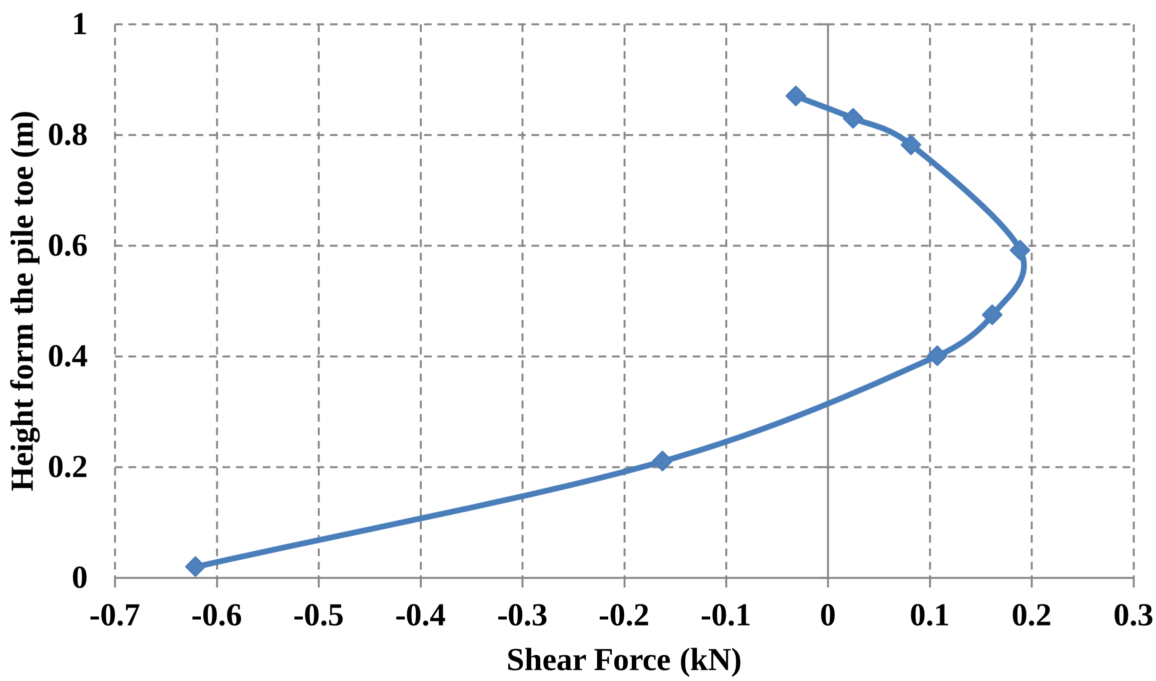

Figure A.55 Shear Force along the Pile for Scour Depth = 500 mm and Slope = 0 Degree

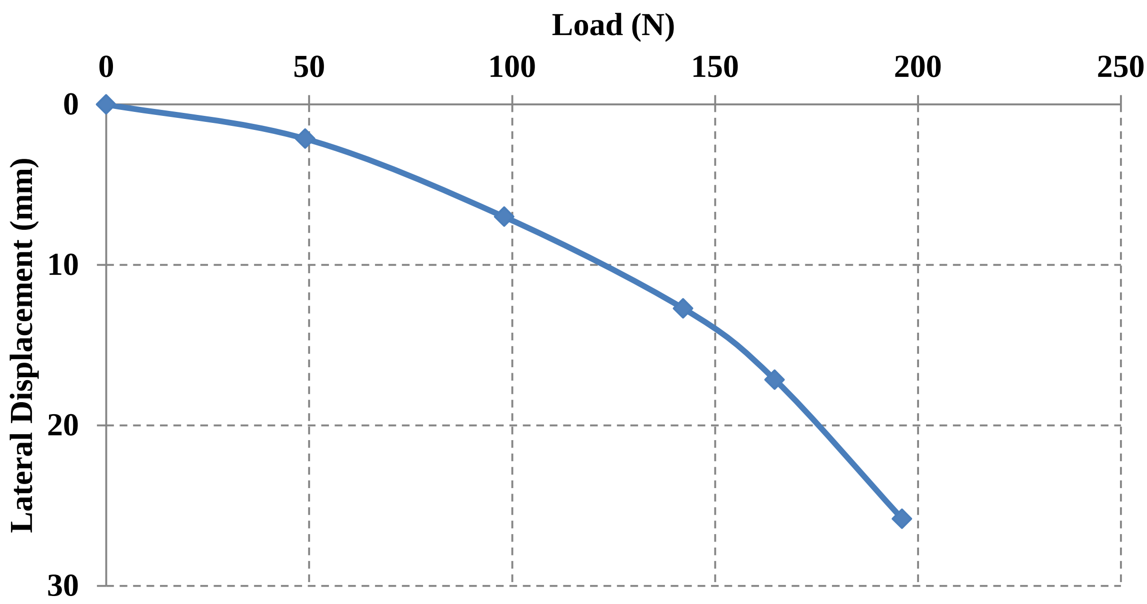

Figure A.56 Lateral Displacements vs. Load for Scour Depth = 500 mm and Slope = 0 Degree

A.3.2.2. 15-degree scour slope

200-mm scour depth

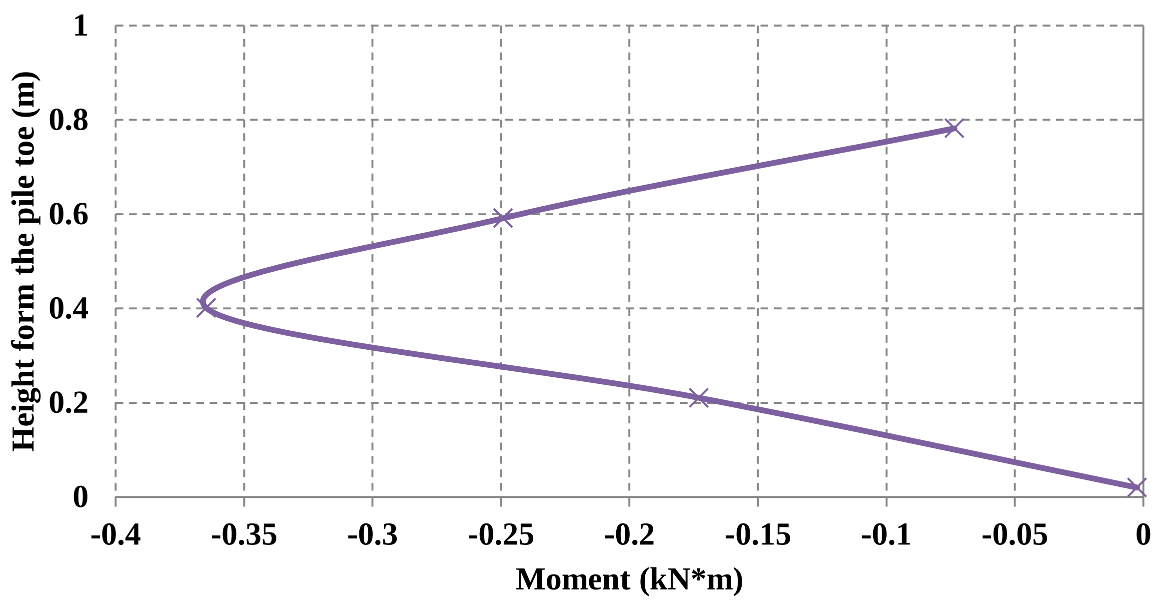

Figure A.57 Moment along the Pile for Scour Depth = 200 mm and Slope = 15 Degrees

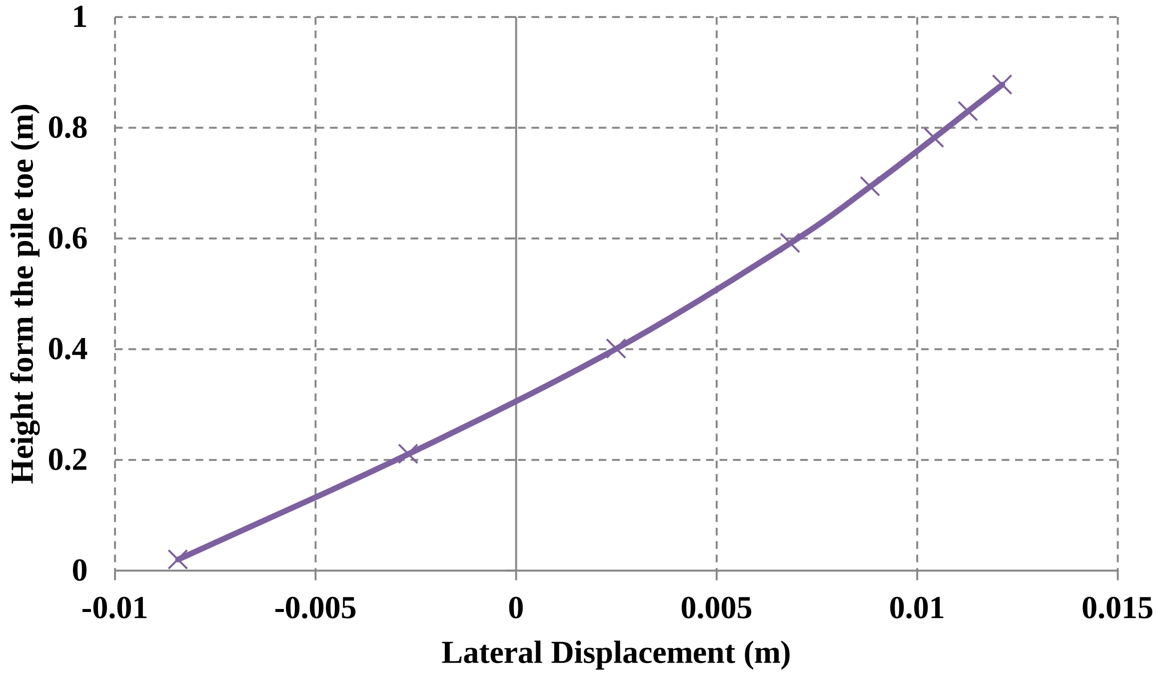

Figure A.58 Lateral Displacement along the Pile for Scour Depth = 200 mm and Slope = 15 Degrees

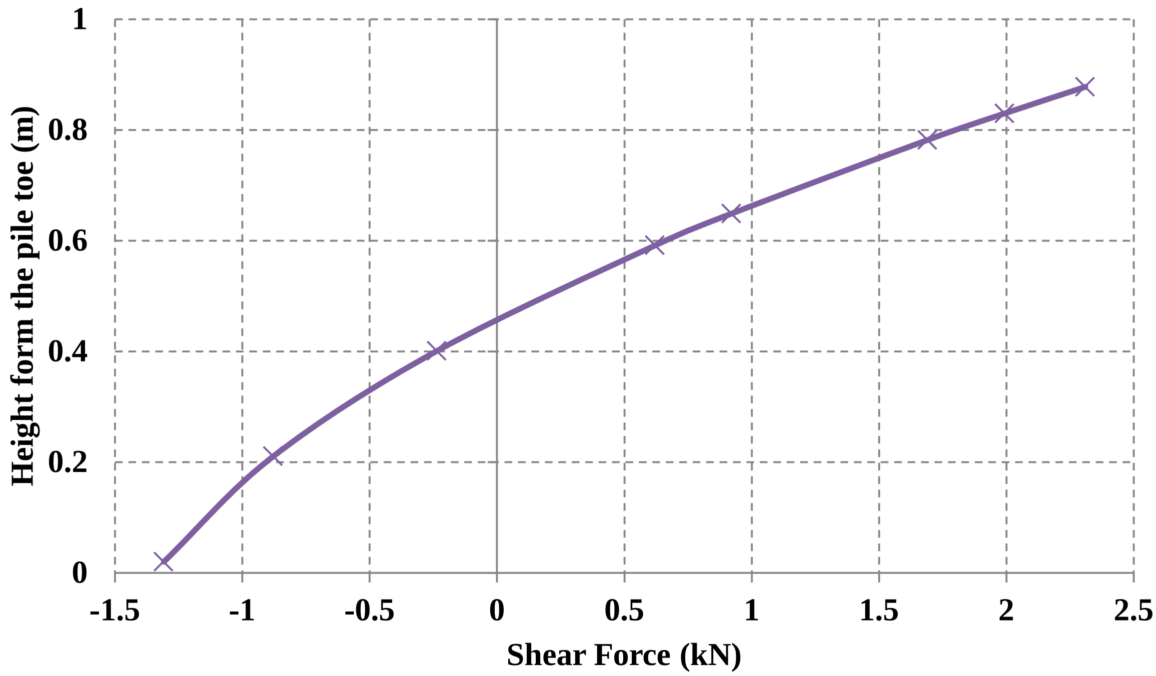

Figure A.59 Shear Force along the Pile for Scour Depth = 200 mm and Slope = 15 Degrees

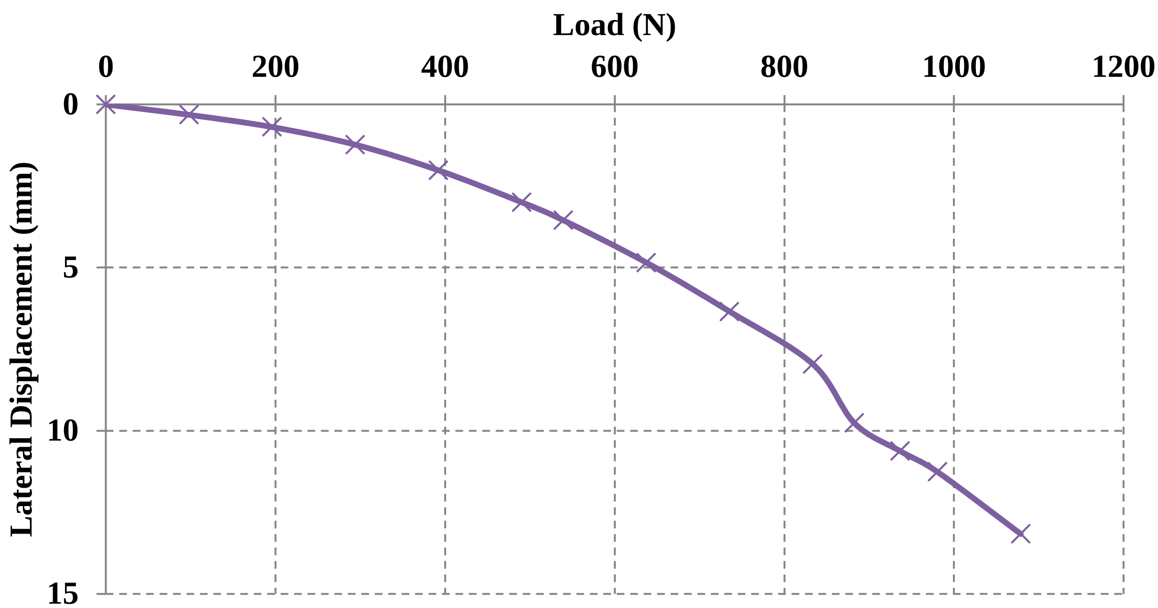

Figure A.60 Lateral Displacements vs. Load for Scour Depth = 200 mm and Slope = 15 Degrees

300-mm scour depth

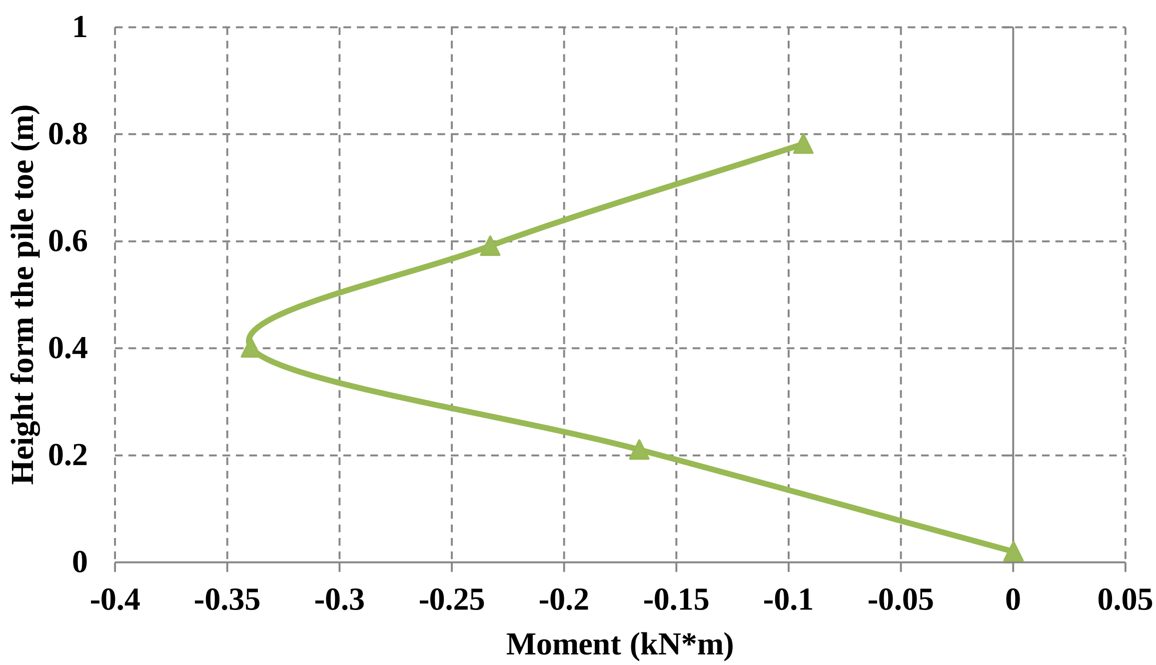

Figure A.61 Moment along the Pile for Scour Depth = 300 mm and Slope = 15 Degrees

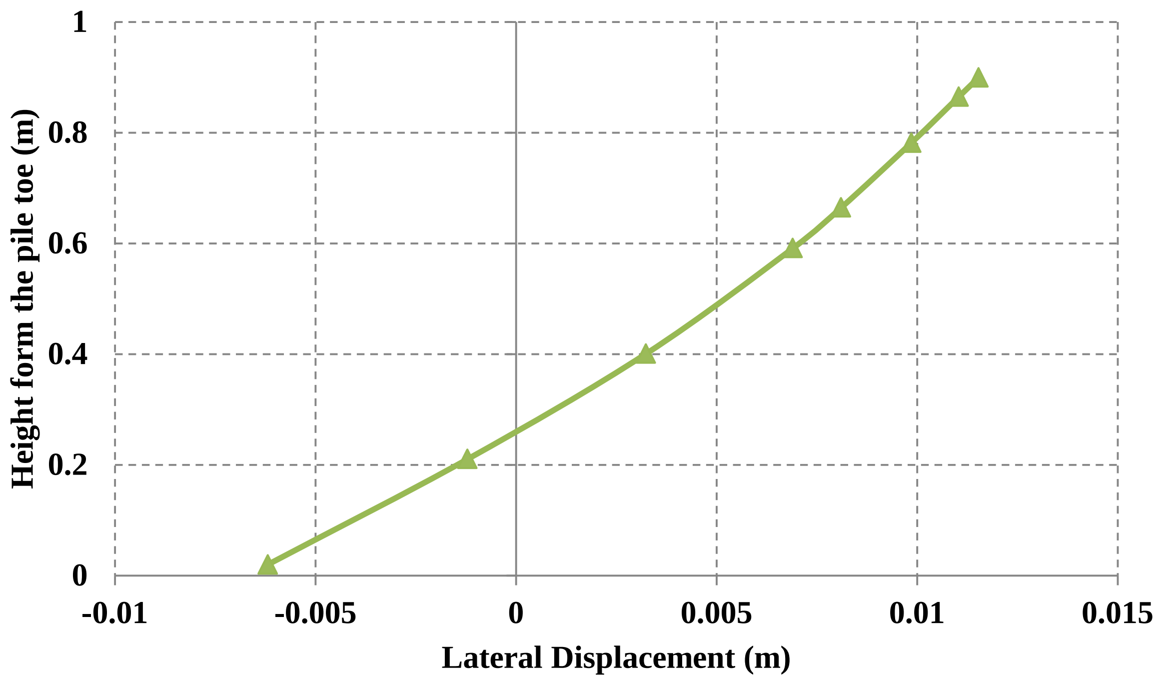

Figure A.62 Lateral Displacement along the Pile for Scour Depth = 300 mm and Slope = 15 Degrees

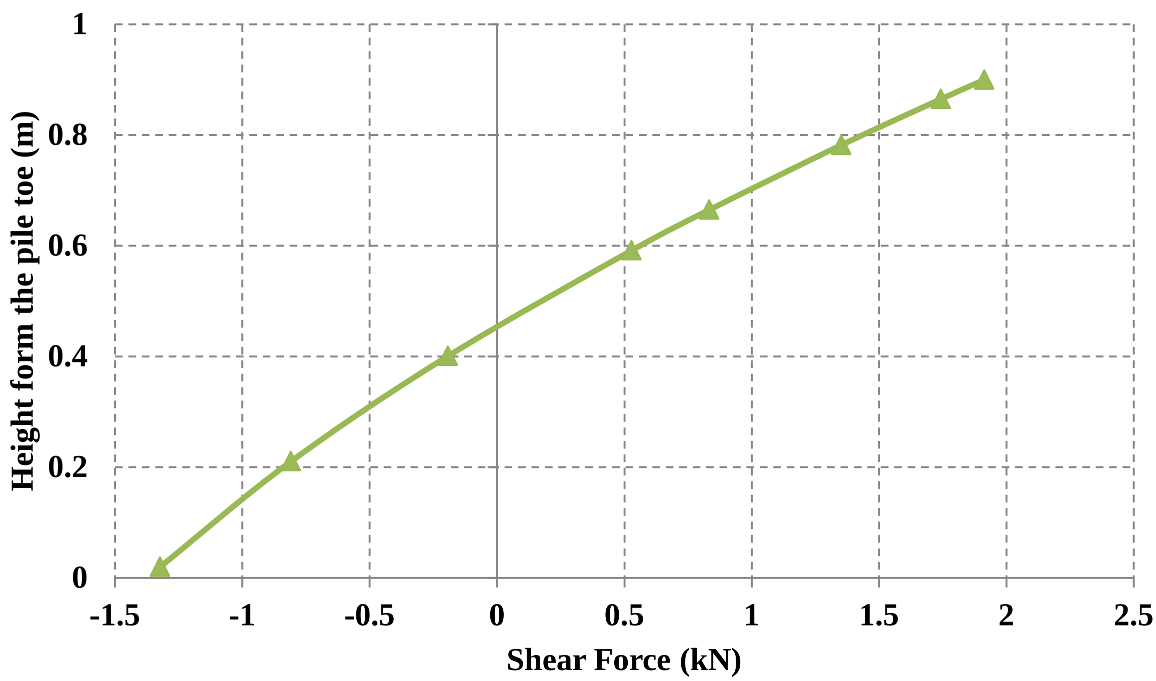

Figure A.63 Shear Force along the Pile for Scour Depth = 300 mm and Slope = 15 Degrees

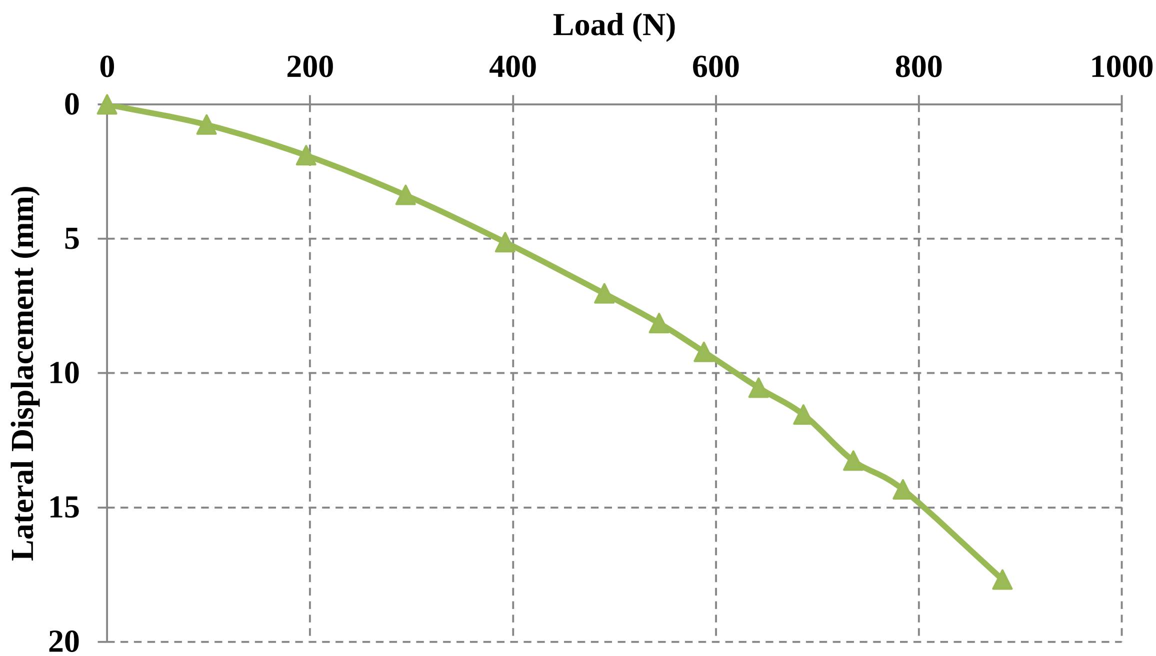

Figure A.64 Lateral Displacements vs. Load for Scour Depth = 300 mm and Slope = 15 Degrees

400-mm scour depth

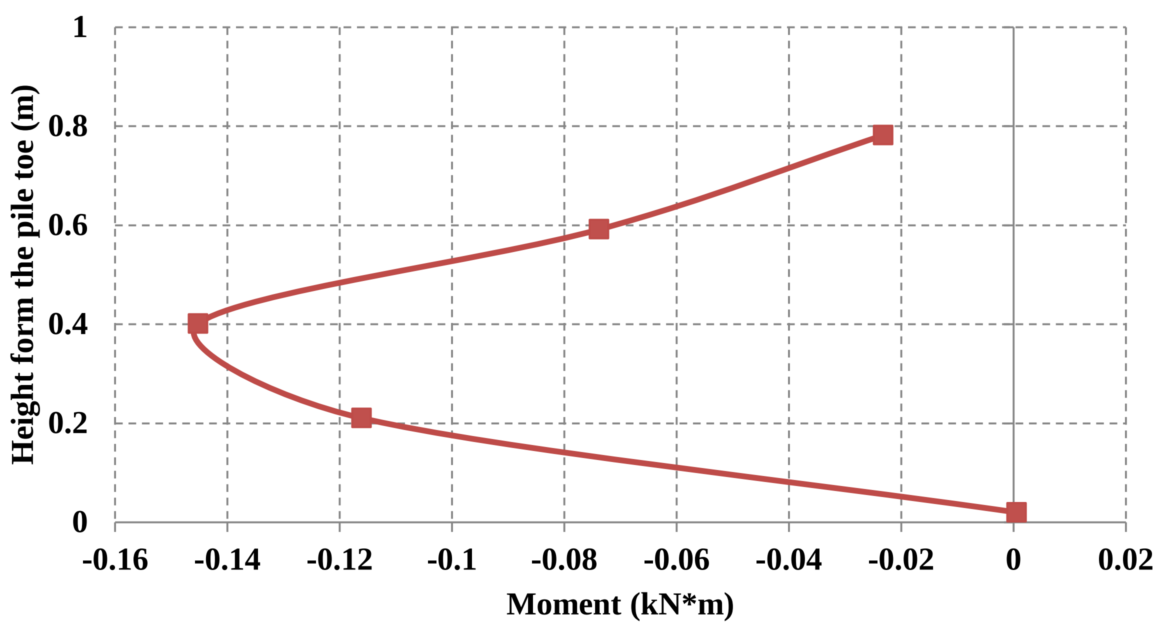

Figure A.65 Moment along the Pile for Scour Depth = 400 mm and Slope = 15 Degrees

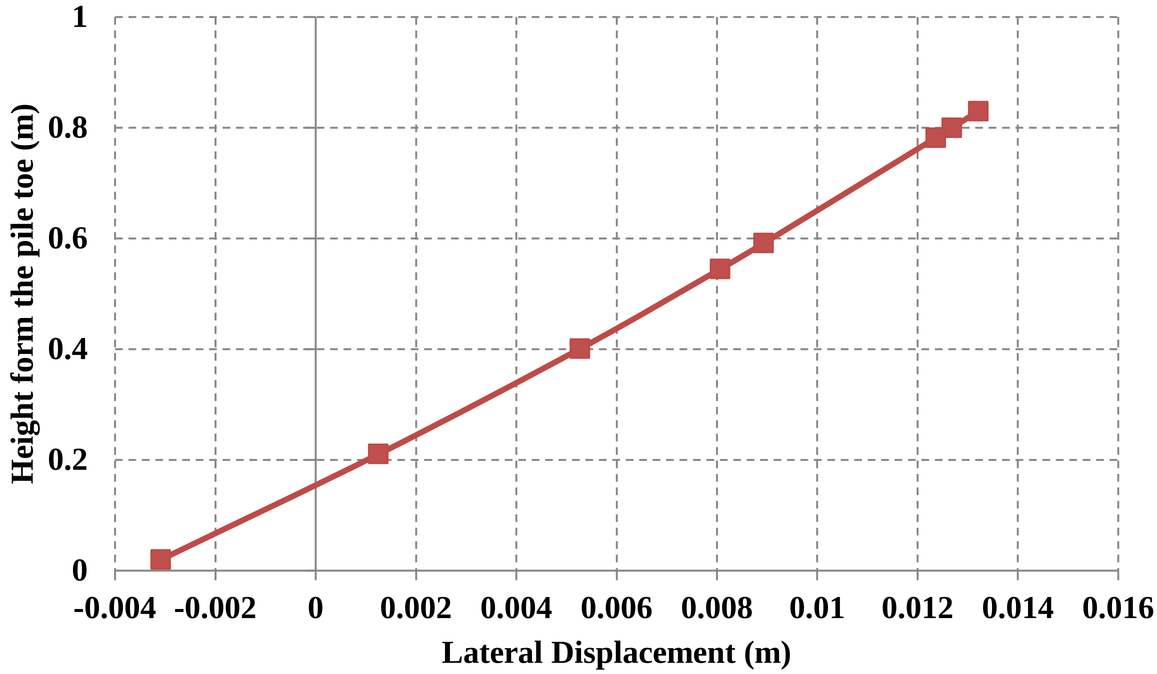

Figure A.66 Lateral Displacement along the Pile for Scour Depth = 400 mm and Slope = 15 Degrees

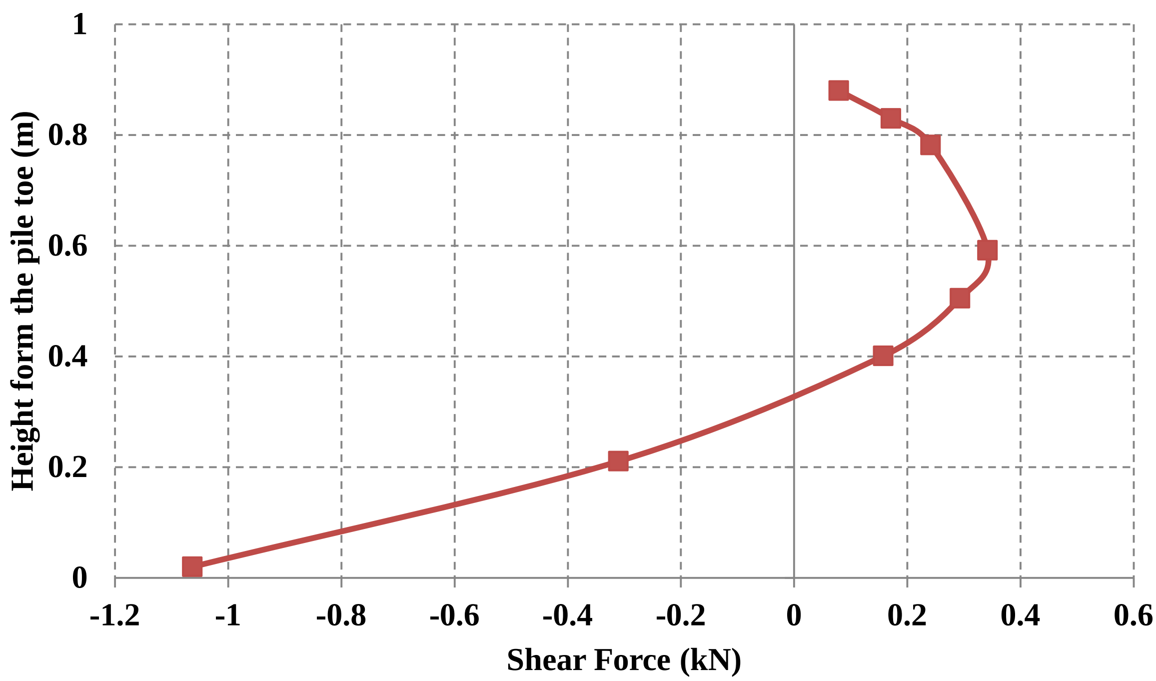

Figure A.67 Shear Force along the Pile for Scour Depth = 400 mm and Slope = 15 Degrees

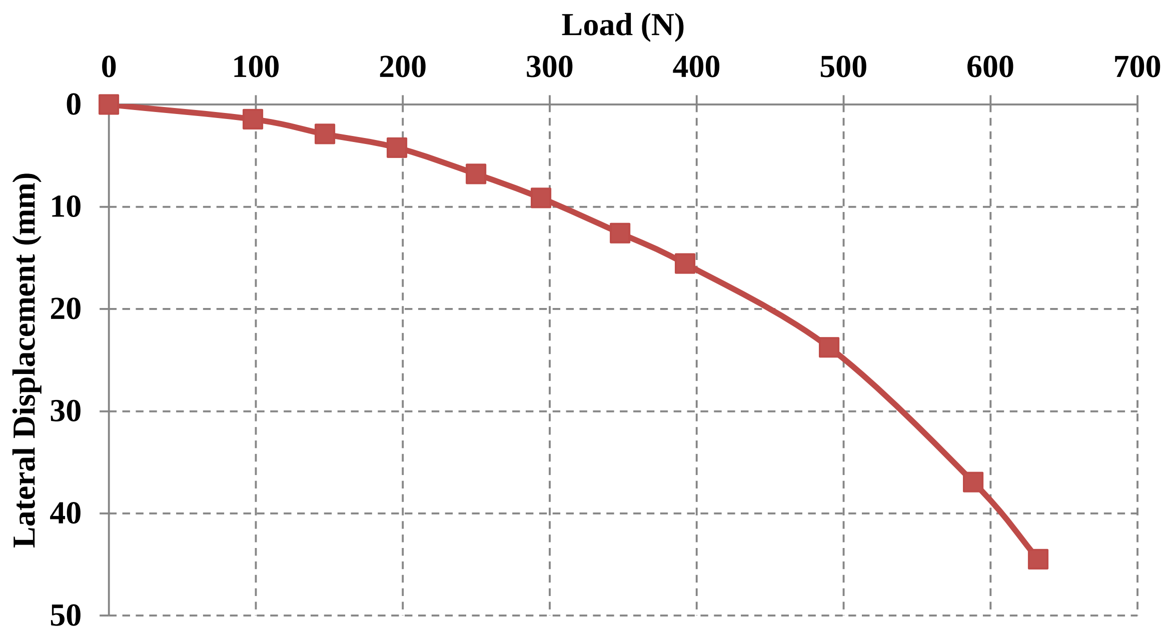

Figure A.68 Lateral Displacements vs. Load for Scour Depth = 400 mm and Slope = 15 Degrees

500-mm scour depth

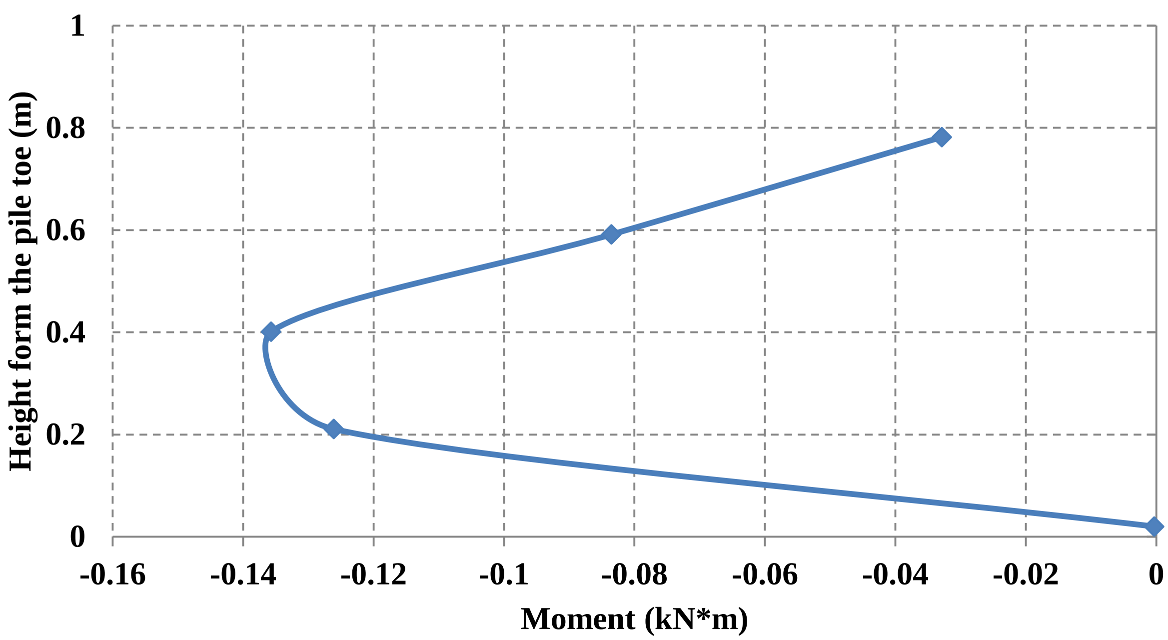

Figure A.69 Moment along the Pile for Scour Depth = 500 mm and Slope = 15 Degrees

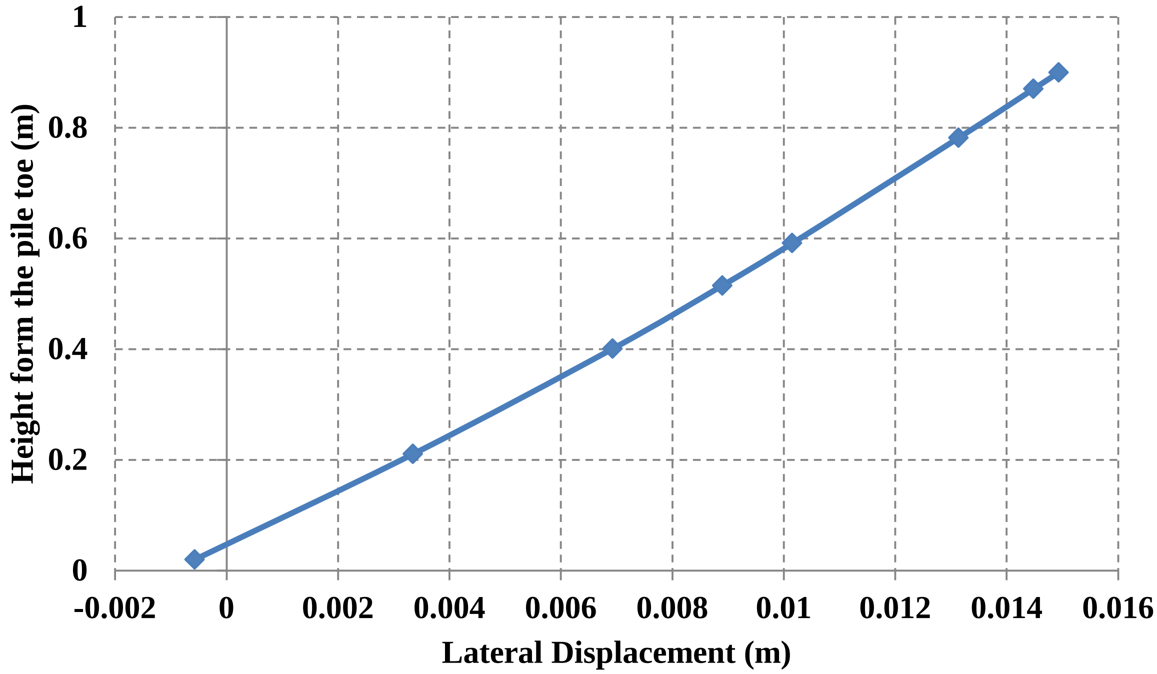

Figure A.70 Lateral Displacement along the Pile for Scour Depth = 500 mm and Slope = 15 Degrees

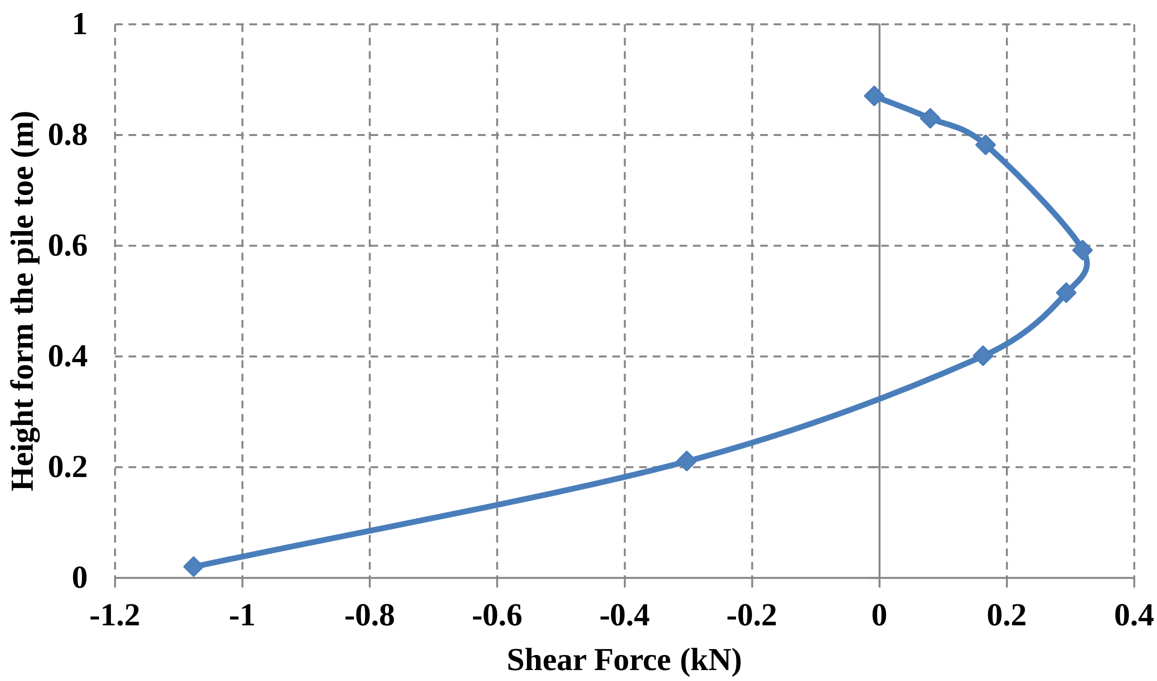

Figure A.71 Shear Force along the Pile for Scour Depth = 500 mm and Slope = 15 Degrees

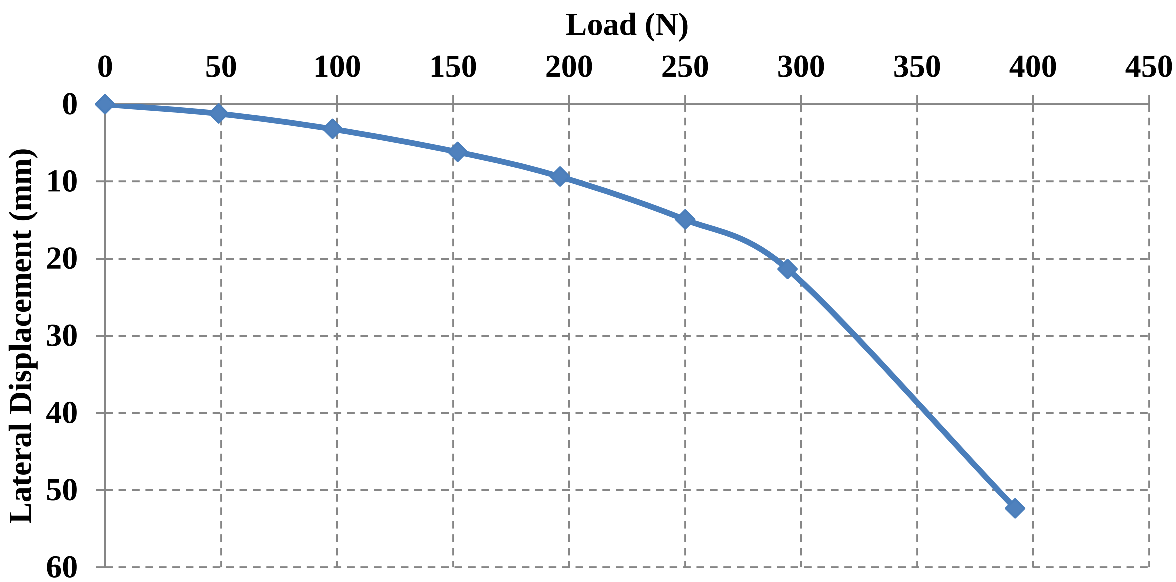

Figure A.72 Lateral Displacements vs. Load for Scour Depth = 500 mm and Slope = 15 Degrees

A.3.2.3. 30-degree scour slope

200-mm scour depth

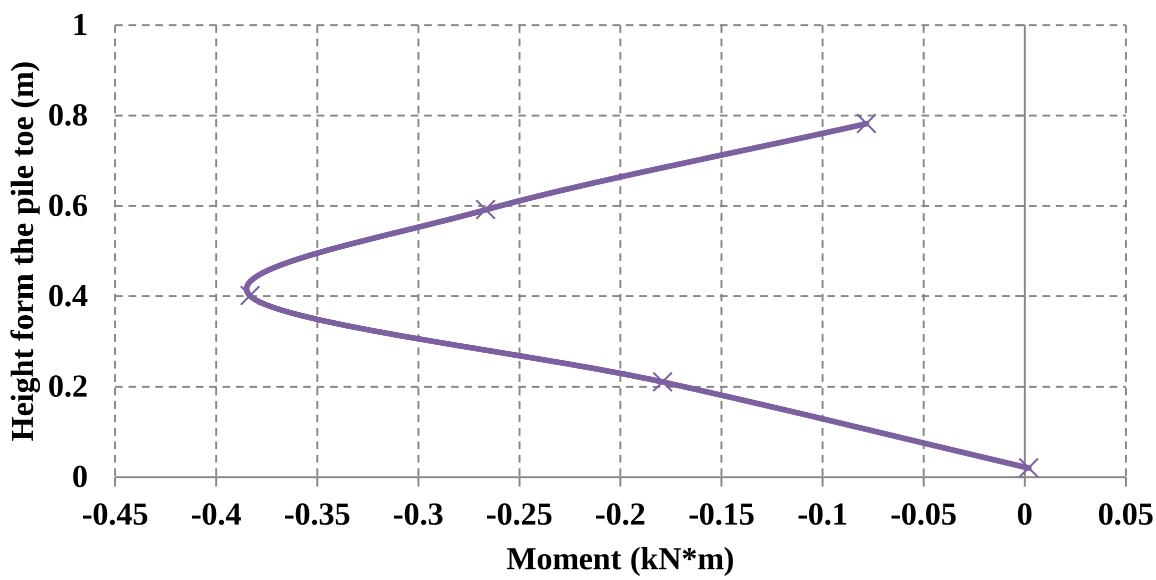

Figure A.73 Moment along the Pile for Scour Depth = 200 mm and Slope = 30 Degrees

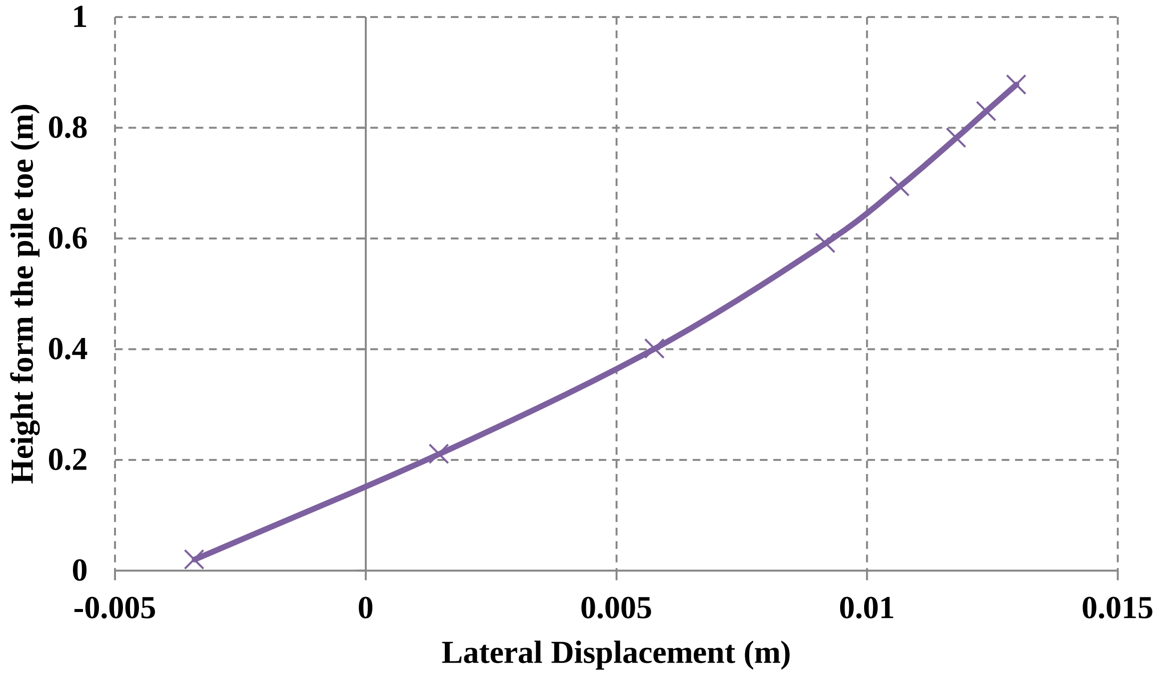

Figure A.74 Lateral Displacement along the Pile for Scour Depth = 200 mm and Slope = 30 Degrees

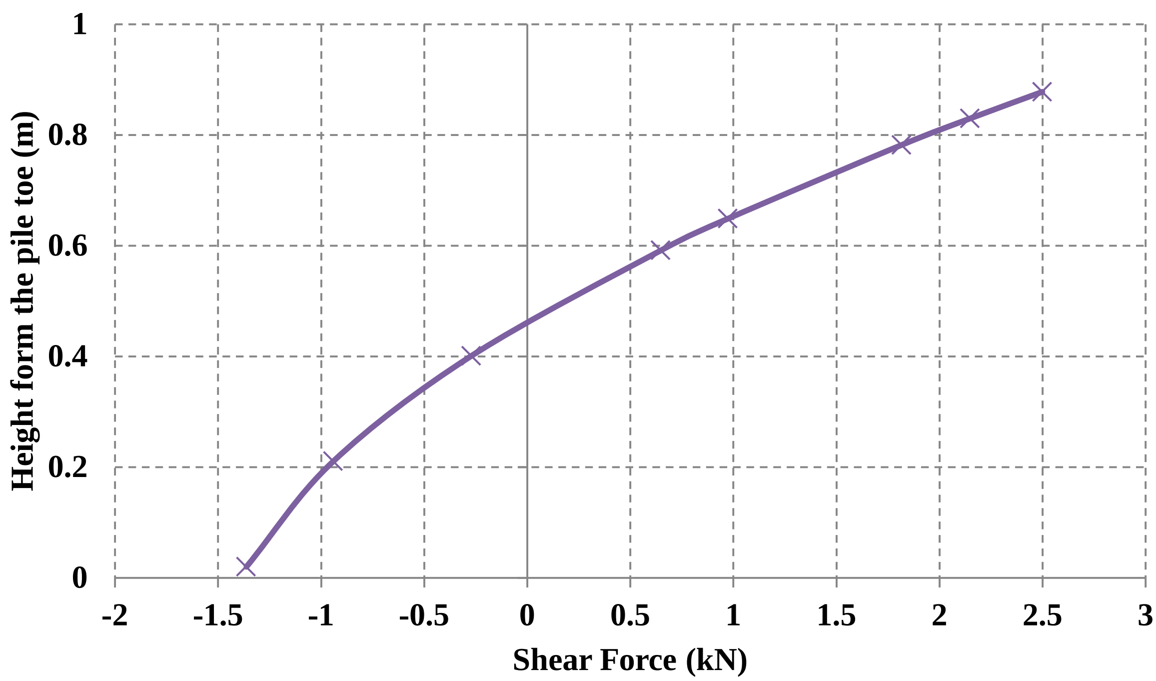

Figure A.75 Shear Force along the Pile for Scour Depth = 200 mm and Slope = 30 Degrees

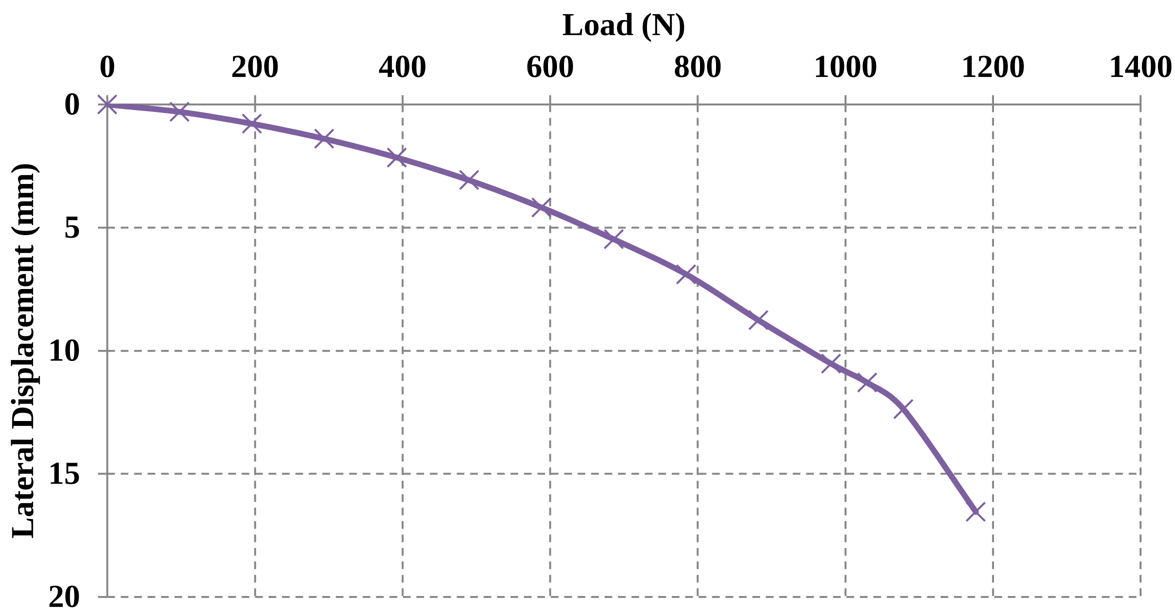

Figure A.76 Lateral Displacements vs. Load for Scour Depth = 200 mm and Slope = 30 Degrees

300-mm scour depth

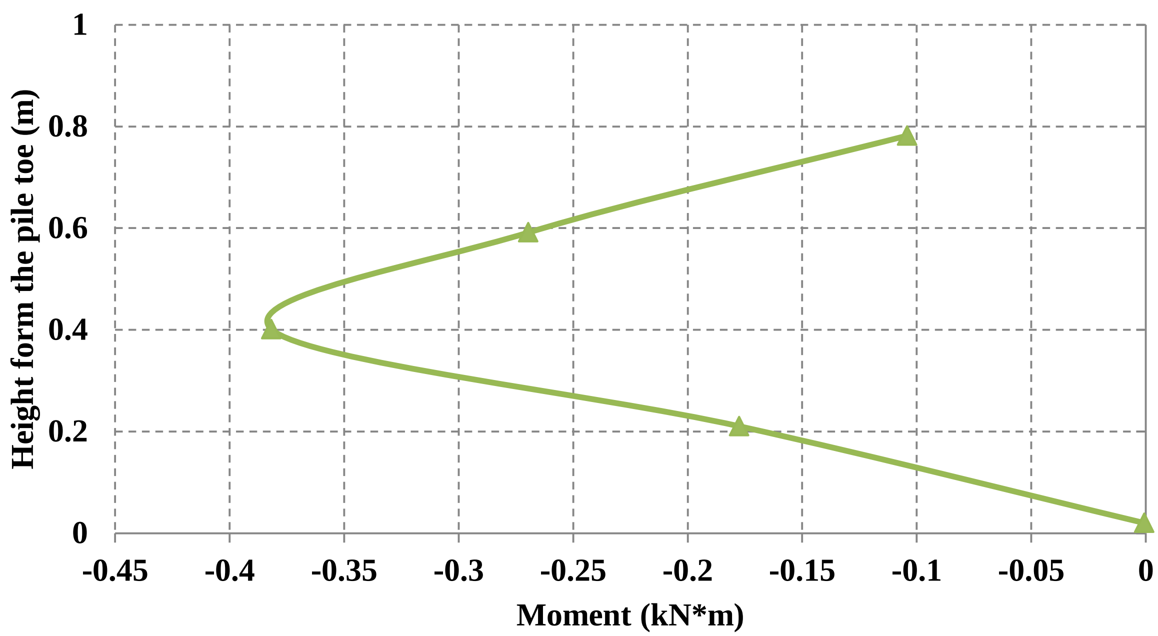

Figure A.77 Moment along the Pile for Scour Depth = 300 mm and Slope = 30 Degrees

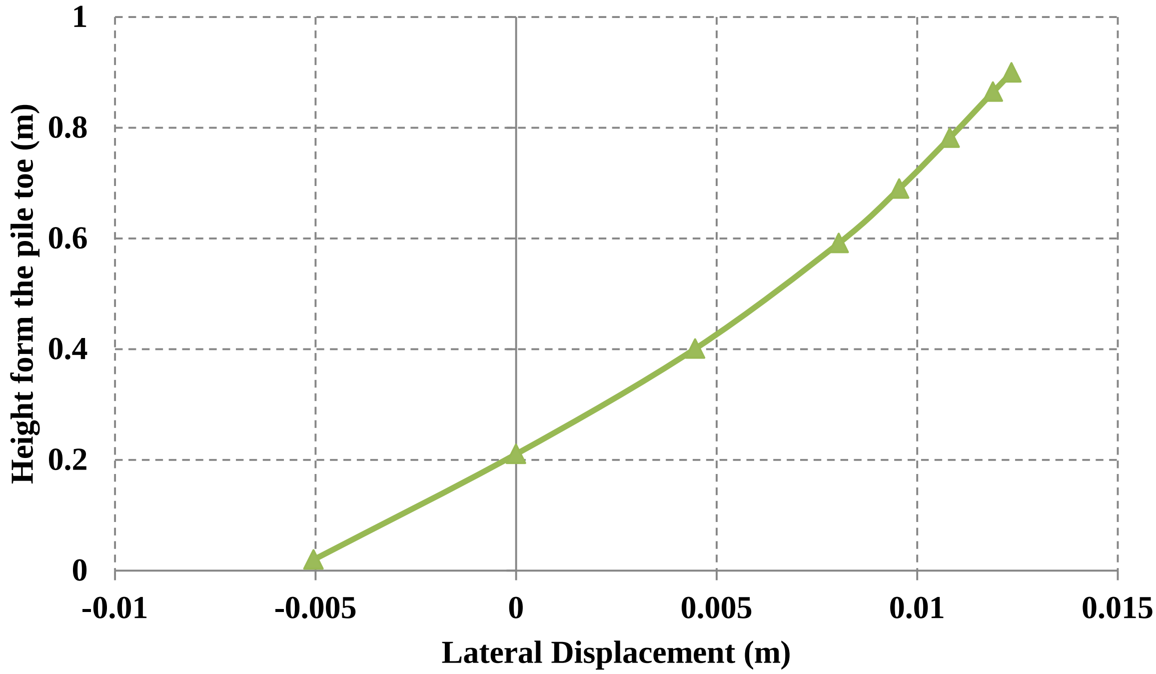

Figure A.78 Lateral Displacement along the Pile for Scour Depth = 300 mm and Slope = 30 Degrees

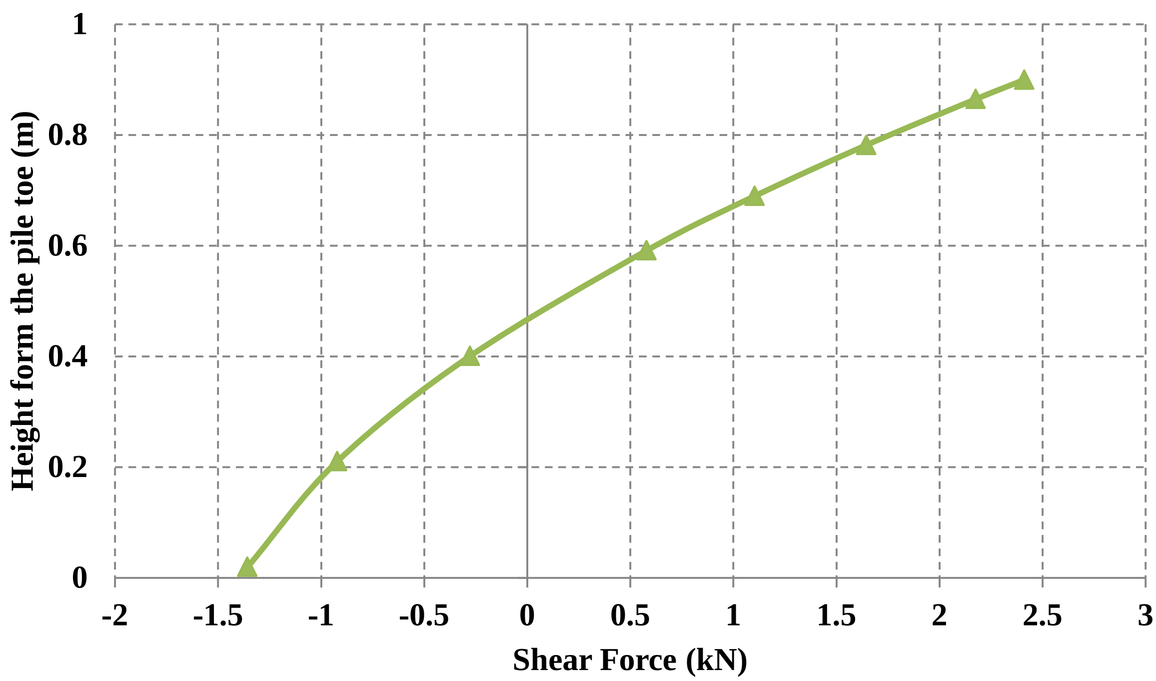

Figure A.79 Shear Force along the Pile for Scour Depth = 300 mm and Slope = 30 Degrees

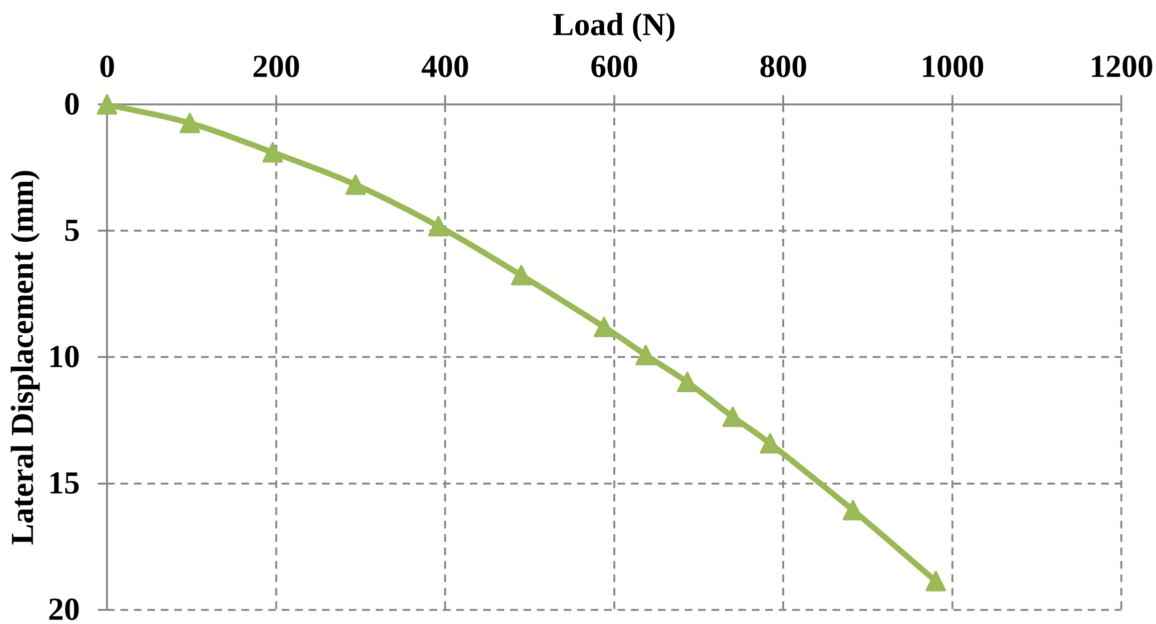

Figure A.80 Lateral Displacements vs. Load for Scour Depth = 300 mm and Slope = 30 Degrees

400-mm scour depth

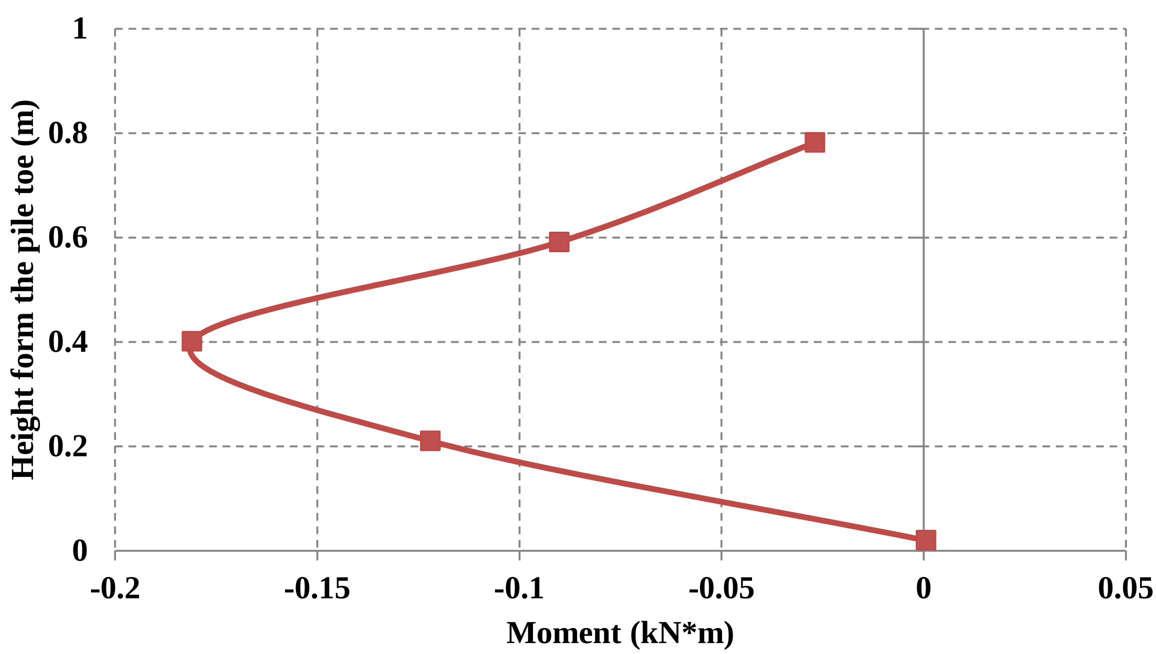

Figure A.81 Moment along the Pile for Scour Depth = 400 mm and Slope = 30 Degrees

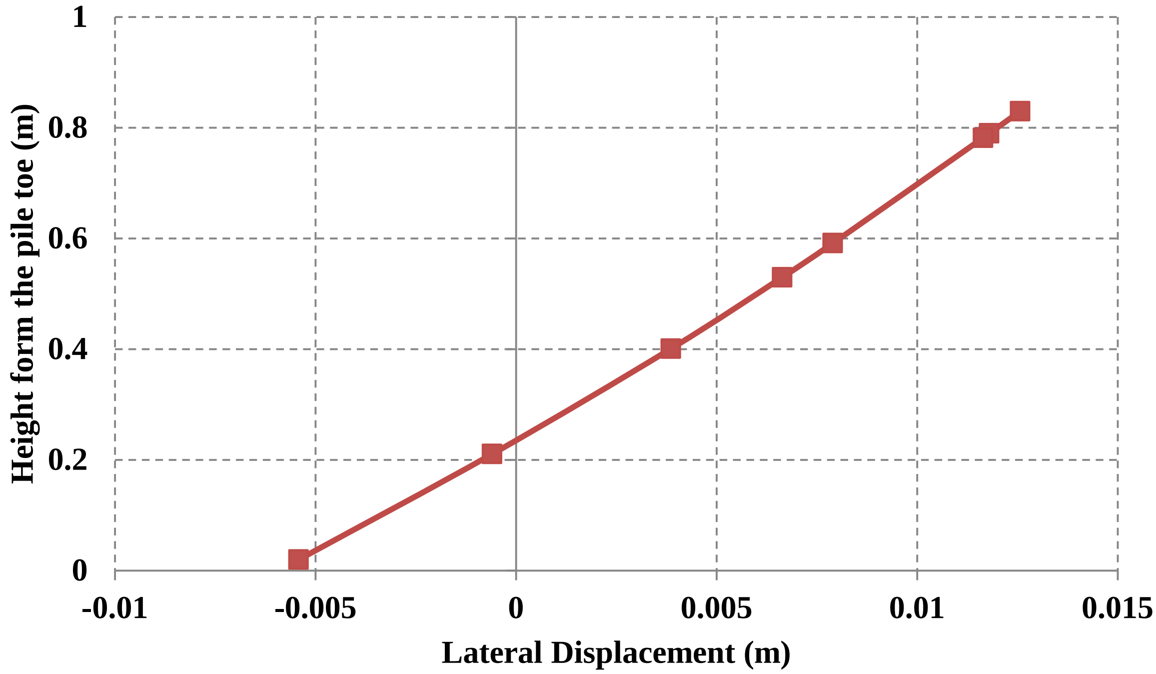

Figure A.82 Lateral Displacement along the Pile for Scour Depth = 400 mm and Slope = 30 Degrees

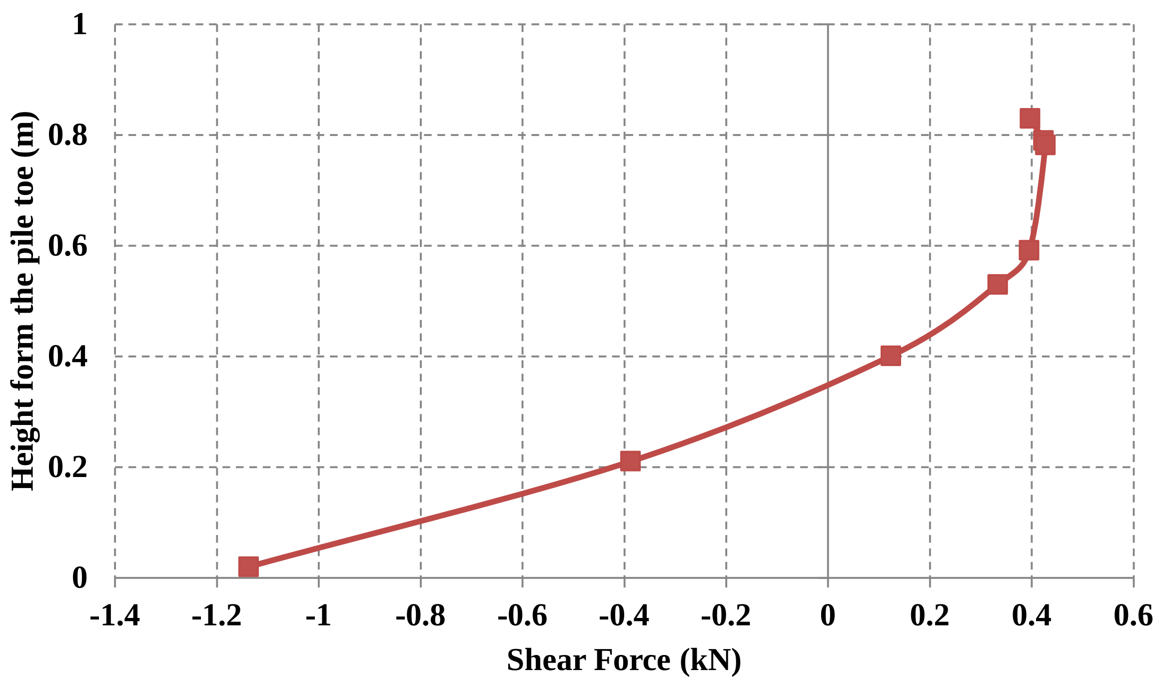

Figure A.83 Shear Force along the Pile for Scour Depth = 400 mm and Slope = 30 Degrees

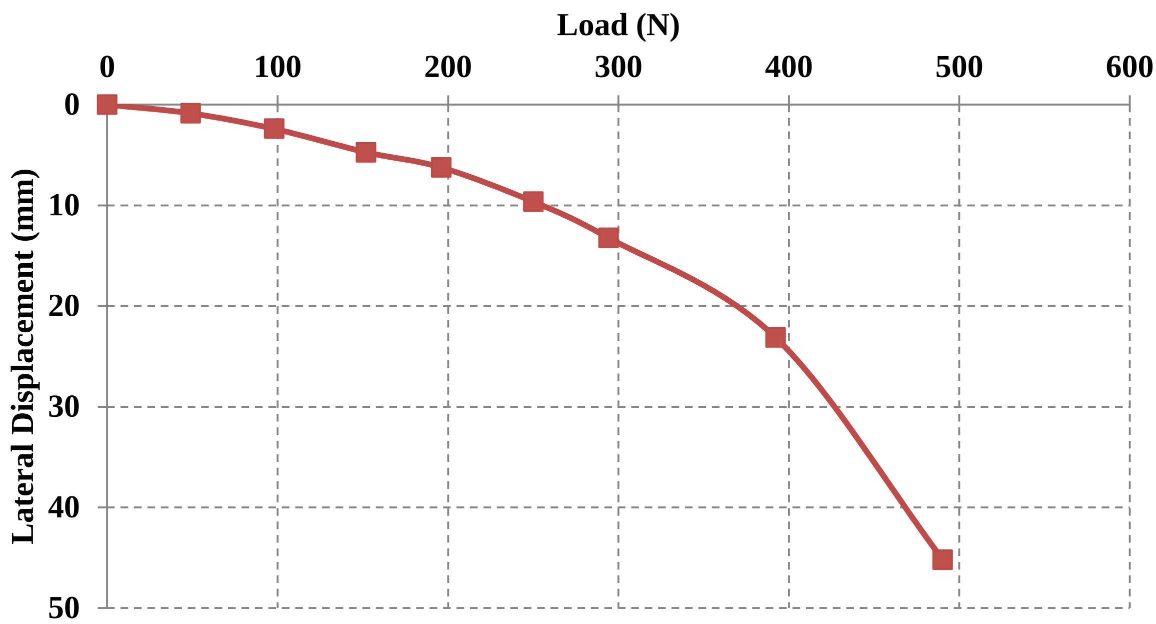

Figure A.84 Lateral Displacements vs. Load for Scour Depth = 400 mm and Slope = 30 Degrees

500-mm scour depth

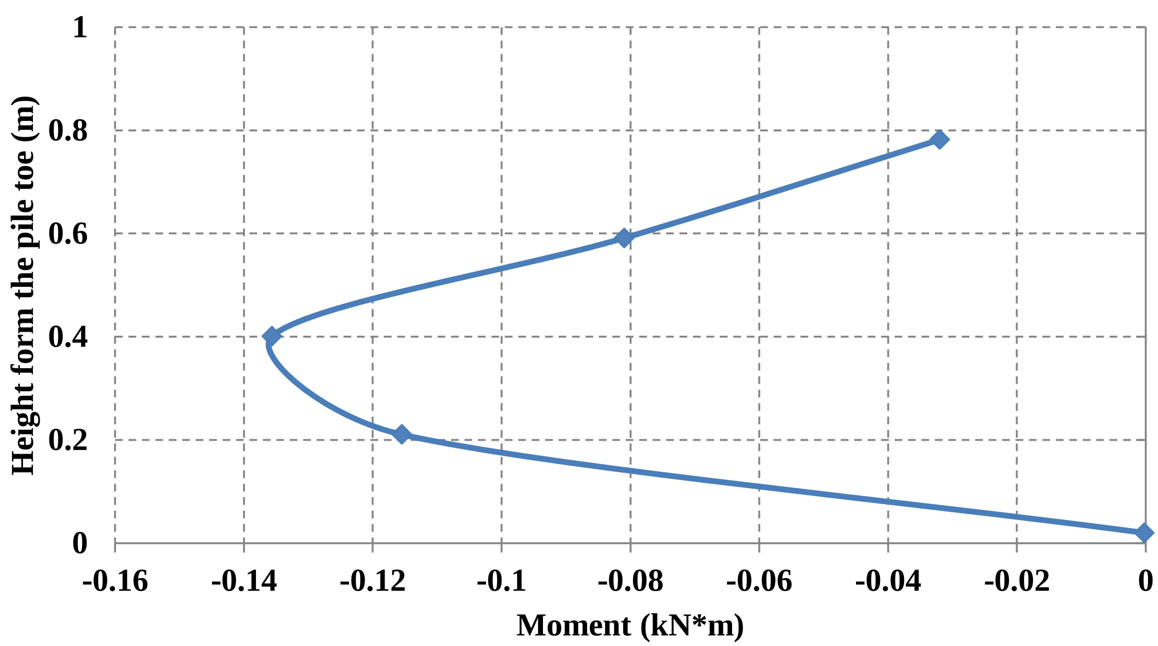

Figure A.85 Moment along the Pile for Scour Depth = 500 mm and Slope = 30 Degrees

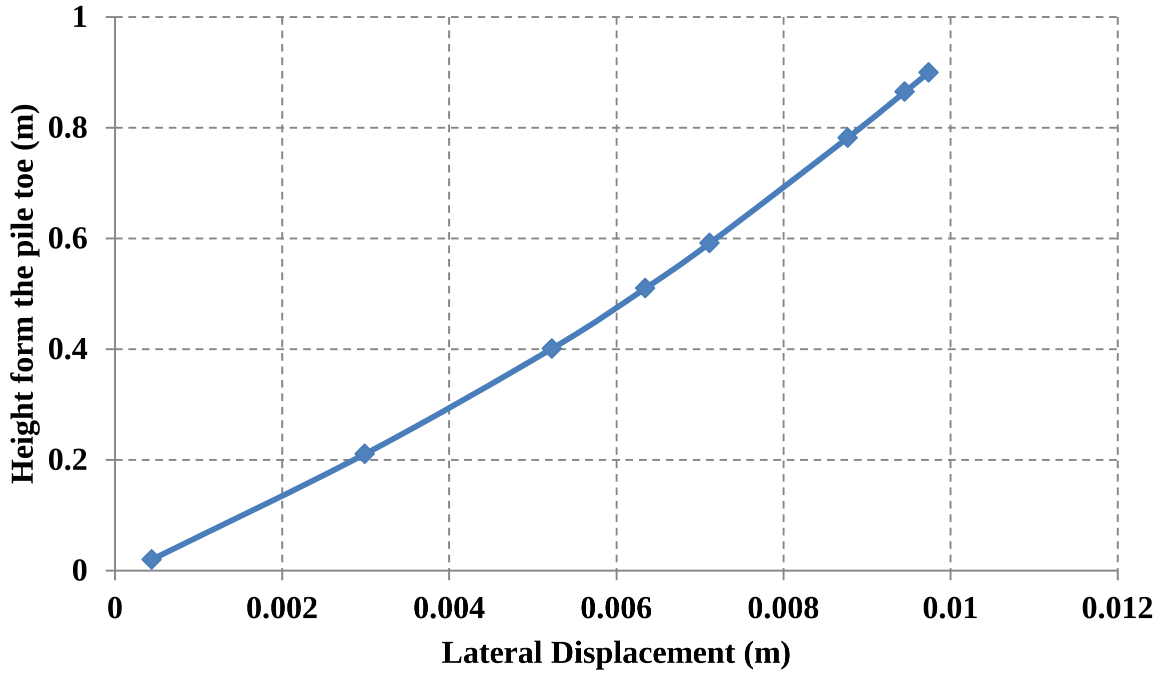

Figure A.86 Lateral Displacement along the Pile for Scour Depth = 500 mm and Slope = 30 Degrees

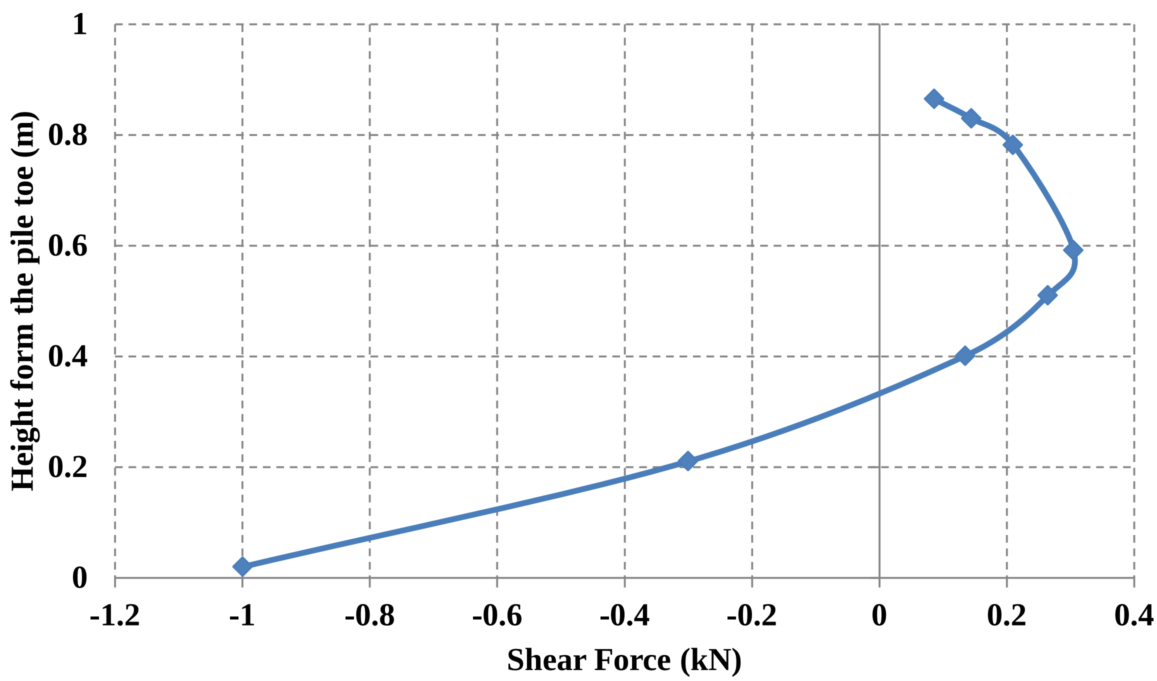

Figure A.87 Shear Force along the Pile for Scour Depth = 500 mm and Slope = 30 Degrees

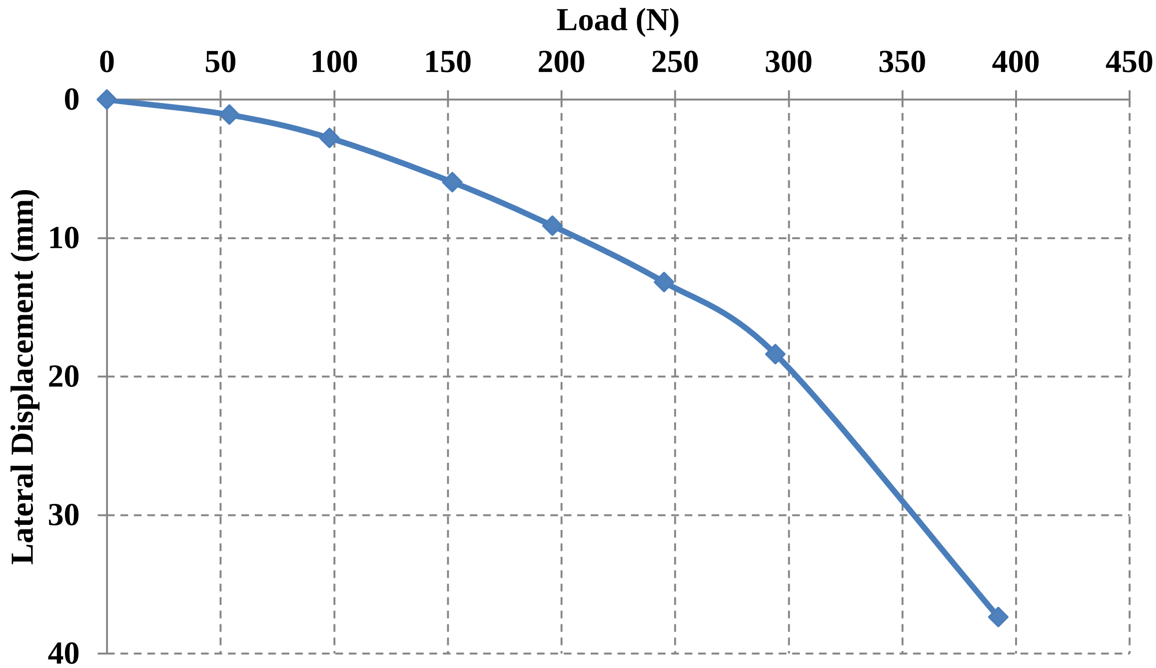

Figure A.88 Lateral Displacements vs. Load for Scour Depth = 500 mm and Slope = 30 Degrees

A.3.3. Combined scour width and scour depth effect

A.3.3.1. 0-mm scour width

200-mm scour depth

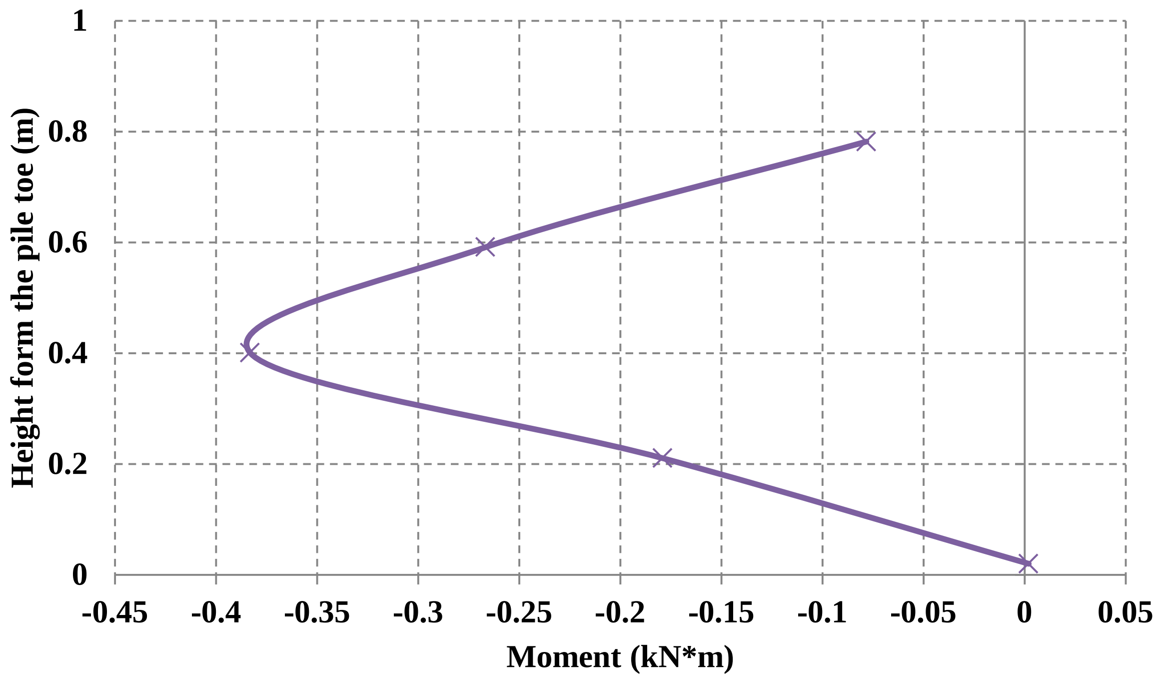

Figure A.89 Moment along the Pile for Scour Depth = 200 mm and Width = 0 mm

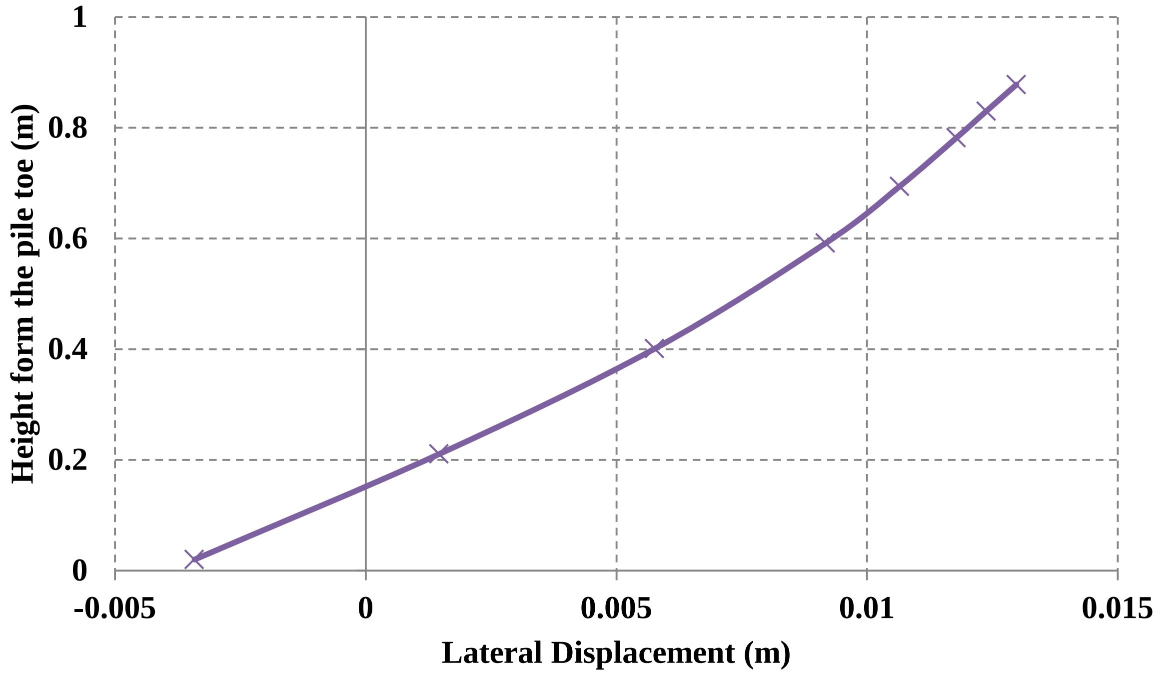

Figure A.90 Lateral Displacement along the Pile for Scour Depth = 200 mm and Width = 0 mm

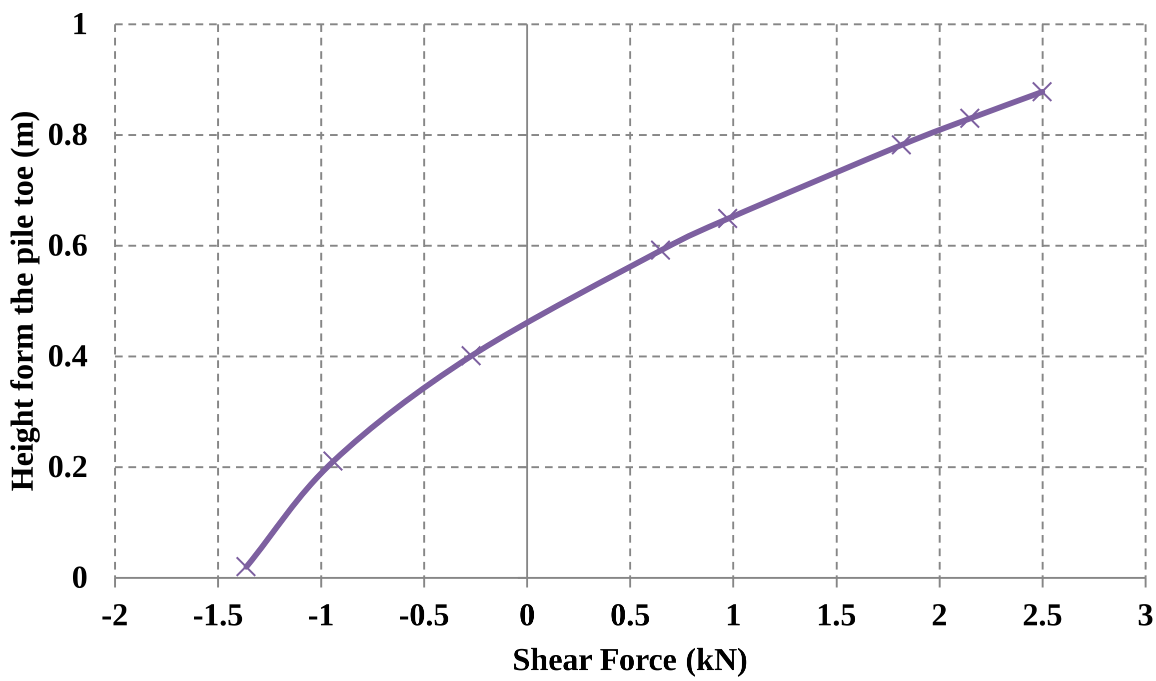

Figure A.91 Shear Force along the Pile for Scour Depth = 200 mm and Width = 0 mm

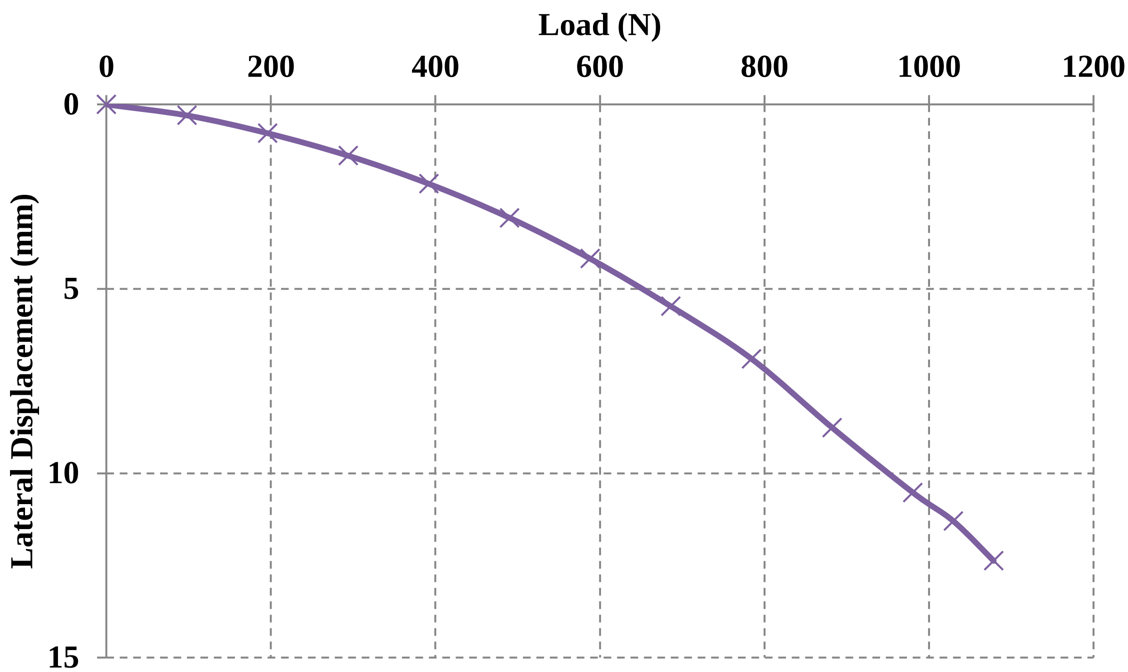

Figure A.92 Lateral Displacements vs. Load for Scour Depth = 200 mm and Width = 0 mm

300-mm scour depth

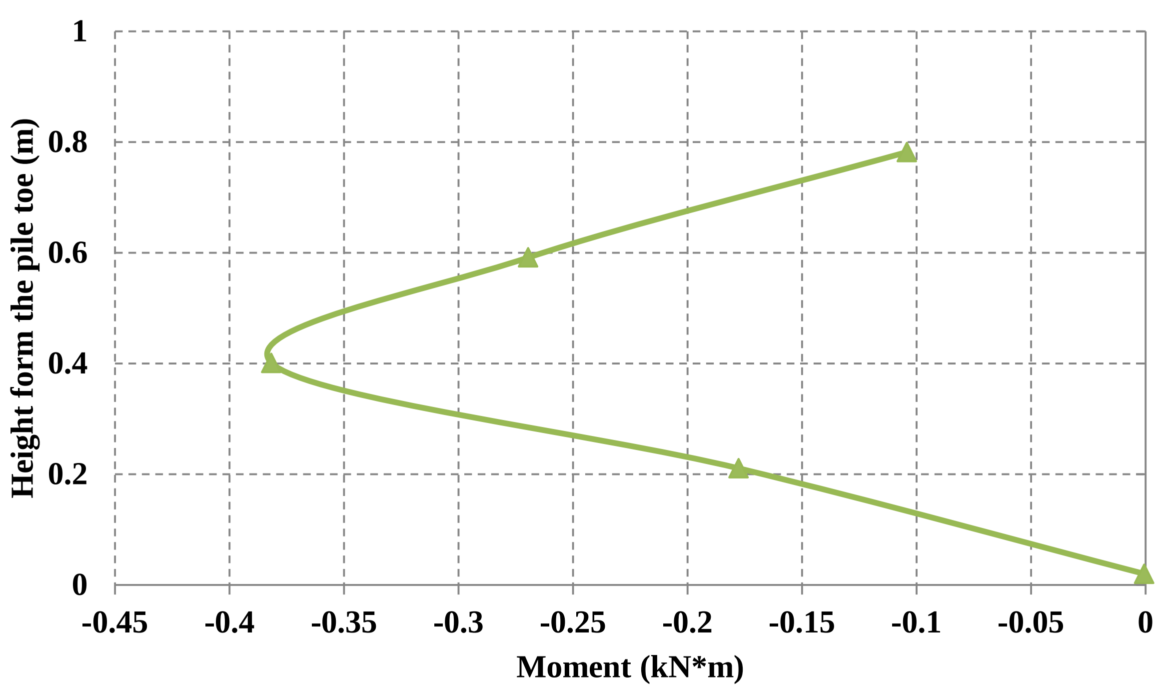

Figure A.93 Moment along the Pile for Scour Depth = 300 mm and Width = 0 mm

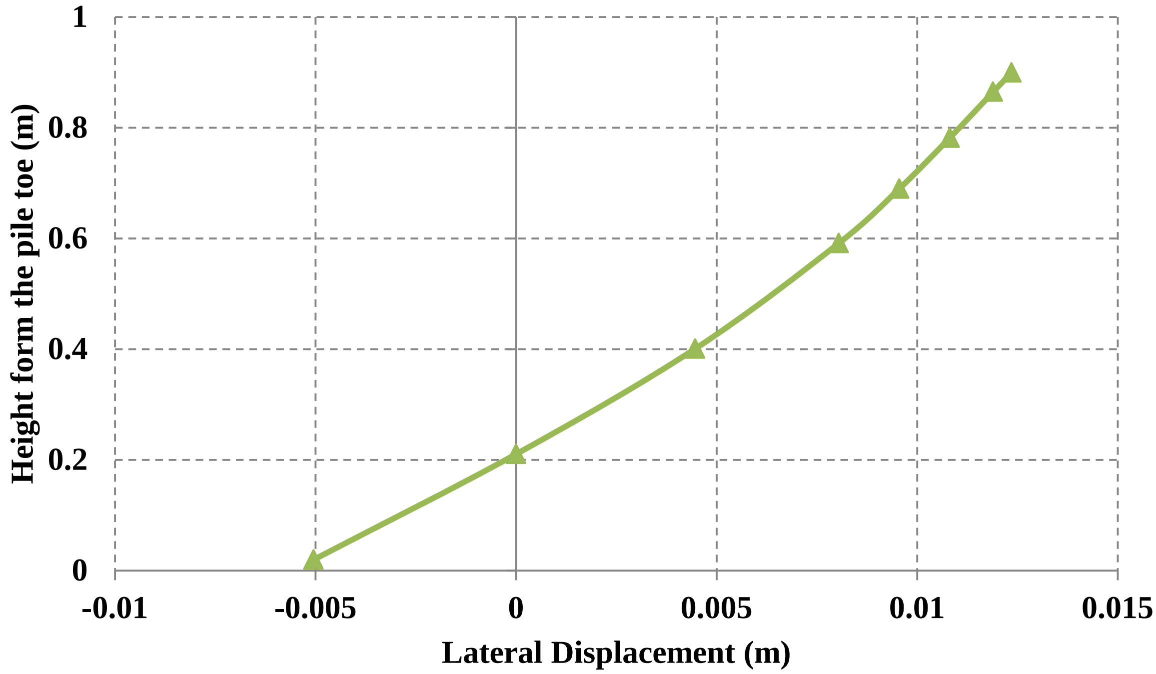

Figure A.94 Lateral Displacement along the Pile for Scour Depth = 300 mm and Width = 0 mm

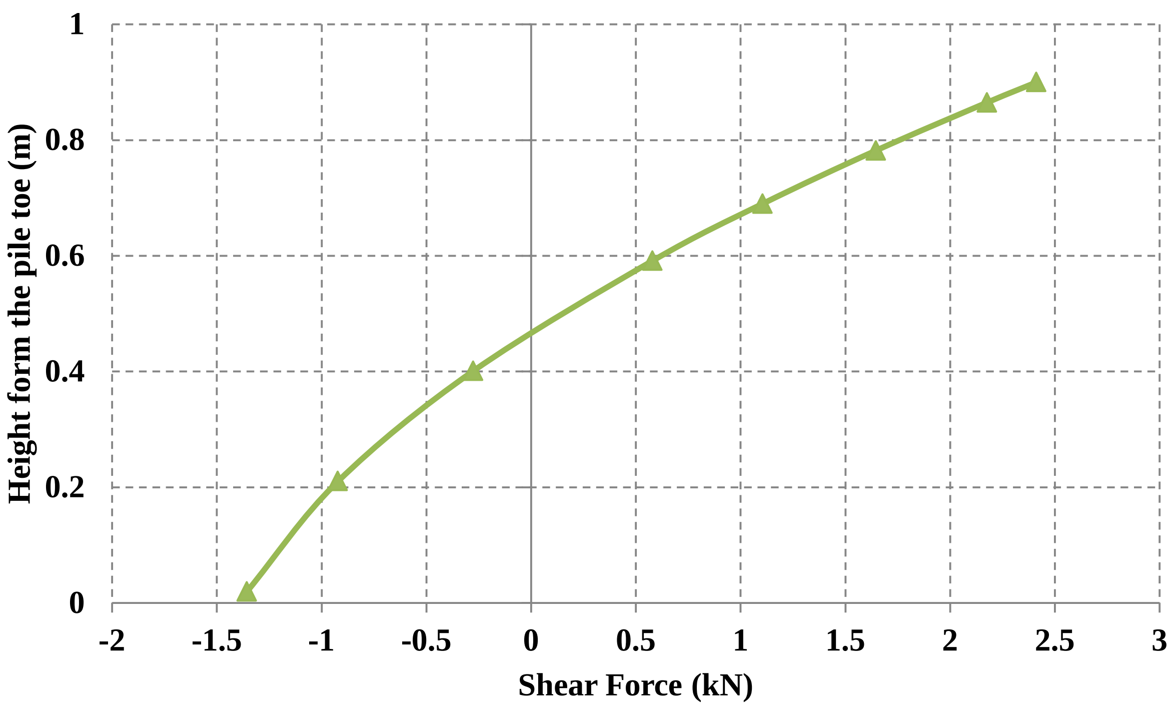

Figure A.95 Shear Force along the Pile for Scour Depth = 300 mm and Width = 0 mm

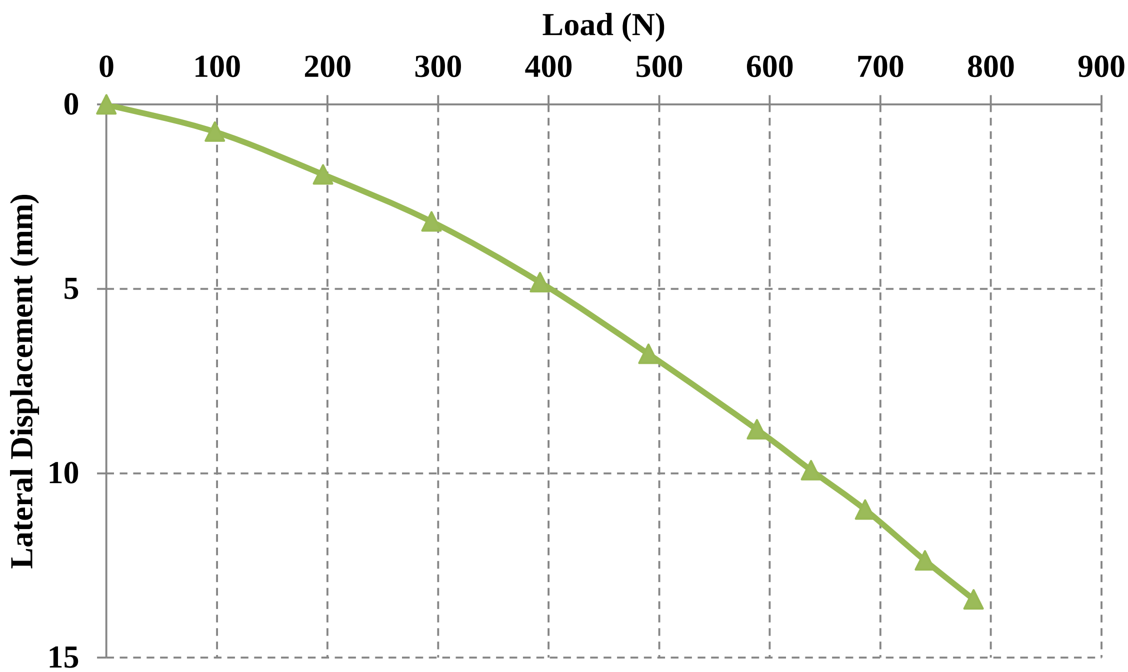

Figure A.96 Lateral Displacements vs. Load for Scour Depth = 300 mm and Width = 0 mm

400-mm scour depth

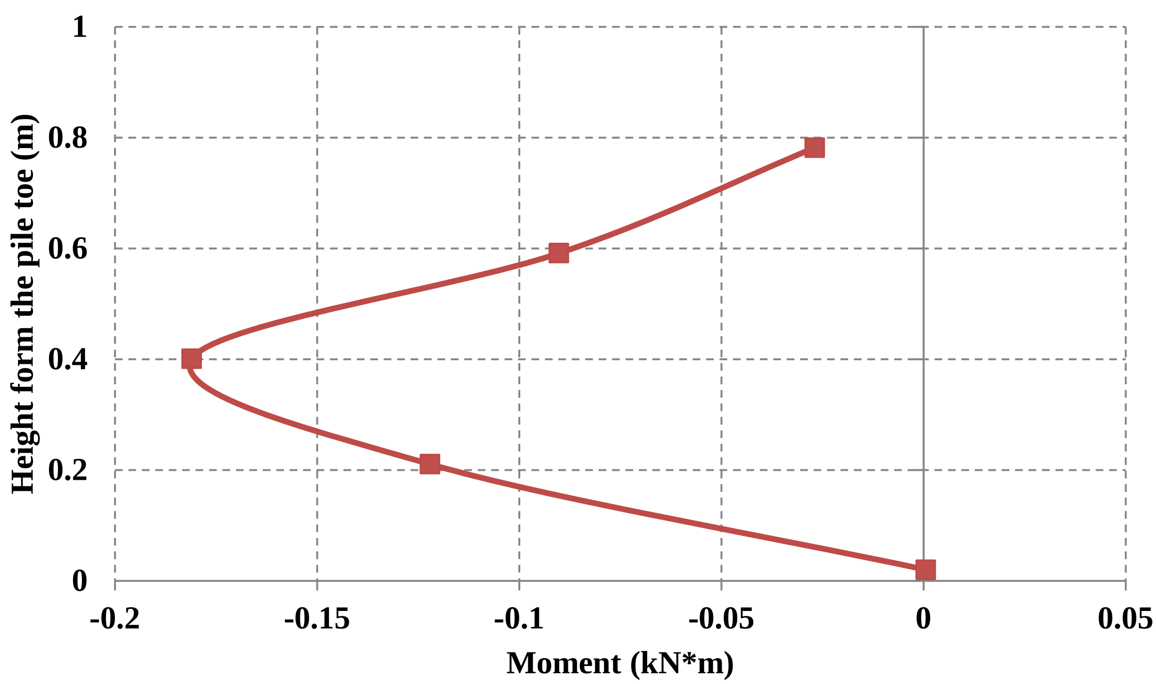

Figure A.97 Moment along the Pile for Scour Depth = 400 mm and Width = 0 mm

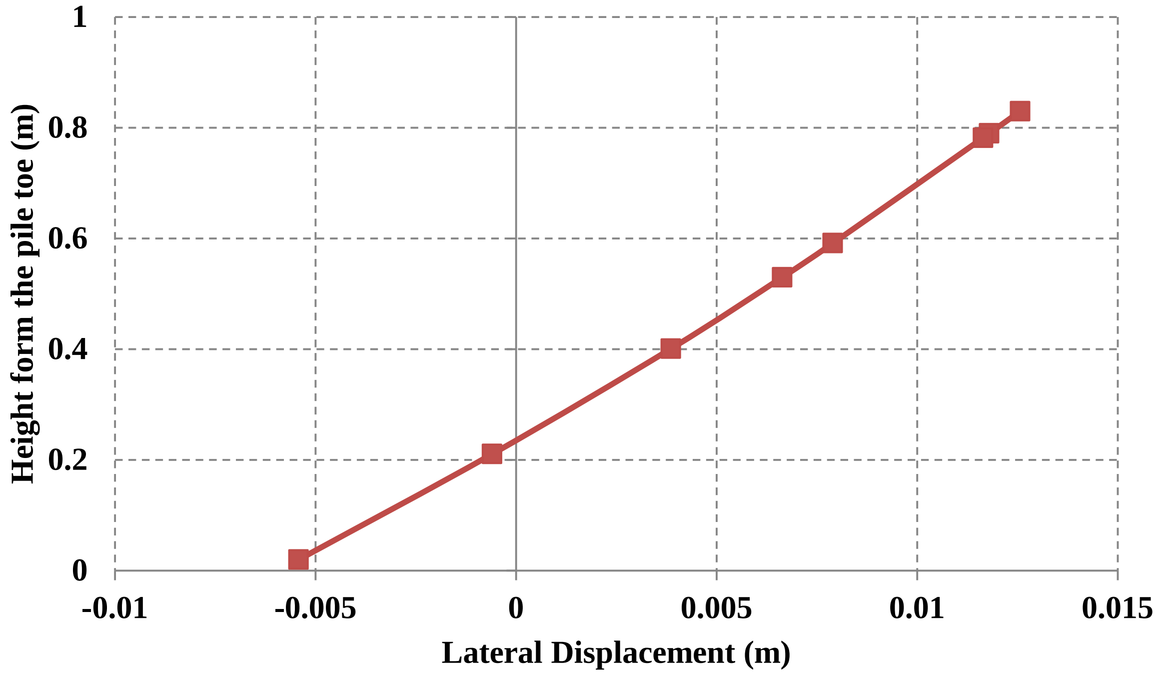

Figure A.98 Lateral Displacement along the Pile for Scour Depth = 400 mm and Width = 0 mm

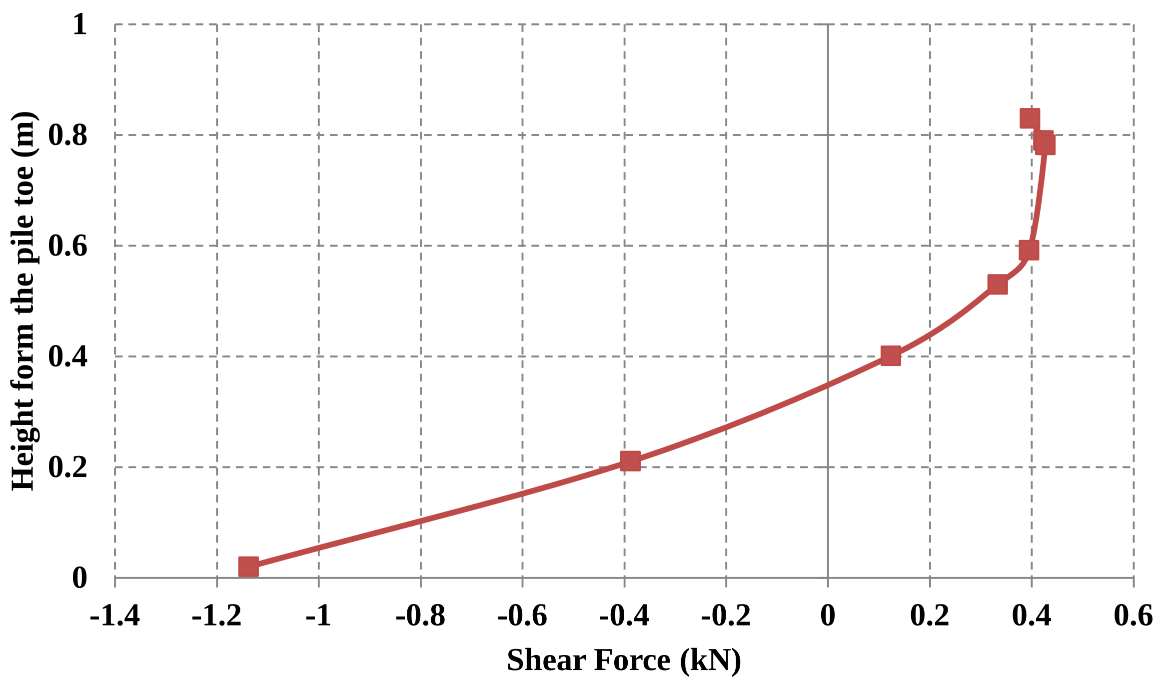

Figure A.99 Shear Force along the Pile for Scour Depth = 400 mm and Width = 0 mm

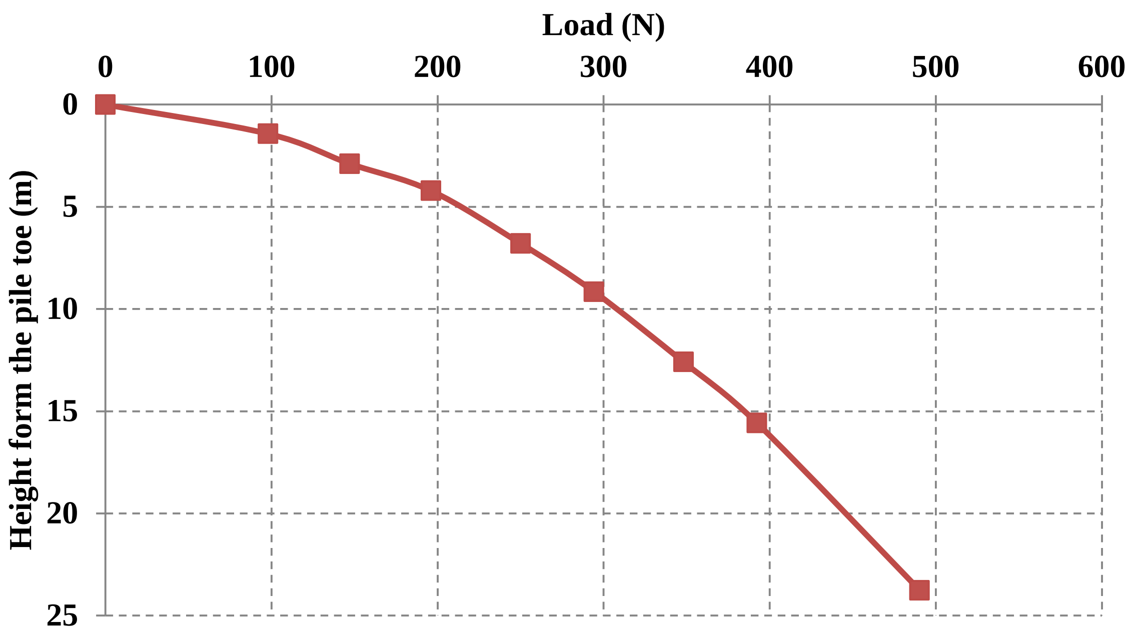

Figure A.100 Lateral Displacements vs. Load for Scour Depth = 400 mm and Width = 0 mm

500-mm scour depth

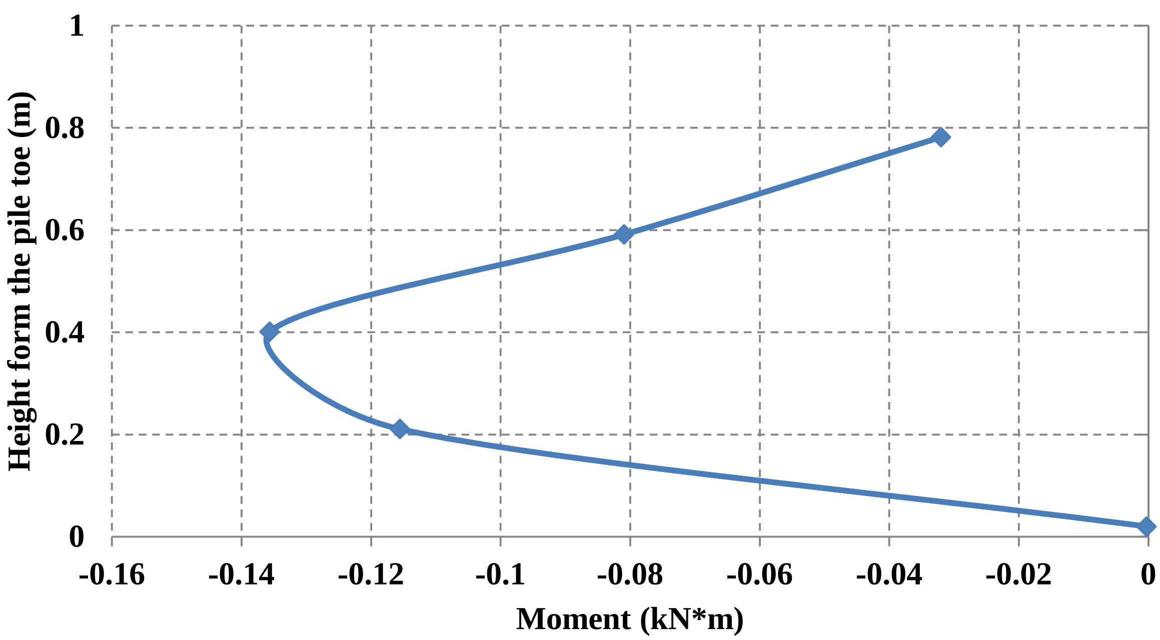

Figure A.101 Moment along the Pile for Scour Depth = 500 mm and Width = 0 mm

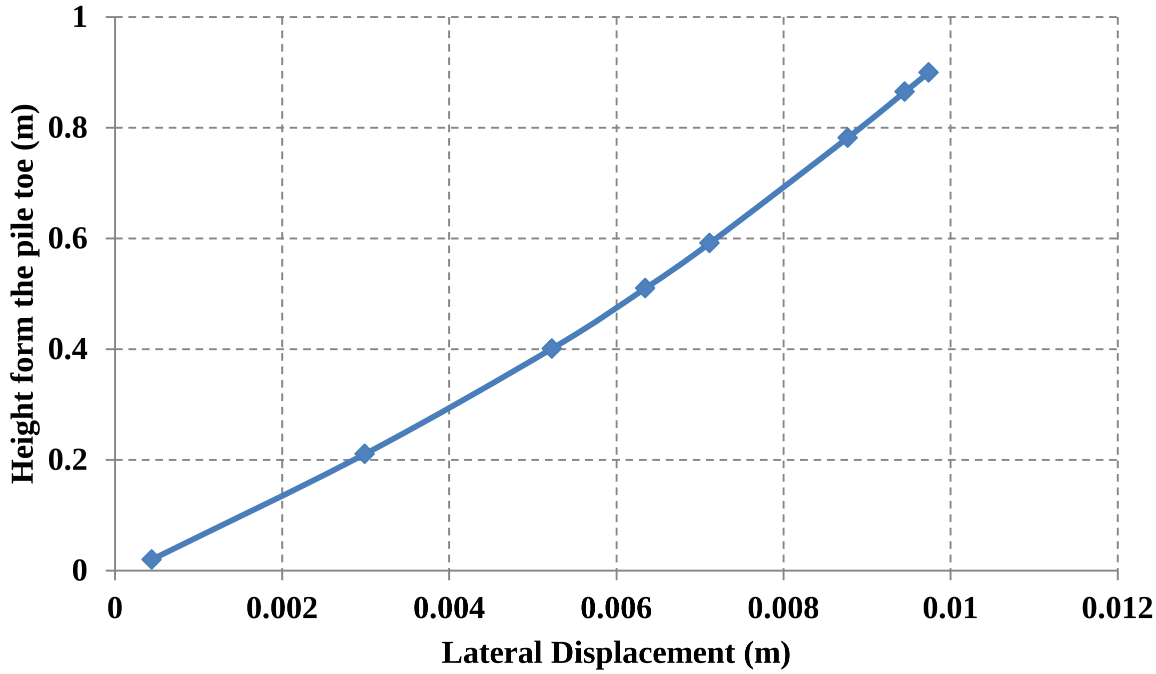

Figure A.102 Lateral Displacement along the Pile for Scour Depth = 500 mm and Width = 0 mm

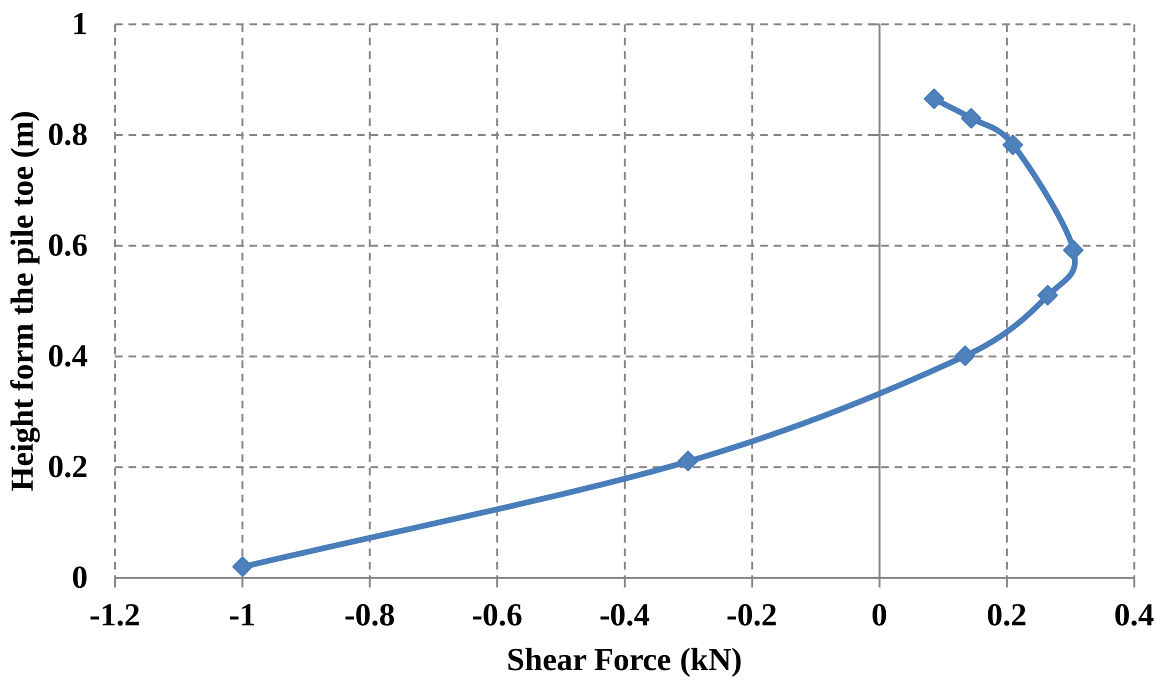

Figure A.103 Shear Force along the Pile for Scour Depth = 500 mm and Width = 0 mm

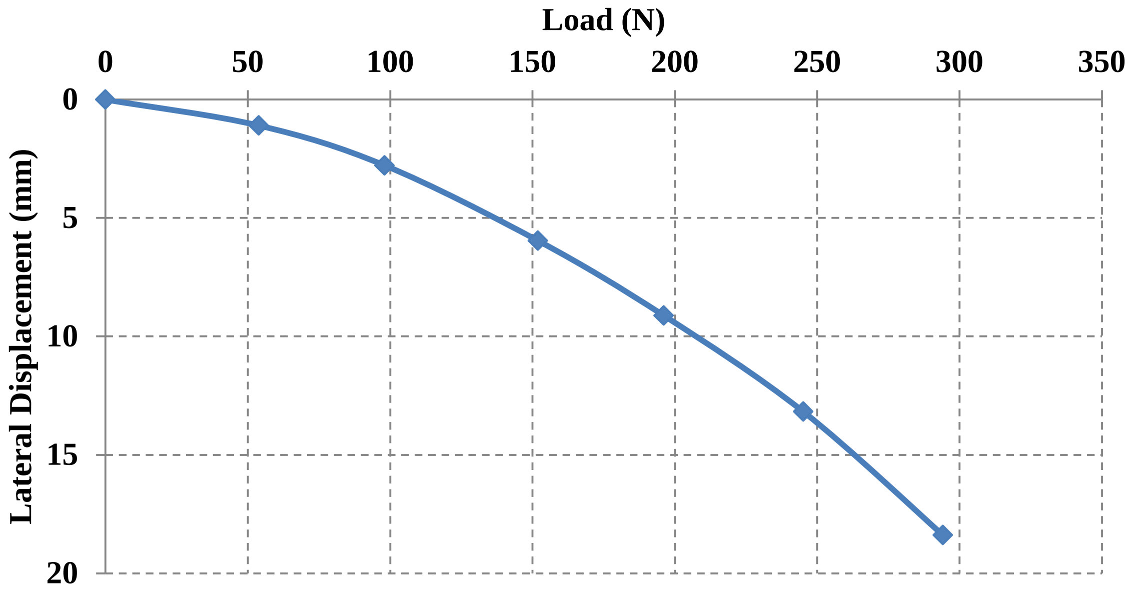

Figure A.104 Lateral Displacements vs. Load for Scour Depth = 500 mm and Width = 0 mm

A.3.3.2. 240-mm scour width

200-mm scour depth

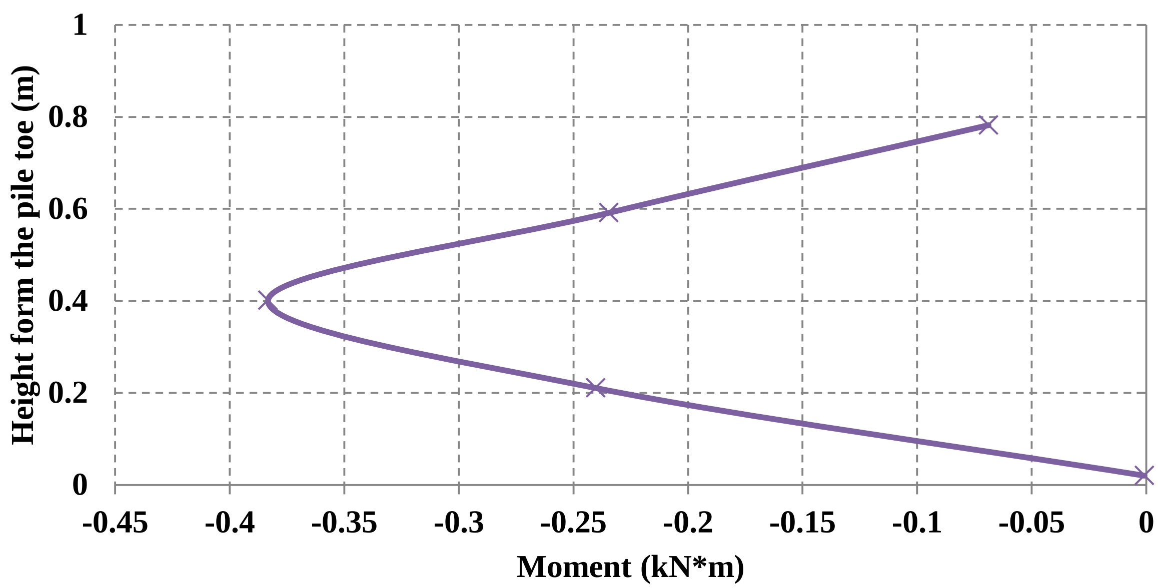

Figure A.105 Moment along the Pile for Scour Depth = 200 mm and Width = 240 mm

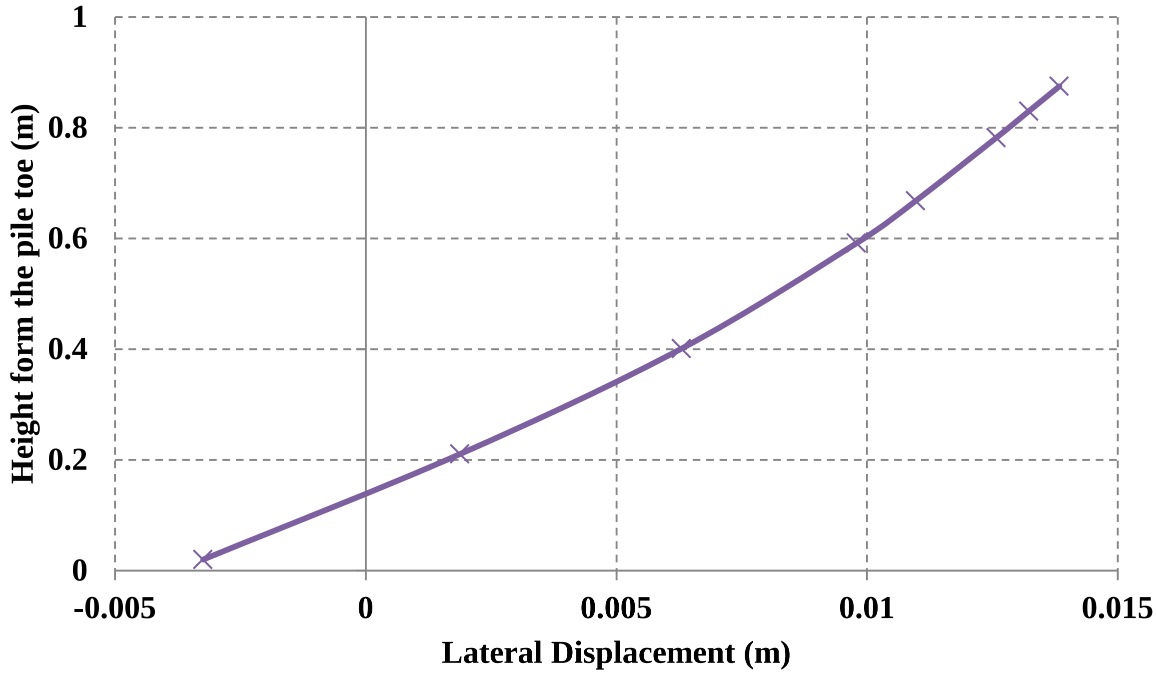

Figure A.106 Lateral Displacement along the Pile for Scour Depth = 200 mm and Width = 240 mm

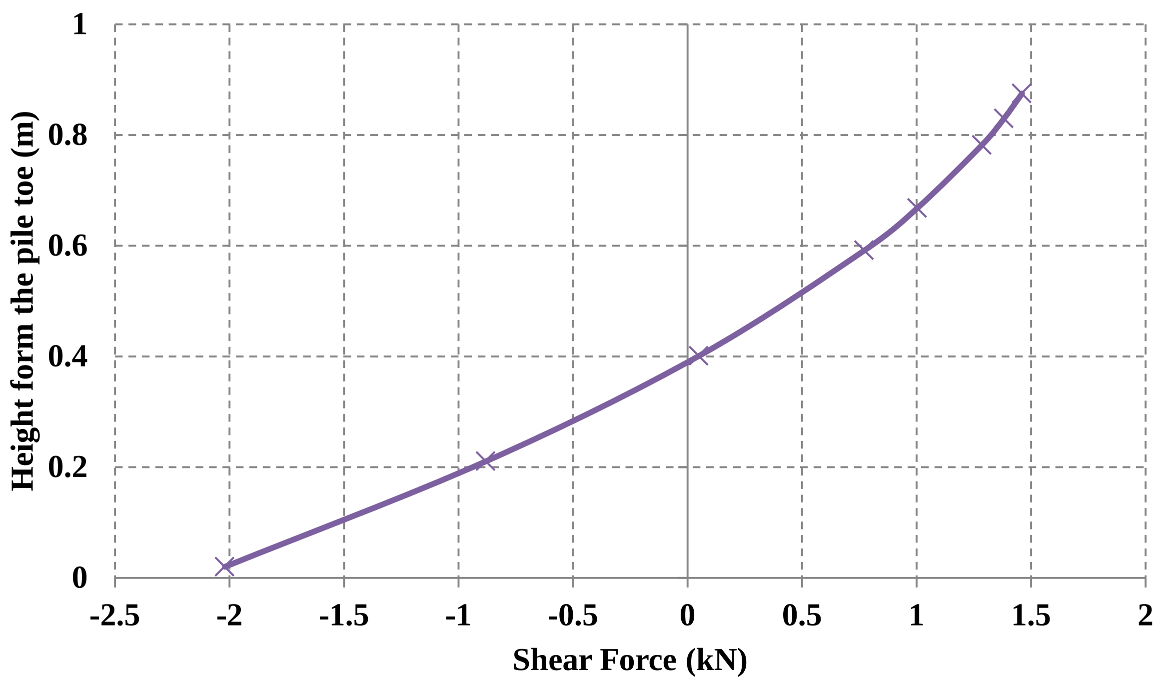

Figure A.107 Shear Force along the Pile for Scour Depth = 200 mm and Width = 240 mm

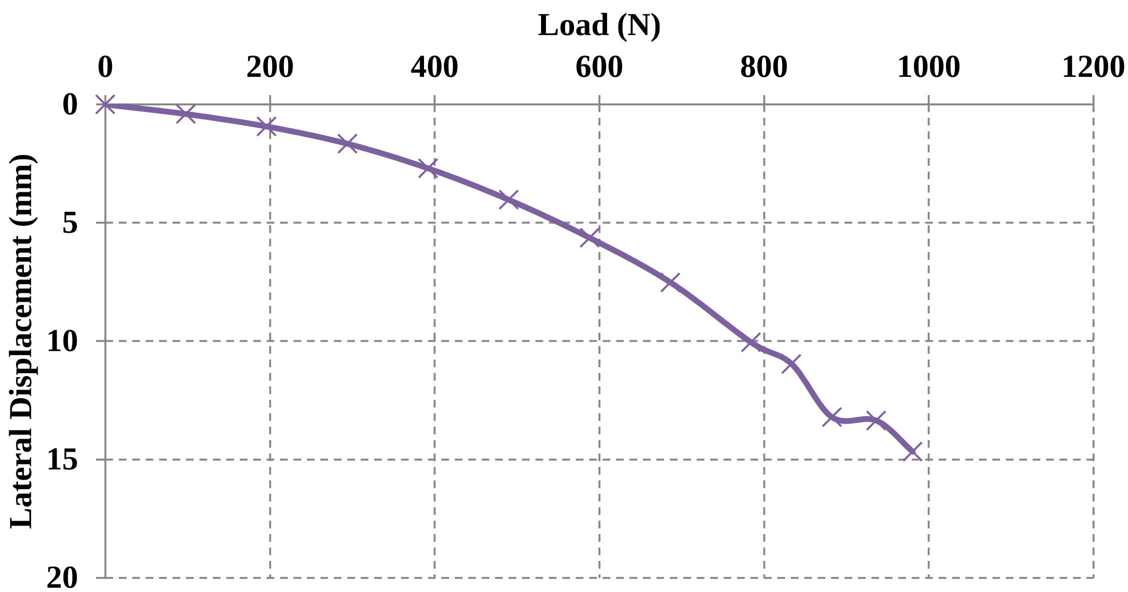

Figure A.108 Lateral Displacements vs. Load for Scour Depth = 200 mm and Width = 240 mm

300-mm scour depth

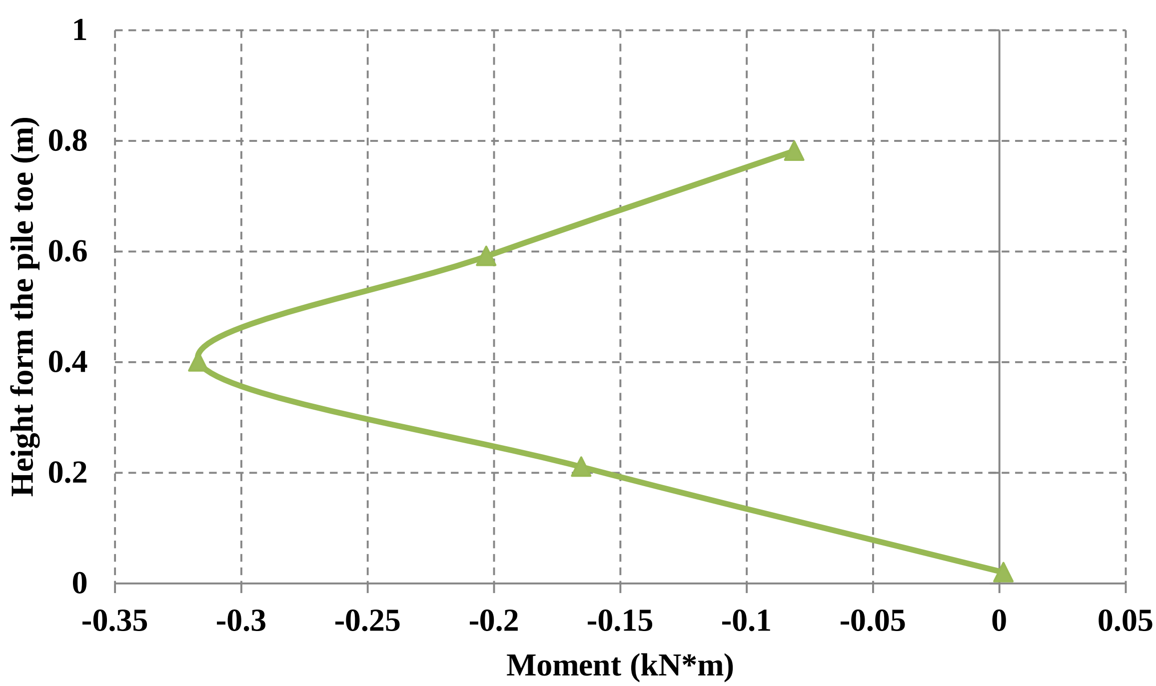

Figure A.109 Moment along the Pile for Scour Depth = 300 mm and Width = 240 mm

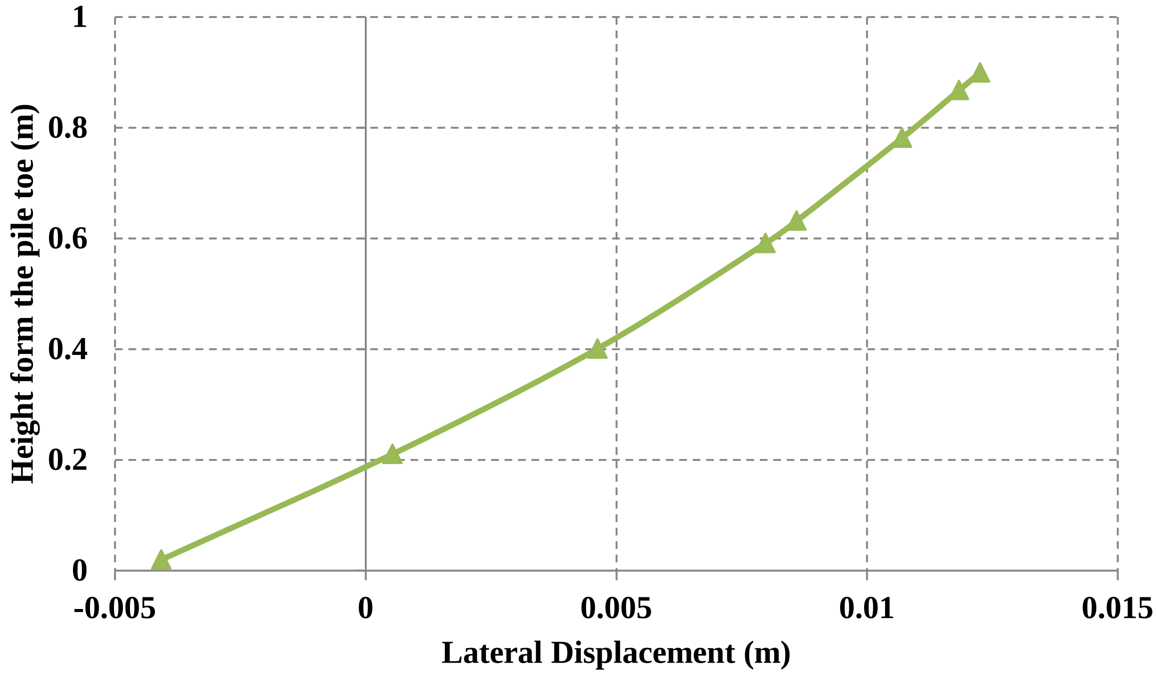

Figure A.110 Lateral Displacement along the Pile for Scour Depth = 300 mm and Width = 240 mm

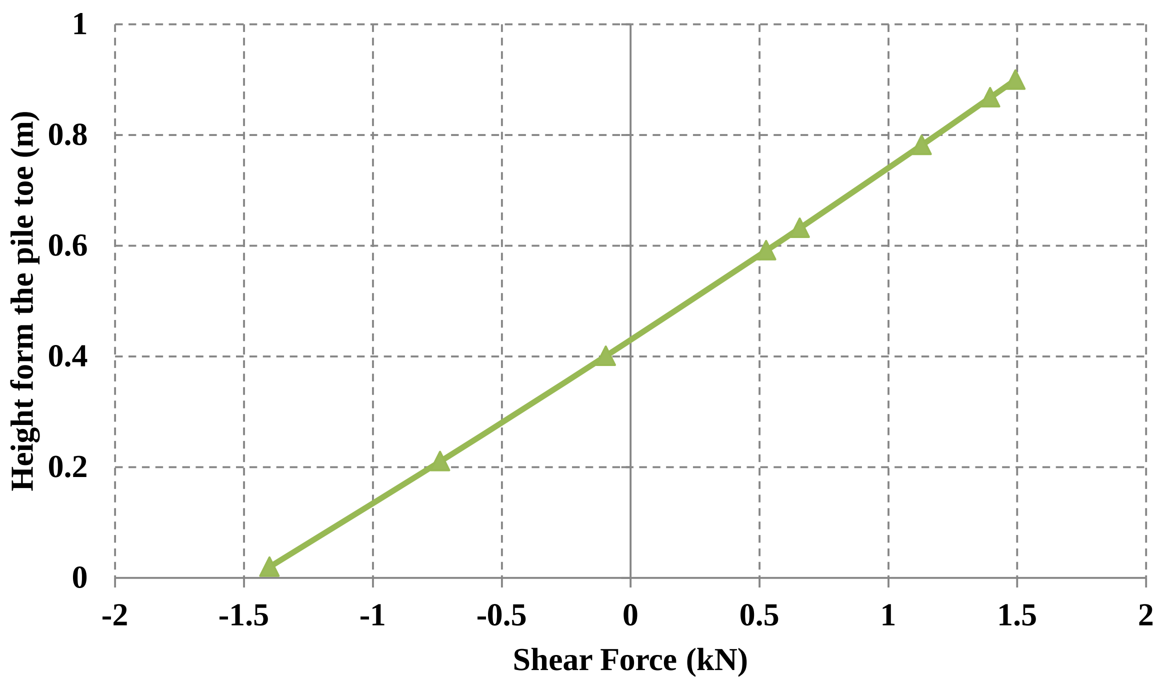

Figure A.111 Shear Force along the Pile for Scour Depth = 300 mm and Width = 240 mm

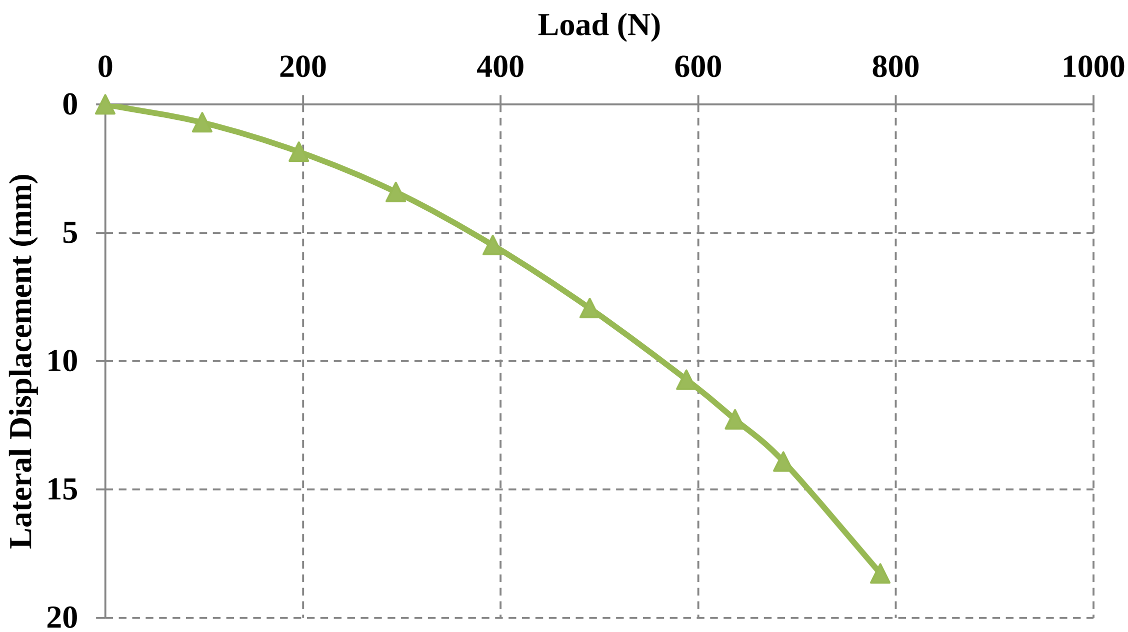

Figure A.112 Lateral Displacements vs. Load for Scour Depth = 300 mm and Width = 240 mm

400-mm scour depth

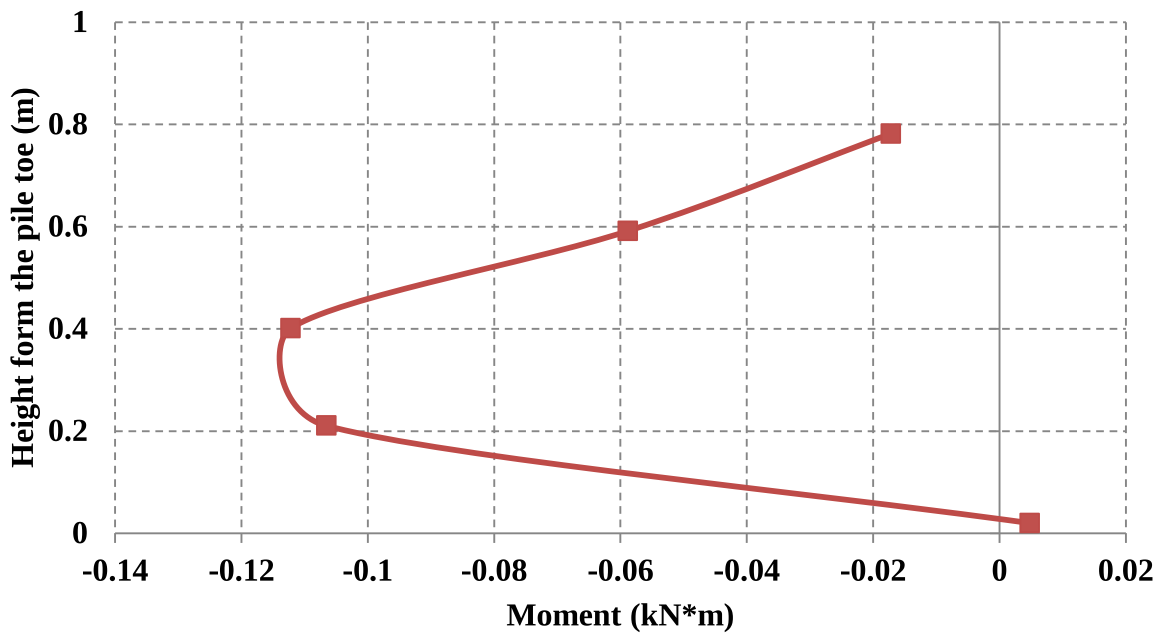

Figure A.113 Moment along the Pile for Scour Depth = 400 mm and Width = 240 mm

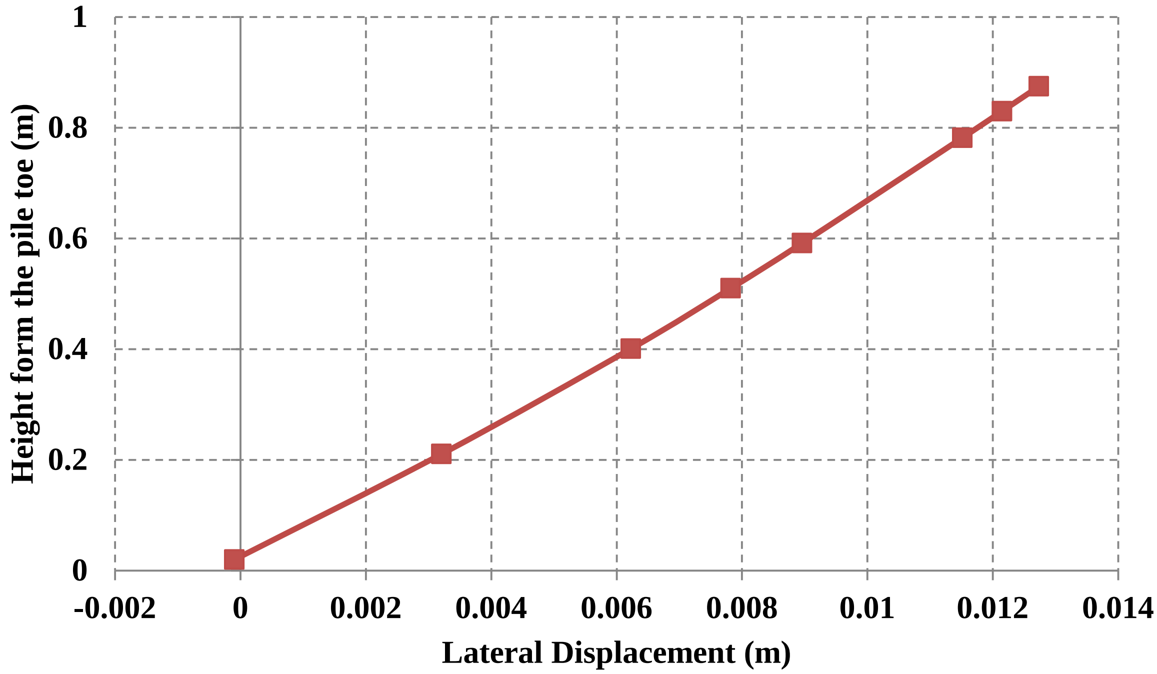

Figure A.114 Lateral Displacement along the Pile for Scour Depth = 400 mm and Width = 240 mm

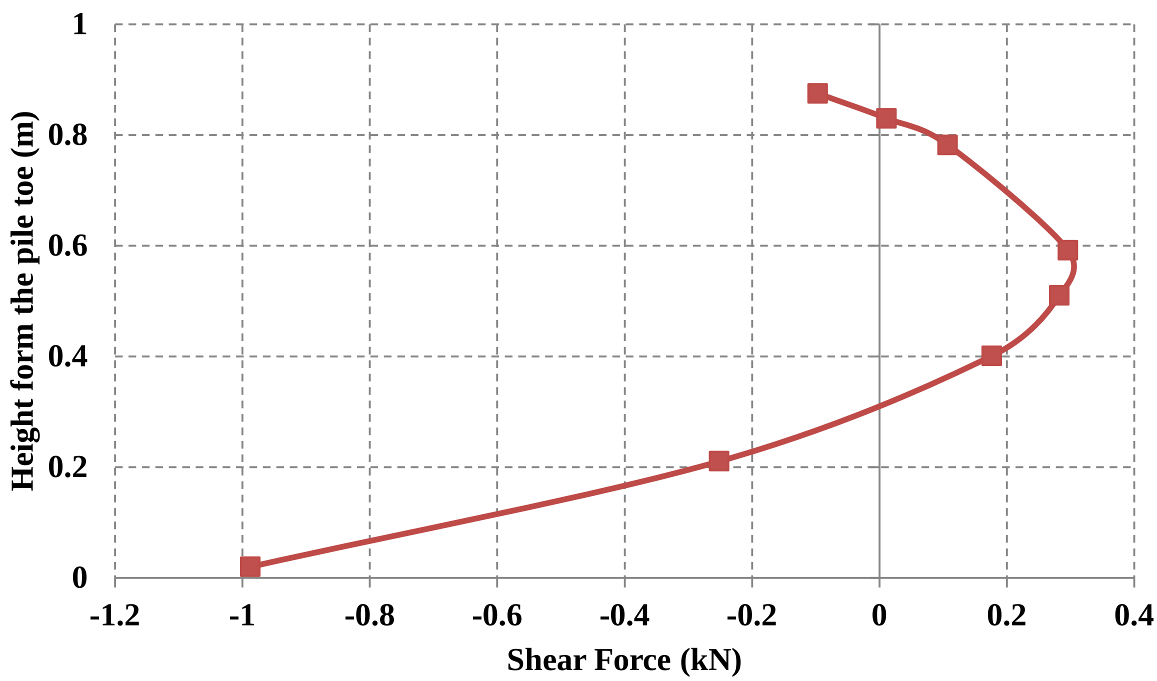

Figure A.115 Shear Force along the Pile for Scour Depth = 400 mm and Width = 240 mm

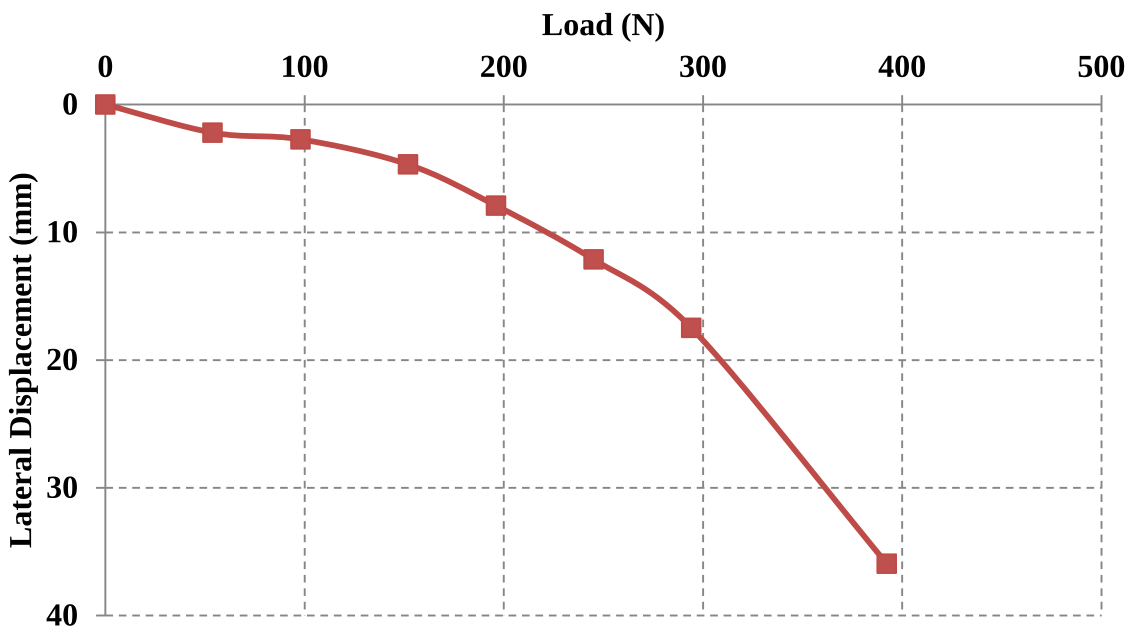

Figure A.116 Lateral Displacements vs. Load for Scour Depth = 400 mm and Width = 240 mm

500-mm scour depth

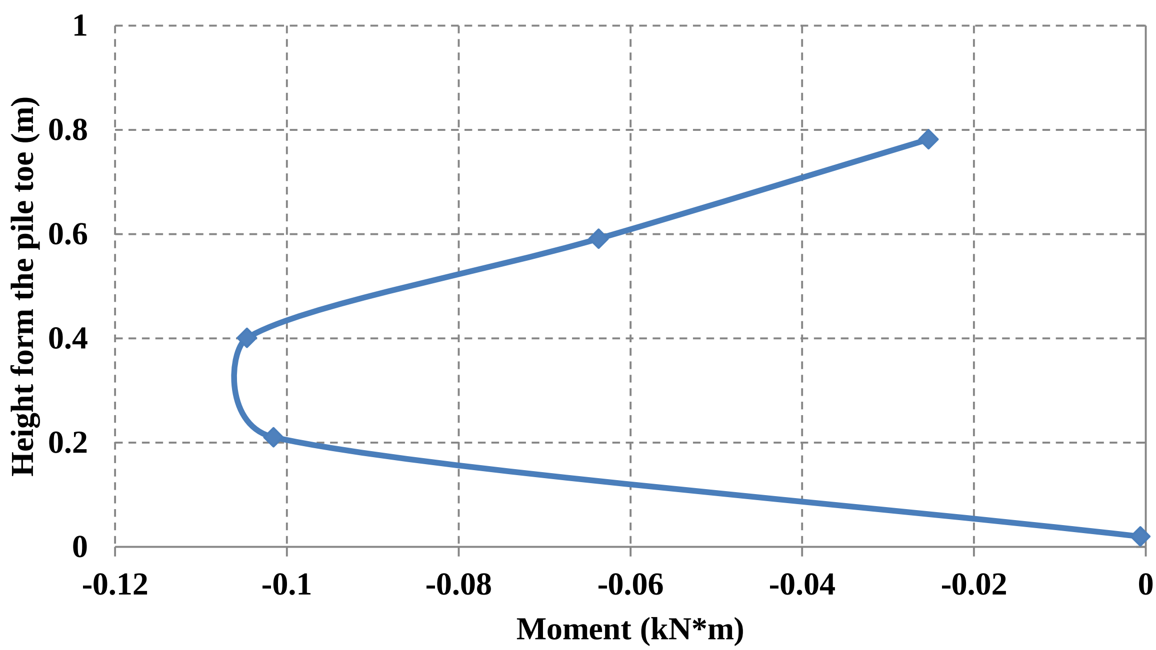

Figure A.117 Moment along the Pile for Scour Depth = 500 mm and Width = 240 mm

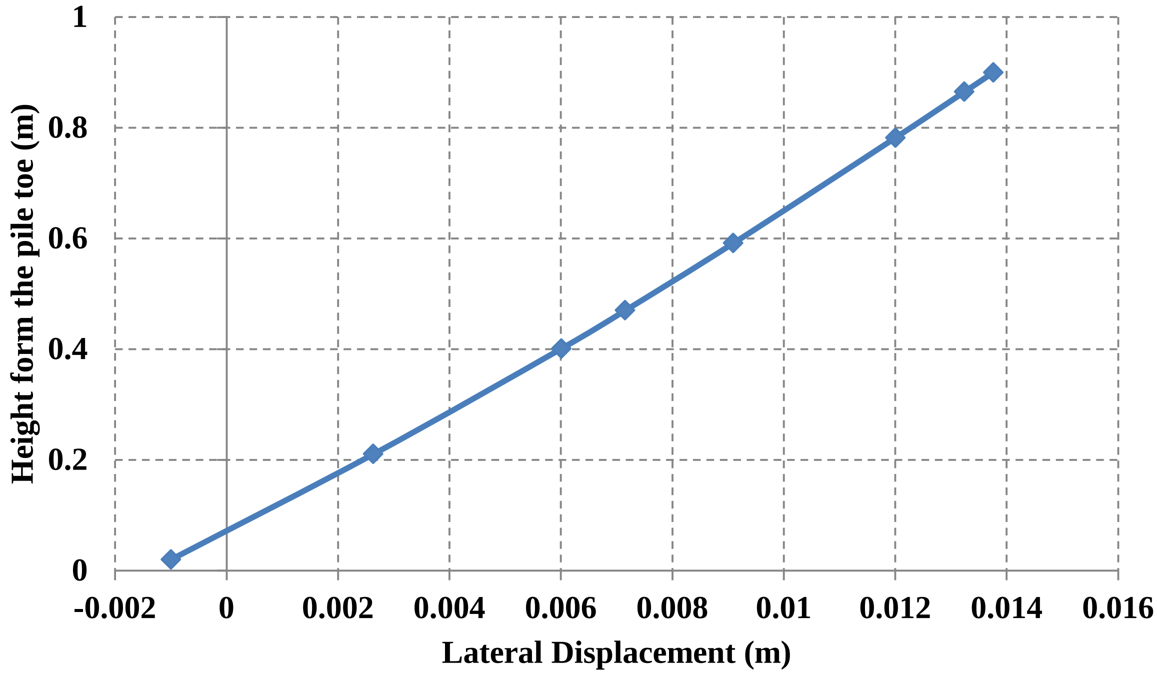

Figure A.118 Lateral Displacement along the Pile for Scour Depth = 500 mm and Width = 240 mm

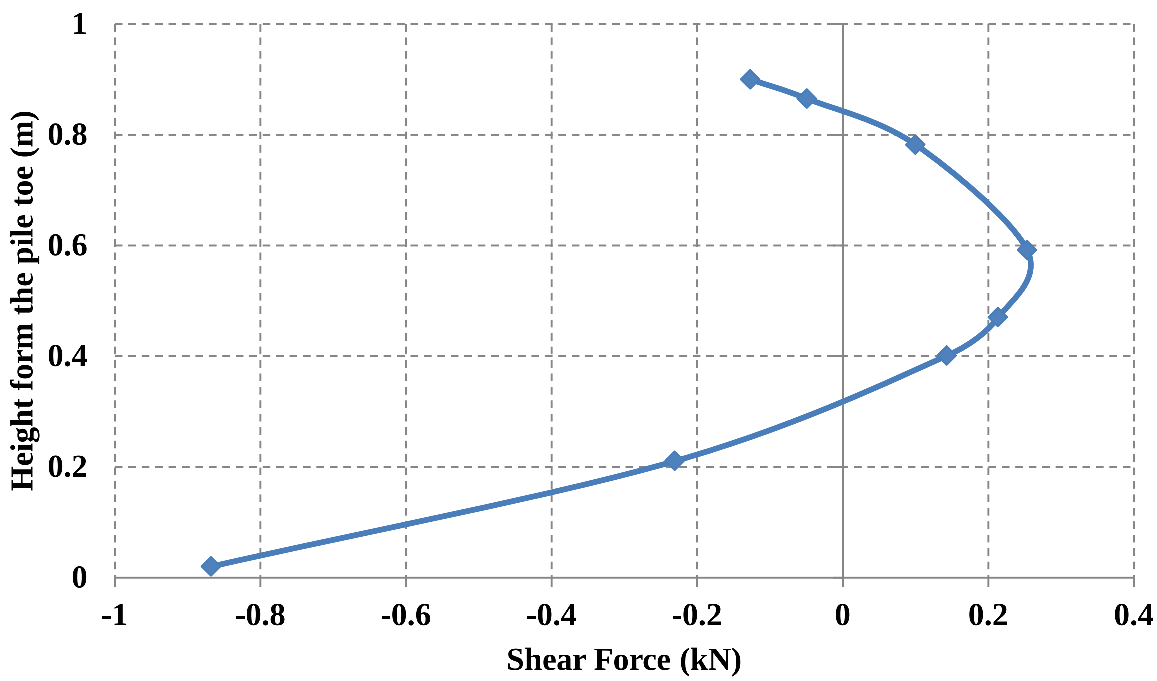

Figure A.119 Shear Force along the Pile for Scour Depth = 500 mm and Width = 240 mm

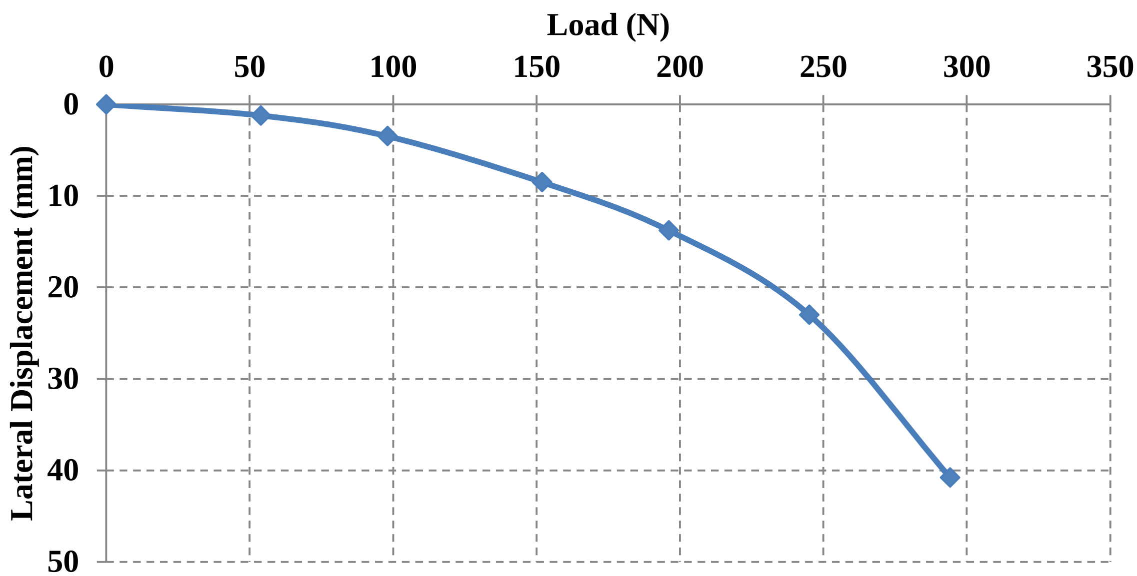

Figure A.120 Lateral Displacements vs. Load for Scour Depth = 500 mm and Width = 240 mm

A.3.3.3. 400-mm scour width

200-mm scour depth

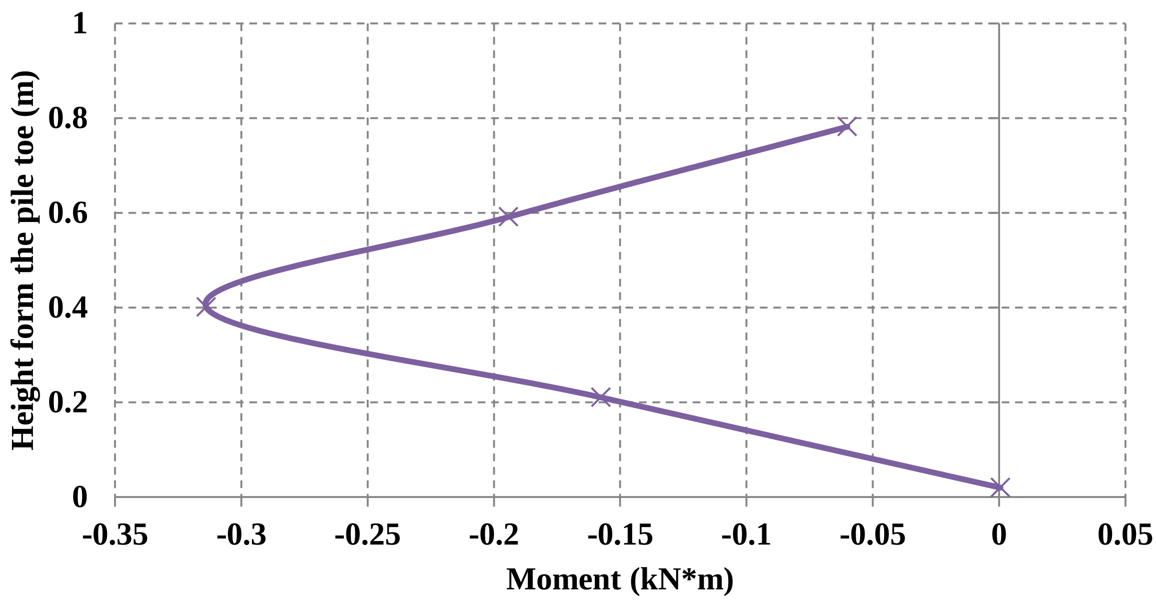

Figure A.121 Moment along the Pile for Scour Depth = 200 mm and Width = 400 mm

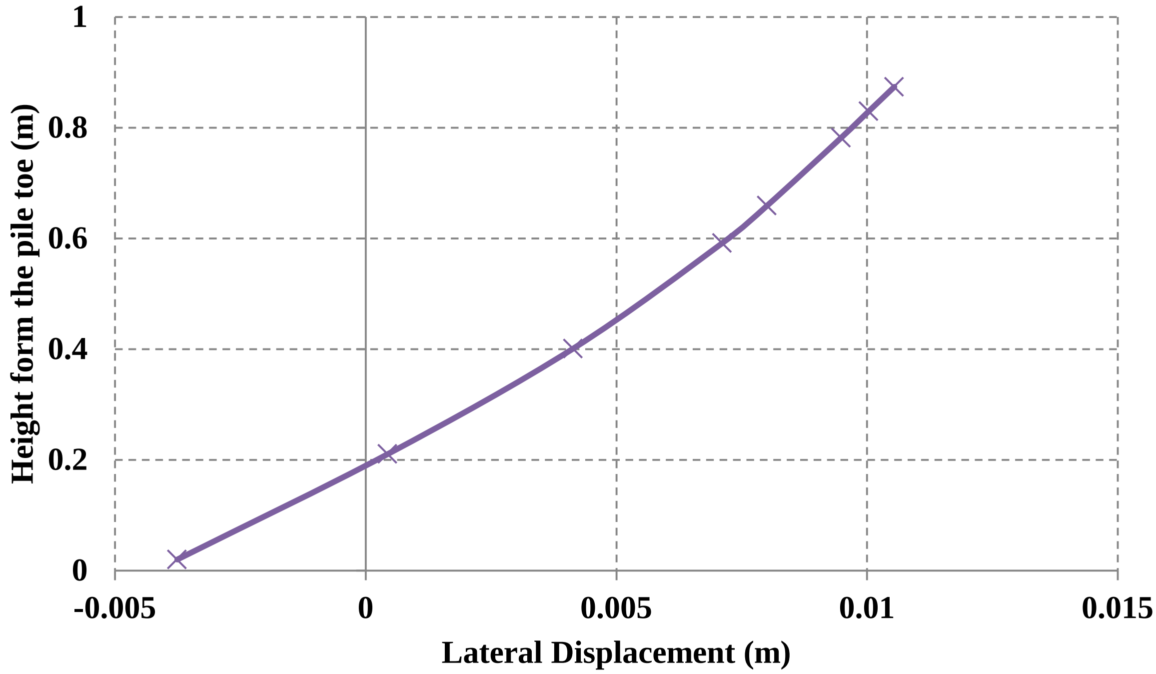

Figure A.122 Lateral Displacement along the Pile for Scour Depth = 200 mm and Width = 400 mm

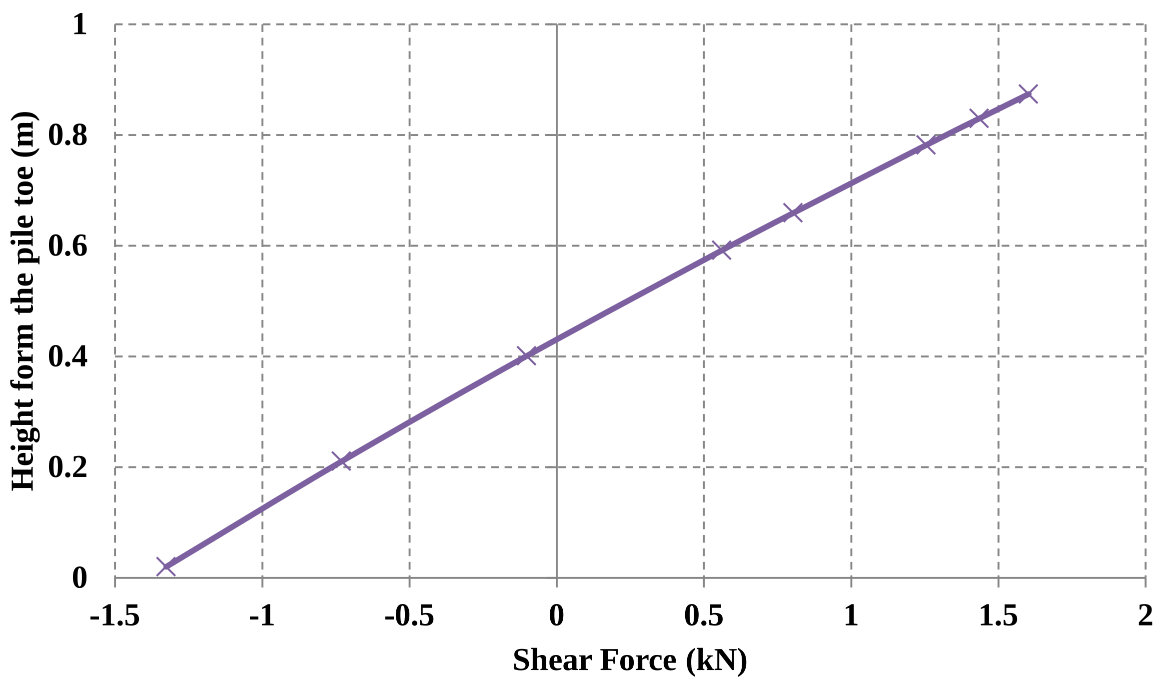

Figure A.123 Shear Force along the Pile for Scour Depth = 200 mm and Width = 400 mm

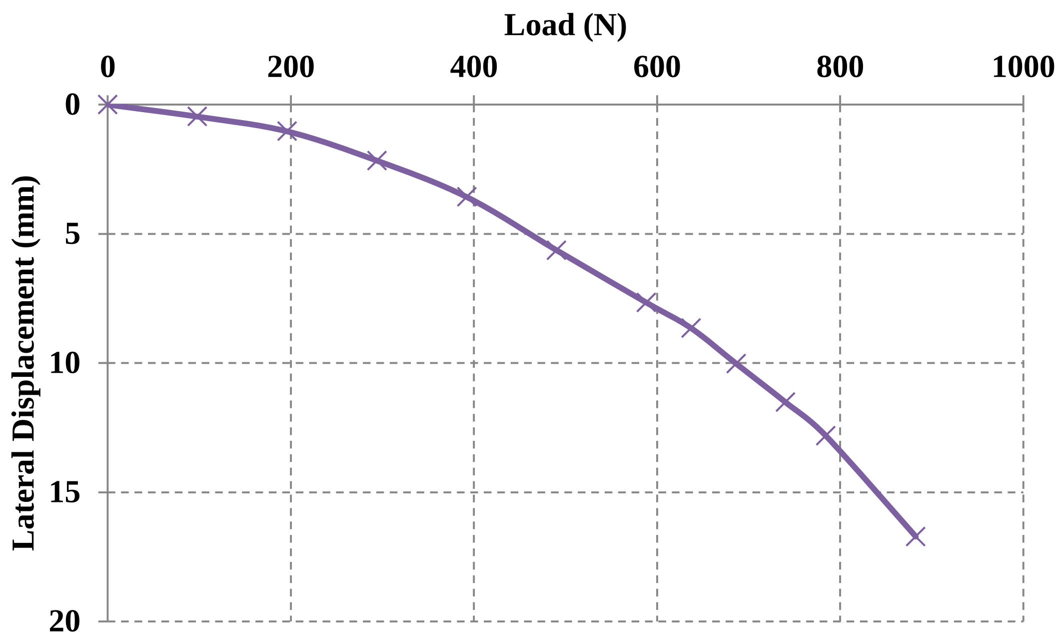

Figure A.124 Lateral Displacements vs. Load for Scour Depth = 200 mm and Width = 400 mm

300-mm scour depth

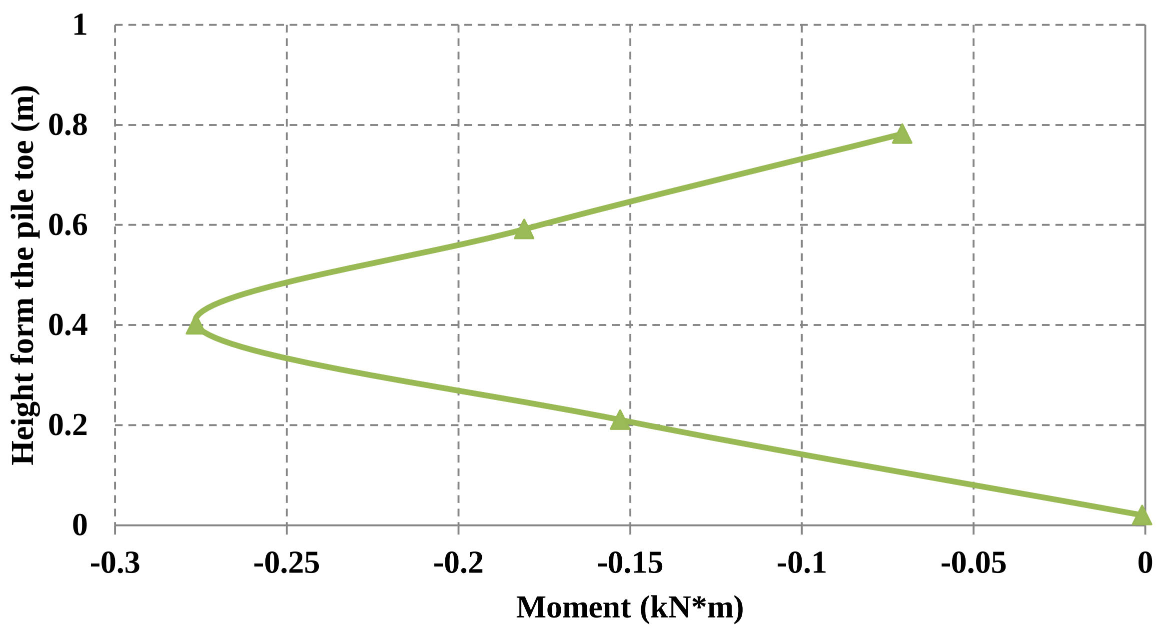

Figure A.125 Moment along the Pile for Scour Depth = 300 mm and Width = 400 mm

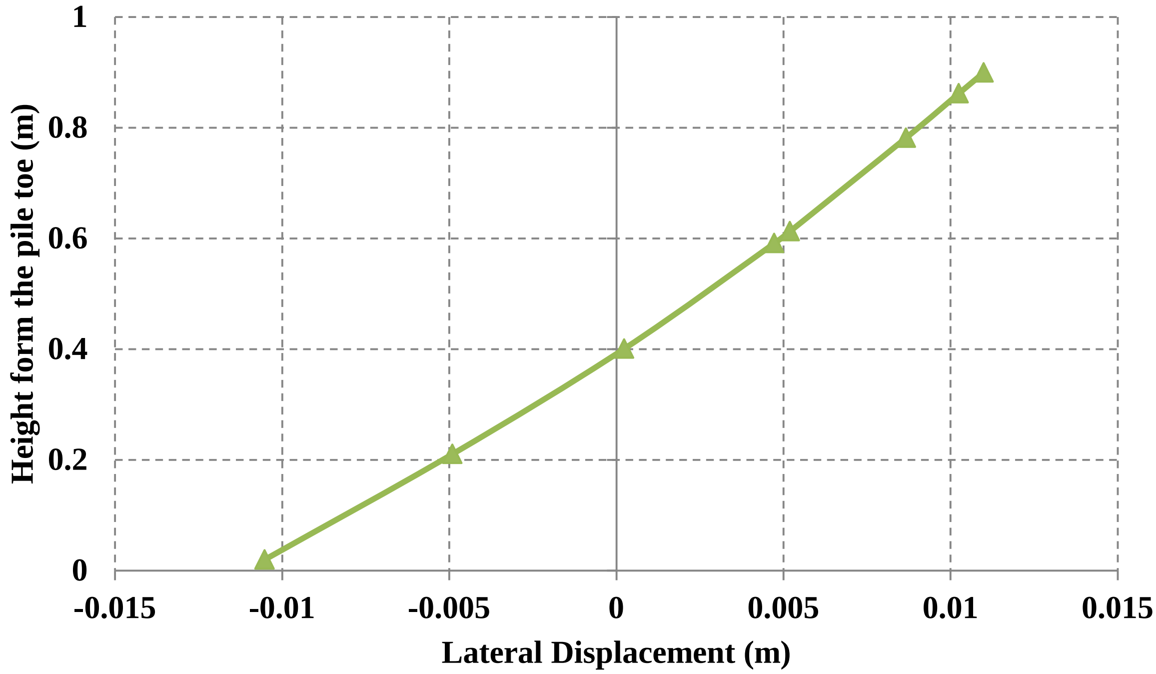

Figure A.126 Lateral Displacement along the Pile for Scour Depth = 300 mm and Width = 400 mm

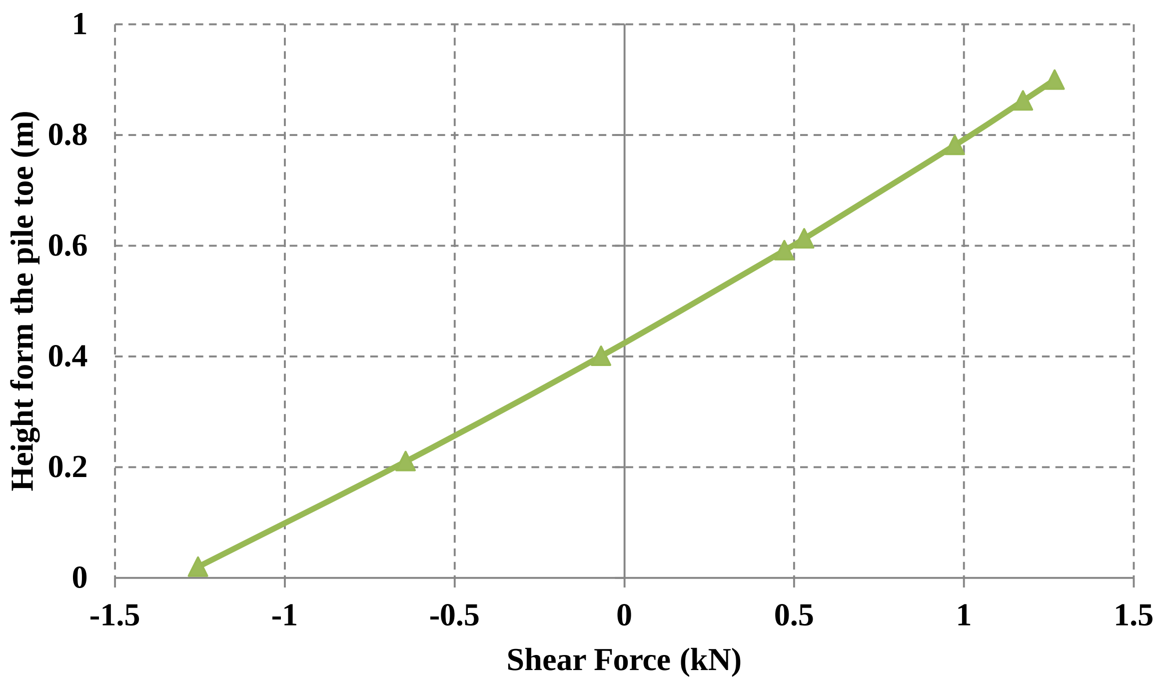

Figure A.127 Shear Force along the Pile for Scour Depth = 300 mm and Width = 400 mm

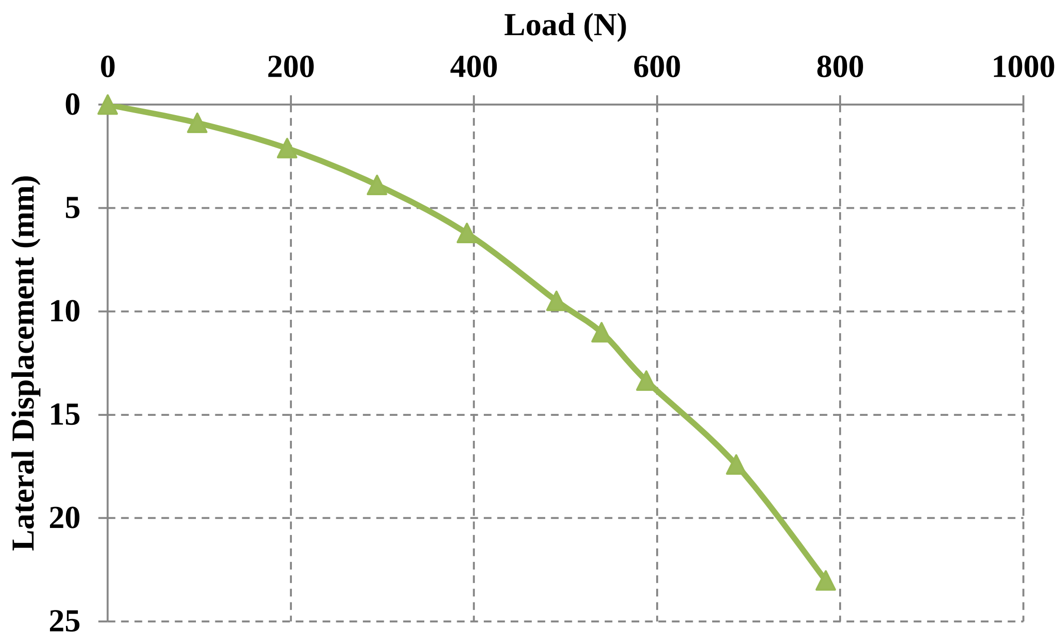

Figure A.128 Lateral Displacements vs. Load for Scour Depth = 300 mm and Width = 400 mm

400-mm scour depth

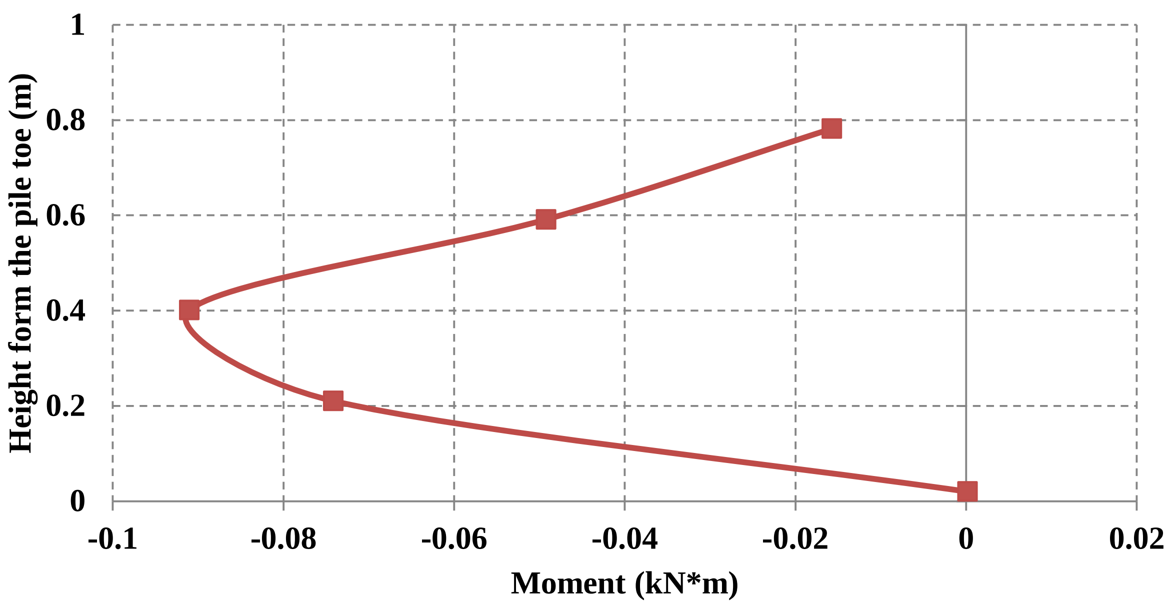

Figure A.125 Moment along the Pile for Scour Depth = 400 mm and Width = 400 mm

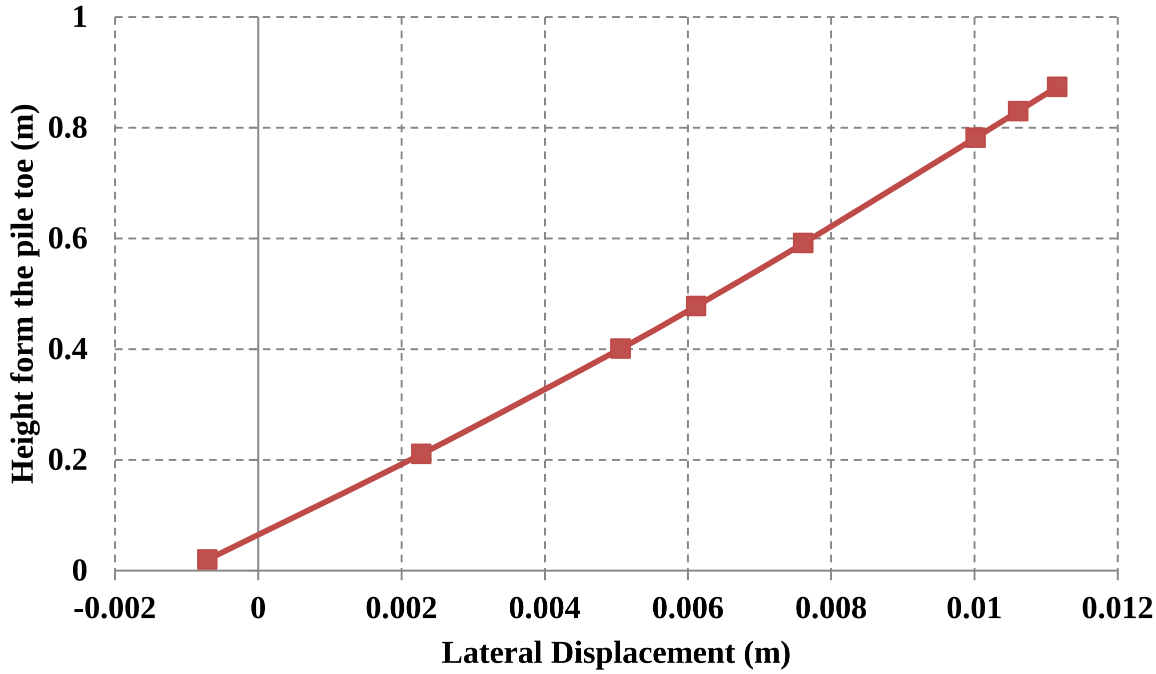

Figure A.126 Lateral Displacement along the Pile for Scour Depth = 400 mm and Width = 400 mm

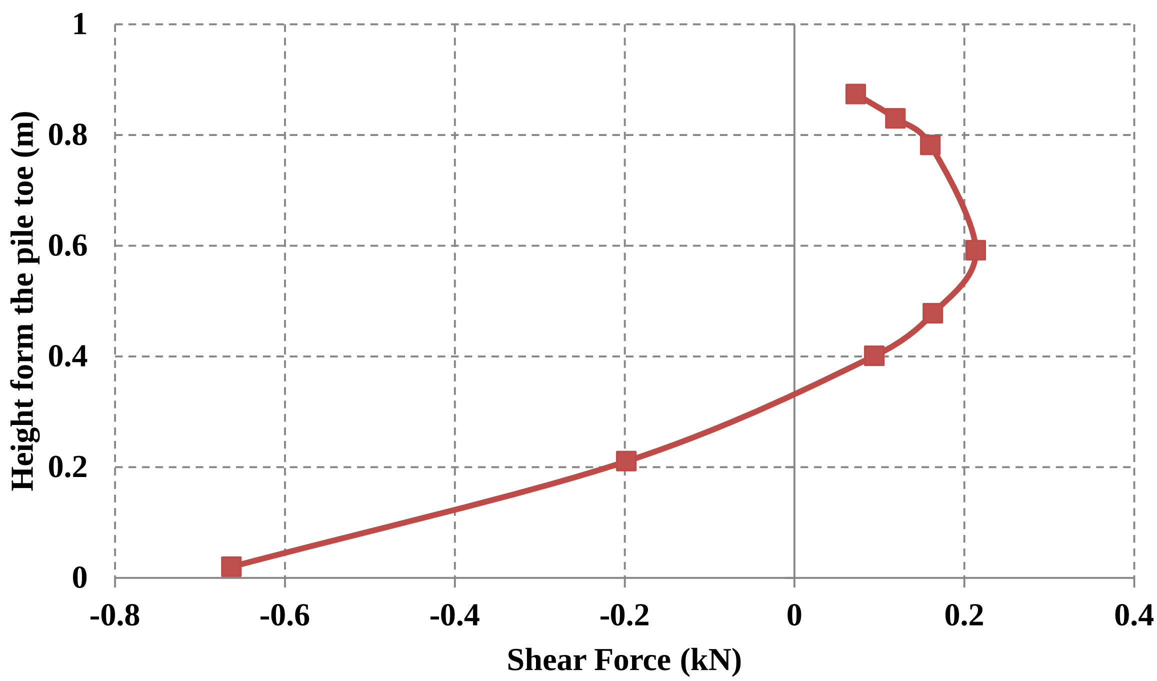

Figure A.127 Shear Force along the Pile for Scour Depth = 400 mm and Width = 400 mm

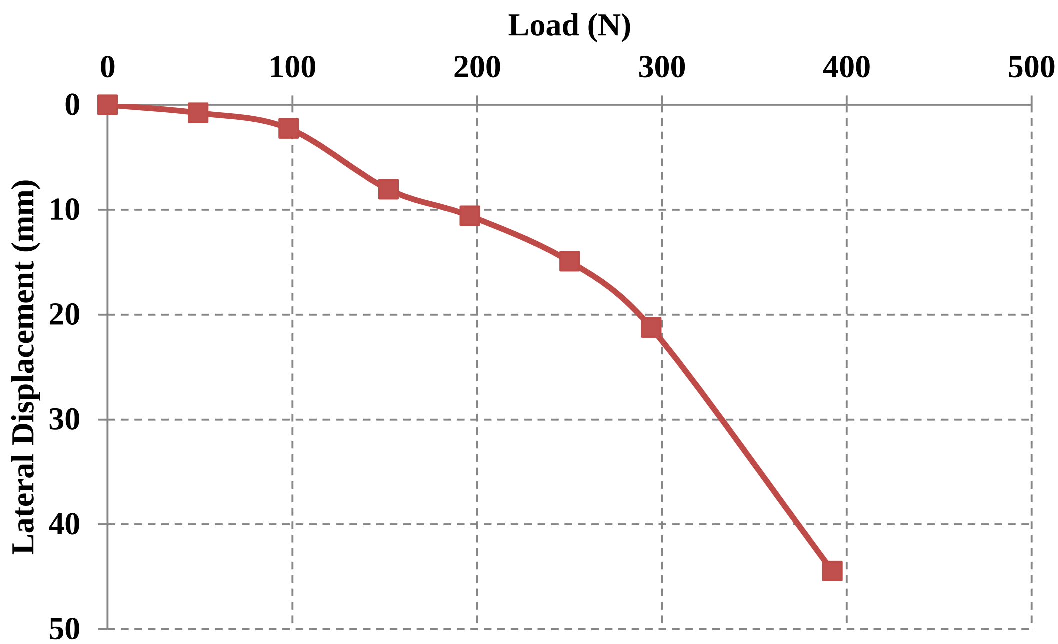

Figure A.128 Lateral Displacements vs. Load for Scour Depth = 400 mm and Width = 400 mm

500-mm scour depth

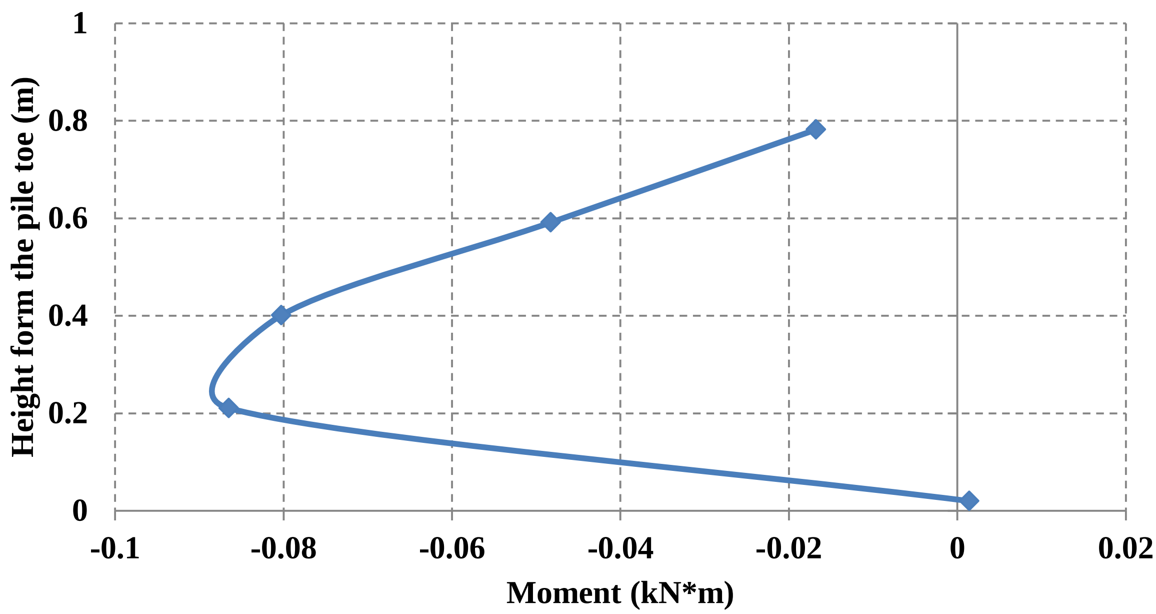

Figure A.129 Moment along the Pile for Scour Depth = 500 mm and Width = 400 mm

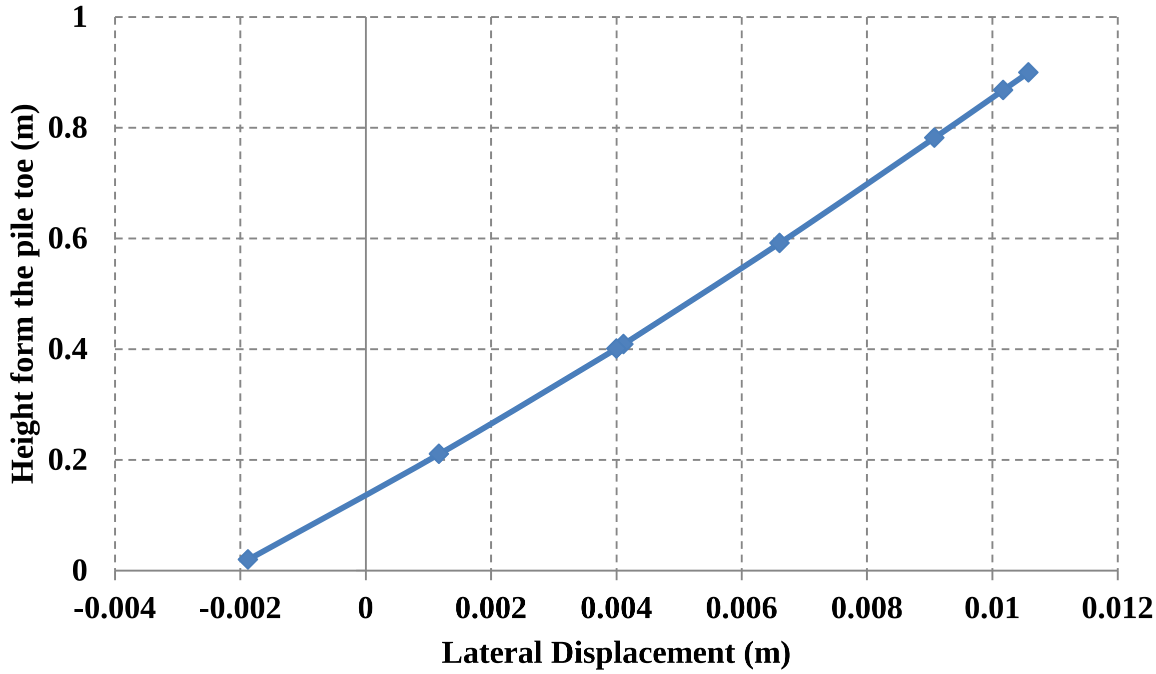

Figure A.130 Lateral Displacement along the Pile for Scour Depth = 500 mm and Width = 400 mm

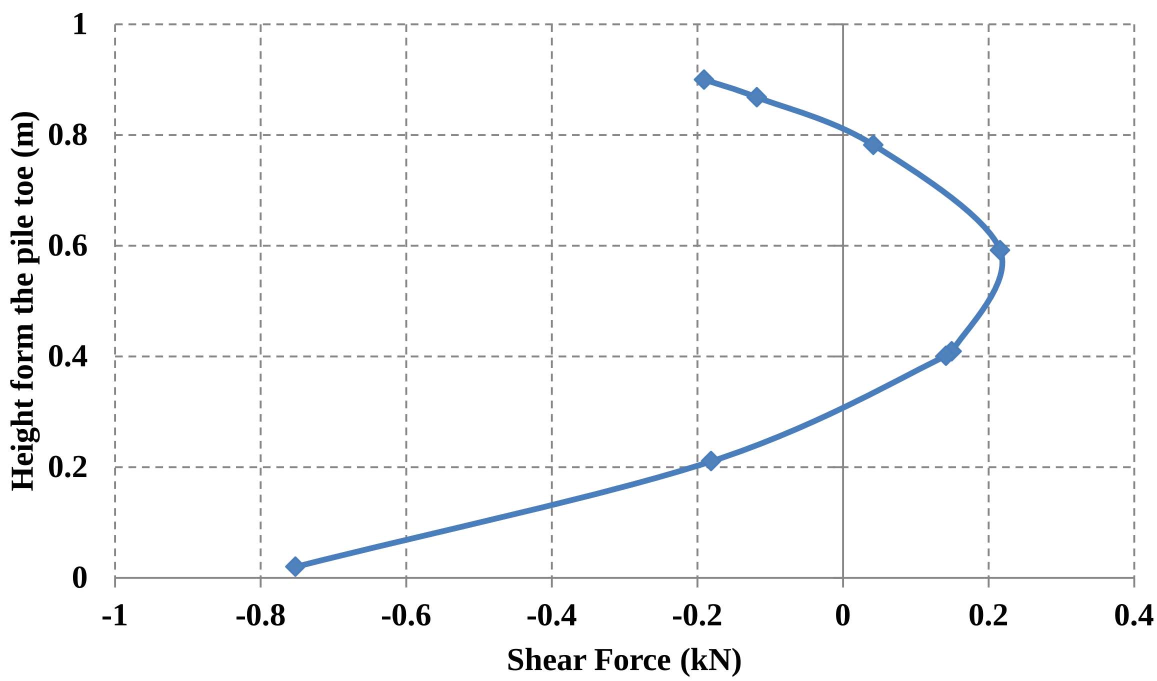

Figure A.131 Shear Force along the Pile for Scour Depth = 500 mm and Width = 400 mm

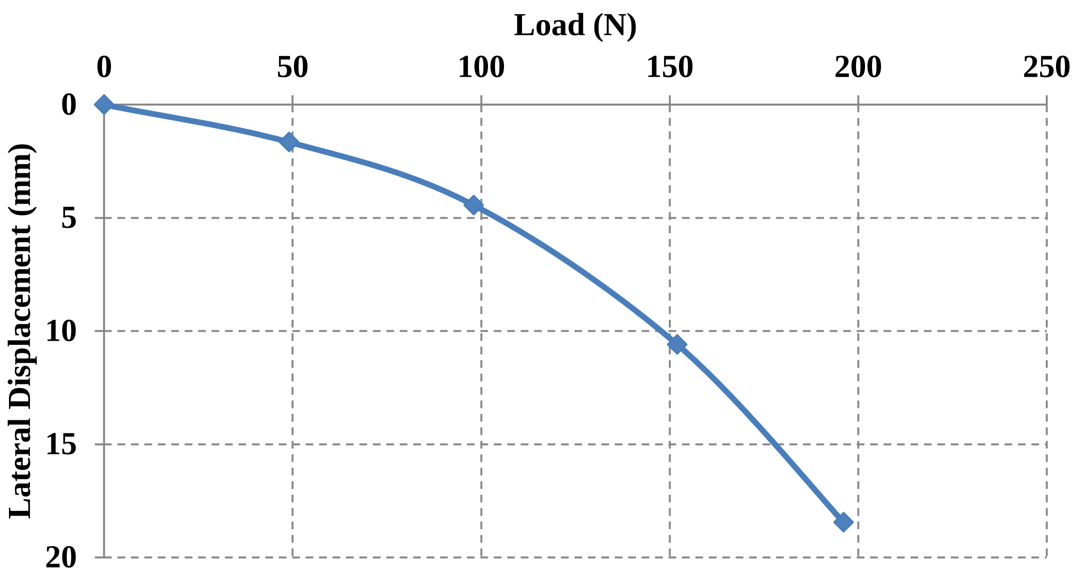

Figure A.132 Lateral Displacements vs. Load for Scour Depth = 500 mm and Width = 400 mm

A.3.3.4. 667-mm scour width

200-mm scour depth

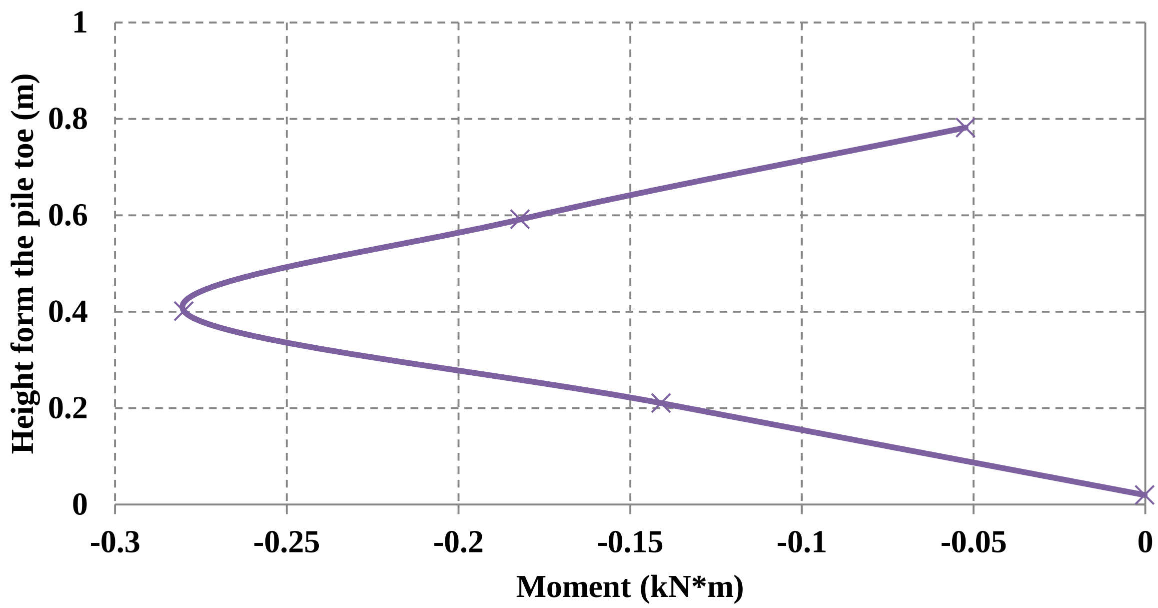

Figure A.133 Moment along the Pile for Scour Depth = 200 mm and Width = 667 mm

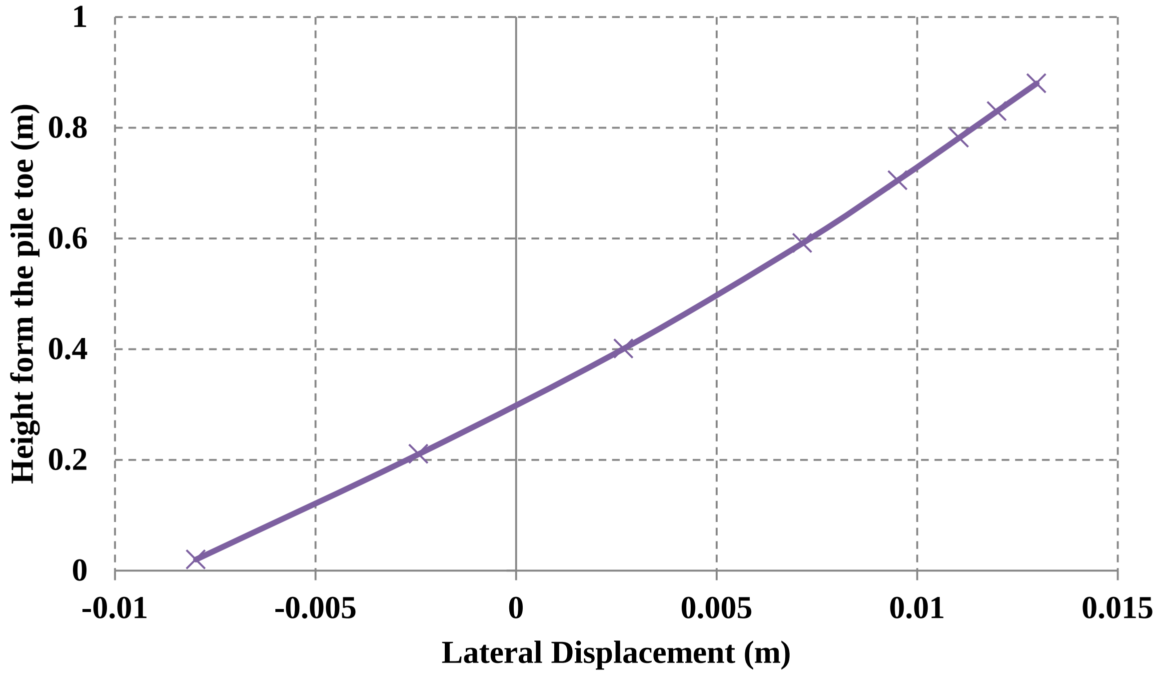

Figure A.134 Lateral Displacement along the Pile for Scour Depth = 200 mm and Width = 667 mm

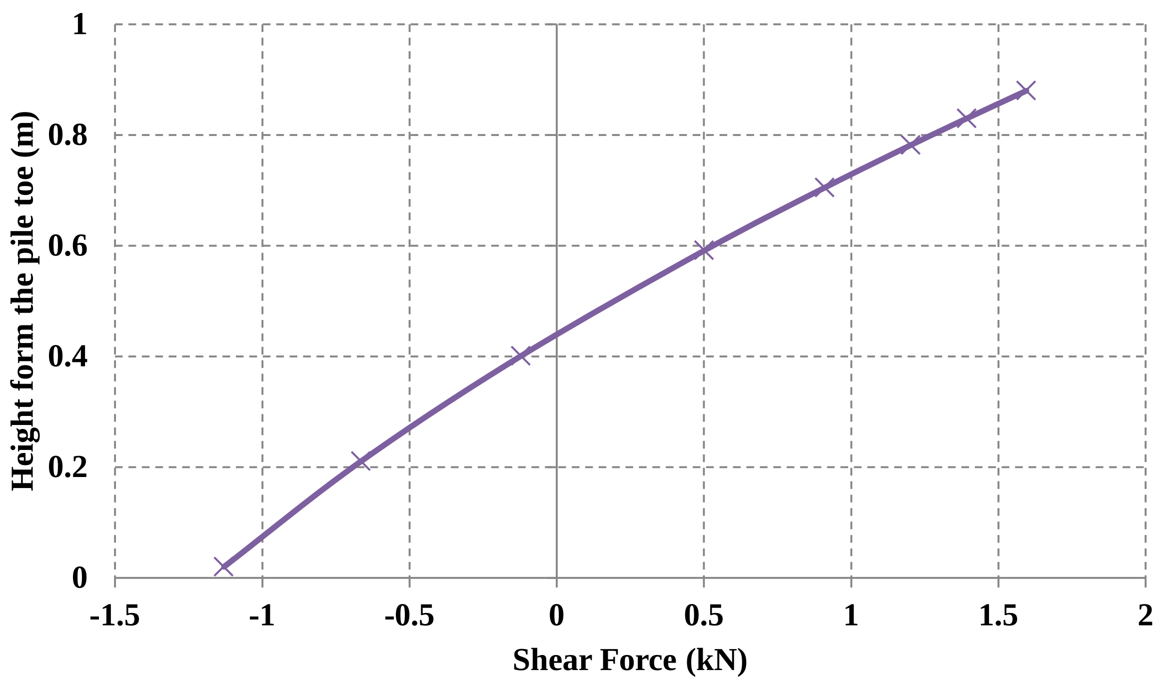

Figure A.135 Shear Force along the Pile for Scour Depth = 200 mm and Width = 667 mm

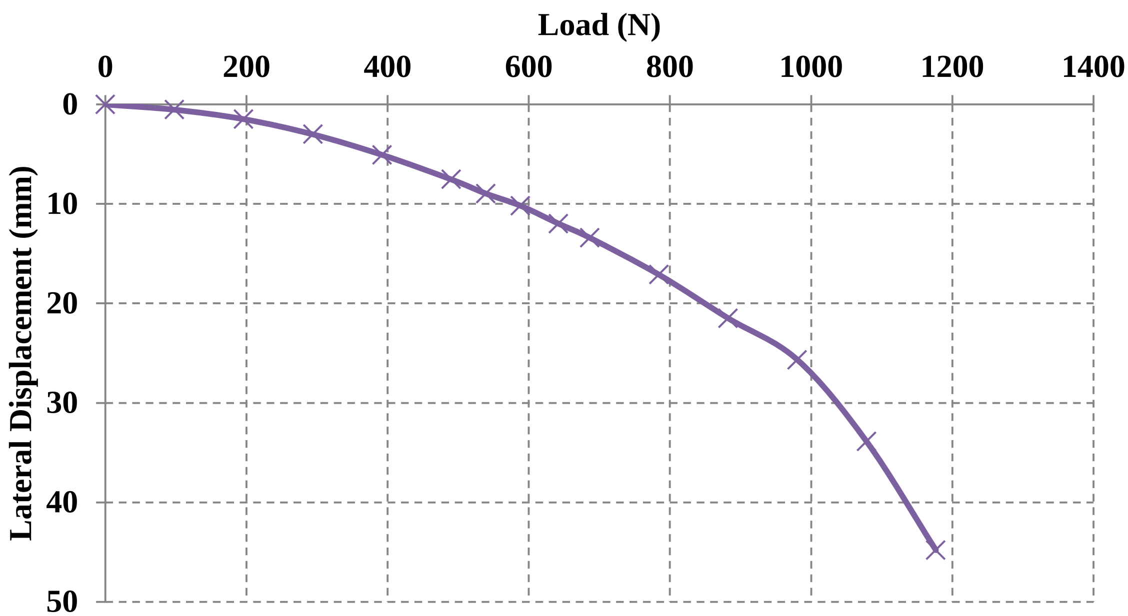

Figure A.136 Lateral Displacements vs. Load for Scour Depth = 200 mm and Width = 667 mm

300-mm scour depth

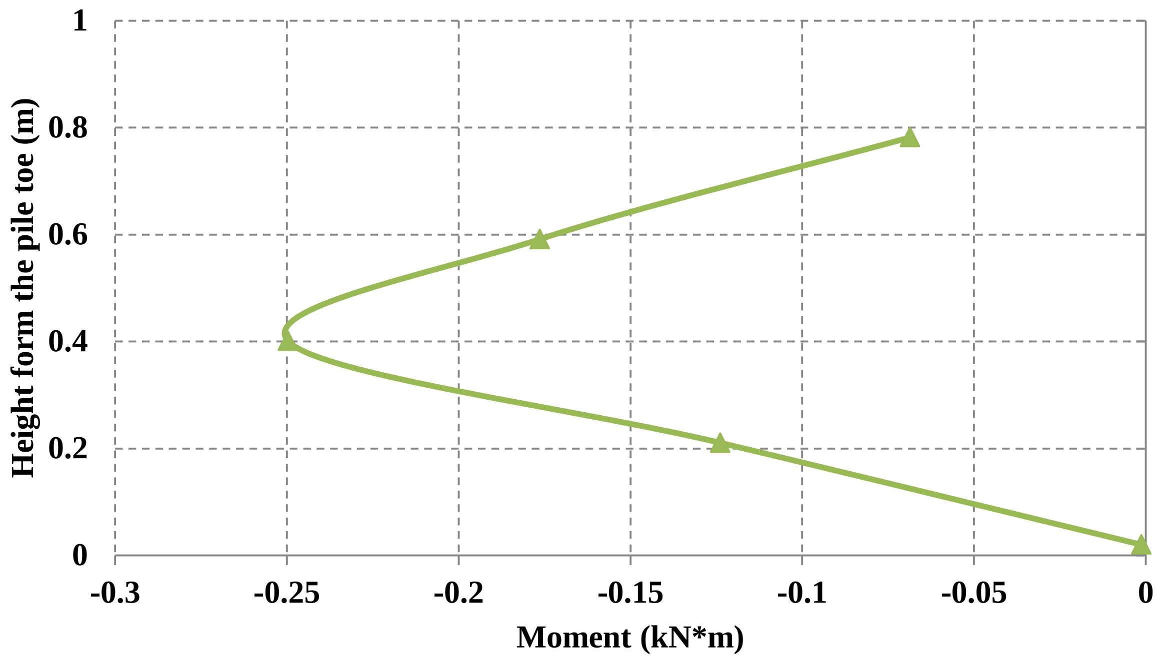

Figure A.137 Moment along the Pile for Scour Depth = 300 mm and Width = 667 mm

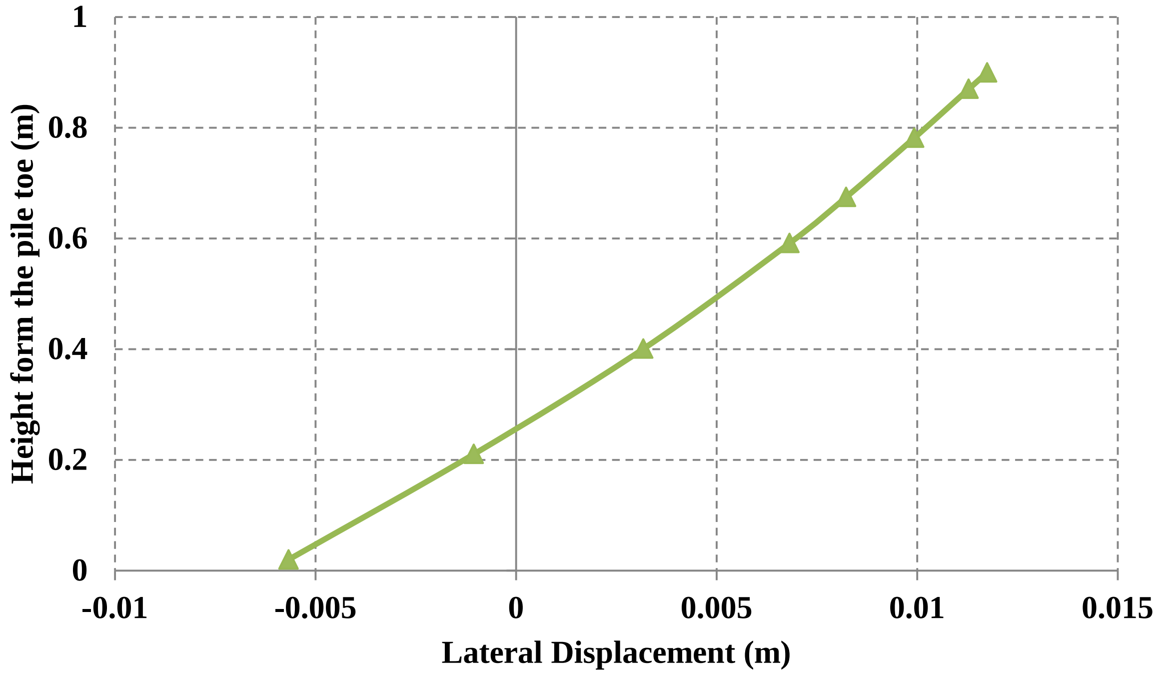

Figure A.138 Lateral Displacement along the Pile for Scour Depth = 300 mm and Width = 667 mm

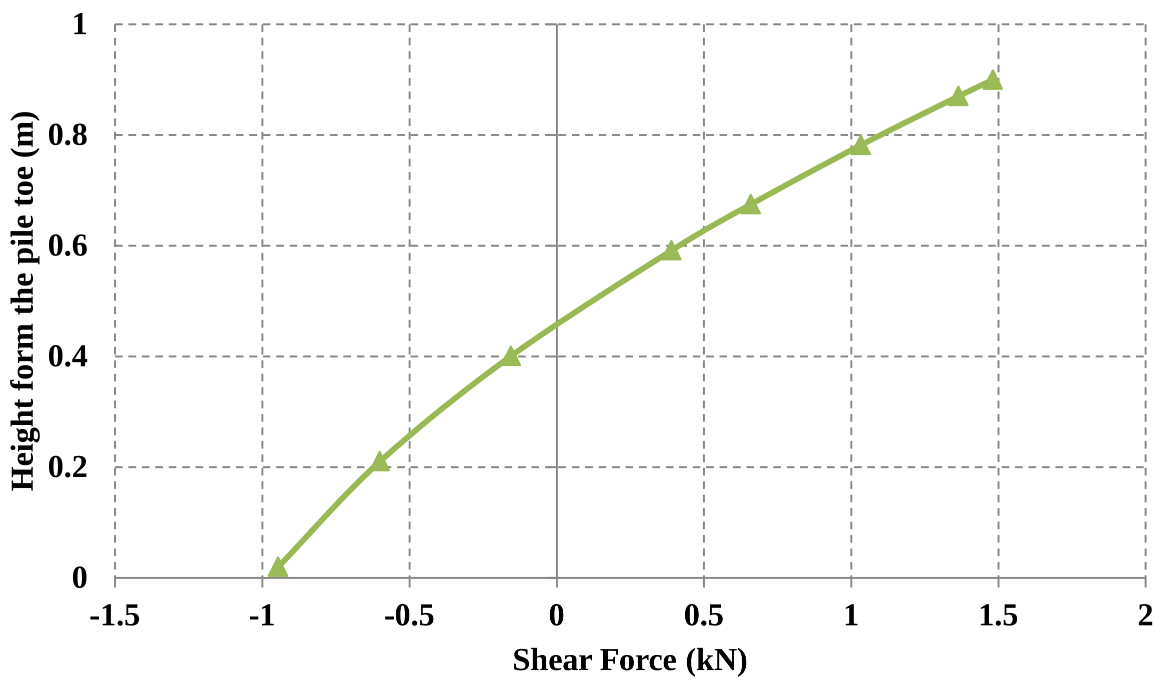

Figure A.139 Shear Force along the Pile for Scour Depth = 300 mm and Width = 667 mm

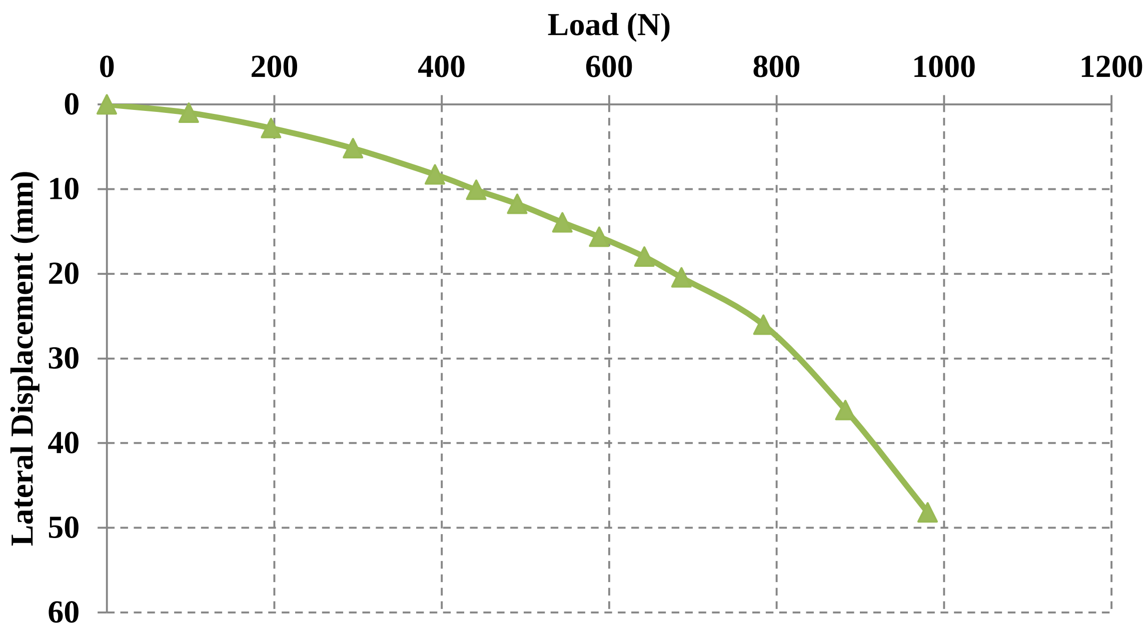

Figure A.140 Lateral Displacements vs. Load for Scour Depth = 300 mm and Width = 667 mm

400-mm scour depth

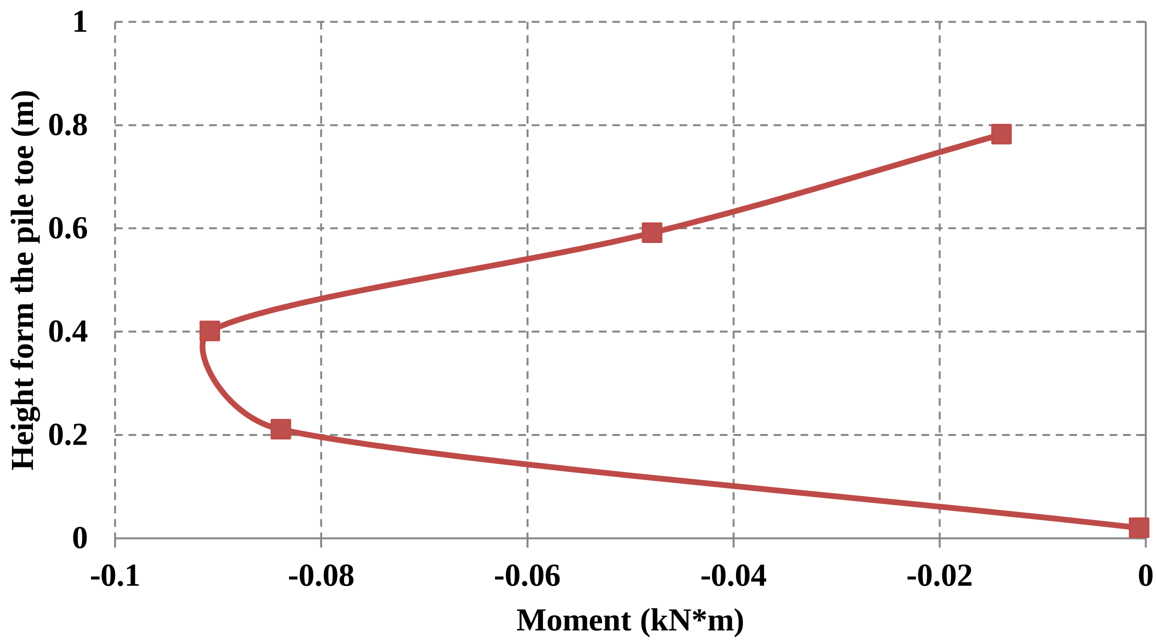

Figure A.141 Moment along the Pile for Scour Depth = 400 mm and Width = 667 mm

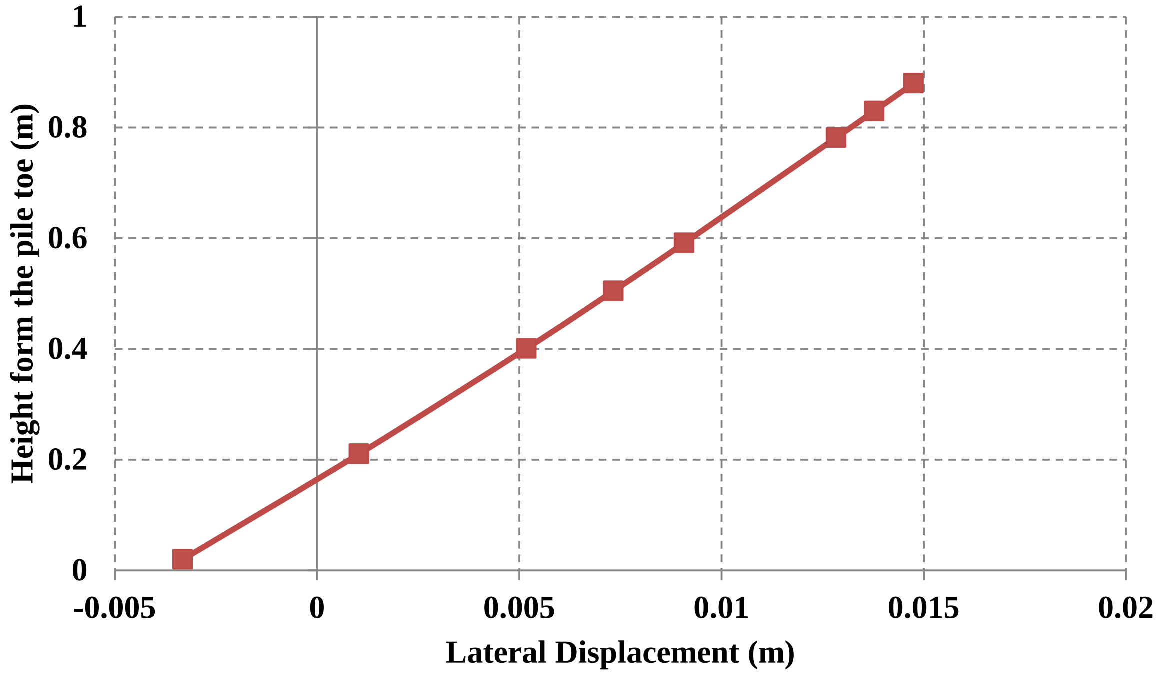

Figure A.142 Lateral Displacement along the Pile for Scour Depth = 400 mm and Width = 667 mm

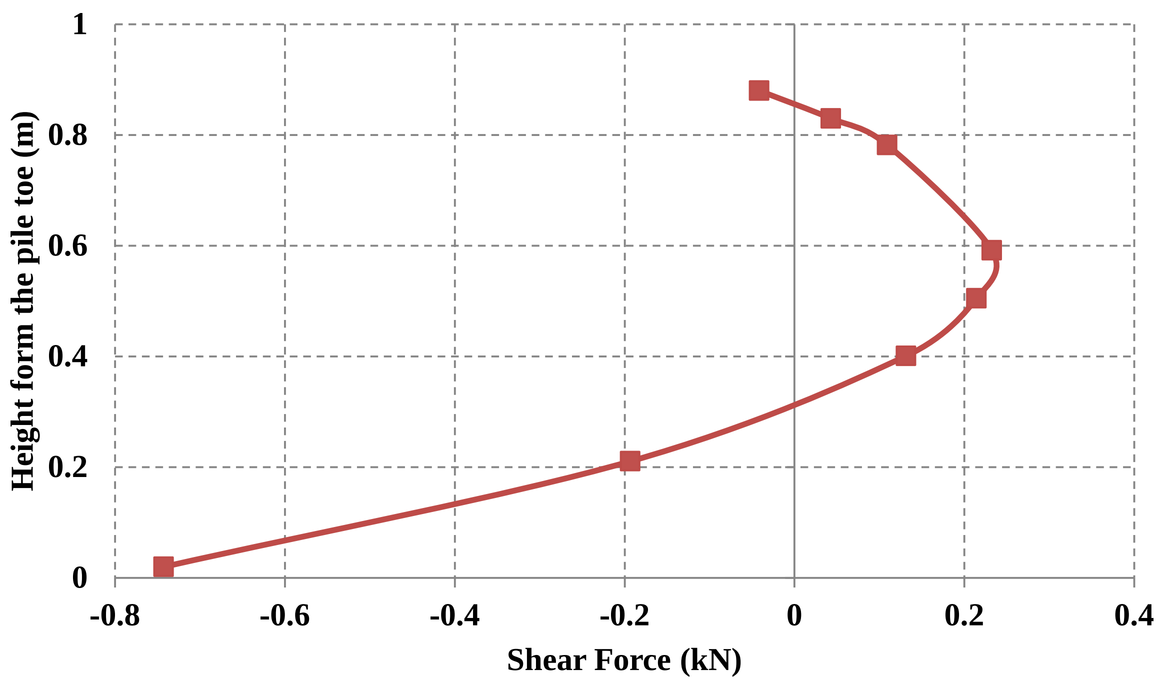

Figure A.143 Shear Force along the Pile for Scour Depth = 400 mm and Width = 667 mm

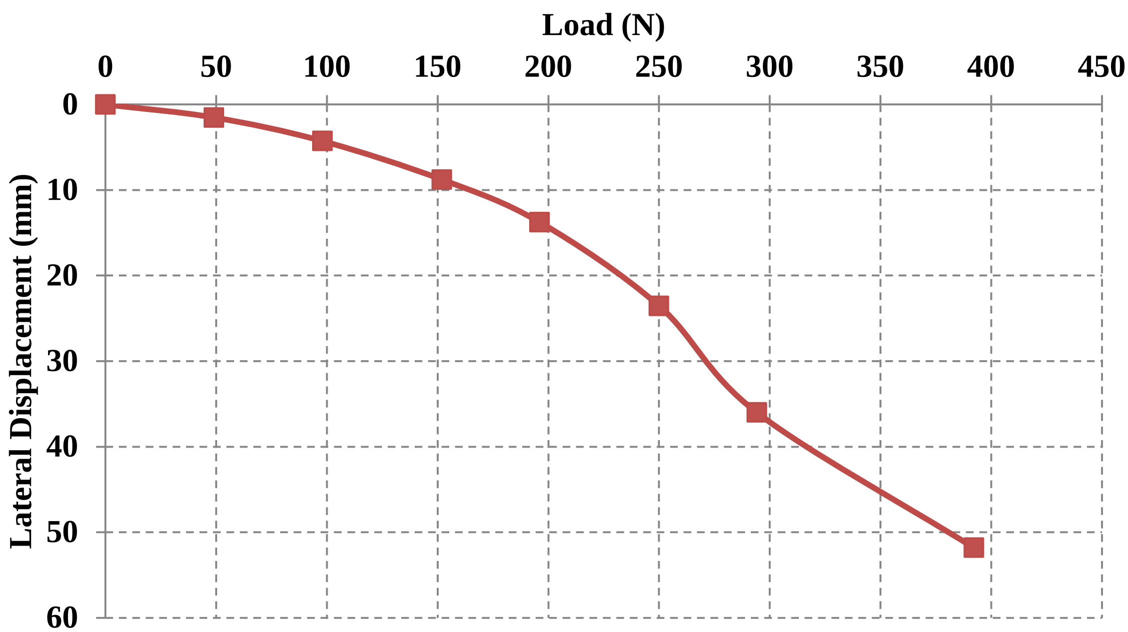

Figure A.144 Lateral Displacements vs. Load for Scour Depth = 400 mm and Width = 667 mm

500-mm scour depth

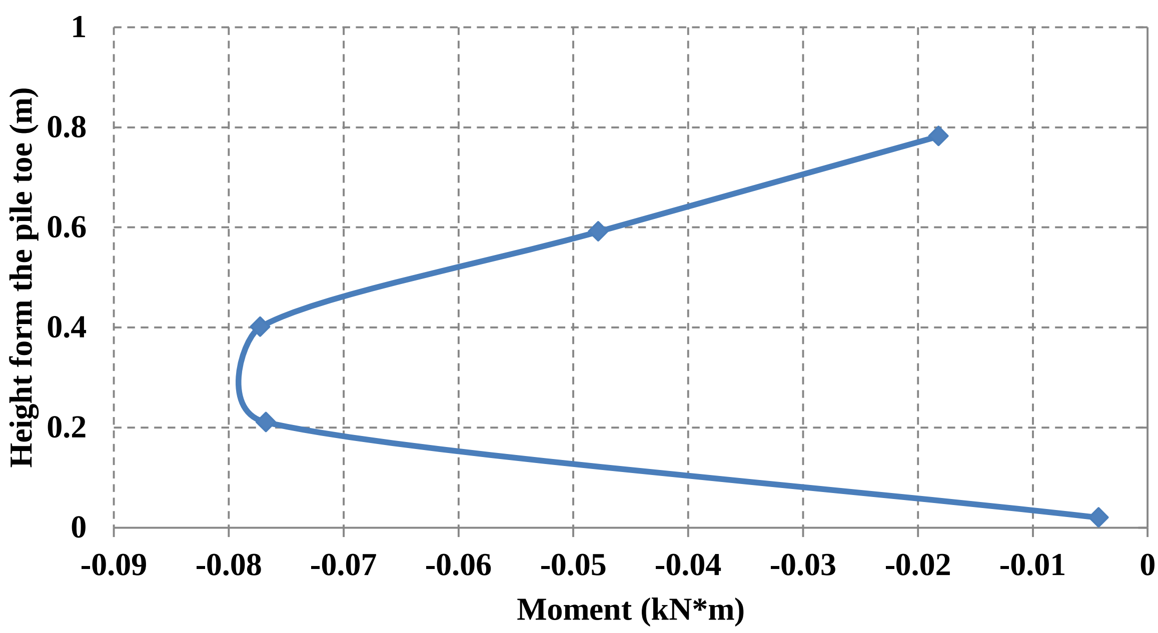

Figure A.145 Moment along the Pile for Scour Depth = 500 mm and Width = 667 mm

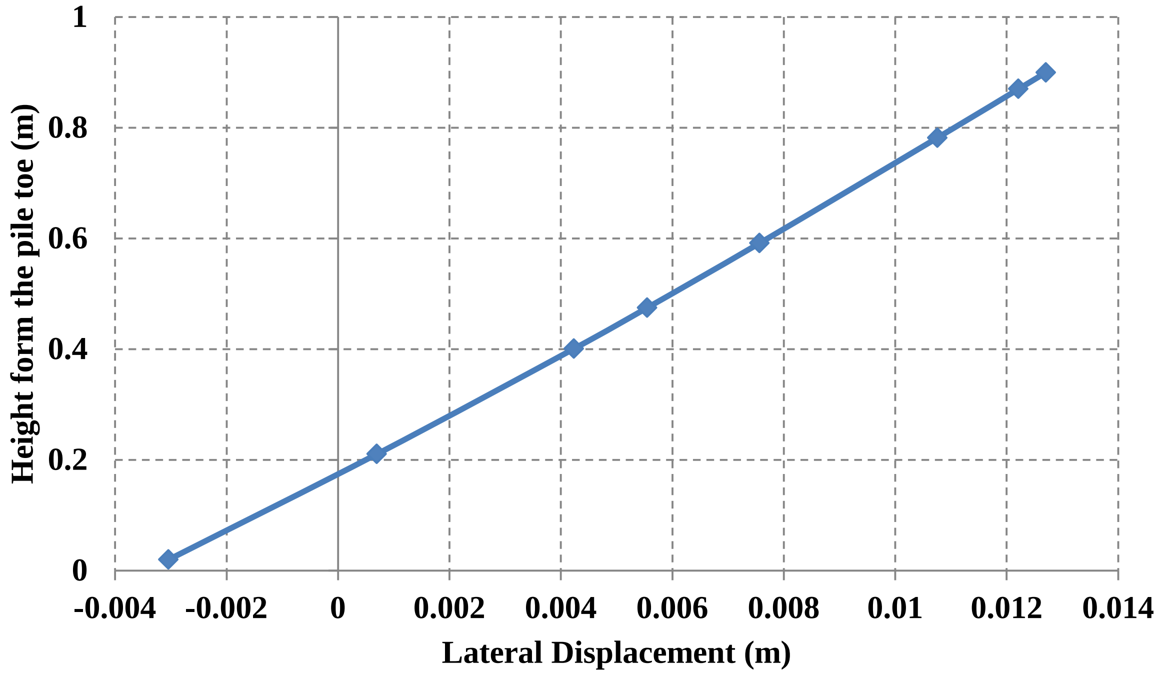

Figure A.146 Lateral Displacement along the Pile for Scour Depth = 500 mm and Width = 667 mm

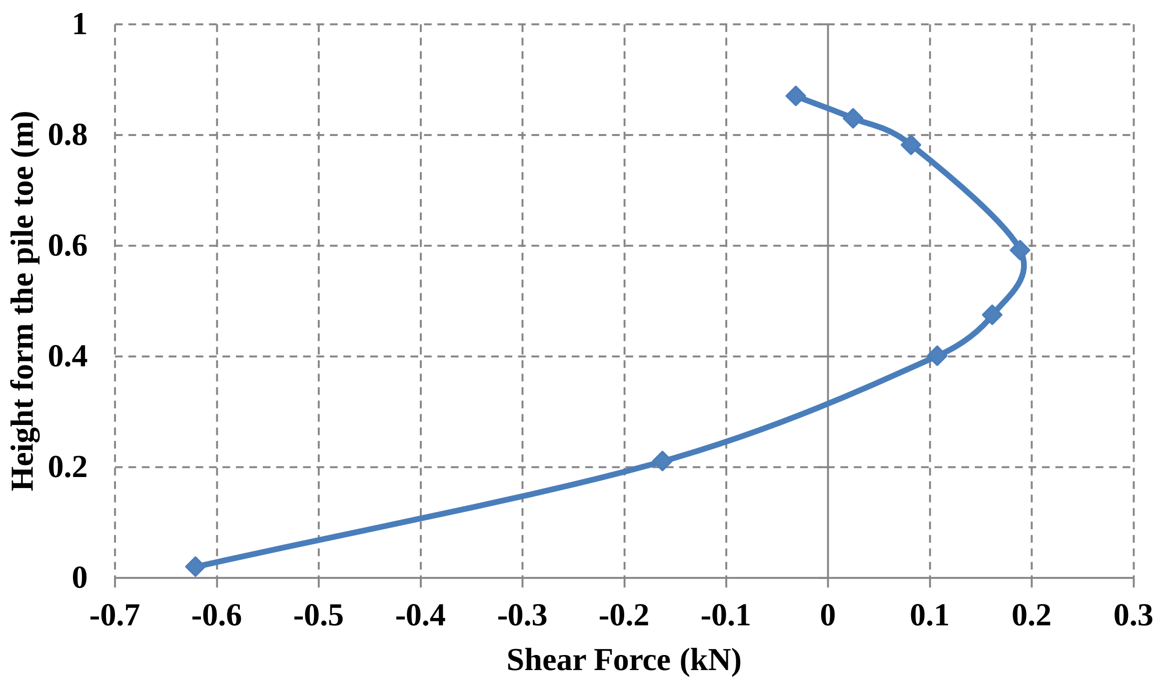

Figure A.147 Shear Force along the Pile for Scour Depth = 500 mm and Width = 667 mm

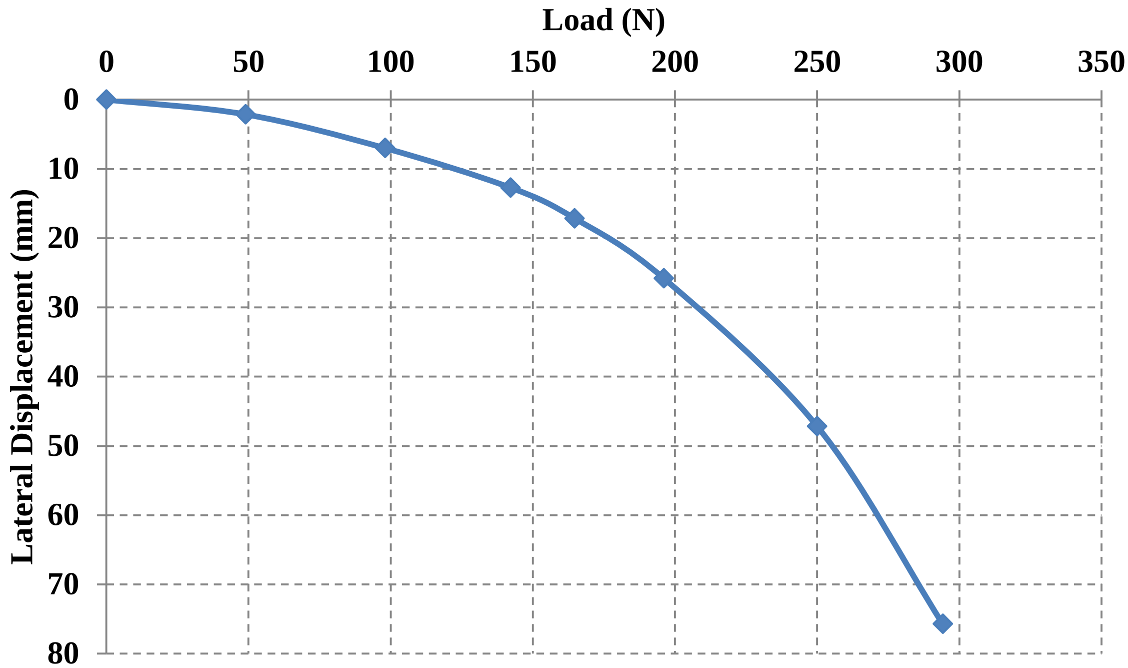

Figure A.148 Lateral Displacements vs. Load for Scour Depth = 500 mm and Width = 667 mm

A.4. Repeated loading experiments

A.4.1. Repeated test 1

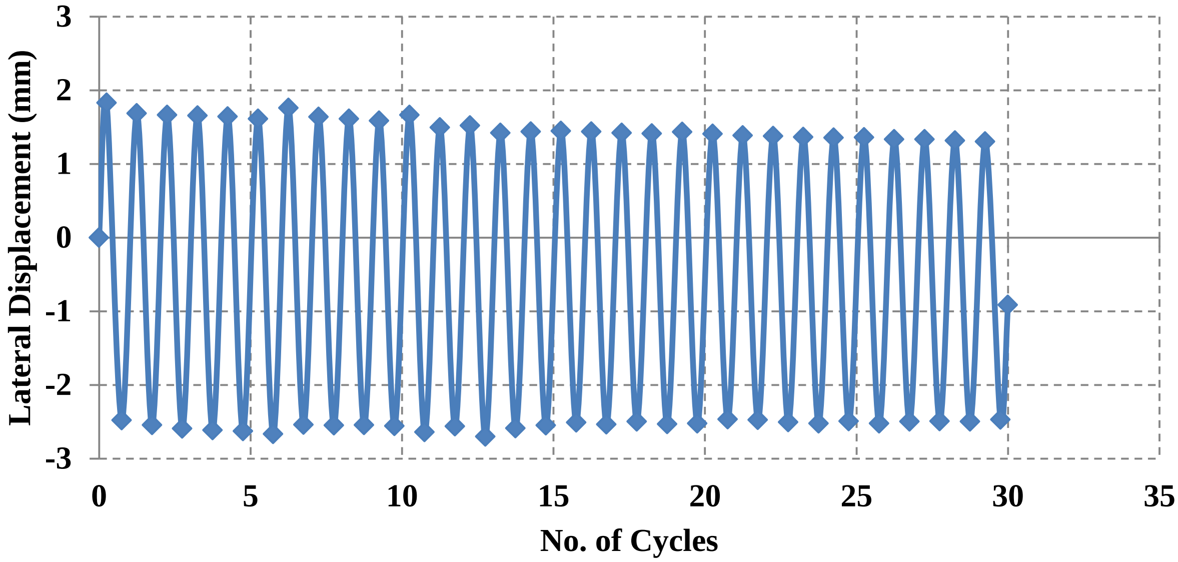

Figure 4.149 Lateral Displacement with No. of Cycles for Repeated Test 1

A.4.2. Repeated test 2

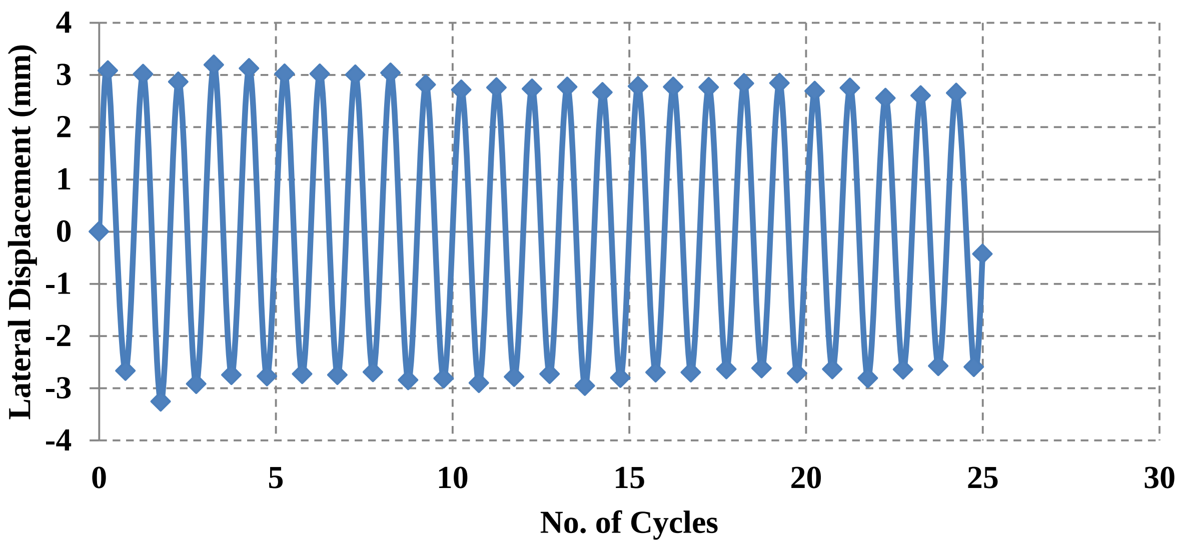

Figure 4.150 Lateral Displacement with No. of Cycles for Repeated Test 2

A.4.3. Repeated test 3

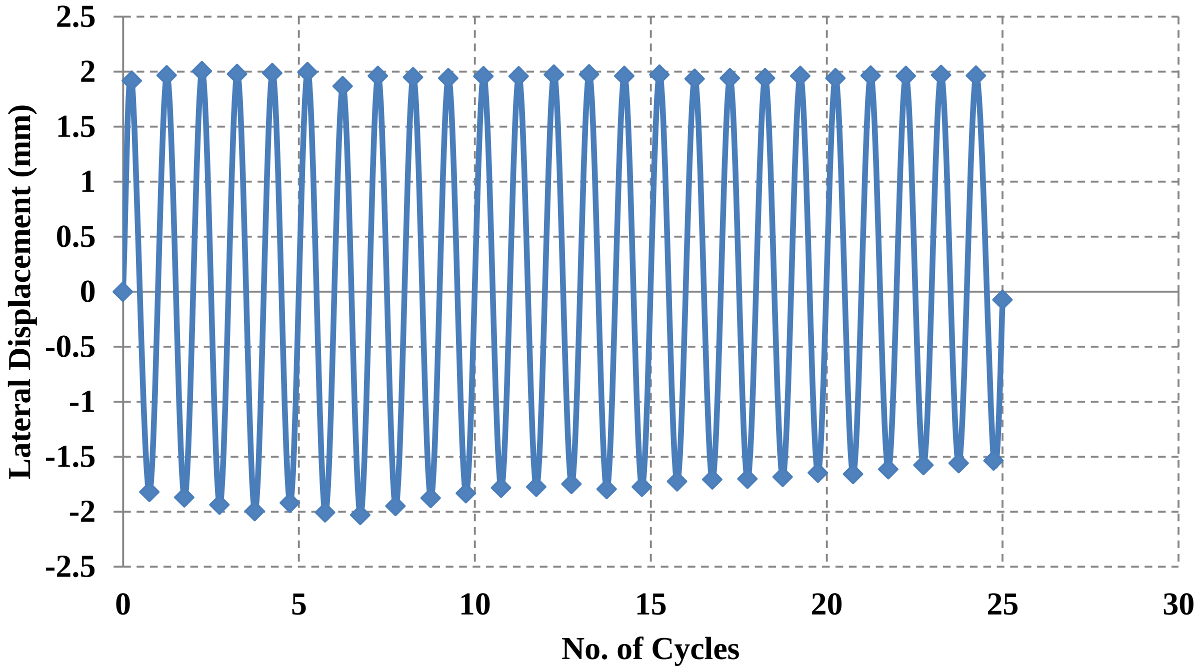

Figure 4.151 Lateral Displacement with No. of Cycles for Repeated Test 3